Transition Metal Catalysis in the Presence of Fluorinating Reagents

Matthew N. Hopkinson

A thesis submitted to the Board of the Faculty of Physical Sciences in partial fulfilment of the requirements for the degree of Doctor of Philosophy at the University of Oxford



Merton College

Trinity Term 2011

Author's Declaration

The work presented in this thesis was conducted at the Chemistry Research Laboratory and the Inorganic Chemistry Laboratory at the University of Oxford and at the GlaxoSmithKline Clinical Imaging Centre at Hammersmith Hospital, London between Michaelmas Term 2007 and Trinity Term 2011 under the supervision of Professor Véronique Gouverneur. All the work is my own, except where otherwise stated, and has not been submitted for any other degree at this or any other university.

Matthew N. Hopkinson

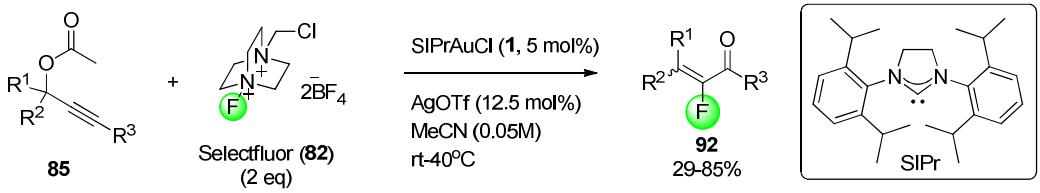
September 2011

Transition Metal Catalysis in the Presence of Fluorinating Reagents

In this thesis, the effect of fluorinating reagents on a selection of transition metal-mediated organic transformations was investigated. The first four chapters are focused on gold-catalysed nucleophilic addition processes performed in the presence of "F^+" sources.

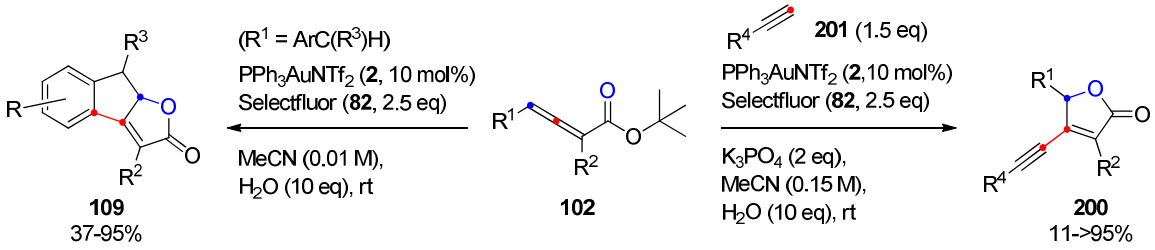
Chapter 1 provides a general introduction to homogeneous gold catalysis and summarises the aims and objectives of the project.

The effect of the electrophilic fluorinating reagent Selectfluor (**82**) on the gold-catalysed rearrangement of propargyl acetates **85** is discussed in **Chapter 2**. α-Fluoroenones **92** resulting from fluorodeacetylation of an allenyl acetate intermediate were delivered as the major products of these reactions (Scheme i).



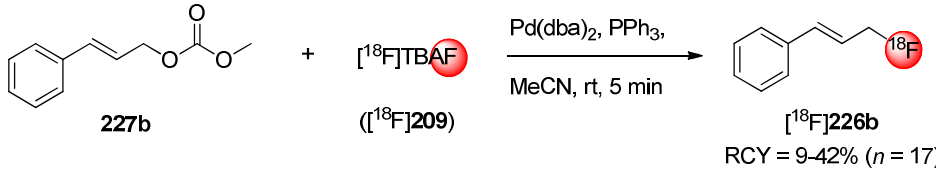
Scheme i Gold-Catalysed Rearrangement-Fluorodeacetylation of Propargyl Acetates **85**.

By contrast, performing the gold(I)-catalysed cyclisation of allenoates **102** in the presence of Selectfluor (**82**) led to products of oxidative coupling. The "F^+" source in these processes most likely acts as an external oxidant in an Au^I/Au^{III} redox cycle. In **Chapter 3**, the cascade cyclisation-intramolecular arylation of benzyl-substituted substrates is discussed whilst the extension of the methodology towards intermolecular homocoupling and intermolecular alkynylation is presented in **Chapter 4** (Scheme ii).



Scheme ii Gold-Catalysed Cyclisation-Oxidative Coupling of *tert*-Butyl Allenoates **102**.

In **Chapter 5**, the feasibility of palladium-catalysed allylic [^{18}F]radiofluorination was investigated using high-specific-activity [^{18}F]fluoride. This study led to the development of the first transition metal-mediated C-^{18}F bond-forming process of relevance for the preparation of radiotracers for PET imaging (Scheme iii).



Scheme iii Palladium-Catalysed Allylic [^{18}F]Radiofluorination of Allylic Methyl Carbonate **227b**.

Chapter 6 gives full experimental procedures and characterisation data for all compounds.

Acknowledgements

My first thanks must go to the people who have directly contributed in some way to the work presented in this thesis. A big thank you to Andy Salisbury and Dr. Arnaud Tessier for starting off the oxidative coupling methodology and providing me with a working project to move onto when PET wasn't going too well. I am also grateful to Jonny Ross for doing a great job on the alkynylation project and for making my job as Part II supervisor very easy. Special thanks must go to Dr. Mickael Huiban for all his help in the 'hot' lab at GlaxoSmithKline working on the palladium project. Sticking with PET, I must also thank Lei Li for spending many long hours with me in the 'hot' labs at GSK and SOMIL and for being a pleasure to work with on the multicomponent project. Thanks to Charley Hollingworth and Amaruka Hazari for validating the 'cold' palladium-catalysed allylic fluorination reaction and providing me with substrates for the 'hot' work. I would also like to thank Dr. Matthew Tredwell for proof reading this thesis and for general advice on all things chemistry.

I am very much indebted to Professor Véronique Gouverneur for all her help and support over the course of my DPhil. Her enthusiasm and encouragement have been an inspiration when things were going well and a comfort when things were not. I am also very grateful for being allowed the freedom to pursue the projects that interested me and come up with my own ideas. On a separate note, I would like to thank Max for many enjoyable walks over the years. I am also greatly indebted to GlaxoSmithKline for funding my DPhil and to my industrial supervisor Professor Tony Gee for all his help and suggestions.

Thank you to Dr. Barbara Odell and the NMR and mass spectrometry services for their assistance with characterisation. A big thanks must also go to Dr. Amber Thompson,

Lorraine Combettes and, especially, Guy Giuffredi for running and analysing all the crystal data presented in this thesis.

I would like to thank all the past and present members of Gouverneur group for making coming into the lab such an enjoyable experience. A special mention must go to Laurence Carroll, Lei Li and the 'Bay 1' occupants Matt Tredwell, Jamie Wolstenhulme and Guy Giuffredi for many good times in and out of the lab. I am particularly grateful to Guy for being a great friend over the past four years whether in the lab, on the football pitch or over one or two cups of tea or pints of beer. I must also thank all the VG footballers who contributed to our glorious victory in the Catalyst Cup.

I would like to take this opportunity to thank my Mum and Dad for all the sacrifices they have made for me over 26 years. I am deeply thankful for all their encouragement and unwavering support in everything I have done. Thank you for being the best parents in the world. Finally, I would like to thank my brother Richard for being my best friend and sharing my time in Oxford as both a graduate and an undergraduate.

Contents

Author's Declaration i
Abstract ii
Acknowledgements iii
Contents v
Abbreviations and Acronyms viii

Chapter 1: Introduction to Homogeneous Gold Catalysis 1

1.1 Gold 1
1.2 General Properties of Gold Catalysts 1
1.3 Nucleophilic Additions to C-C Multiple Bonds 5
1.3.1 Oxygen Nucleophiles 5
1.3.2 Sulfur Nucleophiles 11
1.3.3 Nitrogen Nucleophiles 12
1.3.4 Halide Nucleophiles 15
1.3.5 Carbon Nucleophiles 16
1.4 Demetallation Pathways Beyond Protodeauration 21
1.4.1 Trapping of Gold Carbenoids 22
1.4.2 Nucleophilic Attack of C-Au Bonds 24
1.4.3 Iodo-, Bromo- and Chlorodeauration 27
1.5 Extension of the Methodology Towards Fluorination 29
1.5.1 Fluorodeauration 30
1.5.2 Outline of this Thesis 32

Chapter 2: Gold and F^+: Gold-Catalysed Fluorination 34

2.1 Introduction 34
2.2 Preliminary Studies 37
2.3 Optimisation of the Reaction Conditions 40
2.4 Preparation of Propargyl Acetates **85** 45
2.5 Scope and Limitations of the Fluorination Process 48
2.6 Comments on the Reaction Mechanism 54

2.7 Conclusions 62

Chapter 3: Gold and F^+: Gold-Catalysed Oxidative Coupling I: Intramolecular Coupling 64

3.1 Introduction 64

3.2 Cyclisation-Intramolecular Arylation of Benzyl-Substituted *tert*-Butyl Allenoates 67

3.2.1 Preliminary Studies 67

3.2.2 Literature Examples of Gold-Mediated Oxidative Coupling using Alternative External Oxidants 73

3.2.3 Optimisation of the Reaction Conditions 90

3.2.4 Preparation of *tert*-Butyl Allenoates **102** 98

3.2.5 Scope and Limitations of the Oxidative Coupling Process 103

3.2.6 Comments on the Reaction Mechanism 109

3.2.7 Conclusions 129

Chapter 4: Gold and F^+: Gold-Catalysed Oxidative Coupling II: Intermolecular Coupling 131

4.1 Introduction 131

4.2 Cyclisation-Homodimerisation of *tert*-Butyl Allenoates 132

4.2.1 Introduction 132

4.2.2 Preliminary Studies Using Sub-Stoichiometric Gold 133

4.2.3 Development of the Gold-Catalysed Process Using Selectfluor 141

4.3 Cyclisation-Alkynylation of *tert*-Butyl Allenoates 154

4.3.1 Introduction 154

4.3.2 Preliminary Studies 161

4.3.3 Optimisation of the Reaction Conditions 162

4.3.4 Scope and Limitations of the Cross-Coupling Process 167

4.3.5 Comments on the Reaction Mechanism 175

4.4 Conclusions 183

Chapter 5: Palladium and $^{18}F^-$: Palladium-Catalysed $[^{18}F]$Radiofluorination for PET Imaging 185

5.1 Introduction to PET Imaging and Fluorine-18 185

5.2 Radiolabelling with Fluorine-18 187

5.2.1 General Considerations of Labelling with Short-Half-Life Radioisotopes.....187
5.2.2 Sources of Fluorine-18.....188
5.3 Nucleophilic [^{18}F]Radiofluorination Methods.....190
5.3.1 Aliphatic Nucleophilic [^{18}F]Radiofluorination.....190
5.3.2 Aromatic Nucleophilic [^{18}F]Radiofluorination.....192
5.4 Applying Transition Metal Catalysis to ^{18}F-Radiochemistry.....198
5.4.1 Palladium-Catalysed Allylic Fluorination.....201
5.4.2 Outline of the Project.....203
5.5 Palladium-Mediated Allylic [^{18}F]Radiofluorination.....204
5.5.1 Preliminary Studies.....204
5.5.2 Effect of Different Reaction Conditions.....209
5.5.3 Comparison with Conventional S_N2 [^{18}F]Radiofluorination.....212
5.6 Conclusions.....214

Chapter 6: Experimental Procedures and Characterisation Data.....216

6.1 General Experimental Information.....216
6.2 Experimental Data for Chapter 2.....218
6.3 Experimental Data for Chapter 3.....252
6.4 Experimental Data for Chapter 4.....292
6.5 Experimental Data for Chapter 5.....330

Chapter 7: References.....335

Appendix: X-Ray Crystallography Data.....A-1

Abbreviations and Acronyms

[^{18}F]FDG	2-Deoxy-2-[^{18}F]fluoro-D-glucose
[^{18}F]FDOPA	6-[^{18}F]Fluoro-L-3,4-dihydroxyphenylalanine
[^{18}F]FMISO	[^{18}F]Fluoromisonidazole
Å	Ångström (10^{-10} metres)
Ac	Acetyl
aq	Aqueous
Ar	Aryl
Bn	Benzyl
Bq	Bequerel (s^{-1})
Bu	Butyl
Cbz	Carboxybenzyl
CI	Chemical Ionisation
Cy	Cyclohexyl
dba	Dibenzylideneacetone
DMA	*N*,*N*-Dimethylacetamide
DMF	*N*,*N*-Dimethylformamide
DMSO	Dimethylsulfoxide
dppm	1,1-Bis(diphenylphosphino)methane
dr	Diastereoisomeric Ratio
E^0	Standard Electrode Potential
ee	Enantiomeric Excess
eq	Equivalent(s)
ESI	Electrospray Ionisation
Et	Ethyl
eV	Electron Volt(s)
FI	Field Ionisation
Fmoc	Fluorenylmethyloxycarbonyl
g	Gram(s)
h	Hour(s)
HOESY	Heteronuclear Overhauser Effect Spectroscopy
HPLC	High Performance Liquid Chromatography
HRMS	High Resolution Mass Spectrometry

Hz	Hertz
i	*Iso*
IPr	1,3-Bis(2,6-diisopropylphenyl)imidazol-2-ylidene
IR	Infrared Spectroscopy
Kryptofix 222 (K222)	1,10-Diaza-4,7,13,16,21,24-hexaoxabicyclo[8.8.8]hexacosane
L	Neutral Ligand
LRMS	Low Resolution Mass Spectrometry
LUMO	Lowest Unoccupied Molecular Orbital
M	Moles per cubic decimetre ($moldm^{-3}$)
Me	Methyl
Mes	1,3,5-Trimethylphenyl (Mesityl)
min	Minute(s)
mL	Millilitre(s)
mol	Mole(s)
Mp	Melting Point
Ms	Methanesulfonyl (Mesyl)
n	Normal
NBS	*N*-Bromosuccinimide
NCS	*N*-Chlorosuccinimide
NFSI	*N*-Fluorobenzenesulfonimide
NHC	*N*-Heterocyclic Carbene
NIS	*N*-Iodosuccinimide
NOE	Nuclear Overhauser Effect
NR	No Reaction
$^{n}J_{XY}$	Scalar coupling constant (in NMR Spectra) between nuclei X and Y through n bonds
NMR	Nuclear Magnetic Resonance Spectroscopy
NTf_2	Bis(trifluoromethanesulfonyl)imide
PET	Positron Emission Tomography
Pet. Ether	Petroleum Ether
Ph	Phenyl
PIDA	(Diacetoxyiodo)benzene
Piv	Dimethylpropanoyl (Pivaloyl)
ppm	Parts per Million

Pr	Propyl
QMA	Quaternary Methyl Ammonium
RCY	Radiochemical Yield
R_f	Retention Factor
rt	Room Temperature
SA	Specific Activity
S_EAr	Electrophilic Aromatic Substitution
Selectfluor	1-Chloromethyl-4-fluoro-1,4-diazoniabicyclo[2.2.2]octane bis(tetrafluoroborate)
SIPr	1,3-Bis(2,6-diisopropylphenyl)imidazolidin-2-ylidene
S_NAr	Nucleophilic Aromatic Substitution
Su	Succinimidyl
t	Tertiary (*tert*)
$t_{½}$	Half-Life
TBAF	Tetra-*n*-butylammonium fluoride
TBDPS	*tert*-Butyldiphenylsilyl
TBS	*tert*-Butyldimethylsilyl
t-BuBrettphos	2-(Di(*tert*-butyl)phosphino)3,6-dimethoxy-2′,4′,6′-triisopropyl-1,1′-biphenyl
Tf	Trifluoromethanesulfonyl (Triflyl)
TFA	Trifluoroacetic Acid
THF	Tetrahydrofuran
TLC	Thin Layer Chromatography
Ts	*para*-Toluenesulfonyl (Tosyl)
UV	Ultraviolet
V	Volt(s)
Z	Atomic Number
Z_{eff}	Effective Nuclear Charge
β^+	Positron (Positive Beta Radiation)
δ	Chemical Shift
µL	Microlitre(s)
ºC	Degrees Celcius

Chapter 1

Introduction to Homogeneous Gold Catalysis

1.1 Gold

Gold has captured the imagination of mankind more than perhaps any other element. Attractive in appearance, the acquisition and display of gold has been a consistent feature of human civilisation since the beginning of recorded history. To this day, gold retains many of its traditional uses in jewellery, art and as a store of value and has also found many novel applications in such diverse areas as electronics, medicine, photography and dentistry. Some of this appeal can be attributed to the stability of the elemental Au^0 oxidation state. With a filled 5d-shell and tightly held 6s electron, the first ionisation potential for gold is among the highest in the d-block (E^0 of $Au^0/Au^I = +1.69V$)[1] and Au^0 is resistant to oxidative corrosion and tarnishing. It is perhaps the unreactive nature of gold(0) and the consequent assumption that gold in all its forms is inert that has precluded, until recently, its study as a metal for catalysis. When not in the elemental oxidation state, however, gold is capable of catalysing a wide-range of chemical transformations and nowadays homogeneous gold catalysis represents one of the most dynamic and fast-moving areas of chemical research.[2-12]

1.2 General Properties of Gold Catalysts

A third row transition metal with the ground state electronic configuration $[Xe]4f^{14}5d^{10}6s^1$, the chemistry of gold bears similarities with the other group 11 elements, copper and silver. However, in this part of the periodic table, relativistic effects derived from the increased atomic number *Z* are not insignificant and, as a result, gold possesses many characteristics

not observed with the other 'coinage' metals (Figure 1.1).[13]

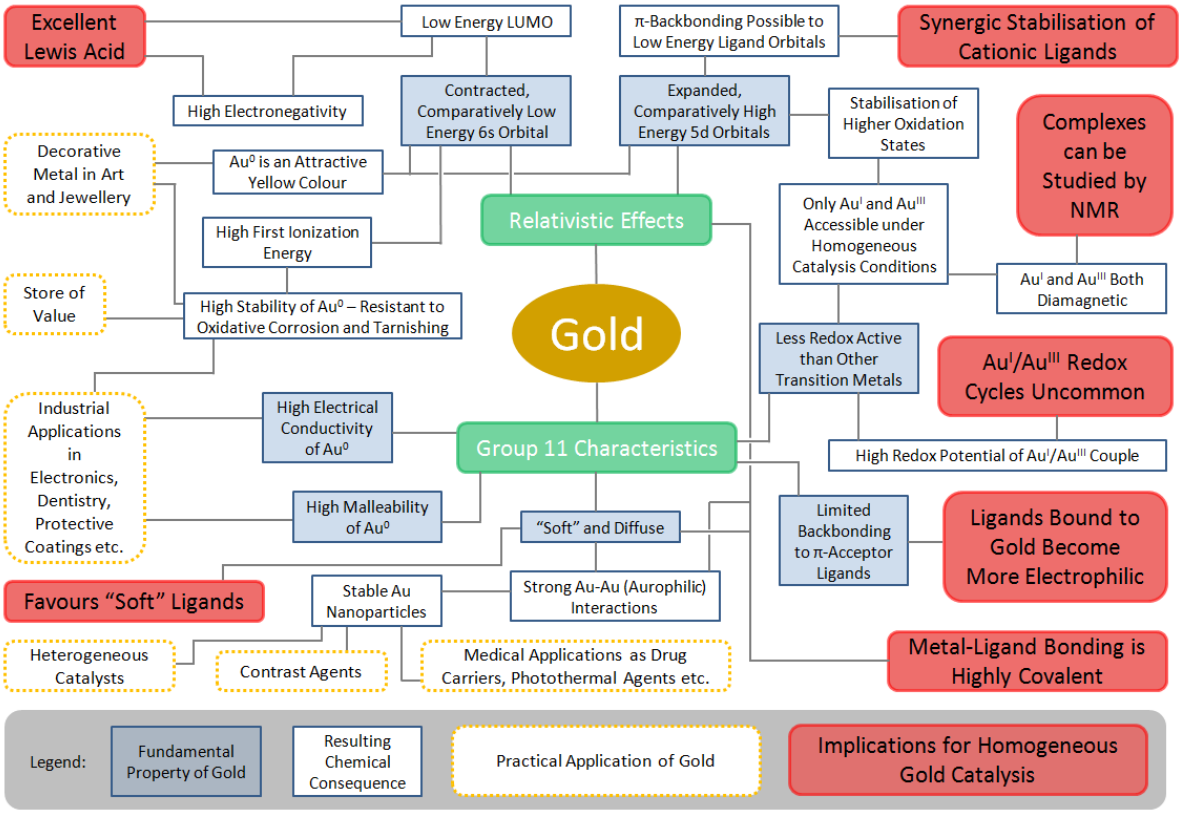


Figure 1.1 Some Fundamental Properties of Gold and their Implications for Homogeneous Catalysis.

The principal consequence of relativity on the atomic properties of gold is the radial contraction of the valence 6s orbital. The resulting energetic stabilisation of the 6s electron due to its greater exposure to the nuclear charge is reflected in the high first ionisation energy of gold and the consequent stability of the elemental oxidation state. A secondary effect of the 6s contraction is the radial expansion and energetic destabilisation of the 5d orbitals. Electrons in these orbitals experience a comparatively small effective nuclear charge (Z_{eff}) due to more efficient shielding by radially contracted s and p electrons. The combined effects of a low 6s and high 5d energy lead to a comparatively small energy barrier for the excitation of a 5d electron to the Fermi level (essentially the 6s band) in gold(0). The bandgap of 2.38 eV corresponds to the absorption of blue visible light and results in the attractive yellow colour of the metal.

The relativistic effects described above also provide a theoretical model for understanding some aspects of the reactivity of gold in higher oxidation states in the presence of organic substrates. In line with the other group 11 metals, the redox chemistry of gold is comparatively limited. However, the relative stabilities of the accessible oxidation states vary for the different 'coinage' elements. Whereas the coordination chemistry of copper and silver is dominated by the +1 and +2 oxidation states, M^{3+} complexes are much more prevalent with the heavier element whilst gold(II) is unstable towards disproportionation. This increased stabilisation of the higher oxidation state can be explained in part by the relativistically destabilised 5d electrons which are relatively easily removed from the metal.[14-15] As a result, only two oxidation states, +1 and +3, are generally observed under homogeneous catalysis conditions. Gold(III) has a $5d^8$ electron configuration and typically adopts a square planar geometry whereas $5d^{10}$ gold(I) generally forms linear species. Au^I and Au^{III} are readily available as the corresponding halides whilst alternative catalysts stabilised by pyridyl (for gold(III)) or *N*-heterocyclic carbene (NHC) or phosphine ligands (for gold(I)) have been reported. Coordinatively-saturated gold(I) complexes of the form [LAuX] (L = neutral ligand eg. phosphine or NHC, X = charged ligand eg. Cl; such as SIPrAuCl, **1**, Figure 1.2) only become catalytically active upon the generation of a free coordination site through the loss of the ligand X. Precatalysts containing halide ligands typically require the addition of a silver(I) co-catalyst whilst more recently-developed complexes bearing less coordinating counter-ions such as $^-NTf_2$ dissociate upon solvation (eg. PPh_3AuNTf_2, **2**, Figure 1.2).

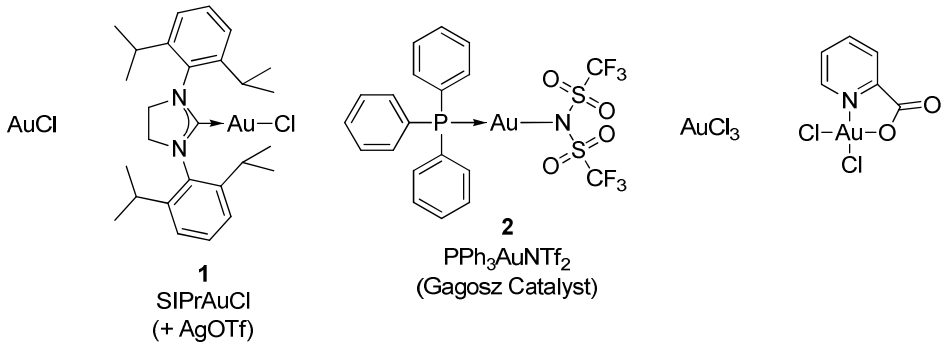


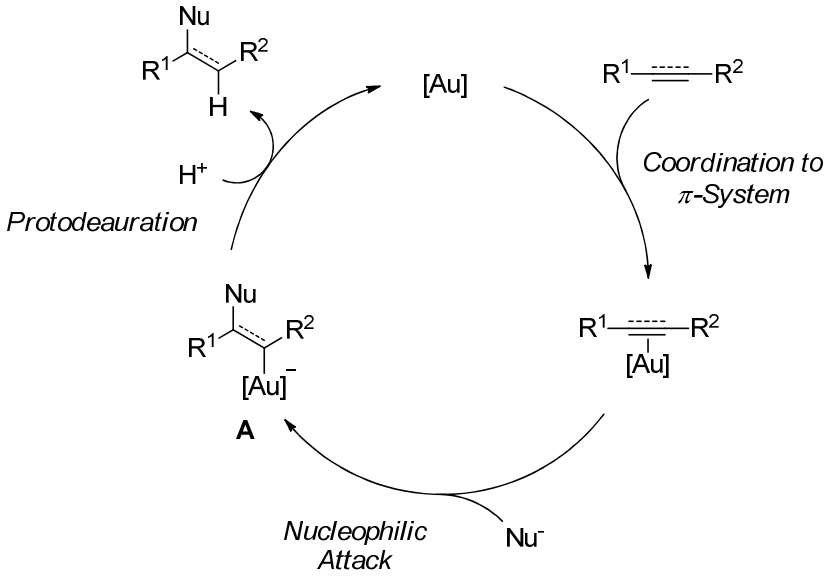
Figure 1.2 Some Common Gold Catalysts and Precatalysts.

The redox potential of the Au^{I}/Au^{III} couple is comparatively high (E^0 = +1.41V)[1] and gold(I) and gold(III) do not generally interconvert under homogeneous catalysis conditions. In particular, gold(I) does not react with molecular oxygen and, as a result, many gold-catalysed transformations can be performed under an atmosphere of air. The lack of redox activity stands in contrast to the chemistry of other late transition metals, such as palladium, which often engage in M^n/M^{n+2} two-electron redox cycles.[16]a Instead, in either the +1 or +3 oxidation state, gold most commonly acts as a redox-neutral Lewis acid towards organic substrates.[b] Moreover, the 'soft' and diffuse nature of the heavy metal leads to a preference for 'soft' ligands whilst metal-ligand bonding is highly covalent. Consequently, in the presence of organic compounds containing multiple functional groups, gold(I) or gold(III) is highly selective for 'softer', carbon-based moieties such as alkynes, allenes or, to a lesser extent, alkenes. Upon coordination to gold, these π-systems become considerably more electrophilic and are activated towards attack by inter- or intramolecular nucleophiles. The combination of the highly σ-accepting character of gold and the lack of synergic 5d-π* back-bonding[17] is thought to lead to an overall reduction of electron density in the

[a] Reactions proceeding via proposed Au^{I}/Au^{III} redox cycles are discussed more thoroughly in Chapter 3 of this thesis.

[b] The proficiency of gold(I) in this role can be rationalised in part by the relativistically contracted 6s orbital, which gives rise to a relatively low energy LUMO.

coordinated π-systems, increasing their electrophilicity. A general catalytic cycle for gold-catalysed nucleophilic additions to C-C multiple bonds is shown in Scheme 1.1.



Scheme 1.1 General Catalytic Cycle for Gold-Catalysed Hydrofunctionalisation Reactions.

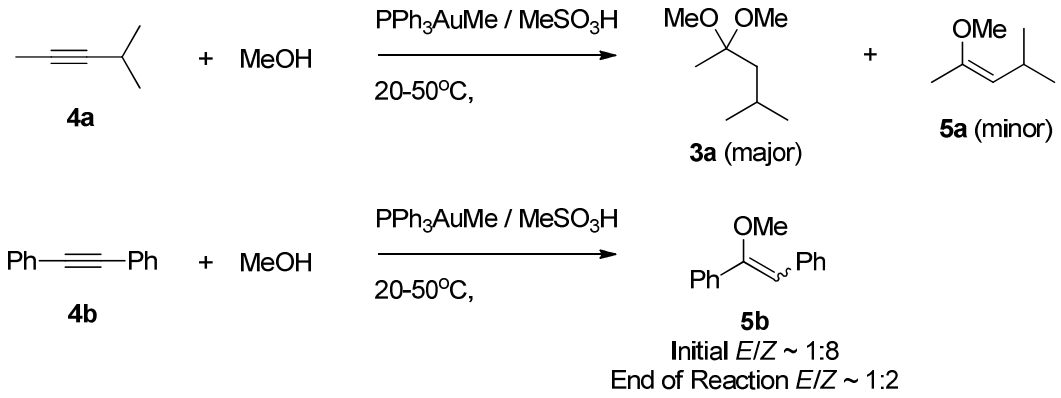
After the initial coordination of either gold(I) or gold(III) to the alkyne, allene or alkene, nucleophilic attack is thought to result in the formation of an organogold intermediate of type **A** where the gold and nucleophile are situated *trans* to each other. In the vast majority of cases these complexes undergo rapid protodeauration to afford the product of *trans*-hydrofunctionalisation and regenerate the catalyst. Reactions of this type make up the largest class of gold-catalysed transformations and, over the last decade, a wide-range of impressive examples involving a variety of nucleophiles and π-systems have been reported.[2-12] In the subsequent sections of this chapter, the development of these processes will be discussed focusing on reactions demonstrating the scope and limitations of the methodology.

1.3 Nucleophilic Additions to C-C Multiple Bonds

1.3.1 Oxygen Nucleophiles

Early studies focused on the addition of water and simple alcohols to alkynes catalysed by gold(III) salts.[18-20] A seminal paper by Teles *et al* in 1998 reported the successful

application of cationic gold(I) complexes as catalysts for this process.[21] Dimethyl acetals **3** were prepared upon reacting simple alkynes **4** with methanol in the presence of [LAuMe] (L = phosphine, phosphite, arsine or NHC) and methanesulfonic acid (Scheme 1.2). The acidic additive serves to cleave the Au-Me bond and generate catalytically-active $[LAu]^+$. The highest turnover numbers were obtained with catalysts bearing the most electron withdrawing ligands L, supporting a mechanism where gold acts as a π-Lewis acid. For the unsymmetrical alkyne **4a**, nucleophilic attack occurred predominantly at the least hindered carbon to afford the dimethyl acetal **3a** as a single regioisomer whilst a small amount of the corresponding enol ether **5a** was also obtained. In the case of diphenylacetylene **4b**, the enol ether **5b** formed upon initial nucleophilic attack did not react further with methanol and was obtained predominantly as the *Z*-diastereoisomer although substantial isomerisation was observed under the reaction conditions.

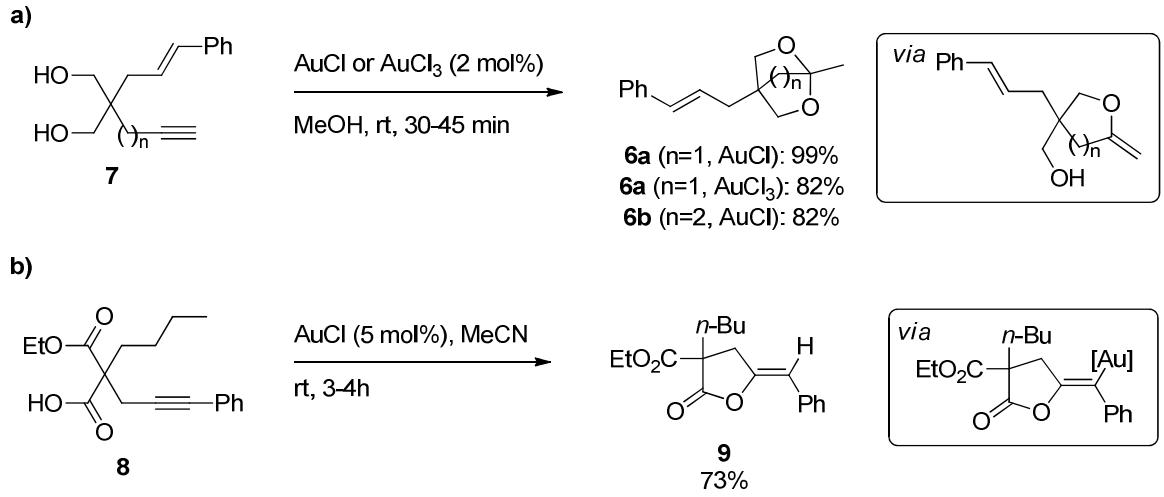


Scheme 1.2 Addition of Methanol across Simple Alkynes **4**.

The use of gold catalysts allows for the alkyne alkoxylation to be performed under mild reaction conditions (20-50ºC) without the need for rigorous extrusion of air or water. In addition, the environmentally and biologically benign nature of gold stands in contrast to the mercury(II) salts traditionally used as catalysts in these processes.[22]

An intramolecular version of this reaction was reported by Genêt and co-workers in 2005.[23] Bicylic ketals **6** were delivered in excellent yield upon cyclising diols **7** in the presence of

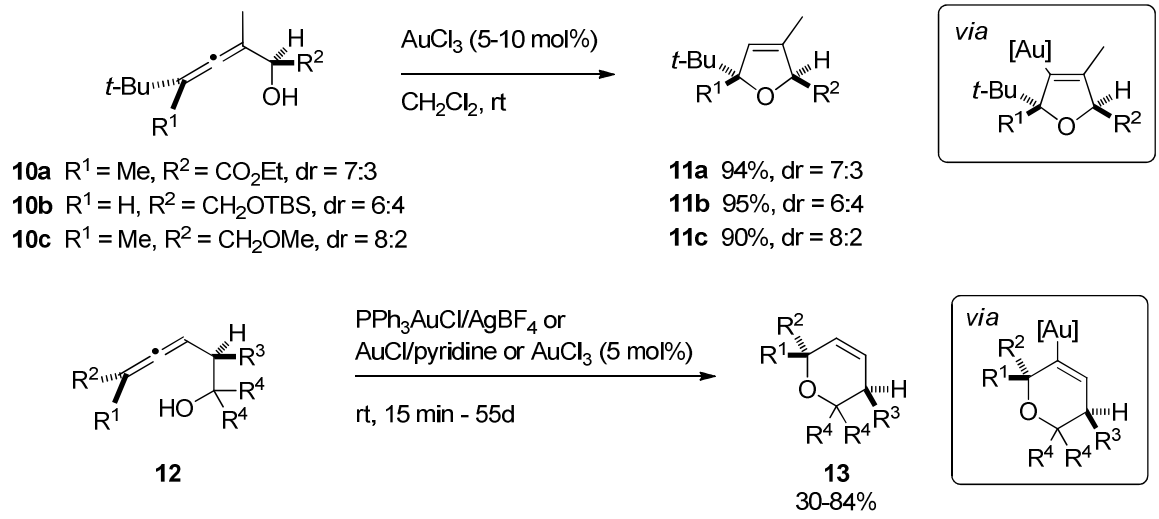
either AuCl or $AuCl_3$ (2 mol%) in methanol (Scheme 1.3a). The reactions were complete within 45 minutes at room temperature whilst no side-products resulting from cyclisation onto the alkene or intermolecular nucleophilic attack of the methanol solvent were observed. In a related process, alkynoic acid **8** cyclised in a 5-*exo*-dig fashion in the presence of AuCl (5 mol%) to afford the corresponding lactone **9** in 73% yield (Scheme 1.3b).[24] The exclusive formation of the *Z*-diastereoisomer is consistent with a *trans*-nucleophilic addition step as depicted in Scheme 1.1 leading to a vinylgold intermediate of type **A**.



Scheme 1.3 a) Intramolecular Cyclisation of a) Diols **7** and b) Alkynoic Acid **8**.

Functionalised α-hydroxyallenes **10** were shown to cyclise in a 5-*endo*-trig fashion in the presence of gold(III) or gold(I) catalysts to afford dihydrofurans **11** in excellent yields (Scheme 1.4).[25-26] Importantly, diastereoisomerically-enriched allenes reacted with complete axis-to-centre chirality transfer. As such, this methodology gives access to valuable heterocyclic motifs under mild conditions in a stereochemically controlled fashion. In addition to increasing the rate of the cyclisation reactions, the use of gold catalysts greatly increases the scope of suitable allene substrates compared to the analogous silver(I)[27] or Brønsted acid catalysed processes.[28] For example, the notoriously sensitive silyl-substituted compound **10b** reacted cleanly with $AuCl_3$ (7 mol%) to afford the corresponding

dihydrofuran **11b** in 95% yield.[25] β-Hydroxyallenes **12** underwent an analogous 6-*endo*-trig cyclisation under similar conditions with $PPh_3AuCl/AgBF_4$, AuCl/pyridine or $AuCl_3$ (5 mol%) to afford dihydropyrans **13** in up to 84% yield.[29] No dihydrofuran products resulting from a potentially competitive 5-*exo*-dig cyclisation were observed.

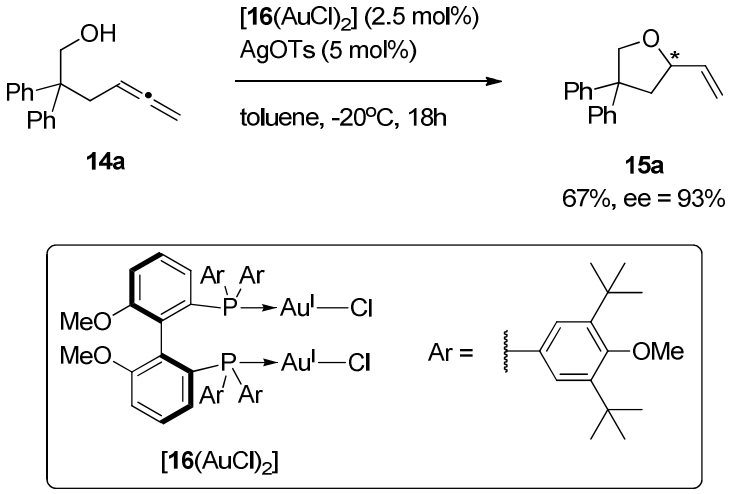


Scheme 1.4 Cyclisation of α- and β-Hydroxyallenes.

The analogous 5- or 6-*exo*-dig cyclisation of γ- or δ-hydroxyallenes **14** to give 2-vinyltetrahydrofurans or pyrans **15** was demonstrated by Widenhoefer *et al* in 2006.[30] A year later, the same group reported an asymmetric version of this reaction leading to enantiomerically-enriched heterocycles directly from prochiral allenes using chiral gold(I) catalysts.[31] Performing asymmetric transformations with gold raises many challenges. In allene or alkene hydrofunctionalisation reactions of the type shown in Scheme 1.1, the π-acidic gold catalyst is situated far from the site of nucleophilic attack and therefore has comparatively little effect in inducing chirality. Moreover, the chiral information present in the ligand is held even further away from the reacting centre with gold(I) complexes by virtue of the linear coordination geometry of the low oxidation state metal.[c] Despite these challenges, many gold(I)-catalysed enantioselective allene or alkene hydrofunctionalisation

[c] Although the square planar geometry of gold(III) is intuitively more suitable for asymmetric catalysis, no enantioselective gold(III)-catalysed hydrofunctionalisation reactions have been reported to date.

reactions have been disclosed. Among the chiral catalysts screened by Widenhoefer and co-workers, the bis(Au^I) species [**16**$(AuCl)_2$] (2.5 mol%) proved most suitable for the asymmetric γ- or δ-hydroxyallene cyclisation process when used in combination with AgOTs (5 mol%). Using this catalytic system, 2-vinyltetrahydrofuran **15a** was prepared from the corresponding γ-hydroxyallene **14a** in 67% yield and 93% enantiomeric excess after 18 hours at −20ºC (Scheme 1.5).

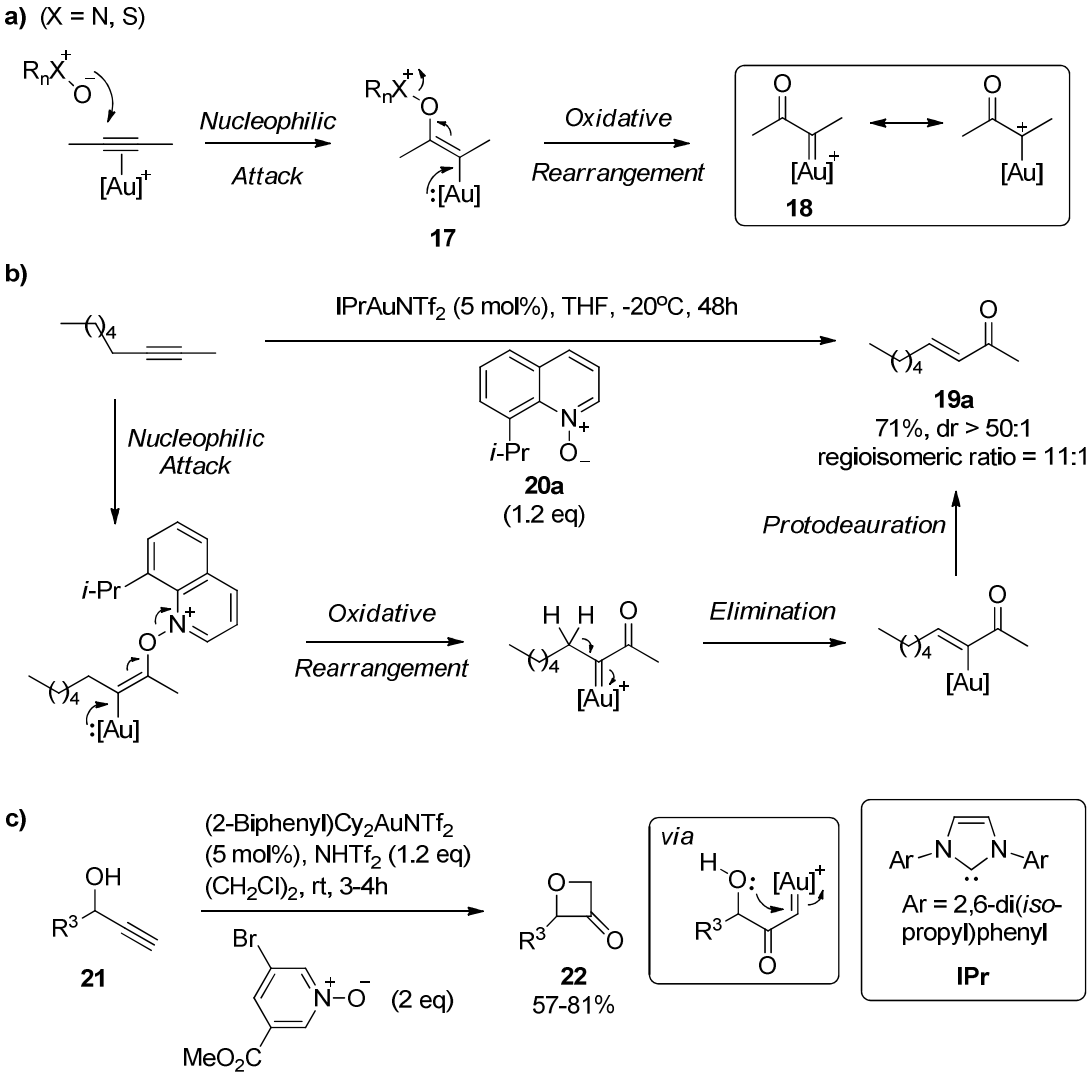


Scheme 1.5 Asymmetric Cyclisation of γ-Hydroxyallene **14a**.

Recently, several research groups have studied the intra- and intermolecular nucleophilic addition reactions of sulfoxides and *N*-oxides with alkynes. In these processes, nucleophilic attack of the oxygen onto the C-C multiple bond leads to a vinylgold intermediate **17** containing a cationic sulfur or nitrogen δ to the gold (Scheme 1.6a). Although the 5d orbitals of gold are generally considered to be too low in energy for meaningful back-bonding into antibonding π* orbitals of classical π-acceptor ligands, the lower energy LUMO of the conjugated cationic system in intermediates of type **17** can allow for synergic donation of electron density from the metal d-orbitals.[13] This π-donation can stabilise intermediates of type **18** formed upon extrusion of a NR_3 or SR_2 motif. The nature of the bonding in gold carbenoid species of this type has been the subject of debate.[32] Theoretical studies on related intermediates from gold-catalysed enyne cycloisomerisation reactions (see section

1.3.5) have indicated that the carbon-gold bond possesses both σ- and π-contributions although the bond order is always less than or equal to one.[33] Organogold intermediates of type **18** may react via a number of different pathways leading to a variety of diversely-functionalised products not accessible via simple nucleophilic attack-protodeauration catalytic cycles of the type shown in Scheme 1.1.[d] In 2010, Zhang and co-workers reported the synthesis of *trans*-α,β-unsaturated ketones **19** directly from alkynes under mild conditions using the gold(I) catalysts IPrAuNTf$_2$ or [(2,4-*t*-Bu$_2$PhO)$_3$P]AuNTf$_2$ (5 mol%) and pyridine *N*-oxides **20** as oxygen transfer reagents (Scheme 1.6b).[34] For alkyl-substituted alkynes, excellent levels of regioselectivity were achieved using the sterically demanding quinoline *N*-oxide **20a** with the nucleophile preferentially attacking the least hindered end of the alkyne. For internal alkynes bearing one aryl and one alkyl substituent, resonance stabilisation of complex **18** by the aryl group governed the observed regioselectivity. By comparison, alternative related alkyne oxidation processes typically require harsh conditions and result in mixtures of regioisomeric compounds in various oxidation states. In this reaction, the intermediate **18** formed upon nucleophilic attack and loss of the quinoline moiety most likely undergoes elimination to give a vinylgold(I) species prior to protodeauration. Alternatively, intermediates of type **18** may react with intramolecular nucleophiles to afford cyclic products. For example, propargyl alcohols **21** were oxidatively cyclised to oxetan-3-ones **22** in generally moderate to good yields upon treatment with gold(I) catalysts and pyridine *N*-oxides (Scheme 1.6c).[35-36]

[d] For a more detailed discussion of gold carbenoid demetallation pathways not involving protodeauration, see Section 1.4.1.

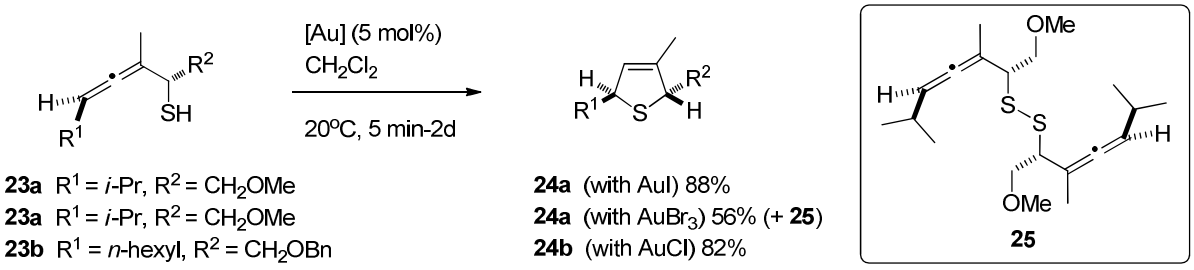


Scheme 1.6 a) General Scheme of α-Oxo Gold Carbenoid Formation. b) Regioselective oxidation of alkynes. c) Oxidative Cyclisation of Propargyl Alcohols.

1.3.2 Sulfur Nucleophiles

In 2006, Krause and co-workers demonstrated that α-thioallenes **23** cyclise in the presence of gold catalysts in a similar manner to the analogous hydroxy-substituted substrates.[37] The successful cyclisation of compounds bearing a free thiol group is somewhat surprising considering the well-known affinity of sulfur for heavy elements such as gold.[38] Using AuI or AuCl as catalyst, a wide-range of dihydrothiophenes **24** could be prepared from the corresponding α-thioallenes **23** with complete axis-to-centre chirality transfer in generally moderate to good yields (Scheme 1.7). When sources of gold(III) were employed as

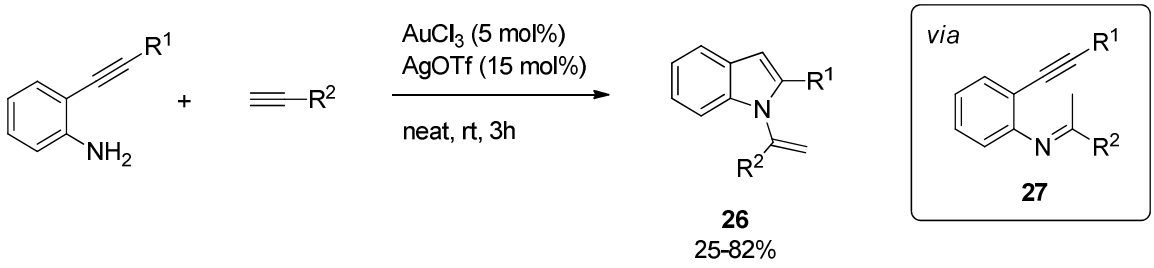
catalysts with α-thioallene **23a**, small amounts of disulfide **25** were observed as a side-product. The formation of this compound most likely results from an oxidative homocoupling process with concomitant reduction of gold(III) to gold(I).



Scheme 1.7 Cyclisation of α-Thioallenes.

1.3.3 Nitrogen Nucleophiles

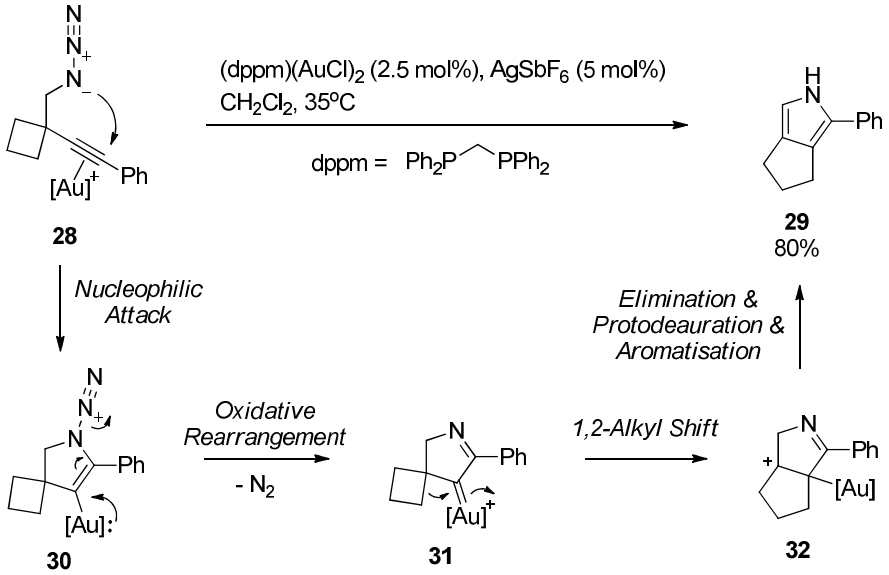
Protected or unprotected nitrogen atoms are also suitable nucleophiles in gold-catalysed alkyne, allene or alkene hydrofunctionalisation reactions. In 2007, Li and co-workers demonstrated that *ortho*-alkynylanilines react with terminal alkynes in a cascade process involving two hydroamination steps to afford *N*-vinylindoles **26** (Scheme 1.8).[39] This transformation is thought to proceed via an initial gold(III)-catalysed intermolecular hydroamination of the terminal alkyne leading to the imine intermediate **27**. Tautomerisation followed by a second gold-mediated hydroamination onto the intramolecular alkyne then delivers the heterocyclic product.



Scheme 1.8 Tandem Hydroamination of Intermolecular and Intramolecular Alkynes.

Azides may react with alkynes in the presence of gold catalysts in a similar fashion to sulfoxides or *N*-oxides leading to gold carbenoid intermediates upon extrusion of N_2. The β-

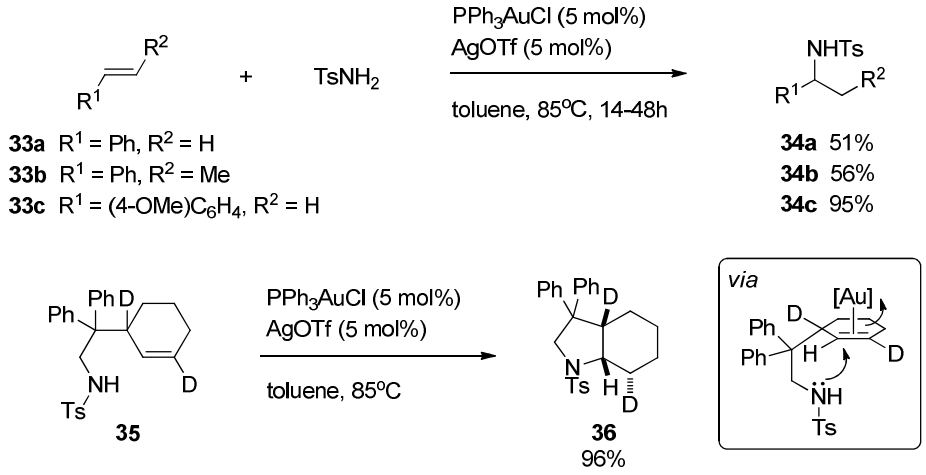
azidoalkyne **28** was cyclised in the presence of the gold(I) catalyst $(dppm)(AuCl)_2$ (2.5 mol%, dppm = 1,1-bis(triphenylphosphino)methane) and $AgSbF_6$ (5 mol%) to afford pyrrole **29** (Scheme 1.9).[40] The formation of this product can be rationalised by an initial 5-*endo*-dig cyclisation to afford the vinylgold complex **30**, which can then undergo an intramolecular oxidative rearrangement leading to the gold carbenoid species **31** and one equivalent of N_2. A 1,2-alkyl shift then delivers the ring expanded cationic intermediate **32** prior to elimination, protodeauration and aromatisation.



Scheme 1.9 Synthesis of Pyrroles from β-Azidoalkynes.

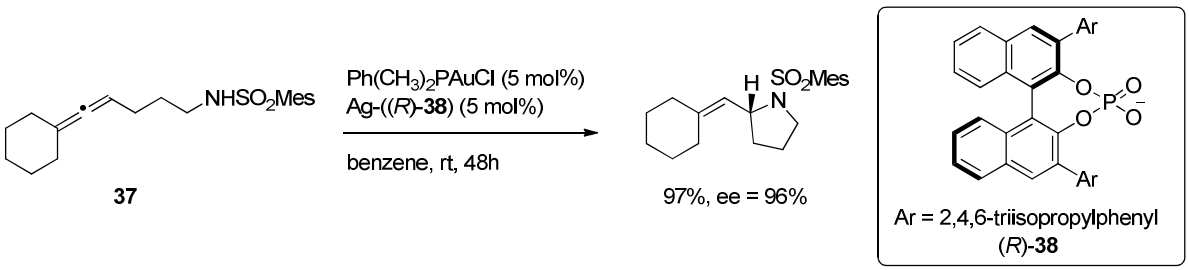
Although hydrofunctionalisation reactions are more commonly observed with alkynes or allenes, gold(I) and gold(III) are capable of activating alkenes towards attack by nucleophiles. In 2006, He and co-workers reported the intra- and intermolecular hydroamination of simple alkenes with sulfonamides.[41] Treating internal or terminal alkenes **33** with *p*-toluenesulfonamide in the presence of PPh_3AuCl (5 mol%) and AgOTf (5 mol%) in toluene led to the corresponding alkylamine products **34** in typically good yields within 48 hours at 85ºC (Scheme 1.10). For unsymmetrical olefins, excellent levels of regioselectivity were observed with the Markownikoff products being favoured. Importantly no side-products resulting from β-hydride elimination from an alkylgold(I) intermediate

were isolated. The *trans*-nature of the hydroamination step was confirmed by the preparation and cyclisation of the deuterated substrate **35**. Under the optimised reaction conditions, this racemic compound led smoothly to the corresponding racemic bicyclic compound **36** as a single diastereoisomer featuring the nitrogen and deuterium atoms in a *syn*-arrangement.



Scheme 1.10 Hydroamination of Alkenes.

Several enantioselective allene hydroamination reactions have been reported using gold(I) catalysts stabilised by chiral phosphine ligands. An alternative approach to asymmetric gold catalysis was reported by Toste *et al* in 2007 using achiral cationic (phosphine)gold(I) catalysts and enantiomerically-pure phosphate counter-ions based on binaphthol.[42] In apolar solvents, the anionic counter-ion forms a tight ion pair with the catalyst-substrate complex which then reacts with the nucleophile in an enantioselective fashion. In this approach, the source of chirality (namely the counter-ion) is thought to be in closer proximity to the site of nucleophilic attack than when using chiral phosphine ligands bound to linear gold(I) catalysts. The 5-*exo*-trig cyclisation of the sulfonyl-protected γ-aminoallene **37** proceeded in 97% yield and 96% ee when treated with $Ph(CH_3)_2PAuCl$ (5 mol%) and the silver(I) salt of the chiral phosphate (*R*)-**38** (5 mol%) in benzene at room temperature for 48 hours (Scheme 1.11).



37

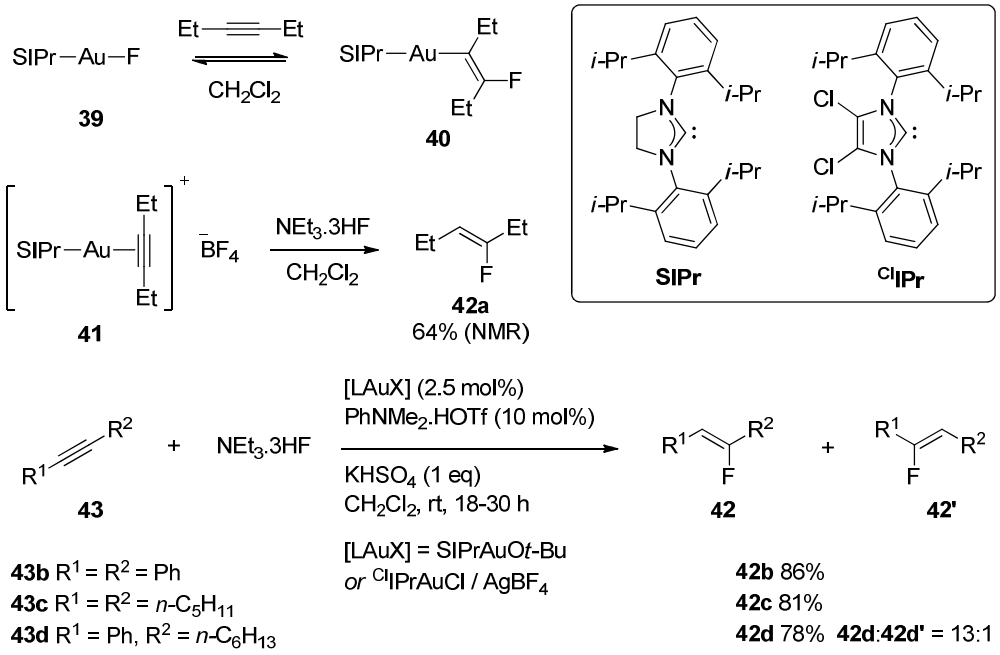
97%, ee = 96%

Scheme 1.11 Asymmetric Cyclisation of a γ-Aminoallene using a Chiral Counterion.

1.3.4 Halide Nucleophiles

The gold(III)-catalysed hydrochlorination of alkynes has been known since the 1970s,[18, 43-44] however alternative halogen nucleophiles have only recently been studied. In 2007, Sadighi and co-workers reported the gold(I)-catalysed hydrofluorination of simple alkynes under mild conditions.[45] This study was preceded by the preparation of the first isolable fluoride complex of gold(I) using the *N*-heterocyclic carbene ligand SIPr (1,3-Bis(2,6-diisopropylphenyl)imidazolidin-2-ylidene).[46] Treatment of this species (**39**) with excess 3-hexyne in dichloromethane led after 10 minutes to the reversible formation of the β-fluorovinyl complex **40** which was observed by ^{19}F NMR (Scheme 1.12). The formation of this species can be rationalised by an initial ligand exchange of the fluoride by the alkyne followed by nucleophilic attack of F^- onto the π-activated triple bond. In support of this hypothesis, the reaction between the η^2-alkynylgold(I) complex **41** with the mildly acidic fluoride source $NEt_3.3HF$ led smoothly to the *trans*-fluoroalkene **42a**. With this result in hand, a catalytic version of the hydrofluorination process was developed using [(NHC)AuX] (X = Cl, *t*-BuO) complexes as catalysts in the presence of various internal alkynes **43** and $NEt_3.3HF$. The use of *N*-heterocyclic carbene ligands was essential for appreciable formation of the fluoroalkene products. Under these conditions, monofluoroalkenes **42** could be furnished as the only fluorinated products in yields up to 86% after 18-30 hours at room temperature. By comparison, alternative alkyne hydrofluorination processes generally

require harsh conditions and result in mixtures of mono-, di- or trifluorinated products. For unsymmetrical alkynes bearing one alkyl and one aryl substituent, moderate to excellent levels of regioselectivity were observed with the β-fluorostyrene products being favoured. In 2009, Miller and co-workers were able to reverse the regioselectivity of this process with alkynes bearing carbonyl-based directing groups.[47]

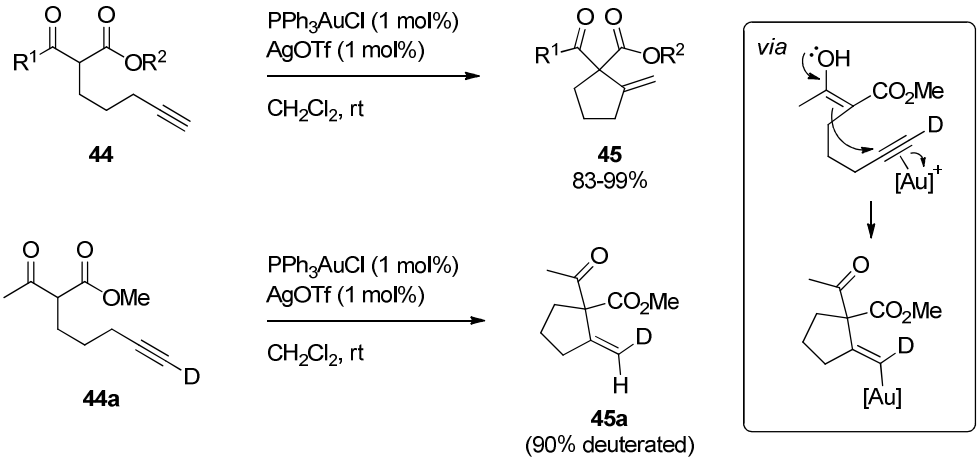


Scheme 1.12 Hydrofluorination of Alkynes.

1.3.5 Carbon Nucleophiles

Carbon-carbon bond-forming reactions are among the most important processes in organic chemistry. As such, novel methodologies which enable the selective formation of C-C bonds under mild conditions are highly sought. The use of intra- and intermolecular carbon nucleophiles in gold-catalysed alkyne, allene and alkene hydrofunctionalisation reactions has been the focus of many research groups. In 2004, Toste and co-workers reported the successful Conia-ene cyclisation of terminal alkynes **44** bearing pendant malonyl groups using the gold(I) catalytic system $PPh_3AuCl/AgOTf$ (1 mol%, Scheme 1.13).[48] Importantly, this reaction proceeded at room temperature, affording carbocyclic compounds

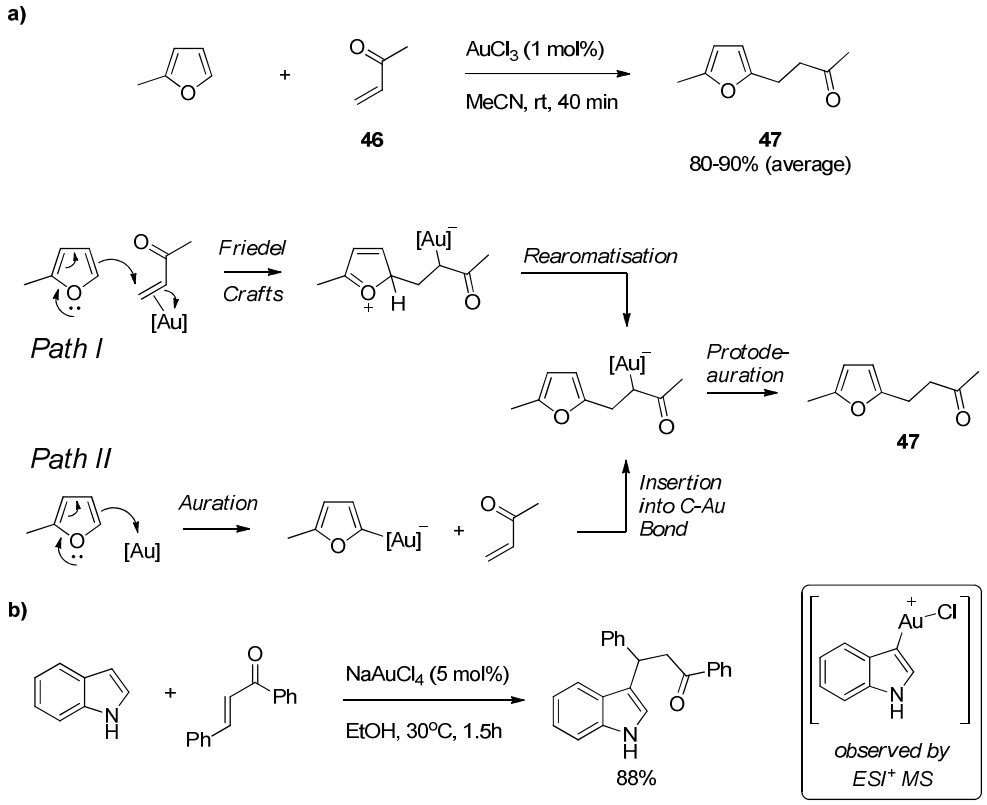
45 in high yields without the need for acidic or basic additives. By contrast, analogous thermally-promoted Conia-ene reactions typically require temperatures greater than 200ºC.[49] The *trans*-nature of the nucleophilic addition process was confirmed by labelling experiments. The selectively deuterated alkyne **44a** afforded the diastereoisomerically-pure carbocycle **45a**, featuring the malonyl carbon and the deuterium *cis*- to each other.



Scheme 1.13 Intramolecular Conia-ene Reaction.

Aromatic groups may also act as nucleophiles in gold-catalysed hydrofunctionalisation reactions. In 2000, Hashmi and co-workers reported the intermolecular coupling of non-activated furans with α,β-unsaturated ketones **46** leading to C2-alkylated heterocycles **47** using gold(III) chloride as catalyst (Scheme 1.14a).[50-51] The formation of these products can be explained by two competing mechanisms. One pathway involves gold(III) acting in its conventional role as a π-Lewis acid, activating the enone towards a Friedel-Crafts-type attack of furan (Scheme 1.14a, Path I). Alternatively, the aromatic nucleophile could react with gold(III) directly to afford a distinct furan(gold) complex, which then reacts with the enone via insertion (Scheme 1.14a, Path II). The direct auration of arenes by gold(III) chloride was first demonstrated in a seminal paper by Kharasch *et al* in 1931.[52] This C-H functionalisation reaction occurs under remarkably mild conditions, delivering arylgold

complexes after only a few minutes at room temperature.[e] In 2004, Arcadi and co-workers reported the analogous coupling of α,β-unsaturated ketones with indoles under similar conditions (Scheme 1.14b).[53] The involvement of an aurated indole intermediate in this process was supported by electrospray mass spectral analysis of a control reaction between indole and a stoichiometric amount of $NaAuCl_4.2H_2O$.

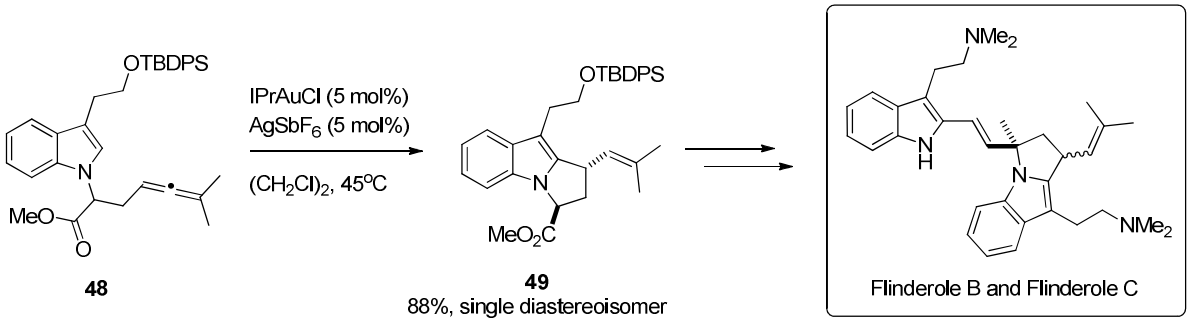


Scheme 1.14 a) C2-Alkylation of Furans. b) C3-Alkylation of Indoles.

A related allene hydroheteroarylation process has been recently applied in the total synthesis of the natural products Flinderole B and Flinderole C.[54] The indole-substituted allene **48** reacted in the presence of the *N*-heterocyclic carbene-stabilised gold(I) catalyst IPrAuCl (5 mol%) and $AgSbF_6$ (5 mol%) to afford the 5-*exo*-trig cyclisation product **49** as a single diastereoisomer in 88% yield (Scheme 1.15). This transformation constitutes the key step in

[e] For a discussion of this process, see Chapter 3 (Section 3.2.2.1).

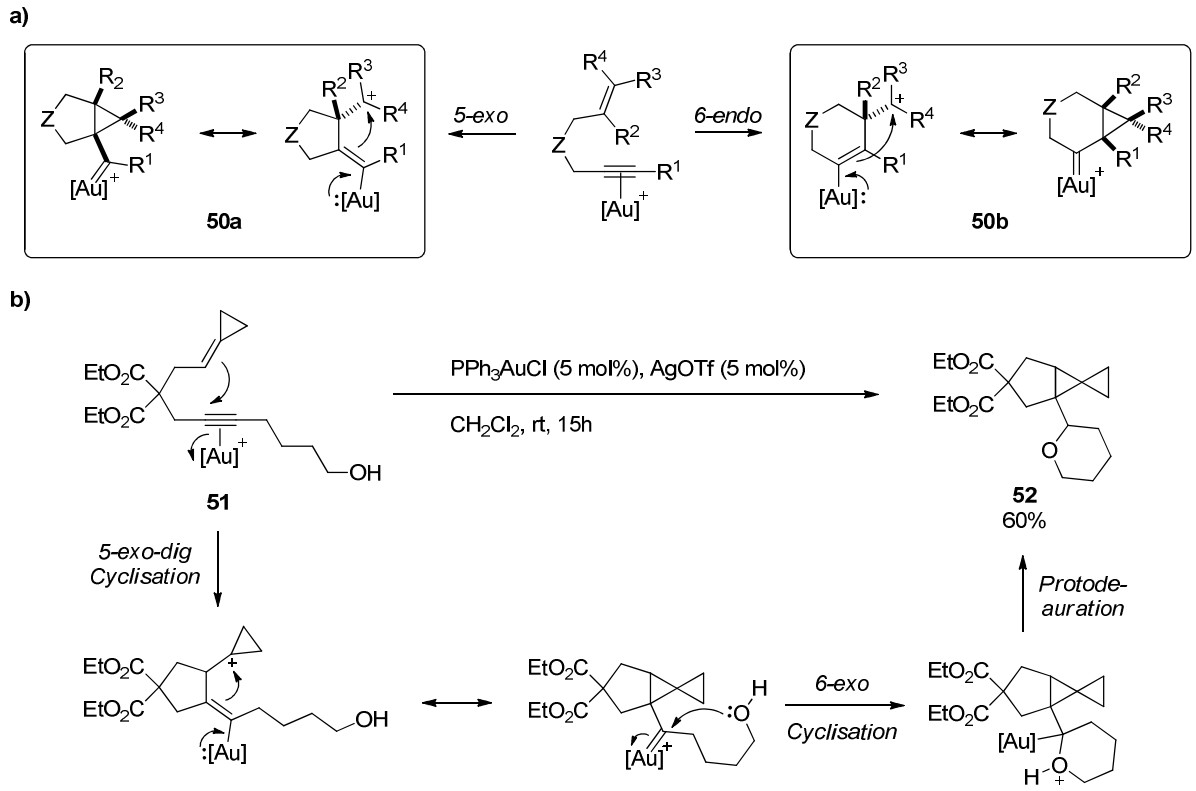
the 18 step synthesis of these two important compounds (overall total synthesis yield = 4%), which have shown promise as potential anti-malarial agents.[55]



Scheme 1.15 Allene Cyclisation in the Total Synthesis of Flinderole B and Flinderole C.

The intramolecular rearrangements of 1,*n*-enynes (*n* = 5-9) are the most widely studied class of gold-catalysed C-C bond-forming reactions. In the presence of other late transition metals such as platinum or ruthenium, enynes commonly react to form dienes in an Alder-ene cycloisomerisation process involving a two-electron M^n/M^{n+2} redox cycle.[56] The reluctance of gold to undergo the necessary oxidation state changes for this kind of transformation as well as the mono-coordinate nature of the $[LAu^I]^+$ fragment make this reactivity mode unfavourable with gold catalysts. Instead, nucleophilic attack of the alkene moiety onto the gold-activated alkyne occurs, leading to intermediates of type **50a** and **50b** (Scheme 1.16a). As previously discussed, the positive charge in species of this type can be stabilised by π-back-bonding from the metal 5d orbitals and, as a result, these complexes are thought to have substantial carbenoid character. Intermediates of type **50a** and **50b** may react further via a number of different pathways and, over the last few years, a multitude of impressive transformations have been disclosed. The cyclopropyl-substituted 1,6-enyne **51** was cyclised in the presence the gold(I) catalytic system PPh_3AuCl / AgOTf (5 mol%) to afford the spirocycle **52** (Scheme 1.16b).[57] The formation of this compound can be rationalised by a cascade sequence involving an initial 5-*exo*-dig enyne cyclisation followed by nucleophilic

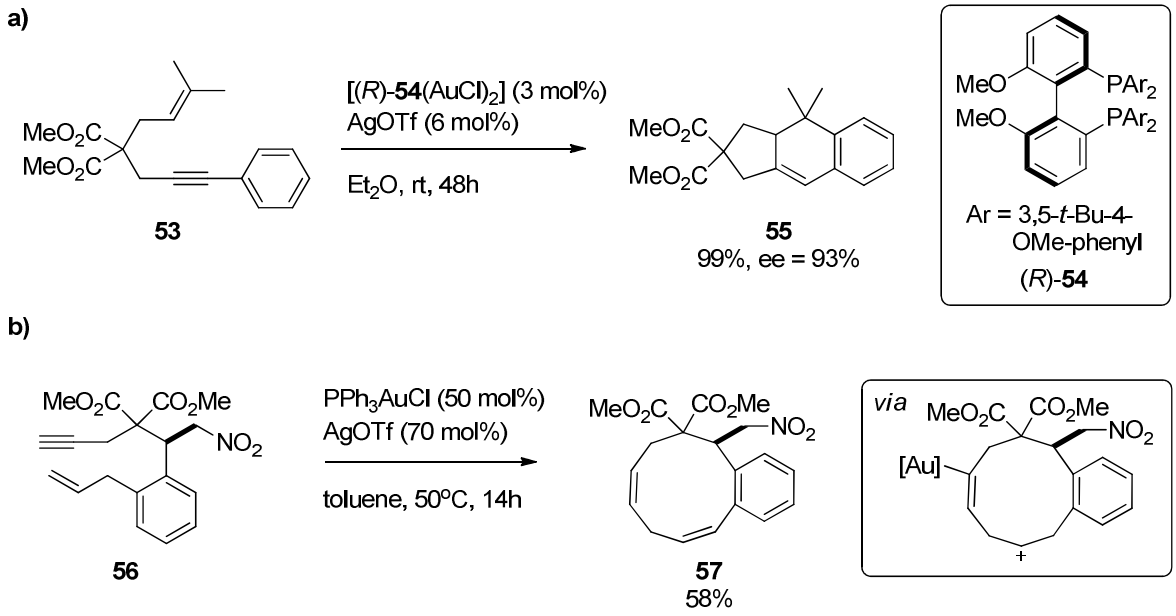
trapping of the resulting gold carbenoid intermediate by the pendant hydroxyl group and protodeauration.



Scheme 1.16 a) General Scheme for the Cycloisomerisation of 1,6-Enynes. b) Cascade Cycloisomerisation-Oxycyclisation of an 1,6-Enyne.

An asymmetric version of a related cycloisomerisation reaction was reported by Michelet *et al* in 2009.[58] 1.6-Enyne **53** bearing a phenyl substituent at the alkynyl position was reacted in the presence of the chiral gold(I) catalyst [(*R*)-**54**$(AuCl)_2$] (3 mol%) and AgOTf (6 mol%) in Et_2O for 48h. This reaction led to the tricyclic compound **55** resulting from a 5-*exo*-dig cyclisation-Friedel-Crafts arylation cascade in 99% yield and 93% ee (Scheme 1.17a). Longer chain enynes may also undergo cycloisomerisation reactions in the presence of gold catalysts. The 1,9-enyne **56** afforded the cycloisomerisation product **57**, featuring a 10-membered carbocyclic ring in 58% yield upon treatment with PPh_3AuCl (50 mol%) and AgOTf (70 mol%) (Scheme 1.17b).[59] The formation of this product is best explained by a

mechanism involving the elimination of a proton from an intermediate of type **50b** formed upon a 10-*endo*-dig cyclisation of the enyne followed by protodeauration.



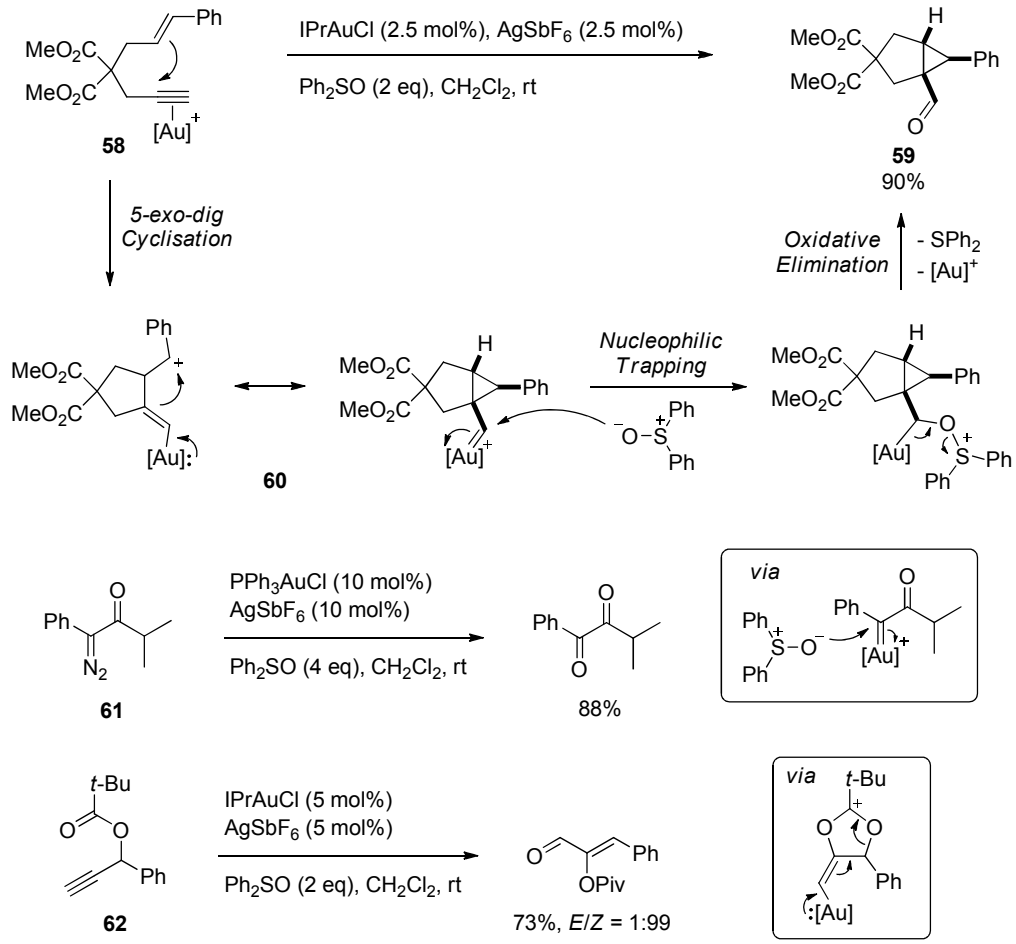
Scheme 1.17 a) Asymmetric Cycloisomerisation of a 1,6-Enyne. b) Cycloisomerisation of a 1,9-Enyne.

1.4 Demetallation Pathways Beyond Protodeauration

In all the gold-catalysed reactions discussed in the previous section, the final step in the catalytic cycle involves the protodeauration of an organogold intermediate. This elementary step is ubiquitous in homogeneous gold catalysis and results in the formation of a new carbon-hydrogen bond. The prevalence of this reactivity pathway, however, limits the scope of organic transformations accessible using gold catalysts. Whereas a multitude of different bonds may be formed upon attack of a nucleophile onto a gold-activated alkyne, allene or alkene, the last stage of these processes is generally limited to C-H bond formation. The scope of these reactions would be vastly increased if protodeauration could be suppressed in favour of alternative demetallation pathways leading to the formation of a new carbon-carbon or carbon-heteroatom bond. Over the last few years, several such processes have been reported and a selection of these are summarised in the following sections.

1.4.1 Trapping of Gold Carbenoids

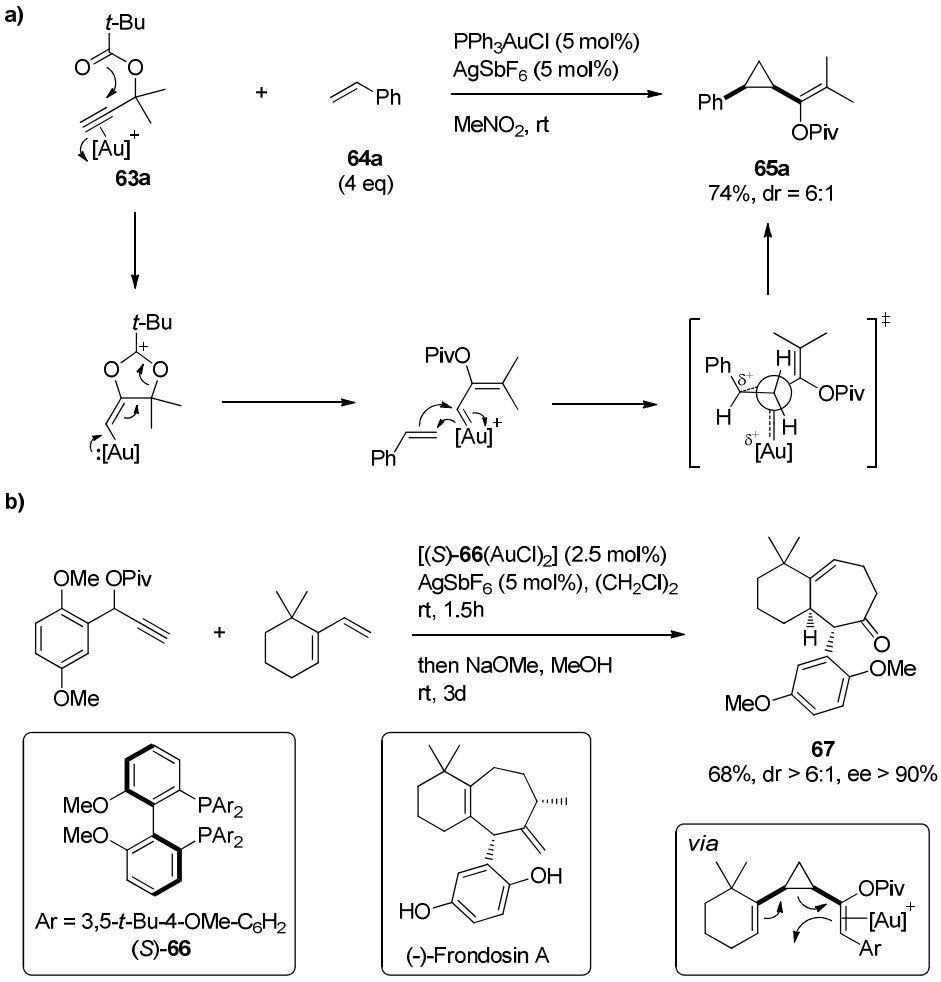
Alternative demetallation pathways to protodeauration may be observed in reactions proceeding via organogold intermediates with carbenoid character. In 2007, Toste and co-workers reported the oxidative trapping of several postulated gold carbenoids using diphenylsulfoxide as an oxygen transfer reagent.[60] Reacting the 1,6-enyne **58** in the presence of IPrAuCl (2.5 mol%), $AgSbF_6$ (2.5 mol%) and two equivalents of the sulfoxide led to the cyclopropyl aldehyde **59** in 90% yield (Scheme 1.18). The formation of this product is best explained by a mechanism involving the nucleophilic attack of the sulfoxide oxygen onto the gold carbenoid enyne cyclisation intermediate **60** followed by extrusion of diphenylsulfide and $[IPrAu]^+$. Similar oxygen transfer processes were also observed with other substrates including α-diazoketones **61** and terminal propargyl esters **62**. With these latter compounds, a gold carbenoid intermediate is formed as a result of a 1,2-shift of the ester group.



Scheme 1.18 Oxidative Trapping of Gold Carbenoid Intermediates.

Organogold intermediates derived from propargyl esters have also been trapped by alkenes to form cyclopropanes. This reactivity pathway is typical of carbenes and serves as evidence for the postulated carbenoid character of these intermediates. Upon treatment with 5 mol% of PPh_3AuCl and $AgSbF_6$ in nitromethane, propargyl pivalates, acetates and benzoates **63** could be coupled with alkenes **64** to afford cyclopropyl enol esters **65** in yields up to 84% (Scheme 1.19a).[61] Moderate to high levels of diastereoselectivity were observed in favour of the *cis*-cyclopropyl products. The preferential formation of these diastereoisomers can be rationalised by a concerted carbene transfer mechanism proceeding via the transition state with the minimised steric demands. Recently, Nevado and co-workers applied this transformation as part of an asymmetric cycloheptannulation cascade approach to the synthesis of the natural product (–)-Frondosin A.[62] The cyclohexene-substituted product

formed upon cyclopropanation of the gold carbenoid intermediate reacted further in the presence of the gold catalyst [(*S*)-**66**$(AuCl)_2$] (2.5 mol%) and $AgSbF_6$ (5 mol%) to afford the ring opened product **67** in 68% yield and greater than 90% ee (Scheme 1.19b). This species features the core structure of the norsesquiterpenoid (−)-Frondosin A, which has shown promising biological activity.

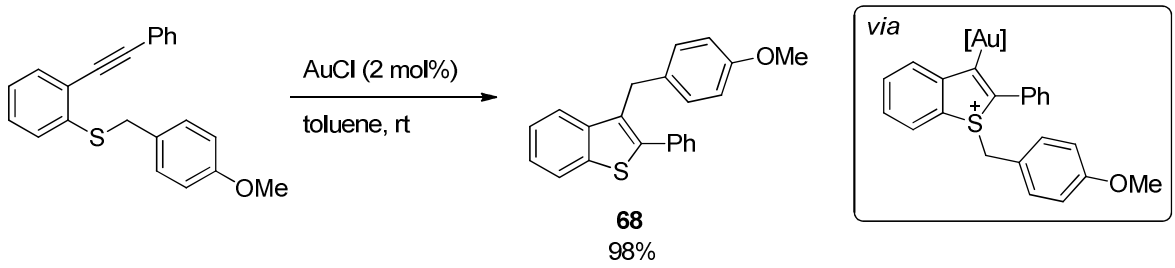


Scheme 1.19 a) Cyclopropanation of Olefins. b) Cascade Cycloheptannulation Approach to Frondosin A.

1.4.2 Nucleophilic Attack of C-Au Bonds

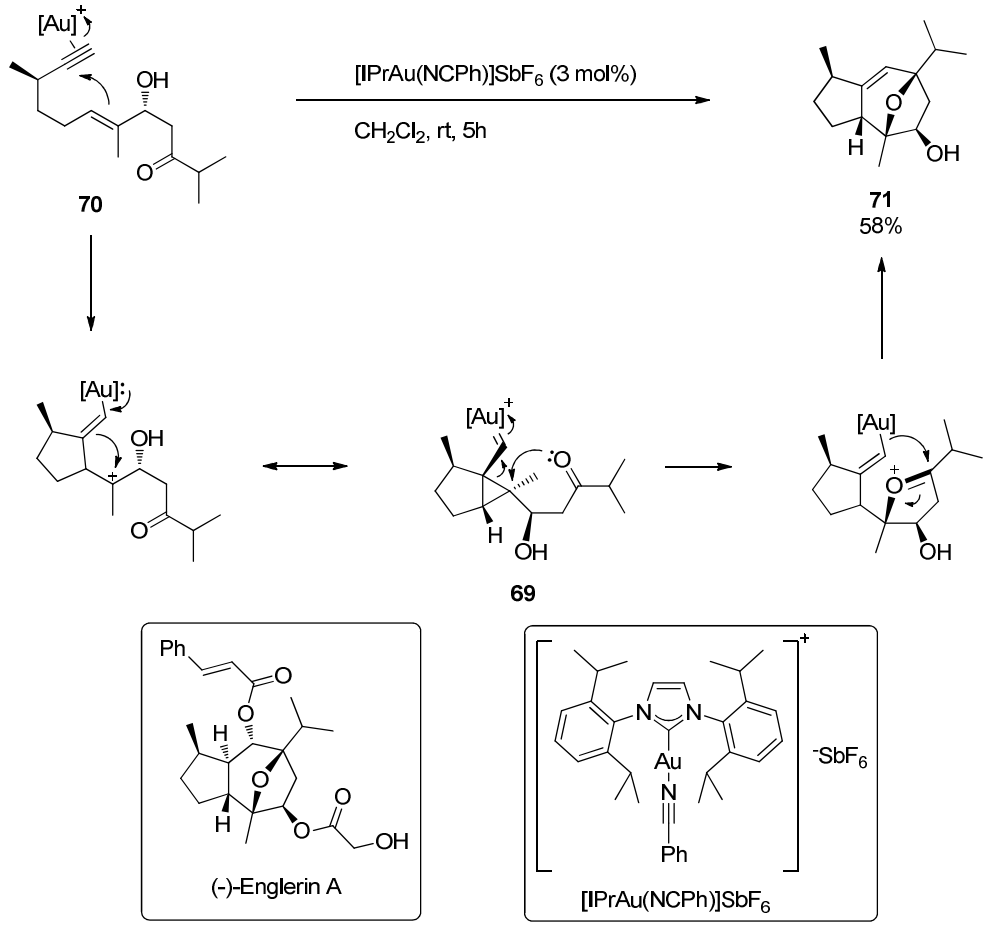
In selected cases, vinylgold intermediates formed upon nucleophilic attack to an activated alkyne or allene may react with intramolecular electrophiles other than a proton. In 2006, Yamamoto and co-workers reported the synthesis of the 3-substituted benzothiophene **68** via a cascade 5-*endo*-dig cyclisation-1,3-alkyl migration process in 98% yield using gold(I)

chloride as catalyst (Scheme 1.20).[63] The vinylgold(I) species formed upon nucleophilic attack of the sulfur onto the activated alkyne is thought to react directly with the intramolecular sulfur substituent leading to the formation of a new carbon-carbon bond. Whether this step occurs with concomitant cleavage of the carbon-gold bond or via nucleophilic attack of the alkene followed by facile elimination of the metal has yet to be determined.



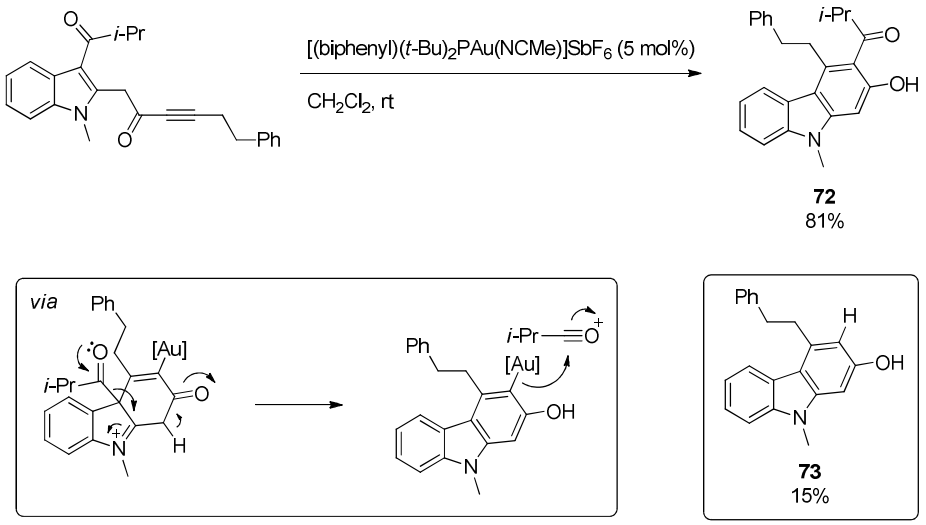
Scheme 1.20 Cyclisation-1,3-Migration of Thioethers.

The vinylgold(I) intermediate **69** formed upon nucleophilic trapping of the gold carbenoid 1,6-enyne cycloisomerisation intermediate of substrate **70** was recently shown by Echavarren *et al* to react with an intramolecular carbonyl electrophile to afford the complex bicyclic structure **71** (Scheme 1.21).[64] This process was employed as the key step in the synthesis of the sesquiterpene diester (−)-Englerin A, which has been shown to inhibit the growth of several renal cancer cell lines.



Scheme 1.21 Synthesis of (–)-Englerin A.

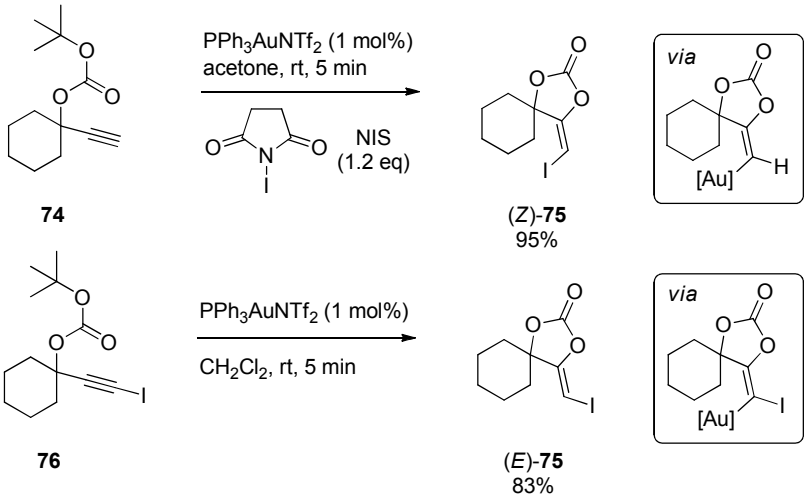
Very recently, a related trapping of an acyl cation by a vinylgold species was reported by Liu and co-workers during the cyclisation of alkynyl-substituted 3-acylindoles **72**.[65] In this process, the organogold intermediate formed upon 6-*endo*-dig cyclisation reacts with an acylium species generated upon rearomatisation of the indole motif (Scheme 1.22). The conventional cyclisation-protodeauration process could not be completely suppressed, however, and considerable amounts of the non-acylated side-products **73** were isolated from the reaction mixtures.



Scheme 1.22 Trapping of an Organogold Intermediate with an Acylium Ion.

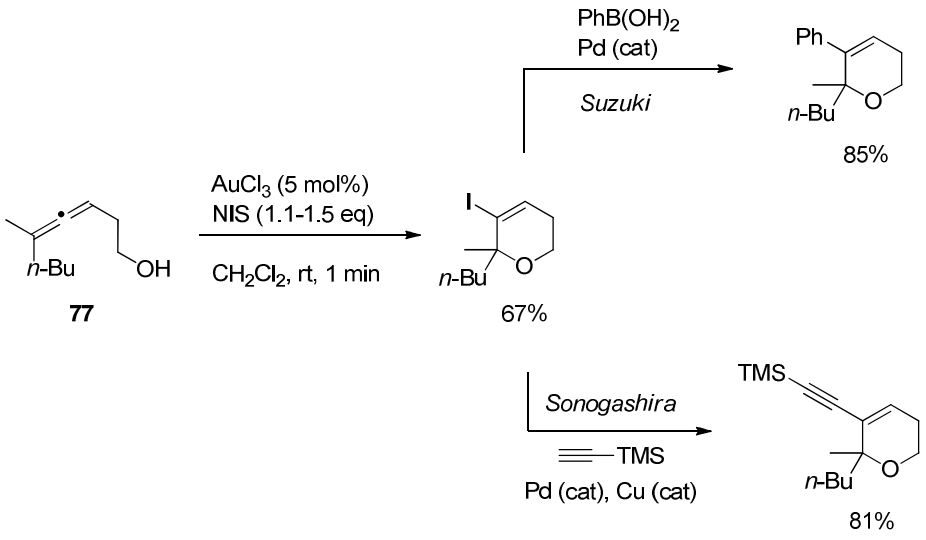
1.4.3 Iodo-, Bromo- and Chlorodeauration

The iododeauration of organogold species in the presence of electrophilic sources of iodine is the most widely reported demetallation pathway other than protodeauration observed with gold catalysts. This process leads to the formation of new carbon-halogen bonds, delivering substrates amenable to further functionalisation (eg. via lithium-halogen exchange or palladium-catalysed coupling). In 2006, Gagosz and co-workers reported the 5-*exo*-dig cyclisation-iododeauration of the *tert*-butyloxy propargyl carbonate **74** in the presence of PPh_3AuNTf_2 (1 mol%) and 1.2 equivalents of the electrophilic iodinating reagent *N*-iodosuccinimide (NIS, Scheme 1.23).[66] This powerful protocol leads to the formation of two new bonds; a carbon-oxygen bond in the nucleophilic addition step followed by a carbon-iodine bond during demetallation. The (*Z*)-iodoalkene product (*Z*)-**75** was formed in 95% isolated yield as a single diastereoisomer after just 5 minutes at room temperature. The formation of the (*Z*)-diastereoisomer is consistent with a *trans*-nucleophilic attack followed by an electrophilic iodination process occurring with retention of stereochemistry. By contrast, the cyclisation-protodeauration of the iodinated substrate **76** performed in the absence of NIS led exclusively to the (*E*)-diastereoisomer (*E*)-**75**.



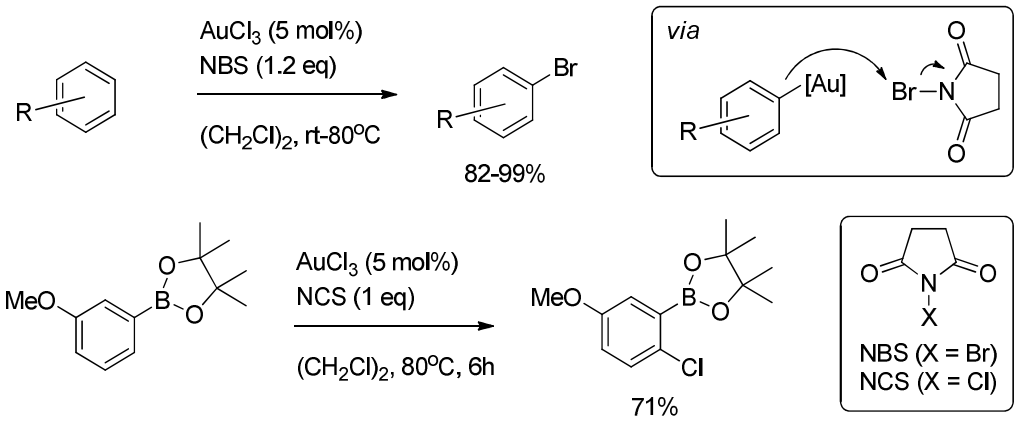
Scheme 1.23 Iododeauration of Vinylgold Intermediates.

Performing the gold-catalysed 6-*endo*-trig cyclisation of β-hydroxyallenes **77** in the presence of NIS led to a dramatic increase in the reaction rate relative to the conventional cyclisation-protodeauration reaction (Scheme 1.24).[67] Whilst the C-H bond-forming process with these substrates took several days, the analogous cyclisation-iododeauration process was complete after just one minute at room temperature. In the absence of gold, the iodocyclisation took two days at room temperature. The iodinated dihydropyran products were amenable to palladium-catalysed Suzuki-Miyaura or Sonogashira coupling reactions with arylboronic acids or terminal alkynes.



Scheme 1.24 Cyclisation-Iododeauration of β-Hydroxyallenes.

Analogous bromodeauration processes have been reported from gold complexes using *N*-bromosuccinimide (NBS).[68-69] In one such transformation, electrophilic halogenation is thought to occur from an arylgold(III) species formed upon aryl C-H functionalisation of non-activated arenes with gold(III) chloride. Aryl bromides were furnished in up to 99% yield whilst the corresponding chlorinated products could also be prepared using *N*-chlorosuccinimide as a source of electrophilic chlorine (Scheme 1.25). However, it should be noted that, in these processes, protodeauration serves only to regenerate the arene starting materials and halodeauration can proceed without competing protonolysis-based side-reactions.



Scheme 1.25 Direct Halogenation of Non-Activated Arenes with *N*-Halosuccinimides.

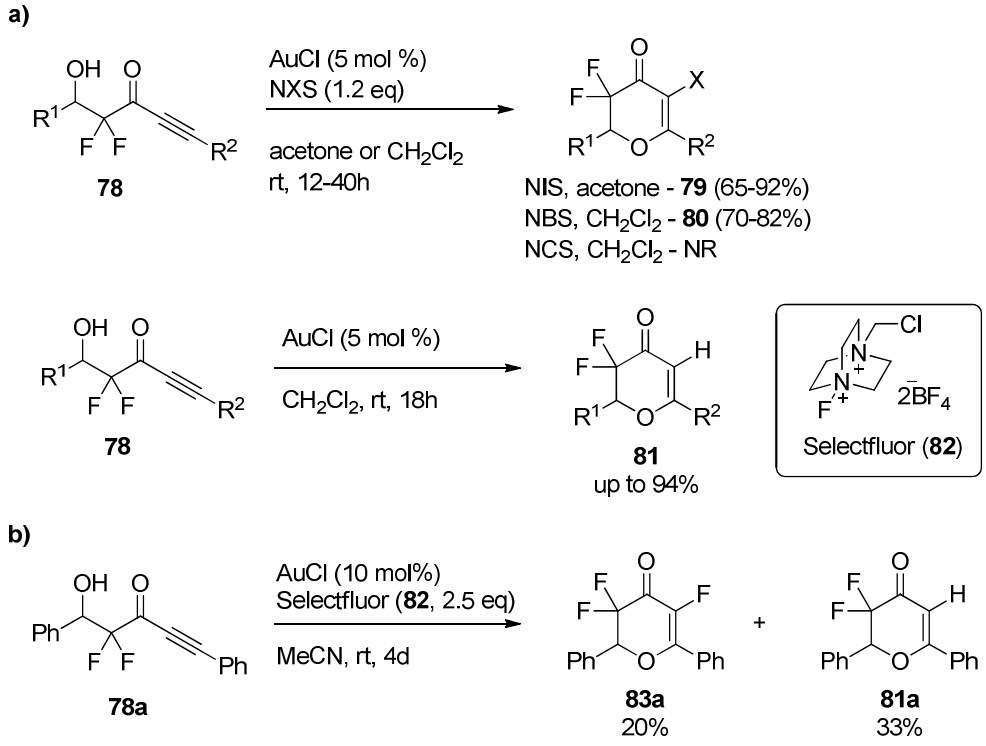
1.5 Extension of the Methodology towards Fluorination

Whilst the halodeauration of organogold complexes is well-established with electrophilic sources of iodine, bromine and, to a lesser extent, chlorine, the extension of this methodology towards fluorination has received less research attention. Fluorinated organic compounds find multiple uses as materials,[70] agrochemicals[71] and pharmaceuticals[72] with ten of the top thirty selling drugs in the USA in 2008 containing at least one fluorine atom.[73] Replacing a hydrogen or hydroxyl group in an organic molecule with a fluorine can have a dramatic effect on the electronic profile of the compound whilst causing minimal

change to its steric properties.[74-75] Fluorinated compounds may exhibit greater bioavailability than their non-fluorinated analogues whilst the high stability of the C-F bond can lead to improved metabolic stability *in vivo*.[72] In addition to these uses, organofluorine compounds labeled with the radioactive isotope fluorine-18 are widely employed as radiotracers for positron emission tomography (PET) imaging.[76] In contrast to the many applications of fluorinated organic molecules, these compounds are extremely scarce in nature.[77] As a result, the preparation of these compounds relies heavily on synthetic organic chemistry and novel fluorination methodologies are highly sought.

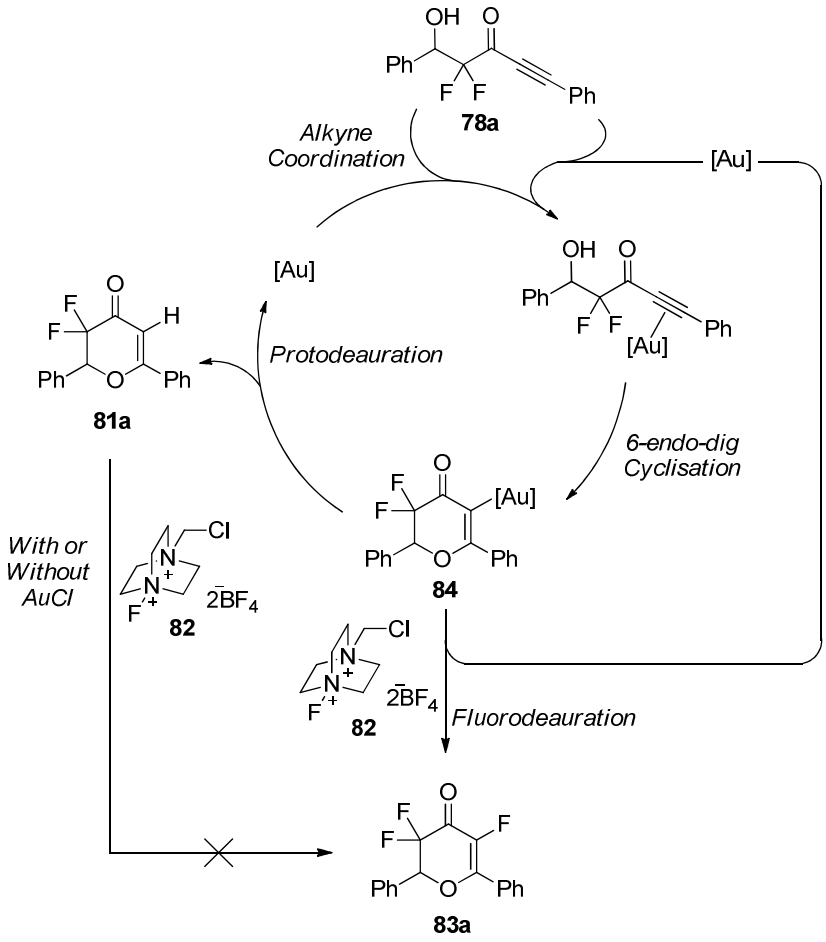
1.5.1 Fluorodeauration

In 2008, our group studied the gold-catalysed 6-*endo*-dig cyclisation of β-hydroxy-α,α-difluoroynones **78** in the presence of a variety of electrophilic halogenation reagents.[78] The reactions with NIS and NBS led to the expected alkoxyiodinated and alkoxybrominated products **79** and **80** respectively whilst the corresponding protodeaurated dihydropyranones **81** were afforded in the absence of a halogen source (Scheme 1.26a). Performing the cyclisation reaction of ynone **78a** with gold(I) chloride in the presence of 2.5 equivalents of the electrophilic fluorinating reagent Selectfluor (**82**) for 4 days at room temperature led to a mixture of two cyclised compounds. Although the cyclisation-protodeauration product **81a** was isolated as the major species in 33% yield, dihydropyranone **83a**, featuring a fluoroolefin motif, could also be isolated from the reaction mixture in 20% yield (Scheme 1.26b). This product results from a formal alkoxyfluorination process involving the formation of one carbon-oxygen bond and one carbon-fluorine bond across the alkyne. Changing the catalyst from AuCl or switching to alternative "F^+" sources led to lower conversions to the trifluorinated product whilst varying the substitution pattern around the β-hydroxy-α,α-difluoroynone substrates had a minimal effect on the reaction efficiency.



Scheme 1.26 Cyclisation-Halodeauration of β-Hydroxy-α,α-difluoroynones.

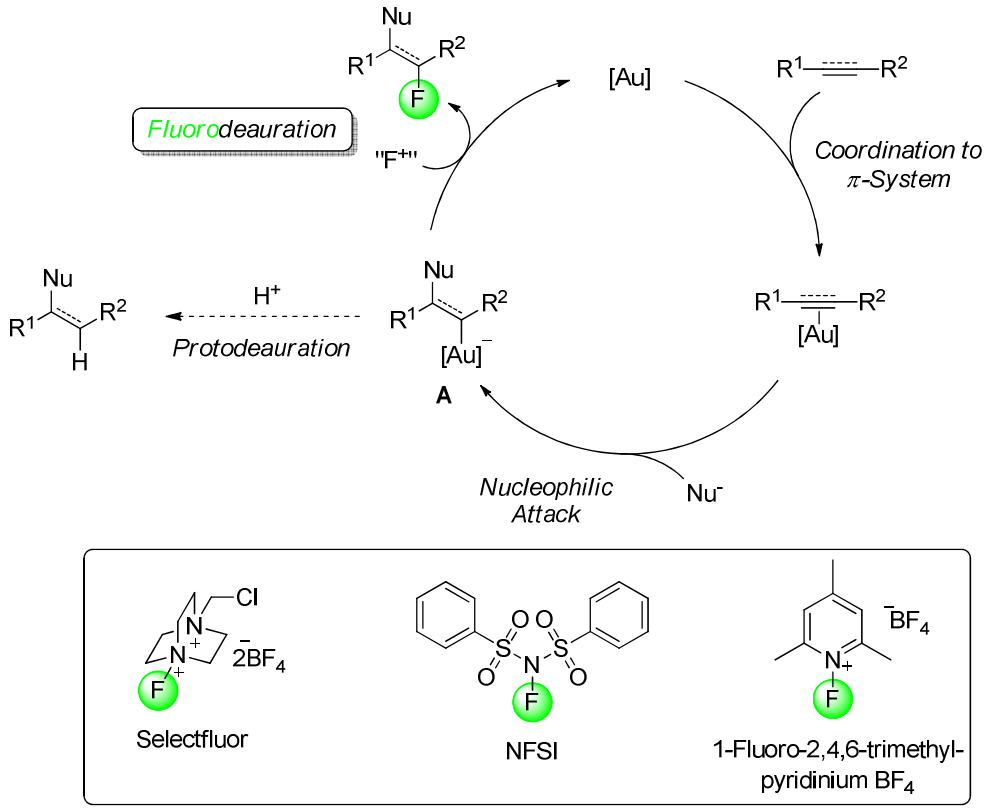
The formation of the trifluorinated dihydropyranone products **83** is consistent with a cyclisation-fluorodeauration mechanism of the type shown in Scheme 1.27. Initial coordination of gold to the alkyne followed by nucleophilic attack of the pendant hydroxy group would lead to the vinylgold intermediate **84**. Protodeauration at this stage would deliver the major *gem*-difluorinated product **81** and regenerate the catalyst. Instead, the organogold complex **84** could react with Selectfluor via an electrophilic fluorodeauration mechanism to afford the trifluorinated product **83**. The involvement of a direct fluorodemetallation process was supported by a control reaction with the difluorinated dihydropyranone **81a**. No trace of **83a** was observed upon treating the protodeaurated product with Selectfluor either with or without gold, suggesting that this compound is not an intermediate in the fluorination process. The exact mechanism of the proposed fluorodeauration step, however, has yet to be fully established.



Scheme 1.27 Proposed Mechanism for the Cyclisation-Fluorodeauration of β-Hydroxy-α,α-difluoroynones.

1.5.2 Outline of this Thesis

The cyclisation-fluorodeauration reaction of β-hydroxy-α,α-difluoroynones discussed above is the first example of a gold-catalysed fluorination process using an electrophilic source of fluorine. The observation that "F^+" could act as an alternative electrophile to H^+ in cleaving gold-carbon bonds could lead to a potentially very powerful new methodology where electrophilic fluorination follows a gold-catalysed nucleophilic addition to a carbon-carbon multiple bond. Considering the large number of these transformations reported over the last few years, this approach could allow for the preparation of an ever-increasing array of diversely substituted fluorinated compounds (Scheme 1.28).



Scheme 1.28 General Mechanism of Nucleophilic Addition-Fluorodeauration Reactions in the Presence of Electrophilic Fluorinating Reagents.

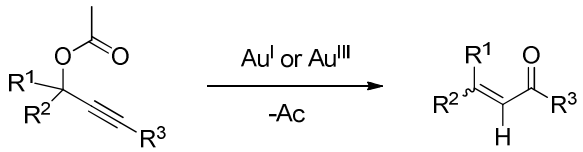
In the subsequent three chapters of this thesis, the reactivity of gold catalysts in the presence of electrophilic fluorinating reagents is investigated focusing on gold-catalysed nucleophilic addition reactions to carbon-carbon multiple bonds. In particular, the scope and limitations of fluorodeauration as a method of C-F bond formation is examined with an emphasis on determining the mechanistic pathways in operation in the studied reaction systems. Chapter 2 summarises the results of our study into the effect of electrophilic fluorinating reagents on the gold(I)-catalysed [3,3]-sigmatropic rearrangement of propargyl acetates. This is followed, in chapters 3 and 4, by a discussion on the reactivity of gold catalysts in the presence of *tert*-butyl allenoates and Selectfluor. This latter study led to the discovery of a novel reactivity pathway for gold catalysts, not leading to fluorinated products.

Chapter 2

Gold and F^+: Gold-Catalysed Fluorination

2.1 Introduction

Following the successful validation of a gold-catalysed nucleophilic addition-fluorodeauration process in the cyclisation of β-hydroxy-α,α-difluoroynones (see Section 1.5.1),[78] we sought to investigate the scope and limitations of this methodology with alternative reaction systems. Following a survey of gold-catalysed alkyne and allene hydrofunctionalisation reactions, we identified the formal [3,3]-sigmatropic rearrangement-protodeacetylation of propargyl acetates **85** as a promising transformation for further study (Scheme 2.1). This process is related to the classical Meyer-Schuster rearrangement and may be catalysed by a number of transition metals including gold.[79]

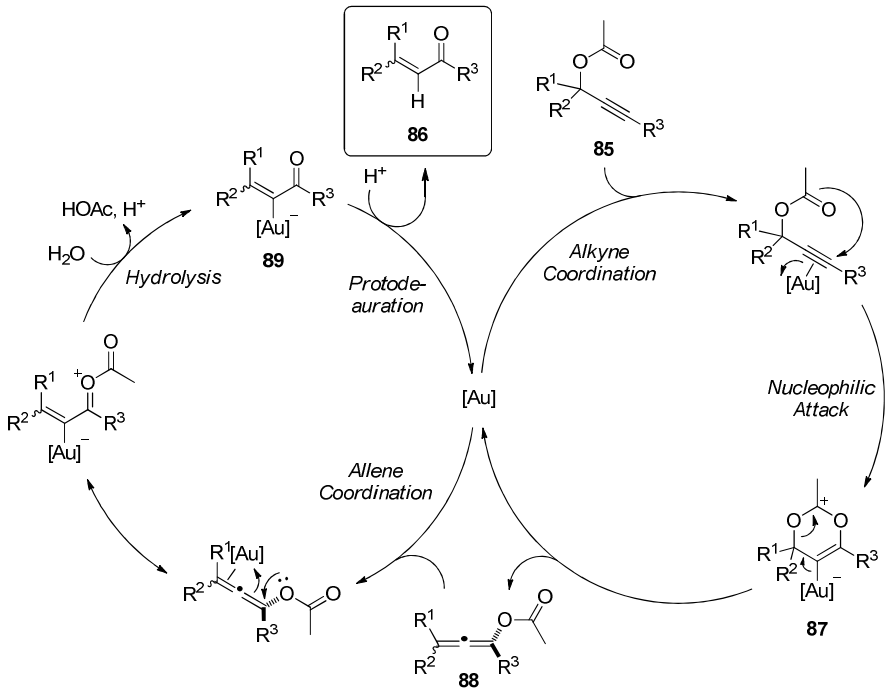


85 **86**

Scheme 2.1 Preparation of Enones **86** from Propargyl Acetates **85**.

A general mechanism for this transformation leading to enones **86** is displayed in Scheme 2.2. In the first step, the alkyne moiety is activated by gold(I) or gold(III) towards intramolecular nucleophilic attack of the acetate group leading to the cyclic intermediate **87**. Ring opening of this species with concomitant loss of the metal affords the formal [3,3]-sigmatropic rearrangement product **88**. At this stage, the strongly π-Lewis acidic gold

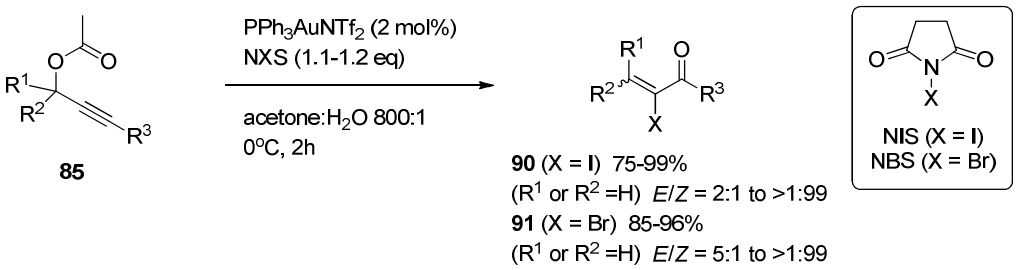
catalyst can re-complex the allene leading to the vinylgold complex **89** upon hydrolysis of the acetyl group. Finally, protodeauration delivers the enone products **86** and regenerates the gold catalyst.



Scheme 2.2 Proposed Mechanism for the Synthesis of Enones via the Formal [3,3]-Sigmatropic Rearrangement of Propargyl Acetates.

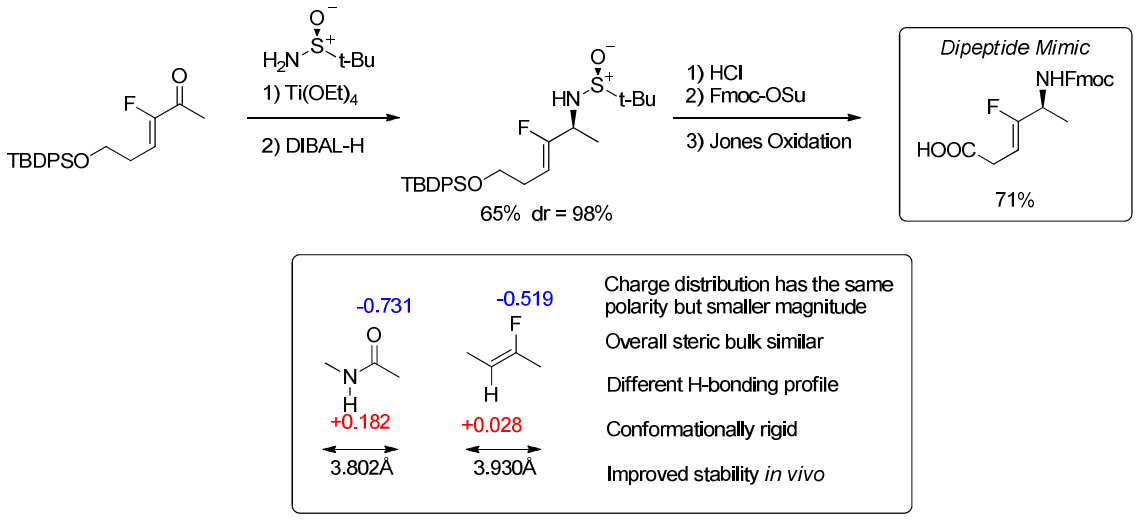
In 2007, Zhang and co-workers reported the synthesis of α-iodoenones **90** directly from propargyl acetates upon treatment with gold catalysts in the presence of the electrophilic iodinating reagent NIS (Scheme 2.3).[80] In this reaction, which was later extended to the preparation of α-bromoenones **91**,[81] the protodeauration step was completely suppressed in favour of halodeauration leading to (*E*)- and (*Z*)-α-haloenones as the only products in high yields under mild conditions. Moreover, the sense and level of diastereoselectivity of the rearrangement-halodeacetylation process with unsymmetrical propargyl acetates offered insights into the mechanisms of the iodo- and bromodeauration steps.[f]

[f] The mechanism of halodeauration proposed in these studies is discussed more thoroughly in Section 2.6.



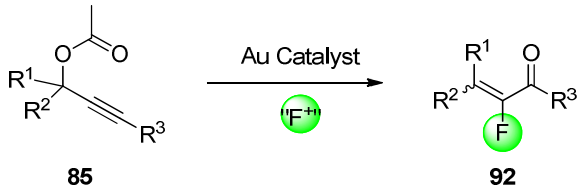
Scheme 2.3 Rearrangement-Halodeacetylation of Propargyl Acetates with *N*-Iodo- and *N*-Bromosuccinimide.

Inspired by these transformations, we sought to investigate whether α-fluoroenones **92** could be prepared via an analogous process performed in the presence of electrophilic fluorinating reagents. As demonstrated by Pannecoucke *et al* in 2007, α-fluoroenones can be further manipulated to afford fluoroalkenes of defined stereochemistry, which have found multiple applications as peptide mimics (Scheme 2.4).[82-83] The CH=CF motif possesses similar electronic and steric properties to the amide group whilst offering greater conformational rigidity and metabolic stability.[84-85] Synthetic routes to α-fluoroenones currently rely on the manipulation of fluorinated building blocks with many methods suffering from low diastereoselectivity.[85-88]



Scheme 2.4 Preparation of Peptidomimetics from α-Fluoroenones.

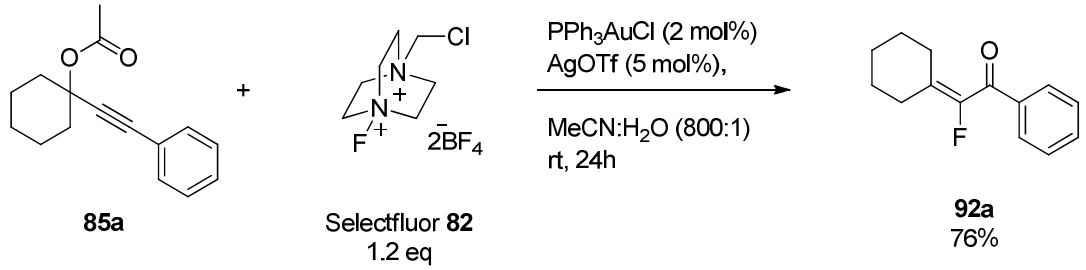
In this chapter, our studies towards the development of a gold-catalysed [3,3]-sigmatropic rearrangement-fluorodeacetylation of propargyl acetates **85** to afford α-fluoroenones **92** are presented (Scheme 2.5). This protocol allowed for the preparation of these useful fluorinated compounds in generally moderate to good yields under mild conditions whilst, in some cases, high levels of diastereoselectivity (up to 93:7) were observed. In addition, the *E*/*Z* selectivity of the process as well as control reactions with proposed intermediates provided insights into the nature of the fluorination step.[89]



Scheme 2.5 Rearrangement-Fluorodeacetylation of Propargyl Acetates **85**.

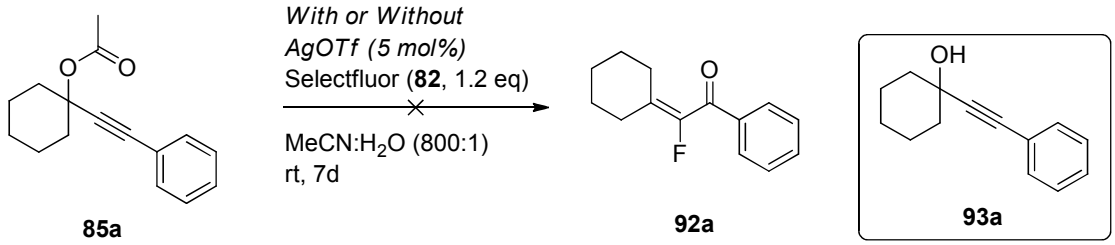
2.2 Preliminary Studies

As a preliminary experiment, the symmetrical propargyl acetate **85a** was reacted with the gold(I) pre-catalyst PPh_3AuCl (2 mol%) and AgOTf (5 mol%) in the presence of 1.2 equivalents of the electrophilic fluorinating reagent Selectfluor (**82**, Scheme 2.6). After stirring in acetonitrile/water (800:1, 0.05M) for 24 hours at room temperature, all the propargyl acetate starting material had been consumed and the reaction was filtered through Celite. NMR Spectroscopic analysis on the crude mixture indicated the formation of a single fluorinated product whilst mass spectral data was consistent with the α-fluoroenone **92a**. The identity of this species was unambiguously confirmed upon purification by column chromatography on silica gel. The desired rearrangement-fluorodeacetylation product was afforded in 76% yield as the only isolable compound. Notably, no products resulting from the conventional rearrangement-protodeacetylation process were observed.



Scheme 2.6 Preliminary Experiment with Propargyl Acetate **85a**.

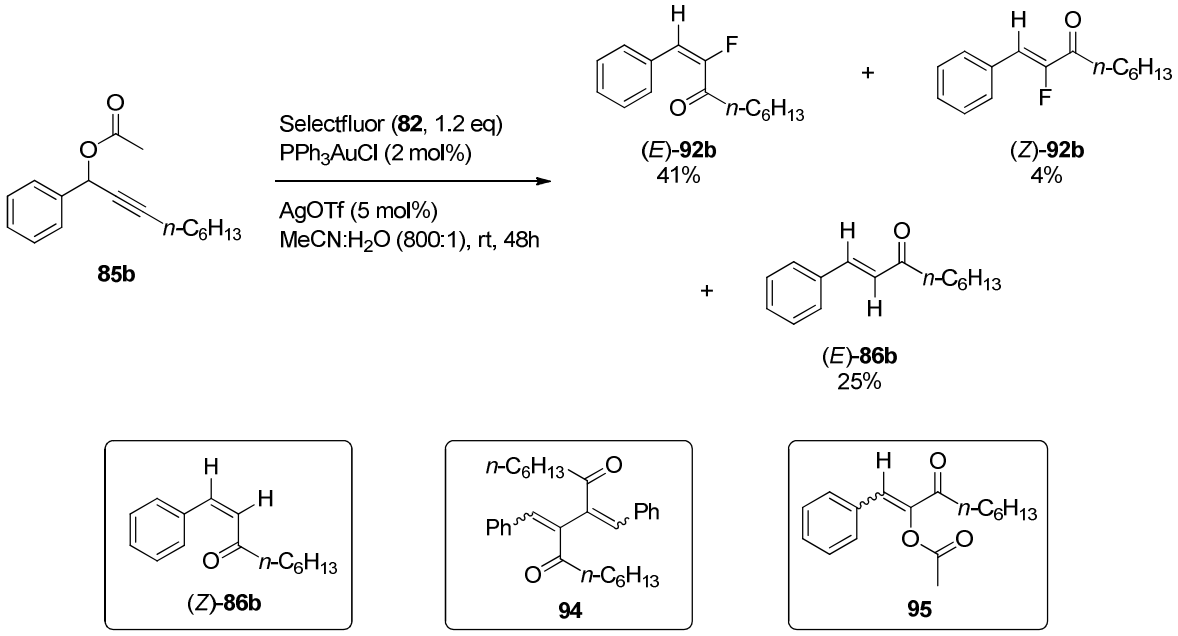
In order to confirm that the observed rearrangement-fluorination process was indeed gold-catalysed, the same reaction was performed in the absence of PPh_3AuCl. After 7 days at room temperature, this reaction led to mainly recovered starting material along with some deacetylated propargyl alcohol **93a** whilst α-fluoroenone **92a** was observed in only a trace amount (< 5%, Scheme 2.7). Similar results were obtained when the reaction was performed in the absence of both PPh_3AuCl and AgOTf.



Scheme 2.7 Control Reactions with Propargyl Acetate **85a**.

With the fluorination reaction successfully validated using the symmetrical tertiary propargyl acetate **85a**, we were poised to investigate the degree of diastereocontrol afforded by the process with starting materials bearing a single propargyl substituent. Thus, the phenyl-substituted secondary propargyl acetate **85b** was reacted under the same conditions with PPh_3AuCl/AgOTf and Selectfluor. After 48 hours at room temperature, the corresponding α-fluoroenones **92b** were delivered in 45% combined isolated yield in a diastereoisomeric ratio of 91:9 favouring the *E*-isomer (*E*)-**92b** (Scheme 2.8). The conventional rearrangement-protodeacetylation process was not completely suppressed

under these conditions and the (*E*)-enone isomer (*E*)-**86b** was also isolated as a minor side-product in 25% yield (*E*/*Z* >20:1) whilst a trace amount of the *Z*-enone (*Z*)-**86b** was detected by NMR spectroscopy. Mass spectrometry and NMR analysis on the crude reaction mixture also indicated the presence of trace amounts of the enone dimer **94** and α-acetylenone **95**. These products result from oxidative homocoupling and C-O bond-forming cross-coupling processes respectively.[g]



Scheme 2.8 Preliminary Experiment with Propargyl Acetate **85b**.

Importantly, the two α-fluoroenone geometric isomers (*E*)-**92b** and (*Z*)-**92b** could be easily separated by column chromatography and isolated as diastereoisomerically-pure compounds. Furthermore, both (*E*)- and (*Z*)-isomers were found to be stable towards isomerisation under the reaction conditions.[h] The stereochemistry of each fluoroolefin (*E* or *Z*) was assigned by analysis of their ^{1}H and ^{19}F NMR spectra. The observed $^{3}J_{HF}$ alkene coupling constant of 25.3 Hz in the ^{1}H and ^{19}F NMR spectra of (*E*)-**92b** is consistent with

[g] Gold-mediated oxidative coupling processes of this type performed in the presence of Selectfluor are discussed more thoroughly in Chapter 3 of this thesis.

[h] Semi-empirical calculations performed by Nevado *et al* (reference [96]) have indicated that (*Z*)-α-fluoroenones are more stable than their (*E*)-counterparts in the order of 5 kcalmol^{-1} implying that the (*E*)-stereoselectivity of the process is not due to thermodynamic factors.

proton-fluorine coupling across a *cis*-double bond. By contrast, a larger $^{3}J_{HF}$ coupling of 36.9 Hz was observed in the ^{1}H and ^{19}F NMR spectra of (*Z*)-**92b**, as would be expected with a *trans*-arrangement of the two spins. In addition, a strong nuclear Overhauser effect was observed between the alkene proton and the fluorine in a ^{1}H-^{19}F HOESY experiment with (*E*)-**92b**, further supporting the assignment of the (*E*)-double bond geometry (Figure 2.1).

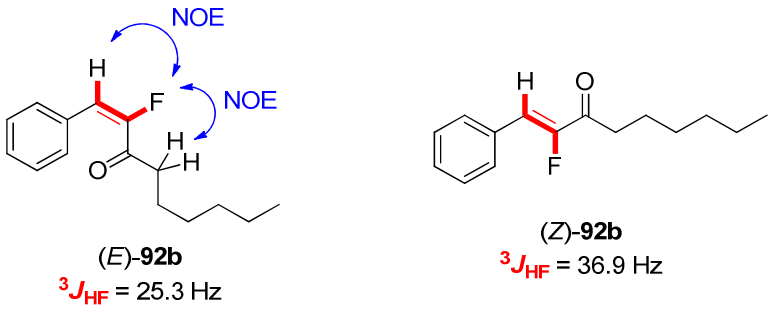
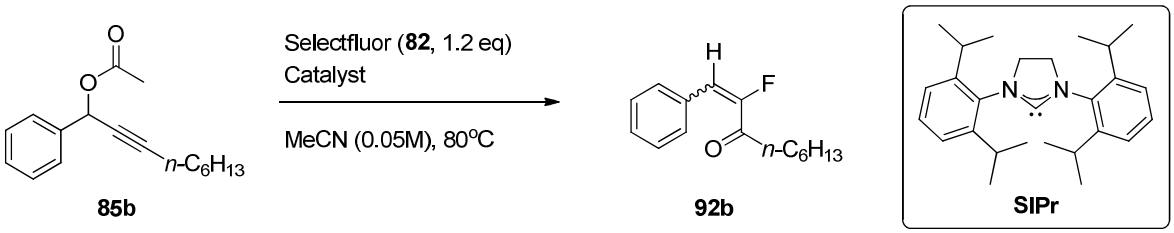


Figure 2.1 NMR Assignment of (*E*)- and (*Z*)-**92b**.

2.3 Optimisation of the Reaction Conditions

With the [3,3]-sigmatropic rearrangement-fluorodeacetylation of propargyl acetates validated, we sought to identify standard reaction conditions which optimised both the yield of α-fluoroenones and, in the case of unsymmetrical substrates, the diastereoselectivity. Firstly, a screen of catalysts was conducted using the phenyl-substituted propargyl acetate **85b** as a model substrate (Table 2.1).



Entry	Catalyst	Time	Yield (%)[a]	*E*/*Z* Ratio[b]
1	PPh_3AuCl (2 mol%) AgOTf (5 mol%)	2h	64 (40)	81:19
2	AgOTf (2 mol%)	66h	---	---
3	No Catalyst	66h	---	---

4	$PtCl_2$ (2 mol%)	66h	Trace	---
5	AuCl (2 mol%)	2h	40	78:22
6	$AuCl_3$ (2 mol%)	2h	4	*Z* Only
7	SIPrAuCl (**1**, 2 mol%) AgOTf (5 mol%)	2h	68 (53)	81:19
8	SIPrAuCl (**1**, 2 mol%)	2h	59	80:20

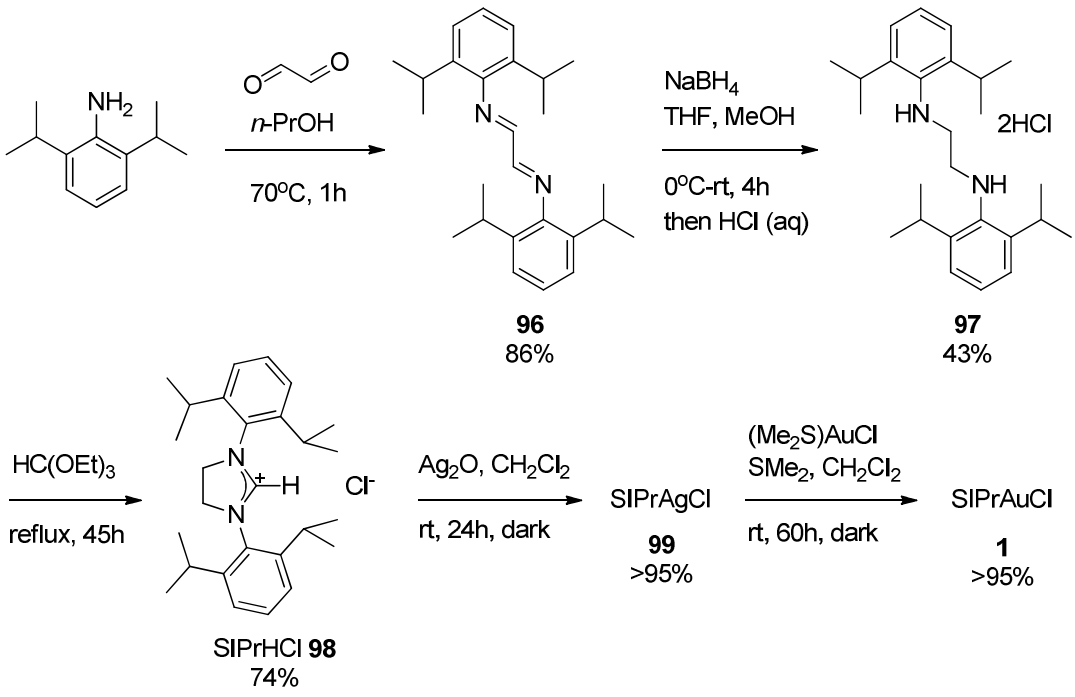
[a] Yield of **92b** estimated by ^{19}F NMR analysis of the crude reaction mixture with fluorobenzene as an internal reference. Isolated yields are in parentheses. [b] *E*/*Z* Determined by ^{19}F NMR analysis of the crude reaction mixture.

Table 2.1 Optimisation of the Catalyst.

In each case, the yield and *E*/*Z* selectivity of the α-fluoroenone products **92b** were determined by ^{19}F NMR analysis of the crude reaction mixture. The yields were estimated by comparing the combined integration of the ^{19}F NMR peaks of (*E*) and (*Z*)-**92b** with the signal corresponding to a known quantity of the added internal reference, fluorobenzene. Isolated yields were obtained where appropriate and these are displayed in parentheses in the table above (Table 2.1). All the reactions were performed with 2 mol% of the catalyst at 80ºC using Selectfluor (**82**, 1.2 eq) as the electrophilic fluorine source. Each experiment was conducted in acetonitrile due to the comparatively good solubility of Selectfluor in this solvent.[i] Under these conditions, the PPh_3AuCl/AgOTf catalysed reaction afforded α-fluoroenones **92b** in 40% isolated yield (64% estimated by ^{19}F NMR) after 2 hours in an *E*/*Z* ratio of 81:19 (Table 2.1, Entry 1). In the absence of PPh_3AuCl, either with or without AgOTf, no fluorinated products were formed after an extended reaction time (Table 2.1, Entries 2-3). The reaction with the platinum(II) salt $PtCl_2$ was similarly unsuccessful, delivering **92b** in only a trace amount (Table 2.1, Entry 4). Although the unstabilised gold(I) source AuCl was a suitable catalyst for the rearrangement-fluorodeacetylation reaction, the α-fluoroenone products were delivered in a lower yield (40% estimated by ^{19}F NMR) and a

[i] Selectfluor is not soluble in the majority of organic solvents (eg dichloromethane, tetrahydrofuran, diethyl ether).

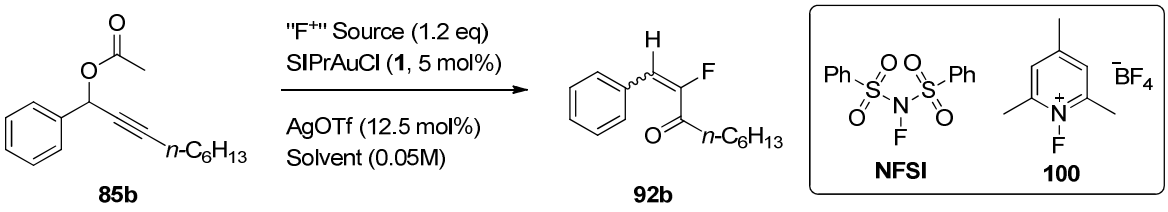
slightly lower diastereoselectivity (*E*/*Z* = 78:22) compared to the $PPh_3AuCl/AgOTf$ catalysed process (Table 2.1, Entry 5). The fluorinated product **92b** was formed in only 4% yield (estimated by ^{19}F NMR) when the gold(III) catalyst $AuCl_3$ was employed (Table 2.1, Entry 6). The highest yield of α-fluoroenones was obtained using the *N*-heterocyclic carbene stabilised gold(I) catalyst SIPrAuCl (**1**). This species was prepared in 5 steps according to the procedures of Arduengo[90] and Sadighi (Scheme 2.9).[46] Firstly glyoxal was reacted in the presence of 2.25 equivalents of diisopropylamine at 70ºC for one hour to afford the corresponding 1,2-diimine compound **96** in 86% yield. Reduction with sodium borohydride to afford the 1,2-diamine **97** followed by construction of the five-membered imidazolidynium ring using triethyl orthoformate led to SIPrHCl (**98**) in 32% yield over two steps. This species was then treated with Ag_2O to afford the silver transfer reagent SIPrAgCl (**99**) in quantitative yield. Finally, transmetalation of the *N*-heterocyclic carbene ligand from silver(I) to gold(I) was performed using $(Me_2S)AuCl$ in the presence of excess dimethyl sulfide in dichloromethane.



Scheme 2.9 Preparation of SIPrAuCl (**1**).

Reacting **85b** with SIPrAuCl (2 mol%) and AgOTf (5 mol%) in the presence of Selectfluor (1.2 eq) at 80ºC for 2 hours led to the α-fluoroenones **92b** in 53% isolated yield (68% estimated by ^{19}F NMR) in a *E*/*Z* ratio of 81:19 (Table 2.1, Entry 7). The reaction was also successful with this catalyst in the absence of AgOTf although the fluorinated products were afforded in a slightly lower yield (59% estimated by ^{19}F NMR) and diastereoselectivity (*E*/*Z* = 80:20, Table 2.1, Entry 8).

With the combination of the gold(I) source SIPrAuCl (**1**) and silver(I) co-catalyst AgOTf identified as the optimum catalytic system for the rearrangement-fluorodeacetylation process, our attention turned to optimising the other reaction parameters (Table 2.2).



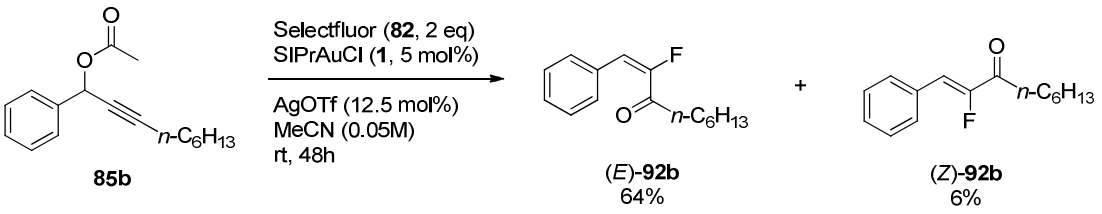
Entry	Conditions	Time	Yield (%)[a]	*E*/*Z* Ratio[b]
1[c]	Selectfluor, MeCN, rt	14h	71	92:8
2	Selectfluor, MeCN, rt	14h	81	91:9
3	Selectfluor, MeCN:H_2O (800:1), rt	48h	69	89:11
4	Selectfluor, acetone, rt	48h	5	20:80
5	NFSI,[d] CH_2Cl_2, rt	48h	---	---
6	**100**,[e] MeCN, rt	48h	---	---
7	Selectfluor (2 eq), MeCN, rt	14h	>95 (70)	93:7

[a] Yield of **92b** estimated by ^{19}F NMR analysis of the crude reaction mixture with fluorobenzene as an internal reference. Isolated yields are in parentheses. [b] *E*/*Z* Determined by ^{19}F NMR analysis of the crude reaction mixture. [c] Reaction performed with SIPrAuCl (**1**, 2 mol%) and AgOTf (5 mol%). [d] NFSI = *N*-Fluorobenzenesulfonimide. [e] **100** = 1-Fluoro-2,4,6-trimethylpyridinium tetrafluoroborate.

Table 2.2 Optimisation of the Reaction Conditions.

In an attempt to increase the diastereoselectivity of the process, the reaction with SIPrAuCl/AgOTf (2 mol%/5 mol%) was conducted at room temperature. Under these

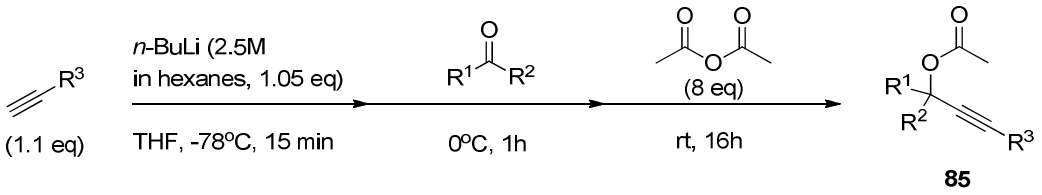
conditions, α-fluoroenones **92b** were delivered in 71% yield (estimated by ^{19}F NMR) in an improved *E*/*Z* ratio of 92:8 (Table 2.2, Entry 1). Increasing the loading of SIPrAuCl and AgOTf to 5 mol% and 12.5 mol% respectively led to an increase in the yield of the fluorinated products to 81% (estimated by ^{19}F NMR, Table 2.2, Entry 2). In the related iodination and bromination reactions reported by Zhang and co-workers, the yields of the halogenated enone products were improved when a small amount of water was added to the acetonitrile solvent.[80-81] However, performing the rearrangement-fluorodeacetylation process in an 800:1 mixture of acetonitrile and water led to a lower yield (69% estimated by ^{19}F NMR) and diastereoselectivity (*E*/*Z* = 89:11) of **92b** (Table 2.2, Entry 3). Changing the solvent to acetone led to a dramatically decreased fluoroenone yield of 5% (estimated by ^{19}F NMR, Table 2.2, Entry 4). This result is possibly due to the poor solubility of Selectfluor in this solvent. The reaction was similarly unsuccessful when alternative electrophilic fluorinating reagents to Selectfluor were employed. Both *N*-fluorobenzenesulfonimide (NFSI) and 1-fluoro-2,4,6-pyridinium BF_4 (**100**) afforded no fluorinated organic products after 48 hours at room temperature in dichloromethane and acetonitrile respectively (Table 2.2, Entry 5-6). Finally, the effect of the stoichiometry of Selectfluor was investigated. Increasing the number of equivalents of the electrophilic fluorinating reagent to two resulted in complete conversion of **85b** to **92b** (>95% conversion estimated by ^{19}F NMR) with an *E*/*Z* ratio of 93:7 after 48 hours at room temperature (Table 2.2, Entry 7). Upon purification by column chromatography on silica gel, the α-fluoroenones could be isolated in 70% combined yield (64% of (*E*)-**92b** and 6% of (*Z*)-**92b**) from this reaction (Scheme 2.10). As previously observed during the preliminary studies, both (*E*)- and (*Z*)-products were stable with respect to isomerisation under these reactions conditions.

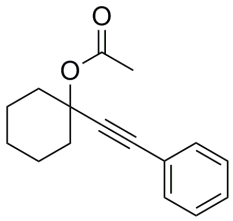
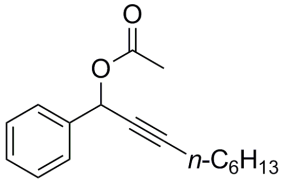
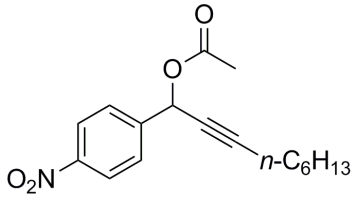
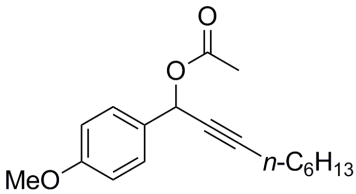


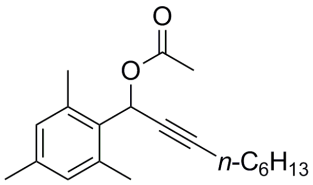
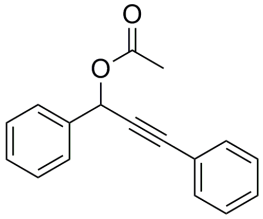
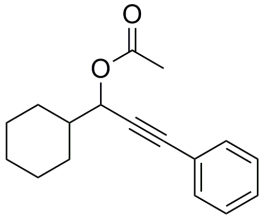
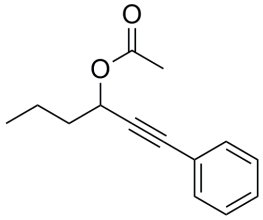
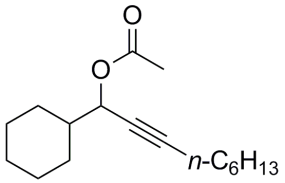
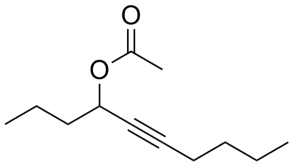
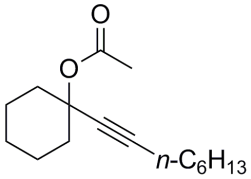
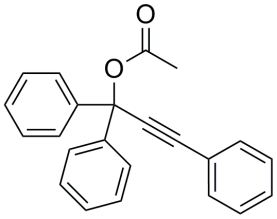
Scheme 2.10 Rearrangement-Fluorodeacetylation of Propargyl Acetate **85b** under the Optimised Reaction Conditions.

2.4 Preparation of Propargyl Acetates 85

Having optimised the reaction conditions, we then set out to evaluate the scope and limitations of the cascade [3,3]-sigmatropic rearrangement-fluorodeacetylation process with a range of different propargyl acetates **85**. These substrates were synthesised in a one-pot procedure analogous to that of Zhang and co-workers (Table 2.3).[80]



Entry	R^1	R^2	R^3	Product **85**	Yield[a]
1[b]	-$(CH_2)_5$-		Ph		**85a** (58%)[c]
2	Ph	H	*n*-C_6H_{13}		**85b** (89%)
3	4-NO_2-C_6H_4	H	*n*-C_6H_{13}		**85c** (72%)
4	4-MeO-C_6H_4	H	*n*-C_6H_{13}		**85d** (61%)

5	Mesityl	H	*n*-C_6H_{13}		**85e** (67%)
6	Ph	H	Ph		**85f** (93%)
7	Cy	H	Ph		**85g** (64%)
8	*n*-C_3H_7	H	Ph		**85h** (86%)
9	Cy	H	*n*-C_6H_{13}		**85i** (58%)
10	*n*-C_3H_7	H	*n*-C_4H_9		**85j** (86%)
11	-(CH_2)-		*n*-C_6H_{13}		**85k** (74%)
12	Ph	Ph	Ph		**85l** (28%)

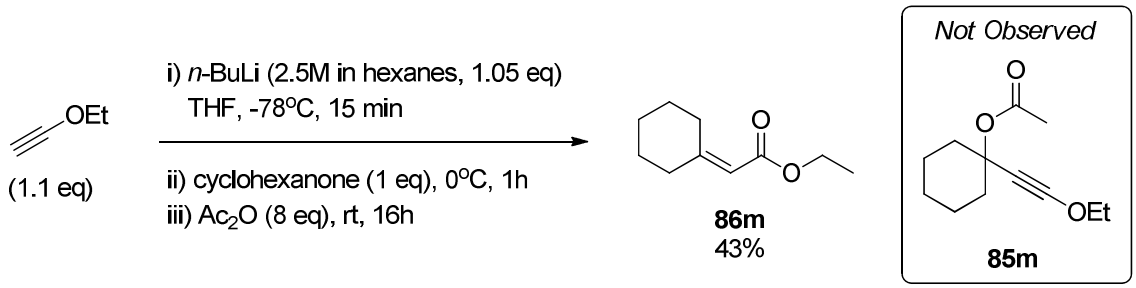
[a] Isolated yield. [b] 4 Equivalents of Ac_2O used. [c] 17% of the corresponding propargyl alcohol **93a** was also isolated.

Table 2.3 Preparation of Propargyl Acetates **85a-l**.

Terminal alkynes (1.1 eq relative to the aldehyde or ketone) bearing aryl or alkyl substituents were first reacted with 1.05 equivalents of *n*-butyllithium in tetrahydrofuran at −78ºC. After 15 minutes, one equivalent of an aldehyde or ketone was added carefully and the mixture was allowed to stir at 0ºC for one hour. Acetic anhydride was then added and the reaction was warmed to room temperature overnight (16h). In the preparation of the test substrate **85a**, 4 equivalents of the acetic anhydride were employed according to the procedure of Zhang.[80] In our hands, however, this quantity of the acetylating reagent resulted in incomplete conversion to the propargyl acetate and 17% of the corresponding propargyl alcohol **93a** was isolated from the reaction mixture along with 58% of **85a** (Table 2.3, Entry 1). Consequently, in all further reactions, 8 equivalents of anhydride were employed to encourage complete acetylation. Under these conditions, propargyl acetates **85b-e** bearing an *n*-hexyl substituent at the alkynyl position and an aryl group at the propargyl position were delivered in good to excellent yields up to 89% (Table 2.3, Entries 2-5). These compounds would enable the effect of the aryl group electronics on the efficiency and diastereoselectivity of the rearrangement-fluorodeacetylation process to be evaluated. A series of substrates featuring a phenylacetylene motif, allowing for an investigation of the effect of various aryl or alkyl substituents at the propargyl position, were also prepared in 64-93% yield (Table 2.3, Entries 6-8). The all alkyl-substituted secondary propargyl acetates **85i** and **85j** were afforded in 58% and 86% yield respectively (Table 2.3, Entries 9-10). Finally, the symmetric tertiary substrates **85k** and **85l** bearing all alkyl and all phenyl substituents respectively were synthesised from the corresponding ketones (Table 2.3, Entries 11-12).

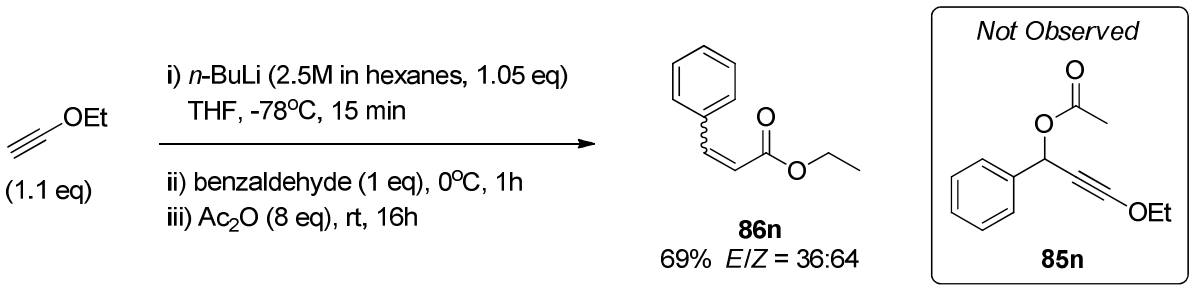
Using the same procedure, the preparation of the ethoxy-substituted propargyl acetate **85m** was attempted. Upon [3,3]-sigmatropic rearrangement-fluorodeacetylation, this substrate would deliver an α-fluoroenone compound with ester functionality. Such a species could

react via transesterification to afford a range of diversely functionalised fluoroenones and, as such, could be an important synthetic intermediate towards fluoroalkene peptidomimetics. The reaction between cyclohexanone, acetic anhydride and ethoxyacetylene, however, did not lead to the desired propargyl acetate **85m** and instead delivered enone **86m** as the only isolable product in 43% yield (Scheme 2.11). This compound presumably results from a spontaneous, non-gold-catalysed [3,3]-sigmatropic rearrangement-protodeacetylation of **85m** under the reaction conditions.



Scheme 2.11 Attempted Preparation of Propargyl Acetate **85m**.

The attempted preparation of the phenyl-substituted substrate **85n** was similarly unsuccessful. The only isolable products from this reaction were the diastereoisomeric enones **86n**, which were afforded as a 36:64 *E*/*Z* mixture in 69% yield (Scheme 2.12).



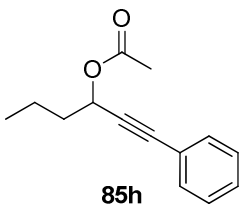
Scheme 2.12 Attempted Preparation of Propargyl Acetate **85n**.

2.5 Scope and Limitations of the Fluorination Process

Propargyl acetates **85a-l** were subjected to the [3,3]-sigmatropic rearrangement-fluorodeacetylation conditions with SIPrAuCl (**1**, 5 mol%), AgOTf (12.5 mol%) and

Selectfluor (**82**, 2 eq) in acetonitrile (0.05M). After preliminary experiments, it became clear that higher temperatures than room temperature were required to ensure complete conversion of the starting material for most substrates. For example, the rearrangement-fluorodeacetylation of propargyl acetate **85h** had not gone to completion after 8 days at room temperature whilst only 49% conversion to α-fluoroenones was observed after 7 days with substrate **85j** (determined by ^{1}H NMR, Scheme 2.13).

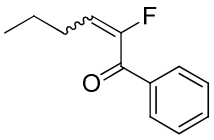
a)



85h

Selectfluor (**82**, 2 eq)
SIPrAuCl (**1**, 5 mol%)

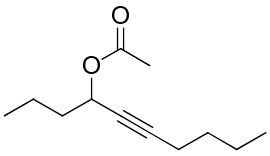
AgOTf (12.5 mol%)
MeCN (0.05M), rt



92h

Time	Conversion
55h	51%
81h	55%
8d	89%

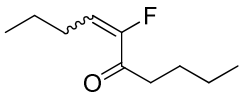
b)



85j

Selectfluor (**82**, 2 eq)
SIPrAuCl (**1**, 5 mol%)

AgOTf (12.5 mol%)
MeCN (0.05M), rt

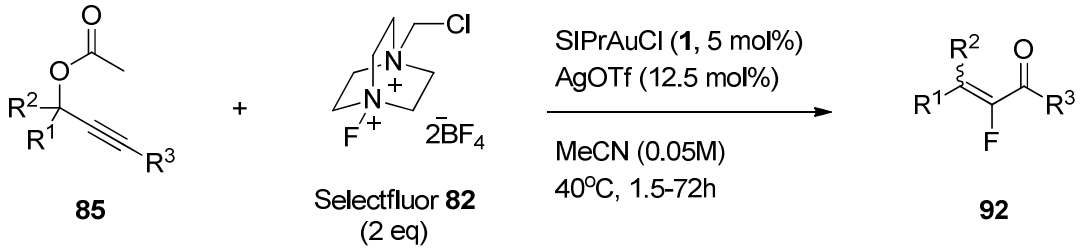


92j

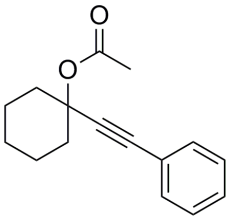
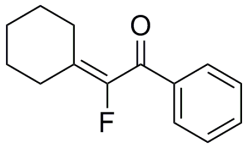
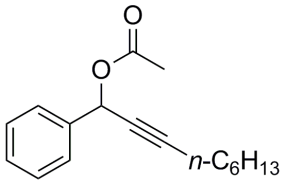
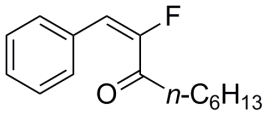
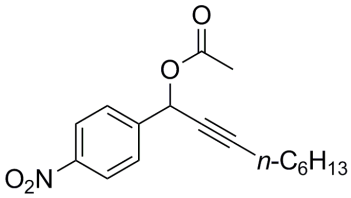
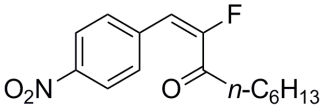
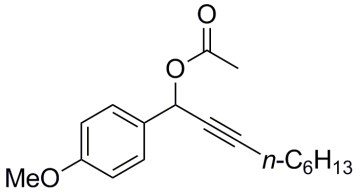
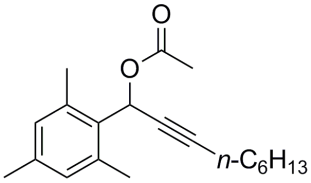
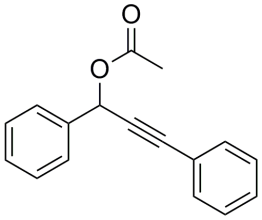
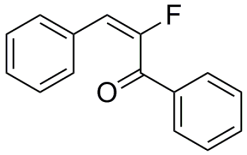
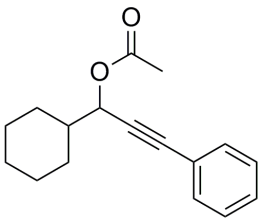
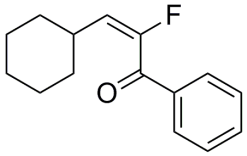
Time	Conversion
16h	10%
29h	23%
62h	32%
90h	42%
7d	49%

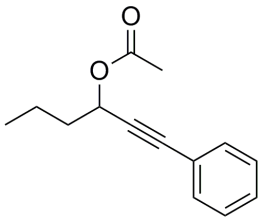
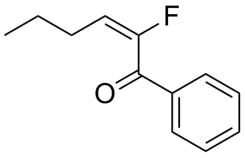
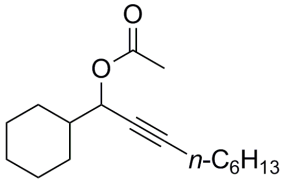
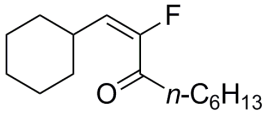
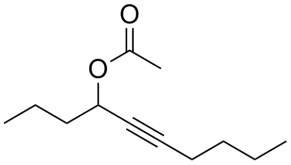
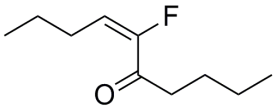
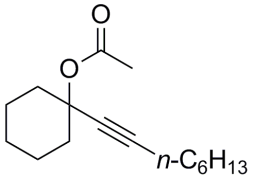
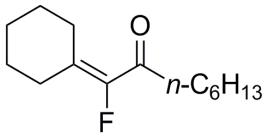
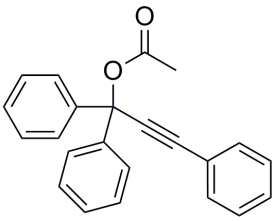
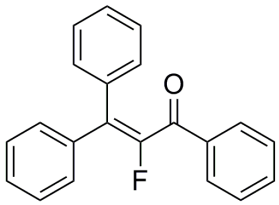
Scheme 2.13 Rearrangement-Fluorodeacetylation of Propargyl Acetates **85h** and **85j** at rt. (Conversions determined by ^{1}H NMR).

Consequently, the [3,3]-sigmatropic rearrangement-fluorodeacetylation reactions were performed at 40ºC to encourage complete conversion of the starting material within a reasonable reaction time (≤72h). The results of these experiments are displayed in Table 2.4.



85 + Selectfluor **82** (2 eq) → **92**

Entry	Propargyl Acetate **85**	Time	Major Product	Yield[a]	*E*/*Z* Ratio[b]
1		1.5h		**92a** 85%	---
2[c]		48h		**92b** 70% (*E*) 64% (*Z*) 6%	93:7
3		20h		**92c** 64% (*E*) only	90:10
4		20h	Complex Reaction Mixture	---	---
5		20h	Complex Reaction Mixture	---	---
6		24h		**95f** 62% (*E*) only	92:8
7		48h		**92g** 80% (*E*) 68% (*Z*) 12%	84:16

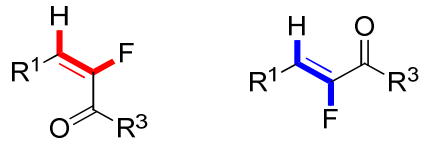
8		72h		**92h** 63% (*E*) 42% (*Z*) 21%	67:33
9		72h		**92i** 29% (*E*) only	77:23
10		72h		**92j** 39% (*E*) 19% (*Z*) 18%	58:42
11		3.5h		**92k** 58%	---
12		24h		**92l** 58%	---

[a] Isolated yield. [b] Determined by ^{19}F NMR of the crude reaction mixture. [c] Reaction performed at room temperature.

Table 2.4 Rearrangement-Fluorodeacetylation of Propargyl Acetates **85a-l**.

The reactions were monitored by thin layer chromatography (TLC) and worked-up upon completion (1.5-72h). With secondary propargyl acetates **82b-j**, bearing only one substituent at the propargyl position, the *E*/*Z* ratio was determined by ^{19}F NMR analysis of the crude reaction mixture. In every case, preferential formation of the (*E*)-diastereoisomer was observed whilst the (*E*) and (*Z*)-α-fluoroenones could be easily separated upon purification by column chromatography on silica gel. The double bond geometry was assigned based on analysis of the ^{1}H and ^{19}F NMR spectra of each isomer. Vicinal $^{3}J_{HF}$ coupling constants of 23-26 Hz were observed between the alkene proton and the fluorine for the (*E*)-isomers whilst larger couplings of 34-37 Hz were observed for the (*Z*)-isomers

(Figure 2.2). These values are consistent with literature precedents for *cis*- and *trans*-α-fluoroenones.[91]



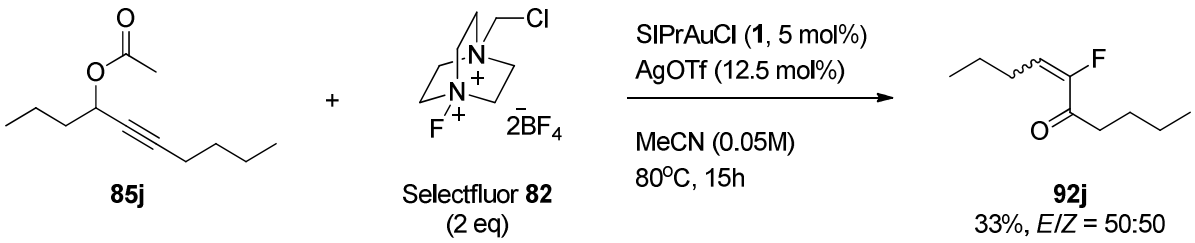
(*E*)-**92** (R^2 = H) $^3J_{HF}$ = 23-26 Hz

(*Z*)-**92** (R^2 = H) $^3J_{HF}$ = 34-37 Hz

Figure 2.2 Assignment of (*E*)- and (*Z*)-α-Fluoroenones **92**.

The highest levels of diastereoselectivity were observed with substrates bearing an aryl substituent at the propargyl position. The *para*-nitrophenyl substituted propargyl acetate **85c** reacted within 20 hours at 40ºC to afford the corresponding α-fluoroenone **92c** in an *E*/*Z* ratio of 90:10. Purification by silica gel column chromatography delivered the (*E*)-isomer (*E*)-**92c** as the only isolable compound in 64% yield (Table 2.4, Entry 3). By contrast, propargyl acetates featuring electron-rich aryl groups were not suitable substrates for the [3,3]-sigmatropic rearrangement-fluorodeacetylation process. The reactions with compounds **85d** and **85e**, bearing *para*-methoxyphenyl and mesityl substituents respectively, led to complex mixtures of fluorinated and non-fluorinated products (Table 2.4, Entries 4-5). Potential side-reactions resulting from direct fluorination of the electron-rich aromatic rings by Selectfluor could explain the low selectivity observed with these substrates. Propargyl acetate **92f**, which bears a phenyl substituent at both the propargyl and alkynyl positions, reacted successfully under the optimised conditions to afford α-fluoroenone **92f** in a 92:8 diastereoisomeric ratio favouring (*E*)-**92f**. This isomer was furnished as the only isolable product in 62% yield upon purification by column chromatography on silica gel (Table 2.4, Entry 6). Phenylacetylene-derived substrates **85g** and **85h**, featuring an alkyl group at the propargyl position, were also amenable to the rearrangement-fluorodeacetylation process. These compounds delivered α-fluoroenones **92g**

and **92h** in combined yields of 80% (68% of (*E*)-**92g** and 12% of (*Z*)-**92g**) and 63% (42% of (*E*)-**92h** and 21% of (*Z*)-**92h**) respectively, although lower levels of diastereoselectivity were observed (*E*/*Z* = 84:16 for **92g** and 67:33 for **92h**, Table 2.4, Entries 7-8). The fluorination reaction was also successful with the all-alkyl substituted propargyl acetates **85i** and **85j**. However, the corresponding α-fluoroenones **92i** and **92j** were afforded with poor diastereoselectivities (*E*/*Z* = 77:23 for **92i** and 58:42 for **92j**) and in comparatively low isolated yields (29% and 39% respectively). Substantial decomposition of the fluorinated products was observed upon work-up and purification with these substrates. Furthermore, in contrast to aryl-substituted α-fluoroenones, noticeable isomerisation (*E*/*Z* > 95:5 to *E*/*Z* = 80:20 over 72 hours) was observed upon reacting a diastereoisomerically-pure sample of (*E*)-**92i** under the optimised conditions at 40ºC. In an attempt to decrease the reaction time from 72 hours, the rearrangement-fluorodeacetylation of propargyl acetate **85j** was repeated at 80ºC. Complete consumption of the starting material was observed after 15 hours at this temperature but the α-fluoroenone products were delivered in a lower yield (33%) and *E*/*Z* ratio (50:50, Scheme 2.14).



Scheme 2.14 Rearrangement-Fluorodeacetylation of **85j** Performed at 80ºC.

Tertiary propargyl acetates reacted readily under the optimised conditions affording the corresponding α-fluoroenones in moderate to excellent yields. The reaction with the test substrate **85a** was complete within 90 minutes and delivered the fluorinated product **92a** in 85% isolated yield upon silica gel column chromatography (Table 2.4, Entry 1). The all

alkyl- and all-phenyl-substituted α-fluoroenones **92k** and **92l** were both furnished in 58% yield after 3.5 and 24 hours respectively (Table 2.4, Entries 11-12). This latter compound (**92l**) was a crystalline solid, allowing for unambiguous assignment of the structure by X-ray crystallographic analysis (Figure 2.3).

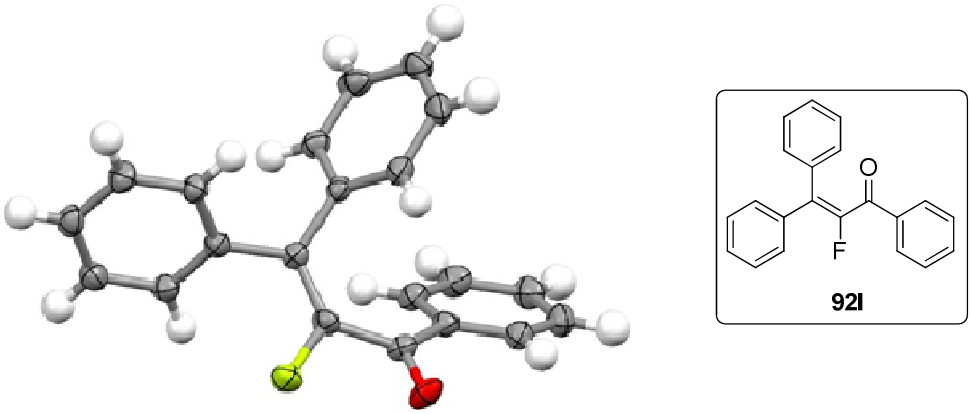
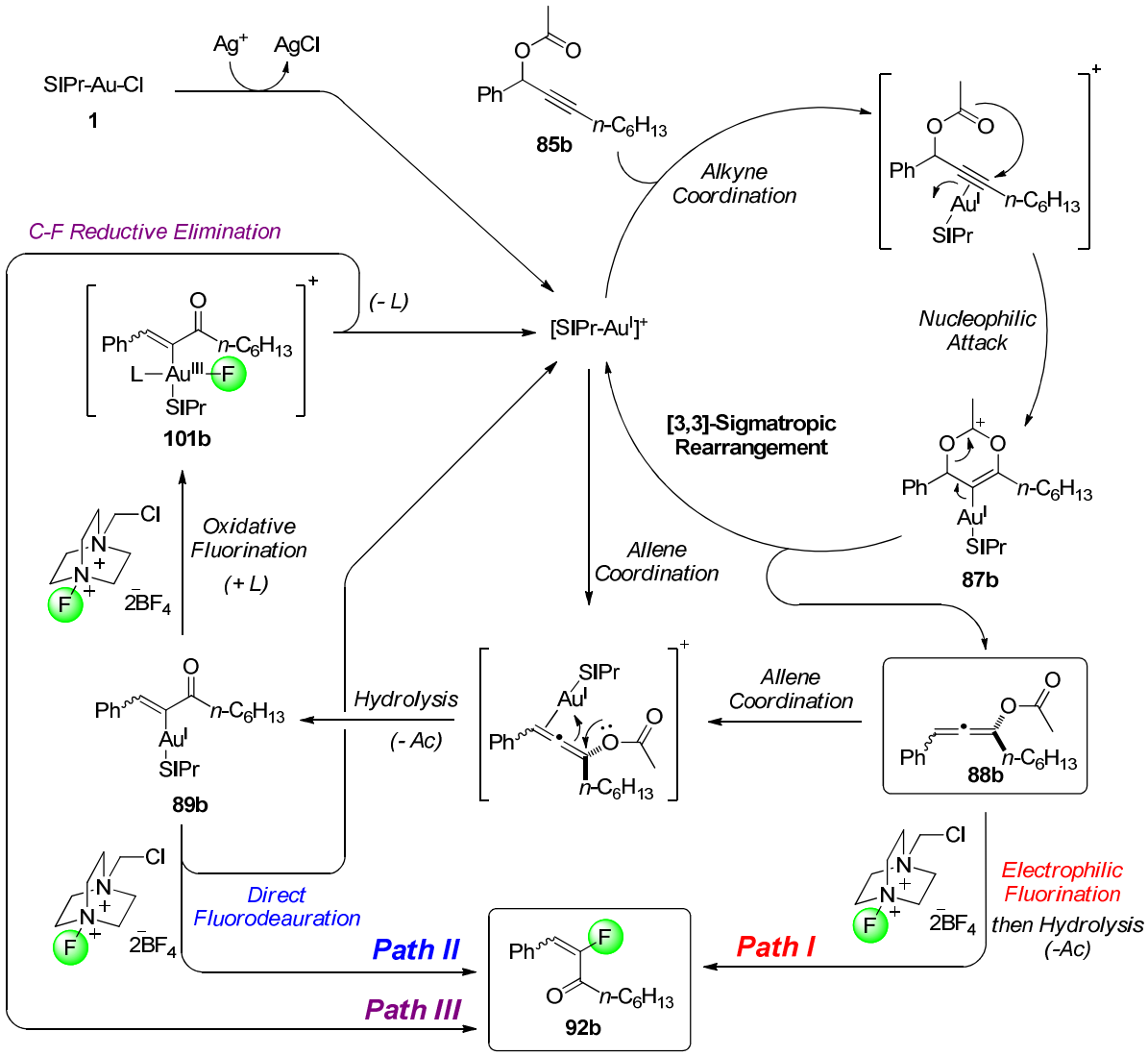


Figure 2.3 X-Ray Crystal Structure of α-Fluoroenone **92l**.

2.6 Comments on the Reaction Mechanism

With the scope and limitations of the gold-catalysed [3,3]-sigmatropic rearrangement-fluorodeacetylation process established, our attention turned to an investigation of the reaction mechanism with a focus on determining the nature of the fluorination step. Three plausible mechanistic pathways for this transformation are summarised in Scheme 2.15 using the preparation of α-fluoroenone **92b** from substrate **85b** as a representative example. In each pathway, the propargyl acetate first undergoes a formal [3,3]-sigmatropic rearrangement mediated by gold to afford the allenyl acetate intermediate **88b**. This process is most likely catalysed by the cationic gold(I) complex $[SIPrAu]^+$ which is formed upon abstraction of the chloride ion of the pre-catalyst SIPrAuCl (**1**) by silver(I). Coordination of this highly π-Lewis acidic species to the alkyne moiety in **85b** followed by intramolecular nucleophilic attack of the pendant acetate oxygen leads to the transient cyclic complex **87b**.

Ring-opening of this species leads to the allenyl acetate **88b** and regenerates the cationic gold(I) catalyst.



Scheme 2.15 Plausible Mechanisms for the Rearrangement-Fluorodeacetylation of Propargyl Acetates **85**. L = Neutral Ligand.

At this stage, the key allenyl acetate intermediate **88b** may react via two distinct pathways. Firstly, this species, which features an enol ether-type moiety, could react directly with the electrophilic fluorinating reagent Selectfluor to afford the α-fluoroenone product **92b** after hydrolysis of the acetate group (Scheme 2.15, Path I).[j] In this pathway, the C-F bond is

[j] Hydrolysis could occur either upon work-up or *in situ* with adventitious water present in the reaction medium.

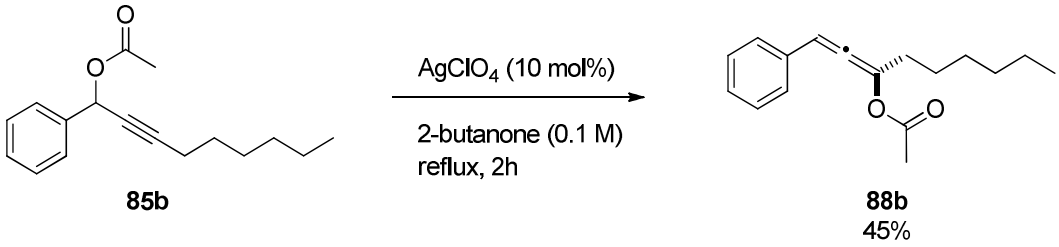
formed via direct electrophilic fluorination without the involvement of the gold catalyst. Alternatively, the cationic gold(I) complex $[SIPrAu]^+$ can coordinate the allene in **88b** leading to the vinylgold(I) species **89b** upon hydrolysis of the acetate group. Direct electrophilic fluorination with concomitant cleavage of the carbon-gold(I) bond in this complex by Selectfluor would lead to **92b** and regenerate the gold(I) catalyst (Scheme 2.15, Path II). This pathway is analogous to the accepted mechanism for the conventional [3,3]-sigmatropic rearrangement-protodeacetylation process with fluorodeauration replacing the protodeauration step (see Scheme 2.2). A similar pathway was tentatively proposed by our group as the operative fluorination mechanism in the previously discussed cyclisation-fluorodeauration of β-hydroxy-α,α-difluoroynones (see Section 1.5.1).[78] A third possible fluorination mechanism involves the "F^+" source acting as a stoichiometric oxidant rather than a conventional fluorinating reagent.[k] Thus, the reaction between the vinylgold(I) complex **89b** and Selectfluor could lead to the gold(III) fluoride complex **101b** resulting from a formal oxidation of gold(I) to gold(III). Carbon-fluorine bond-forming reductive elimination from this species would then afford the α-fluoroenone product and regenerate the active gold(I) catalyst (Scheme 2.15, Path III).

In order to distinguish between Path I and Paths II/III, we sought to independently prepare the key allenyl acetate intermediate **88b** as a mechanistic probe. If the direct electrophilic fluorination mechanism (Path I) is feasible, reacting this compound with Selectfluor should lead to the α-fluoroenones **92b** without the presence of SIPrAuCl and AgOTf.

Allenyl acetate **88b** was prepared directly from the corresponding propargyl acetate via a silver(I)-catalysed [3,3]-sigmatropic rearrangement according to the procedure of Zhang *et al*.[92] Reacting **85b** with $AgClO_4$ (10 mol%) in 2-butanone at reflux for 2 hours led to the key intermediate in 45% yield upon silica gel column chromatography (Scheme 2.16). The

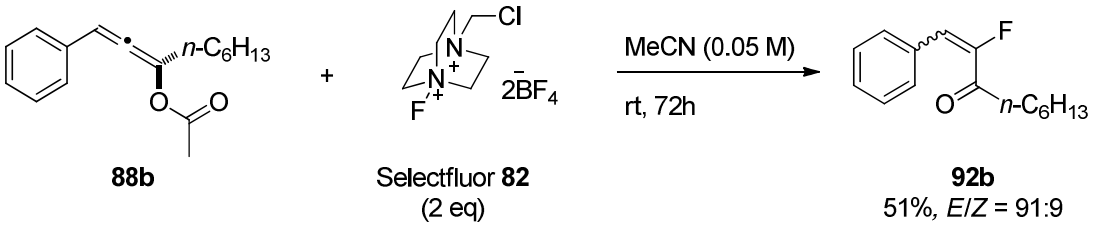
[k] Gold-catalysed reactions proceeding via mechanisms involving postulated Au^I/Au^{III} redox cycles where Selectfluor acts as a stoichiometric oxidant are discussed in Chapters 3 and 4 of this thesis.

structure of this compound was assigned based on analysis of its ^{13}C NMR and IR spectra. The observation of a highly deshielded resonance at δ = 196.7 ppm in the ^{13}C NMR spectrum is consistent with a sp-hybridised allenyl carbon whilst a characteristic allene stretch at λ = 1965 cm^{-1} was observed in the IR spectrum.



Scheme 2.16 Preparation of Allenyl Acetate **88b**.

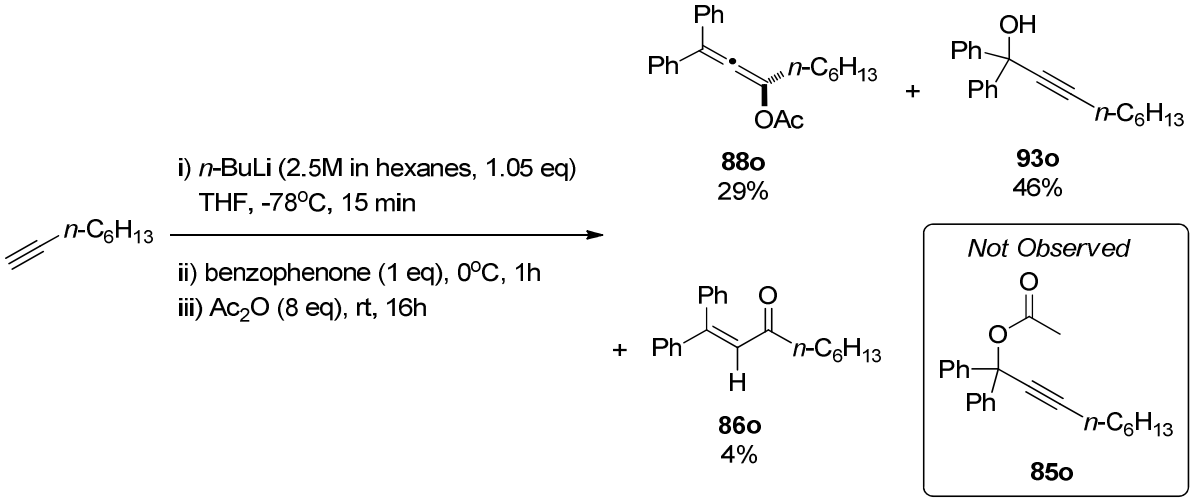
Compound **88b** was reacted with two equivalents of the electrophilic fluorinating reagent Selectfluor (**82**) in acetonitrile (0.05M) at room temperature. This reaction led, after 72 hours, to the α-fluoroenones **92b** in an isolated yield of 51% upon purification by column chromatography on silica gel (Scheme 2.17). The successful preparation of these compounds from **88b** in the absence of gold suggests that Path I is at least feasible under the optimised reaction conditions. Moreover, the fluorinated products were afforded in a similar *E*/*Z* ratio (*E*/*Z* = 91:9) as in the gold-catalysed process (*E*/*Z* = 93:7), suggesting that the origin of the (*E*)-diastereoselectivity in both reactions could be due to the same considerations.



Scheme 2.17 Fluorination of Allenyl Acetate **88b** without Gold.

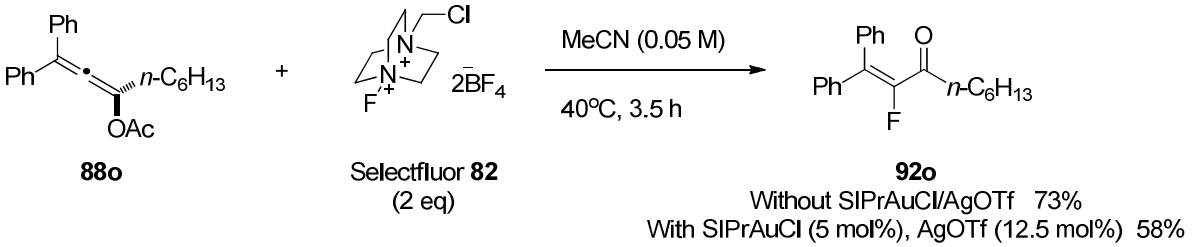
Further support for the involvement of a non-gold-catalysed fluorination step from allenyl acetate intermediates in the rearrangement-fluorodeacetylation process was provided by

compound **88o**. This species was isolated in 29% yield during the attempted preparation of the corresponding propargyl acetate **85o** from 1-octyne and benzophenone according to the procedure discussed in Section 2.4 (Scheme 2.18). The formation of **88o** presumably results from a spontaneous [3,3]-sigmatropic rearrangement of **85o** under the reaction conditions.



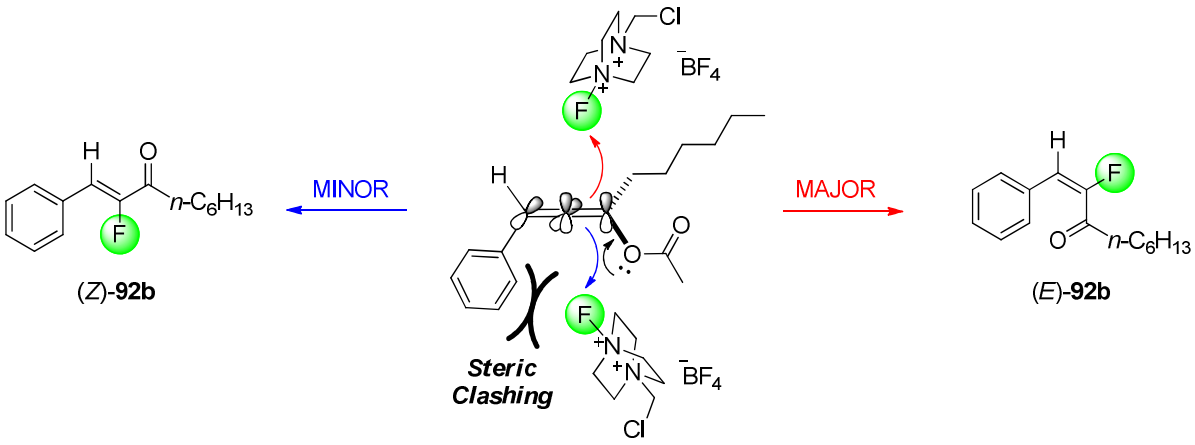
Scheme 2.18 Preparation of Allenyl Acetate **88o**.

Reacting this substrate with Selectfluor (2 eq) under the optimised conditions at 40ºC without SIPrAuCl or AgOTf, led smoothly to the corresponding α-fluoroenone **92o** in 73% isolated yield within 3.5 hours (Scheme 2.19). Furthermore, when this reaction was repeated in the presence of SIPrAuCl (**1**, 5 mol%) and AgOTf (12.5 mol%), **92o** was delivered in a lower yield of 58%.



Scheme 2.19 Fluorination of Allenyl Acetate **88o** With and Without Gold.

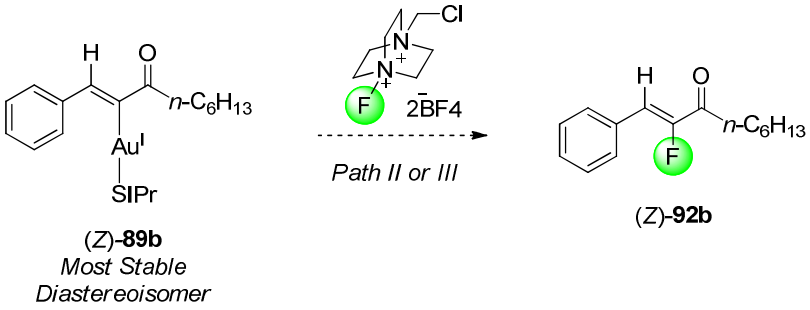
These control reactions imply that a mechanism consisting of an initial gold-catalysed formal [3,3]-sigmatropic rearrangement of the propargyl acetate followed by a direct electrophilic fluorination of the allenyl acetate intermediate not mediated by gold is at least feasible under the optimised conditions (Scheme 2.15, Path I). This mechanistic pathway is also consistent with the (*E*)-diastereoselectivity observed throughout this study. As demonstrated for allenyl acetate **88b** in Scheme 2.20, the electrophilic fluorinating reagent Selectfluor is expected to approach the allene preferentially from the least hindered face leading to α-fluoroenone products with (*E*)-geometry. This rationale is supported by the 91:9 *E*/*Z* selectivity observed in the direct fluorination reaction of allenyl acetate **88b** with Selectfluor (Scheme 2.17).



Scheme 2.20 Preferential Formation of (*E*)-**92b** via Direct Electrophilic Fluorination of **88b**.

In the related [3,3]-sigmatropic rearrangement-halodeacetylation reactions of propargyl acetates in the presence of electrophilic sources of iodine and bromine, a general preference for the (*Z*)-α-haloenones **90** and **91** was observed.[80-81] The halogenation step in these processes was proposed to occur via the direct halodeauration of a vinylgold(I) intermediate of type **89** proceeding with retention of stereochemistry in a mechanism analogous to Path II in Scheme 2.14. The (*Z*)-selectivity of the process was then explained by the preferential formation of the (*Z*)-diastereoisomer of complex **89**. This species is expected to experience

less steric clashing than the corresponding (*E*)-isomer by virtue of the comparatively long carbon-gold bond length.[80-81] (*Z*)-Vinylgold(I) intermediates of this type have been proposed as reactive intermediates in a number of related gold-catalysed transformations of propargyl acetates.[92-95] By analogy, therefore, if Paths II or III (Scheme 2.14) were operative, the [3,3]-sigmatropic rearrangement-fluorodeacetylation of propargyl acetates would be expected to proceed with preferential (*Z*)-diastereoselectivity rather than the (*E*)-selectivity observed throughout the study (Scheme 2.21).

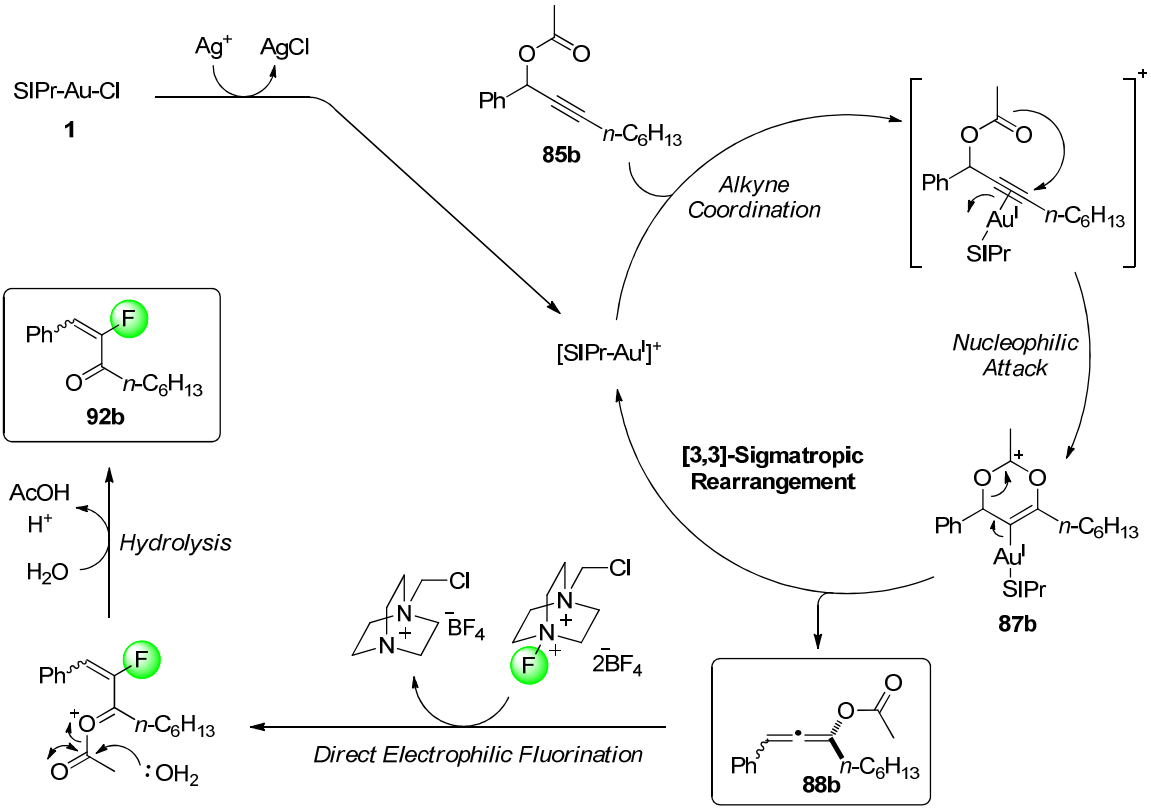


(*Z*)-**89b**
Most Stable Diastereoisomer

(*Z*)-**92b**

Scheme 2.21 Preferential Formation of (*Z*)-α-Fluoroenones via Path II of III.

Taken together, the control reactions with allenyl acetate intermediates and the consistent (*E*)-diastereoselectivity of the [3,3]-sigmatropic rearrangement-fluorodeacetylation reaction mitigate in favour of the mechanism shown in Scheme 2.22. In this process, the gold catalyst is not directly involved in C-F bond formation and merely delivers an allenyl acetate intermediate amenable to direct electrophilic fluorination with Selectfluor. It should be noted that, although this mechanism appears to be favoured under these conditions, gold-mediated fluorination processes such as Path II and Path III (Scheme 2.14) could be operating as minor pathways. Indeed, the direct electrophilic fluorination of allenyl acetates **88** with Selectfluor is seemingly a highly favourable process, out-competing conventional protodeacetylation under these conditions.

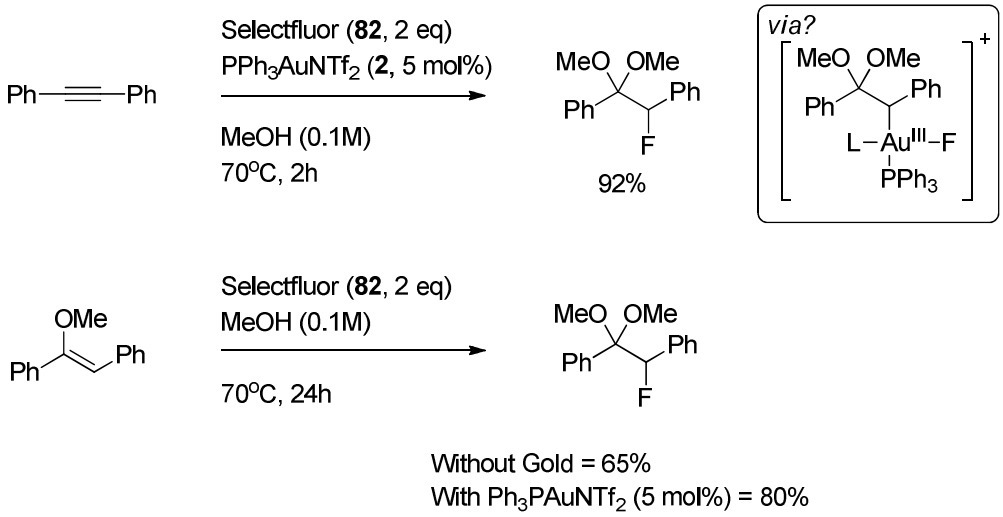


Scheme 2.22 Proposed Reaction Mechanism.

While we were preparing the results of this study for publication,[89] a paper appeared in the literature by de Haro and Nevado reporting the same gold-catalysed (*E*)-selective [3,3]-sigmatropic rearrangement-fluorodeacetylation of propargyl acetates performed in the presence of Selectfluor.[96] In this report, a Au^{I}/Au^{III} redox mechanism analogous to Path III in Scheme 2.14 involving a C-F bond-forming reductive elimination was proposed although no evidence in support of this pathway was provided. Whilst the oxidative fluorination of gold(I) to gold(III) by electrophilic fluorinating reagents has been demonstrated in the literature,[97] C-F bond forming reductive elimination from the resulting $5d^8$ gold(III) fluoride complex was not observed.[I] The analogous reductive elimination from $4d^8$ palladium(II) complexes is a notoriously challenging operation with unambiguous C-F bond formation only recently being disclosed by Buchwald and co-workers.[98]

[I] Gold-catalysed reactions involving proposed Au^{I}/Au^{III} redox cycles performed in the presence of electrophilic fluorinating reagents are discussed more thoroughly in Chapter 3 of this thesis.

A similar Au^{I}/Au^{III} redox mechanism was proposed by the same group in a more recent study focusing on the gold-catalysed alkoxylation-fluorination of simple alkynes in the presence of Selectfluor (Scheme 2.23).[99] Control reactions performed in the absence of gold, however, showed that a direct electrophilic fluorination of the proposed enol ether intermediate by Selectfluor was feasible under the reaction conditions. Adding 5 mol% of the gold(I) catalyst PPh_3AuNTf_2 (**2**) to this reaction led to an increase in the yield of the α-fluoroacetal products from 65% to 80% suggesting that gold could have a role to play in the fluorination process. However, further studies are required to determine the origins of this increase in the reaction efficiency.



Scheme 2.23 Alkoxylation-Fluorination of Alkynes with Selectfluor.

2.7 Conclusions

In summary, an investigation into the effect of electrophilic fluorinating reagents on the gold-catalysed formal [3,3]-sigmatropic rearrangement of propargyl acetates **85** led to the discovery of a novel reaction pathway leading to α-fluoroenones **92**. The combination of the *N*-heterocyclic carbene stabilised gold(I) catalyst SIPrAuCl (**1**) and AgOTf led to the highest yields of the fluorinated products whilst Selectfluor (**82**) was identified as the fluorinating reagent of choice. Unsymmetrical propargyl acetates typically reacted with

moderate to high levels of diastereoselectivity with the (*E*)-geometric isomers (*E*)-**92** being preferentially formed in all cases. Under the optimised reaction conditions, α-fluoroenones **92** were generally afforded in good to excellent yields whilst the easy separation of the (*E*) and (*Z*) isomers upon silica gel column chromatography allowed for the isolation of the fluorinated products as diastereoisomerically-pure compounds. The propargyl acetate starting materials **85** were readily prepared in a one-pot procedure from widely-available stock chemicals and, consequently, this methodology represents a mild and operationally simple two-step route to these fluorinated building blocks.

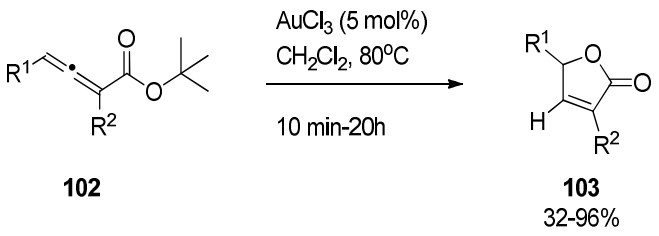
The (*E*)-diastereoselectivity of the process as well as control reactions with allene intermediates **88** suggest that the gold catalyst is not directly involved in the fluorination step in this process. Instead gold(I) most likely catalyses the initial [3,3]-sigmatropic rearrangement process delivering an allenyl acetate intermediate amenable to direct electrophilic fluorination with Selectfluor.

Chapter 3

Gold and F^+: Gold-Catalysed Oxidative Coupling I – Intramolecular Coupling

3.1 Introduction

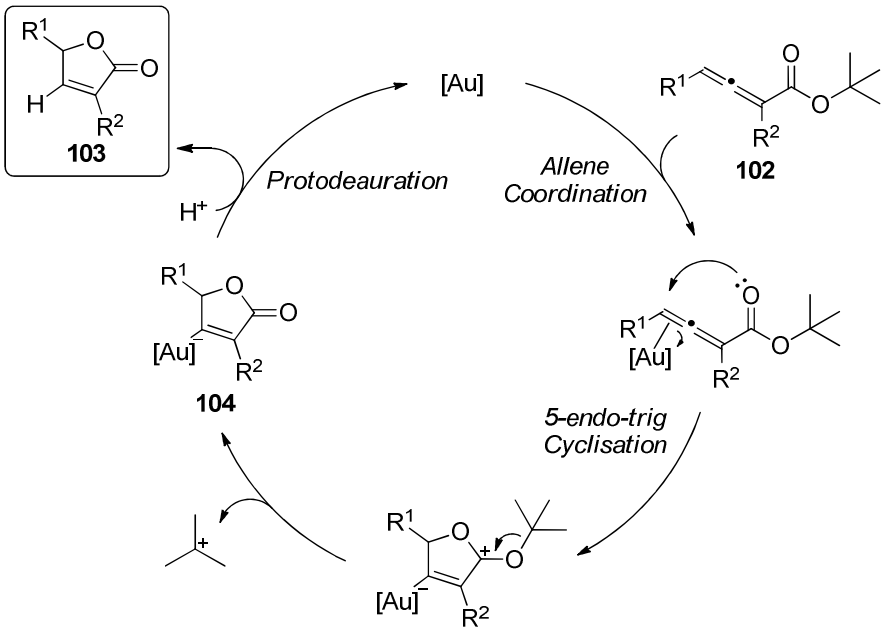
Although the gold(I)-catalysed rearrangement-fluorodeacetylation of propargyl acetates presented in Chapter 2 of this thesis was synthetically successful, mechanistic studies indicated that the fluorination step in this process was not itself mediated by gold.[89] Instead, the direct electrophilic fluorination of an allenyl acetate intermediate by Selectfluor (**82**) was found to be the most likely C-F bond-forming pathway, out-competing any potential gold-mediated fluorination. Consequently, in order to investigate the feasibility of fluorodeauration as a means of C-F bond-formation, our attention turned to alternative reaction systems not proceeding via intermediates susceptible to direct electrophilic fluorination in the presence of an "F^+" source. Following a survey of the literature, we identified the gold-catalysed 5-*endo*-trig cyclisation of *tert*-buyl allenoates **102** as a promising transformation for further study (Scheme 3.1). This allene hydrofunctionalisation process, which was first reported by Shin and co-workers in 2005,[100] delivers γ-butenolides **103** in generally high yields from the corresponding allenoates using $AuCl_3$ as catalyst.



102 **103** 32-96%

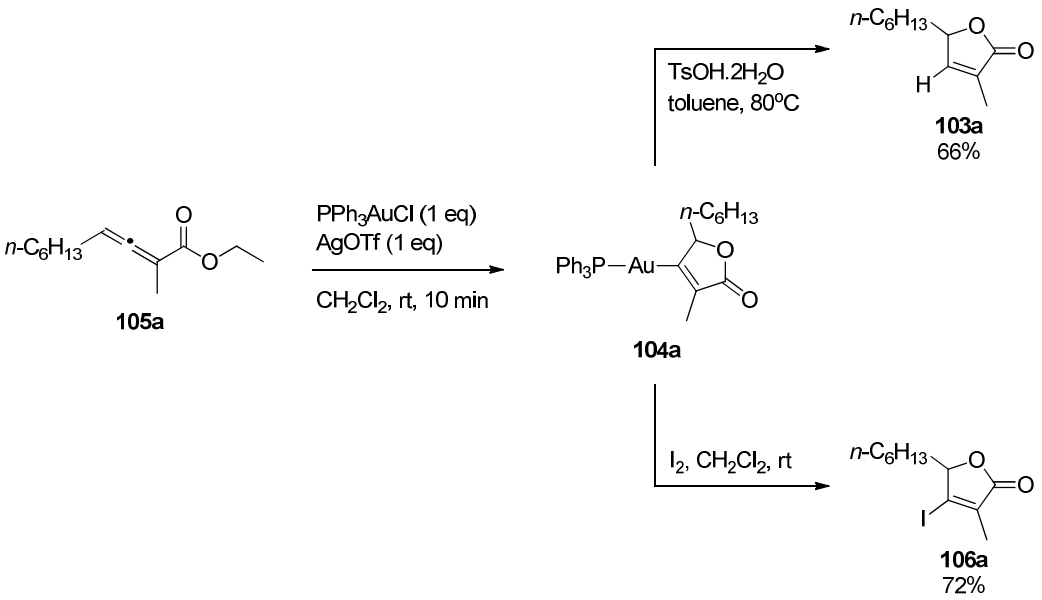
Scheme 3.1 Cyclisation of *tert*-Butyl Allenoates **102**.

A general mechanism for this process is shown in Scheme 3.2. In the first step, the π-Lewis acidic gold(III) coordinates the allene moiety in **102**, activating it towards intramolecular attack of the pendant ester oxygen. At this stage, loss of the *tert*-butyl cation delivers the (butenolide)gold complex **104**, which can then undergo protodeauration to afford the γ-butenolide product **103** and regenerate the gold catalyst.



Scheme 3.2 General Mechanism for the Cyclisation of *tert*-Butyl Allenoates.

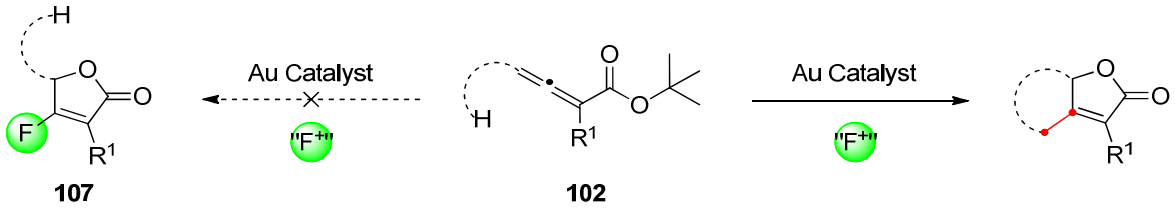
Support for a mechanism involving (butenolide)gold complexes of type **104** was provided by Hammond and co-workers in 2008.[101-102] Performing the related gold-mediated cyclisation of ethyl allenoates **105** in the presence of stoichiometric amounts of the gold(I) source PPh_3AuCl and AgOTf allowed for the isolation and full characterisation of (butenolide)gold complexes **104** featuring a $[PPh_3Au]$ moiety (Scheme 3.3). Treating these species with *para*-toluenesulfonic acid led smoothly to the corresponding protodeaurated γ-butenolides **103** whilst selective iododeauration to afford β-iodo-γ-butenolides **106** was observed in the presence of iodine.



Scheme 3.3 Isolation of a (Butenolide)gold(I) Complex **104**.

As part of our study into the effect of electrophilic fluorinating reagents on gold-catalysed nucleophilic addition reactions to alkynes and allenes, we sought to investigate whether the protodeauration step in this process could be rerouted in favour of fluorodeauration leading to β-fluoro-γ-butenolides **107** in the presence of an "F^+" source. Whilst the γ-butenolide motif features prominently in several natural products,[103] synthetic routes to fluorinated analogues of these compounds are scarce. In addition, the possibility of preparing the proposed vinylgold intermediate independently would enable any observed fluorodeauration step to be investigated directly.

In the following two chapters, the results of our investigation into the effect of electrophilic fluorinating reagents on the gold-catalysed 5-*endo*-trig cyclisation of *tert*-butyl allenoates **102** are presented. This study led to the discovery of an unexpected reactivity pathway not leading to fluorinated products (Scheme 3.4).



Scheme 3.4 Oxidative Coupling Reactions Performed in the Presence of "F^+" Sources.

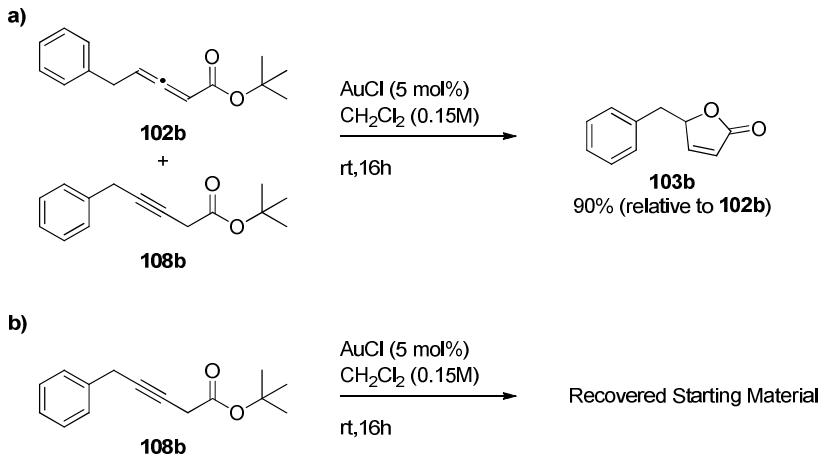
3.2 Cyclisation-Intramolecular Arylation of Benzyl-Substituted *tert*-Butyl Allenoates

Some of the work in this section was conducted in collaboration with Andrew Salisbury (Part II, University of Oxford, 2008)[104] and Dr. Arnaud Tessier (University of Oxford).[105]

3.2.1 Preliminary Studies

The benzyl-substituted *tert*-butyl allenoate **102b** was selected as the test substrate for use in the gold catalysis reactions and was prepared as a mixture with its alkyne isomer **108b** according to literature procedures from 3-phenylpropanoyl chloride and *tert*-butyl (triphenylphosphoranylidene)acetate.[100] Attempts to separate **102b** from **108b** or isomerise the alkyne proved unsuccessful with only partial enrichment possible upon very careful silica gel column chromatography (see Section 3.2.4 for more details). Reacting this mixture (**102b**:**108b** = 2.2:1) with AuCl (5 mol%) in dichloromethane (0.15M) for 16 hours led smoothly to the corresponding protodeaurated γ-butenolide **103b** in 90% yield relative to the allenoate (Scheme 3.5a).[m] The alkyne contaminant **108b**, which could be prepared independently in >95% yield according to the procedure of Fu *et al*,[106] was inert under the reaction conditions and was completely recovered after 24 hours at room temperature. (Scheme 3.5b).

[m] The amounts were calculated with respect to the combined amount of **102b** and alkyne **108b**.

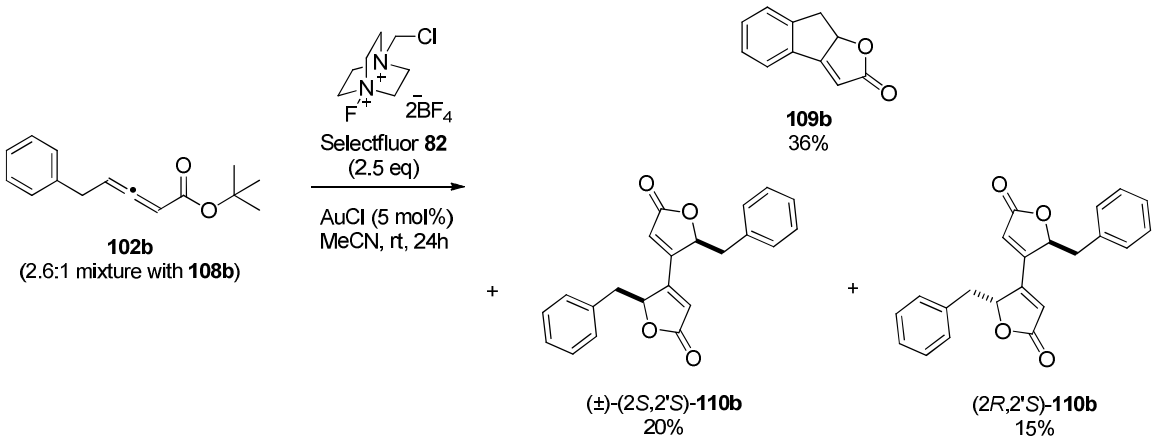


Scheme 3.5 Cyclisation of Benzyl-Substituted *tert*-Butyl Allenoate **102b**.

Having validated the conventional cyclisation-protodeauration reaction with this substrate, our attention turned to investigating the effect of electrophilic fluorinating reagents on the gold(I)-catalysed process. Thus, allenoate **102b** (as a mixture with its isomeric alkyne **108b**, **102b**:**108b** = 2.6:1) was reacted with AuCl (5 mol%) and 2.5 equivalents of Selectfluor (**82**) in acetonitrile (0.15M) at room temperature.[n] After 24 hours, complete consumption of the allenoate was observed and the reaction was filtered through Celite. ^{1}H NMR Analysis of the crude reaction mixture indicated that the protodeaurated γ-butenolide **103b** was not formed during the reaction whilst the ^{19}F NMR spectrum showed no peaks consistent with an organofluorine compound. Purification by column chromatography on silica gel led to the isolation of three compounds, formed in 36%, 20% and 15% yield, relative to the allenoate, respectively (Scheme 3.6). The major product, formed in 36% yield, was the tricyclic indeno[2,1-*b*]furanone **109b** whilst the separable bibutenolide diastereoisomers (±)-(2*S*,2'*S*)-**110b** and (2*R*,2'*S*)-**110b** were formed as minor side-products. Compounds **109b** and **110b** were fully characterised by NMR, IR and mass spectrometry with the identity of each species being unambiguously confirmed by X-ray crystallographic analysis (Figure 3.1). A

[n] The amounts were calculated with respect to the combined amount of **102b** and alkyne **108b**.

control experiment with the pure alkyne **108b** resulted in complete decomposition of the starting material with no formation of **109b** or **110b**.



Scheme 3.6 Cyclisation of Allenoate **102b** Performed in the Presence of Selectfluor.

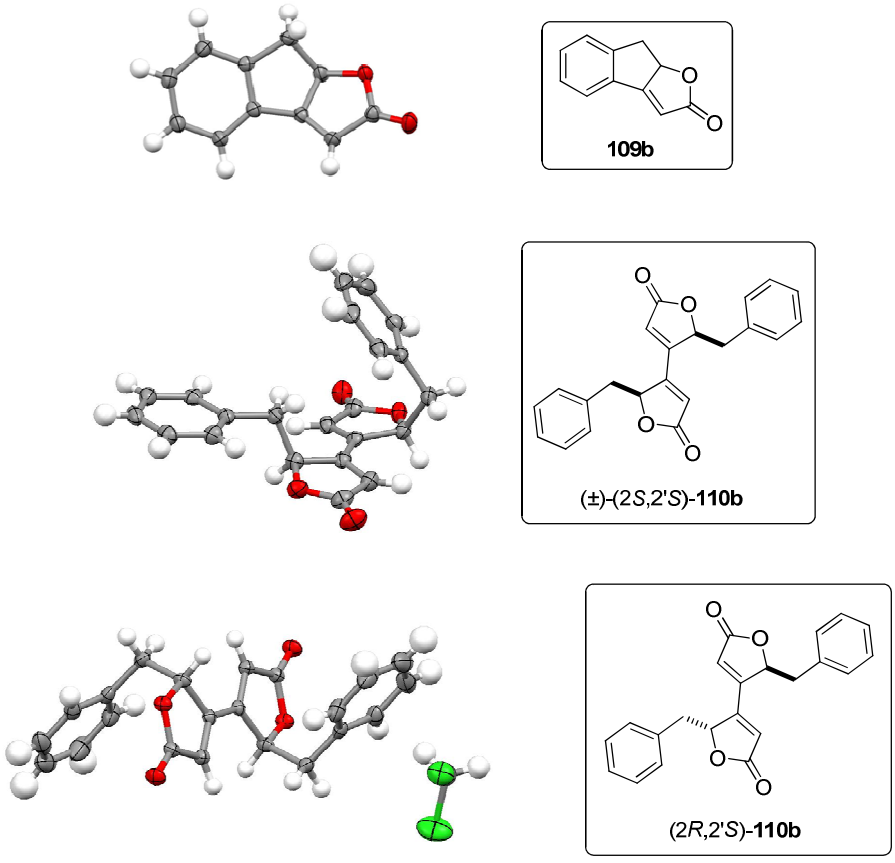
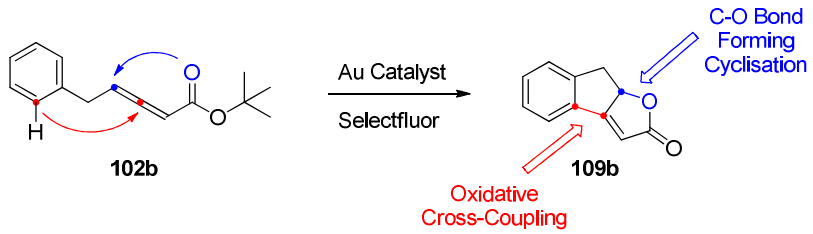


Figure 3.1 X-Ray Crystal Structures of Compounds **109b** and **110b**.

Compounds **109b** and **110b** both result from cascade processes where the initial 5-*endo*-trig allenoate cyclisation is followed by oxidative coupling. In the case of the diastereoisomeric

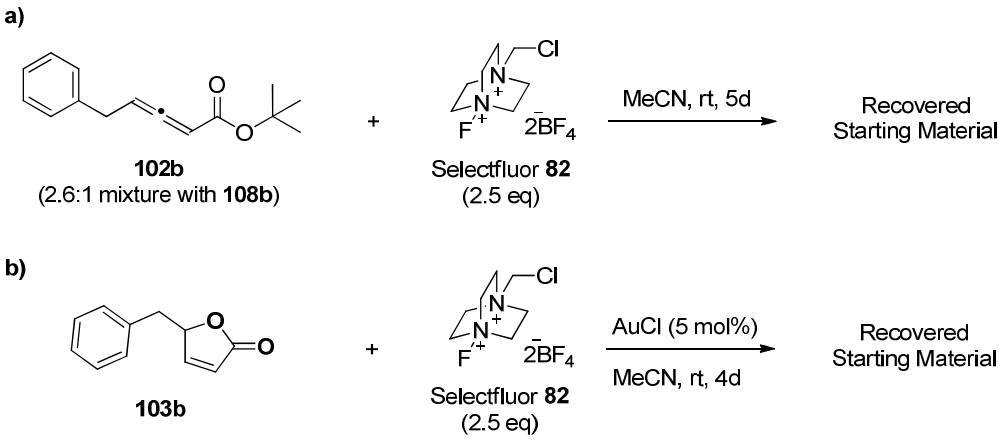
bibutenolides (±)-(2*S*,2'*S*)-**110b** and (2*R*,2'*S*)-**110b**, the conventional protodeauration pathway observed in the absence of Selectfluor is rerouted in favour of oxidative homodimerisation leading to the formation of a new carbon-carbon bond between two butenolide fragments.[o] The formation of the major indenofuranone product **109b** can be explained by an oxidative cross-coupling process where the carbon-oxygen bond-forming allenoate cyclisation is followed by arylation with the intramolecular benzyl group (Scheme 3.7). Compounds of type **109b** are surprisingly scarce in the literature although the structural core bears similarities with that of several cadinane sesquiterpenoids isolated from *Heritiera littoralis*.[107]



Scheme 3.7 Cascade Cyclisation-Oxidative Intramolecular Arylation of Allenoate **102b**.

In order to confirm that the formation of compounds **109b** and **110b** was not mediated by the electrophilic fluorinating reagent alone, allenoate **102b** was reacted under the same conditions in the absence of AuCl. This control experiment led to only recovered starting material after 5 days implying that the cascade cyclisation-oxidative coupling reaction requires the presence of both Selectfluor and gold in order to proceed (Scheme 3.8a). Furthermore, γ-butenolide **103b** was unreactive when treated with AuCl (5 mol%) and Selectfluor (2.5 eq) at room temperature for 4 days suggesting that the cyclisation-protodeauration product is not an intermediate in the oxidative coupling process (Scheme 3.8b).

[o] The cascade cyclisation-oxidative homodimerisation of allenoates is discussed more thoroughly Chapter 4 of this thesis.

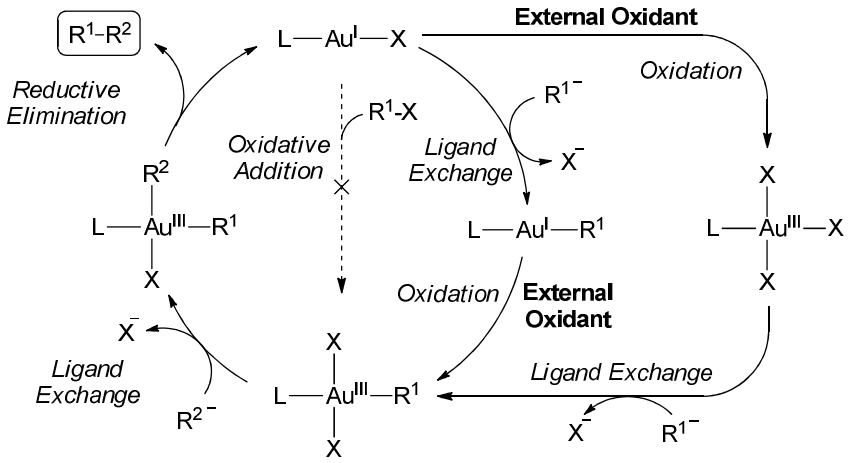


Scheme 3.8 a) Control Experiment Performed in the Absence of Gold. b) Control Experiment with γ-Butenolide **103b**.

The apparent ability of Selectfluor to promote gold-catalysed oxidative coupling reactions is potentially very significant. As previously discussed, M^n/M^{n+2} redox cycles of the type usually implicated in homo- and cross-coupling reactions mediated by other late transition metals are not generally accessible to gold catalysts by virtue of the comparatively high redox potential of the Au^I/Au^{III} couple (E^0 = +1.41V).[1] In particular, the oxidative addition of organic halides or equivalents commonly observed in palladium-catalysed coupling reactions is challenging for gold(I) and has only been unambiguously validated for electron-rich alkylgold(I) complexes with simple alkyl iodides.[108-113] Moreover, whilst gold(I)-catalysed analogues of the Suzuki-Miyaura and Sonogashira reactions have been reported with aryl iodides,[114-118] the involvement of Au^I/Au^{III} redox cycles in these processes has been the subject of debate.[119] A recent report by Corma and co-workers suggested that heterogeneous gold nanoparticles formed upon *in situ* decomposition of the gold(I) source could be responsible for the observed reactivity in these processes.[120]

Over the last few years, however, a handful of homo- and cross-coupling reactions mediated by gold catalysts have appeared in the literature.[121-124] The majority of these transformations are thought to proceed via Au^I/Au^{III} redox cycles of the type shown in

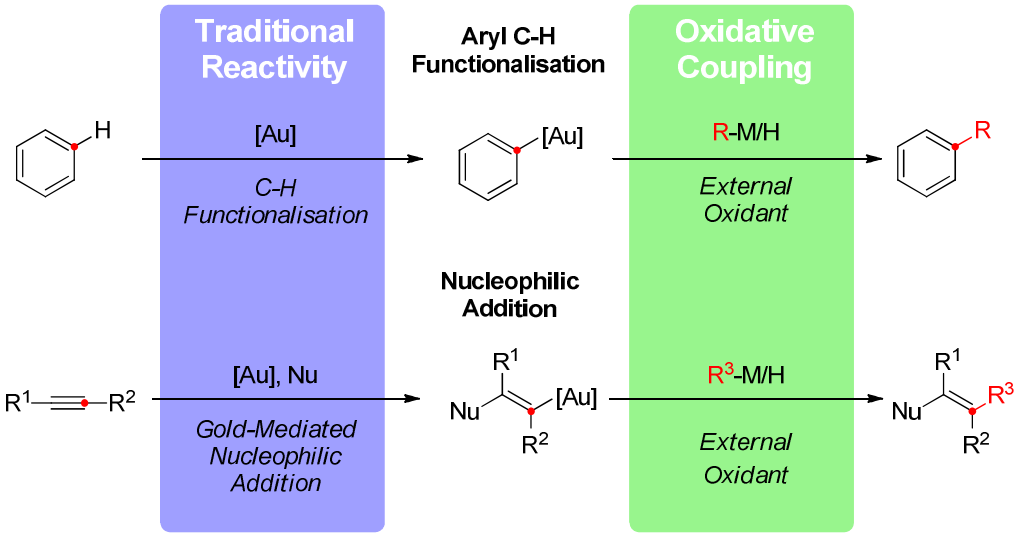
Scheme 3.9 where the key oxidation of gold(I) to gold(III) is performed by a strong external oxidant present in the reaction mixture.



Scheme 3.9 General Catalytic Cycle for Gold-Catalysed Oxidative Coupling Reactions.

In oxidative transformations of this type, each coupling partner coordinates to the high oxidation state metal via a redox-neutral "ligand exchange" process such as transmetalation to afford a doubly-organic substituted gold(III) complex amenable to reductive elimination. Whilst gold may react with organometallic reagents commonly used in palladium catalysed coupling reactions (eg. arylboronic acids), one or both coupling partners may instead coordinate to the metal following an organic transformation mediated by gold. In particular, the well-established ability of gold(III) to selectively react with aryl C-H bonds under mild conditions has been exploited in the development of gold-catalysed coupling reactions of non-activated arenes. Alternatively, oxidative homo- or cross-coupling can replace protodeauration as the last step in gold-catalysed nucleophilic addition reactions to carbon-carbon multiple bonds. Cascade reactions of this type lead to the formation of two new bonds across the alkyne, allene or alkene. The first bond is constructed upon nucleophilic addition mediated by gold acting in its traditional role as a soft π-Lewis acid whilst the second bond results from a Au^{I}/Au^{III} redox process. As such, this potentially powerful

methodology could allow for the preparation of a wide-range of synthetically appealing organic compounds in a time-efficient and step-economical manner (Scheme 3.10).



Scheme 3.10 Cascade C-H Functionalisation/Nucleophilic Addition-Oxidative Coupling Reactions.

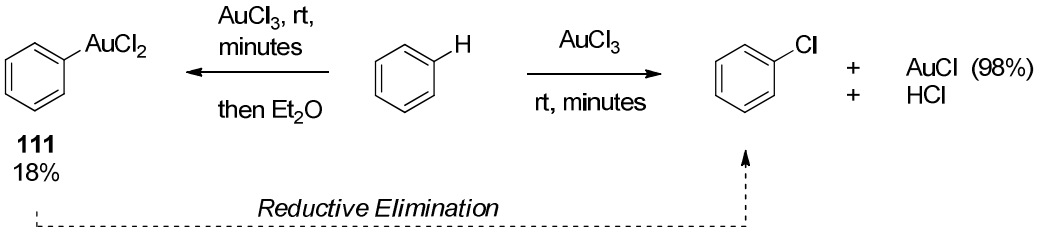
3.2.2 Literature Examples of Gold-Mediated Oxidative Coupling using Alternative External Oxidants

Building on seminal earlier work using stoichiometric gold(III), a number of gold-catalysed oxidative coupling reactions have been reported in the last few years using a range of external oxidants.[121-124] In this section, the development of these processes is discussed focusing on the mechanistic aspects of each transformation. In the first part, oxidative arylation processes involving the direct C-H bond functionalisation of non-activated arenes are presented. This is followed by a summary of gold-mediated oxidative coupling reactions where one or both coupling partners are derived from a nucleophilic addition to a C-C multiple bond.

3.2.2.1 Coupling Reactions Involving Aryl C-H Bond Functionalisation

The direct functionalisation of an aryl C-H bond by gold(III) was first reported in 1931 by Kharash and Isbell.[52] Reacting $AuCl_3$ with benzene at room temperature led, after a few minutes, to the formation of a red solution with the evolution of hydrogen chloride gas. Leaving the mixture for a few minutes longer resulted in the precipitation of yellow gold(I)

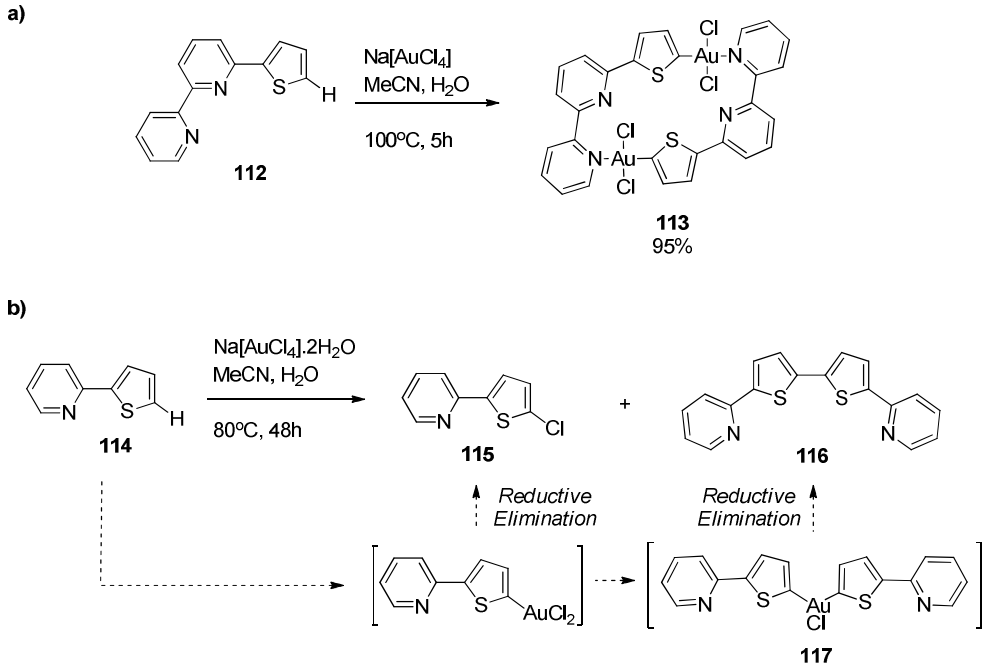
chloride, which was collected by filtration in 98% yield relative to $AuCl_3$. Analysis of the filtrate revealed the presence of the oxidative chlorination product, chlorobenzene (Scheme 3.11). The formation of this compound can be rationalised by a mechanism involving C-Cl bond-forming reductive elimination from the arylgold(III) complex **111**, generated upon Friedel-Crafts-type arylation of gold(III) by benzene. This species could be isolated in 18% yield upon quenching the reaction with diethyl ether prior to the precipitation of AuCl. The generation of arylgold(III) complexes directly from non-activated arenes is a remarkable transformation. Unlike many aryl C-H bond functionalisation processes mediated by other transition metals, this auration step occurs after just a few minutes at room temperature and does not require the presence of a directing group on the arene.[125] Notably, when the oxidative chlorination reaction was performed in the presence of chlorine gas, chlorobenzene could be produced using catalytic amounts of gold(III). In this process, Cl_2 could be acting as a stoichiometric external oxidant, converting the AuCl formed upon reductive elimination back to $AuCl_3$.



Scheme 3.11 Oxidative Chlorination of Benzene.

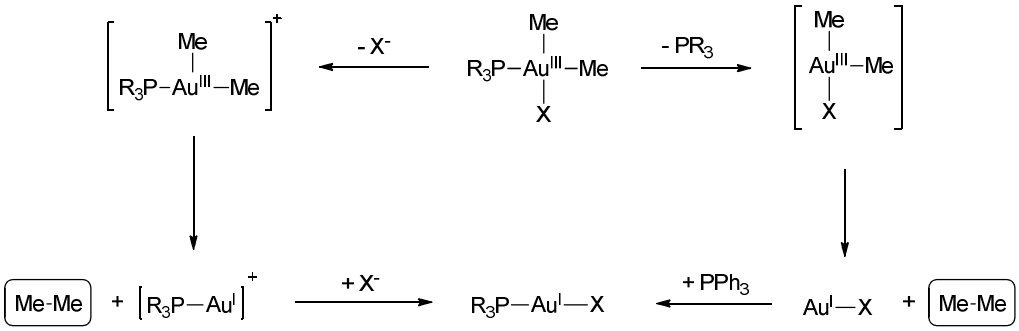
A similar aromatic auration was reported by Constable and co-workers upon heating the 6-(2''-thienyl)-2,2'-bipyridine ligand (Htbpy, **112**) with $Na[AuCl_4]$ in acetonitrile/water.[126-127] Selective C-H bond functionalisation at the 5'-position of the thiophene ring was observed leading to the dimeric complex **113** after 5 hours at 100ºC (Scheme 3.12a). Reacting the related 2-(2'-thienyl)pyridine ligand (Hthpy, **114**) under similar conditions led instead to the formation of a range of gold complexes and free ligands including Clthpy (**115**) and pttp

(**116**, Scheme 3.12b).[128] These compounds result from oxidative chlorination and homodimerisation at the 5'-position of Hthpy respectively. This latter C(sp^2)-C(sp^2) bond-forming pathway is thought to proceed via reductive elimination from a doubly-organic substituted gold(III) complex **117** formed either upon sequential C-H functionalisation of two Hthpy ligands or via transmetalation between gold complexes.



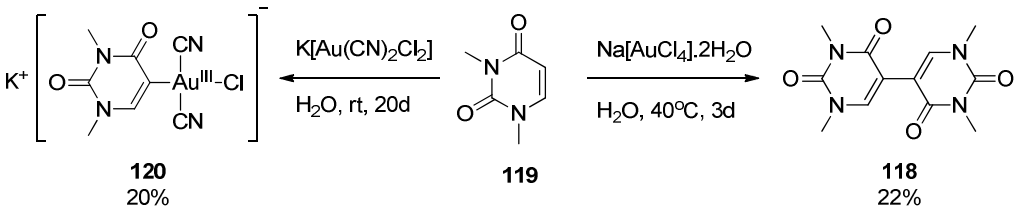
Scheme 3.12 a) Auration at the 5' Position of Htbpy (**112**). b) Oxidative Chlorination and Homodimerisation of Hthpy (**114**).

Carbon-carbon bond-forming reductive elimination from gold(III) complexes has been demonstrated by a number of research groups.[108, 112-113, 129-143] This elementary step is thought to proceed via a dissociative mechanism where one ligand around the metal is lost to afford a three-coordinate species prior to C-C bond-formation (Scheme 3.13).[133] For example, the release of ethane from dimethylgold(III) complexes of the form [PR_3AuMe_2X] (R = alkyl, aryl) occurs at a much faster rate with less strongly-coordinating phosphine ligands and counter-ions X. C-C bonds have also been formed between (sp^2)- and (sp)-hybridised carbons in this manner.



Scheme 3.13 Proposed Mechanism of Reductive Elimination from Diorganogold(III) Complexes.

The ability of gold(III) salts to homodimerise aromatic compounds was exploited by Lippert *et al* in 1999. The nucleobase dimer **118** was formed in 22% isolated yield upon treating 1,3-dimethyluracil **119** with one equivalent of $Na[AuCl_4].2H_2O$ in water at 40ºC (Scheme 3.14).[144] The intermediacy of a selectively aurated (5-uracilyl)gold(III) complex in this process was supported by the isolation of the related complex **120** when *trans*-$K[Au(CN)_2Cl_2]$ was used as the gold(III) source.[145] This species decomposed slowly over 3 months to afford the corresponding 5-cyano-nucleobase via $C(sp^2)$-C(sp) bond-forming reductive elimination.



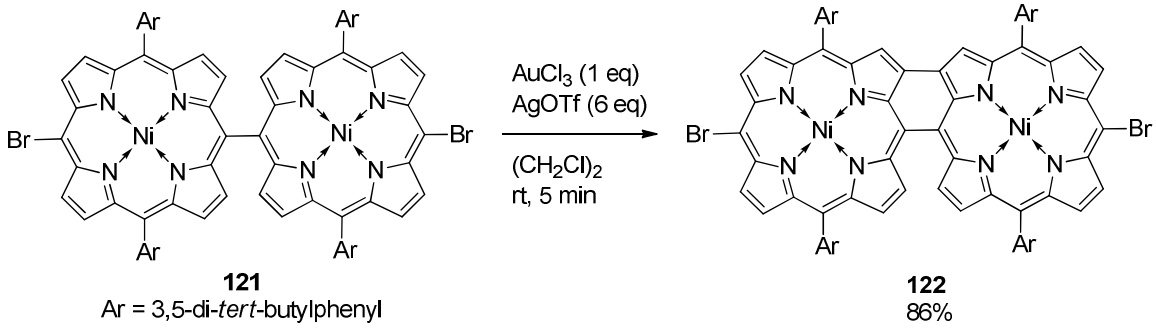
120
20%

119

118
22%

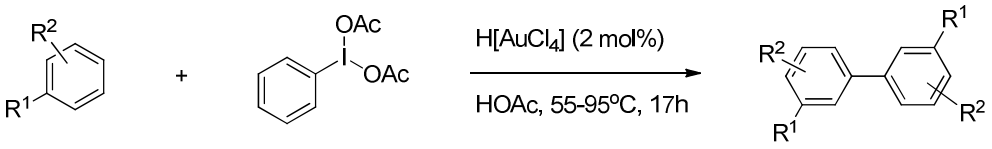
Scheme 3.14 Oxidative Homodimerisation of 1,3-Dimethyluracil **119**.

A second carbon-carbon bond was formed between the two porphyrin groups in nickel(II) complex **121** upon treatment with one equivalent of $AuCl_3$ and 6 equivalents of AgOTf (Scheme 3.15).[146] Reacting the product **122** with another equivalent of gold(III) resulted in the formation of a third linkage between the two macrocyclic units.



Scheme 3.15 Oxidative Homocoupling of two Porphyrin Units in Nickel(II) Complex **121**.

The first oxidative arene homodimerisation reaction performed in the presence of catalytic amounts of gold was reported by Tse and co-workers in 2008.[147] The key to catalytic turnover in this process was the use of $PhI(OAc)_2$ (PIDA) as a sacrificial external oxidant. Reacting non-activated benzene-derivatives **123** in the presence of the oxidant and 2 mol% of $H[AuCl_4]$ in acetic acid at 55-95ºC led to the corresponding biaryls **124** in generally moderate to good yields relative to PIDA (Scheme 3.16). The oxidative homocoupling of non-activated arenes represents an elegant alternative to the palladium-catalysed Suzuki-Miyaura reactions typically used to synthesise biaryls. Unlike the gold-catalysed reaction, these latter processes require the pre-activation of each aryl coupling partner as either an aryl halide or boronic acid prior to coupling. The $H[AuCl_4]$-catalysed homodimerisation reaction was successful with a range of arenes **123** bearing both electron-withdrawing and electron-donating substituents. Notably, aryl iodides and bromides reacted to form the corresponding biaryls with no loss of the halogen functionality. The regioselectivity of the coupling process is consistent with a mechanism involving arylgold(III) intermediates formed upon Friedel-Crafts-type attack of the arene on gold(III). Reductive elimination from a diarylgold(III) complex formed upon Friedel-Crafts auration of a second arene or transmetalation between arylgold complexes best explains the formation of the biaryl products **124**. The gold(I) formed during this process is then oxidised back to the catalytically active gold(III) by PIDA to complete the catalytic cycle.



123 excess

PIDA (1 eq)

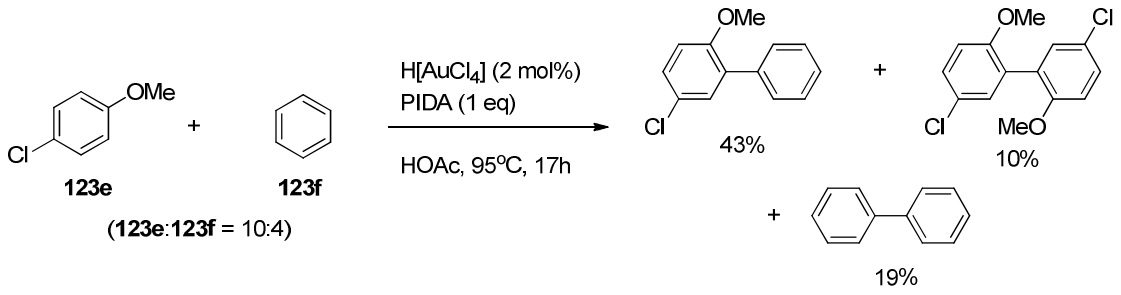
124

123a R^1 = Me, R^2 = *p*-Me
123b R^1 = CO_2Me, R^2 = *p*-Me
123c R^1 = Br, R^2 = *p*-OMe
123d R^1 = I, R^2 = *o*-OMe

124a 81% (GC yield)
124b 78%
124c 56%
124d 69% (+10% *para*-*ortho*)

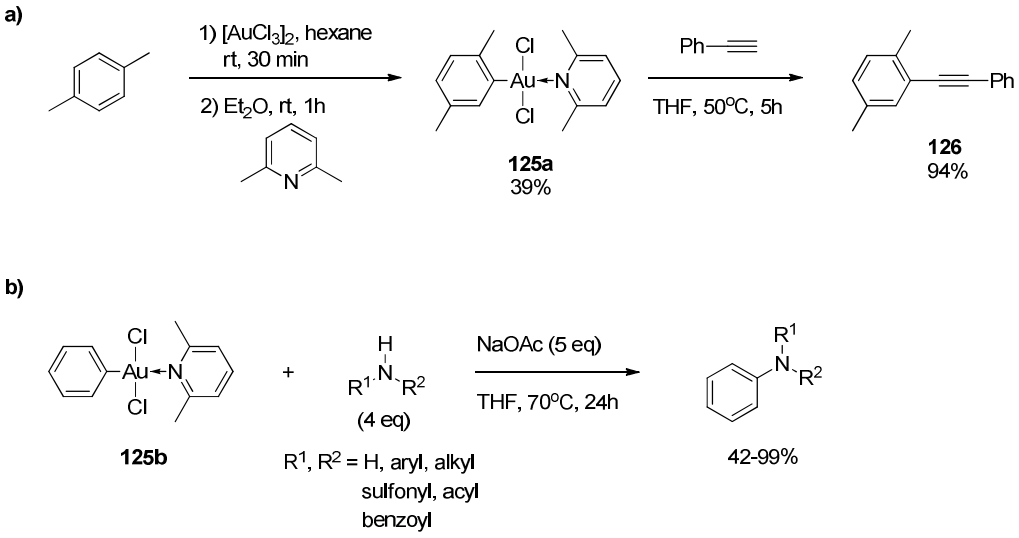
Scheme 3.16 Oxidative Homodimerisation of Non-Activated Arenes.

Extending this methodology to oxidative cross-coupling raises the additional challenge of controlling selectivity for the cross-coupled product over the homodimers of each coupling partner. Coupling methodologies involving an oxidative addition step have an inherent selectivity for the cross-coupled product by virtue of the different methods by which each coupling partner coordinates to the metal centre. Coupling can only occur after oxidative addition to afford a M^{n+2} species has occurred whilst a second such process from the high oxidation state complex is generally not possible. In the case of oxidative coupling reactions where the key oxidation of M^n to M^{n+2} in the cycle is performed by an external oxidant, both coupling partners coordinate to the metal via a redox-neutral "ligand exchange" process. As such, if the rates of "ligand exchange" of both fragments are not significantly different to each other at both coordination stages, homocoupling can occur via the same mechanism as cross-coupling without the requirement for intermolecular scrambling between M^{n+2} complexes. For example, reacting two separate arenes under the optimised $H[AuCl_4]$-catalysed coupling conditions described above led to mixtures of cross-coupled and homocoupled biaryls (Scheme 3.17).[148]



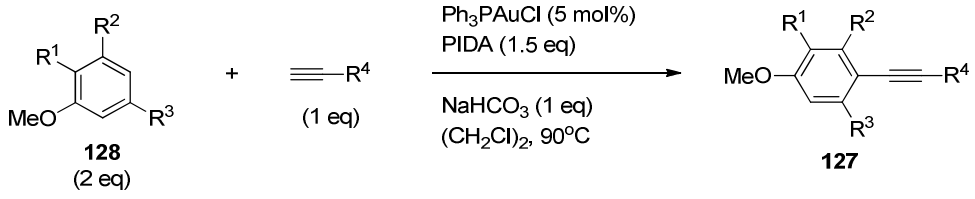
Scheme 3.17 Competing Homocoupling and Cross-Coupling of Non-Activated Arenes.

An oxidative cross-coupling reaction between terminal alkynes and stoichiometric arylgold(III) complexes was reported by Fuchita and co-workers in 2001.[149] Reacting *para*-xylene with gold(III) chloride in hexane at room temperature led to the isolable (*para*-xylyl)gold(III) species **125** in 39% yield upon addition of 2,6-lutidine. Treating this complex with phenylacetylene in tetrahydrofuran at 50ºC led to the corresponding diarylacetylene **126** in 94% yield after 5 hours (Scheme 3.18a). Recently, Limbach and co-workers reported the selective amination of arylgold(III) complexes of type **125** with a variety of primary and secondary amines (Scheme 3.18b).[150] The presence of sodium acetate as a basic additive was found to be essential for appreciable formation of the aniline products.



Scheme 3.18 a) Oxidative Alkynylation and b) Oxidative Amination of Arylgold(III) Complexes **125**.

In 2003, Reetz and co-workers attempted to develop a catalytic variant of the alkynylation process from non-activated arenes and alkynes.[151] However, after screening several strong oxidants, only styrene products resulting from redox-neutral alkyne hydroarylation could be isolated from the reaction mixtures. In 2010, de Haro and Nevado revisited this chemistry using PIDA as a stoichiometric external oxidant.[152] In the presence of this reagent, internal acetylene **127a** could be furnished in 81% yield from 1,3,5-trimethoxybenzene **128a** and methylpropiolate using just 5 mol% of the gold(I) catalyst PPh_3AuCl (Scheme 3.19). Notably, no products resulting from hydroarylation of the alkyne[151] or homodimerisation of the arene[147] or alkyne[116] were observed. The preparation of internal acetylenes **127** directly from non-activated arenes and terminal alkynes via C-H bond functionalisation of both components is a remarkable transformation. In contrast to the palladium-catalysed Sonogashira reaction, this alkynylation process does not require the pre-activation of the arene coupling partner whilst no copper co-catalyst is required to activate the alkyne. The scope of arene and alkyne coupling partners also complements that observed in the palladium-catalysed process. The combination of electron-rich arenes and electron-deficient alkynes led to the best cross-coupling yields whilst aromatic compounds without electron-donating groups and alkynes without ester or ketone substituents were generally unreactive.

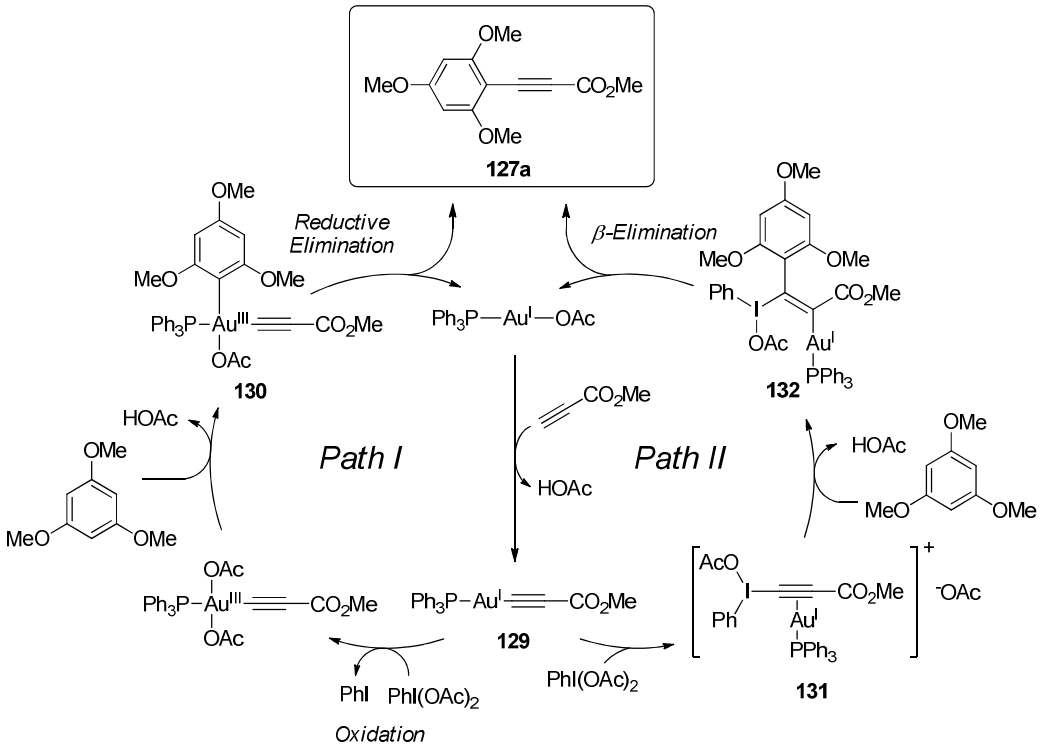


128a $R^2 = R^3 = OMe$, $R^4 = CO_2Me$ — **127a** 81%
128b $R^2 = R^3 = OMe$, $R^4 = Ph$ — **127b** 25%
128c $R^2 = OMe$, $R^4 = CO_2Me$ — **127c** 52%
128d $R^1 = Me$, $R^2 = R^3 = OMe$, $R^4 = CO_2Me$ — **127d** 60%

Scheme 3.19 Oxidative Alkynylation of Non-activated Arenes **128**.

Two plausible mechanisms for this transformation are shown in Scheme 3.20. Both pathways involve the initial formation of the alkynylgold(I) complex **129**, which was

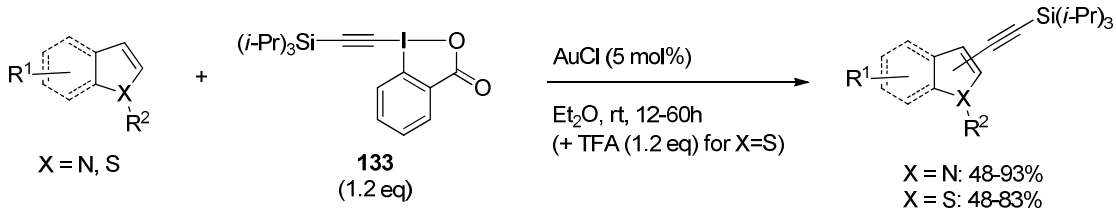
observed by ^{1}H and ^{31}P NMR spectroscopy. Oxidation of this species by PIDA followed by a Friedel-Crafts-type ligand exchange with the arene would lead to the gold(III) complex **130** bearing both the aryl and alkynyl coupling partners. Reductive elimination from this species would then deliver the cross-coupled product **127** and regenerate gold(I) (Scheme 3.20, Path I). Alternatively, the alkynyl ligand in complex **129** could instead act as nucleophile leading to the gold(I)-activated (alkynyl)iodonium salt **131**. Friedel-Crafts-type attack of the arene onto the alkyne would then lead to the vinylgold(I) complex **132** which could deliver the product upon β-elimination (Scheme 3.20, Path II). This latter pathway does not involve a Au^{I}/Au^{III} redox cycle.



Scheme 3.20 Plausible Mechanisms for the Oxidative Alkynylation of Non-activated Arenes **128**.

A similar gold(I)-catalysed alkynylation process of non-activated indoles, pyrroles and thiophenes was reported by Waser and co-workers (Scheme 3.21).[153-154] In these reactions, the alkynyl coupling partner is derived from the (alkynyl)iodonium salt **133**. As in the arene alkynylation reaction discussed above, a π-activation mechanism involving Friedel-Crafts

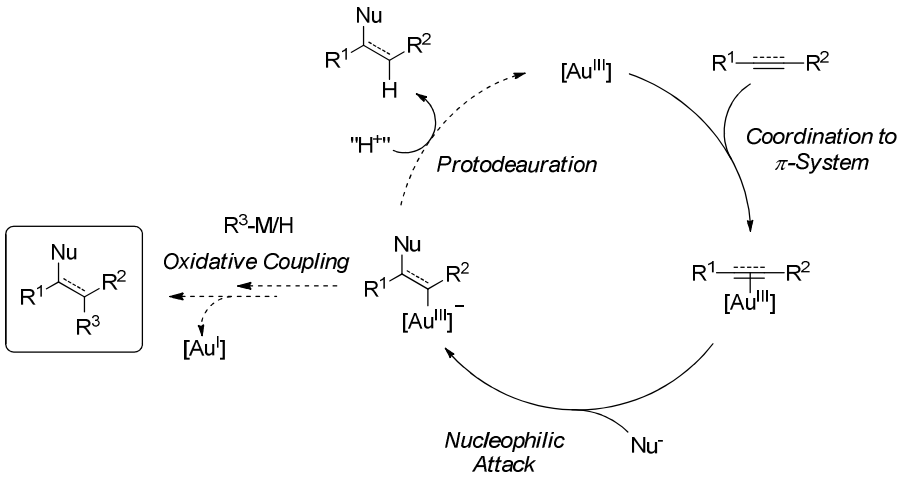
attack of the heteroarene onto compound **133** followed by β-elimination could explain the observed reactivity. Alternatively, the iodonium salt could react with gold(I) in an oxidative addition process leading to a Au^{I}/Au^{III} redox cycle. Further mechanistic studies are required to determine which pathway is operating.



Scheme 3.21 Oxidative Alkynylation of Heteroarenes with (Alkynyl)iodonium Salt **133**.

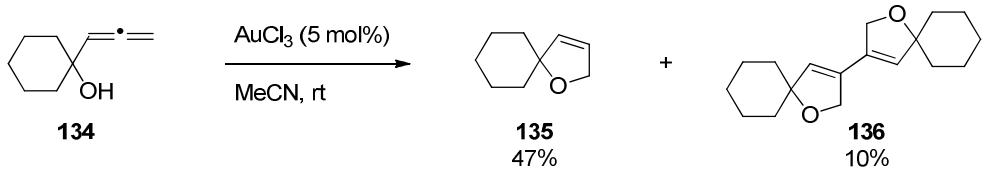
3.2.2.2 Cascade Nucleophilic Addition-Oxidative Coupling Reactions

In all the transformations discussed in the previous section, competitive protodeauration serves only to regenerate the arene starting materials and coupling can proceed without significant side-reactions. However, when one or both coupling partners are derived from a gold-mediated nucleophilic addition to a carbon-carbon multiple bond, reductive elimination from a suitably substituted organogold(III) complex must favourably compete with protodeauration in order for coupled products to be observed (Scheme 3.22).



Scheme 3.22 Competition between Protodeauration and Oxidative Coupling in Gold(III)-Mediated Nucleophilic Addition Reactions to C-C Multiple Bonds.

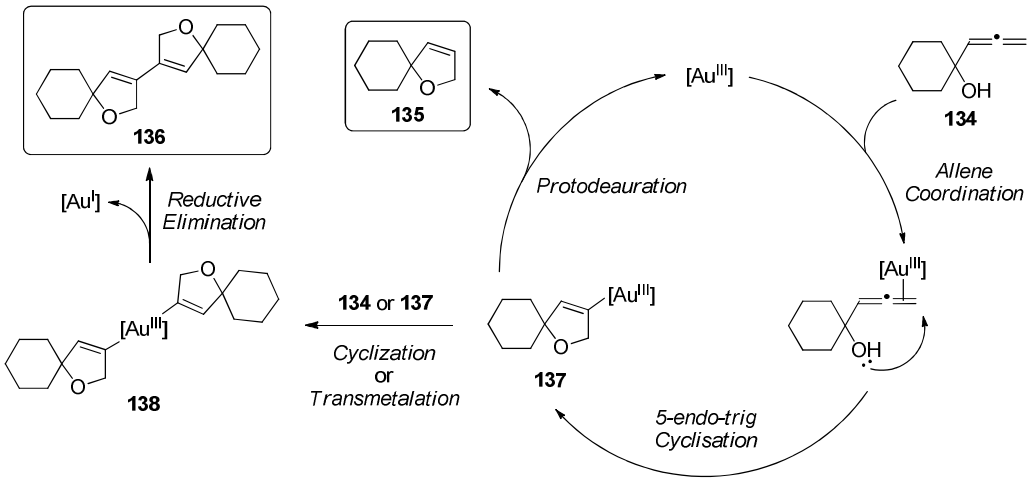
Competitive oxidative homocoupling during a gold(III)-catalysed nucleophilic addition reaction was first observed by Hashmi and co-workers in 2006.[155] Reacting the allenyl carbinol **134** with 5 mol% of $AuCl_3$ in acetonitrile at room temperature led to the formation of two products. Whilst the major species, formed in 47% yield, was the expected cyclisation-protodeauration product **135**, the dihydrofuran dimer **136** was also isolated in 10% yield (Scheme 3.23).



134 **135** 47% **136** 10%

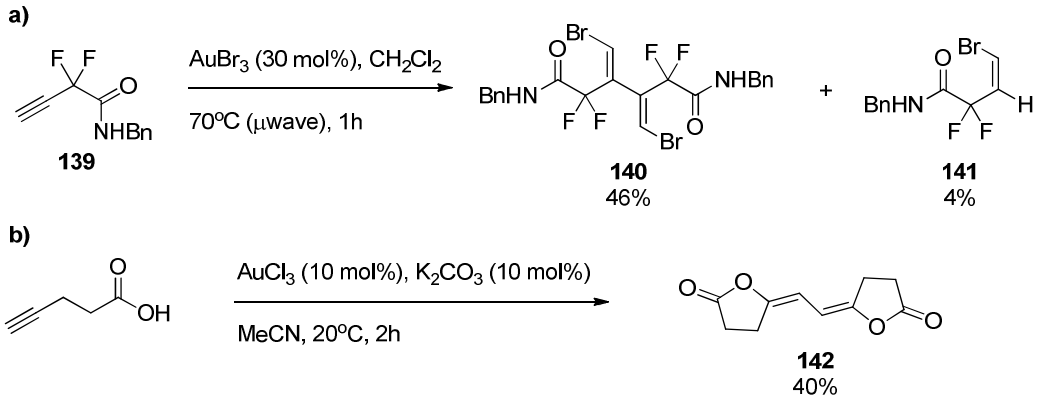
Scheme 3.23 Cyclisation-Homocoupling of Allenyl Carbinol **134**.

The formation of this compound can be rationalised by the mechanism shown in Scheme 3.24. After coordination of gold(III) to the allene, nucleophilic attack of the pendant alcohol would lead to the vinylgold(III) species **137**. Protodeauration at this stage delivers the major dihydrofuran product **135** and regenerates gold(III). Alternatively, complex **137** can react with another molecule of the allenyl carbinol **134** to afford the doubly organic substituted gold(III) species **138**. This intermediate could instead result from transmetalation of a dihhydrofuran motif between organogold complexes **137**. $C(sp^2)$-$C(sp^2)$ Bond-forming reductive elimination from **138** would then furnish the minor coupled product **136** and gold(I). The 10% yield of dimer **136** observed in this process is consistent with the above mechanism as one equivalent of the $AuCl_3$ catalyst is converted into gold(I) for every two molecules of allenyl carbinol converted into dimer **136**. Increasing the amount of gold(III) from 5 mol% to 15 mol% resulted in an increase in the yield of the coupled product to 23%.



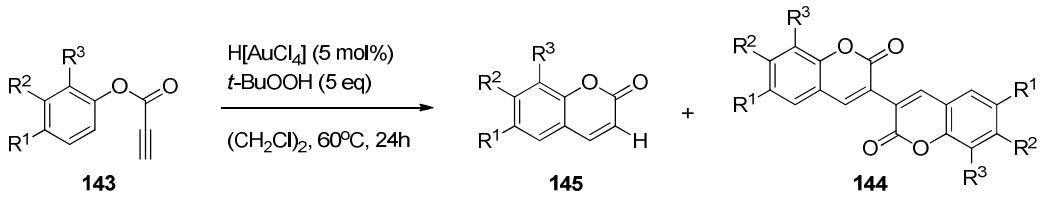
Scheme 3.24 Plausible Mechanism for the Cyclisation-Homodimerisation of Allenyl Carbinol **134**.

Related cascade nucleophilic addition-homodimerisation reactions performed in the presence of sub-stoichiometric gold(III) were reported by the groups of Fustero[156] and Pale.[157] Treating the *gem*-difluorinated propargylic amide **139** with gold(III) bromide (30 mol%, Scheme 3.25a) in dichloromethane led to the dibrominated diene **140** in 46% yield. Alkene **141,** resulting from a conventional hydrofunctionalisation process was isolated in only 4% yield from this reaction. Similarly, dienol lactone **142** could be synthesised directly from the corresponding alkynoic acid as the only isolable product via a cascade cyclisation-oxidative dimerisation process upon treatment with $AuCl_3$ (10 mol%, Scheme 3.25b). The observed yield of 40% for the homocoupling product **142** in this process is not consistent with a mechanism of the type shown in Scheme 3.24 based on a 10 mol% loading of gold(III).



Scheme 3.25 Oxidative Homocoupling Following Nucleophilic Addition to a) *Gem*-difluorinated Propargyl Amides and b) Alkynoic Acids.

The first cascade nucleophilic addition-oxidative homodimerisation reaction performed using catalytic amounts of gold was reported by Wegner and co-workers in 2008 upon reacting arylpropionic esters **143** with $H[AuCl_4]$ (5 mol%).[158] *tert*-Butyl hydroperoxide (5 eq) was identified as the external oxidant of choice for this transformation, delivering dicoumarins **144** in up to 67% isolated yield after 24 hours at 60ºC (Scheme 3.26). In this process, gold mediates the formation of two new carbon-carbon bonds across the alkyne. Under these conditions, however, the conventional hydrofunctionalisation process could not be completely suppressed and coumarins **145** were formed as minor side-products.

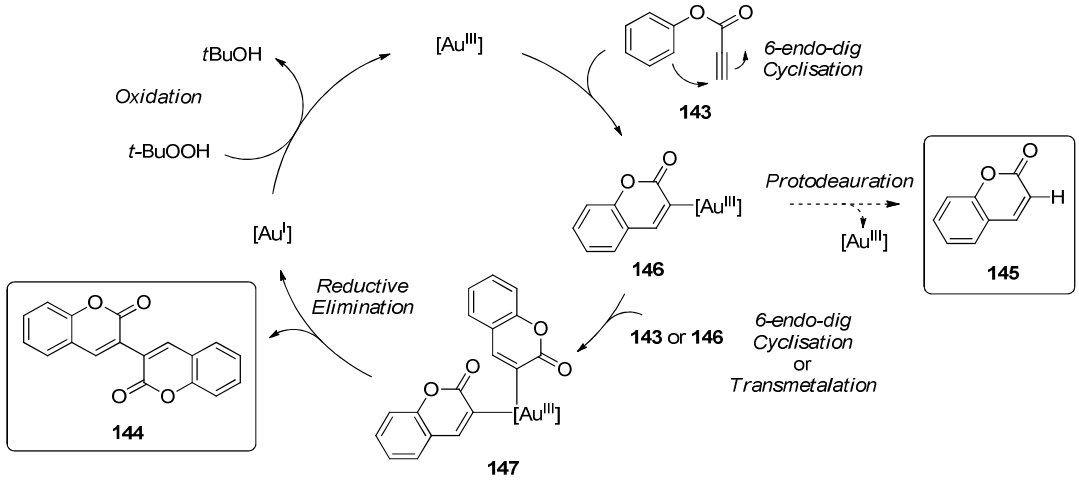


143a	R^1 = *t*Bu, R^2 = R^3 = H	**145a**	32%	**144a**	55%
143b	R^1 = R^2 = R^3 = H	**145b**	40%	**144b**	27%
143c	R^3 = Ph, R^1 = R^2 = H	**145c**	18%	**144c**	37%
143d	R^2 = OMe, R^1 = R^3 = H	**145d**	23%	**144d**	40%

Scheme 3.26 Cyclisation-Oxidative Homodimerisation of Arylpropionic Esters **143**.

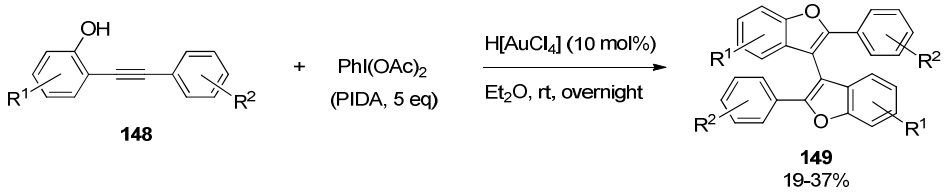
A feasible mechanism for this reaction is shown in Scheme 3.27. The vinylgold(III) intermediate **146** formed upon initial 6-*endo*-dig cyclisation of the starting material may undergo protodeauration to afford the coumarin product **145** and regenerate gold(III).

Alternatively this species could react with another molecule of **143** or undergo transmetalation with another (coumarin)gold complex to generate the doubly-substituted organogold(III) intermediate **147**. Reductive elimination from this species would then deliver the $C(sp^2)$-$C(sp^2)$ bonded product **144** and one equivalent of gold(I). The catalytic cycle is then completed by the re-oxidation of low valent metal back to gold(III) by *tert*-butyl hydroperoxide.



Scheme 3.27 Proposed Mechanism for the Cyclisation-Oxidative Homodimerisation of Arylpropionic Esters.

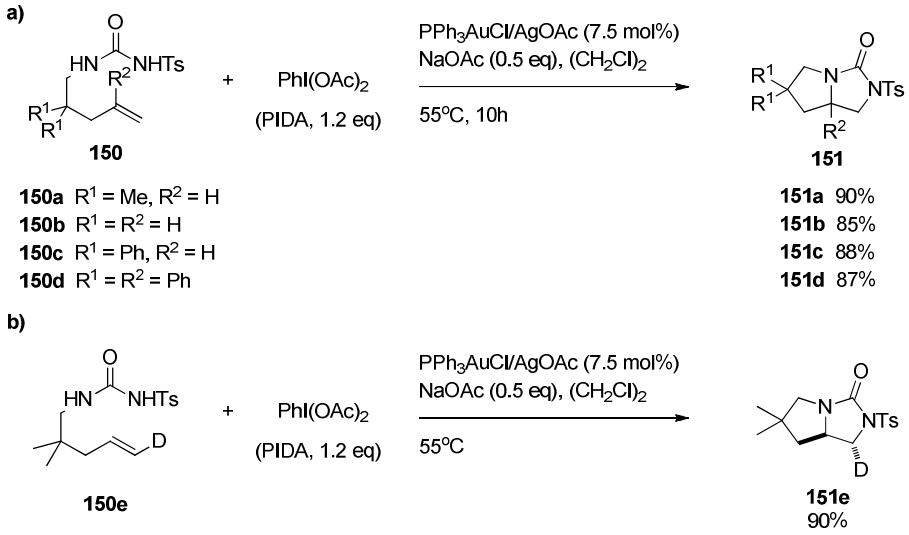
The same research group reported a similar cascade cyclisation-homodimerisation process upon reacting *ortho*-alkynylphenols **148** with $H[AuCl_4]$.[159] With these substrates, PIDA proved to be the most successful oxidant, delivering 3,3'-bis(arylbenzofurans) **149** in up to 37% yield (Scheme 3.28). The low efficiency of this process can be explained in part by competitive oxidation of the phenol starting materials by PIDA leading to quinone side-products.



Scheme 3.28 Cyclisation-Oxidative Homodimerisation of *ortho*-Alkynylphenols.

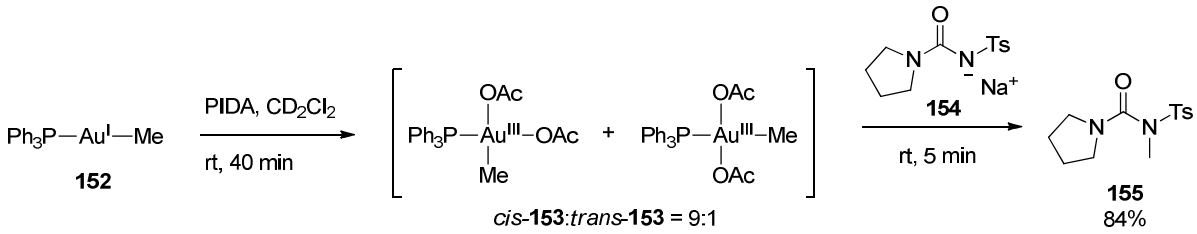
In 2009, Iglesias and Muñiz reported the oxidative diamination of alkenes **150** using a gold(I) catalyst in the presence of PIDA.[160] In this process, an initial gold-mediated 5-*exo*-trig cyclisation is followed by oxidative amination with the pendant urea nitrogen. Upon treatment with PPh_3AuCl/AgOAc (7.5 mol%) and 1.5 equivalents of the oxidant, alkenes **150** afforded a range of cyclic 1,2-diamines **151** in generally excellent yields (Scheme 3.29a). Notably, no products resulting either from protodeauration or from β-hydride elimination of an alkylgold intermediate were observed under these conditions. Whilst β-hydride elimination is commonly observed with other late transition metals, alkylgold complexes do not generally demetalate via this pathway. As a result, gold-catalysed homo- and cross-coupling reactions with sp^3-hybridised organic fragments can proceed in high selectivity without competition from elimination-derived side-reactions.

The oxidative diamination of the deuterated substrate **150e** led smoothly to the diastereoisomerically pure cyclic urea **151e** in 90% yield (Scheme 3.29b). The formation of this product is consistent with a mechanism involving an initial *trans*-aminoauration step followed by an oxidative coupling step proceeding with inversion of stereochemistry (eg. via S_N2-type nucleophilic substitution). Alternatively, an oxidative coupling process occurring with retention of stereochemistry (eg. via reductive elimination from gold(III)) could follow a *syn*-aminoauration step.



Scheme 3.29 Oxidative Diamination of Alkenes.

A reaction mechanism involving the *in situ* oxidation of an alkylgold(I) intermediate by PIDA was supported by NMR studies. Treating PPh_3AuMe **152** with PIDA in dichloromethane led to the formation of a 9:1 mixture of two organogold complexes within 40 minutes at room temperature. Although these species escaped isolation, analysis of the crude NMR spectra enabled their assignment as the *cis*- and *trans*-isomers of the gold(III) complex **153**. Subjecting this mixture to a nitrogen nucleophile in the form of urea **154** led to the formation of the expected *N*-methylated species **155** in 84% yield after 5 minutes (Scheme 3.30).



Scheme 3.30 *In situ* Oxidation of PPh_3AuMe by PIDA.

Although the field of gold-catalysed oxidative coupling remains in its infancy, the examples reported over the last couple of years demonstrate the potential of this methodology to

enable the rapid construction of complex organic molecules. In particular, the ability of gold(III) to selectively functionalise aryl C-H bonds under mild conditions has allowed for oxidative homocoupling and alkynylation reactions to be performed with non-activated aryl coupling partners. Organogold complexes formed upon nucleophilic attack onto a gold-activated carbon-carbon multiple bond may also engage in oxidative homocoupling and cross-coupling reactions. These processes combine the 'traditional' reactivity of gold as a π-Lewis acid with oxidative coupling in a single transformation involving the formation of two carbon-carbon or carbon-heteroatom bonds across the alkyne, allene or alkene.

The cyclisation-intramolecular arylation process observed upon treating the benzyl-substituted *tert*-butyl allenoate **102b** with catalytic AuCl in the presence of Selectfluor (**82**) (see Section 3.2.1) combines both of these activation pathways in a single coupling process. The butenolide coupling partner is delivered as a result of a 5-*endo*-trig cyclisation onto the gold-activated allene whilst the aryl coupling partner is derived from the intramolecular non-activated arene via direct C(sp^2)-H bond functionalisation (Figure 3.2).

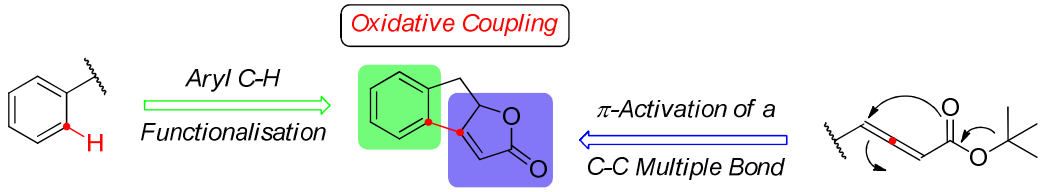
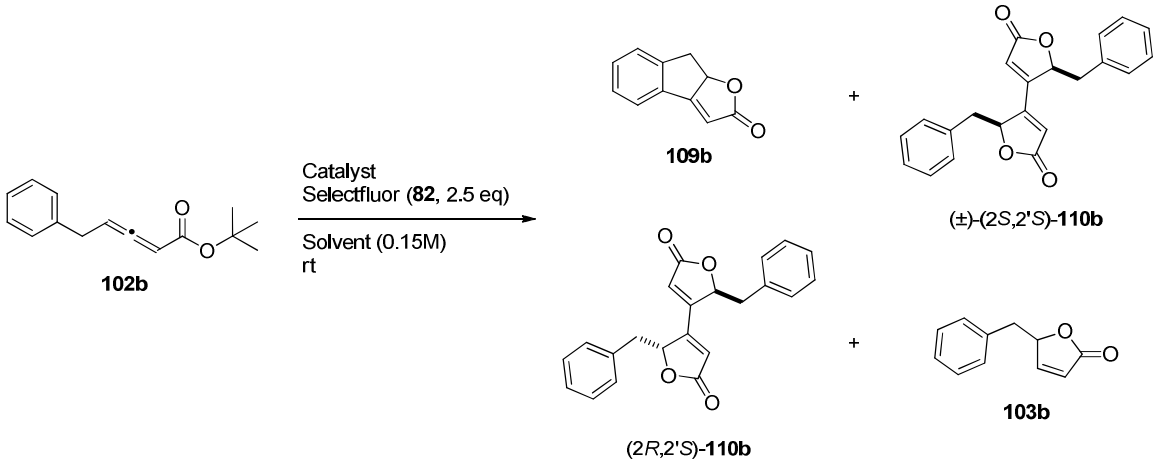


Figure 3.2 Oxidative Coupling between Coupling Partners Derived from Aryl C-H Functionalisation and Nucleophilic addition to an Allene.

In the remainder of this chapter, the development of this cascade cyclisation-intramolecular arylation reaction is discussed. Along with synthetic studies evaluating the scope and limitations of the gold-catalysed oxidative coupling reaction, this study also included an investigation of the reaction mechanism focused on determining the role of the electrophilic fluorinating reagent.

3.2.3 Optimisation of the Reaction Conditions

Having validated a gold-catalysed oxidative coupling process in the presence of Selectfluor, our attention turned to identifying optimised reaction conditions which maximised the yield of the indenofuranone products. Using the benzyl-substituted *tert*-butyl allenoate **102b** as a model substrate, the efficiency of a range of catalysts was tested (Table 3.1).



Entry	Catalyst, Solvent[a]	Time	Product Distribution (%)[b]				
			109b	(±)-(2*R*,2'*S*)-**110b**	(2*S*,2'*S*)-**110b**	**103b**	**102b**
1	AuCl (5 mol%), MeCN	24h	45 (36)	30 (20)	25 (15)	0 ---	0 ---
2	No Catalyst, MeCN	5d	0	0	0	0	100
3	$AuCl_3$ (5 mol%), MeCN	5d	26 (20)	38 (29)	36 (15)	0 ---	0 ---
4	$SIPrAuNTf_2$ (**156**, 5 mol%), MeCN	5d	0	0	0	0	100
5	$PtCl_2$ (5 mol%), MeCN	5d	0	0	0	0	100[c]
6	AgOTf (5 mol%), MeCN	5d	0	0	0	Trace	100[c]
7	CuOAc (5 mol%), MeCN	16h	0	0	0	0	0[c][d]
8	H_2SO_4 (5 mol%), MeCN	5d	0	0	0	0	100
9	$Pd(OAc)_2$ (5 mol%), MeCN	16h	0	45 (28)	55 (30)	0	0
10	AuCl (10 mol%), MeCN	24h	57 (56)	26 ---	17 ---	0	0

11	AuCl (10 mol%), MeCN, H_2O (10 eq)	24h	67 (58)	20 ---	13 ---	0	0
12	IPrAuCl (**158**, 10 mol%), AgOTf (12.5 mol%), MeCN, H_2O (10 eq)	5d	0	0	0	Trace	100
13	PPh_3AuNTf_2 (**2**, 10 mol%), MeCN, H_2O (10 eq)	4h	80 (62)	13 ---	7 ---	0 ---	0 ---

[a] Reaction conditions: allenoate **102b** (1 eq, as a mixture with alkyne **108b**, **102b**:**108b** = 3.3:1), Selectfluor (**82**, 2.5 eq), Solvent (0.15M), rt. The amounts were calculated with respect to the combined amount of **102b** and alkyne **108b**. [b] Product ratio based on **102b** as a percentage estimated by ^{1}H NMR on the crude reaction mixture. Isolated yields (relative to **102b**) are displayed in parentheses where appropriate. [c] Complex reaction mixture. [d] Complete decomposition of **102b** observed.

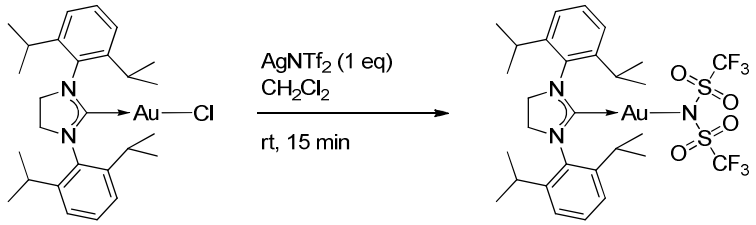
Table 3.1 Optimisation of the Catalyst.

In each reaction, the allenoate **102b** (as a mixture with its isomeric alkyne **108b**, **102b**:**108b** = 3.3:1) was treated with 5 mol% of the catalyst and Selectfluor (**82**, 2.5 eq) in acetonitrile at room temperature.[p] The mixture was monitored by thin layer chromatography and filtered through Celite upon complete consumption of the allenoate or after 5 days. The product distribution was then determined by ^{1}H NMR analysis of the crude reaction mixture whilst isolated yields were obtained where appropriate. For each reaction which led to isolable products, a control experiment with a pure sample of the alkyne impurity **108b** was performed. Compounds **109b**, **110b** or **103b** were formed in no case and consequently the isolated yields were calculated with respect to the amount of allenoate present. These values are displayed in parentheses in the table above.

In an initial experiment, the reaction was performed with gold(III) chloride (5 mol%) as catalyst. The oxidative coupling products **109b** and **110b** were delivered as the only isolable species under these conditions with no products resulting from cyclisation-protodeauration (**103b**) or cyclisation-fluorodeauration (**107b**) detectable by NMR or mass spectrometry (Table 3.1, Entry 3). In comparison to the AuCl-catalysed process (Table 3.1, Entry 1), however, a lower selectivity for the intramolecular cross-coupled product **109b** was

[p] The amounts were calculated with respect to the combined amount of **102b** and alkyne **108b**.

observed. Whilst ^{1}H NMR analysis of the crude reaction mixture indicated a **109b**:**110b** ratio of 45:65 when the gold(I) salt was employed as catalyst, this ratio decreased to 26:74 in the presence of the gold(III) species. The *N*-heterocyclic carbene-stabilised gold(I) source SIPrAuNTf$_2$ (**156**) was not a suitable catalyst for the cascade cyclisation-oxidative coupling process. This complex, which was prepared in 90% yield from the corresponding chloride SIPrAuCl (**1**, Scheme 3.31),[161] afforded no cyclised products after 5 days at room temperature with only recovered starting material being detected by crude ^{1}H NMR (Table 3.1, Entry 4).

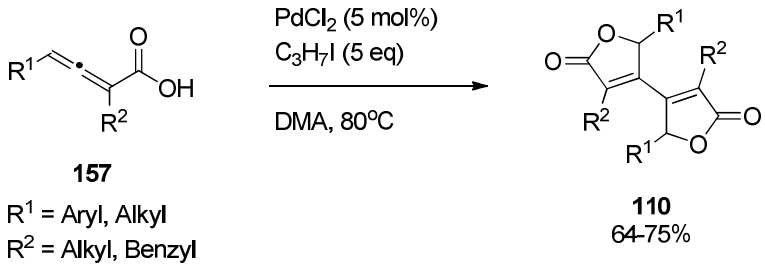


1 **156** 90%

Scheme 3.31 Preparation of SIPrAuNTf$_2$ (**156**).

Sources of platinum(II), silver(I) and copper(I) were similarly unsuitable catalysts for the cascade cyclisation-oxidative coupling reaction. With $PtCl_2$ (5 mol%), only recovered starting material could be detected after 5 days at room temperature with some decomposition of the allenoate observed (Table 3.1, Entry 5). A trace amount of the protodeaurated product **103b** was afforded as the only cyclised compound when AgOTf (5 mol%) was employed as catalyst whilst complete decomposition of the allenoate was observed with CuOAc (5 mol%, Table 3.1, Entries 6-7). The Brønsted acid H_2SO_4 (5 mol%) led to recovered starting material with no cyclisation of the allenoate observed after 5 days at room temperature (Table 3.1, Entry 8). In contrast to these catalysts, the palladium(II) source $Pd(OAc)_2$ was more successful in mediating the allenoate cyclisation process. Treating allenoate **102b** with 5 mol% of this salt in the presence of Selectfluor led smoothly

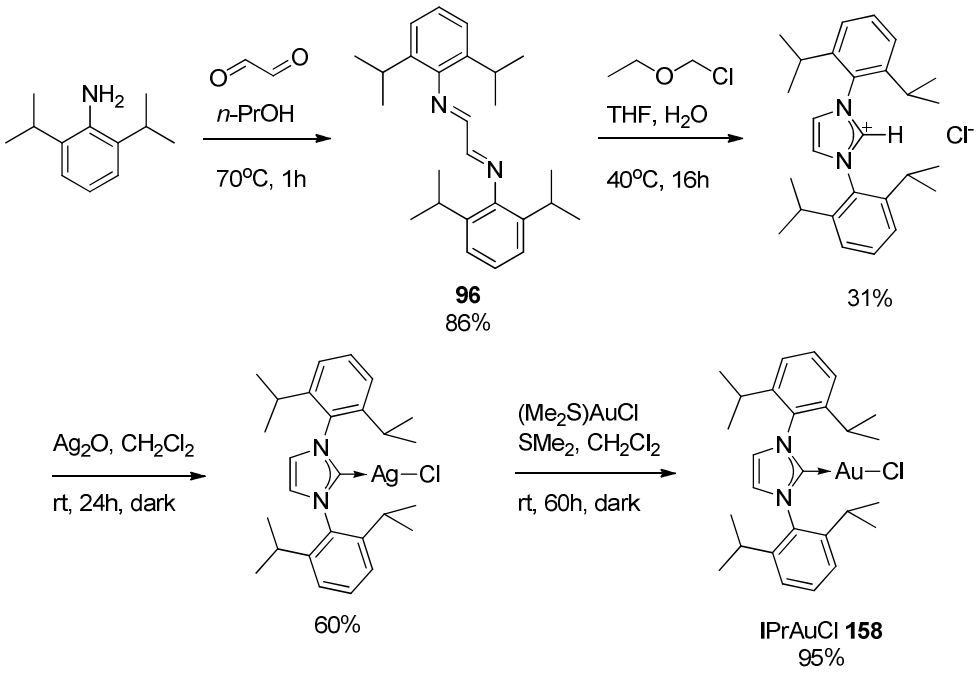
to the bibutenolides (±)-(2*S*,2'*S*)-**110b** and (2*R*,2'*S*)-**110b** in a combined isolated yield of 58% after 16 hours at room temperature (Table 3.1, Entry 9). However, the desired cross-coupled indenofuranone product **109b** was not observed under these conditions. The palladium(II)-catalysed cyclisation-oxidative homodimerisation of allenic acids **157** under aerobic conditions to form bibutenolides **110** was previously reported by Ma and Yu in 2003 (Scheme 3.32).[162-164]



Scheme 3.32 Palladium(II)-Catalysed Cyclisation-Oxidative Homodimerisation of Allenic Acids.

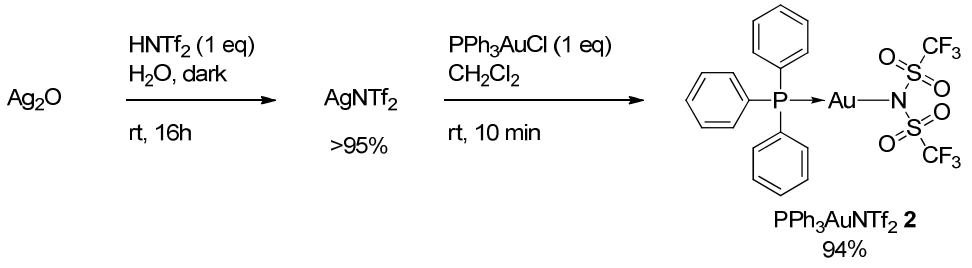
Having identified a gold(I) salt as the optimum catalyst for the preparation of the tricyclic product **109b**, we then evaluated the effect of increasing the catalyst loading on the reaction efficiency. Performing the allenoate cyclisation reaction with 10 mol% of AuCl in the presence of 2.5 equivalents of Selectfluor led to a greater selectivity for the cross-coupled product. The indenofuranone **109b** was delivered in 56% isolated yield under these conditions from a crude **109b**:**110b** ratio of 57:43 (Table 3.1, Entry 10). The selectivity for the intramolecular arylation product was further increased to 67:33 (**109b**:**110b**, isolated yield of **109b** = 58%) when 10 equivalents of water were added to the reaction mixture (Table 3.1, Entry 11). At this stage, alternative sources of gold(I) were evaluated as catalysts in the cyclisation-oxidative arylation process. Performing the reaction with the *N*-heterocyclic carbene containing species IPrAuCl (**158**, 10 mol%) along with AgOTf (12.5 mol%) did not lead to **109b** or **110b** after 5 days at room temperature (Table 3.1, Entry 11).

Complex **158** was prepared in 3 steps from the 1,2-diimine **96** (see Section 2.3) according to the procedures of Arduengo[90] and Nolan (Scheme 3.33).[165-166]



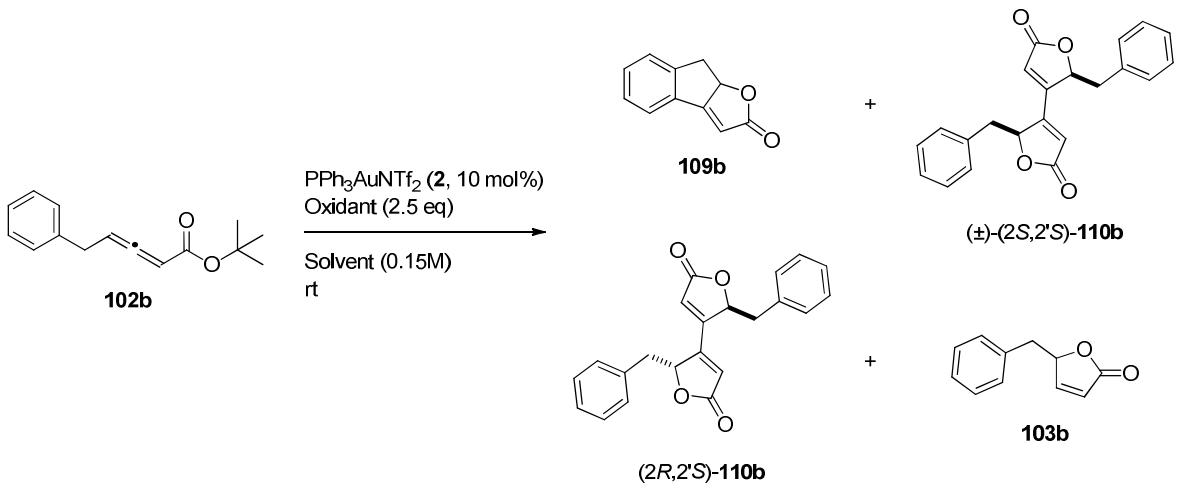
Scheme 3.33 Preparation of IPrAuCl (**158**).

The highest yield of the cross-coupled product **109b** was obtained with the phosphine-stabilised gold(I) catalyst PPh_3AuNTf_2 (**2**). This compound was prepared in one step from the commercially available chloride PPh_3AuCl via counter-ion exchange with $AgNTf_2$ according to the procedure of Gagosz (Scheme 3.34).[167] Treating allenoate **102b** with 10 mol% of this catalyst and 2.5 equivalents of Selectfluor in acetonitrile (0.15M) and water (10 eq) led smoothly to the cyclisation-oxidative coupling products **109b** and **110b** in a crude ratio of 80:20 (isolated yield of **109b** = 62%) after just 4 hours at room temperature.



Scheme 3.34 Preparation of PPh_3AuNTf_2 (**2**).

With PPh_3AuNTf_2 (**2**) identified as the catalyst of choice for this transformation, we sought to investigate the effect of a range of external oxidants on the reaction efficiency (Table 3.2).



Entry	Oxidant, Solvent[a]	Time	Product Distribution (%)[b]				
			109b	(±)-(2*R*,2'*S*)-**110b**	(2*S*,2'*S*)-**110b**	**103b**	**102b**
1	NFSI,[c] MeCN, H_2O (10 eq)	72h	38 (20)	40 (33)	22 (12)	0 ---	0 ---
2	NFSI,[c] CH_2Cl_2	16h	0 ---	0 ---	0 ---	100 (57)	0 ---
3	**100**,[d] MeCN, H_2O (10 eq)	5d	0	0	0	Trace	100[e]
4	*t*-BuOOH, MeCN, H_2O (10 eq)	6d	0	0	0	50	50
5	$PhI(OAc)_2$, MeCN, H_2O (10 eq)	48h	0 ---	52 (9)	48 (14)	0 ---	0[e] ---
6	Ph_2SO, MeCN, H_2O (10 eq)	6d	0	0	0	69	31
7	Oxone,[f] MeCN, H_2O (10 eq)	6d	12 (10)	25 (11)	63 (35)	Trace ---	0 ---

[a] Reaction conditions: allenoate **102b** (1 eq, as a mixture with alkyne **108b**, **102b**:**108b** = 3.3:1), PPh_3AuNTf_2 (10 mol%), Oxidant (2.5 eq), Solvent (0.15M), rt. The amounts were calculated with respect to the combined amount of **102b** and alkyne **108b**. [b] Product ratio based on **102b** as a percentage estimated by ^1H NMR on the crude reaction mixture. Isolated yields (relative to **102b**) are displayed in parentheses where appropriate. [c] NFSI = *N*-Fluorobenzenesulfonimide. [d] **100** = 1-Fluoro-2,4,6-trimethylpyridinium tetrafluoroborate. [e] Complex reaction mixture. [f] Oxone = $KHSO_5.½KHSO_4.½K_2SO_4$.

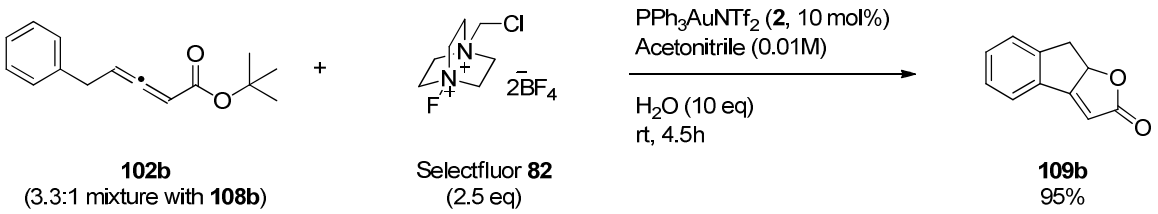
Table 3.2 Optimisation of the External Oxidant.

As a first experiment, the allenoate cyclisation process was performed in the presence of the electrophilic fluorinating reagent *N*-fluorobenzenesulfonimide (NFSI, 2.5 eq) in place of Selectfluor. Whilst this reaction delivered the oxidative coupling products **109b** and **110b** as the only isolable species, a lower selectivity for the desired indenofuranone was observed. Under these conditions, the tricyclic product **109b** was delivered in 20% isolated yield from a crude **109b**:**110b** ratio of 38:62 (Table 3.2, Entry 1). The cyclisation-oxidative coupling process was also considerably slower when NFSI was employed instead of Selectfluor with complete consumption of the allenoate only observed after 72 hours at room temperature. Interestingly, when the reaction was performed under the same conditions but with dichloromethane (0.15M) as solvent, complete conversion of the allenoate into the cyclisation-protodeauration product **103b** (isolated yield = 57%) was observed with no formation of **109b** or **110b** (Table 3.2, Entry 2). The collidinium-derived electrophilic fluorinating reagent 1-fluoro-2,4,6-trimethylpyridinium tetrafluoroborate (**100**) was not compatible with the allenoate cyclisation process. The reaction with this compound in acetonitrile (0.15M) and water (10 eq) led to mostly recovered starting material after 5 days with only a trace amount of the protodeaurated product **103b** detected by crude ^{1}H NMR (Table 3.2, Entry 3).

At this stage, external two-electron oxidants employed in previously reported gold-catalysed oxidative coupling reactions were tested (see Section 3.2.2). Treating allenoate **102b** with PPh_3AuNTf_2 (10 mol%) and 2.5 equivalents of *tert*-butyl hydroperoxide in acetonitrile (0.15M) and water (10 eq) did not lead to coupled products. Instead, slow conversion of the allenoate into the protodeaurated γ-butenolide **103b** was observed under these conditions (Table 3.2, Entry 4). The hypervalent iodine reagent $PhI(OAc)_2$ (PIDA), which has been previously employed in gold-mediated homo- and cross-coupling reactions involving aryl C-H functionalisation, was more successful in promoting oxidative coupling. In the

presence of 2.5 equivalents of this compound, the bibutenolides **110b** were produced in 23% isolated yield from allenoate **102b** after 48 hours at room temperature (Table 3.2, Entry 5). However, the indenofuranone **109b** was not formed under these conditions and significant decomposition of the allenoate starting material was observed. Performing the allenoate cyclisation reaction in the presence of the sulfoxide oxidant Ph_2SO (2.5 eq) resulted in no formation of the homo- or cross-coupled products. The cyclisation-protodeauration product **103b** was afforded as the major species from this reaction after 6 days at room temperature (Table 3.2, Entry 6). Indenofuranone **109b** was formed as a minor product in 10% isolated yield upon performing the PPh_3AuNTf_2-catalysed reaction in the presence of the strong oxidising agent Oxone ($KHSO_5.½KHSO_4.½K_2SO_4$, 2.5 eq, Table 3.2, Entry 7). The diastereoisomeric bibutenolides **110b** were afforded as the major products of this reaction in 46% combined yield whilst a trace amount of the protodeaurated γ-butenolide **103b** was detected by ^{1}H NMR.

With the (phosphine)gold(I) complex PPh_3AuNTf_2 (**2**) and the electrophilic fluorinating reagent Selectfluor (**82**) identified as the optimum catalyst and external oxidant combination for the allenoate cyclisation-intramolecular arylation process, our attention turned to optimising the other reaction parameters. In an attempt to encourage the formation of the intramolecular, cross-coupled product **109b** over the intermolecular homodimers **110b**, the reaction was performed at the lower solvent concentration of 0.01M. Under these conditions, complete conversion of the allenoate **102b** to the tricyclic indenofuranone **109b** was observed with only trace amounts of the diastereoisomeric bibutenolides **110b** being detected by crude ^{1}H NMR. Compound **109b** was isolated in 95% yield relative to the allenoate after 4 hours at room temperature from this reaction (Scheme 3.34). A control experiment with the pure alkyne impurity **108b** resulted in complete decomposition of the starting material with no formation of **109b**.

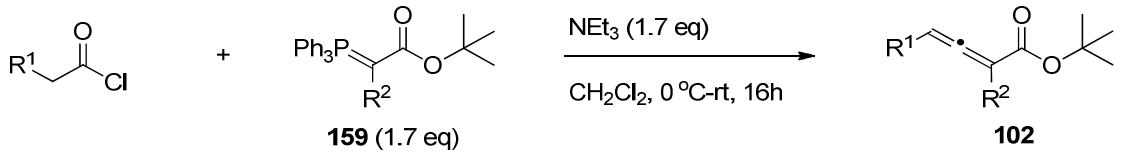


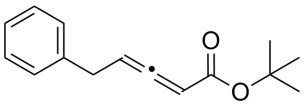
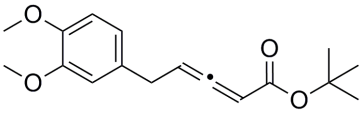
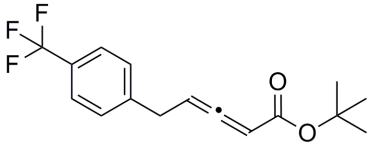
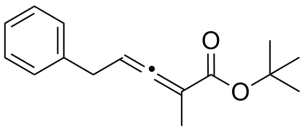
Scheme 3.34 Cyclisation-Intramolecular Arylation of Allenoate **102b** with PPh_3AuNTf_2 and Selectfluor.

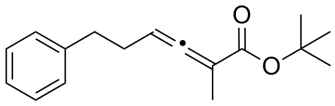
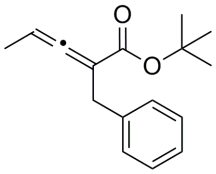
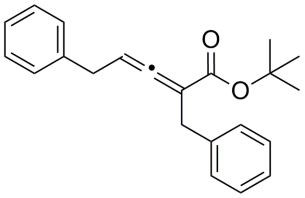
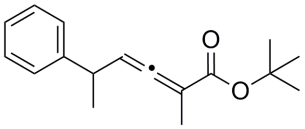
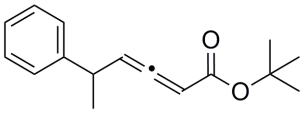
Reducing the amount of the electrophilic fluorinating reagent Selectfluor to two equivalents resulted in a lower conversion to the indenofuranone product **109b**. This compound was delivered in 81% yield after 4.5 hours under these conditions.

3.2.4 Preparation of *tert*-Butyl Allenoates 102

With a set of standard reaction conditions established, we sought to investigate the scope of the cyclisation-intramolecular oxidative arylation process with a range of *tert*-butyl allenoates **102**. These compounds were synthesised via a Wittig-type process between *tert*-butyl-ester-substituted phosphorus ylids **159** and *in situ* prepared ketenes according to the procedure of Shin and co-workers (Table 3.3).[100]



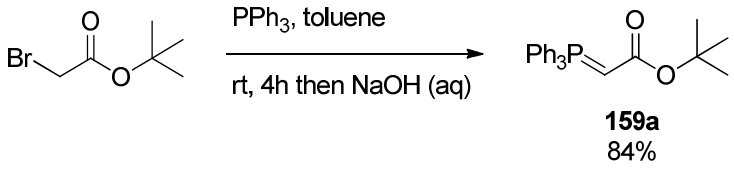
Entry	R^1	R^2	Product **102**	Yield[a]
1	$PhCH_2$	H		**102b** 55%[b]
2	$[(m,p\text{-}OMe)C_6H_3]CH_2$	H		**102c** 29%[c][d]
3	$[(p\text{-}CF_3)C_6H_4]CH_2$	H		**102d** 34%[c][e]
4	$PhCH_2$	Me		**102e** 93%

5	$PhCH_2CH_2$	Me		**102f** 57%[c]
6	Me	$PhCH_2$		**102g** >95%
7	$PhCH_2$	$PhCH_2$		**102h** 78%
8	PhCH(Me)	Me		**102i** 84%[c][f]
9	PhCH(Me)	H		**102j** 22%[c][g]

[a] Isolated yield of the allenoate. In cases where the allenoate **102** was isolated in a mixture with its isomeric alkyne **108**, the yield refers to the amount of allenoate present. [b] Isolated as a 2.9:1 mixture with its isomeric alkyne **108b**. [c] The acid chloride was prepared from the corresponding carboxylic acid and thus the yield was calculated over two steps. [d] Isolated as a 3.5:1 mixture with its isomeric alkyne **108c**. [e] Isolated as a 2.5:1 mixture with its isomeric alkyne **108d**. [f] Diastereoisomeric ratio = 50:50. [g] The allenoate diastereoisomers and the alkyne impurity **108j** were partially separable by column chromatography.

Table 3.3 Preparation of *tert*-Butyl Allenoates **102**.

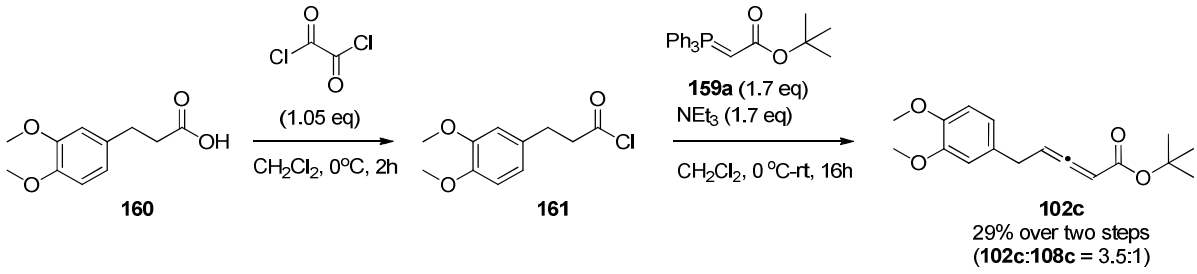
In each case, the *tert*-butyl ester-substituted phosphorus ylid **159** was stirred in the presence of triethylamine (1.7 eq) in dichloromethane at room temperature for 15 minutes. The reaction mixture was then cooled to 0ºC and a solution of an acid chloride in dichloromethane was added dropwise over 30 minutes. After being allowed to warm to room temperature overnight, the mixture was concentrated *in vacuo*. Pentane was added and the slurry was left to stand for two hours with periodic shaking. Filtration of the phosphine oxide by-product followed by column chromatography on silica gel afforded the desired allenoate **102** as an oil. Under these conditions, the test substrate **102b** was furnished in 55% yield from 3-phenylpropanoyl choride and ylid **159a** (Table 3.3, Entry 1). This latter species was prepared in 84% yield from *tert*-butyl bromoacetate and triphenylphosphine (Scheme 3.35).



Scheme 3.35 Preparation of Phosphorus Ylid **159a**.

Allenoate **102b** was isolated as a 2.9:1 mixture with its co-spotting isomeric alkyne **108b**. Extensive efforts to separate the two isomers by silica gel column chromatography were unsuccessful with only partial enrichment of the allenoate possible using very long columns with slow solvent gradients. Chromatography on basic alumina was similarly ineffective whilst attempts at distillation resulted in the decomposition of both isomers. Treating the mixture of **102b** and **108b** with excess triethylamine in dichloromethane had no effect on the isomeric ratio with complete recovery of starting material possible after 16 hours at room temperature.

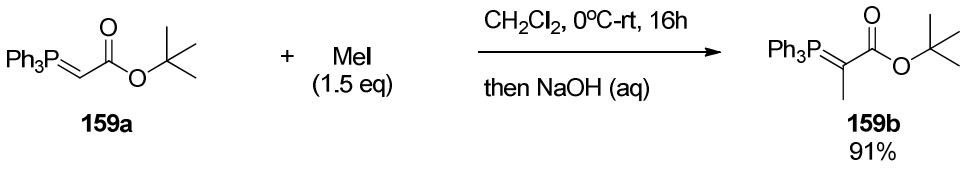
Allenoate **102c**, bearing two methoxy substituents on the aromatic ring, was prepared in a two-step sequence from carboxylic acid **160**. This species was treated with oxalyl chloride in dichloromethane for two hours at 0ºC to afford the corresponding acid chloride **161** (Scheme 3.36). Reacting this compound under the standard Wittig conditions delivered the allenoate **102c** in 29% yield over two steps as a 3.5:1 mixture with its isomeric alkyne **108c** (Table 3.3, Entry 2).



Scheme 3.36 Two-step Preparation of Allenoate **102c**.

The trifluoromethyl-substituted substrate **102d** was prepared in a similar fashion from the appropriate carboxylic acid. This compound was delivered in 34% yield over two steps as a 2.5:1 mixture with its isomeric alkyne **108d** (Table 3.3, Entry 3). Taken together, substrates **102b-d** should allow for the effect of the aryl group electronics on the cyclisation-intramolecular arylation process to be evaluated.

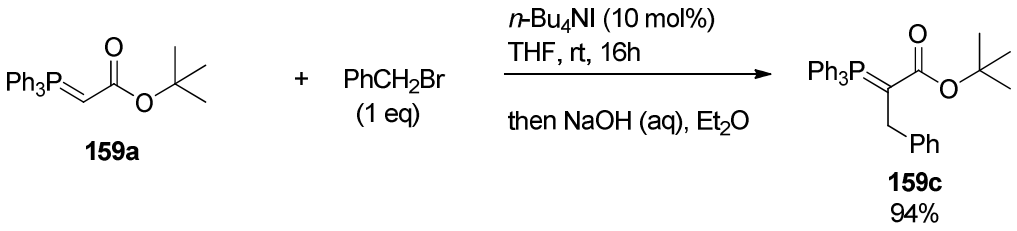
The synthesis of *tert*-butyl allenoates featuring a methyl group α- to the carbonyl was achieved using phosphorus ylid **159b**. This compound was delivered in 91% yield upon methylation of ylid **159a** with methyl iodide in dichloromethane (Scheme 3.37). Reacting ylid **159b** with 3-phenylpropanoyl chloride under the standard conditions afforded allenoate **102e** in 93% isolated yield (Table 3.3, Entry 4). Notably, the isomeric alkyne side-product **108** observed with allenoates derived from ylid **159a** was not formed during this reaction and the allenoate was isolated as a pure compound.



Scheme 3.37 Preparation of Phosphorus Ylid **159b**.

The homobenzyl-substituted allenoate **102f** was synthesised in 57% yield over two steps from the corresponding carboxylic acid (Table 3.3, Entry 5). This compound was again delivered as a pure compound without contamination with its isomeric alkyne **108**. These side-products were also not formed during the synthesis of allenoates **102g** and **102h** featuring a benzyl substituent α- to the carbonyl. Cyclisation-intramolecular arylation of these substrates would lead to tricyclic products **162** containing the indeno-[2,1-*c*]-furanone structural core. Allenoate **102g** was delivered in >95% yield upon treating propanoyl chloride with phosphorus ylid **159c** under the standard Wittig conditions (Table 3.3, Entry

6). Compound **159c** was prepared in 94% yield from **159a** via benzylation with benzyl bromide in the presence of a phase-transfer catalyst (Scheme 3.38).



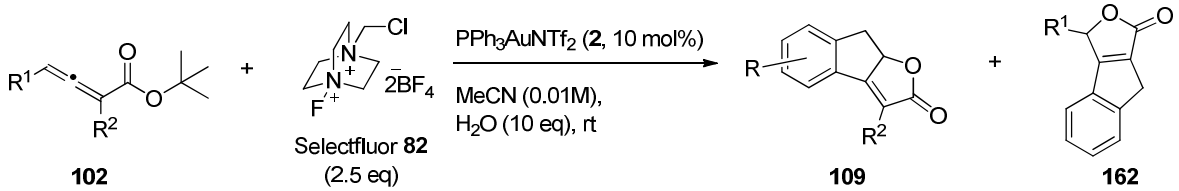
Scheme 3.38 Preparation of Phosphorus Ylid **159c**.

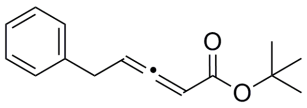
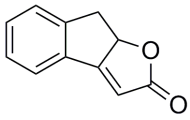
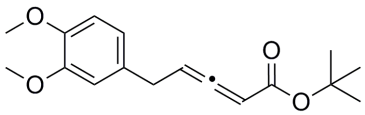
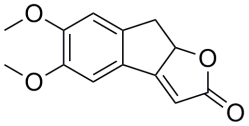
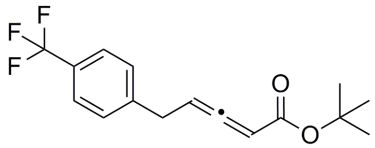
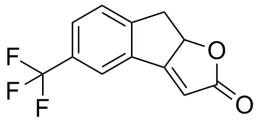
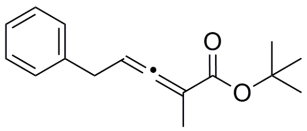
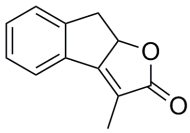
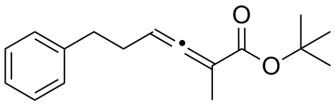
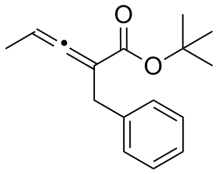
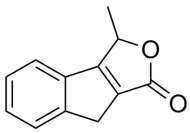
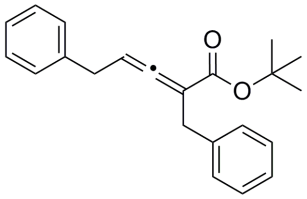
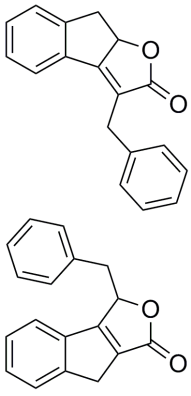
Reacting 3-phenylpropanoyl chloride with phosphorus ylid **159c** under the standard conditions led allenoate **102h**, featuring a benzyl group at both the 2- and 4-positions, in 78% isolated yield (Table 3.3, Entry 7).

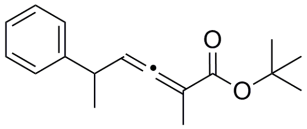
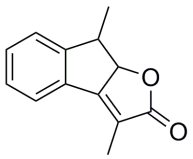
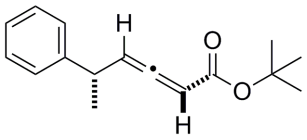
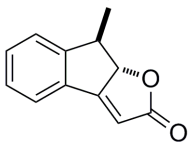
tert-Butyl allenoates derived from 3-phenylbutanoyl chloride were afforded as mixtures of diastereoisomers. The methyl-substituted allenoate **102i** was prepared in 84% isolated yield over two steps from 3-phenylbutanoic acid as an inseparable 50:50 diastereoisomeric mixture (Table 3.3, Entry 8). Although the analogous synthesis of substrate **102j** from ylid **159a** suffered from competitive formation of the isomeric alkyne side-product **108j**, the allenoate diastereoisomers could be partially separated from both each other and the alkyne impurity upon careful silica gel column chromatography (Table 3.3, Entry 9). A pure sample of a single diastereoisomer of **102j** was isolated in 7% yield over two steps from 3-phenylbutanoic acid whilst the combined yield of the allenoate (both diastereoisomers) was 22%.

3.2.5 Scope and Limitations of the Oxidative Coupling Process

tert-Butyl allenoates **102b-j** were reacted under the optimised cyclisation-intramolecular arylation conditions with PPh_3AuNTf_2 (**2**) and Selectfluor (**82**). The results of these experiments are presented in Table 3.4.



Entry[a]	Allenoate **102**	Time	Product(s)	Yield[b]
1[c]		4.5h		**109b** 95%[d]
2[e]		1.5h		**109c** 84%[d]
3[f]		22h		**109d** 37%[d]
4		16h		**109e** 70%
5		24h	Complex Reaction Mixture	---
6		24h		**162g** 57%
7		24h		**109h** 27% **162h** 43%

8[g]		5h		**109i** 81% dr = 55:45
9[h]		4h		(±)-(8*R*,8a*S*)-**109j** 83%

[a] Reaction conditions: PPh_3AuNTf_2 (**2**, 10 mol%), Selectfluor (**82**, 2.5 eq), MeCN (0.01M), H_2O (10 eq), rt. In cases where the allenoate was employed as mixture with its isomeric alkyne, the amounts were calculated with respect to the combined amount of **102** and **108**. [b] Isolated yield. [c] Allenoate **102b** employed as a 3.3:1 mixture with its isomeric alkyne **108b**. [d] Yield calculated relative to the allenoate **102**. [e] Allenoate **102c** employed as a 3:1 mixture with its isomeric alkyne **108c**. [f] Allenoate **102d** employed as a 7:1 mixture with its isomeric alkyne **108d**. [g] Allenoate **102i** employed as a 52:48 mixture of diastereoisomers. [h] Allenoate (±)-(2*S*,5'*S*)-**102j** employed as a single diastereoisomer.

Table 3.4 Cyclisation-Intramolecular Arylation of *tert*-Butyl Allenoates **102b-j**.

In each case, the allenoate was reacted with 10 mol% of PPh_3AuNTf_2 (**2**) and 2.5 equivalents of Selectfluor (**82**) in acetonitrile (0.01M) and water (10 eq).[q] The mixture was stirred at room temperature until TLC analysis showed complete consumption of the allenoate (1.5-24h). After the addition of dichloromethane to encourage precipitation of the fluorinating reagent, the mixture was filtered through Celite and purified by column chromatography on a short pad of silica gel.

Firstly, the effect of the aryl group electronics on the reaction efficiency was investigated. The cyclisation-intramolecular arylation of the dimethoxy-substituted substrate **102c** was a remarkably fast process. Under the optimised conditions, this compound was consumed within 90 minutes to afford the corresponding tricyclic indenofuranone **109c** in 84% yield relative to the allenoate (Table 3.4, Entry 2). By contrast, allenoate **102d**, which bears an electron-withdrawing trifluoromethyl group, was less readily cyclised, delivering indenofuranone **109d** in only 37% yield relative to the allenoate after an extended reaction time of 24 hours (Table 3.4, Entry 3). The structure of this compound was unambiguously confirmed by X-ray crystallography (Figure 3.3)

[q] In cases where the allenoate was employed as mixture with its isomeric alkyne, the amounts were calculated with respect to the combined amount of **102** and **108**.

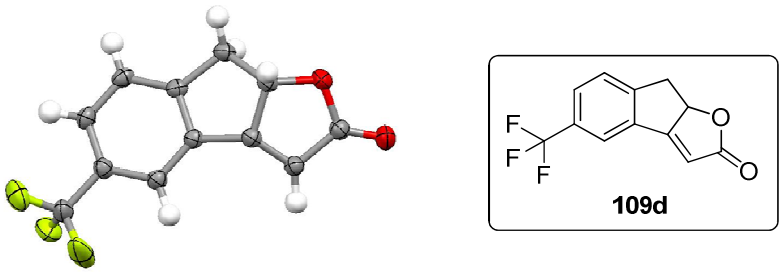


Figure 3.3 X-Ray Crystal Structure of **109d**.

Allenoate **102e** featuring a methyl group α- to the carbonyl was also susceptible to the cyclisation-intramolecular arylation process. This reaction delivered the corresponding indenofuranone **109e** featuring a tetra-substituted alkene in 70% yield after 16 hours at room temperature (Table 3.4, Entry 4). Again, X-ray crystallography allowed for unambiguous structural assignment of the cross-coupled product (Figure 3.4).

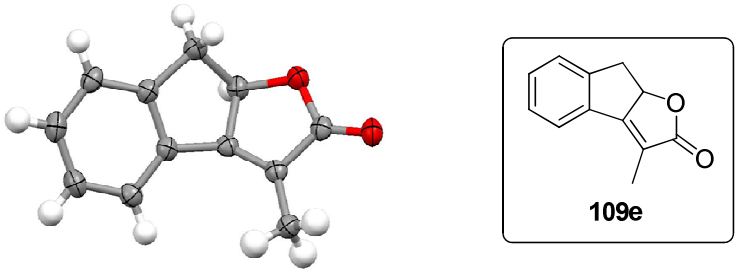


Figure 3.4 X-Ray Crystal Structure of **109e**.

The cascade cyclisation-intramolecular arylation of *tert*-butyl allenoate **102f**, which contains an extra CH_2 unit between the allene moiety and the phenyl group, would deliver the dihydronaphthofuranone **163**. This structural core is present in the cadinane sesquiterpenoid heritol whilst related heterocyclic motifs feature prominently in several other natural products isolated from *Heritiera littoralis*.[107] Reacting **102f** under the optimised conditions, however, led to a complex mixture of cyclised and non-cyclised products (Table 3.4, Entry 5). Whilst small amounts of the desired dihydronaphthofuranone product **164** and the cyclisation-homodimerisation products **110f** were observed by ^{1}H NMR spectroscopy and

mass spectrometry, these compounds could not be isolated from the reaction mixture (Figure 3.5).

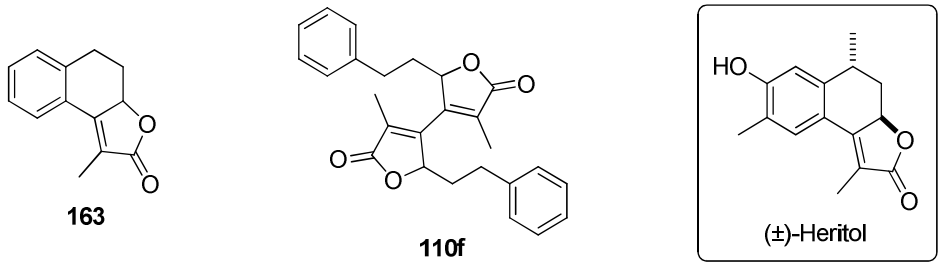
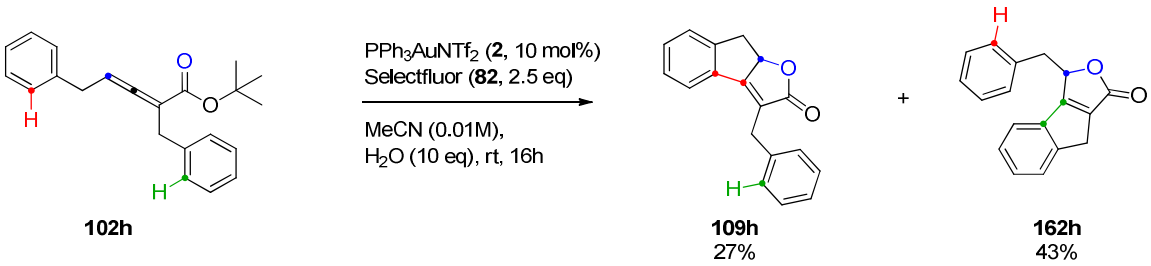


Figure 3.5 Structures of **163**, **110f** and (±)-Heritol.

Treating allenoate **102g** with PPh_3AuNTf_2 (**2**) and Selectfluor (**82**) under the optimised conditions led to the indeno-[2,1-*c*]-furanone **162g** resulting from intramolecular arylation with the benzyl group situated at the 2-position. This compound was delivered in 57% yield after 24 hours at room temperature (Table 3.4, Entry 6). When allenoate **102h** was employed, competition between arylation with the intramolecular 2-benzyl and 4-benzyl groups was observed (Scheme 3.39). The indeno-[2,1-*b*]-furanone **109h** resulting from cascade cyclisation-intramolecular arylation with the 4-benzyl substituent was delivered in 27% yield from this reaction whilst the structural isomer **162h** was afforded in 43% yield (Table 3.4, Entry 7). The indeno-[2,1-*c*]-furanone structure of **162h** was confirmed upon X-ray analysis of a crystal grown from dichloromethane/hexane (Figure 3.6).



Scheme 3.39 Competitive Cyclisation-Intramolecular Arylation of *tert*-Butyl Allenoate **102h**.

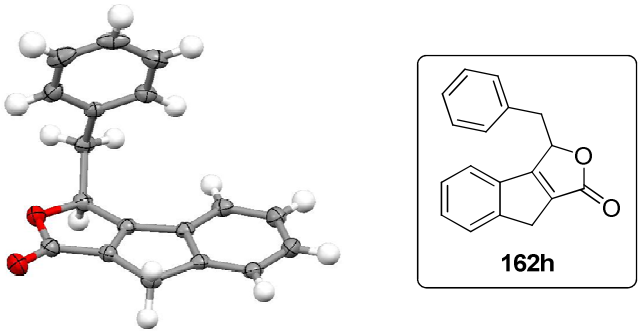


Figure 3.6 X-Ray Crystal Structure of **162h**.

The methyl-substituted *tert*-butyl allenoate **102i** was subjected to the optimised reaction conditions as a 52:48 mixture of diastereoisomers. This reaction led smoothly to a 55:45 diastereoisomeric mixture of the corresponding indenofuranone **109i** in 81% isolated yield after 5 hours at room temperature (Table 3.4, Entry 8). X-Ray analysis of a single crystal grown from this mixture confirmed the tricyclic structure of the product (Figure 3.7).

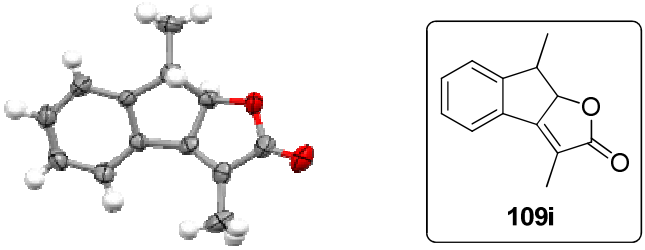


Figure 3.7 X-Ray Crystal Structure of **109i**.

As discussed in Section 3.2.4, the diastereoisomers of substrate **102j** could be separated upon silica gel column chromatography and consequently a pure sample of a single diastereoisomer of the allenoate was reacted under the cyclisation-intramolecular arylation conditions. Smooth conversion to a single diastereoisomer of the cross-coupled product was observed within 4 hours at room temperature implying that the cascade process occurs without loss of stereochemical information. The indenofuranone **109j** could be isolated in 83% yield from this reaction upon purification by column chromatography on a short pad of silica gel (Table 3.4, Entry 9). The relative stereochemistry of this product was

unambiguously assigned as (±)-(8*R*,8a*S*) by X-ray crystallography (Figure 3.8). Assuming complete stereochemical inversion does not occur under the reaction conditions, the relative stereochemistry of the allenoate **109j** can be assigned as (±)-(2*S*,5*S*) based on the cyclisation mechanism shown in Scheme 3.40.

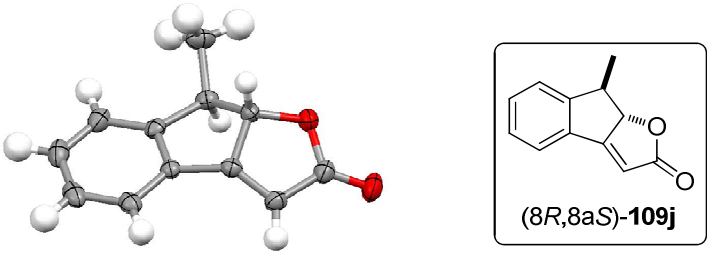
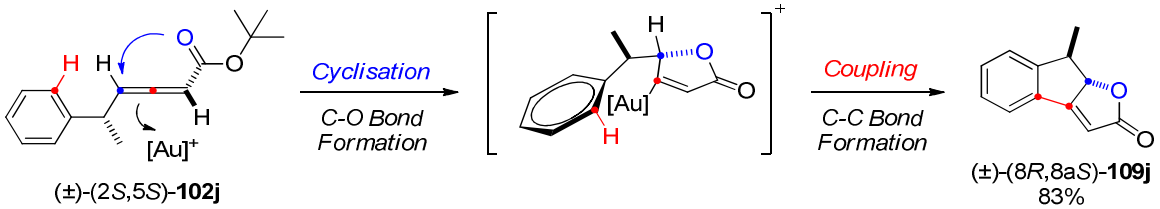
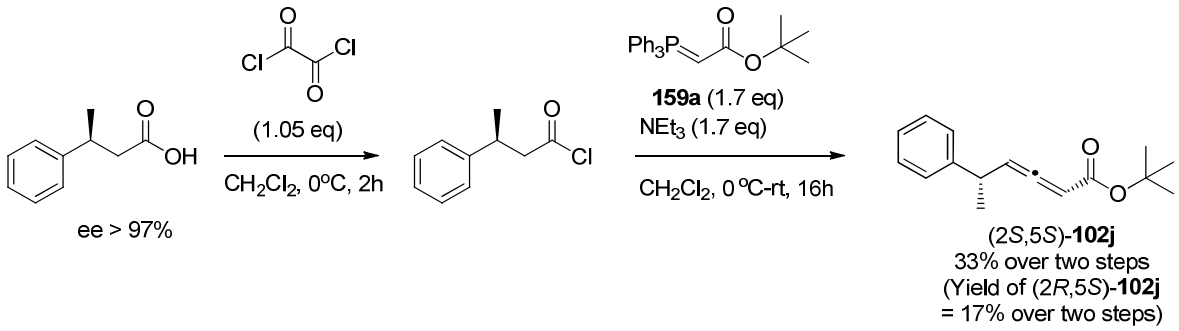


Figure 3.8 X-Ray Crystal Structure of (8*R*,8a*S*)-**109j**.



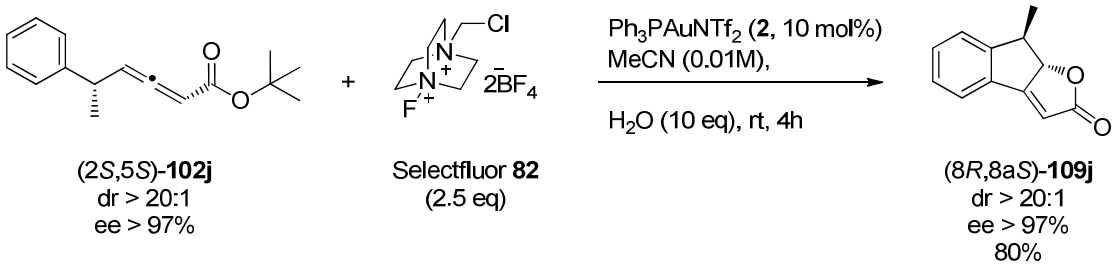
Scheme 3.40 Cyclisation-Intramolecular Arylation of (±)-(2*S*,5*S*)-**102j** into (±)-(8*R*,8a*S*)-**109j**.

The clean transfer of stereochemical information observed in the cyclisation-intramolecular arylation reaction of (±)-(2*S*,5*S*)-**102j** encouraged us to investigate whether enantiopure *tert*-butyl allenoates could be converted into the corresponding indenofuranones without erosion of enantiomeric excess. The enantioenriched allenoate (2*S*,5*S*)-**102j** was prepared via the standard Wittig method discussed in Section 3.2.4 using phosphorus ylid **159a** and (*S*)-3-phenylbutanoyl chloride (Scheme 3.41). This latter reagent was prepared from the commercially available carboxylic acid (Sigma-Aldrich, ee > 97%) using oxalyl chloride. Partial separation of the allenoate diastereoisomers and the isomeric alkyne impurity was possible by silica gel column chromatography and a pure sample of enantioenriched (2*S*,5*S*)-**102j** was isolated in 17% yield over two steps (total yield of (2*S*,5*S*)-**102j** = 33%).



Scheme 3.41 Preparation of (2*S*,5*S*)-**102j** from (*S*)-3-Phenylbutanoic Acid.

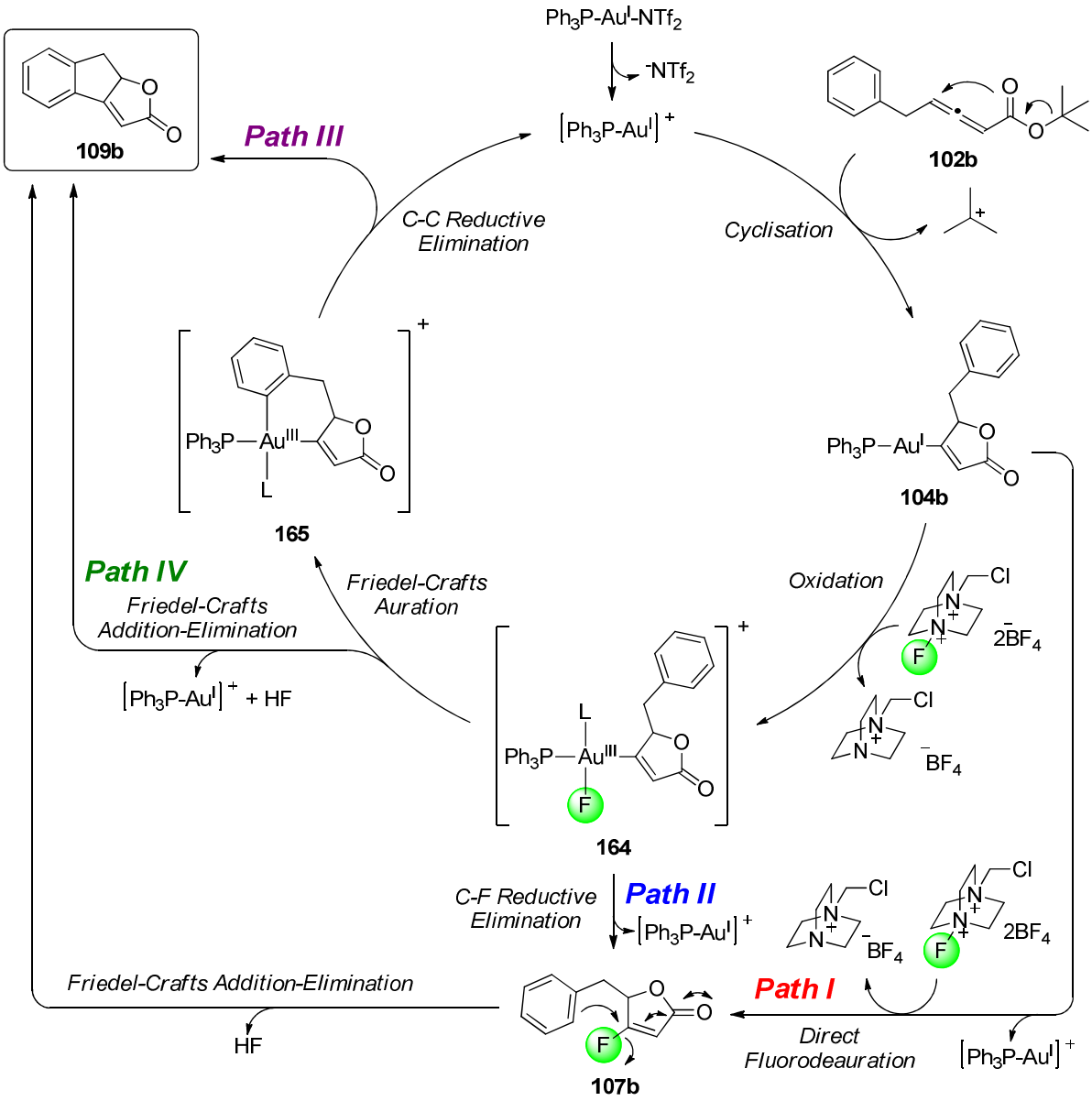
Treating (2*S*,5*S*)-**102j** with PPh_3AuNTf_2 (**2**) and Selectfluor (**82**) under the optimised cyclisation-intramolecular arylation conditions led smoothly to the corresponding indenofuranone (8*R*,8a*S*)-**109j** as a single diastereoisomer in 80% yield. Furthermore, analysis of the tricyclic product by chiral high performance liquid chromatography (HPLC, CHIRALCEL OJ-H, hexane:isopropanol 97:3, flow rate 1 mL/min) indicated that the oxidative coupling reaction proceeded with complete axis-to-centre chirality transfer, delivering (8*R*,8a*S*)-**109j** in > 97% ee (Scheme 3.42).



Scheme 3.42 Axis-to-Centre Chirality Transfer in the Cyclisation-Arylation of (2*S*,5*S*)-**102j**.

3.2.6 Comments on the Reaction Mechanism

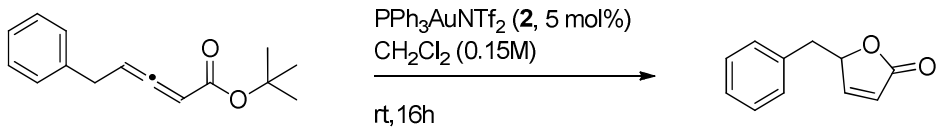
With the scope and limitations of the cascade cyclisation-intramolecular arylation process established, our attention turned to an investigation of the reaction mechanism with a focus on determining the role of the electrophilic fluorinating reagent Selectfluor (**82**). Three plausible mechanistic pathways for the transformation of *tert*-butyl allenoate **102b** into indenofuranone **109b** are displayed in Scheme 3.43.



Scheme 3.43 Plausible Reaction Mechanisms for the Cascade Cyclisation-Intramolecular Oxidative Arylation of *tert*-Butyl Allenoates **102**.

The first stage of the cascade process involves the *in situ* generation of the active gold(I) catalyst from complex **2**. In an organic solvent, the weakly coordinating $^{-}NTf_2$ counter-ion dissociates from the gold(I) source to afford the phosphine-stabilised cationic species $[PPh_3Au]^+$. This complex has a free coordination site and can act as a π-Lewis acid, activating the allene moiety of the allenoate **102b** towards nucleophilic attack of the intramolecular ester oxygen. Concomitant loss of a *tert*-butyl cation leads to the

(butenolide)gold(I) complex **104b** resulting from a formal 5-*endo*-trig cyclisation of **102b**. Protodeauration at this stage would lead to the conventional γ-butenolide product **103b** and regenerate the cationic gold(I) catalyst (see Scheme 3.2). This compound was afforded as the major product in 91% yield (relative to the allenoate) when **102b** was reacted with PPh_3AuNTf_2 (**2**, 5 mol%) in the absence of Selectfluor (**82**, Scheme 3.44).[r]



102b
(3.3:1 mixture with **108b**)

103b
91% (relative to **102b**)

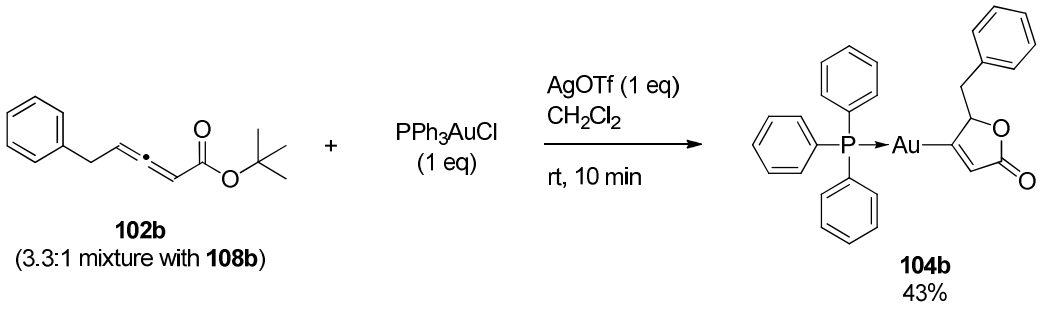
Scheme 3.44 Cyclisation-Protodeauration of Allenoate **102b** with PPh_3AuNTf_2 (**2**).

However, when the reaction is performed in the presence of Selectfluor, intermediate **104b** does not protodeaurate and may instead react with the electrophilic fluorinating reagent. One possible mechanistic pathway involves the formation of the β-fluoro-γ-butenolide intermediate **107b** resulting from a direct fluorodeauration of complex **104b**. A similar cascade cyclisation-fluorination mechanism was tentatively proposed by our group as the operative pathway in the gold(I)-catalysed synthesis of trifluorinated dihydropyranones **83** discussed in Section 1.5.1 of this thesis. Indeed, β-fluoro-γ-butenolides **107** resulting from a cascade 5-*endo*-trig allenoate cyclisation-fluorodeauration process were the original target compounds of this study. γ-Butenolides of this type are expected to be excellent Michael acceptors and **107b** could feasibly react with the intramolecular arene in a Friedel-Crafts addition-elimination process to afford the indenofuranone product **109b** and one equivalent of hydrogen fluoride (Scheme 3.43, Path I). An electrophilic aromatic substitution (S_EAr)-type arylation step is consistent with the scope and limitation studies where higher yields and shorter reaction times were observed for allenoates bearing more electron rich arene substituents (see Section 3.2.5). Alternatively, the reaction between the vinylgold(I)

[r] The isomeric alkyne impurity **108b** was unreactive under the reaction conditions and did not lead to **103b**.

intermediate **104b** and the electrophilic fluorinating reagent could lead to the gold(III) fluoride complex **164**. This species results from a formal two-electron oxidation of gold(I) with Selectfluor acting as a stoichiometric external oxidant. Carbon-fluorine bond-forming reductive elimination from intermediate **164** would lead to the β-fluoro-γ-butenolide **107b** which could then deliver the oxidative coupling product **109b** upon Friedel-Crafts addition-elimination (Scheme 3.43, Path II). Instead, the aryl group in complex **164** could react with the electron-deficient gold(III) centre in an intramolecular Friedel-Crafts auration process leading to the auracyclic gold(III) species **165**. An electrophilic aromatic substitution (S_EAr) mechanism of this type has been implicated in related arene C(sp^2)-H functionalisation reactions with gold(III) (see Section 3.2.2.1). Carbon-carbon bond-forming reductive elimination from complex **165** would deliver the cross-coupled indenofuranone product **109b** and regenerate the cationic gold(I) catalyst $[PPh_3Au]^+$ (Scheme 3.43, Path III). In a fourth possible pathway, indenofuranone **109b** could be afforded directly from the gold(III) fluoride complex **164** in a Friedel-Crafts addition-elimination process with gold acting as a leaving group (Scheme 3.43, Path IV).

Following the successful isolation of a (butenolide)gold(I) complex by Hammond and co-workers in their study on the related gold-catalysed cyclisation of ethyl allenoates (see Scheme 3.3),[101-102] we sought to prepare the proposed intermediate **104b** independently using PPh_3AuCl and AgOTf. Treating *tert*-butyl allenoate **102b** (as a mixture with **108b**, **102b**:**108b** = 3.3:1, 1.2 eq of allenoate) with one equivalent of each of these reagents in dichloromethane for 10 minutes led to a mixture of **104b** and the corresponding protodeaurated γ-butenolide **103b**.[102] The desired organogold(I) complex could be isolated in 43% yield relative to PPh_3AuCl upon careful column chromatography on silica gel (Scheme 3.45).

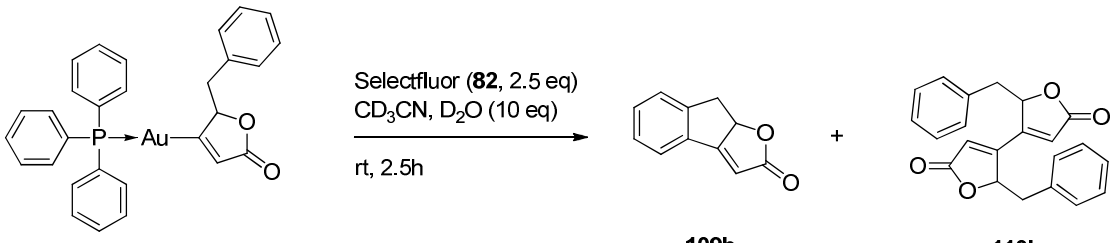


102b
(3.3:1 mixture with **108b**)

104b
43%

Scheme 3.45 Preparation of (Butenolide)gold(I) Complex **104b**.

Complex **104b** was added to a solution of the electrophilic fluorinating reagent Selectfluor (**82**, 2.5 eq) in deuterated acetonitrile (0.15M) and D_2O (10 eq) and the reaction was monitored by NMR spectroscopy. Under these conditions, complex **104b** was smoothly converted into the homo- and cross-coupled products **110b** and **109b** within 15 minutes at room temperature. Notably, the cyclisation-protodeauration product **103b** was not formed during the reaction whilst the crude ^{1}H and ^{19}F NMR spectra contained no peaks consistent with an organofluorine compound. Silica gel column chromatography after 2.5 hours allowed for the isolation of compounds **109b** and **110b** in 37% and 60% yield respectively (Scheme 3.46). The successful preparation of the cross-coupled product **109b** from complex **104b** implies that a cyclisation-intramolecular arylation mechanism involving the (butenolide)gold(I) species is possible under the reaction conditions.



104b

109b
37%

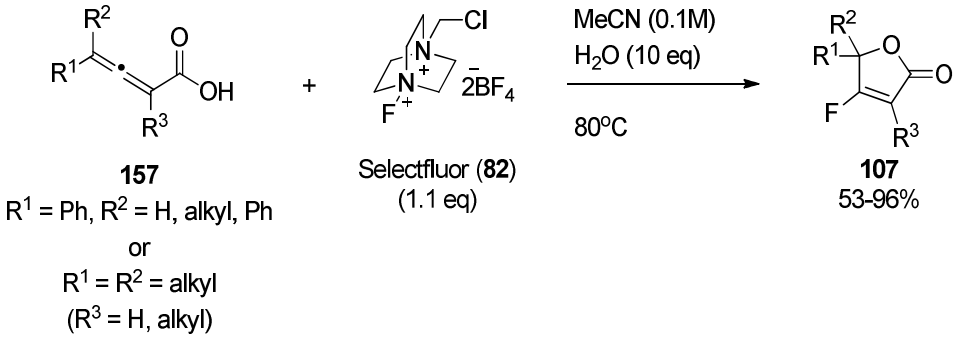
110b
60% dr = 63:37

Scheme 3.46 Oxidative Homo- and Cross-Coupling of Organogold(I) Complex **104b**.

At this stage, our attention turned to elucidating the role of the electrophilic fluorinating reagent in the oxidative coupling process. In order to distinguish between Paths I/II and

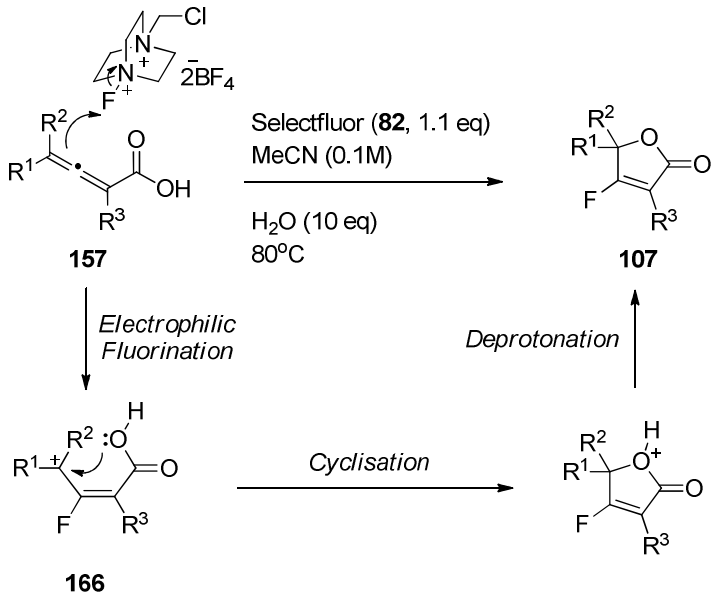
III/IV in Scheme 3.43, we sought to independently prepare a β-fluoro-γ-butenolide **107** for use as a mechanistic probe. If an oxidative cyclisation mechanism analogous to Path I or Path II in Scheme 3.43 is operative, this compound should lead to the indenofuranone **109** or **162** via an intramolecular Friedel-Crafts addition-elimination process under the standard cyclisation-arylation conditions.

β-Fluoro-γ-butenolides **107** are scarce in the literature and, to date, only one synthetic route to these compounds has been reported. In 2008, Ma and co-workers demonstrated that allenic acids **157** can react with Selectfluor (**82**) to afford fluorocyclised products of type **107** when heated to 80ºC in acetonitrile and water (Scheme 3.47).[168]



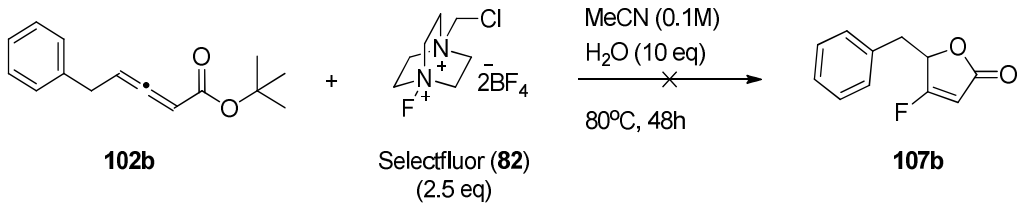
Scheme 3.47 Fluorocyclisation of Allenic Acids **157**.

A cascade fluorination-cyclisation mechanism of the type shown in Scheme 3.48 was proposed for this transformation. In the first step, the electrophilic fluorinating reagent Selectfluor (**82**) reacts with the allene moiety of the starting material **157** to afford the cationic fluorinated intermediate **166**. This species then undergoes an intramolecular cyclisation with the carboxylic acid leading to the fluorocyclised product **107** upon deprotonation.



Scheme 3.48 Proposed Mechanism for the Fluorocyclisation of Allenic Acids **157**.

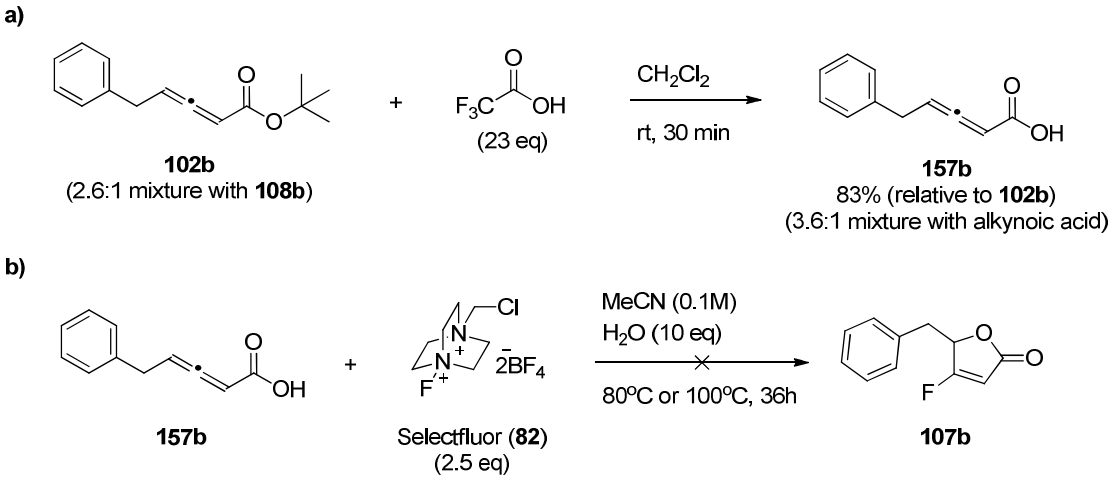
The scope of allenic acid starting materials in this process was somewhat limited with only substrates bearing either an aryl group or two alkyl groups at the 4-position leading to the fluorocyclised products. These substituents offer greater resonance and/or inductive stabilisation of the cationic charge in intermediate **166**, leading to a more favourable initial electrophilic fluorination step (see Scheme 3.48).[168] In accordance with these observations, the mono-benzyl substituted allene **102b** was not a suitable substrate for the fluorocyclisation reaction. Heating the *tert*-butyl allenoate **102b** to 80ºC with Selectfluor in acetonitrile and water led only to recovered starting material after 48 hours with no formation of the β-fluoro-γ-butenolide **107b** (Scheme 3.49).[s]



Scheme 3.49 Attempted Fluorocyclisation of *tert*-Butyl Allenoate **102b**.

[s] This reaction was conducted by Andrew Salisbury (Part II, University of Oxford, 2008). reference [104]

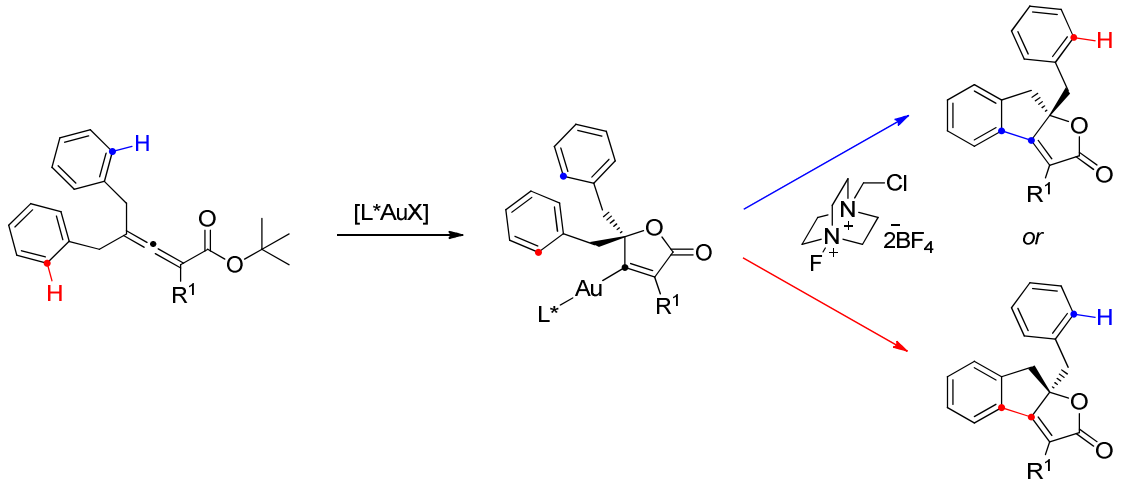
The attempted fluorocyclisation of the corresponding allenic acid **157b** was similarly unsuccessful. This compound was prepared in 83% yield from *tert*-butyl allenoate **102b** and then treated with Selectfluor in acetonitrile and water (Scheme 3.50a). Complete recovery of the starting material was observed after 36 hours at 80ºC whilst increasing the reaction temperature to 100ºC did not encourage fluorocyclisation (Scheme 3.50b).[t]



Scheme 3.50 a) Preparation of Allenic Acid **157b**. b) Attempted Fluorocyclisation of Allenic Acid **157b**.

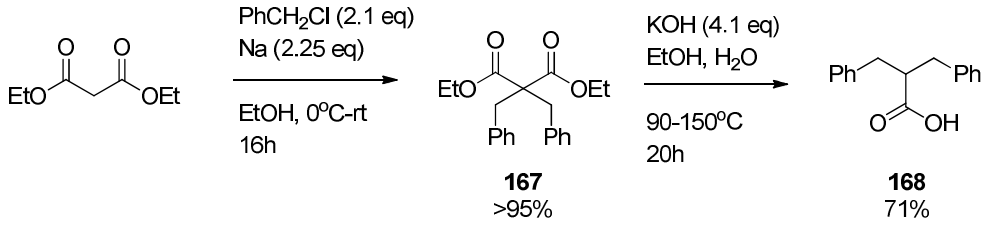
With the fluorocyclisation of a mono benzyl-substituted allene proving challenging, our attention turned to the synthesis of a fluorinated butenolide from an allenic acid precursor bearing two benzyl groups at the 4-position. These compounds are expected to be better suited to the cascade fluorination-cyclisation process as they offer improved inductive stabilisation of the positive charge generated upon electrophilic fluorination. In addition, the prochiral nature of dibenzyl-substituted *tert*-butyl allenoates could potentially lead to the development of an asymmetric variant of the cyclisation-intramolecular arylation process using gold(I) catalysts bearing chiral ligands or counter-ions (Scheme 3.51).

[t] This reaction was conducted by Andrew Salisbury (Part II, University of Oxford, 2008). reference [104]



Scheme 3.51 Potential Development of an Asymmetric Variant of the Cyclisation-Intramolecular Arylation Process (L* = Chiral Ligand).

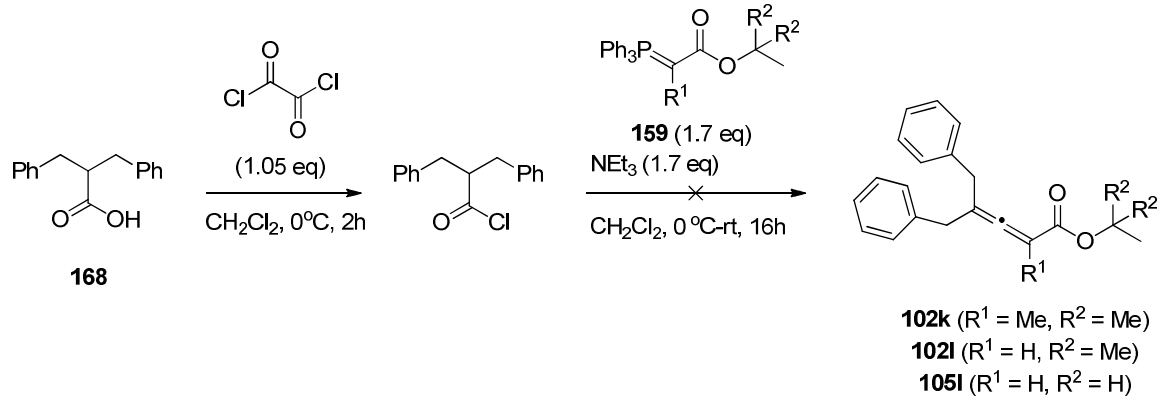
The synthesis of the dibenzyl-substituted *tert*-butyl allenoate **102k** was attempted starting from commercially-available diethyl malonate. Treatment of this compound with 2.1 equivalents of benzyl chloride in the presence of *in situ*-prepared sodium ethoxide led to the dibenzylated product **167** in quantitative yield. Hydrolysis of the ethyl esters with potassium hydroxide and subsequent decarboxylation at 150ºC delivered the corresponding dibenzyl-substituted carboxylic acid **168** in 71% yield after 20 hours (Scheme 3.52).



Scheme 3.52 Preparation of Dibenzyl-Substituted Carboxylic Acid **168**.

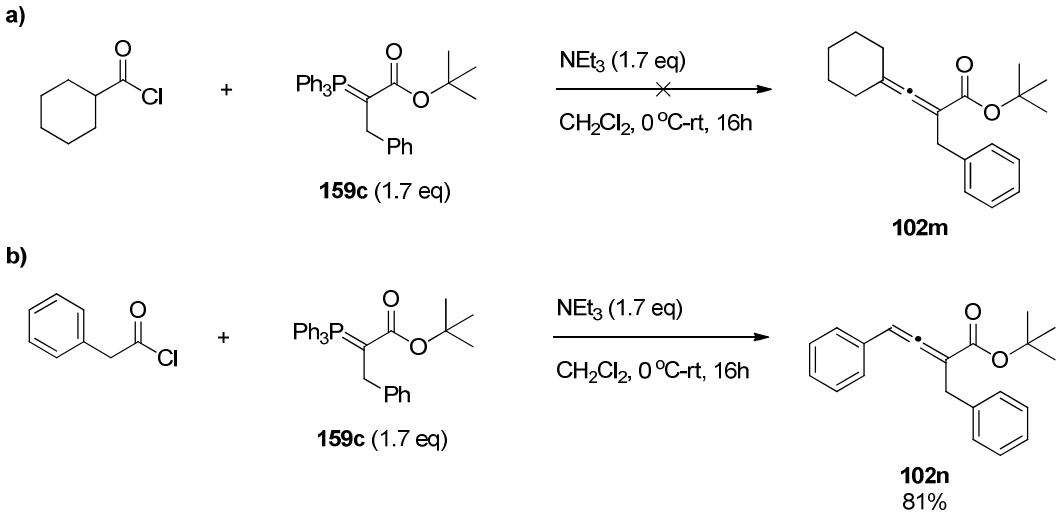
Compound **168** was converted into the corresponding acid chloride using oxalyl chloride and then subjected to the standard Wittig conditions with phosphorus ylid **159b** (see Section 3.2.4). Disappointingly, this reaction led to a complex mixture of products with no formation of the desired allenoate **102k** observed either by crude NMR analysis or upon silica gel column chromatography. The attempted syntheses of the related *tert*-butyl and

ethyl allenoates **102l** and **105l** were similarly unsuccessful with no allene-containing products detectable by crude NMR (Scheme 3.53).



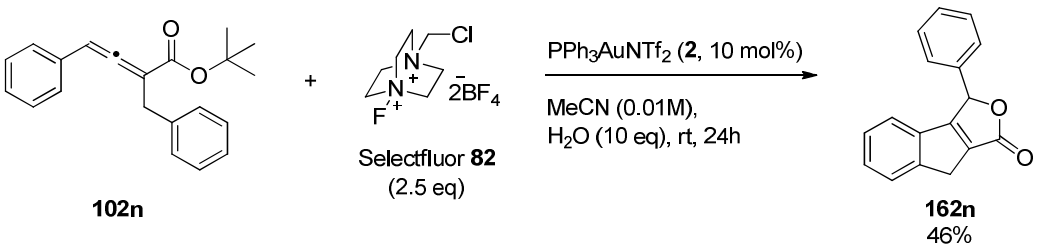
Scheme 3.53 Attempted Preparation of Dibenzyl-Substituted Allenoates **102k**, **102l** and **105l**.

The unsuccessful preparation of allenoates bearing two benzyl-substituents at the 4-position led us to identify alternative substrates amenable to fluorocyclisation. The *tert*-butyl allenoates **102m** and **102n**, bearing 4,4-dialkyl and 4-phenyl substituents respectively, were selected as promising candidates for further study. These compounds feature a benzyl group at the 2-position of the allene and would lead to tricyclic indeno-[2,1-*c*]-furanone products **162** upon cyclisation-intramolecular arylation. In an initial experiment, commercially-available cyclohexanecarbonyl chloride was reacted with the benzyl-substituted phosphorus ylid **159c** under the standard Wittig conditions discussed in Section 3.2.4. This reaction led to a complex mixture of products with no formation of *tert*-butyl allenoate **102m** detected by crude NMR (Scheme 3.54a).The analogous synthesis of the phenyl-substituted allenoate **102n**, however, was more successful. Treating phenylacetyl chloride with ylid **159c** under the same conditions led smoothly to the desired compound **102n** in 81% yield after 16 hours (Scheme 3.54b).



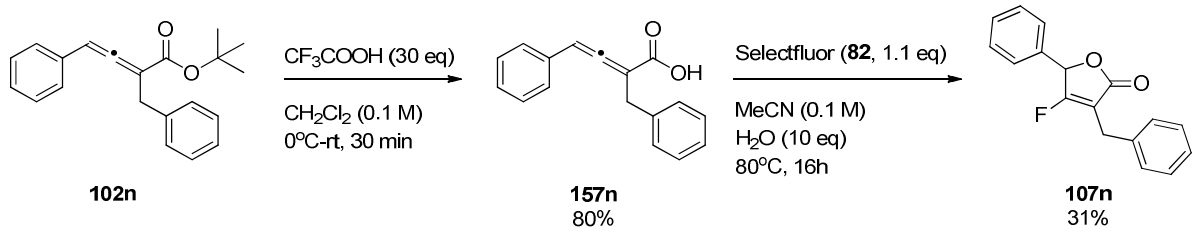
Scheme 3.54 a) Attempted Preparation of Allenoate **102m**. b) Preparation of Allenoate **102n**.

tert-Butyl allenoate **102n** was successfully converted into the corresponding indeno-[2,1-*c*]-furanone **162n** upon treatment with PPh_3AuNTf_2 (**2**, 10 mol%) and Selectfluor (**82**, 2.5 eq) under the standard cyclisation-intramolecular arylation conditions. The tricyclic compound was delivered in 46% isolated yield from this reaction upon purification by silica gel column chromatography (Scheme 3.55).



Scheme 3.55 Cyclisation-Intramolecular Arylation of *tert*-Butyl Allenoate **162n**.

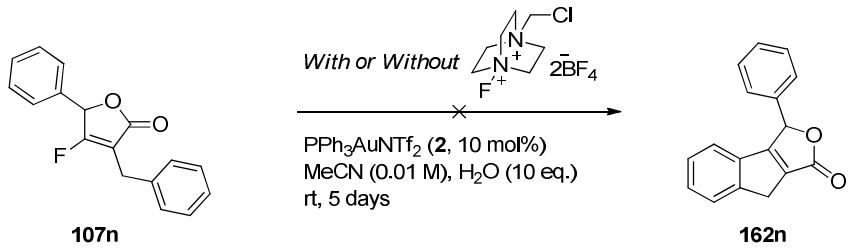
Hydrolysis of *tert*-butyl allenoate **102n** with trifluoroacetic acid afforded the corresponding allenic acid **157n**, which was then treated with Selectfluor (**82**, 1.1 eq) in acetonitrile (0.1M) and water (10 eq) at 80ºC for 16 hours. Although several products were formed in this reaction, the ^{1}H and ^{19}F NMR spectra of the crude mixture contained peaks consistent with the desired β-fluoro-γ-butenolide **107n**. Pleasingly, this compound was isolated in 31% yield upon purification by silica gel column chromatography (Scheme 3.56).



Scheme 3.56 Preparation of the β-Fluoro-γ-butenolide **107n**.

With the benzyl-substituted β-fluoro-γ-butenolide **107n** in hand, we were poised to investigate whether this compound would undergo an intramolecular Friedel-Crafts addition-elimination under the optimised cyclisation-intramolecular arylation conditions. The fluorinated species **107n** was reacted with PPh_3AuNTf_2 (**2**, 5 mol%) and Selectfluor (**82**, 2.5 eq) in acetonitrile (0.01M) and water (10 eq) at room temperature for 24 hours. NMR Analysis of the crude reaction mixture indicated that the β-fluoro-γ-butenolide was inert under these conditions with no peaks consistent with the indenofuranone product **162n** being observed in the ^{1}H NMR spectrum. Even after 5 days at room temperature, no trace of the tricyclic product was detected and the β-fluoro-γ-butenolide starting material **107n** could be recovered from the reaction mixture as the only isolable material. Similar results were obtained upon reacting **107n** under the same conditions but in the absence of Selectfluor. Indenofuranone **162n** was not produced in this reaction with only starting material being observed after 5 days at room temperature (Scheme 3.57). In a third control experiment, an equimolar mixture of the β-fluoro-γ-butenolide **107n** and the *tert*-butyl allenoate **102n** was treated with PPh_3AuNTf_2 (**2**) and Selectfluor (**82**) under the optimised conditions. Whilst smooth conversion of the allenoate into the tricyclic indenofuranone **162n** was observed after 48 hours at room temperature, ^{1}H and ^{19}F NMR analysis indicated that the fluorinated butenolide remained intact during this reaction.[u]

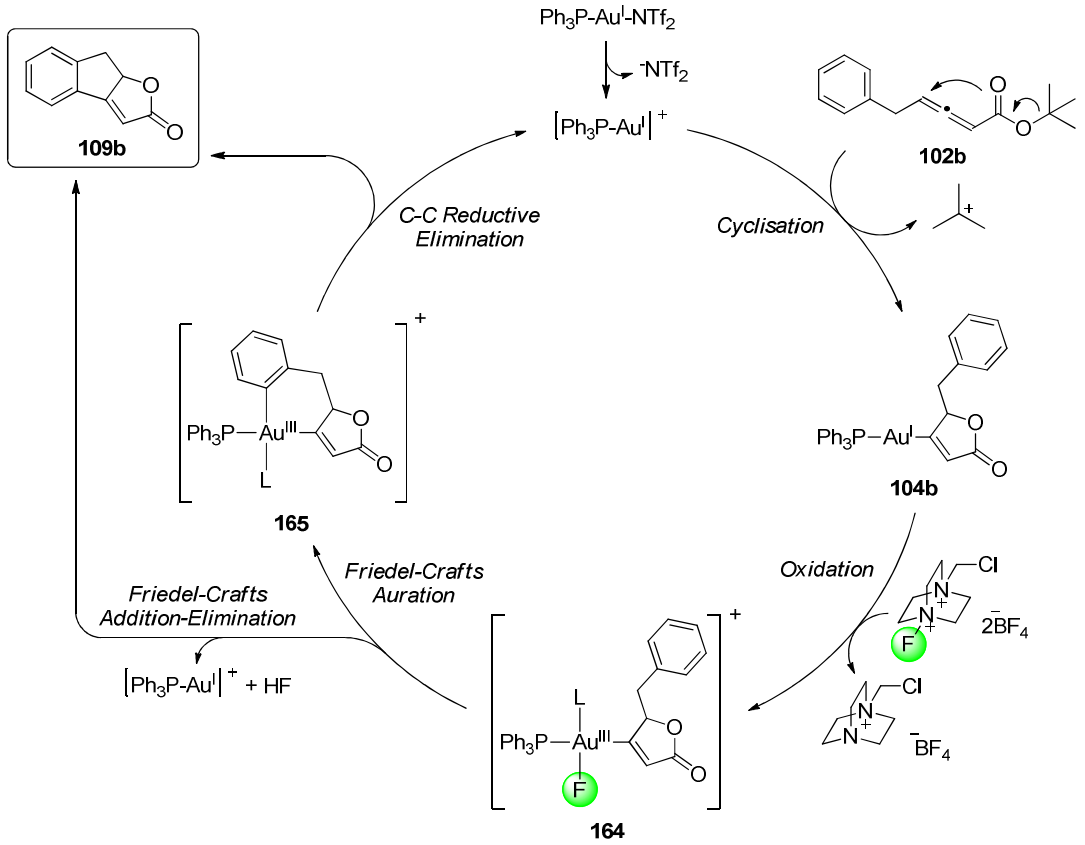
[u] Hexafluorobenzene was used as an internal reference in the ^{19}F NMR spectra.



Scheme 3.57 Attempted Arylation of β-Fluoro-γ-Butenolide **107n**.

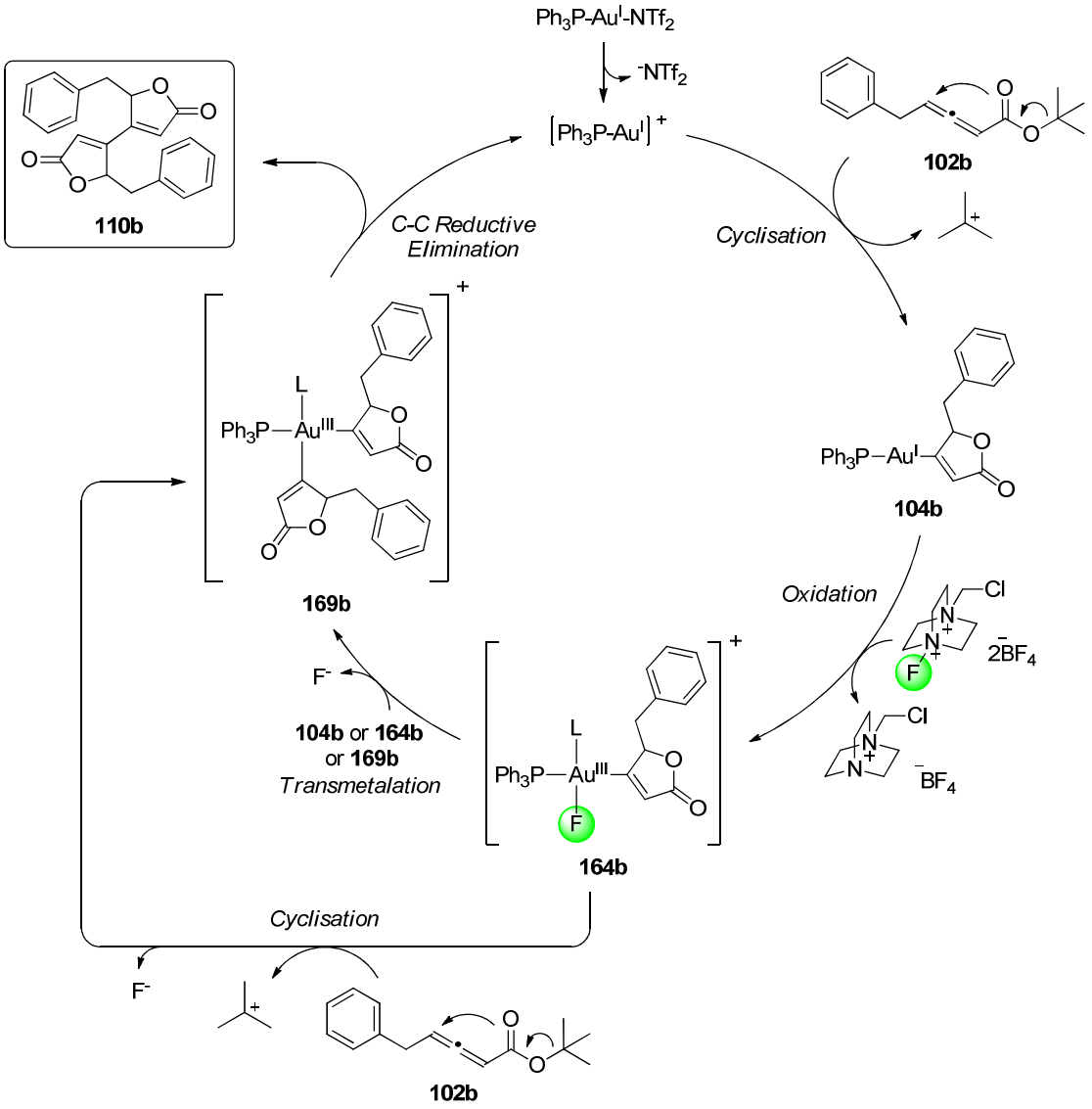
The apparent stability of the benzyl-substituted β-fluoro-γ-butenolide **107n** towards intramolecular Friedel-Crafts addition-elimination suggests that compounds of this type are unlikely to be intermediates in the cyclisation-oxidative arylation process. The lack of fluorinated organic side-products observed during our optimisation and scope and limitations studies is also consistent with this interpretation. β-Fluoro-γ-butenolides of the type implicated in Paths I and II in Scheme 3.43 were not isolated from any reaction mixture during the course of this investigation whilst the fluorodeaurated product **107b** was not observed when the (butenolide)gold(I) complex **104b** was treated with Selectfluor (see Scheme 3.46).

Taken together, these observations mitigate in favour of a cyclisation-intramolecular arylation mechanism involving an Au^{I}/Au^{III} redox cycle (Scheme 3.58). In this process, Selectfluor acts as a stoichiometric external oxidant rather than a conventional fluorinating reagent, converting the (butenolide)gold(I) complex formed upon cyclisation of the allenoate to the gold(III) fluoride intermediate **164**. Friedel-Crafts attack of the intramolecular aryl group onto the gold(III) centre followed by C-C bond-forming reductive elimination would then lead to the indenofuranone product **109**. Alternatively, a Friedel-Crafts addition-elimination of the aryl substituent onto complex **164** would also lead to the same product with gold acting as a leaving group.



Scheme 3.58 Proposed Mechanism for the Cyclisation-Intramolecular Arylation of *tert*-Butyl Allenoates **102** (Depicted for Allenoate **102b**).

The formation of the bibutenolide side-products **110b** can also be explained by this mechanism (Scheme 3.59). Activation of a second molecule of the *tert*-butyl allenoate starting material by complex **164** would lead to the gold(III) species **169**, bearing two butenolide groups. Carbon-carbon bond-forming reductive elimination from this complex would then deliver the homodimerised product and regenerate the active gold(I) catalyst. Alternatively, the doubly organic-substituted gold(III) intermediate **169** could be formed upon transmetalation of a butenolide fragment in complex **104**, **164** or **169** onto the gold(III) fluoride species **164**.

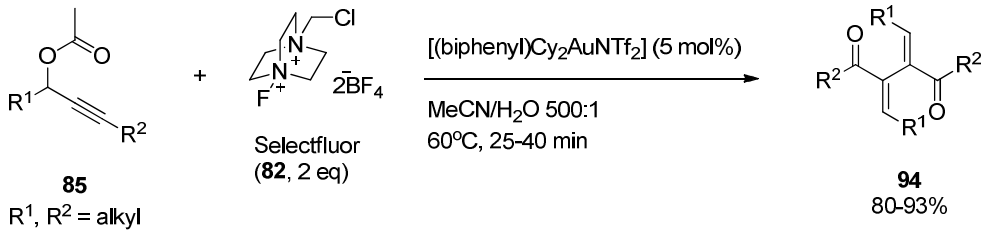


Scheme 3.59 Proposed Mechanism for the Cyclisation-Homodimerisation of *tert*-Butyl Allenoate **102b**.

The formation of the homodimerised side-product **110b** is less readily explained by a mechanism involving the β-fluoro-γ-butenolide intermediate **107b**. Such a pathway would involve an intermolecular Michael-type attack of a nucleophilic butenolide unit onto the fluorinated α,β-unsaturated ester. Whilst nucleophilic addition reactions involving organic ligands coordinated to gold(I) have been reported in the literature, intermolecular examples onto carbon-electrophiles are scarce.[v]

[v] The gold-mediated cyclisation-homodimerisation of *tert*-butyl allenoates is discussed more thoroughly in Chapter 4 of this thesis.

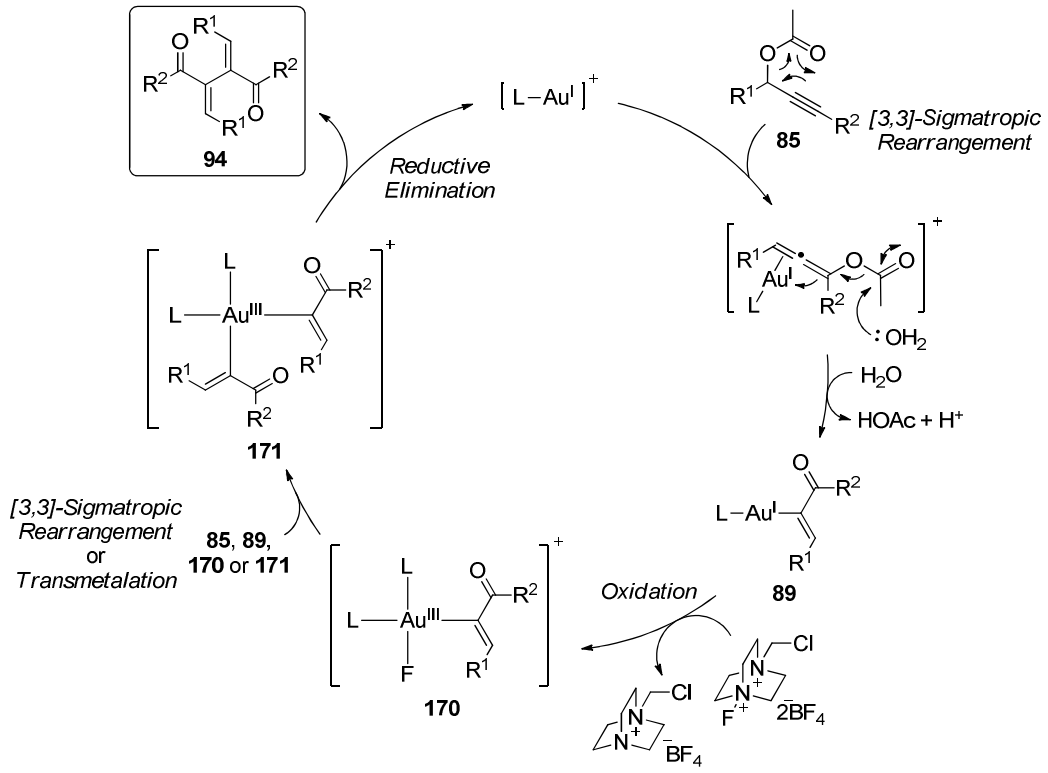
Whilst we were conducting this investigation, Zhang and co-workers reported a similar gold(I)-catalysed cascade nucleophilic addition-oxidative coupling reaction performed in the presence of Selectfluor (**82**).[169] Propargyl acetates **85** were converted into the (*E*,*E*)-enone dimers **94** as single diastereoisomers in up to 93% yield upon treatment with the gold(I) source [(biphenyl)$Cy_2PAuNTf_2$] (5 mol%) and two equivalents of the electrophilic fluorinating reagent in acetonitrile/water (500:1) at 60ºC (Scheme 3.60). Notably, the conventional [3,3]-sigmatropic rearrangement-protodeacetylation process was completely suppressed with no formation of enones **86** observed. In addition, no α-fluoroenones **92** resulting from rearrangement-fluorodeacetylation were produced during the reaction implying that oxidative homocoupling was a more favourable process under these conditions.[89, 96] The enone dimer **94b** was observed in a trace amount during our preliminary studies into the rearrangement-fluorodeacetylation of propargyl acetate **85b** using PPh_3AuCl/AgOTf as catalyst (see Scheme 2.8). In all further reactions in our investigation, however, no homocoupled enone products were observed (see Chapter 2).



Scheme 3.60 Rearrangement-Homodimerisation of Propargyl Acetates.

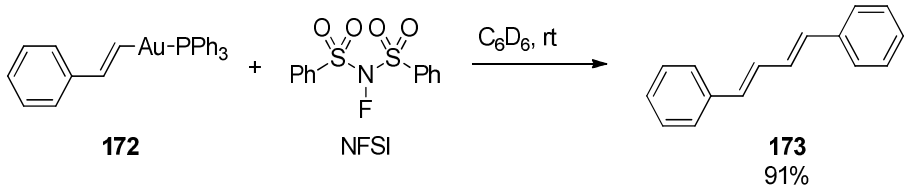
The observed reactivity is best explained by an Au^I/Au^{III} redox cycle analogous to that shown in Scheme 3.59, with Selectfluor acting as a stoichiometric external oxidant (Scheme 3.61). After the initial [3,3]-sigmatropic rearrangement (see Scheme 2.2), gold is thought to complex the allene moiety of the allenyl acetate intermediate leading to the vinylgold(I) complex **89** upon hydrolysis of the acetyl group. This species is then oxidised to the (enone)gold(III) fluoride complex **170** by the electrophilic fluorinating reagent. Activation

of another molecule of the starting material or transmetalation between gold complexes would then deliver a gold(III) complex **171** amenable to $C(sp^2)$-$C(sp^2)$ bond-forming reductive elimination.



Scheme 3.61 Proposed Mechanism for the Rearrangement-Homocoupling of Propargyl Acetates.

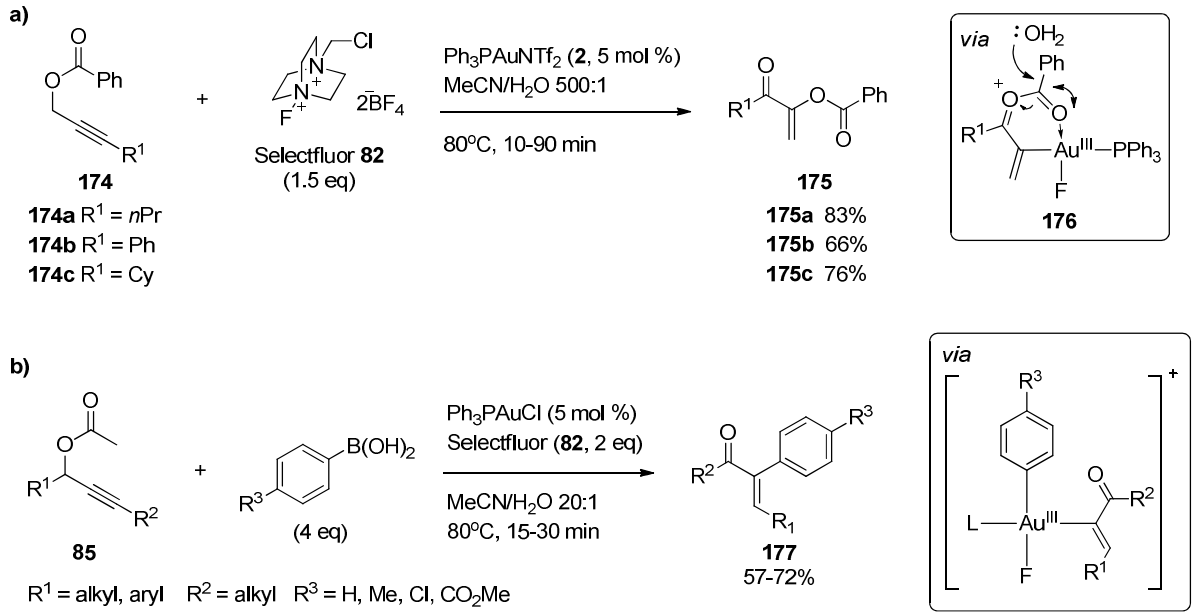
The ability of Selectfluor to promote homocoupling from organogold(I) complexes was also demonstrated by Hashmi and co-workers.[170-171] Whereas electrophilic sources of bromine, iodine and chlorine reacted with the η^1-(styryl)gold(I) complex **172** to afford the corresponding halogenated styrenes, no fluorodeauration was observed with the mild electrophilic fluorinating reagent NFSI. Instead, diene **173** was furnished as the only product in 91% yield from this reaction (Scheme 3.62). A mechanism involving the oxidation of gold(I) to gold(III) by the "F^+" source followed by transmetalation and reductive elimination can again explain the observed reactivity.



172 NFSI **173** 91%

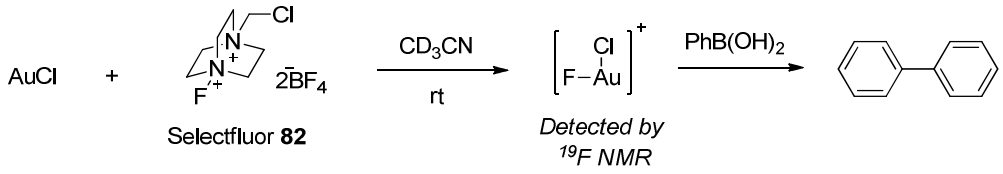
Scheme 3.62 Homocoupling of Organic Ligands Coordinated to Gold(I) Complexes.

The cyclisation-homocoupling of propargyl esters could be rerouted in favour of oxidative cross-coupling in the presence of a suitable intra- or intermolecular coupling partner. Propargyl benzoates **174** were converted into the corresponding α-benzoylenones **175** upon treatment with PPh_3AuNTf_2 (**2**) and Selectfluor (**82**) in acetonitrile/water (500:1) at 80ºC (Scheme 3.63a).[172] The oxygen coupling partner in this process is most likely generated upon hydrolysis of the intramolecular benzoate group in a gold(III) intermediate of type **176**. Performing the [3,3]-sigmatropic rearrangement of propargyl acetates **85** in the presence of arylboronic acids led to (*E*)-α-arylenones **177** resulting from a cascade rearrangement-oxidative intermolecular arylation process (Scheme 3.63b).[173] Fluoride ions derived from the electrophilic fluorinating reagent are thought to encourage the transmetalation of the aryl coupling partner in this process through the formation of a boronates complex. The cross-coupled enones **177** were delivered in generally moderate yields upon treatment with PPh_3AuCl (5 mol%) and two equivalents of Selectfluor (**82**) although competitive formation of the protodeaurated, fluorodeaurated or homocoupled side-products, **86**, **92** or **94** could not be completely suppressed. An Au^I/Au^{III} redox cycle was again proposed as operative mechanism for this transformation with the oxidation of a gold(I) complex to a gold(III) fluoride species being the key elementary step.



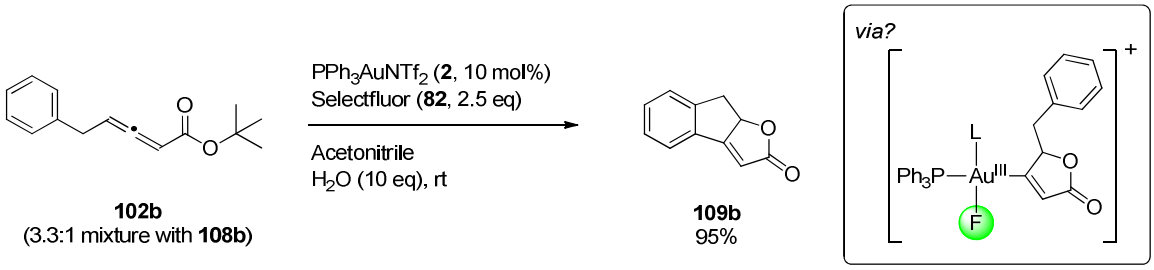
Scheme 3.63 a) Rearrangement-Oxidative Ester Migration of Propargyl Benzoates. b) Rearranegement-Oxidative Arylation of Propargyl Acetates.

More recently, spectroscopic evidence for the formation of a gold(III) fluoride complex was reported by Hammond and co-workers upon treating the gold(I) source AuCl with Selectfluor (**82**) in deuterated acetonitrile.[174] After a few minutes at room temperature, a new peak appeared at $\delta = -184$ ppm in the ^{19}F NMR spectrum of this mixture. Leaving the reaction for a few minutes longer resulted in an increase in the relative intensity of this resonance whilst the mass spectrum contained peaks consistent with gold(III) complexes. When phenylboronic acid was added, the ^{19}F NMR peak at $\delta = -184$ ppm immediately disappeared and the homocoupling product biphenyl could be detected in the crude reaction mixture (Scheme 3.64).



Scheme 3.64 *In Situ* Formation of a Gold(III) Fluoride Complex from AuCl.

A similar peak was observed when the cascade cyclisation-intramolecular arylation of *tert*-butyl allenoate **102b** was followed by ^{19}F NMR. After 10 minutes at room temperature, a small resonance was detected at $\delta = -181$ ppm which slowly disappeared over the course of the reaction (Figure 3.9). This peak was also observed when the (butenolide)gold(I) complex **104b** was treated with Selectfluor (see Scheme 3.46). Efforts to isolate this fluorinated intermediate were unsuccessful, however, and further studies would be required to confirm the tentative assignment of this peak as a gold(III) fluoride complex.



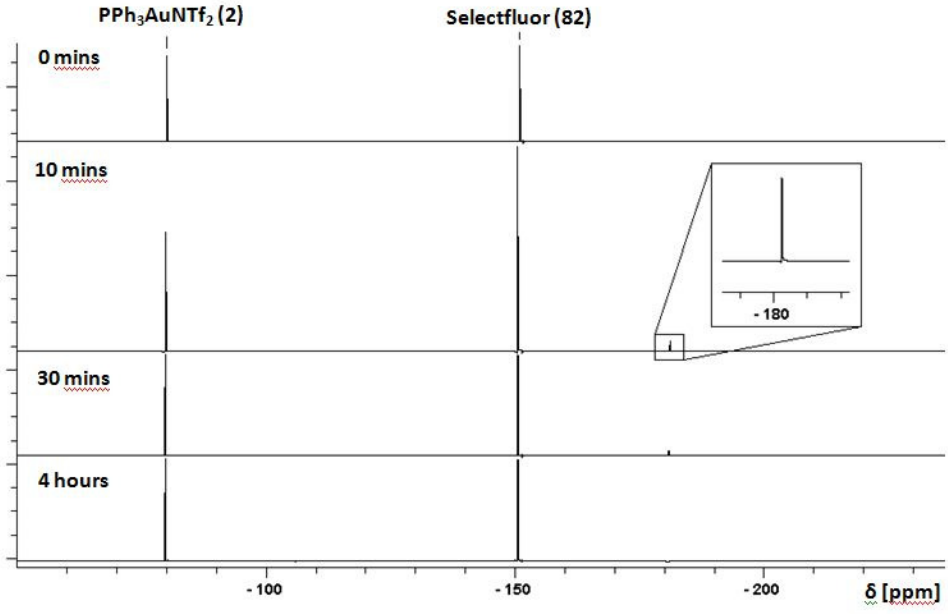
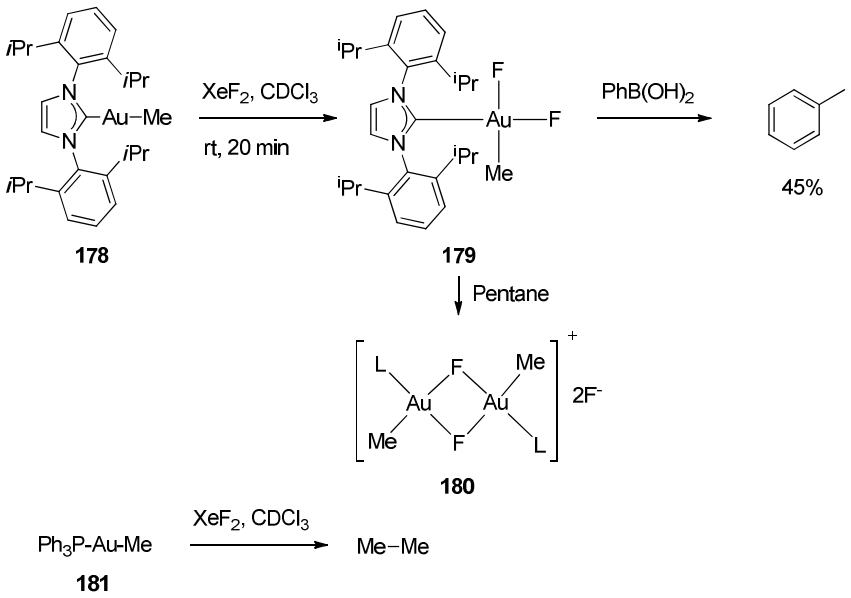


Figure 3.9 ^{19}F NMR Analysis of the Cyclisation-Intramolecular Arylation of Allenoate **102b**.

Unambiguous evidence for the oxidation of gold(I) to gold(III) by electrophilic fluorinating reagents was recently provided by Mankad and Toste.[97] The formation of two new fluorinated species was observed by ^{19}F NMR when the (methyl)gold(I) complex **178** was treated with the "F^+" source XeF_2 in deuterated chloroform. These compounds were

tentatively assigned as the *cis*- and *trans*-isomers of the difluorinated gold(III) complex **179** resulting from oxidative fluorination of the (methyl)gold(I) species. Diffusion of pentane into the reaction mixture allowed of the isolation and unambiguous characterisation of the corresponding dimeric complex **180** by X-ray crystallography. When an aryl coupling partner in the form of phenylboronic acid was added to the solution of **179**, rapid formation of the cross-coupling product toluene was observed (Scheme 3.65). The use of the *N*-heterocyclic carbene ligand IPr was essential in stabilising the gold(III) fluoride complex. Reacting the analogous phosphine-stabilised gold(I) species **181** under the same conditions led to the $C(sp^3)$-$C(sp^3)$ homocoupled product ethane.



Scheme 3.65 Preparation of a Gold(III) Fluoride upon Reacting a Gold(I) Complex with XeF_2.

3.2.7 Conclusions

In conclusion, performing the gold-catalysed 5-*endo*-trig cyclisation of benzyl-substituted *tert*-butyl allenoates **102** in the presence of the electrophilic fluorinating reagent Selectfluor (**82**) did not lead to fluorinated organic products. Instead, this reaction delivered indenofuranone products **109** and **162** resulting from a cascade cyclisation-oxidative cross-coupling process involving $C(sp^2)$-H functionalisation of the intramolecular benzyl

substituent. The phosphine-stabilised gold(I) source PPh_3AuNTf_2 (**2**) was identified as the catalyst of choice for this transformation whilst alternative external oxidants to Selectfluor were less efficient in promoting the cross-coupling process. The formation of bibutenolide side-products **110** could be completely suppressed upon performing the reaction at low concentrations. Under these conditions, indenofuranones **109** and **162** were generally delivered in moderate to excellent yields up to 95%. In addition, complete axis-to-center chirality transfer was observed when diastereoisomerically and enantiomerically-enriched allenoate starting materials were employed.

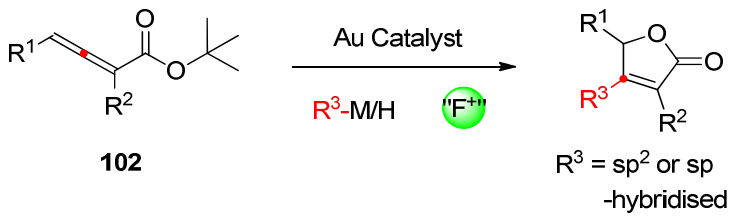
Control reactions with the proposed (butenolide)gold(I) intermediate **104b** and β-fluoro-γ-butenolide **107n** are consistent with a reaction mechanism involving a Au^I/Au^{III} redox cycle. In this process, Selectfluor is thought to act as a stoichiometric external oxidant, performing the key oxidation of gold(I) to gold(III) in the catalytic cycle.

Chapter 4

Gold and F^+: Gold-Catalysed Oxidative Coupling II – Intermolecular Coupling

4.1 Introduction

With a cascade nucleophilic addition-intramolecular oxidative coupling reaction validated with benzyl-substituted *tert*-butyl allenoates **102**,[105] we sought to investigate the scope and limitations of gold-catalysed coupling reactions performed in the presence of the electrophilic fluorinating reagent Selectfluor (**82**). Using the 5-*endo*-trig cyclisation of *tert*-butyl allenoates **102** as a model transformation, the viability of gold-catalysed homo- and cross-coupling reactions with a selection of intermolecular coupling partners was examined (Scheme 4.1). In the first section of this chapter, the cyclisation-homodimerisation of allenoates performed both in the absence and in the presence of Selectfluor is discussed. This is followed in the subsequent section by the results of our study into intermolecular oxidative cross-coupling with non-activated alkyne coupling partners.

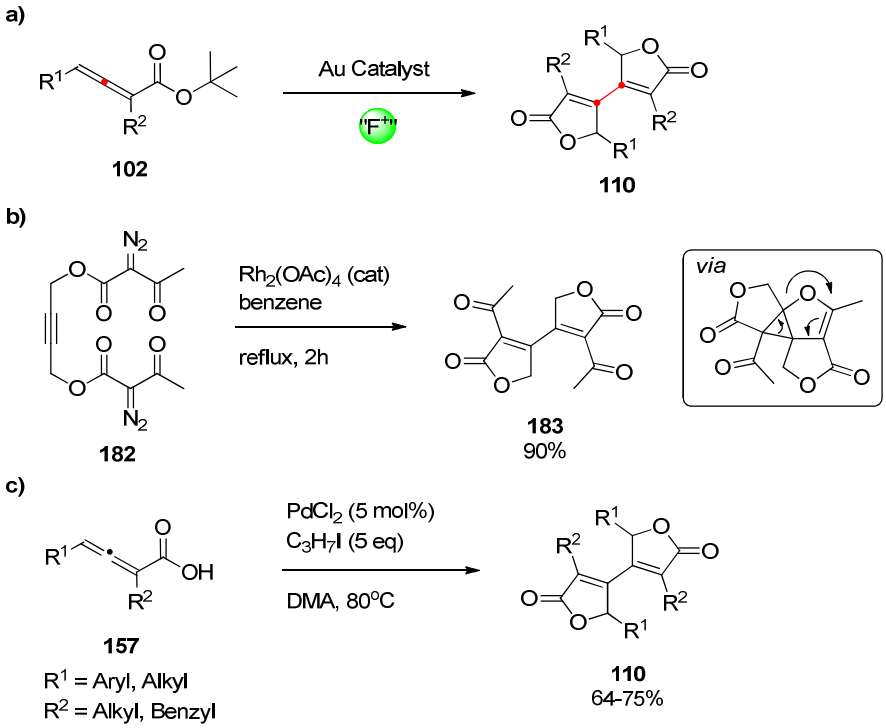


Scheme 4.1 Cascade Cyclisation-Intermolecular Coupling of Allenoates.

4.2 Cyclisation-Homodimerisation of *tert*-Butyl Allenoates

4.2.1 Introduction

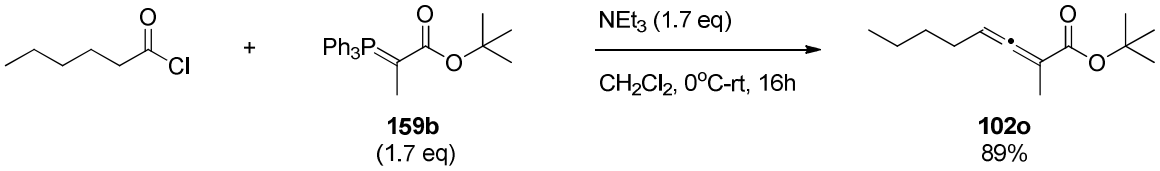
During our preliminary studies into the cascade cyclisation-intramolecular arylation of benzyl-substituted *tert*-butyl allenoates **102** (see Chapter 3),[105] bibutenolides **110** resulting from a cyclisation-homodimerisation process were often observed as minor side-products. As an initial study, we sought to investigate whether *tert*-butyl allenoates could be selectively transformed into these homocoupled compounds in the absence of a competing intramolecular coupling pathway (Scheme 4.2a). Synthetic routes towards bibutenolides **110** are extremely scarce in the literature. In 1990, Kinder and Padwa reported the synthesis of the 2-acetyl-substituted bibutenolide **182** upon treating the bis(diazo)ester **183** with catalytic amounts of $Rh_2(OAc)_4$ (Scheme 4.2b).[175-176] More recently, palladium(II) catalysts have been shown to mediate the cascade cyclisation-homodimerisation of allenic acids **157** to afford bibutenolide compounds in the presence of external oxidants (see Scheme 4.2c).[162-164]



Scheme 4.2 a) Gold and "F+"-Mediated Cyclisation-Homodimerisation of *tert*-Butyl Allenoates. b) Rhodium-Catalysed Cyclisation of Bis(diazo)ester **182**. c) Palladium-Catalysed Cyclisation-Homodimerisation of Allenic Acids.

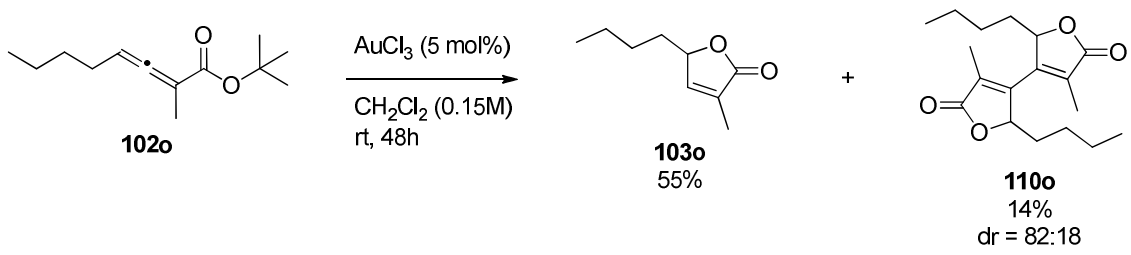
4.2.2 Preliminary Studies Using Sub-Stoichiometric Gold

The alkyl-substituted *tert*-butyl allenoate **102o** was identified as a suitable test substrate for use in our preliminary investigations. This compound was prepared in 89% yield from hexanoyl chloride and phosphorus ylid **159b** according to the standard Wittig method discussed in Section 3.2.4 (Scheme 4.3). In accordance with the benzyl-substituted substrates prepared from ylid **159b**, compound **102o** was isolated as a pure allenoate without contamination with its alkyne isomer.



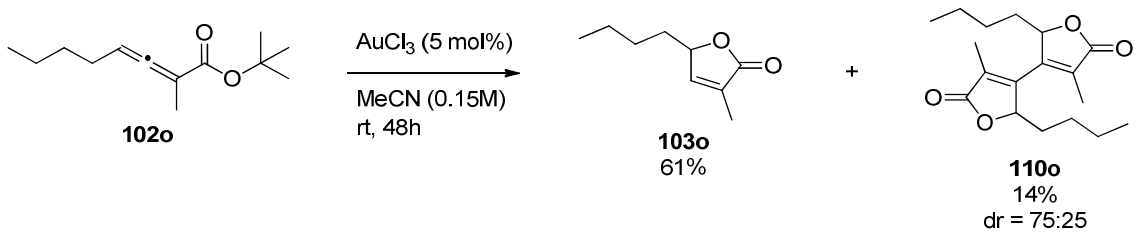
Scheme 4.3 Preparation of *tert*-Butyl Allenoate **102o**.

As an initial experiment, the allenoate **102o** was reacted with 5 mol% of gold(III) chloride in dichloromethane under the conventional cyclisation-protodeauration conditions reported by Shin and co-workers (see Scheme 3.1).[100] After stirring at room temperature for 48 hours, the expected γ-butenolide **103o** was isolated in 55% yield upon purification by silica gel column chromatography. To our surprise, however, the cyclisation-protodeauration product was not the only compound produced during this reaction. An 82:18 mixture of the separable bibutenolide diastereoisomers **110o** resulting from a cascade cyclisation-homodimerisation process were also isolated in 14% yield (Scheme 4.4).



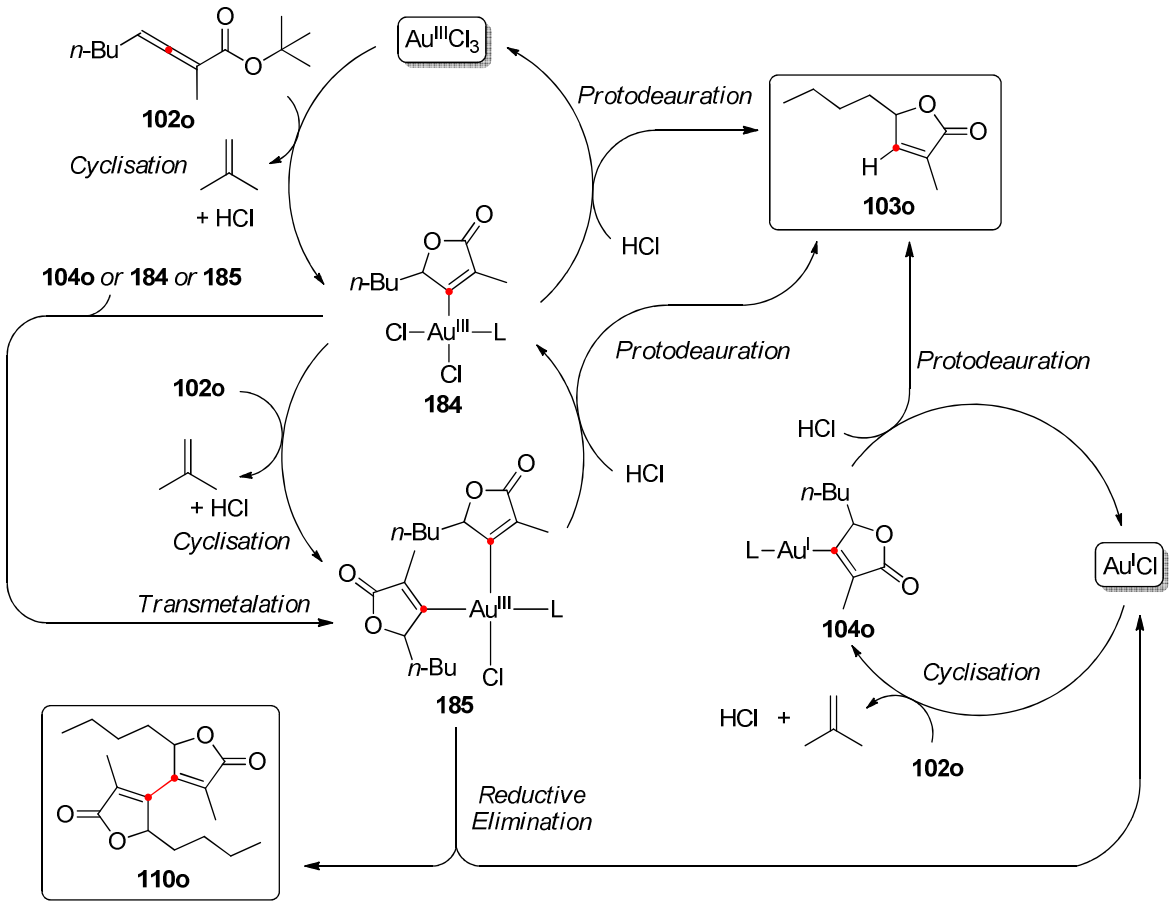
Scheme 4.4 Cyclisation-Homocoupling of Allenoate **102o** Mediated by 5 mol% of Gold(III) in Dichloromethane.

Similar results were obtained upon performing the reaction in acetonitrile. The diastereoisomeric bibutenolides **110o** were delivered in a combined yield of 14% under these conditions (dr = 75:25) whilst the cyclisation-protodeauration product **103o** was isolated in 61% yield (Scheme 4.5).



Scheme 4.5 Cyclisation-Homocoupling of Allenoate **102o** Mediated by 5 mol% of Gold(III) in Acetonitrile.

In these reactions, homodimerisation of the butenolide units formed upon cyclisation of the allenoate seemingly competes with the conventional protodeauration pathway. Similar reactivity was observed by the groups of Hashmi,[155] Pale[157] and Fustero[156] upon performing alkyne and allene nucleophilic addition reactions in the presence of gold(III) salts (see Section 3.2.2.2). A homocoupling mechanism involving a reductive elimination step from a diorganogold(III) complex was proposed for these processes and, at first glance, an analogous pathway can be assumed for the formation of the bibutenolides **110o** (Scheme 4.6).



Scheme 4.6 Proposed Mechanism for the Formation of γ-Butenolide **103o** and Bibutenolide **110o**. L = Neutral Ligand.

In the first stage of this mechanism, the gold(III) ion activates the allene moiety in substrate **102o** towards intramolecular nucleophilic attack of the pendant ester oxygen leading to the (butenolide)gold(III) complex **184**.[w] Protodeauration of this species in the presence of hydrochloric acid would deliver the major γ-butenolide product **103o** and regenerate $AuCl_3$. Alternatively, the gold(III) species **184** could mediate the 5-*endo*-trig cyclisation of a second molecule of the starting material leading to the doubly butenolide-substituted gold(III) complex **185**. Transmetalation of a butenolide unit from any one of the (butenolide)gold species **184**, **185** or **104o** onto complex **184** would also lead to the same intermediate. Protodeauration of complex **185** would again deliver the hydrofunctionalisation product

[w] The fourth coordination site in the square-planar complex is most likely occupied by a neutral ligand present in the reaction mixture.

103o and regenerate the (butenolide)gold(III) species **184**. However, the bis(butenolide)gold(III) species **185** could instead undergo carbon-carbon bond-forming reductive elimination to afford the homocoupled bibutenolide product **110o**. This elementary step also results in the formation of one molecule of gold(I) chloride, which can itself mediate the conventional 5-*endo*-trig cyclisation process leading to γ-butenolide **103o** upon protodeauration of the (butenolide)gold(I) complex **104o**.

On closer inspection, however, the mechanism shown in Scheme 4.6 cannot fully account for the product distribution observed upon treating allenoate **102o** with catalytic $AuCl_3$. For every two molecules of allenoate **102o** converted into the bibutenolide **110o**, one molecule of the gold(III) salt is reduced to gold(I) chloride. As such, in the absence of an external oxidant, the maximum possible yield of the oxidative homocoupling product is equal to twice the loading of the gold(III) catalyst. The 14% isolated yield of the bibutenolide **110o** is, therefore, not consistent with the above mechanism based on a 5 mol% loading of $AuCl_3$.

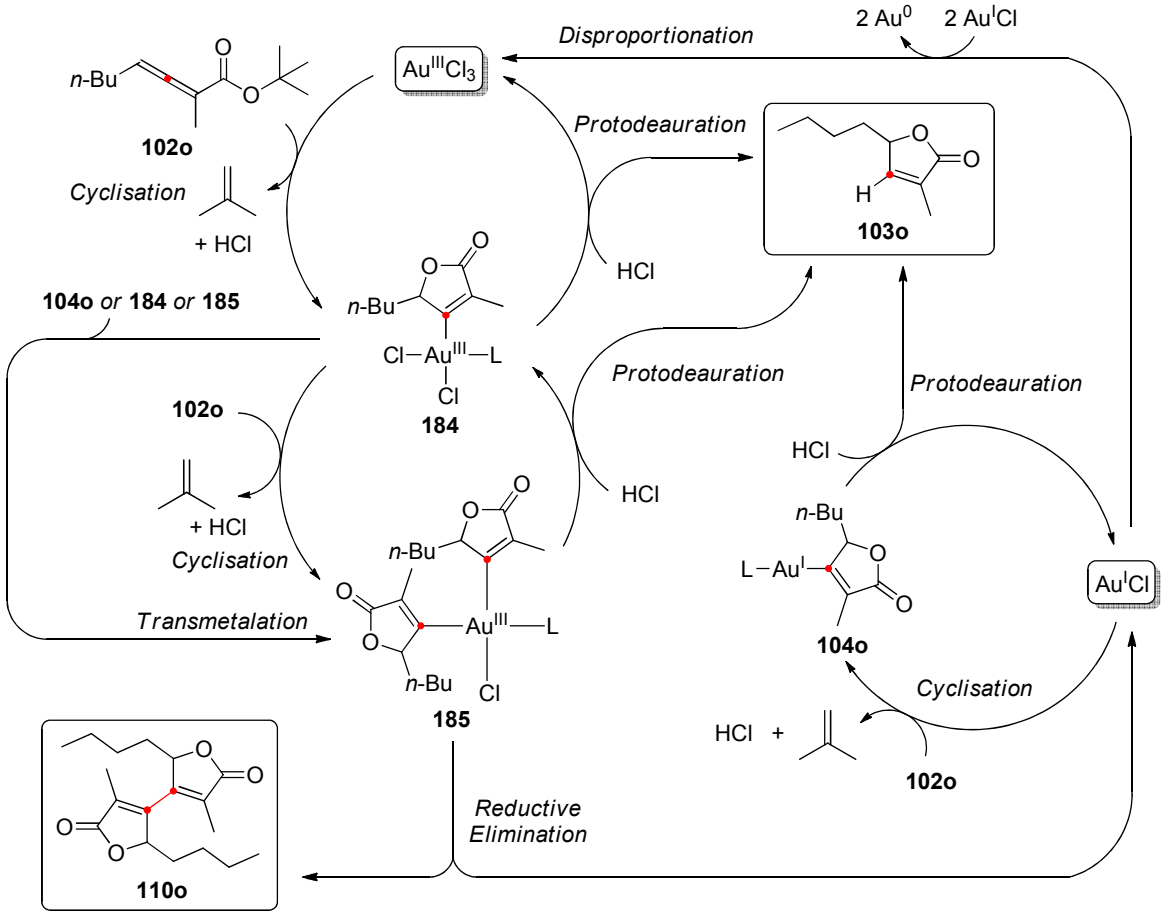
An amended mechanistic explanation for the reaction between *tert*-butyl allenoate **102o** and catalytic $AuCl_3$ is shown in Scheme 4.7. As well as mediating the conventional cyclisation-protodeauration process, the gold(I) chloride formed upon reductive elimination from complex **185** could feasibly disproportionate under the reaction conditions to afford elemental gold(0) and $AuCl_3$. Colloids of gold were generated during the course of the allenoate cyclisation process whilst a mirror of Au^0 was deposited on the walls of the reaction vessel. The gold(III) formed upon disproportionation could then mediate the cyclisation-oxidative homodimerisation process accounting for the higher than expected observed yield of the bibutenolide **110o**. The maximum theoretical yield of the homocoupled product in this case can be calculated using the following equation.

$$\text{Maximum Theoretical Yield of } \mathbf{110o} = (5 \times 2)\left[1 + \sum_{n}^{\infty}\left(\frac{1}{3}\right)^{n}\right]\%$$

$$= 10\left[1 + \frac{1}{2}\right]\%$$

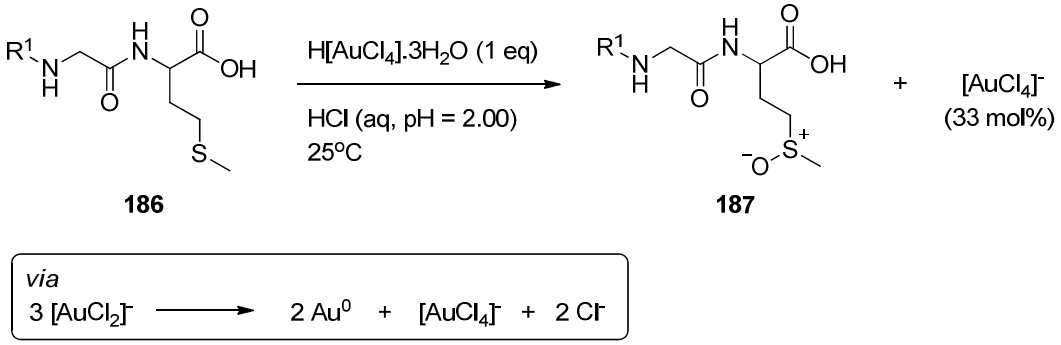
$$= 15\%$$

The disproportionation of three molecules of gold(I) chloride results in the formation of two equivalents of gold(0) and one molecule of gold(III) chloride. As such, a third of the gold(I) generated upon reductive elimination can itself mediate the conversion of two more molecules of the allenoate into bibutenolide **110o**. Overall, this pathway can account for the formation of 5% of the homocoupled product leading to a total maximum yield of 15% based on a 5 mol% loading of the gold(III) chloride catalyst.



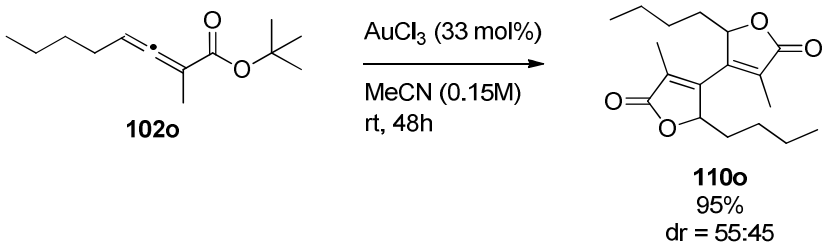
Scheme 4.7 Amended Mechanism for the Formation of γ-Butenolide **103o** and Bibutenolide **110o**. L = Neutral Ligand.

The disproportionation of gold(I) is an energetically favourable process and has been widely documented in aqueous solutions.[177-180] The *in situ* formation of $[AuCl_4]^-$ and Au^0 from $[AuCl_2]^-$ was recently reported by Djuran and co-workers during the gold(III)-mediated oxidation of methionine residues in glycyl-D,L-methionine derivatives **186**.[181] Treating these compounds with one equivalent of $H[AuCl_4].3H_2O$ resulted in the quantitative formation of the corresponding sulfoxides **187** (Scheme 4.8). However, no gold(I) species were observed in the reaction mixture and UV-visible spectroscopy indicated that approximately 33% of the $[AuCl_4]^-$ remained present in the solution.



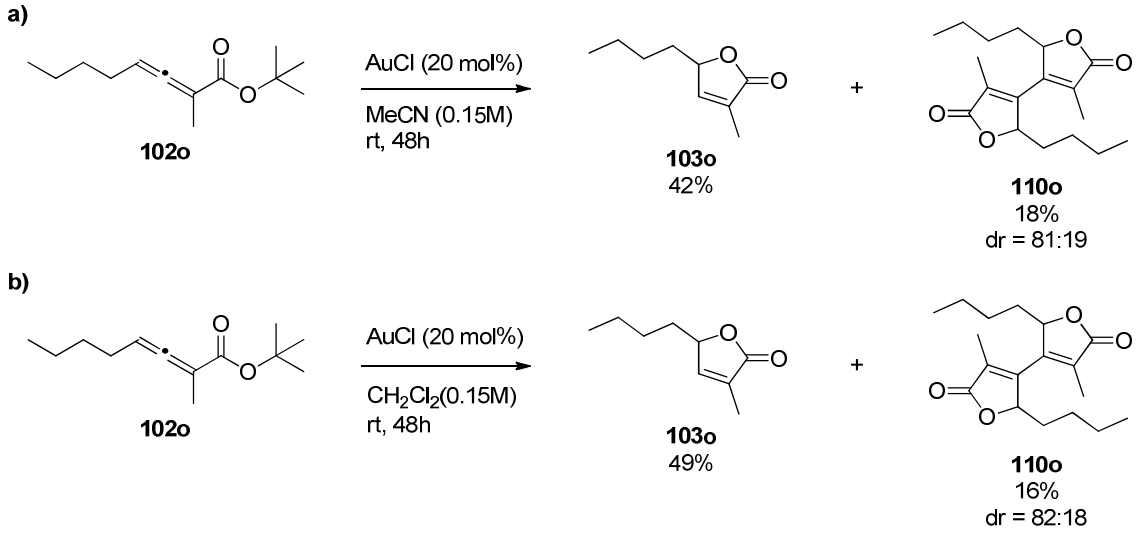
Scheme 4.8 Proposed Disproportionation of Gold(I) During the Gold(III)-Mediated Oxidation of Methionine.

If a mechanism of the type shown in Scheme 4.7 is operative, the homocoupled bibutenolide product **110o** could theoretically be delivered in quantitative yield upon increasing the gold(III) loading to 33 mol%. In order to test this hypothesis, *tert*-butyl allenoate **102o** was reacted with this quantity of $AuCl_3$ in acetonitrile at room temperature. After 48 hours, only a trace amount of the cyclisation-protodeauration product could be detected by crude NMR analysis with the majority of the allenoate substrate being smoothly converted into the bibutenolide **110o** (Scheme 4.9). This compound was isolated in 95% yield as a 55:45 diastereoisomeric mixture upon purification by silica gel column chromatography.



Scheme 4.9 Cyclisation-Homocoupling of Allenoate **102p** Mediated by 33 mol% of Gold(III) in Acetonitrile.

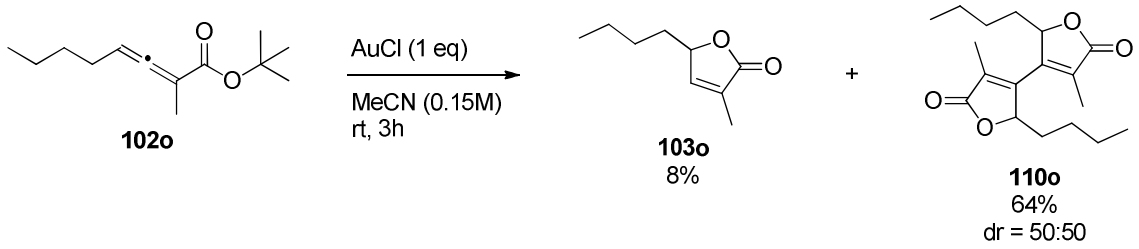
Further support for a mechanism involving the disproportionation of gold(I) into gold(III) was provided upon treating the allenoate with AuCl. After 48 hours at room temperature, the reaction between substrate **102o** and 20 mol% of the gold(I) source in acetonitrile delivered the bibutenolide **110o** in 18% isolated yield (dr = 81:19, Scheme 4.10a). A maximum theoretical homocoupling yield of 20% would be predicted for this process based on an Au^{I} loading of 20 mol%. The bibutenolide **110o** was isolated in 16% yield (dr = 82:18) upon performing the reaction under the same conditions in dichloromethane (Scheme 4.10b).



Scheme 4.10 Cyclisation-Homocoupling of Allenoate **102o** Mediated by 20 mol% of Gold(I) in a) Acetonitrile and b) Dichloromethane.

Moreover, when *tert*-butyl allenoate **102o** was treated with one equivalent of gold(I) chloride in acetonitrile at room temperature, the cascade cyclisation-homocoupling process was observed as the major reaction pathway. Bibutenolide **110o** was furnished in 64% yield

under these conditions (dr = 50:50) with only 8% of the cyclisation-protodeauration product **103o** being isolated upon silica gel column chromatography (Scheme 4.11). To the best of our knowledge, these reactions are the first examples of a cascade cyclisation-oxidative coupling process performed only in the presence of a gold(I) source.



Scheme 4.11 Cyclisation-Homocoupling of Allenoate **102o** Mediated by one Equivalent of Gold(I) in Acetonitrile.

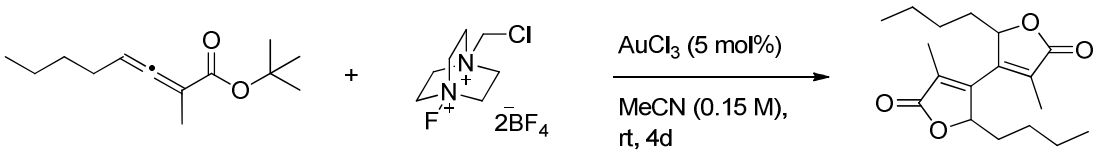
Taken together, these reactions indicate that the cascade cyclisation-homodimerisation of allenoate **102o** is a more favourable process than the conventional cyclisation-protodeauration pathway in the presence of $AuCl_3$. Furthermore, the gold(I) formed during the coupling process can itself mediate the formation of the bibutenolide products with the homocoupling reaction actually out-competing hydrofunctionalisation under these conditions. Whilst further studies are required to determine the exact mechanism by which Au^I mediates the oxidative coupling process, a pathway involving the disproportionation of the low-valent metal into Au^0 and Au^{III} is consistent with the results obtained during this study. Alternatively, a reaction mechanism involving a bimetallic reductive elimination from two (butenolide)gold(I) complexes of type **104o** could explain the observed reactivity. Similar pathways have been proposed by Ritter and co-workers in the coupling reactions of palladium(III) and silver(II) species.[182-188] However, bimetallic reductive elimination has not been validated for Au^I and further mechanistic work would be required to determine the feasibility of this pathway from (butenolide)gold(I) complexes **104**. A heterogeneous coupling mechanism catalysed by colloidal gold formed during the reaction can also not be ruled out. A cascade cyclisation-oxidative homocoupling reaction proceeding via this

pathway was recently reported by Stratakis and co-workers upon reacting aryl propargyl ethers in the presence of gold nanoparticles supported on titanium oxide.[189] However, a heterogeneous catalysis mechanism of this type would not account for the correlation between the bibutenolide yield and the catalyst loading observed during this study.

4.2.3 Development of the Gold-Catalysed Process Using Selectfluor

4.2.3.1 Preliminary Studies

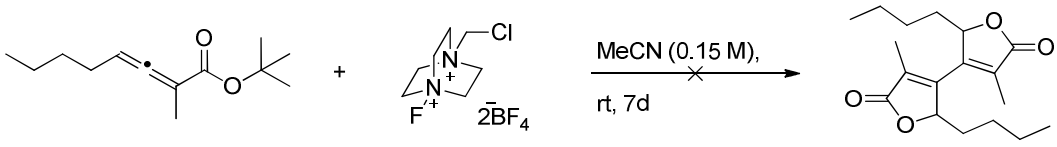
With the feasibility of the cascade cyclisation-oxidative homodimerisation reaction established using sub-stoichiometric amounts of gold, our attention turned to the development of the gold-catalysed process performed in the presence of the electrophilic fluorinating reagent Selectfluor (**82**). As a preliminary experiment, 2.5 equivalents of the "F^+" source were added to a solution of the alkyl-substituted *tert*-butyl allenoate **102o** and gold(III) chloride (5 mol%) in acetonitrile. Pleasingly, smooth conversion into the bibutenolide **110o** was observed after 4 days at room temperature with no trace of the cyclisation-protodeauration product **103o** detected by crude NMR analysis. The homocoupled product was isolated as a 57:43 diastereoisomeric mixture in 64% yield upon purification by silica gel column chromatography (Scheme 4.12).



102o + Selectfluor **82** (2.5 eq) → **110o** 64% dr = 57:43

Scheme 4.12 Cyclisation-Homodimerisation of Allenoate **102o** Catalysed by $AuCl_3$ in the Presence of Selectfluor.

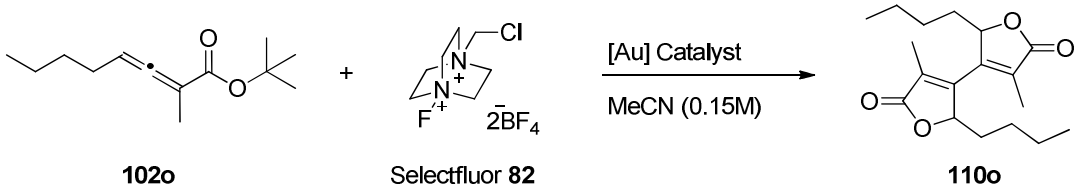
In order to confirm that the homocoupling process was indeed catalysed by gold, *tert*-butyl allenoate **102o** was treated under the same conditions in the absence of $AuCl_3$. This reaction led only to recovered starting material after 7 days at room temperature with no cyclised products detected upon crude NMR analysis (Scheme 4.13).



Scheme 4.13 Control Reaction Performed in the Absence of $AuCl_3$.

4.2.3.2 Optimisation of the Reaction Conditions

Having established the feasibility of the gold-catalysed oxidative homocoupling process, a brief optimisation study was carried out with the aim of identifying standard reaction conditions (Table 4.1).



Entry	Catalyst	Equivalents of Selectfluor (**82**)	Temp.	Time	Yield (dr)[a]
1	$AuCl_3$ (5 mol%)	2.5	rt	4d	64% (57:43)
2	No Catalyst	2.5	rt	7d	---[b]
3	PPh_3AuCl (5 mol%)	2.5	rt	5d	52% (66:34)
4	IPrAuCl (**158**, 5 mol%)	2.5	rt	7d	---[b]
5	PPh_3AuNTf_2 (**2**, 5 mol%)	2.5	rt	4d	---[c]
6	$AuCl_3$ (5 mol%)	2.5	80ºC	1h	78% (52:48)
7	$AuCl_3$ (5 mol%)	1.2	80ºC	1h	73% (50:50)
8	$AuCl_3$ (1 mol%)	2.5	80ºC	16h	14% (50:50)

[a] Isolated yields. Diastereoisomeric ratio of the purified products determined by ^{1}H NMR. [b] No consumption of the allenoate observed. [c] Complex reaction mixture.

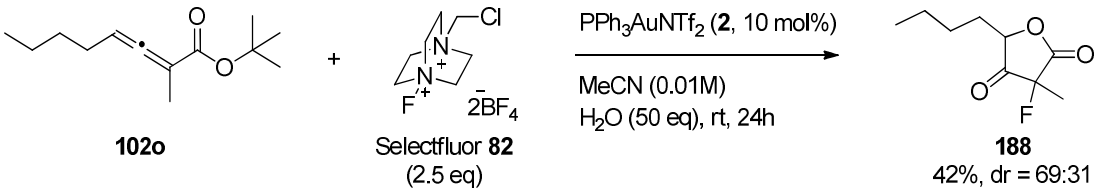
Table 4.1 Optimisation of the Reaction Conditions.

In each case, the gold catalyst and Selectfluor (**82**) were stirred with the *tert*-butyl allenoate **102o** (1 eq) in acetonitrile (0.15M) at the designated temperature. Upon complete

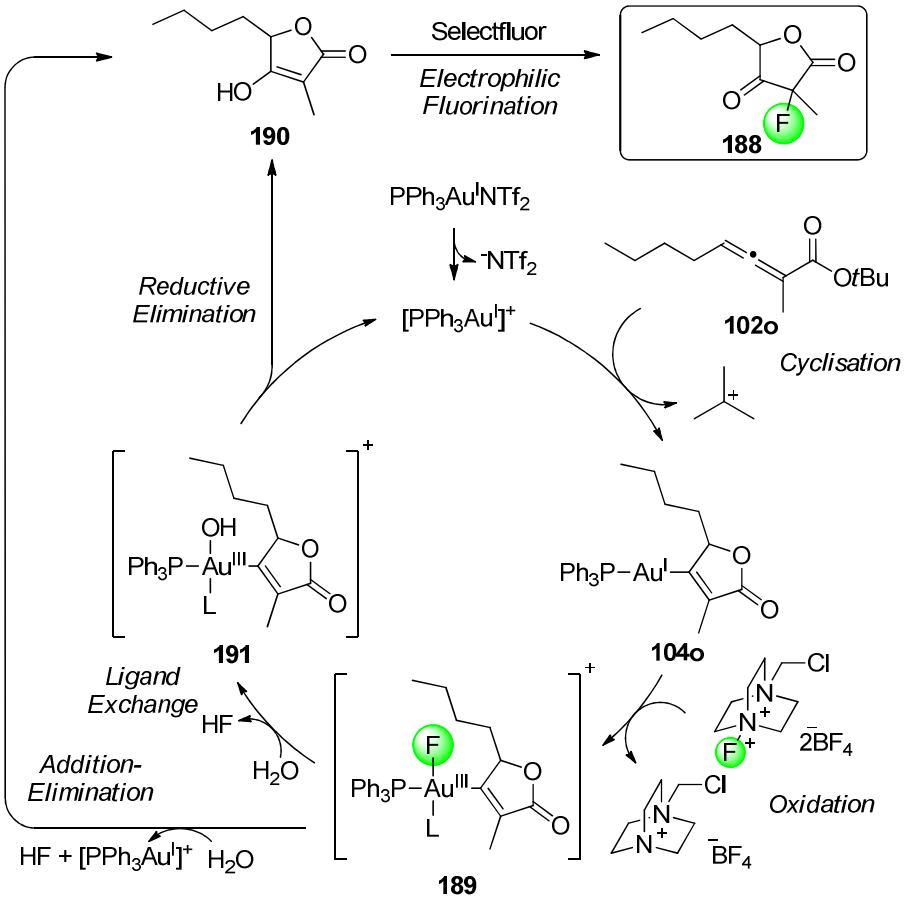
consumption of the starting material or after 7 days, the crude reaction mixture was filtered through Celite, concentrated *in vacuo* and purified by column chromatography on silica gel. As an initial study, the efficiency of a selection of gold catalysts was investigated. Performing the cyclisation-oxidative homodimerisation reaction in the presence of the commercially-available gold(I) source PPh_3AuCl (5 mol%) led to the desired bibutenolide **110o** as the only product after 5 days at room temperature (Table 4.1, Entry 3). However, the homocoupled compound was furnished in a lower isolated yield of 52% (dr = 66:34) using this catalyst. By contrast, the *N*-heterocyclic carbene-stabilised gold(I) source IPrAuCl (**158**) did not catalyse the oxidative coupling process when reacted with substrate **102o** and 2.5 equivalents of Selectfluor (**82**) in acetonitrile. The allenoate starting material remained unreacted after 7 days at room temperature under these conditions (Table 4.1, Entry 4). In our previous study on the related cascade cyclisation-intramolecular arylation of benzyl-substituted *tert*-butyl allenoates, the highest yields of the cross-coupled products were obtained using the phosphine-stabilised gold(I) complex PPh_3AuNTf_2 (**2**, see Section 3.2.3). This species, however, was not a suitable catalyst for the cascade cyclisation-homocoupling process. Treating allenoate **102o** with Selectfluor (2.5 eq) and 5 mol% of complex **2** in acetonitrile (0.15M) led to a complex mixture of organic products with only a trace amount of the desired bibutenolide **110o** (Table 4.1, Entry 5). Interestingly, this reaction delivered trace amounts of the fluorinated cyclic β-ketoester **188** resulting from a cascade cyclisation-oxidative hydrolysis-fluorination process. This compound was delivered as the major product in up to 42% isolated yield (dr = 67:33) when the allenoate cyclisation process was conducted in the presence of water (50 eq, Scheme 4.14).

The formation of this product is consistent with the mechanism shown in Scheme 4.15. Activation of the allene moiety in the allenoate by gold(I) followed by intramolecular nucleophilic attack would lead to the (butenolide)gold(I) complex **104o**. Oxidation of this

species in the presence of Selectfluor (**82**) would then deliver the gold(III) fluoride intermediate **189**. This species could feasibly react with water in a Michael-type addition-elimination process leading to the cyclic enol **190**. Alternatively, water could first coordinate to the gold(III) centre to afford the hydroxide complex **191** prior to C-O bond-forming reductive elimination. Direct electrophilic fluorination of enol **190** by a second equivalent of Selectfluor would then deliver the α-fluoro-β-ketoester **188**.

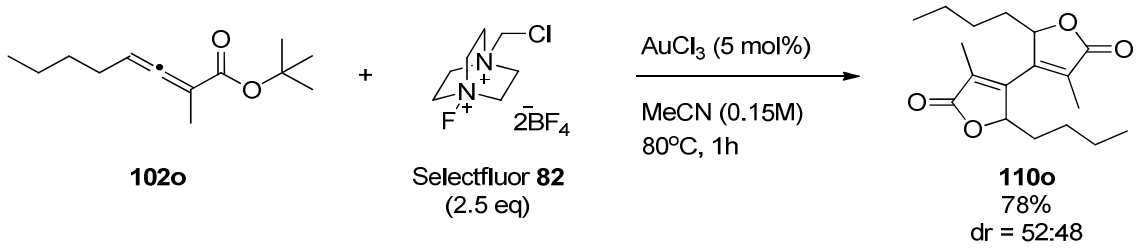


Scheme 4.14 Formation of the Fluorinated Cyclic β-Ketoester **188** from Allenoate **102o**.



Scheme 4.15 Proposed Mechanism for the Formation of the Cyclic α-Fluoro-β-ketoester **188**.

Having identified gold(III) chloride as the optimum catalyst for the homodimerisation reaction, our attention turned to the other reaction parameters. With the aim of shortening the reaction time, the cascade cyclisation-oxidative homocoupling process was conducted at elevated temperatures. Complete consumption of the allenoate starting material was observed within one hour when substrate **102o** was reacted with $AuCl_3$ (5 mol%) and Selectfluor (**82**, 2.5 eq) in acetonitrile (0.15M) at 80ºC (Table 4.1, Entry 6). The corresponding separable bibutenolides **110o** were isolated as a 52:48 diastereoisomeric mixture in a combined yield of 78% from this reaction (Scheme 4.16).

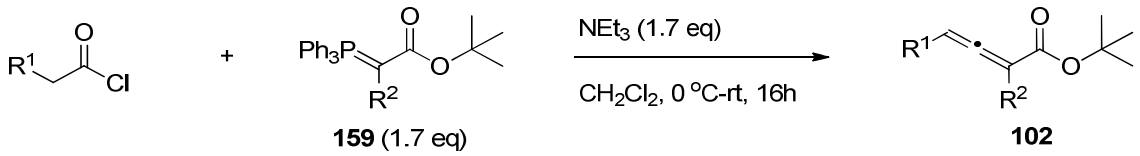


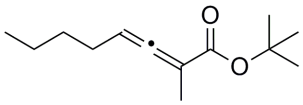
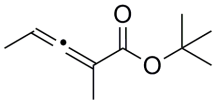
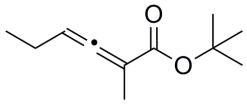
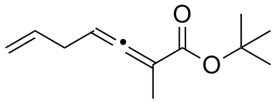
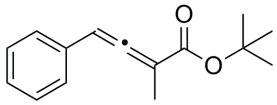
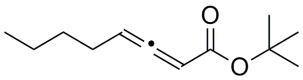
Scheme 4.16 Cyclisation-Homodimerisation of Allenoate **102o** at 80ºC.

Decreasing the amount of Selectfluor (**82**) to 1.2 equivalents had little effect on the reaction efficiency. The bibutenolide **110o** was isolated in a slightly lower yield of 73% (dr = 50:50) under these conditions (Table 4.1, Entry7). By contrast, reducing the loading of the gold(III) catalyst to 1 mol% resulted in a significantly messier reaction with the desired cyclisation-homocoupling product being delivered in only 14% yield after 16 hours (Table 4.1, Entry 8).

4.2.3.3 Preparation of *tert*-Butyl Allenoates 102o-t

Having established standard reaction conditions, we sought to investigate the scope and limitations of the cascade cyclisation-homodimerisation process with a range of *tert*-butyl allenoates **102**. These compounds were prepared according to the general Wittig procedure discussed in Section 3.2.4 (Table 4.2).

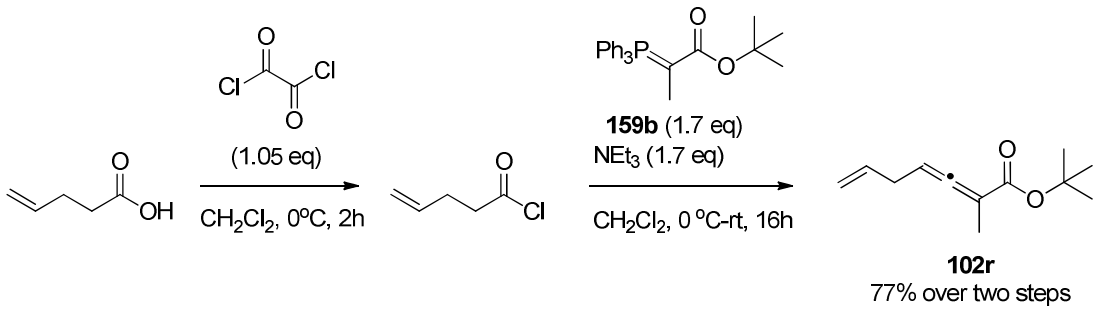


Entry	R^1	R^2	Product **102**	Yield[a]
1	*n*-C_4H_9	Me		**102o** 89%
2	Me	Me		**102p** 40%
3	C_2H_5	Me		**102q** 26%
4	$CH_2CH{=}CH_2$	Me		**102r** 77%[b]
5	Ph	Me		**102s** 20%
6	*n*-C_4H_9	H		**102t** 36%[c]

[a] Isolated yield. [b] The acid chloride was prepared from the corresponding carboxylic acid and thus the yield was calculated over two steps. [c] Isolated as a 3.5:1 mixture with its isomeric alkyne **108t**. Yield refers to the amount of allenoate **102t** present.

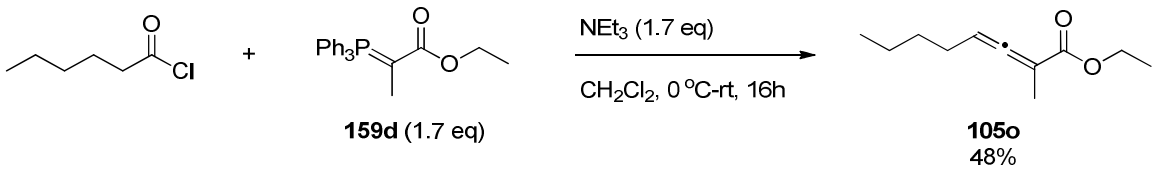
Table 4.2 Preparation of *tert*-Butyl Allenoates **102o-t**.

The majority of the substrates were prepared from the methyl-substituted phosphorus ylid **159b** as these allenoates do not suffer from contamination with the isomeric alkyne impurities **108** (see Section 3.2.4). The methyl and ethyl-substituted *tert*-butyl allenoates **102p** and **102q** were synthesised from ylid **159b** and the corresponding acid chlorides in 40% and 26% yield respectively (Table 4.2, Entries 2-3). Substrate **102r** bearing an allyl substituent at the 4-position was prepared via the two-step protocol shown in Scheme 4.17. Firstly, pent-4-enoic acid was treated with oxalyl chloride to afford the corresponding acid chloride amenable to the Wittig process with phosphorus ylid **159b**. The desired allenoate was delivered in 77% yield over two steps upon purification by silica gel chromatography (Table 4.2, Entry 4).



Scheme 4.17 Preparation of *tert*-Butyl Allenoate **102r**.

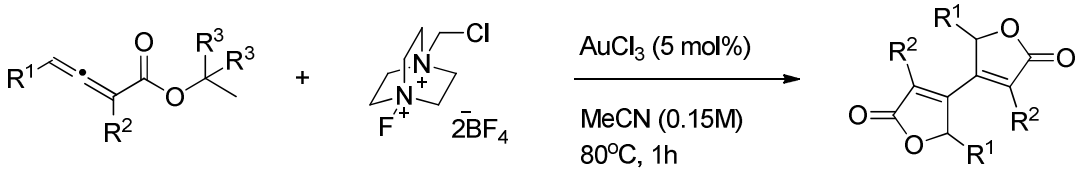
The phenyl-substituted allenoate **102s** was furnished in 20% yield upon reacting phenylacetyl chloride with phosphorus ylid **159b** under the standard conditions (Table 4.2, Entry 5). In accordance with the benzyl-substituted allenoates bearing a hydrogen at the 2-position (see Section 3.2.4), substrate **102t** was prepared as a mixture with its isomeric alkyne **108t** (**102t**:**108t** = 3.5:1). The desired allenoate was delivered in a corrected yield of 36% yield from hexanoyl chloride and phosphorus ylid **159a**. In order to probe the effect the ester substituent, the ethyl allenoate **105o** was synthesised in 48% yield using the commercially-available phosphorus ylid **159d** (Scheme 4.18).



Scheme 4.18 Preparation of Ethyl Allenoate **105o**.

4.2.3.4 Scope and Limitations of the Coupling Process

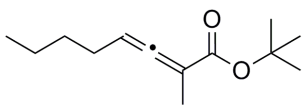
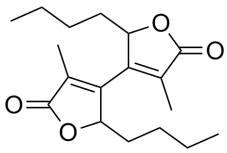
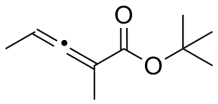
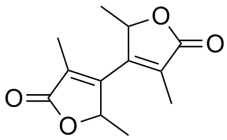
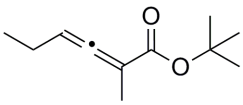
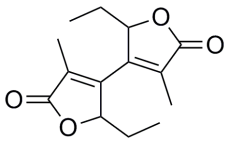
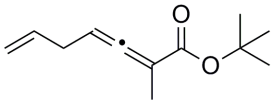
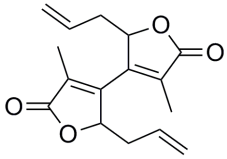
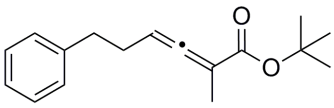
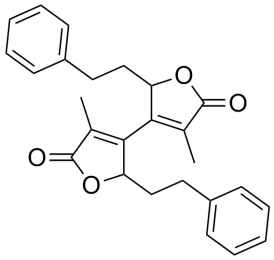
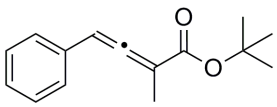
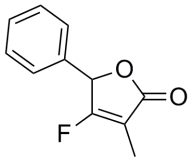
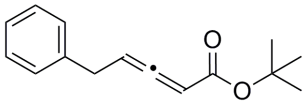
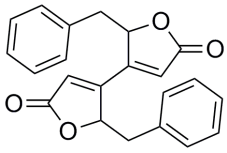
With a range of allenoates in hand, the scope and limitations of the gold-catalysed cascade cyclisation-oxidative homodimerisation process were investigated. The results of these experiments are summarised in Table 4.3.

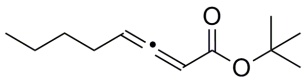
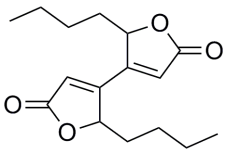
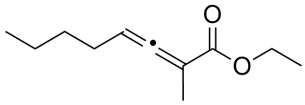


102 (R^3 = Me)
105 (R^3 = H)

Selectfluor **82** (2.5 eq)

110

Entry	Allenoate **102** or **105**	Major Product	Yield[a]	dr[b]
1			**110o** 78%	52:48
2			**110p** 36%[c]	50:50
3[f]			**110q** 79%[c]	55:45
4			**110r** 46%[c]	50:50
5			**110f** 43%	50:50
6[d]			**107s** 26%	---
7[e]			**110b** 60%[f][g]	52:48

8[h]			**110t** 91%[f]	52:48
9[i]		Complex Reaction Mixture	---	---

[a] Isolated yield. [b] Diastereoisomeric ratio of the purified products determined by ^{1}H NMR. [c] The diastereoisomers were inseparable by silica gel column chromatography. [d] The reaction was stirred for two hours. [e] Allenoate **102b** employed as a 2.6:1 mixture with its isomeric alkyne **108b**. The amounts of the reagents were calculated with respect to the combined amount of **102b** and **108b**. [f] Yield calculated relative to the allenoate **102**. [g] The indenofuranone **109b** was also produced in 37% yield (relative to **102b**) in this reaction. [h] Allenoate **102t** employed as a 3.5:1 mixture with its isomeric alkyne **108t**. The amounts of the reagents were calculated with respect to the combined amount of **102t** and **108t**. [i] The reaction was stirred for 16 hours.

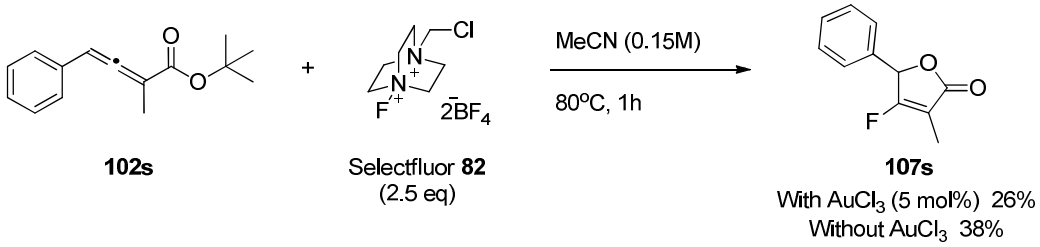
Table 4.3 Cyclisation-Homodimerisation of Allenoates **102** and **105**.

In each case, the allenoate was treated with gold(III) chloride (5 mol%) and Selectfluor (**82**, 2.5 eq) in acetonitrile (0.15M) at 80ºC. The reactions were monitored by TLC and complete consumption of the starting material was observed after one hour in most cases. After cooling to room temperature and filtration through Celite, the crude reaction mixtures were analysed by NMR spectroscopy and purified. Whilst the bibutenolide products **110** were generally delivered with low levels of diastereoselectivity, in some cases, the isomers could be at least partially separated upon silica gel column chromatography.

The alkyl-substituted *tert*-butyl allenoates **102p** and **102q** were readily transformed into the corresponding bibutenolides **110p** and **110q** under these conditions. Whilst the ethyl-substituted homodimer **110q** was delivered in 79% yield, the related bibutenolide **110p** was noticeably unstable on silica gel and was isolated in only 36% yield (Table 4.3, Entries 2-3). *tert*-Butyl allenoate **102r**, bearing an allyl substituent at the 4-position, was also amenable to the cyclisation-homodimerisation process. The corresponding bibutenolide **110r** was delivered as a 50:50 mixture of diastereoisomers in 46% yield upon silica gel column chromatography (Table 4.3, Entry 4). Whilst the homobenzyl-substituted allenoate **102f** was not a suitable substrate for the cascade cyclisation-intramolecular arylation process (see

Section 3.2.5), reacting this substrate with $AuCl_3$ and Selectfluor led smoothly to the corresponding bibutenolide **110f** in 43% yield after one hour at 80ºC (Table 4.3, Entry 5).[x]

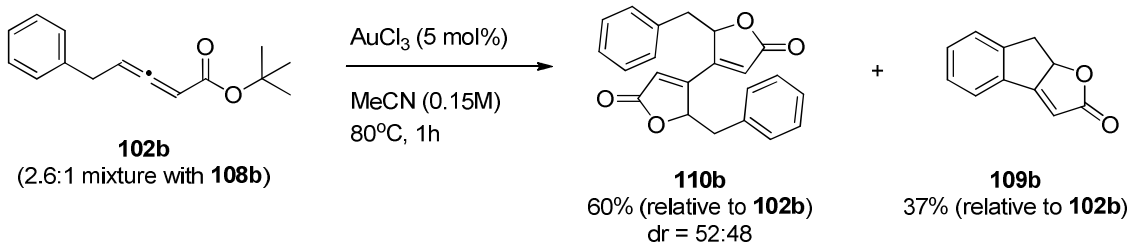
At this stage, the efficiency of the cascade cyclisation-homodimerisation process with an allenoate bearing a phenyl group at the 4-position was investigated. *tert*-Butyl allenoate **102s** was treated with $AuCl_3$ and Selectfluor in acetonitrile under the standard oxidative cyclisation conditions at 80ºC. Whilst complete consumption of the allenoate was observed by TLC after two hours, the NMR spectra of the crude reaction mixture contained no peaks consistent with the bibutenolide **110s**. Instead, the major product of this reaction was the β-fluoro-γ-butenolide **107s** resulting from a fluorocyclisation process. This species was isolated in 26% yield upon purification by silica gel column chromatography (Table 4.3, Entry 6). In order to determine whether the fluorinated butenolide results from a gold-catalysed cyclisation-fluorination process, allenoate **102s** was reacted under the same conditions in the absence of $AuCl_3$. Complete consumption of the starting material was observed after two hours at 80ºC under these conditions and the β-fluoro-γ-butenolide **107s** was isolated in a higher yield of 38% upon silica gel column chromatography (Scheme 4.19). As such, the fluorinated butenolide product most likely results from a fluorocyclisation mechanism of the type shown in Scheme 3.48 where an initial electrophilic fluorination delivers a phenyl-stabilised cationic intermediate amenable to cyclisation.



Scheme 4.19 Fluorocyclisation of Allenoate **102s** in the Presence or Absence of $AuCl_3$.

[x] For the preparation of *tert*-butyl allenoate **102f**, see Section 3.2.4.

Treating the benzyl-substituted *tert*-butyl allenoate **102b** with $AuCl_3$ and Selectfluor led to a mixture of products resulting from oxidative homocoupling (**110b**) and intramolecular oxidative arylation (**109b**, see Section 3.2, Table 4.3, Entry 7).[y] The bibutenolide **110b** was delivered in 60% yield relative to the allenoate (dr = 52:48) upon silica gel column chromatography whilst indenofuranone **109b** was afforded in 37% yield relative to **102b** (Scheme 4.20). A control experiment with a pure sample of the isomeric alkyne impurity **108b** did not lead to **109b** or **110b**.



Scheme 4.20 Cyclisation-Homodimerisation and Oxidative Arylation of Allenoate **102b**.

The butyl-substituted allenoate **102t** was also employed as a mixture with its isomeric alkyne impurity **108t**. Upon treatment with $AuCl_3$ and Selectfluor under the standard oxidative cyclisation conditions, this mixture was converted into the corresponding bibutenolides **110t** in a combined yield of 91% relative to the allenoate (Table 4.3, Entry 8).[z] Reacting a pure sample of the independently prepared alkyne impurity **108t**[106] under the same conditions resulted in decomposition of the starting material with no formation of the homodimerised product. The bibutenolide diastereoisomers were easily separated by silica gel column chromatography and X-ray crystallographic analysis of one isomer enabled the assignment of the relative stereochemistry (Figure 4.1).

[y] A mixture of the allenoate **102b** and its inseparable isomeric alkyne impurity **108b** was employed in the reaction (**102b**:**108b** = 2.6:1). The amounts of the reagents were calculated with respect to the combined amount of **102b** and **108b**.

[z] The amounts of the reagents were calculated with respect to the combined amount of **102t** and **108t**.

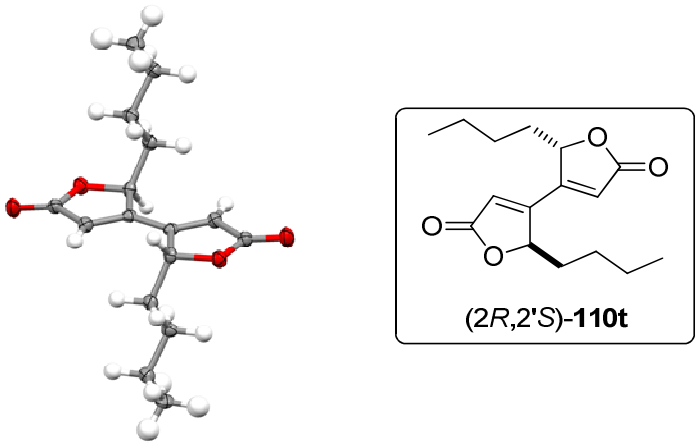
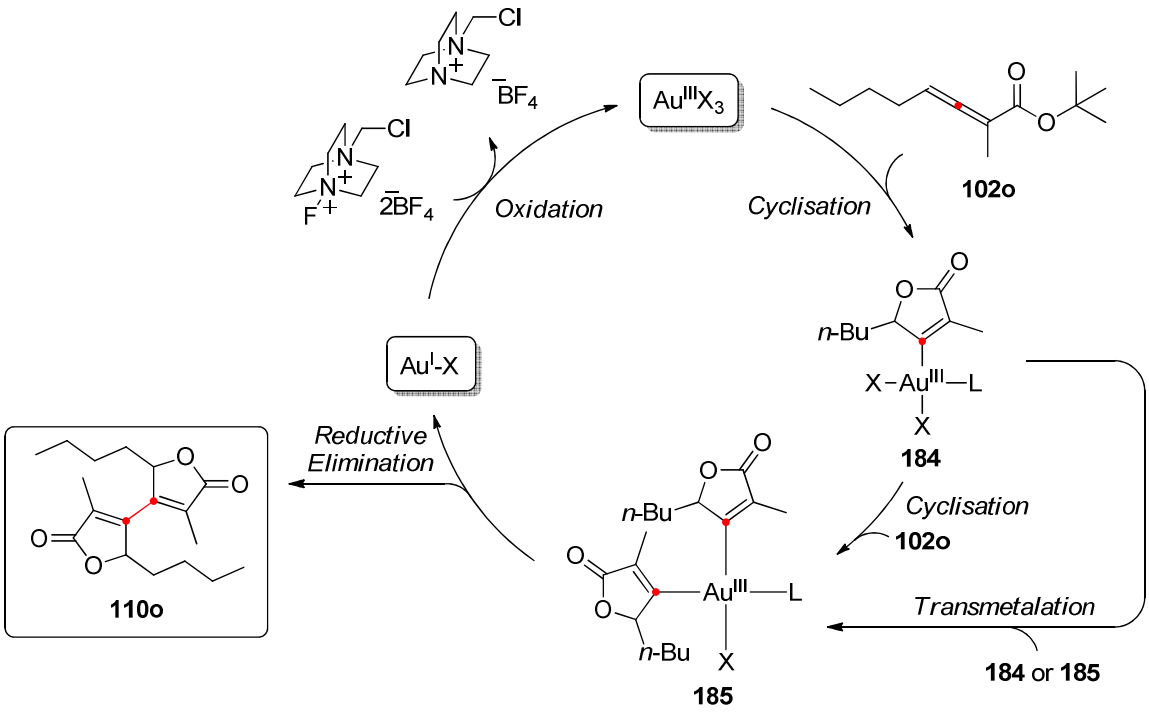


Figure 4.1 X-Ray Crystal Structure of (2*R*,2'*S*)-**110t**.

Finally, the ethyl allenoate **105o** was subjected to the standard conditions with gold(III) chloride and the electrophilic fluorinating reagent. In contrast to the analogous *tert*-butyl allenoate **102o**, this compound was not a suitable substrate for the cyclisation-oxidative homodimerisation process, delivering a complex mixture of products after 16 hours at 80ºC (Table 4.3, Entry 9).

4.2.3.5 Comments on the Reaction Mechanism

In accordance with the postulated mechanism for the related intramolecular arylation process, the gold(III)-catalysed cascade cyclisation-oxidative homodimerisation of *tert*-butyl allenoates **102** can be explained by Au^{I}/Au^{III} redox cycle where Selectfluor (**82**) acts as a stoichiometric external oxidant (Scheme 4.21).



Scheme 4.21 Proposed Mechanism for the Gold(III)-Catalysed Cyclisation-Homodimerisation of *tert*-Butyl Allenoates **102** in the Presence of Selectfluor (**82**). X = Cl or F, L = Neutral Ligand.

Activation of the allene by gold(III) followed by intramolecular nucleophilic attack of the ester oxygen would deliver the (butenolide)gold(III) complex **184**. Cyclisation of another molecule of the allenoate or transmetalation of a butenolide unit between organogold intermediates would then afford the doubly organic-substituted gold(III) species **185**. At this stage, reductive elimination would lead to the bibutenolide product **110** and one molecule of a gold(I) salt. The catalytic cycle is then completed by oxidation of the low valent metal back to the active gold(III) catalyst by Selectfluor (**82**).

A reaction mechanism involving a β-fluoro-γ-butenolide intermediate **107** is considered unlikely as this pathway would require a butenolide fragment to act as an intermolecular nucleophile at the β-position (see Section 3.2.6). Whilst the fluorinated butenolide **107t** was observed as the major product when the phenyl-substituted allenoate **102t** was reacted with $AuCl_3$ and Selectfluor, this compound did not react further to afford the corresponding

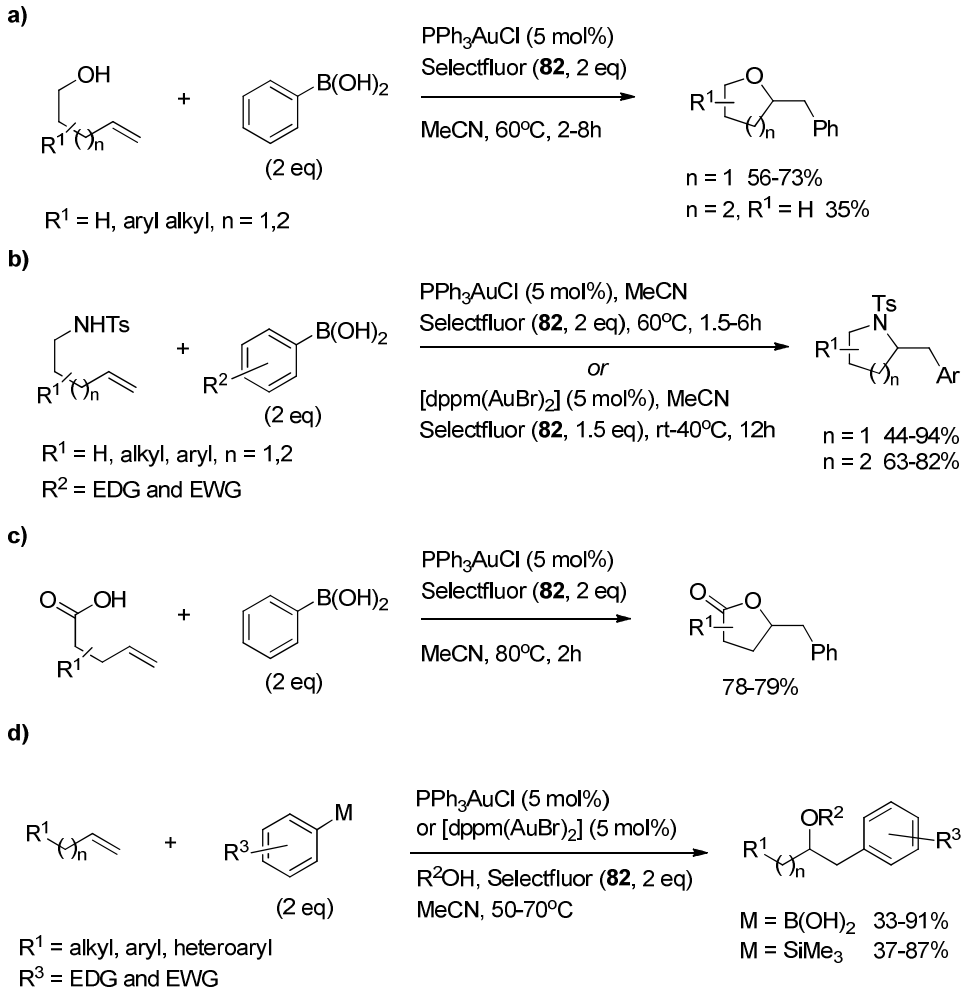
bibutenolide under the standard conditions. Furthermore, β-fluoro-γ-butenolides **107** were not observed in any other reaction mixture during the course of our study.

4.3 Cyclisation-Alkynylation of *tert*-Butyl Allenoates

4.3.1 Introduction

Performing intermolecular cross-coupling reactions under oxidative catalysis conditions raises the additional challenge of controlling selectivity for the cross-coupled product over the homodimers of each coupling partner. Despite this extra complexity, several impressive intermolecular oxidative cross-coupling reactions mediated by gold-catalysts in the presence of Selectfluor have been disclosed recently.

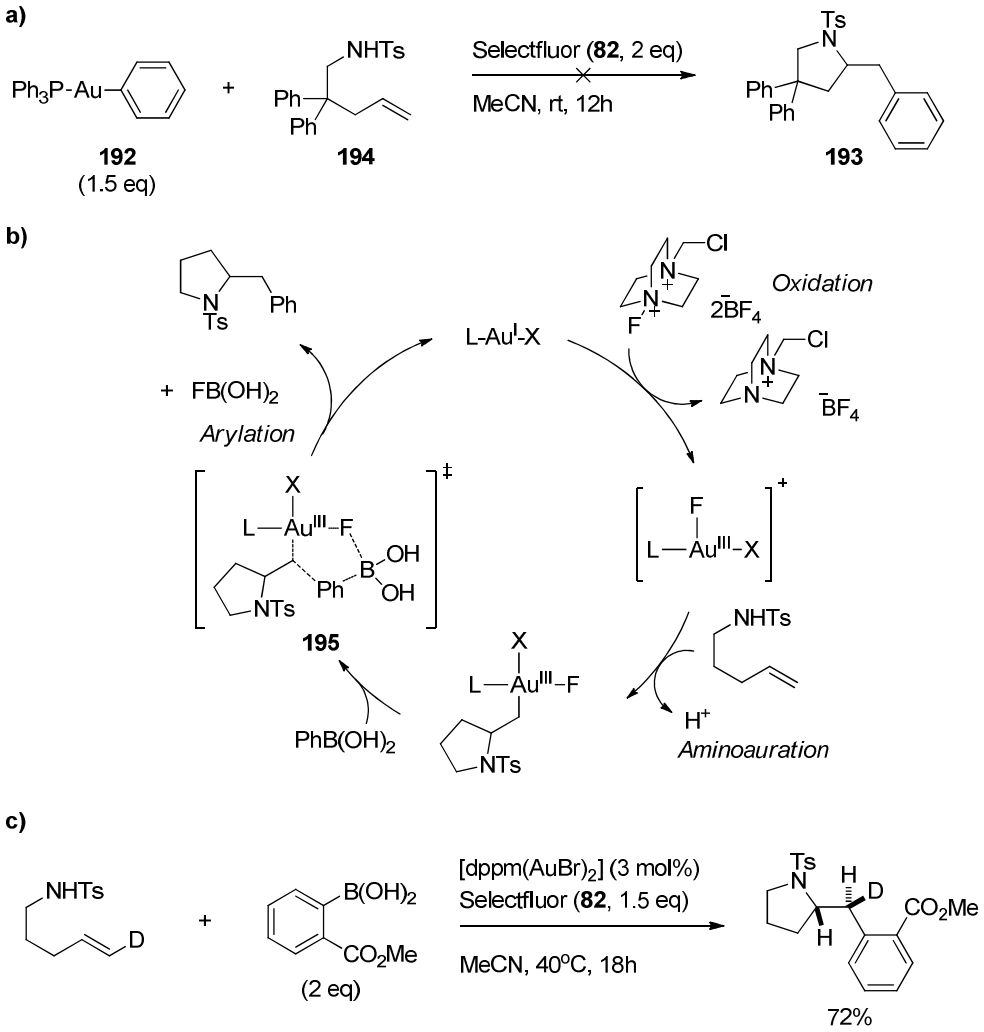
Following the successful intermolecular arylation reaction reported by Zhang and co-workers (see Section 3.2.6),[173] the groups of Zhang,[190] Toste[191-193] and Russell[194] independently disclosed a series of inter-related gold-catalysed cascade cyclisation-intermolecular oxidative arylation reactions performed in the presence of Selectfluor (**82**). In these impressive processes, one coupling partner is delivered as a result of a gold-mediated nucleophilic addition onto an alkene whilst the aryl fragment is derived from either an arylboronic acid[190-192] or an arylsilane.[193-194] In general, the alkylated arene products were delivered in moderate to good yields whilst no side-products resulting from β-hydride elimination were observed (Scheme 4.22). As previously discussed, this feature of gold catalysts is potentially very significant as homo- and cross-coupling processes of sp^3-hybridised organic fragments catalysed by other transition metals typically suffer from β-hydride elimination-derived side-reactions.



Scheme 4.22 Gold-Catalysed Cyclisation-Intermolecular Arylation of Alkenes Performed in the Presence of Selectfluor.

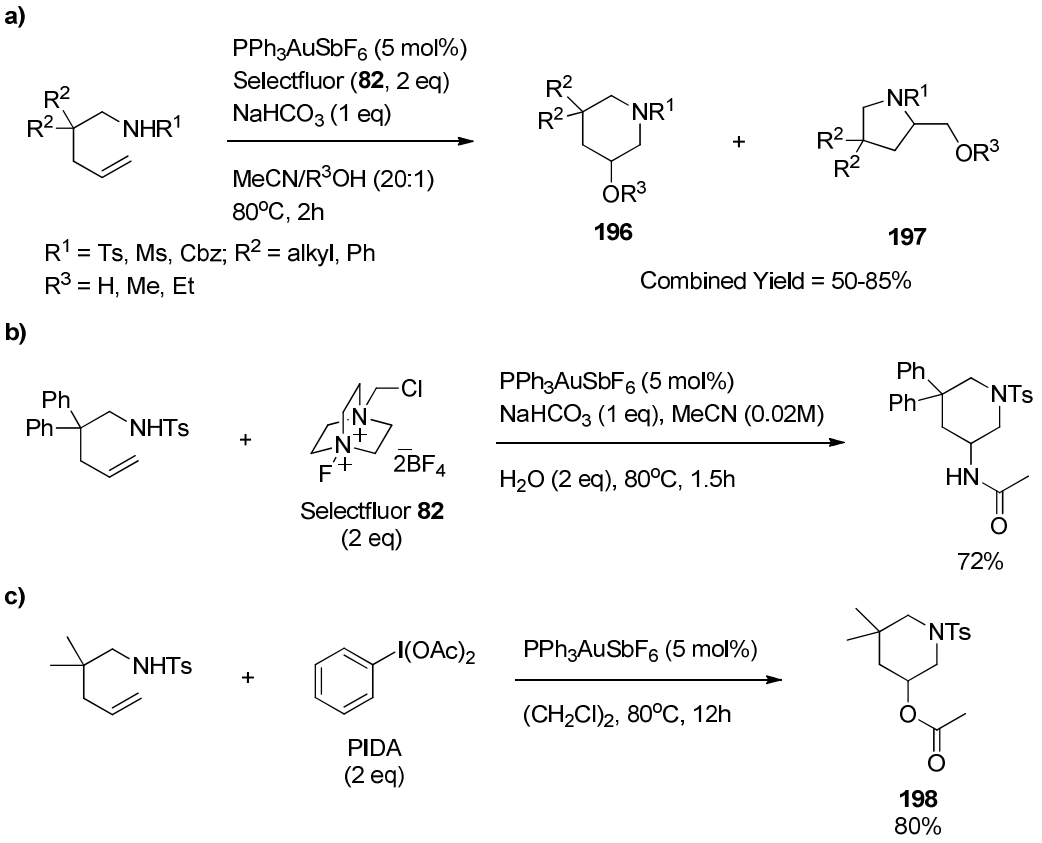
Mechanistic studies conducted by Toste and co-workers indicated that the $C(sp^2)$-$C(sp^3)$ bond is not formed as a result of a reductive elimination from a gold(III) complex.[191] The independently-prepared phenylgold(I) species **192**[195] did not deliver the cross-coupled product **193** when reacted with alkene **194** and Selectfluor in the absence of phenylboronic acid (Scheme 4.23a). Adding $PhB(OH)_2$ to the reaction mixture restored the cascade cyclisation-intermolecular arylation process implying that the aryl group involved in coupling derived directly from the boronic acid without the intermediacy of a distinct arylgold species. Consequently, a nucleophilic addition-type step involving the five-centered concerted transition state **195** was proposed as the most likely arylation pathway

(Scheme 4.23b). In this mechanism, the fluoride ion coordinated to gold(III) activates the boronic acid component through the formation of a B-F bond. Deuterium labelling experiments were consistent with an overall *anti*-addition across the alkene (Scheme 4.23c).[190-191] This stereochemical preference could result from either an initial *anti*-amino- or oxyauration followed by an arylation step proceeding with retention of configuration (eg. S_Ni-type nucleophilic substitution). Alternatively, an S_N2-type arylation process could follow a *syn*-selective addition to the alkene.



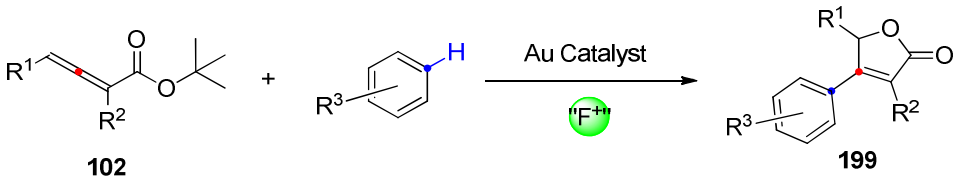
Scheme 4.23 a) Control Reaction with Phenylgold(I) Complex **192**. b) Proposed Mechanism for the Cyclisation-Intermolecular Arylation Process. c) Deuterium-Labelling Studies. L = Neutral Ligand, X = Negatively Charged Ligand.

Recently, de Haro and Nevado extended the scope of the oxidative alkene cyclisation process towards oxygen and nitrogen coupling partners.[196] Treating a range of different alcohols γ-aminoalkenes with water, methanol or ethanol in the presence of 5 mol% of PPh_3AuSbF_6 and two equivalents of Selectfluor (**82**) led predominantly to the corresponding 6-*endo*-trig cyclised products **196** in generally good yields after two hours at 80ºC (Scheme 4.24a). In some cases, pyrrolidines **197** resulting from a 5-*exo*-trig cyclisation were formed as minor side-products. When the reaction was performed under the same conditions but in a mixture of acetonitrile and water (2 eq), the C-O bond-forming process was rerouted in favour of C-N bond formation with acetonitrile acting as the nitrogen coupling partner (Scheme 4.24b). Furthermore, switching the oxidant to PIDA led selectively to the corresponding acetylated products **198** (Scheme 4.24c).



Scheme 4.28 a) Cyclisation-Oxidative Hydroxylation or Alkoxylation of Alkenes. b) Amidation in the Presence of Acetonitrile. c) Acetylation when using PIDA as the Oxidant.

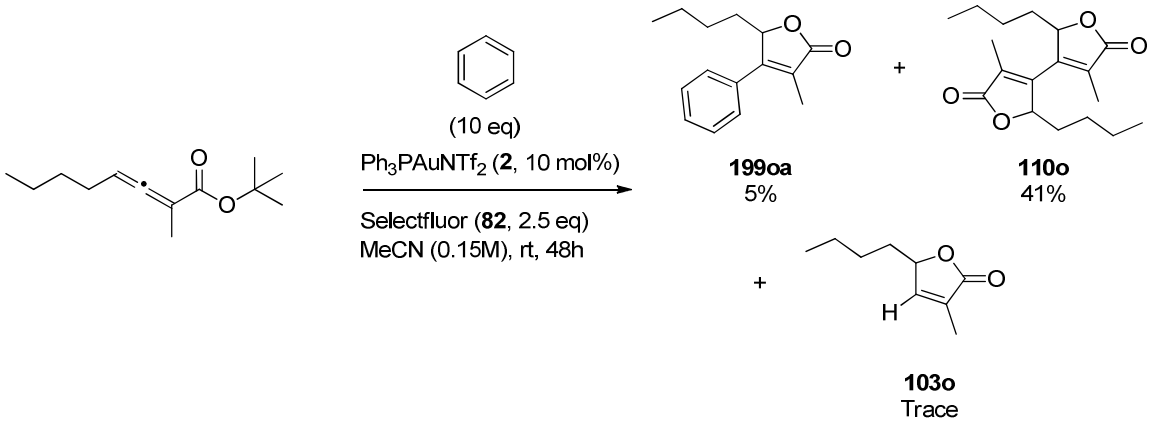
Inspired by these reactions,[aa] we sought to investigate whether an intermolecular oxidative arylation process could follow the gold-mediated 5-*endo*-trig cyclisation of *tert*-butyl allenoates **102**. Instead of using arylboronic acids or silanes as the source of the aryl coupling partner, however, our previous studies on the related cyclisation-intramolecular arylation of benzyl-substituted substrates encouraged us to investigate the feasibility of employing non-activated arenes in this reaction. In this case, one coupling partner is delivered as a result of a gold-mediated nucleophilic addition to a carbon-carbon multiple bond whilst the other derives from C(sp^2)-H bond functionalisation (Scheme 4.25).



Scheme 4.25 Cyclisation-Intermolecular Arylation of *tert*-Butyl Allenoates **102** with Non-Activated Arenes.

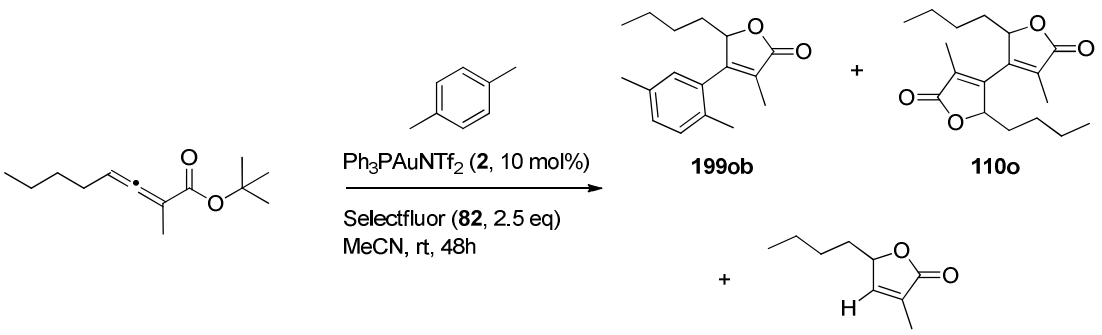
In a preliminary experiment, the alkyl-substituted *tert*-butyl allenoate **102o** was reacted with the gold(I) catalyst PPh_3AuNTf_2 (**2**, 10 mol%) and Selectfluor (**82**, 2.5 eq) in the presence of 10 equivalents of benzene. After 48 hours at room temperature, NMR analysis of the crude reaction mixture indicated that several products had been formed. Although the homocoupled bibutenolide **110o** was afforded as the major product upon silica gel column chromatography (yield = 41%, dr = 56:44), the cross-coupled β-aryl-γ-butenolide **199oa** was also isolated in 5% yield from the crude reaction mixture (Scheme 4.26).

[aa] Related cascade nucleophilic addition-intermolecular arylation processes with arylboronic acids were previously discussed in Section 3.2.6. references [173] and [174]



Scheme 4.26 Cyclisation-Intermolecular Arylation of *tert*-Butyl Allenoate **102o** with Benzene.

Switching to the more electron-rich arene, *para*-xylene, led to a slight increase in the cross-coupling yield. Treating allenoate **102o** under the same conditions in the presence of 10 equivalents of this arene delivered the corresponding β-aryl-γ-butenolide **199ob** in 12% yield after 48 hours at room temperature. The allenoate homocoupling process was again observed as the major pathway in this reaction and bibutenolide **110o** was isolated in 40% yield upon silica gel column chromatography (dr = 60:40). Increasing the number of equivalents of the arene to 50 had a detrimental effect of the reaction efficiency with poor solubility of the electrophilic fluorinating reagent Selectfluor (**82**) observed. β-Aryl-γ-butenolide **199ob** was furnished in only 9% yield under these conditions (estimated by ^{1}H NMR) whilst the major products were the homocoupled bibutenolide **110o** (yield = 24%, dr = 50:50, estimated by ^{1}H NMR) and the protodeaurated γ-butenolide **103o** (yield = 67%, estimated by ^{1}H NMR). In an attempt to suppress the competitive intermolecular homodimerisation pathway, the reaction concentration was reduced to 0.01M whilst the number of equivalents of *para*-xylene was maintained at 50. Disappointingly, this reaction led to a complex mixture of products with no trace of the desired β-aryl-γ-butenolide isolable upon silica gel column chromatography (Scheme 4.27).

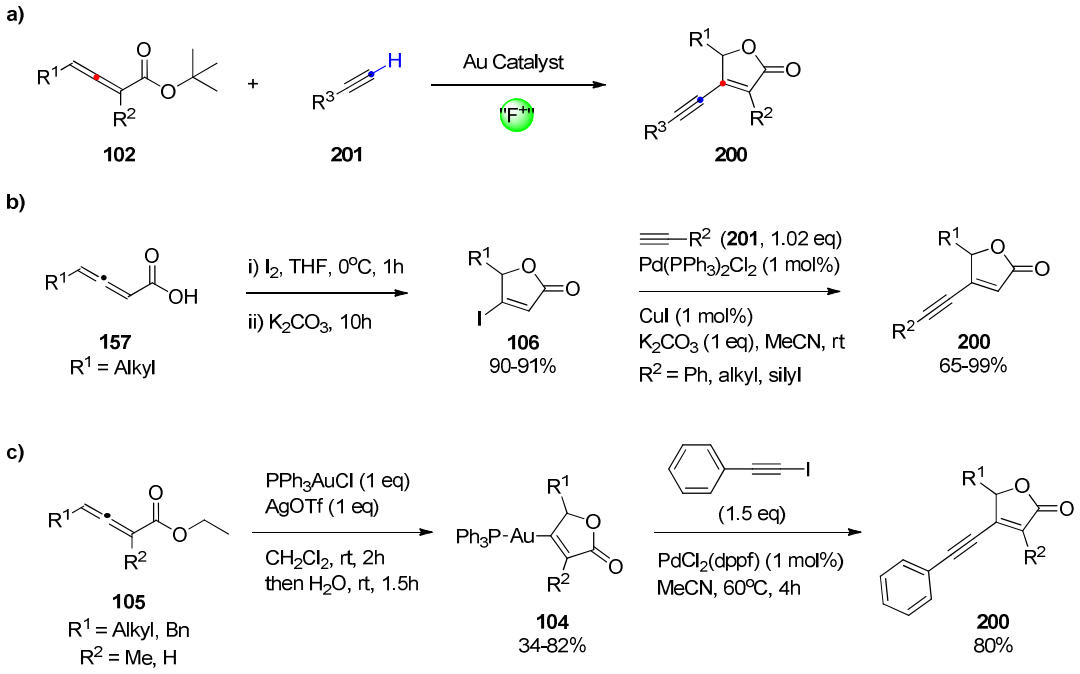


	199ob :	110o :	103o
MeCN (0.15M), *p*-xylene (10 eq)	12%	40%	7%
MeCN (0.15M), *p*-xylene (50 eq) (NMR Yields)	9%	24%	67%
MeCN (0.01M), *p*-xylene (50 eq)	Complex Reaction Mixture		

Scheme 4.27 Cyclisation-Intermolecular Arylation of *tert*-Butyl Allenoate **102o** with *p*-Xylene.

The low selectivity for the cross-coupled β-aryl-γ-butenolide products observed during these preliminary studies encouraged us to investigate alternative intermolecular coupling partners in the oxidative allenoate cyclisation process. Following a survey of the literature, our attention was drawn to the well-established ability of gold complexes to activate C(sp)-H bonds of terminal alkynes.[197-199] This reactivity has been exploited in the gold-catalysed multicomponent synthesis of propargyl amides[200] whilst gold salts have been employed as alternative co-catalysts to copper(I) in palladium-catalysed Sonogashira reactions.[201-203] The cascade cyclisation-intermolecular oxidative alkynylation of *tert*-butyl allenoates **102** would give access to β-alkynyl-γ-butenolides **200** in a single transformation from non-activated starting materials using a catalytic amount of a single metal (Scheme 4.28a). Current synthetic routes to these compounds rely on two-step protocols where the allenoate cyclisation and alkynylation steps are performed separately. In 1999, Ma and co-workers demonstrated that β-iodo-γ-butenolides **106**, formed upon iodocyclisation of allenic acids **157**, can be successfully alkynylated under palladium-catalysed Sonogashira conditions (Scheme 4.28b).[204] More recently, Hashmi et al reported a similar Sonogashira-based

approach to these compounds using iodinated alkynes and stoichiometric (butenolide)gold(I) complexes of type **104** (Scheme 4.28c).[205]



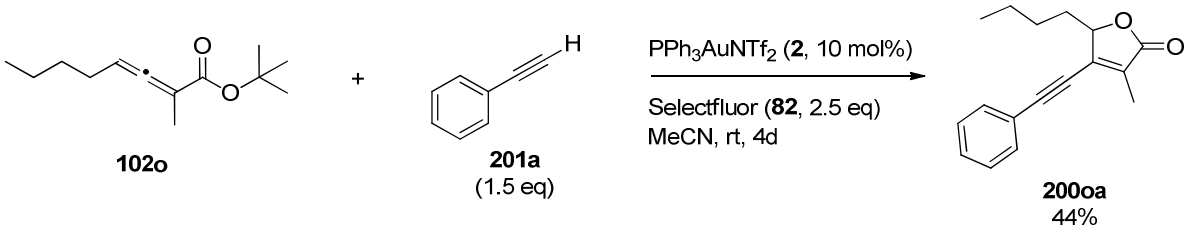
Scheme 4.28 a) Cyclisation-Intermolecular Alkynylation of Allenoates **102**. b) Preparation of β-Alkynyl-γ-Butenolides **200** from β-Iodo-γ-Butenolides. c) Preparation of β-Alkynyl-γ-Butenolides **200** from (Butenolide)gold(I) Comlexes **104**.

The majority of the experimental work in this study was conducted by Jonathan E. Ross (Part II, University of Oxford, 2010)[206] and this section provides a summary of the results.[207]

4.3.2 Preliminary Studies

As a preliminary experiment, the alkyl-substituted *tert*-butyl allenoate **102o** was treated with phenylacetylene (**201a**, 1.5 eq) and PPh_3AuNTf_2 (**2**, 10 mol%) in the presence of Selectfluor (**82**, 2.5 eq) in acetonitrile (0.15M) and water (10 eq). After 4 days at room temperature, NMR analysis of the crude reaction mixture indicated that approximately 50% of the starting material had been converted into a single cyclised product. This compound was identified as the desired β-alkynyl-γ-butenolide **200oa** upon purification by silica gel column chromatography (Scheme 4.29). The $C(sp^2)$-C(sp) cross-coupled product was

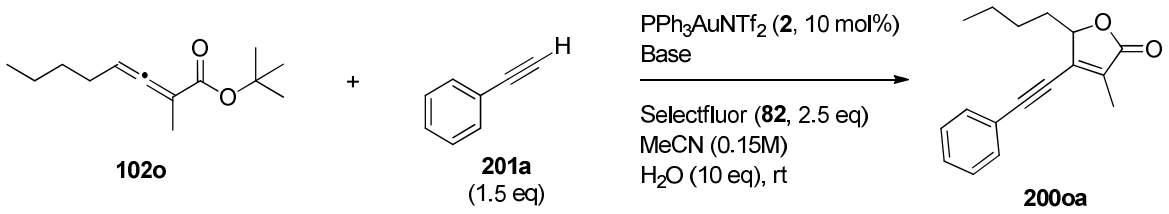
isolated in 44% yield from this reaction whilst no products resulting from the conventional cyclisation-protodeauration process or homodimerisation of either the alkyne or the allenoate were observed.



Scheme 4.29 Cyclisation-Intermolecular Alkynylation of *tert*-Butyl Allenoate **102o** with Alkyne **201a**.

4.3.3 Optimisation of the Reaction Conditions

With the feasibility of the cascade cyclisation-intermolecular oxidative alkynylation process established, our attention turned to optimising the reaction conditions using the conversion of allenoate **102o** and alkyne **201a** into β-alkynyl-γ-butenolide **200oa** as a model transformation. As an initial study, the effect of various basic additives on the efficiency of the cross-coupling process was investigated (Table 4.4).



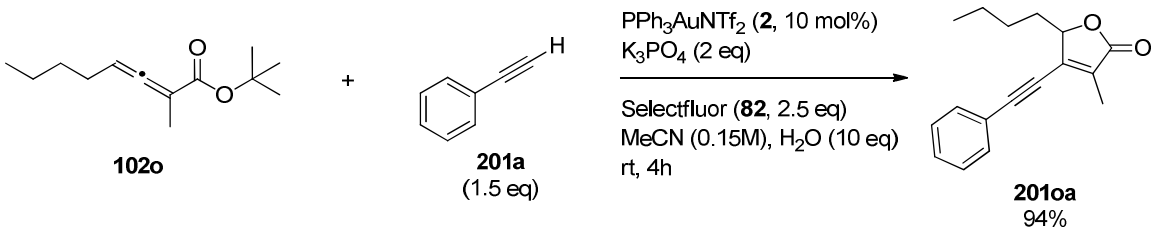
Entry	Base	Loading (eq)	Time	Yield[a] (Conversion)[b]
1	No base	---	4d	44% (50%)
2	K_3PO_4	2	4h	94% (100%)
3	K_3PO_4	0.2	48h	49% (59%)
4	K_3PO_4	1	4.5h	33% (100%)[c]
5	K_2CO_3	4	5d	---[d] (25%)
6	KO*t*-Bu	2	48h	73% (90%)

7	NEt_3	3.5	48h	Decomposition

[a] Isolated yield. [b] Determined by ^1H NMR on the crude reaction mixture. [c] Complex reaction mixture. [d] Isolated yield not determined.

Table 4.4 Effect of Basic Additives.

In each case, a mixture of allenoate **102o** and alkyne **201a** were stirred in acetonitrile (0.15M) and water (10 eq) in the presence of 10 mol% of PPh_3AuNTf_2 (**2**), Selectfluor (**82**, 2.5 eq) and the basic additive at room temperature.[bb] The conversion of the allenoate starting material was determined by NMR analysis of the crude reaction mixture prior to isolation of the cross-coupled product **200oa** upon silica gel column chromatography. The addition of two equivalents of potassium phosphate tribasic to the reaction mixture led to an immediate increase in the yield of the β-alkynyl-γ-butenolide (Table 4.4, Entry 2). Under these conditions, complete consumption of the allenoate was observed after just 4 hours with the cross-coupled product **200oa** being furnished in 94% yield (Scheme 4.30). The presence of K_3PO_4 presumably ensures that the reaction medium is sufficiently basic for deprotonation of the alkyne component to occur throughout the coupling process.[cc]



Scheme 4.30 Cyclisation-Intermolecular Alkynylation of *tert*-Butyl Allenoate **102o** with Alkyne **201a** in the Presence of K_3PO_4 (2 eq).

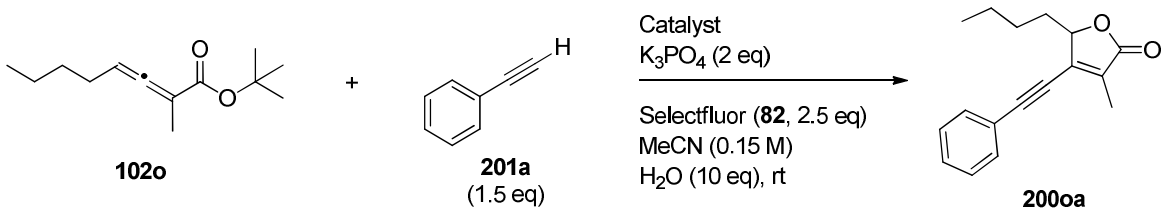
Performing the cyclisation-intermolecular alkynylation process in the presence of catalytic amounts of the same base led to a decrease in the reaction efficiency. Only 54% conversion of the starting material was observed after 48 hours when 20 mol% of K_3PO_4 was employed

[bb] The addition of 10 equivalents of water to the reaction mixtures aided the solvation of the basic additives and Selectfluor (**82**).

[cc] Hydrofluoric acid is likely generated as a side-product of the coupling process. See Section 4.3.5 for a more detailed discussion of the reaction mechanism.

(yield of **200oa** = 49%, Table 4.4, Entry 3). The β-alkynyl-γ-butenolide **200oa** was isolated in a lower yield of 33% when the reaction was performed in the presence of one equivalent of the base (Table 4.4, Entry 4). The alternative inorganic base, potassium carbonate was not effective in promoting in the cyclisation-intermolecular alkynylation process. NMR Analysis of the crude reaction mixture indicated that only 25% of the allenoate **102o** had been consumed after 5 days when four equivalents of this base were employed under the standard conditions (Table 4.4, Entry 5). Whilst the stronger base, potassium *tert*-butoxide (2 eq), was more successful in mediating the oxidative cross-coupling process, the isolated yield of the β-alkynyl-γ-butenolide product **200oa** (73%) was lower than that obtained with K_3PO_4 (Table 4.4, Entry 6). Finally, the ability of the organic base triethylamine to promote the gold-catalysed coupling process was investigated. This compound is commonly employed as a basic additive in palladium-catalysed Sonogashira reactions. When reacted with allenoate **102o** and alkyne **201a** under the standard conditions with PPh_3AuNTf_2 (**2**) and Selectfluor (**82**), however, complete decomposition of the starting materials was detected (Table 4.4, Entry 7). Poisoning of the gold catalyst by triethylamine could explain the lack of coupling reactivity observed with this reagent.

At this stage, the suitability of a range of alternative catalysts for the cyclisation-intermolecular alkynylation process was investigated (Table 4.5).



Entry	Catalyst	Loading (mol%)	Time	Yield[a] (Conversion)[b]
1	PPh_3AuNTf_2 (**2**)	10	4h	94% (100%)
2	No Catalyst	---	10d	No Reaction

3	AgOTf	10	10d	No Reaction
4	CuOAc	10	10d	No Reaction
5	$PtCl_2$	10	10d	No Reaction
6	H_2SO_4	10	10d	No Reaction
7	$Pd(OAc)_2$ / CuOAc	10[c]	24h	Decomposition
8	SIPrAuCl (**1**) / AgOTf	10[d]	10d	No Reaction
9	$AuCl_3$	10	6d	22% (45%)
10	PPh_3AuNTf_2 (**2**)	5	24h	72% (93%)

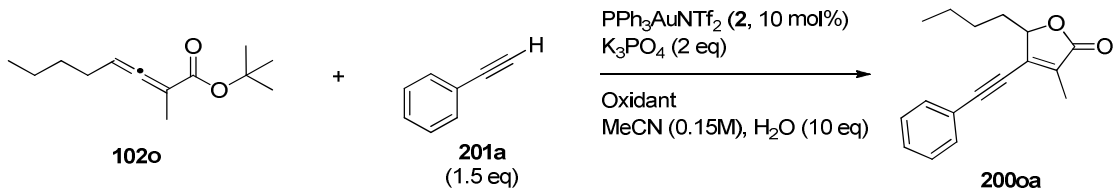
[a] Isolated yield. [b] Determined by ^1H NMR analysis of the crude reaction mixture. [c] 10 mol% of both $Pd(OAc)_2$ and CuOAc. [d] 10 mol% of both SIPrAuCl (**1**) and AgOTf.

Table 4.5 Optimisation of the Reaction Catalyst.

Firstly, the cyclisation-oxidative cross-coupling reaction between *tert*-butyl allenoate **102o** and alkyne **201a** was conducted in the absence of a catalyst. As expected, this reaction led only to recovered starting material after 10 days at room temperature, confirming that the cross-coupling process is indeed gold-catalysed (Table 4.5, Entry 2). No β-alkynyl-γ-butenolide products were formed when inorganic salts of transition metals other than gold were employed as catalysts. Silver(I) trifluoromethanesulfonate, copper(I) acetate and platinum(II) acetate all led to only recovered starting material when employed under the optimised conditions after 10 days at room temperature (Table 4.5, Entries 3-5). The Brønsted acid catalyst H_2SO_4 was similarly unreactive under the standard conditions with Selectfluor (**82**) and K_3PO_4 (Table 4.5, Entry 6). At this stage, a palladium/copper co-catalytic system of the type commonly employed in Sonogashira reactions was investigated. Treating allenoate **102o** and alkyne **201a** in the presence of Selectfluor (**82**, 2.5 eq), K_3PO_4 (2 eq) and 10 mol% of both palladium(II) acetate and copper(I) acetate led to complete decomposition of the allenoate with no formation of **200oa** after 24 hours at room temperature (Table 4.5, Entry 7). The suitability of alternative gold catalysts to PPh_3AuNTf_2

was then studied. Subjecting allenoate **102o** and alkyne **201a** to the standard conditions with 10 mol% of both AgOTf and the *N*-heterocyclic carbene-stabilised gold(I) source SIPrAuCl (**1**) led to only recovered starting material after 10 days at room temperature (Table 4.5, Entry 8). This result is in line with our previous studies on the intramolecular arylation and homodimerisation reactions where NHC-stabilised gold(I) sources were also found to be unsuitable catalysts. Whilst the gold(III) catalyst $AuCl_3$ did lead to the β-alkynyl-γ-butenolide **200oa** when reacted under the standard conditions, the cross-coupled product was delivered in only 22% yield after an extended reaction time of 6 days (Table 4.5, Entry 9). Finally, the effect of decreasing the loading of the PPh_3AuNTf_2 catalyst to 5 mol% was investigated. Under these conditions the β-alkynyl-γ-butenolide product was furnished in a slightly lower yield of 72% after 24 hours at room temperature (Table 4.5, Entry 10).

Having established PPh_3AuNTf_2 (**2**, 10 mol%) as the catalyst of choice for this transformation, our attention turned to investigating the range of suitable external oxidants for the cross-coupling process (Table 4.6).



Entry	Oxidant	Time	Yield[a] (Conversion)[b]
1	Selectfluor (**82**, 2.5 eq)	4h	94% (100%)
2	NFSI[c] (2.5 eq)	7d	---[d] (54%)
3	PIDA (2.5 eq)	7d	No Reaction
4	Oxone[e] (2.5 eq)	7d	No Reaction
5	*t*-BuOOH	7d	No Reaction
6	Selectfluor (**82**, 2 eq)	7h	39% (100%)

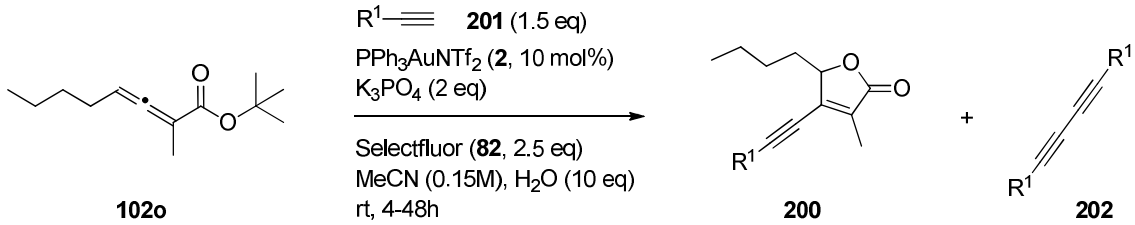
[a] Isolated yield. [b] Determined by ^{1}H NMR analysis of the crude reaction mixture. [c] NFSi = *N*-Fluorobenzenesulfonimide. [d] Isolated yield not determined. [e] Oxone = $KHSO_5.½KHSO_4.½K_2SO_4$.

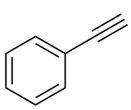
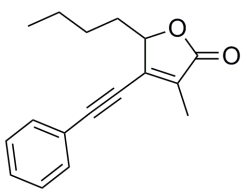
Table 4.6 Effect of the Oxidant.

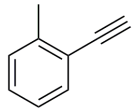
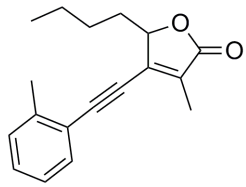
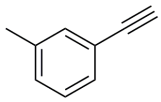
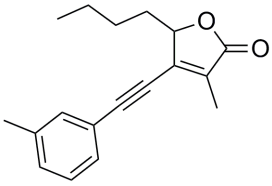
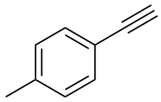
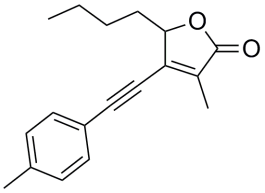
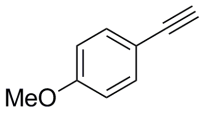
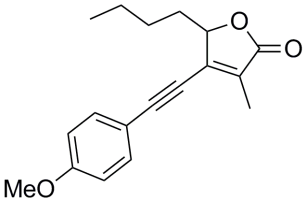
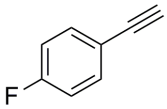
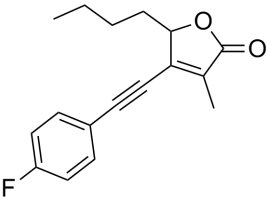
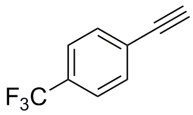
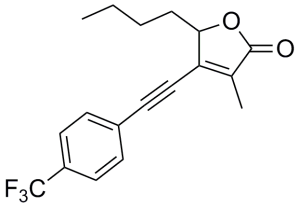
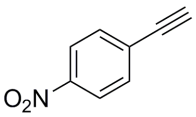
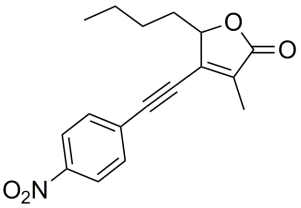
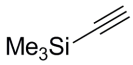
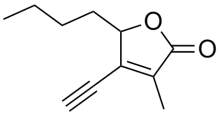
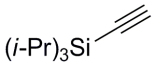
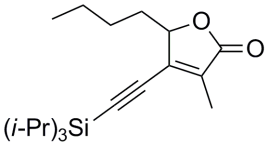
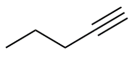
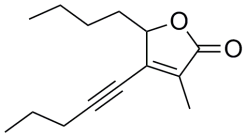
As an initial experiment, allenoate **102o** and alkyne **201a** were reacted under the standard conditions with 2.5 equivalents of the electrophilic fluorinating reagent NFSI (*N*-fluorobenzenesulfonimide) in place of Selectfluor (**82**). NMR Analysis of the crude reaction mixture after 7 days at room temperature indicated that the desired β-alkynyl-γ-butenolide **200oa** had been formed using this oxidant although a substantial amount of the starting material had remained unreacted (conversion = 54%, Table 4.6. Entry 2). Switching to PIDA, Oxone ($KHSO_5$.½$KHSO_4$.½K_2SO_4) or *t*-BuOOH led only to recovered starting material after 7 days at room temperature with no formation of the desired cross-coupled product (Table 4.6, Entries 3-5). With Selectfluor (**82**) identified as the optimum external oxidant for the gold-catalysed process, the effect of decreasing the loading of this reagent to two equivalents was investigated. This reaction led to a lower yield of the cross-coupled product (39%) after a longer reaction time of 7 hours (Table 4.6, Entry 6).

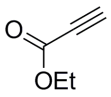
4.3.4 Scope and Limitations of the Cross-Coupling Process

With a set of optimised reaction conditions in hand, we were poised to investigate the scope and limitations of the cascade cyclisation-intermolecular alkynylation process with a range of allenoate and alkyne coupling partners. The results of the oxidative cyclisation of *tert*-butyl allenoate **102o** with a selection of terminal alkynes **201** are summarised in Table 4.7.



Entry	Alkyne **201**	Major Product	Yield of **200**[a]	Yield of **202**[b]
1			**200oa** 94%	**---**

2			**200ob** 42%	**202b** 11%
3			**200oc** 71%	**202c** 16%
4			**200od** >95%	**202d** 5%
5			**200oe** 88%	**---**
6[d]			**200of** 78%	**202f** 5%
7[e]			**200og** 63%	**202g** 5%
8			**200oh** 45%	**---**
9			**200oi** 12%	**---**
10			**200oj** 11%	**---**
11			**200ok** 14%	**---**

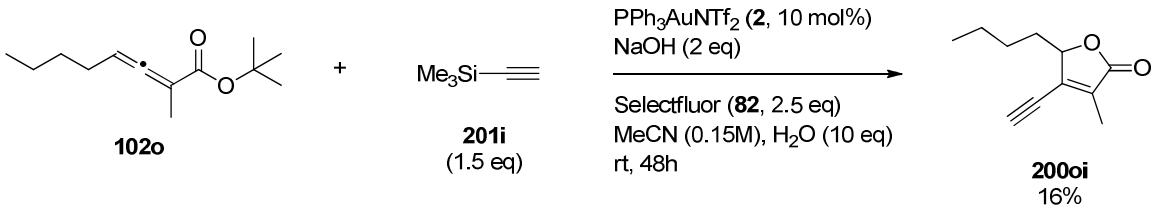
12		Decomposition	---	---

[a] Isolated yield relative to allenoate **102o**. [b] Isolated yield relative to alkyne **201**.

Table 4.7 Cyclisation-Intermolecular Oxidative Alkynylation of Allenoate **102o** with Alkynes **201**.

In each case, the *tert*-butyl allenoate was treated with the alkyne (**201**, 1.5 eq), PPh_3AuNTf_2 (**2**, 10 mol%), Selectfluor (**82**, 2.5 eq) and K_3PO_4 (2 eq) in acetonitrile (0.15M) and water (10 eq). The reactions were stirred at room temperature and complete consumption of the allenoate was observed within 48 hours. After filtration through Celite, the crude mixture was purified by column chromatography on silica gel. In an initial study, the efficiency of a range of substituted arylacetylenes **201a-h** in the cyclisation-intermolecular alkynylation process was investigated. The reaction was tolerant of arylacetylenes bearing *ortho*-, *meta*- and *para*-methyl groups around the aromatic ring with the highest yield being obtained with the *para*-substituted alkyne **201d**. The β-alkynyl-γ-butenolide **200od** was afforded in >95% yield from this reaction upon purification by silica gel column chromatography. In contrast to the reaction with phenylacetylene **201a**, however, competitive homocoupling of the arylacetylene **201d** was observed as a minor side-reaction during the coupling process and diyne **202d** was also isolated in 5% yield relative to **201d** (Table 4.7, Entry 4). Diynes **202b** and **202c** resulting from homodimerisation of the alkyne were also observed with the *ortho*- and *meta*-substituted arylacetylenes **201b** and **201c**. The cross-coupled products **200ob** and **200oc** were delivered in 42% and 71% yields respectively with these substrates whilst the diyne side-products were isolated in 11% and 16% yield relative to the alkynes (Table 4.7, Entries 2,3). Arylacetylene **201e**, bearing an electron-donating *para*-methoxy group, reacted smoothly under the optimised conditions to afford the corresponding β-alkynyl-γ-butenolide **200oe** in 88% yield after 48 hours at room temperature (Table 4.7, Entry 5). Electron-neutral or electron-poor arylacetylenes were also tolerated, delivering the *para*-fluoro, *para*-trifluoromethyl and *para*-nitro-substituted alkynylated butenolide products **200of**, **200og**

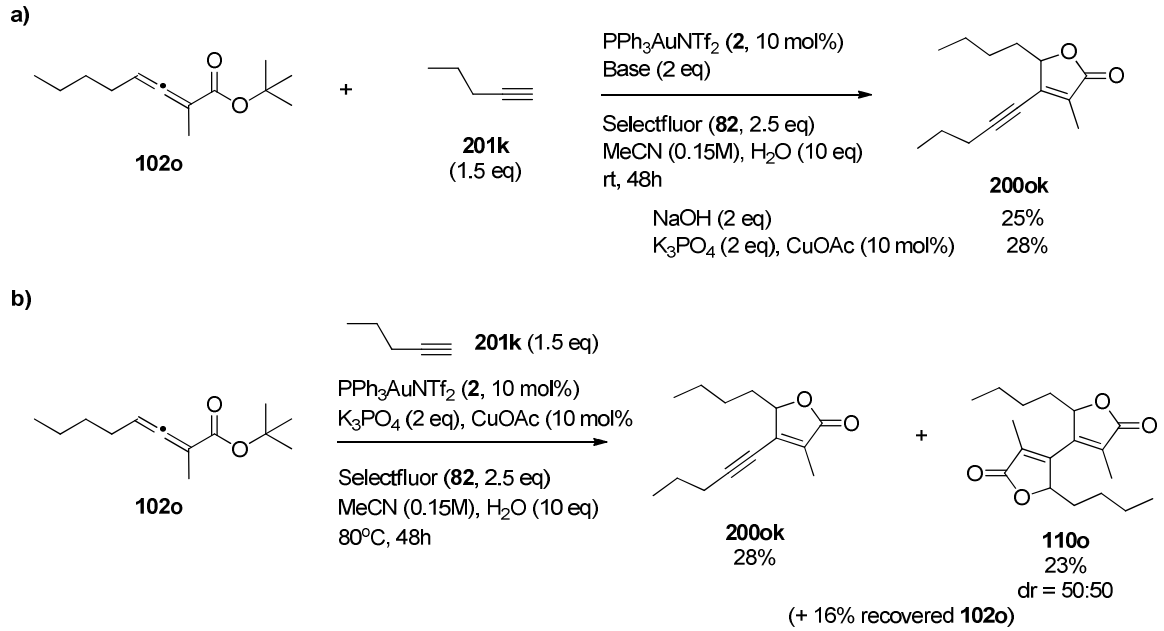
and **200oh** in 78%, 63% and 45% yield respectively (Table 4.7, Entries 6-8). Diynes **202f** and **202g** resulting from competitive oxidative homocoupling of alkynes **201f** and **201g** were both isolated in 5% yield relative to the alkynes from these reactions. The analogous nitro-substituted diyne **202h**, however, was not observed when alkyne **201h** was reacted with allenoate **102o**. In contrast to arylacetylenes, alkyne substrates featuring silyl substituents led to low yields of the cross-coupled products. Treating *tert*-butyl allenoate **102o** with trimethylsilylacetylene **201i** under the optimised conditions with PPh_3AuNTf_2 and Selectfluor led to a complex mixture of products. Purification by silica gel column chromatography delivered the desilylated β-alkynyl-γ-butenolide **200oi** as the only isolable compound in 12% yield (Table 4.7, Entry 9). This species presumably results from an *in situ* cleavage of the silyl group by fluoride ions derived from the electrophilic fluorinating reagent Selectfluor (**82**). Switching the basic additive from K_3PO_4 to sodium hydroxide (2 eq) led to a slight increase in the yield of the cross-coupled product. The β-alkynyl-γ-butenolide **200oi** was isolated in 16% yield after 48 hours at room temperature under these conditions (Scheme 4.31).



Scheme 4.31 Cyclisation-Intermolecular Alkynylation of Allenoate **102o** with Alkyne **201i** in the Presence of NaOH.

In contrast to the reaction with the trimethylsilyl-substituted alkyne **201i**, substrate **201j**, featuring a bulkier tri(*iso*-propyl)silyl group, reacted with allenoate **102o** to afford the corresponding β-alkynyl-γ-butenolide **200oj** without deprotection of the silyl substituent. The cross-coupling efficiency was again low with this substrate, however, and butenolide **200oj** was isolated in only 11% yield after 48 hours at room temperature (Table 4.7, Entry

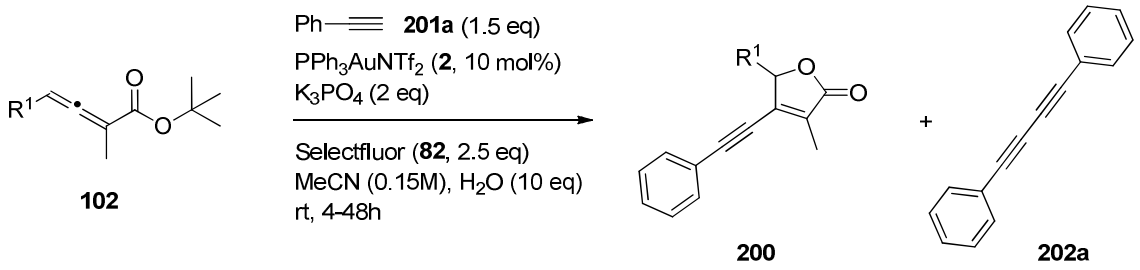
10). No improvement in the yield of the cross-coupled product was observed upon performing the reaction with sodium hydroxide (2 eq) as the basic additive. The cascade allenoate cyclisation-oxidative alkynylation process was similarly inefficient with the alkyl-substituted alkyne 1-pentyne (**201k**). The reaction between allenoate **102o** and this substrate under the standard oxidative cyclisation conditions with PPh_3AuNTf_2, Selectfluor and K_3PO_4 led to the corresponding β-alkynyl-γ-butenolide **200ok** in only 14% yield after 48 hours at room temperature (Table 4.7, Entry 11). The yield of **200ok** was increased to 25% upon using sodium hydroxide as the basic additive (2 eq). The addition of copper(I) acetate (10 mol%) to the reaction mixture led to a further improvement in the cross-coupling yield to 28% although 43% of the allenoate starting material was recovered from the reaction mixture under these conditions (Scheme 4.32a). The copper(I) presumably aids the deprotonation of the alkyne component through the intermediate formation of an η^1-(alkynyl)copper species. Only 16% of allenoate **102o** was recovered upon silica gel column chromatography when the reaction was conducted at 80ºC whilst the cross-coupled β-alkynyl-γ-butenolide product **200ok** was again delivered in 28% yield. Under these conditions, competitive cyclisation-homodimerisation of the allenoate was also observed and bibutenolide **110o** was isolated in 23% yield as a 50:50 mixture of diastereoisomers (Scheme 4.32b).

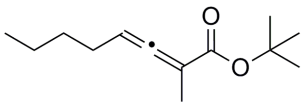
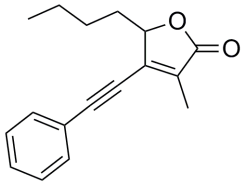
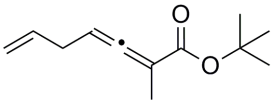
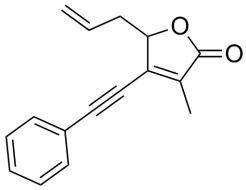
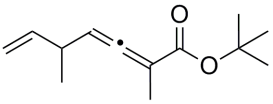
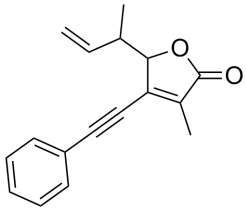
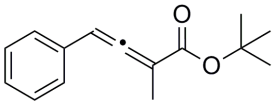


Scheme 4.32 Cyclisation-Intermolecular Alkynylation of *tert*-Butyl Allenoate**102o** with Alkyne **201k** a) with NaOH. b) with CuOAc Co-Catalyst.

Finally, the ester-substituted alkyne **201l** was subjected to the standard oxidative cyclisation conditions with allenoate **102o**. After 48 hours at room temperature, only decomposition of the starting material was observed with no trace of the desired β-alkynyl-γ-butenolide **200ol** detectable by crude NMR analysis (Table 4.7, Entry 12).

At this stage, the scope and limitations of the allenoate component in the cyclisation-intermolecular oxidative alkynylation process was investigated using phenylacetylene **201a** as the alkyne coupling partner (Table 4.8).



Entry	Allenoate **102**	Major Product	Yield of **200**[a]	Yield of **202a**[b]
1			**200oa** 94%	**---**
2			**200ra** 45%	29%
3[c]			**200ua** 33% dr = 55:45[d]	23%
4		No Reaction	**---**	**---**

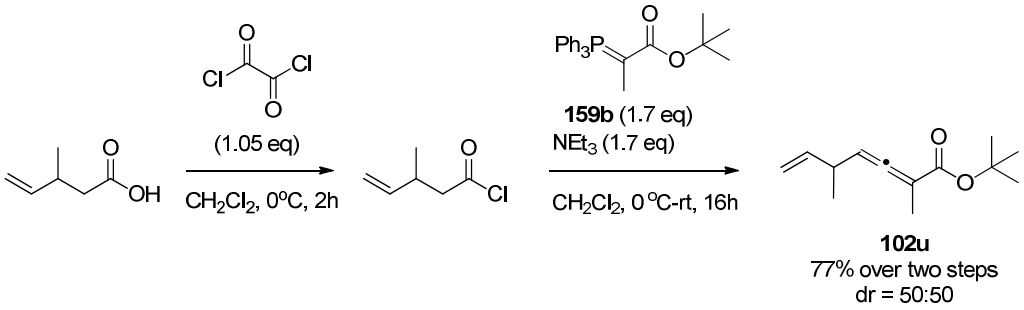
[a] Isolated yield relative to allenoate **102**. [b] Isolated yield relative to alkyne **201a**. [c] 50:50 Diastereoisomeric mixture of allenoate **102u** employed. [d] Determined by ^{1}H NMR analysis of the crude reaction mixture.

Table 4.8 Cyclisation-Intermolecular Alkynylation of Allenoates **102** or **105** with Alkyne **201a**.

Alkyne **201a** was reacted under standard oxidative cyclisation conditions with a selection of *tert*-butyl allenoates prepared from the methyl-substituted phosphorus ylid **159b**. These substrates do not suffer from complications arising from the isomeric alkynes **108** often observed as minor impurities with other *tert*-butyl allenoates.[dd] The allyl-substituted substrate **102r** reacted smoothly to afford the corresponding β-alkynyl-γ-butenolide **200ra** in 45% yield after 48 hours at room temperature (Table 4.8, Entry 2). In comparison with the *n*-butyl-substituted substrate **102o**, however, a lower selectivity for the cross-coupled

[dd] For the preparation of allenoates **102o**, **102r** and **102s**, see Section 4.2.3.3.

product was observed and diyne **202a** was delivered in 29% yield relative to **201a**. A mixture of the cross- and homocoupled products was also observed with *tert*-butyl allenoate **102u**. This substrate was prepared in 77% yield over steps (dr = 50:50) from 3-methylpent-4-enoic acid according to the standard Wittig method discussed in Section 3.2.4 (Scheme 4.33).

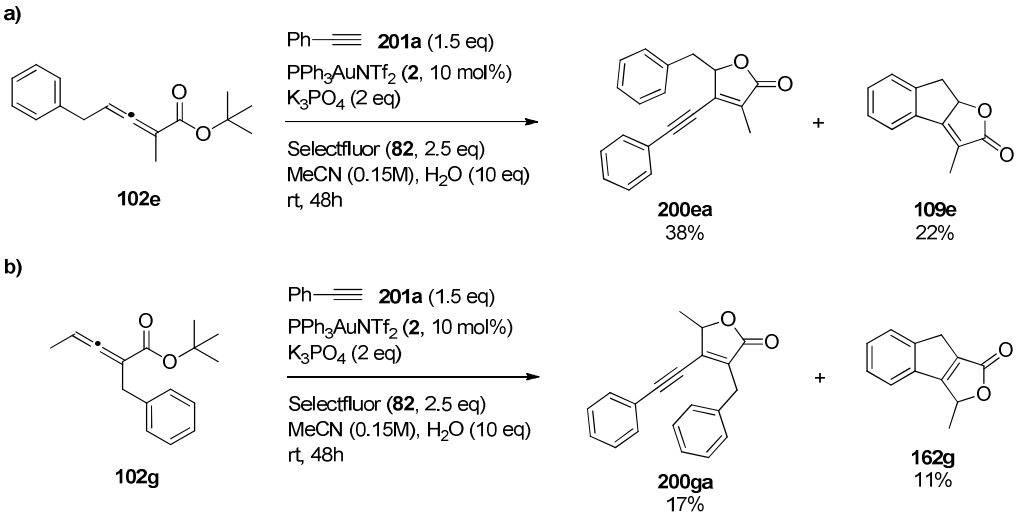


Scheme 4.33 Preparation of *tert*-Butyl Allenoate **102u**.

Upon treatment with phenylacetylene (**201a**, 1.5 eq), PPh_3AuNTf_2 (**2**, 10 mol%), Selectfluor (**82**, 2.5 eq) and K_3PO_4 (2 eq) under the optimised conditions, this compound delivered β-alkynyl-γ-butenolide **200ua** in 33% yield whilst diyne **202a** was furnished in 23% yield relative to the alkyne (Table 4.8, Entry 3). By contrast, the phenyl-substituted allenoate **102s** failed to react under the standard conditions and only starting material could be detected by crude NMR analysis after 48 hours at room temperature (Table 4.8, Entry 4). Surprisingly, the alkyne homodimerisation pathway was also suppressed during this reaction.

Reacting benzyl-substituted allenoates **102e** and **102g** with alkyne **201a** under the optimised conditions led to mixtures of β-alkynyl-γ-butenolides and indenofuranones resulting from intermolecular alkynylation and intramolecular arylation of the cyclised allenoates respectively. The reaction with substrate **102e** delivered the intermolecular cross-coupling product **200ea** in 38% yield after 48 hours at room temperature whilst indeno[2,1-*b*]furanone **109e** was isolated in 22% yield (Scheme 4.34a). β-Alkynyl-γ-butenolide **200ea** was a crystalline solid and thus allowed for unambiguous assignment of the structure by X-

ray crystallographic analysis (Figure 4.2). A slight preference for the intermolecular alkynylation product was also observed when *tert*-butyl allenoate **102g** was subjected to the standard conditions with alkyne **201a**. β-Alkynyl-γ-butenolide **200ga** and indeno[2,1-*c*]furanone **162g** were isolated in 17% and 11% yield from this reaction respectively upon purification by silica gel column chromatography (Scheme 4.34b).



Scheme 4.34 Competition Between Intermolecular Alkynylation and Intramolecular Arylation of Allenoates a) **102e** and b) **102g**.

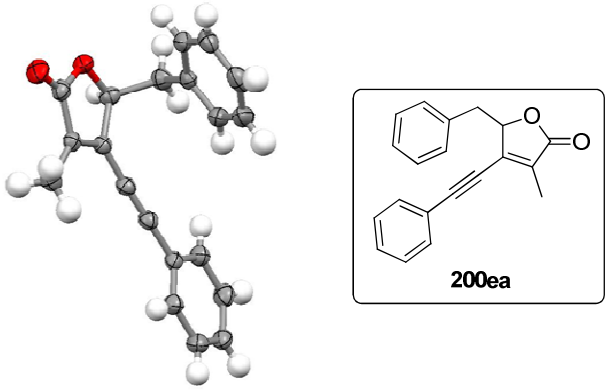
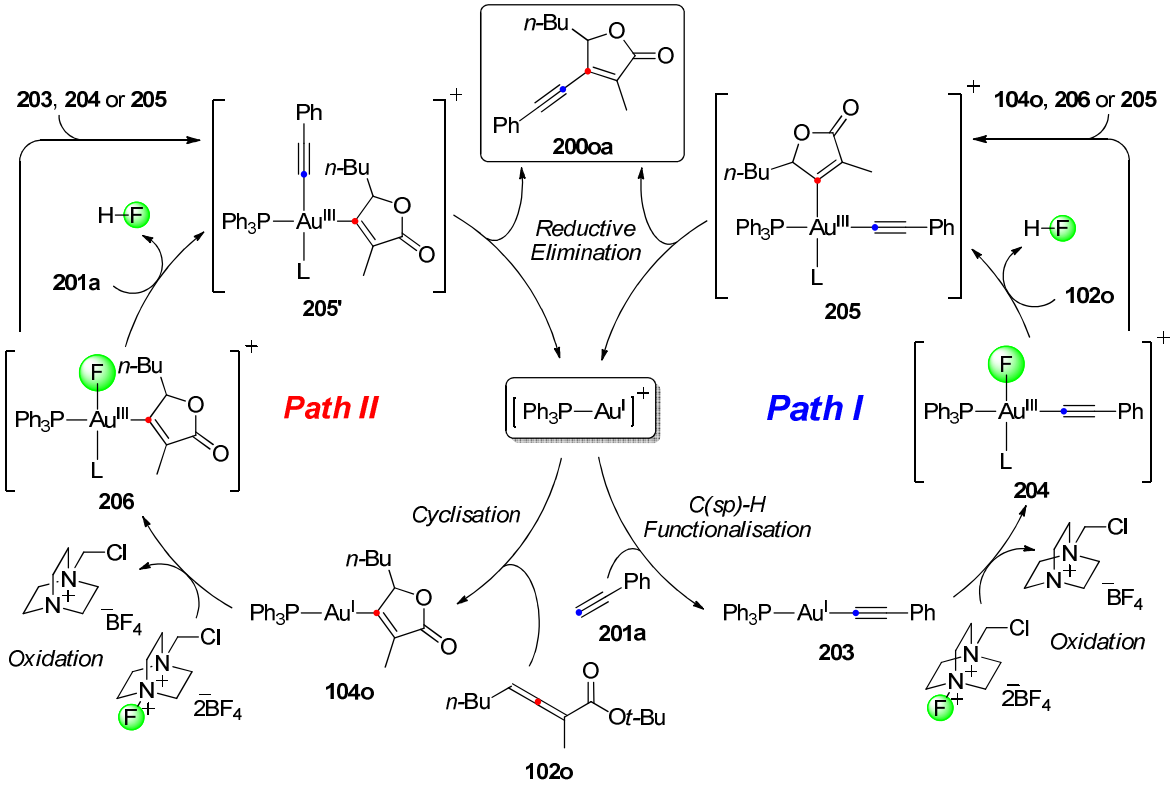


Figure 4.2 X-Ray Crystal Structure of β-Alkynyl-γ-Butenolide **200ea**.

4.3.5 Comments on the Reaction Mechanism

In accordance with our previous studies and the recent literature on related gold-catalysed coupling reactions performed in the presence of Selectfluor (**82**), the two Au^{I}/Au^{III} redox

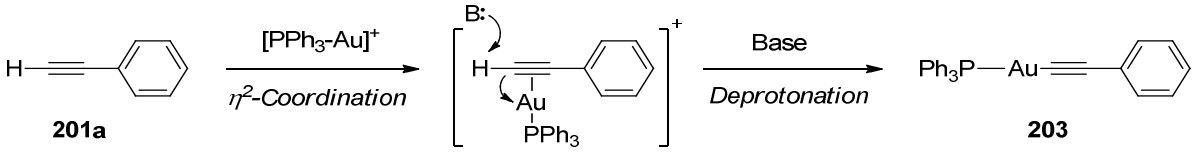
mechanisms shown in Scheme 4.35 can be postulated for the cascade cyclisation-intermolecular alkynylation reaction.



Scheme 4.35 Proposed Mechanisms for the Cyclisation-Intermolecular Alkynylation of Allenoates. L = Neutral Ligand.

In both of these pathways, the gold catalyst performs three separate functions. Acting in its traditional role as a π-Lewis acid, gold is thought to both mediate the cyclisation of the allenoate component and aid the deprotonation of the alkyne coupling partner prior to facilitating the coupling process itself. The order in which these processes are conducted, however, is not clear and two possible options are shown as Paths I and II in Scheme 4.39. In Path I, the cationic gold(I) source $[PPh_3Au]^+$ formed upon dissociation of the $^-NTf_2$ ligand in precatalyst **2**, first mediates the C(sp)-H functionalisation of the alkyne component leading to the η^1-(alkynyl)gold(I) complex **203**. The formation of this species is thought to occur via the mechanism shown in Scheme 4.36 where gold first coordinates the alkyne in an η^2 fashion. This π-activation effectively increases the lability of the alkynyl proton and

leads to the formation of the η^1-coordinated complex **203** upon treatment with a base present in the reaction mixture.



Scheme 4.36 Proposed Mechanism of C(sp)-H Functionalisation.

Oxidation of the (alkynyl)gold(I) complex **203** by the electrophilic fluorinating reagent Selectfluor would lead to the cationic gold(III) fluoride species **204**. Coordination of this intermediate to the allene moiety of the allenoate **102o** followed by intramolecular nucleophilic attack of the pendant *tert*-butyl ester would then deliver the gold(III) species **205** featuring both an alkynyl and a butenolide ligand.[ee,ff] The same intermediate could also be formed via transmetalation of a butenolide unit from a (butenolide)gold species onto complex **204**. C(sp^2)-C(sp) Bond-forming reductive elimination from complex **205** would then furnish the cross-coupled β-alkynyl-γ-butenolide product and regenerate the active gold(I) catalyst $[PPh_3Au]^+$ (Scheme 4.35, Path I). Alternatively, the allenoate cyclisation could occur prior to the alkyne coordination step. In this case, the (butenolide)gold(I) complex **104** formed upon initial 5-*endo*-trig cyclisation of the allenoate would be oxidised to the gold(III) fluoride complex **206** by Selectfluor. Complexation of the alkynyl component either directly from the alkyne **201** or via transmetalation from an (alkynyl)gold species would then deliver the doubly organic-substituted complex **205'**.[gg] Reductive

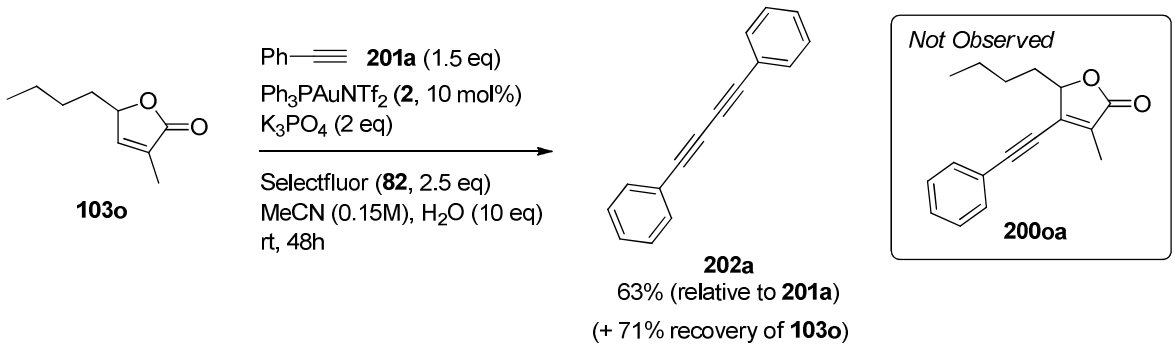
[ee] The basic additive K_3PO_4 could play a role in neutralising the hydrofluoric acid produced as a by-product of this process.

[ff] The fourth coordination site in the square-planar complex is most likely occupied by a neutral ligand such as acetonitrile present in the reaction mixture.

[gg] The geometries of the proposed square planar gold(III) fluoride complexes **204**, **205**, **205'** and **206** shown in Scheme 4.35 are speculatively assigned. Whilst intermediates **205** and **205'** are depicted as isomers, either of these species could feasibly result from Path I or Path II depending on the stereochemical preference of the oxidation or alkyne/butenolide coordination steps. In any case, reductive elimination from gold(III)

elimination from this species would again furnish the cross-coupled product **200** and regenerate the gold(I) catalyst (Scheme 4.35, Path II). Whilst a mechanism involving a β-fluoro-γ-butenolide intermediate **107** cannot be unequivocally ruled out for this transformation, our previous studies on the related cyclisation-intramolecular arylation of benzyl-substituted allenoates mitigate against such a pathway. β-Fluoro-γ-butenolides were not observed in any reaction mixture during the course of this study.

In order to provide support for the mechanisms shown in Scheme 4.35, several control reactions were conducted. In a preliminary experiment, γ-butenolide **103o** was reacted under the optimised conditions in the presence of phenylacetylene **201a**. The NMR spectra of the crude reaction mixture after 48 hours at room temperature contained no peaks consistent with the β-alkynyl-γ-butenolide **200oa** indicating that the cyclisation-protodeauration product is not an intermediate in the oxidative alkynylation process.[hh] Instead, γ-butenolide **103o** was recovered in 71% yield upon purification by silica gel column chromatography whilst diyne **202a**, resulting from oxidative homocoupling of the alkyne, was isolated in 63% yield relative to **201a** (Scheme 4.37).



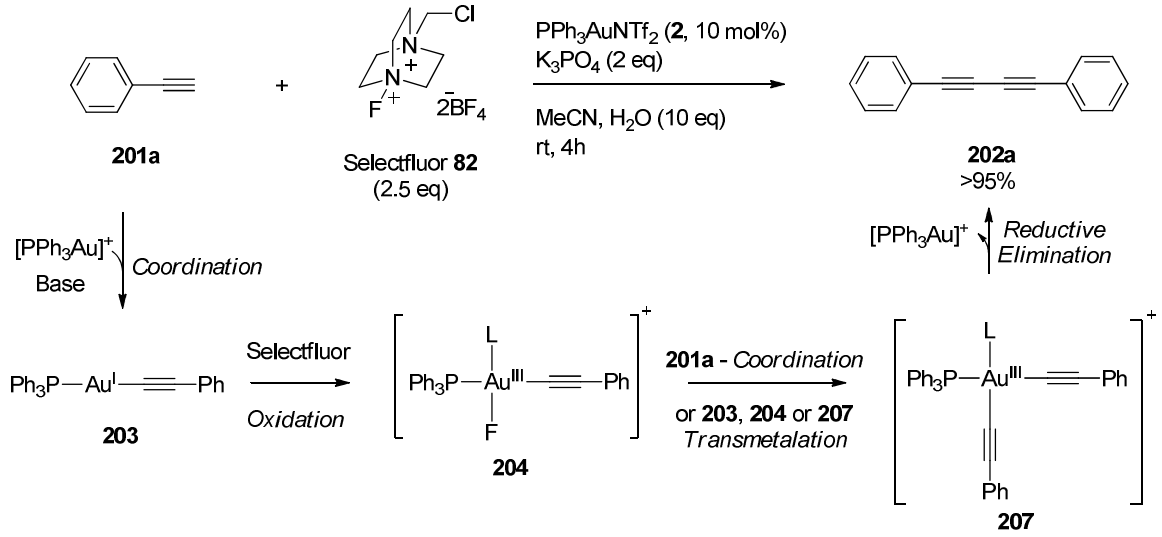
Scheme 4.37 Control Reaction with γ-Butenolide **103o**.

To distinguish between Paths I and II, alkyne **201a** and allenoate **102o** were reacted under the optimised conditions in the absence of an allenoate and an alkyne respectively. Treating

complexes is thought occur via a dissociative mechanism and thus the initial geometry of **205** or **205'** may be of little significance to the overall reactivity (see Section 3.2.2).

[hh] The butenolide homocoupling product **110o** was also not observed during this reaction (see Section 4.2).

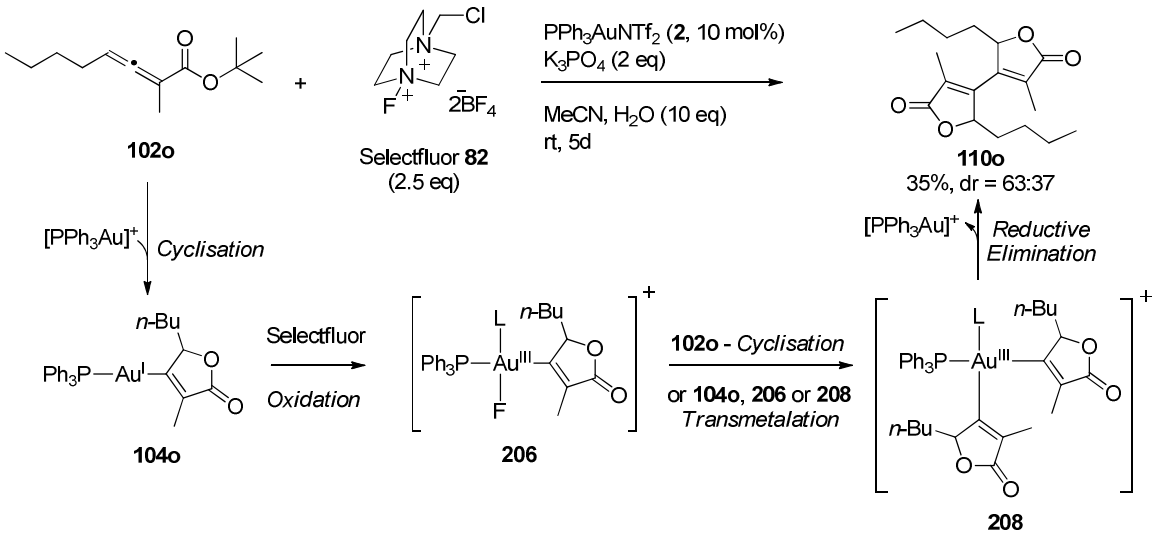
phenylacetylene **201a** with PPh_3AuNTf_2 (**2**, 10 mol%), Selectfluor (**82**, 2.5 eq) and K_3PO_4 (2 eq) in the absence of the allenoate led smoothly to the homodimerisation product **202a** in >95% yield after 4 hours at room temperature. The formation of the diyne product can be rationalised by a mechanism analogous to Path I in Scheme 4.39 where the (alkynyl)gold(III) fluoride complex **204** activates a second molecule of the alkyne to afford the doubly alkyne-substituted gold(III) complex **207** amenable to C(sp)-C(sp) bond-forming reductive elimination (Scheme 4.38).



Scheme 4.38 Homodimerisation of Alkyne **201a**.

Reacting *tert*-butyl allenoate **102o** under the same conditions in the absence of the alkyne led to the cyclisation-oxidative homodimerisation product **110o** in 35% yield (dr = 63:37) after 5 days at room temperature (Scheme 4.39). The formation of this compound is consistent with an Au^I/Au^{III} redox mechanism analogous to that shown in Path II in Scheme 4.35. In this case, the coordination of a second butenolide fragment onto complex **206** would lead to the gold(III) species **208** featuring two butenolide ligands.[ii]

[ii] A mechanistic explanation for the gold-catalysed formation of bibutenolides **110** from *tert*-butyl allenoates **102** is shown in Scheme 4.21 (see also Scheme 3.59).

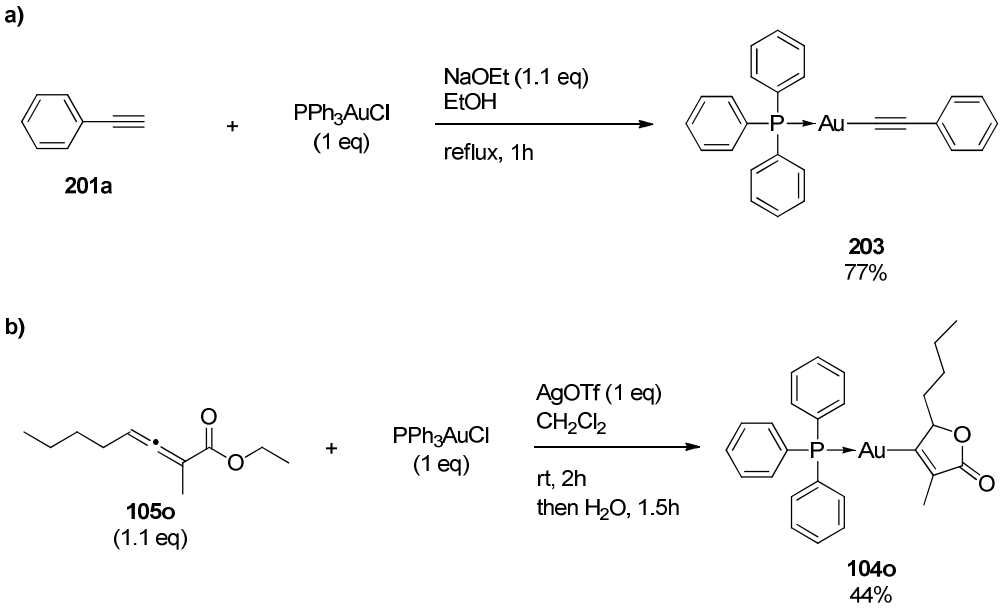


Scheme 4.39 Cyclisation-Homodimerisation of *tert*-Butyl Allenoate **102o**.

The long reaction time and low yield of allenoate homodimerisation process in comparison to the alkyne homocoupling reaction above suggests that Path I could be a more favourable pathway than Path II under the standard conditions. This interpretation is also consistent with our scope and limitation studies where diynes resulting from competitive homodimerisation of the alkyne components were often isolated as minor side-products. Conversely, the allenoate cyclisation-homocoupling products **110** were generally not observed during these reactions.[jj]

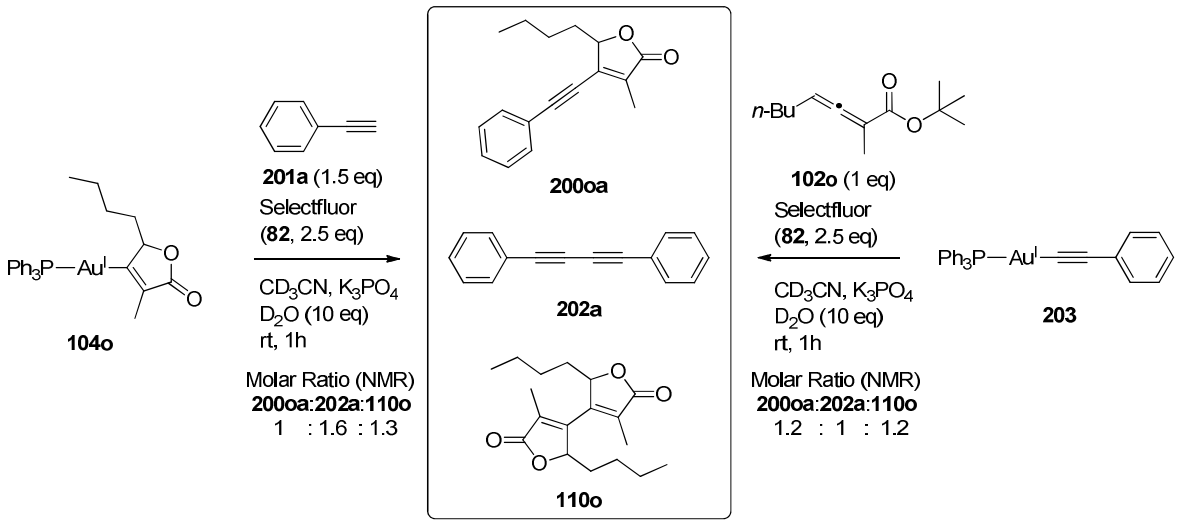
To support a mechanism involving the η^1-(alkynyl)gold(I) and (butenolide)gold(I) complexes **203** and **104o**, these species was prepared independently according to the procedures of Hashmi and co-workers and subjected to the standard oxidative cross-coupling conditions with allenoate **102o** and alkyne **201a** respectively (Scheme 4.40).[205, 208]

[jj] Bibutenolide **110o** was isolated 23% yield when allenoate **102o** was reacted with 1-pentyne **201k** at 80°C (see Scheme 4.32b). However, the elevated temperature of this reaction and the copper(I) acetate (10 mol%) co-catalyst could both have a role to play in the formation of the allenoate homodimerisation product.



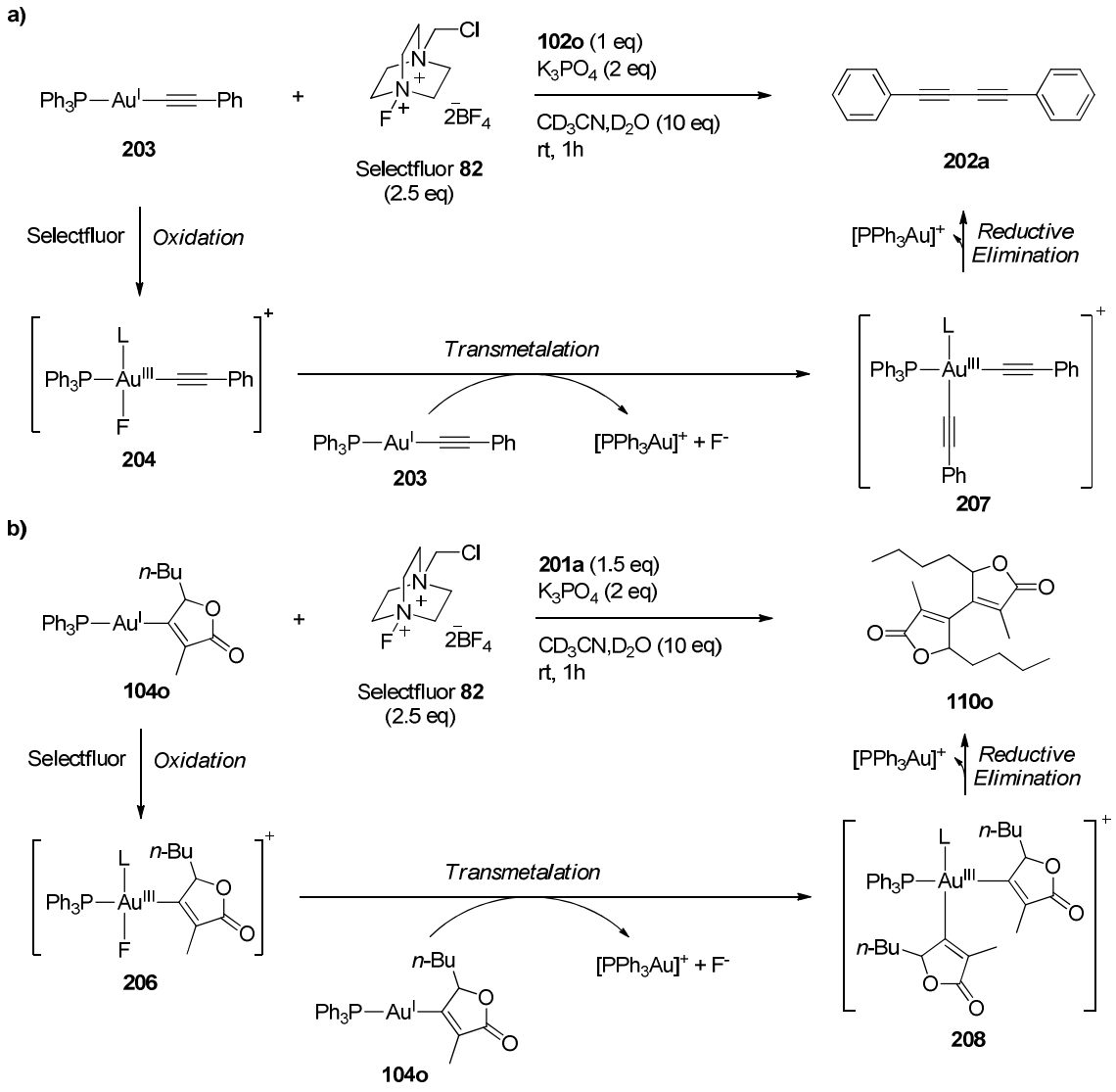
Scheme 4.40 Preparation of Organogold(I) Complexes **203** and **104o**.

NMR Analysis of the crude reaction mixtures after one hour at room temperature in deuterated acetonitrile and D_2O (10 eq) indicated that the cross-coupled β-alkynyl-γ-butenolide product **200oa** had been formed in both cases. Interestingly, the diyne **202a** and bibutenolide **110o**, resulting from oxidative homocoupling of the alkyne and allenoate respectively, were also formed during both reactions (Scheme 4.41).



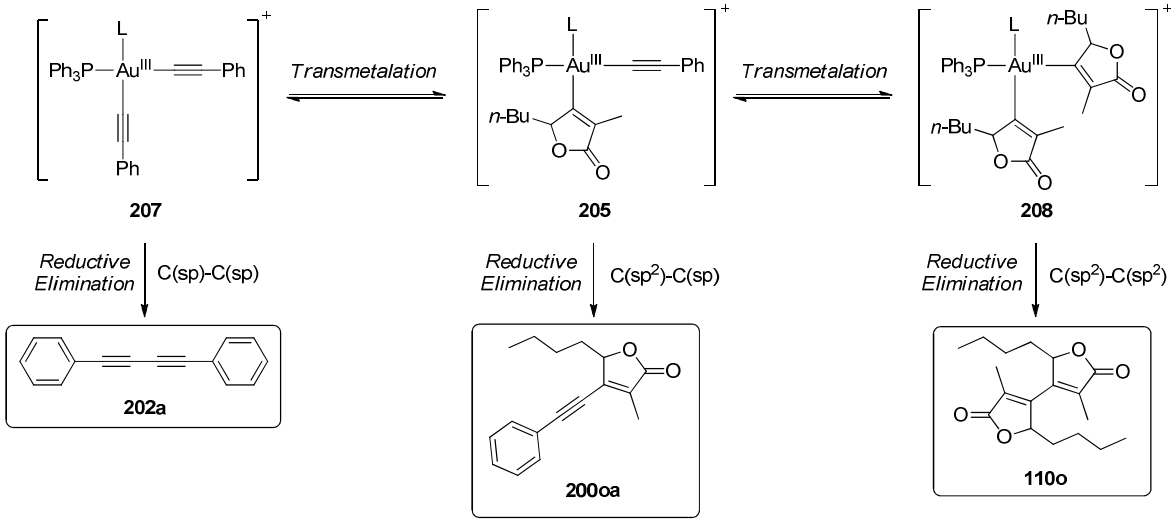
Scheme 4.41 Formation of Cross-Coupled and Homocoupled Products from Organogold(I) Complexes **104o** and **203** (molar ratio estimated by ^{1}H NMR).

The formation of diyne **202a** from η^1-(alkynyl)gold(I) complex **203** in the absence of added alkyne **201a** is best explained by the mechanism shown in Scheme 4.42a. In this pathway, the alkynyl ligand in complex **203** transmetalates onto the (alkynyl)gold(III) fluoride species **204** to afford a doubly alkynyl-substituted gold (III) intermediate amenable to C(sp)-C(sp) bond-forming reductive elimination. A similar transmetalation of a butenolide unit from complex **104o** onto the gold(III) fluoride species **206** can explain the formation of bibutenolide **110** from the gold(I) complex **104o** in the absence of allenoate **102o** (Scheme 4.42b).



Scheme 4.42 Formation of Homodimerised Products from a) η^1-(Alkynyl)gold(I) Complex **203**. b) (Butenolide)gold(I) Complex **104o**.

If intermolecular ligand exchange processes of this type between organogold intermediates are sufficiently fast under the reaction conditions, each product **200**, **201** or **110** could feasibly be formed regardless of the initial coordination and oxidation steps. In this case, the product distribution would depend on the relative rates of ligand exchange and reductive elimination at each of the doubly organic-substituted gold(III) complexes **205**, **207** or **208** (Scheme 4.43).



Scheme 4.43 Intermolecular Ligand Exchange between Gold(III) Complexes.

4.4 Conclusions

In conclusion, the combination of gold catalysts and the electrophilic fluorinating reagent Selectfluor (**82**) is capable of mediating cascade cyclisation-oxidative coupling reactions between *tert*-butyl allenoates **102** and intermolecular coupling partners. Treating alkyl- and allyl-substituted substrates with 5 mol% of gold(III) chloride and 2.5 equivalents of the "F^+" source led smoothly to bibutenolides **110** resulting from a 5-*endo*-trig cyclisation-oxidative homodimerisation cascade. The $C(sp^2)$-$C(sp^2)$ bonded products were afforded in generally moderate to good yields upon purification by silica gel column chromatography whilst side-products resulting from cyclisation-protodeauration or cyclisation-fluorodeauration were not observed.

The homocoupled product **110o** was also furnished upon treating allenoate **102o** with sub-stoichiometric amounts of gold(III) in the absence of Selectfluor. The unexpectedly high yields of the bibutenolide **110o** produced in these reactions can be rationalised by a mechanism involving the disproportionation of the gold(I) generated upon carbon-carbon bond-forming reductive elimination into gold(0) and gold(III).

The scope of the methodology could be extended to intermolecular cross-coupling upon performing the reactions in the presence of terminal alkynes. This process gave access to β-alkynyl-γ-butenolides **200** directly from non-activated precursors using a catalytic amount of a single transition metal. The highest yields of the cross-coupled products were obtained with arylacetylenes bearing electron-donating substituents with the *para*-tolyl-substituted compound **200od** being delivered in >95% yield after 48 hours at room temperature. Electron-neutral and electron-poor arylacetylenes were also tolerated although alkyl and silyl-substituted alkynes led to low yields of the cross-coupled products. The scope of the allenoate substrates was also low with significant amounts of diyne side-products, resulting from competitive homocoupling of the alkyne components, being observed. As in our previous studies, the formation of these compounds is best-explained by an Au^{I}/Au^{III} redox mechanism where Selectfluor performs the key oxidation of gold(I) to gold(III) in the catalytic cycle.

Chapter 5

Palladium and $^{18}F^-$: Palladium-Catalysed [^{18}F]Radiofluorination for PET Imaging

5.1 Introduction to PET Imaging and Fluorine-18

Positron emission tomography (PET) imaging is a non-invasive imaging modality which allows for the quantitative investigation of biological function *in vivo*.[209-211] The technique relies on the detection of radioactivity emitted by a biologically relevant radiotracer compound labelled with a positron-emitting radioisotope (β^+ emitter). A small amount of this species (typically ≈ 400 MBq of activity for ^{18}F-labelled tracers) is administered to the patient prior to the scan and allowed to incubate for a given time depending on the radiotracer employed and the physiological process under investigation. Upon decay of the radioisotope, the emitted positron travels a short distance in the body before colliding with an electron and forming two coincident gamma (γ) rays oriented approximately 180º from each other (energy = 511 keV for ^{18}F). These gamma photons are detected by the scanner and, after millions of such annihilation events, are computed to form a 2D or a 3D image detailing the spatial distribution of the radioisotope *in vivo*. PET Images of this type have been used in the diagnosis of a wide range of medical conditions including cancer,[212] neurological diseases such as Alzheimer's or Parkinson's disease[213] and cardiovascular disorders.[214] Furthermore, a comparison of PET scans recorded after diagnosis can provide valuable information on the efficacy of any treatment program undertaken. In addition to these clinical roles, PET imaging has also found many applications as a research tool,

providing quantitative information on both the function of biologically relevant compounds in the body and their subsequent metabolic fate (Figure 5.1).

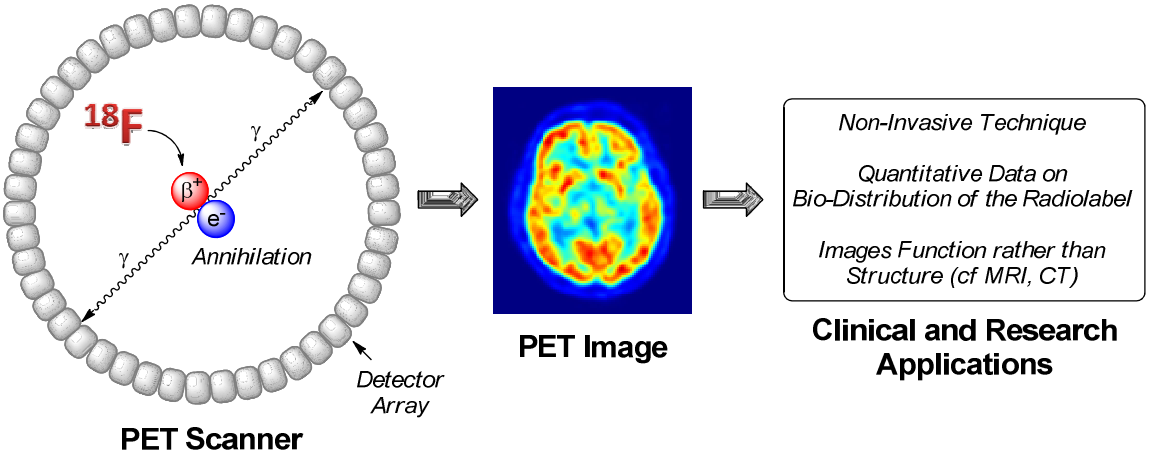


Figure 5.1 Schematic Diagram of Positron Emission Tomography (PET) Imaging.

A selection of positron-emitting radioisotopes commonly employed as the radiolabel in PET tracers are displayed in Table 5.1.[209] A key feature of these isotopes is their relatively short half-lives (< 3 hours),[kk] which both reduce the overall dose of radioactivity received by the patient and allow for several different scans to be undertaken over the course of a few days.[76] The most widely used β^+ emitter in PET radiotracers is fluorine-18 (Figure 5.2). The comparatively long half-life of this isotope ($t_{½}$ = 109.7 min) allows for the preparation of complex radiotracers requiring several synthetic steps after incorporation of the radiolabel. Whilst organofluorine compounds are scarce in nature, these species are commonly employed as pharmaceuticals with the fluorine atom acting as an isostere for a hydrogen or hydroxyl group. Furthermore, the half-life of fluorine-18 allows for radiotracers to be prepared at a dedicated radioisotope production facility and then transported to the

[kk] Longer half-life isotopes such as copper-64 ($t_{½}$ = 12.7 hours) and iodine-124 ($t_{½}$ = 4.18 days) are occasionally used for imaging biological processes with long timescales.

hospital or research centre, enabling PET scans to be performed at locations without access to cyclotrons or radiochemistry laboratories on site.[ll]

Radionuclide	Nuclear Reaction of Preparation[a]	Half-Life ($t_{½}$, min)	Decay Product	Maximum Positron Energy (MeV)
^{11}C	^{14}N(p,α)^{11}C	20.4	^{11}B	0.96
^{13}N	^{16}O(p,α)^{13}N	9.97	^{13}C	1.19
^{15}O	^{15}N(p,n)^{15}O	2.04	^{15}N	1.72
^{19}F	^{18}O(p,n)^{18}F	109.7	^{18}O	0.64

[a] Nuclear reaction is of the form: [Bombarded nuclide](cyclotron beam, side-product of nuclear reaction)[Product nuclide]. p = proton, n = neutron, α = alpha particle.

Table 5.1 Properties of some Common PET Radioisotopes.

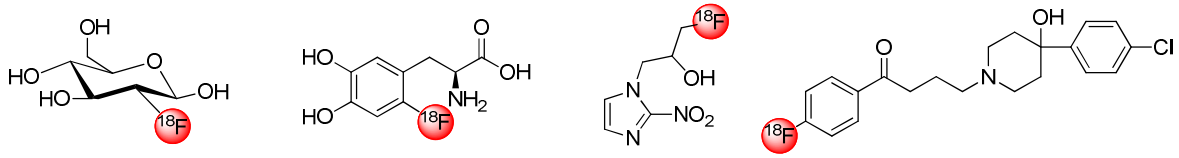


Figure 5.2 A Selection of ^{18}F-Labelled PET Radiotracers.

5.2 Radiolabelling with Fluorine-18

5.2.1 General Considerations of Labelling with Short Half-Life Radioisotopes

In addition to the environmental and safety implications inherent to working with ionising radiation, the labelling of organic compounds with short half-life radioisotopes such as fluorine-18 raises significant challenges not encountered in conventional organic synthesis. In order to minimise decay of the β^+ emitter prior to the PET scan, the total time between production of the radioisotope in the cyclotron and delivery of the clinical dose of the

[ll] The comparatively low energy of the positrons emitted from fluorine-18 also leads to higher resolution PET images as the average distance between the site of radioisotope decay and the annihilation event detected by the scanner is reduced. Whilst of limited practical significance at present, this effect is expected to become important as the resolution of PET scanners increases. [Current PET scanner resolutions are typically in the order of 4-8 mm].

labelled radiotracer to the patient should not generally exceed three half-lives of the isotope (ie ≈ 6 hours for ^{18}F). In addition to the [^{18}F]radiofluorination event and any subsequent synthetic steps, the initial preparation of the radiofluorinating reagent, the purification and analysis of the ^{18}F-labelled compound and the final delivery of the tracer to the PET imaging site must also occur within this timeframe. As such, synthetic routes towards PET radiotracers that incorporate the fluorine at as late a stage as possible are preferred whilst the [^{18}F]radiofluorination reactions themselves should be clean and rapid processes (typically ≤ 30 minutes). In addition, purification of the labelled tracer from the crude reaction mixture should be fast and operationally simple. The relative stoichiometry of the fluorinating reagent and the precursor must also be considered when selecting a radiolabelling methodology. Fluorine-18 is produced in typically picomolar to nanomolar amounts whilst the tracer precursor substrates are present in much larger quantities (generally micromolar concentrations). As such, fluorination processes that require equimolar or excess amounts of the fluorine source are not suitable for radiochemical applications whilst yields are calculated with respect to the amount of ^{18}F (radiochemical yield = RCY) rather than the non-radioactive precursor.

5.2.2 Sources of Fluorine-18

Fluorine-18 is most commonly produced via the ^{18}O(p,n)^{18}F nuclear reaction whereby an oxygen-18 target nucleus is bombarded with a beam of protons accelerated in a cyclotron.[215]mm Irradiation of ^{18}O-labelled water under these conditions leads to the formation of [^{18}F]fluoride ions, which are collected from the cyclotron in an $H_2{}^{18}O$-solution with various metal cations originating from the walls of the target chamber. When oxygen-18 gas is used as the target material, the generated fluorine-18 adheres to the sides of the

[mm] Alternative nuclear reactions are very occasionally employed to prepare fluorine-18. The most prevalent among these is the ^{20}Ne(d,α)^{18}F (d = deuteron) reaction which was traditionally the method of choice for the generation of [^{18}F]F_2 gas. Nowadays, however, this process has been largely supplanted by the ^{18}O(p,n)^{18}F reaction.

cyclotron chamber and must be removed by irradiation with an inert gas containing a small amount of non-radioactive 'carrier' $^{19}F_2$. The electrophilic radiofluorinating reagent [^{18}F]F_2 produced via this method is therefore 'contaminated' with fluorine-19 and, consequently, has an inherently lower specific activity (SA) than the nucleophilic reagent, [^{18}F]fluoride.[216]nn This parameter, which is defined as the activity of a radioactive material per unit mass (unit = GBq/μmol), is of key importance for PET imaging as low SA tracers must be administered in higher doses. The presence of non-radioactive contaminants can result in the saturation of receptor sites *in vivo*, leading to low uptake of the ^{18}F-labelled tracer at the region of interest and poor signal-to-noise ratios. The larger quantities of potentially cytotoxic material administered prior to the PET scan may also have general safety implications for the patient. Another drawback to the use of [^{18}F]F_2 as a radiofluorinating reagent is the maximum theoretical radiochemical yield of 50% achievable with this species. Furthermore, the use of fluorine gas requires specialist equipment and training due to its high toxicity and reactivity whilst electrophilic radiofluorination reactions with [^{18}F]F_2 are often highly unspecific and difficult to control.[217-218]oo

As a result of these factors, the majority of ^{18}F-labelled compounds are synthesised via a nucleophilic [^{18}F]radiofluorination strategy using high specific activity [^{18}F]fluoride. The range of nucleophilic strategies for C-^{18}F bond formation currently available to radiochemists are briefly summarised in the following section focusing on examples which highlight the current limitations of each methodology.[219]

nn [^{18}F]Fluoride is typically produced with a specific activity of > 100 GBq/μmol whereas the SA of [^{18}F]F_2 is < 0.6 MBq/μmol. This value has been increased to 55 GBq/μmol using the post-target procedure developed by Solin and co-workers at the Turku PET Centre. reference [216]

oo Several alternative electrophilic ^{18}F-radiofluorinating reagents have been prepared from [^{18}F]F_2. Recently, our group has reported the successful preparation and use of ^{18}F-labelled variants of the widely-used F^+ sources, NFSI (reference [217]) and Selectfluor (**82**, reference [218]). These milder reagents are easier to handle than [^{18}F]F_2 and can be transported from the site of production to a PET centre without access to a cyclotron or F_2 gas rig.

5.3 Nucleophilic [^{18}F]Radiofluorination Methods

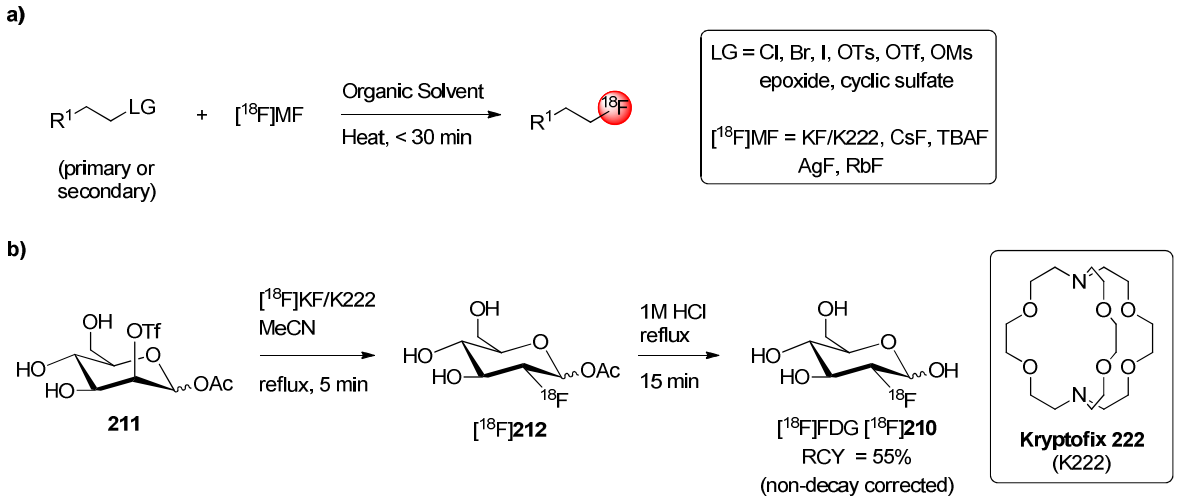
[^{18}F]Fluoride is delivered from the cyclotron in a $H_2{}^{18}O$ solution with various heavy metal cations and must be first converted into an organic soluble fluoride source suitable for use in the radiofluorination reactions.[pp] In most cases, the radioactive fluoride ion is trapped on an anion exchange cartridge and then eluted with an acetonitrile or acetonitrile/water solution containing a suitable cation. Removal of the remaining water upon azeotropic drying with anhydrous acetonitrile then delivers the organic-soluble [^{18}F]radiofluorinating reagent for use in the labelling reactions. The [^{18}F]fluoride source of choice for most applications is potassium [^{18}F]fluoride although alternative reagents such as caesium [^{18}F]fluoride and tetra-*n*-butylammonium [^{18}F]fluoride ([^{18}F]TBAF, [^{18}F]**209**) have also received significant research attention. [^{18}F]KF is typically used in combination with the phase-transfer catalyst Kryptofix 222 (K222), which improves the solubility of the fluoride source in organic solvents through the formation of a [cryptand-K^+] complex.

5.3.1 Aliphatic Nucleophilic [^{18}F]Radiofluorination

The most widely reported [^{18}F]radiofluorination method is the S_N2-type nucleophilic substitution of aliphatic sulfonyl esters with [^{18}F]fluoride (Scheme 5.1a).[220] A C(sp^3)-^{18}F bond-forming process of this type has been applied to the synthesis of the PET tracer 2-[^{18}F]fluoro-2-deoxy-D-glucose ([^{18}F]FDG, [^{18}F]**210**). Treating the trifluoromethanesulfonyl mannose derivative **211** with [^{18}F]KF/K222 in acetonitrile led smoothly to the peracetylated glucopyranoside [^{18}F]**212** after 5 minutes at reflux. The deprotected radiotracer [^{18}F]**210** was delivered in 55% non-decay corrected radiochemical yield over two steps upon hydrolysis of the acetate groups with hydrochloric acid at reflux for 15 minutes (Scheme 5.1b).[221] [^{18}F]FDG ([^{18}F]**210**) has found multiple applications as an imaging agent for glucose up-regulation in a variety of medical conditions, including cancer.[222] Similar nucleophilic

[pp] Fluoride is highly hydrated in aqueous solutions and is consequently a poor nucleophile.

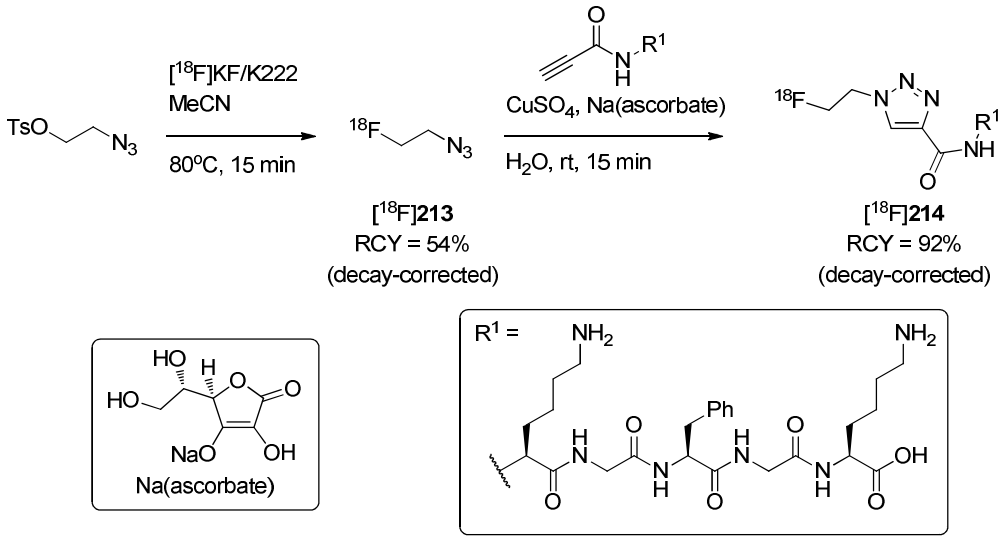
[^{18}F]substitution reactions have been reported with halide, mesylate and tosylate leaving groups whilst S_N2-type ring-opening of cyclic sulfates and epoxides has also been demonstrated.



Scheme 5.1 a) S_N2 Nucleophilic [^{18}F]Radiofluorination of Aliphatic Substrates. b) Preparation of [^{18}F]FDG ([^{18}F]**210**).

Whilst S_N2 reactions are the ^{18}F-labelling method of choice for a wide range of radiotracer targets, the high temperatures typically required for C(sp^3)-^{18}F bond construction to occur at a reasonable rate in these processes are not compatible with many sensitive substrates. In particular, peptides and proteins are susceptible to denaturation under typical [^{18}F]radiofluorination conditions whilst the organic solvents required for labelling with fluoride are not compatible with many biomolecules. In addition, large, complex substrates bearing nucleophilic moieties could undergo competitive intramolecular substitution processes with reactive halide or sulfonyl ester leaving groups. As a result of these limitations, oligonucleotides, peptides and proteins are most commonly labelled via an indirect approach involving an intermediate prosthetic group.[223-224] This species is prepared via conventional nucleophilic [^{18}F]radiofluorination performed at elevated temperatures in an organic solvent and, after purification is attached to the rest of the compound in a mild

and rapid ligation step compatible with the sensitive substrate of interest. [qq] Commonly employed coupling strategies include the condensation of ^{18}F-labelled benzaldehyde prosthetic groups (see Section 5.3.2) with peptide *N*-termini and the Huisgen ('click') 1,3-dipolar cycloaddition of terminal alkynes with 2-[^{18}F]fluoroethylazide ([^{18}F]**213**). Using this latter approach, Årstad and co-workers were able to efficiently synthesise the labelled peptide fragment [^{18}F]**214** in 92% decay corrected RCY from the prosthetic group after only 15 minutes at room temperature (Scheme 5.2).[225] In contrast to direct [^{18}F]radiofluorination, however, the indirect labelling of sensitive substrates with fluorine-18 is a time-consuming and labour-intensive process, requiring additional ligation and purification steps.



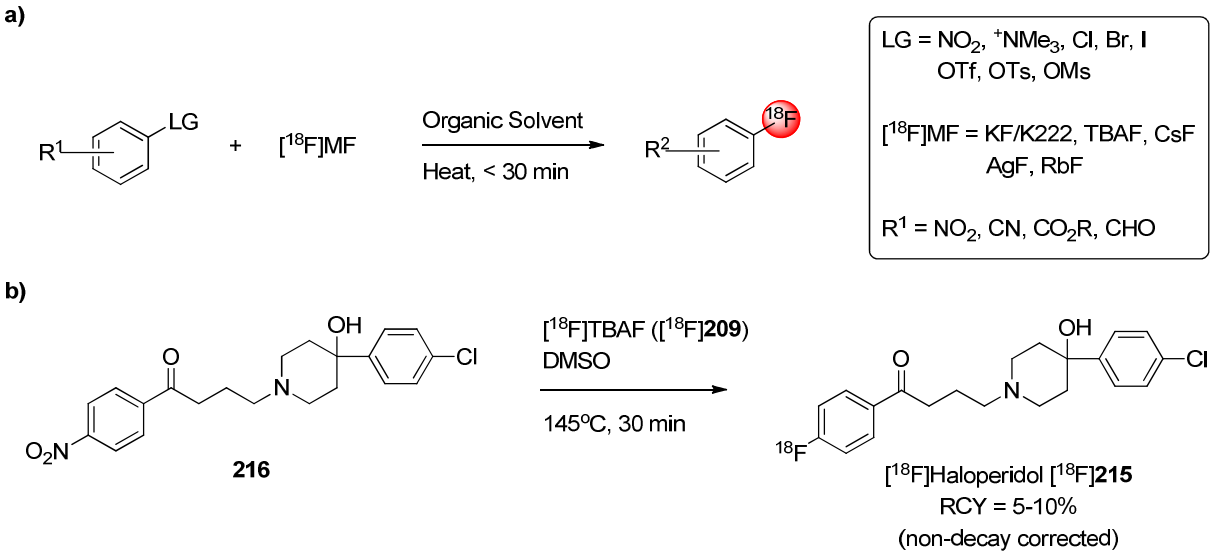
Scheme 5.2 Indirect Labelling of a Peptide using a 'Click' Reaction.

5.3.2 Aromatic Nucleophilic [^{18}F]Radiofluorination

Fluorinated aromatic rings feature prominently in pharmaceuticals and are thus common motifs in radiotracer targets. In accordance with aliphatic [^{18}F]radiofluorination, the installation of an aromatic ^{18}F-substituent is most often achieved using a nucleophilic displacement strategy. Aromatic substitution (S_NAr) reactions of this type with non-carrier-

[qq] [^{18}F]Fluoroalkyl and [^{18}F]fluoroaromatic prosthetic groups are prepared via S_N2 and S_NAr nucleophilic fluorination respectively. (see Section 5.3.2 for a discussion of S_NAr nucleophilic aromatic fluorination).

added [^{18}F]fluoride are often highly efficient processes, delivering ^{18}F-labelled arenes in good radiochemical yields within 30 minutes (Scheme 5.3a).[220] Aromatic precursors bearing nitro- or trimethylammonium salt leaving groups generally lead to the highest RCYs of the ^{18}F-labelled products although aromatic halides and sulfonyl esters have also been successfully employed.[226][rr] The use of trimethylammonium salt precursors has the added advantage of facile separation of the ^{18}F-labelled products from the unreacted starting materials by simple chromatographic methods.[ss] An S_NAr [^{18}F]radiofluorination process was applied by Kilbourn and co-workers to the synthesis of [^{18}F]haloperidol ([^{18}F]**215**).[227] This radiotracer, which is used in the study of dopamine receptors in the brain, was delivered in one step upon treating the nitroarene precursor **216** with [^{18}F]TBAF ([^{18}F]**209**) in DMSO for 30 minutes at 145ºC (Scheme 5.3b).



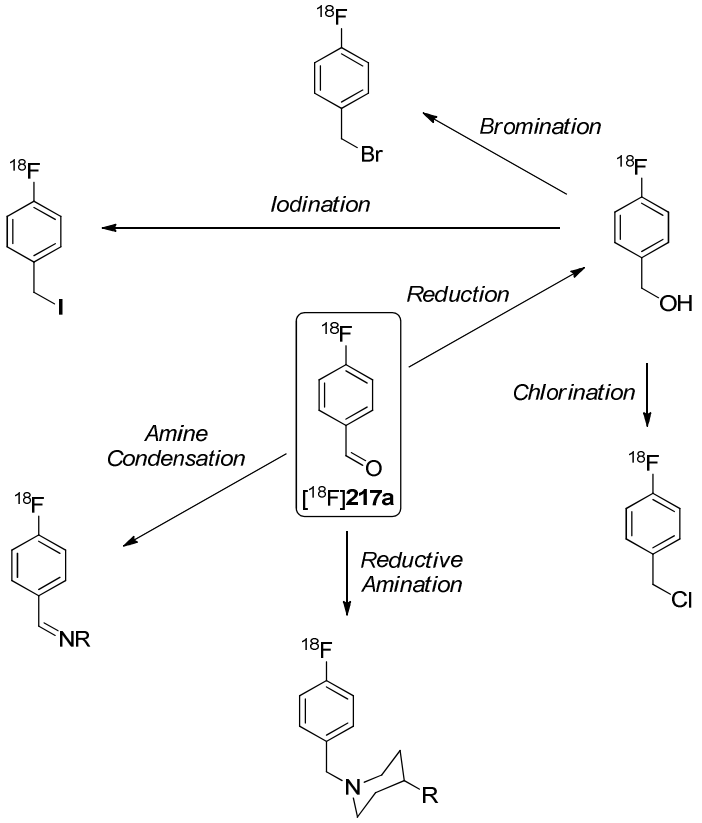
Scheme 5.3 a) S_NAr Nucleophilic Aromatic [^{18}F]Radiofluorination of Aromatic Substrates. b) Preparation of [^{18}F]Haloperidol ([^{18}F]**215**).

The scope of arenes suitable for nucleophilic aromatic [^{18}F]radiofluorination, however, is limited to substrates able to stabilise the negative charge generated by the attack of

[rr] ^{18}F-Labelled pyridines are also synthesised using an S_NAr approach. These motifs have been used as prosthetic groups for the indirect ^{18}F-labelling of several radiotracer targets. reference [226]

[ss] By contrast, nitro- or haloarene precursors often possess similar chromatographic properties to the [^{18}F]fluoroaromatic products leading to complications during purification.

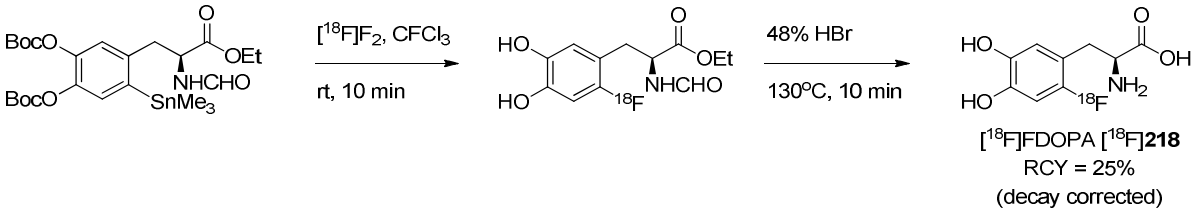
[^{18}F]fluoride. In order for C(sp^2)-^{18}F bond formation to occur at a reasonable rate, at least one electron-withdrawing substituent, such as a carbonyl, nitrile or nitro group, must be present at the *ortho* or *para*-positions of the arene ring. As such, the preparation of PET radiotracers featuring an electron-rich fluorinated arene motif relies heavily on indirect labelling methodologies involving electron-poor [^{18}F]fluoroaromatic prosthetic groups such as 4-[^{18}F]fluorobenzaldehyde ([^{18}F]**217a**, Scheme 5.4). The synthesis of complex radiotracers via this method often requires several manipulations to be performed on the prosthetic group after [^{18}F]radiofluorination, resulting in long overall synthesis times and substantial decay of the radiolabel.



Scheme 5.4 Selected Modifications of 4-[^{18}F]Fluorobenzaldehyde [^{18}F]**217a**.

In fact, electrophilic strategies are still the ^{18}F-labelling methods of choice for many radiotracers featuring electron-rich aromatic motifs despite the previously discussed disadvantages associated with $^{18}F^+$ sources (see Section 5.2.2). For example, an electrophilic

[^{18}F]fluorodestannylation reaction with [^{18}F]F_2 is currently used to prepare the dopamine metabolism imaging agent [^{18}F]FDOPA ([^{18}F]**218**) (Scheme 5.5).[228]

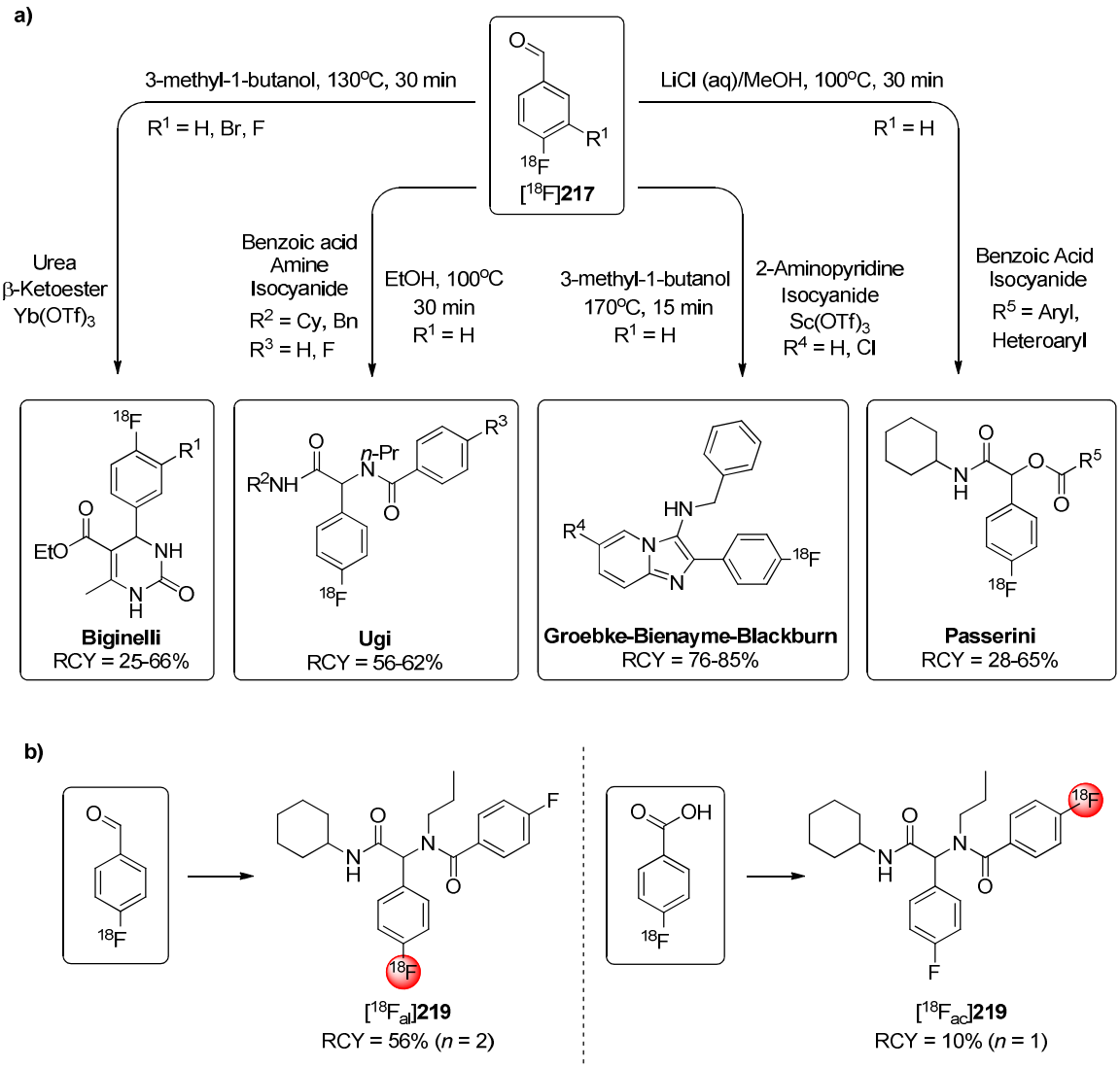


Scheme 5.5 Preparation of [^{18}F]FDOPA ([^{18}F]**218**).

The preparation of [^{18}F]fluoroaromatic motifs from high specific activity [^{18}F]fluoride remains a significant challenge for PET radiochemists. Alongside synthetic investigations aimed at identifying novel direct routes to these compounds, several research groups have focused on improving the efficiency and scope of indirect labelling methodologies involving electron-deficient [^{18}F]fluoroaromatic prosthetic groups. As part of our studies into novel ^{18}F-labelling strategies, we demonstrated that [^{18}F]fluorobenzaldehyde ([^{18}F]**217**) or benzoic acid building blocks can constitute one component in a multicomponent reaction leading to complex fluoroaromatic compounds in a single step from the prosthetic group (Scheme 5.6a).[229][tt] Using the Biginelli,[230] Ugi,[231] Passerini[232] and Groebke-Bienaymé-Blackburn[233-235] reactions as representative convergent processes, a selection of heterocyclic and peptide-like ^{18}F-labelled molecules featuring electron-rich [^{18}F]fluoroaromatic motifs were synthesised in two steps from [^{18}F]KF/K222 in moderate to excellent radiochemical yields. For each multicomponent reaction, a range of diversely-substituted labelled compounds could be prepared using a single set of optimised conditions with only minor variations in the reaction efficiency observed using different non-radioactive components. Furthermore, the Ugi coupling product [^{18}F]**219** could be

[tt] This work was performed in collaboration with Lei Li (DPhil, University of Oxford, **2011**), Dr. Rodrigue Leuma Yona (University of Oxford) and Dr. Romain Bejot (University of Oxford).

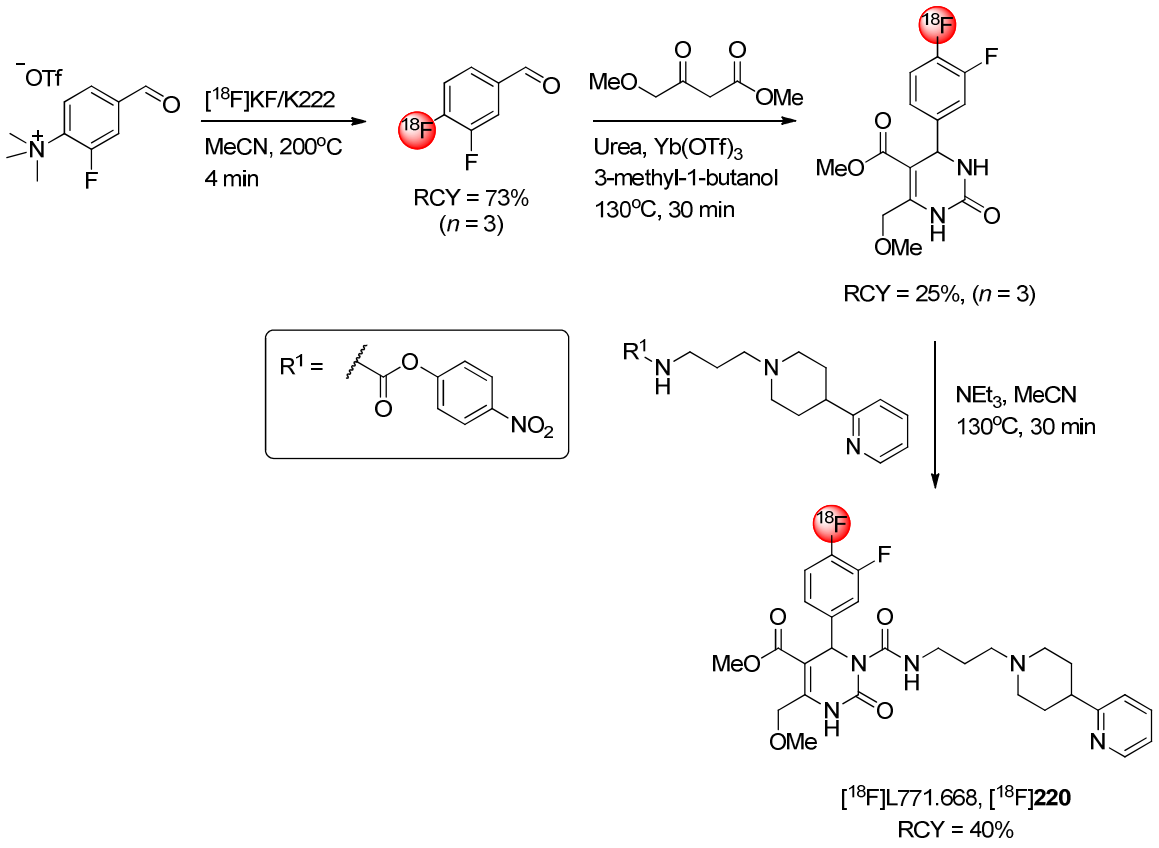
successfully radiolabelled at two different positions depending on whether the benzaldehyde or benzoic acid component was labelled with fluorine-18 (Scheme 5.6b).[uu]



Scheme 5.6 a) Convergent ^{18}F-Radiosynthesis using [^{18}F]Fluoroaromatic Prosthetic Groups. b) Labelling of the Ugi Product [^{18}F]**219** at Two Different Positions.

The potential of this strategy to prepare pharmaceutical targets was demonstrated by the concise synthesis of the α_{1A} adrenoceptor antagonist [^{18}F]L881,668 ([^{18}F]**220**)[236] using a three-component Biginelli reaction as the key step (Scheme 5.7).

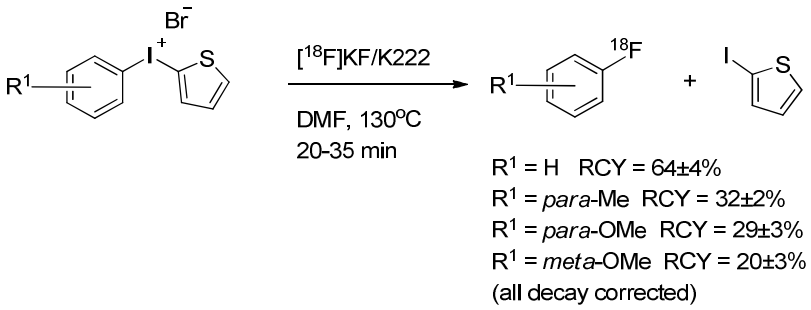
[uu] The Ugi reaction of [^{18}F]4-fluorobenzoic acid was less efficient, however, and required the addition of a small amount of the non-radioactive fluorinated acid in order to proceed. reference[229]



Scheme 5.7 Radiosynthesis of [^{18}F]L771,668 ([^{18}F]**220**) using a Biginelli Reaction.

Whilst indirect strategies with ^{18}F-labelled prosthetic groups remain the most widely used method to prepare high specific activity electron-rich [^{18}F]fluoroaromatic compounds, a more elegant approach to these compounds would involve the direct nucleophilic [^{18}F]radiofluorination of non-activated substrates with [^{18}F]fluoride. Several research groups have focused on the development of novel ^{18}F-labelling methodologies of this type with the most promising results reported to date centering on the use of diaryliodonium salt precursors.[237-240] In 2007, Coenen and co-workers reported the successful preparation of a range of [^{18}F]fluoroaromatics upon treating iodine(III) reagents bearing one thiophene substituent and one aryl group with [^{18}F]KF/K222 in *N*,*N*-dimethylformamide at 130ºC.[241] Notably, the reaction was successful with precursors featuring electron-neutral and electron-donating substituents around the arene ring with the *para*-methyl and *para*-methoxy substituted aromatics being delivered in 32±2% and 29±3% radiochemical yield

respectively (Scheme 5.8). In addition to acting as the leaving group in these reactions, the positively-charged iodonium group also removes electron density from the arene ring, activating it towards nucleophilic attack. The application of this methodology towards more complicated substrates, however, has proved challenging and, to date, no radiotracers containing electron-rich aromatic motifs have been labelled directly from iodonium salt precursors.



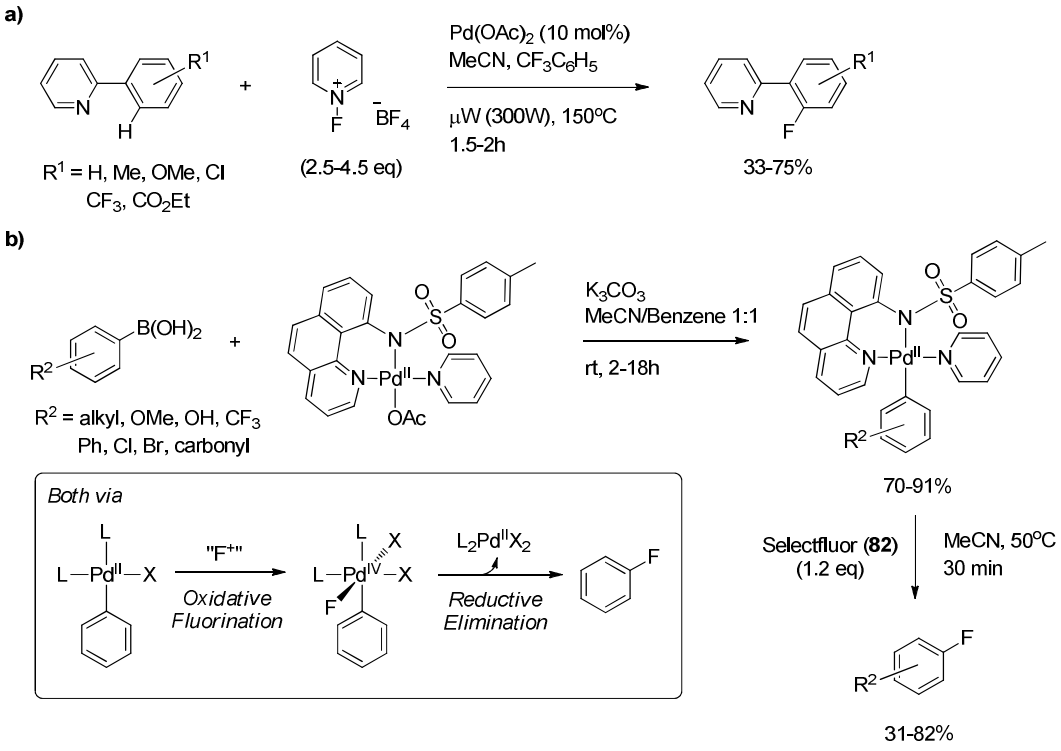
Scheme 5.8 Nucleophilic Aromatic [^{18}F]Radiofluorination of Iodonium Salts.

5.4 Applying Transition Metal Catalysis to ^{18}F-Radiochemistry

As discussed in the previous section, the labelling of organic compounds with fluorine-18 is dominated by nucleophilic substitution processes whereby an aliphatic or aromatic leaving group is replaced by high specific activity [^{18}F]fluoride.[219] Labelling methodologies of this type, however, generally require elevated reaction temperatures and the use of highly reactive leaving groups in order for C-^{18}F bond formation to occur within the timeframe imposed by the radioisotope half-life. Sensitive substrates such as biomolecules must therefore be labelled via lengthy, indirect protocols where ^{18}F-labelled prosthetic groups are prepared independently, purified and subsequently coupled to the rest of the molecule.[223-224] Furthermore, electron-rich ^{18}F-labelled aromatic motifs are not accessible via direct S_NAr nucleophilic [^{18}F]radiofluorination and must instead be prepared either upon functional group manipulation of electron-poor aromatic prosthetic groups or via direct electrophilic fluorination using low specific activity "$^{18}F^+$".

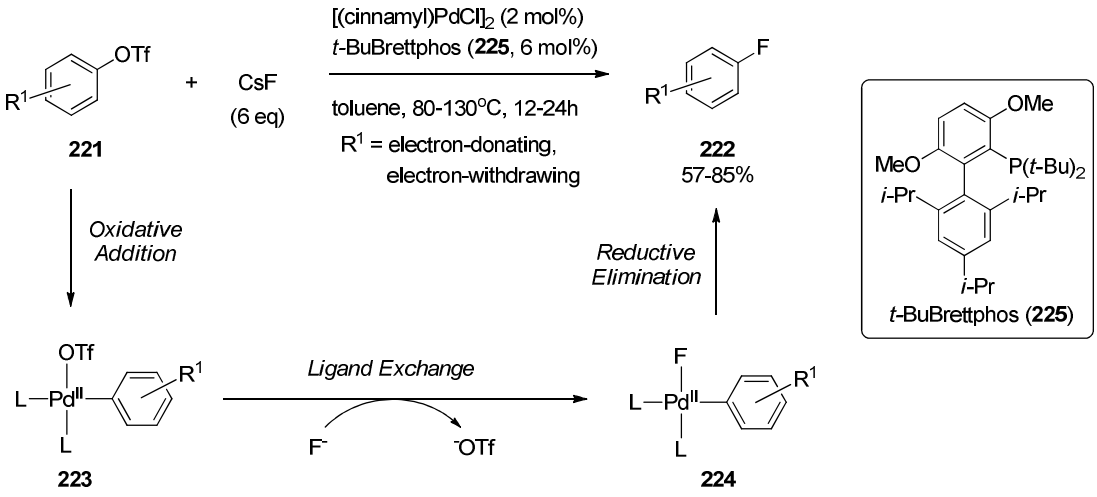
Over the last few years, significant research attention has focused on the development of novel nucleophilic [^{18}F]radiofluorination methods that could potentially overcome these limitations. As part of our studies into the effect of fluorinating reagents of the reactivity of transition metal catalysts, we sought to investigate whether C-^{18}F bonds could be formed directly from high specific activity [^{18}F]fluoride in the presence of palladium catalysts.

Palladium-catalysed fluorination has been demonstrated by a number of research groups using both electrophilic and nucleophilic sources of 'cold' fluorine.[242] The selective fluorination of arylboronic acids[243] and non-activated arenes[244-245] using palladium(II) sources and a range electrophilic fluorinating reagents were reported by the groups of Ritter and Sanford respectively. Mechanistic studies on proposed reaction intermediates indicated that the "F^+" sources in these processes act as stoichiometric oxidants, leading to (aryl)palladium(IV) complexes amenable to C(sp^2)-F bond-forming reductive elimination (Scheme 5.9).[246-248]



Scheme 5.9 a) Palladium-Catalysed Electrophilic Fluorination of Non-Activated Arenes. b) Palladium-Mediated Electrophilic Fluorination of Arylboronic Acids.

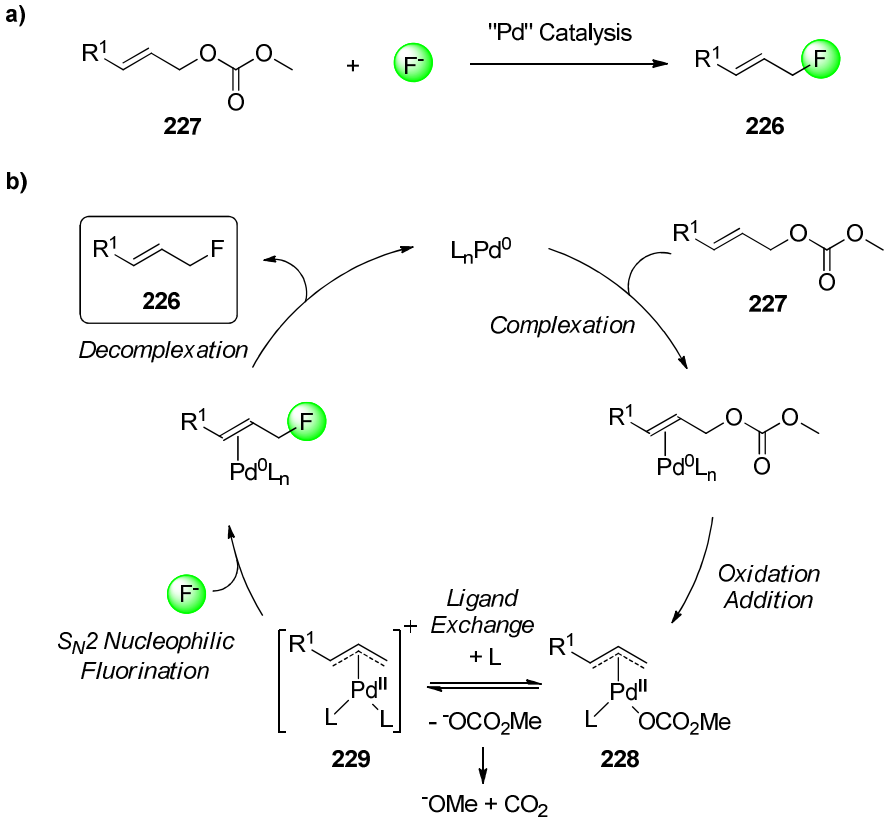
The first palladium-catalysed fluorination reaction using a nucleophilic source of fluorine was reported by Buchwald and co-workers in 2009.[98] A range of aryl triflates **221** bearing electron-withdrawing and donating substituents were converted into the corresponding fluoroarenes **222** in generally excellent yields upon treatment with palladium catalysts and 6 equivalents of caesium fluoride (Scheme 5.10). This reaction is thought to proceed via a Pd(0)/Pd(II) redox cycle involving the initial oxidative addition of the starting material onto palladium(0). Substitution of the triflate group in complex **223** by a fluoride ion would deliver the (aryl)palladium(II) fluoride species **224** amenable to C(sp^2)-F bond-forming reductive elimination. As demonstrated in a series of experimental and theoretical studies by Grushin[249] and Yandulov,[250] this latter step is a challenging operation from palladium(II) with P-F bond forming reductive elimination between the fluoride ion and a phosphine ligand being a more favoured process under most conditions. The key to encouraging C(sp^2)-F bond formation in this process was the use of palladium catalysts bearing the recently-developed ligand *t*-BuBrettphos (**225**). Related sterically-hindered mono-phosphine ligands have proved effective in facilitating challenging C-N,[251] C-O[252] and C-CF_3[253] bond-forming reductive elimination processes from palladium(II) complexes.



Scheme 5.10 Palladium-Catalysed Nucleophilic Fluorination of Aryl Triflates **221**.

5.4.1 Palladium-Catalysed Allylic Fluorination

In 2009, our group demonstrated that palladium(0) catalysts can react with allylic fluorides **226** to afford allylic substitution products resulting from C(sp^3)-F bond cleavage.[254] A series of competition experiments indicated that fluoride was a superior leaving group to acetate in these reactions although methyl carbonate-substituted starting materials were the most reactive. In principle, therefore, treating allyl methyl carbonates **227** with fluoride should deliver the C(sp^3)-F bonded products **226** provided suitable reaction conditions can be identified (Scheme 5.11a). A plausible mechanistic explanation for the palladium-catalysed nucleophilic allylic fluorination process is shown in Scheme 5.11b. Initial coordination of palladium(0) to the alkene moiety in the starting material followed by oxidative addition into the carbon-oxygen bond would afford the (allyl)palladium(II) complex **228**. The species is in equilibrium with the cationic complex **229** resulting from dissociation of the leaving group from the palladium centre. S_N2-Type nucleophilic attack of a fluoride ion onto the allyl ligand of either palladium(II) complex would result in the formation of a new C(sp^3)-F bond with concomitant reduction of the transition metal. Decomplexation of the palladium(0) from the alkene moiety would then deliver the allylic fluoride product and regenerate the active catalyst. Alternatively, the fluoride ion could attack the palladium centre of the cationic complex **229** directly to afford a palladium(II) fluoride intermediate, which would deliver the product upon C(sp^3)-F bond-forming reductive elimination. This pathway seems unlikely, however, due to the previously-discussed difficulty in encouraging C-F bond formation from palladium(II) complexes.

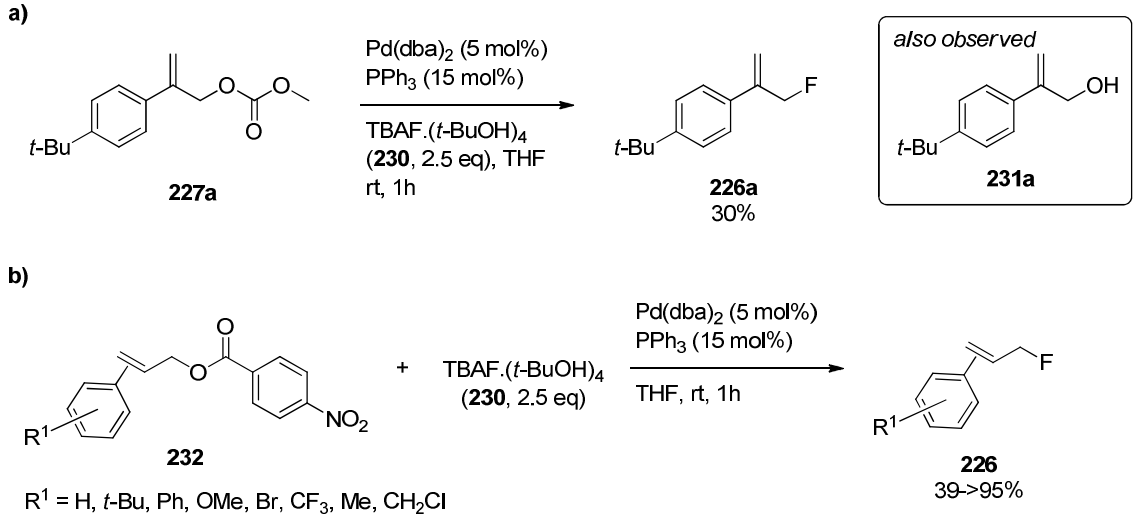


Scheme 5.11 a) Palladium-Catalysed Allylic Fluorination of Allylic Methyl Carbonates **227**. b) Plausible Mechanism for the Palladium-Catalysed Allylic Fluorination Reaction.

As a preliminary experiment, allyl methyl carbonate **227a** was reacted with $Pd(dba)_2$ (dba = dibenzylideneacetone, 5 mol%) and triphenylphosphine (15 mol%) in the presence of 2.5 equivalents of the recently-developed fluoride source TBAF.(*t*-BuOH)$_4$ (**230**) in tetrahydrofuran.[255-257] After one hour at room temperature, 89% of the starting material had been consumed with ^{1}H NMR analysis of the crude reaction mixture indicating that two products had been formed. The desired allylic fluoride **226a** was delivered as a single regioisomer in 30% isolated yield upon silica gel column chromatography whilst alcohol **231a** resulting from hydrolysis of the carbonate leaving group was also observed (Scheme 5.12a).[vv] The formation of this side-product was dramatically reduced upon switching the leaving group to *para*-nitrobenzoate. Using this substrate (**232a**), the allylic fluoride product

[vv] Competitive palladium-catalysed C-O bond formation with adventitious water could also explain the formation of the alcohol side-product.

226a was isolated in >95% yield whilst a range of diversely-substituted linear allylic *para*-nitrobenzoates **232** based on 1- or 2-arylprop-2-en-1-ols were also readily converted into the corresponding C(sp^3)-F bonded compounds (Scheme 5.12b). In each case, the nucleophilic fluorination reaction was complete within one hour at room temperature whilst complete regioselectivity for the linear allylic fluoride product was observed.

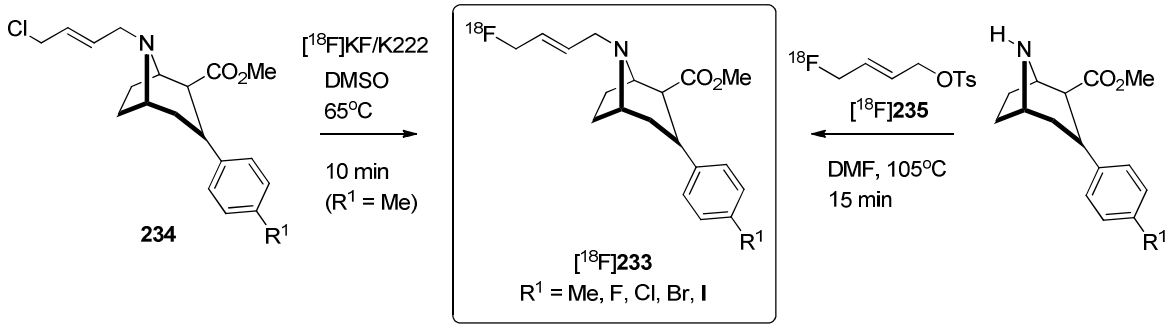


Scheme 5.12 a) Palladium-Catalysed Allylic Fluorination of Allylic Methyl Carbonate **227a**. b) Palladium-Catalysed Allylic Fluorination of Allylic *para*-Nitrobenzoates **232**.

5.4.2 Outline of the Project

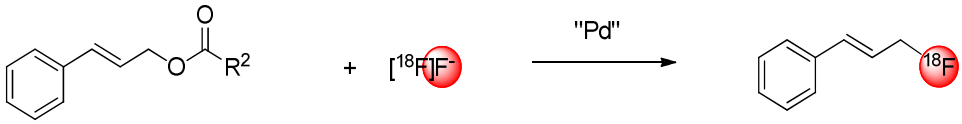
Inspired by the successful development of a palladium-catalysed allylic fluorination process using nucleophilic sources of fluorine, we sought to investigate whether this methodology could be extended to the synthesis of ^{18}F-labelled linear allylic fluoride motifs from high specific activity [^{18}F]fluoride. Although transition metal catalysed reactions are ubiquitous in conventional organic synthesis, these transformations are extremely scarce in the context of PET radiochemistry.[258] In particular, no transition metal-mediated C-^{18}F bond-forming processes have been reported to date whilst the reactivity of palladium complexes in the presence of ^{18}F sources has yet to be established. A family of radiotracer targets [^{18}F]**233** featuring an [^{18}F]allylic fluoride motif were recently reported by the groups of Dollé[259] and Goodman.[260] These compounds have shown promise as PET imaging agents for dopamine

transport in the brain and were synthesised directly from the allylic chlorides **234** or indirectly using the ^{18}F-labelled prosthetic group [^{18}F]**235** (Scheme 5.13).



Scheme 5.13 Current Synthetic Routes Towards the Dopamine Transport Imaging Agents [^{18}F]**233**.

In the remainder of this chapter, our preliminary studies towards the development of a palladium-catalysed allylic [^{18}F]radiofluorination reaction using high specific activity [^{18}F]fluoride are presented. These investigations led to the validation of the first transition metal mediated carbon-fluorine bond-forming process performed under radiosynthetic conditions (Scheme 5.14).[255]



227b (R^2 = OMe)
232b (*p*-$NO_2C_6H_4$)

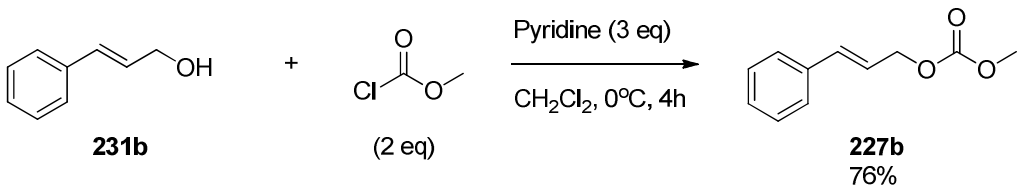
[^{18}F]**226b**

Scheme 5.14 Palladium-Mediated Allylic [^{18}F]Radiofluorination.

5.5 Palladium-Mediated Allylic [^{18}F]Radiofluorination

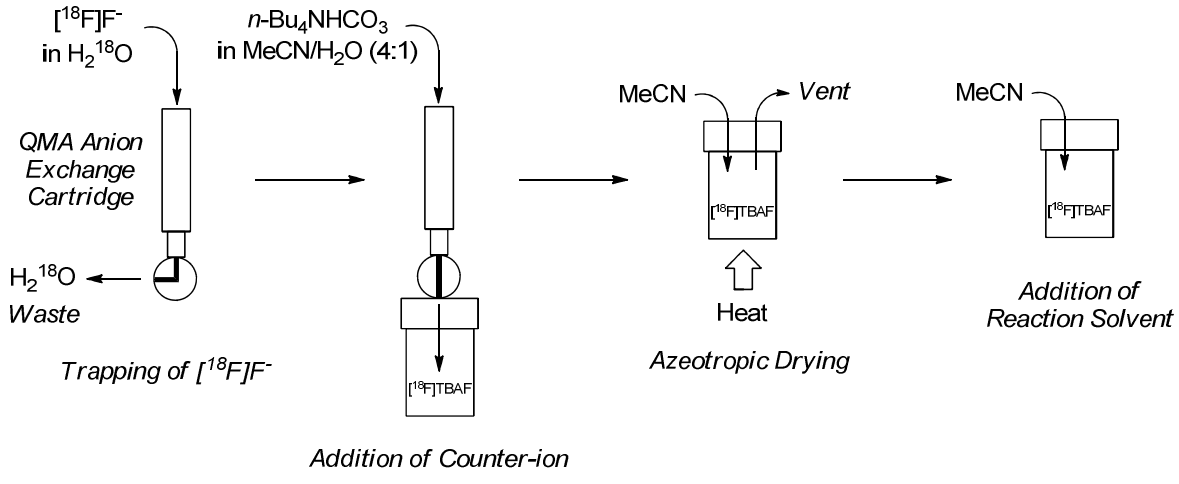
5.5.1 Preliminary Studies

The primary allylic methyl carbonate **227b** was selected as the test substrate for use in our preliminary ^{18}F-labelling experiments. This compound was prepared in 76% yield upon treating the commercially-available alchohol **231b** with two equivalents of methyl chloroformate in dichloromethane and pyridine (Scheme 5.15).



Scheme 5.15 Preparation of Allylic Methyl Carbonate **227b**.

As a first experiment, 5±1 mg of substrate **227b** was mixed with the palladium(0) source $Pd(dba)_2$ (2±1 mg) and triphenylphosphine (2±1 mg) in 450μL of acetonitrile in a dry borosilicate glass vial containing a v-shaped stirring bar. Acetonitrile is sufficiently polar to dissolve most [^{18}F]fluoride sources and is commonly employed as a solvent in nucleophilic S_N2 and S_NAr radiolabelling reactions. Furthermore, the widespread use of MeCN/H_2O as the mobile phase in reverse phase high performance liquid chromatography (HPLC) simplifies purification of the crude radiolabelled product upon completion of the reaction. The mixture of non-radioactive reagents was transferred to a lead-shielded hot cell and 50 μL of an acetonitrile solution containing [^{18}F]TBAF ([^{18}F]**209**) was added. This reagent was prepared from cyclotron-produced [^{18}F]F^-(aq) according to the counter-ion exchange/azeotropic drying procedure described in Section 5.3 (Scheme 5.16).



Scheme 5.16 Preparation of [^{18}F]TBAF ([^{18}F]**209**).

The [^{18}F]fluoride obtained from the cyclotron was separated from oxygen-18 enriched water using a quaternary methyl ammonium (QMA) anion exchange cartridge. A solution of tetra-*n*-butylammonium bicarbonate ($TBAHCO_3$, 13 mg) in acetonitrile/water (4:1, 0.5 mL) was then passed through the cartridge to afford [^{18}F]TBAF ([^{18}F]**209**), which was subsequently dried at 120ºC under a gentle stream of nitrogen with successive additions of acetonitrile (2×0.5 mL). A comparison of the total radioactivity of [^{18}F]fluoride obtained from the cyclotron with that of the dry [^{18}F]TBAF indicated that >98% of the fluoride (decay corrected) had been maintained during the counter-ion exchange and azeotropic drying process.

The dry [^{18}F]TBAF was dissolved in acetonitrile and transferred by lead-shielded syringe to the borosilicate glass vial containing the allylic methyl carbonate **227b**, $Pd(dba)_2$ and triphenylphosphine. After 5 minutes stirring at room temperature, the reaction was quenched with water (0.5 mL) and the crude mixture was injected onto the HPLC (Phenomenex NX 5µm C18 column, MeCN/H_2O, Gradient A, 1 mL/min).[ww] Analysis of the radioactivity trace indicated the presence of only one ^{18}F-labelled organic product with the remainder of the radioactive material being unreacted [^{18}F]TBAF. Moreover, the retention time of the ^{18}F-labelled organic product (14.7 min) was consistent with the UV trace of the non-radioactive linear allylic fluoride **226b** (14.5 min, Figure 5.3).[xx] This reference compound was prepared from the corresponding allylic bromide **236b** in 14% isolated yield after distillation under reduced pressure (Scheme 5.17). The identity of the ^{18}F-labelled product was confirmed upon spiking with the 'cold' reference sample whilst analysis of the crude reaction mixture by radio-TLC (eluent: MeCN/H_2O, 95:5) indicated that [^{18}F]**226** had been delivered in 19% decay corrected radiochemical yield (Scheme 5.18).

[ww] See chapter 6 for details of the HPLC system.

[xx] The UV and radioactivity detectors of the HPLC system are in series and, consequently, the retention times of the radioactive peaks are ≈0.2 minutes later than the corresponding UV peaks.

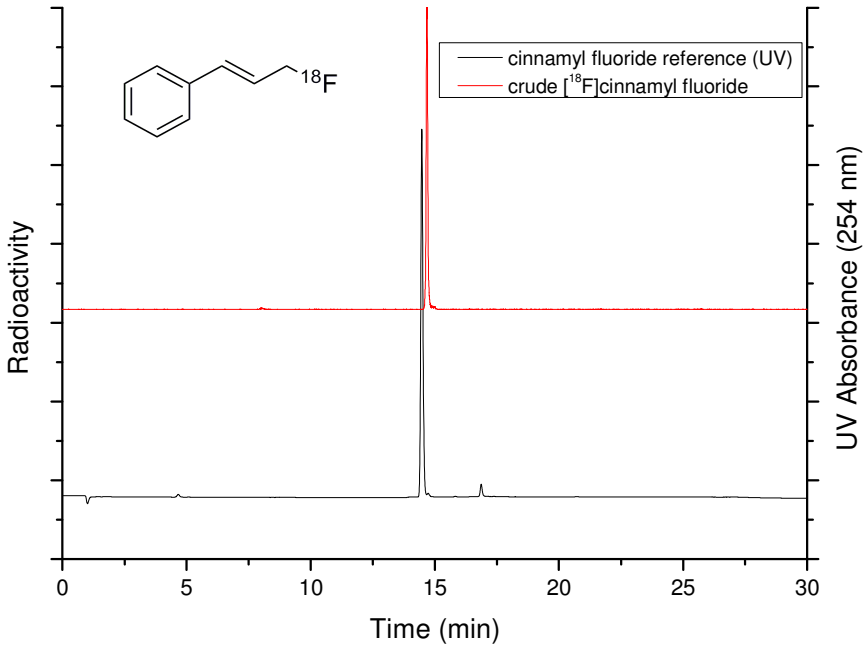
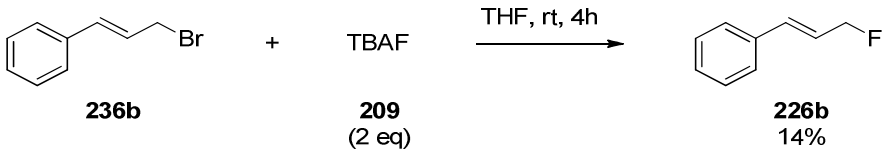
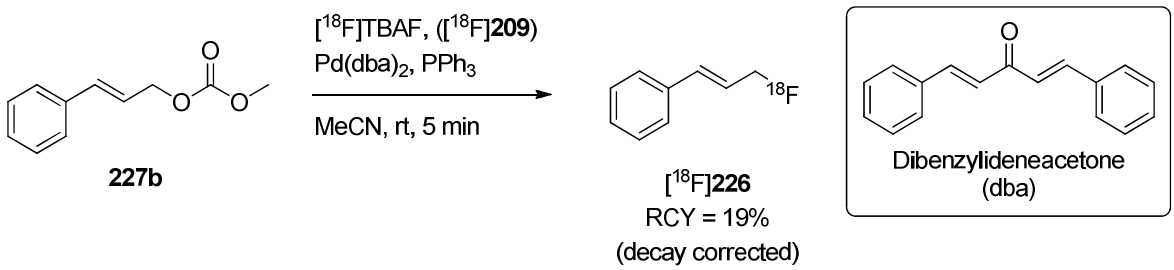


Figure 5.3 HPLC Traces. Red Line: Radioactivity Trace of the Crude [^{18}F]Radiofluorination Reaction Mixture. Black Line: UV Trace of the 'Cold' Allylic Fluoride **226b**.



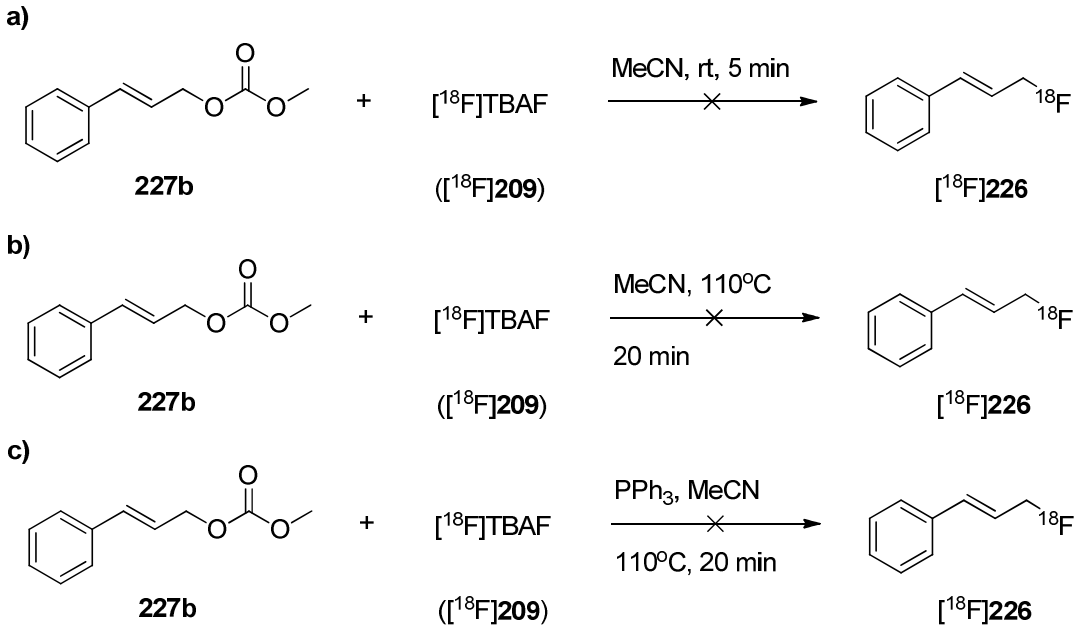
Scheme 5.17 Preparation of 'Cold' Allylic Fluoride **226b**.



Scheme 5.18 Palladium-Mediated Allylic [^{18}F]Radiofluorination of Allylic Methyl Carbonate **227b**.

In order to confirm that the observed [^{18}F]radiofluorination process was indeed palladium-mediated, the reaction was repeated under the same the conditions in the absence of $Pd(dba)_2$ and PPh_3. HPLC analysis of the crude reaction mixture after 5 minutes at room temperature indicated that no ^{18}F-labelled organic products had been formed whilst only

unreacted [^{18}F]TBAF was detected by radio-TLC (Scheme 5.19a). Similarly, no trace of the ^{18}F-labelled allylic fluoride was observed when the reaction was heated to 110ºC for 20 minutes in the absence of the transition metal (Scheme 5.19b,c).

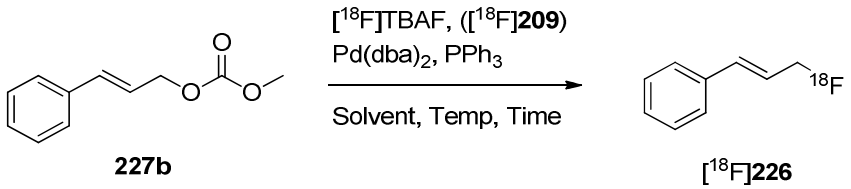


Scheme 5.19 Control Reactions Performed in the Absence of Palladium or PPh_3.

To the best of our knowledge, the formation of the ^{18}F-labelled allylic fluoride [^{18}F]**226** from allylic methyl carbonate **227b** and high specific activity [^{18}F]TBAF ([^{18}F]**209**) represents the first example of a transition metal-mediated C-^{18}F bond forming process. The palladium-mediated [^{18}F]radiofluorination process is a remarkably clean and rapid transformation, delivering the ^{18}F-labelled allylic fluoride as the only radioactive organic material in a respectable radiochemical yield of 19% (decay corrected) after just 5 minutes. Furthermore, the mild reaction conditions and benign nature of the carbonate precursors could be of relevance for the direct aliphatic ^{18}F-labelling of sensitive substrates currently prepared using indirect prosthetic group-based strategies.

5.5.2 Effect of Different Reaction Conditions

Having validated the palladium-mediated allylic [^{18}F]radiofluorination of methyl carbonate **227b**, we sought to investigate the efficiency of the ^{18}F-labelling process under a variety of different reaction conditions (Table 5.2).



227b [^{18}F]**226**

Entry[a]	Solvent	Temp	Time (min)	Radiochemical Yield (RCY)[b]
1	MeCN/*t*-BuOH (9:1)	rt	5	7-32% (*n* = 7)
2[c]	MeCN/*t*-BuOH (9:1)	rt	5	---
3	MeCN	rt	5	9-42% (*n* = 17)
4	MeCN/*t*-BuOH (9:1)	rt	10	9-46% (*n* = 5)
5	MeCN	rt	10	11-13% (*n* = 2)
6	MeCN/*t*-BuOH (9:1)	rt	15	17-19% (*n* = 2)
7	MeCN/*t*-BuOH (9:1)	rt	30	10-22 (*n* = 2)
8	MeCN	rt	30	10-52 (*n* = 7)
9	MeCN/*t*-BuOH (9:1)	rt	1	4-7% (*n* = 2)
10	MeCN/*t*-BuOH (9:1)	rt	2	6-20% (*n* = 2)
11	MeCN/*t*-BuOH (9:1)	100ºC	5	6% (*n* = 1)
12	THF	rt	5	---

[a] Reaction conditions: Carbonate **227b** (5±1 mg), $Pd(dba)_2$ (2±1 mg), PPh_3 (2±1 mg), [^{18}F]TBAF ([^{18}F]**209**, typical activity = 10-50 MBq), solvent (0.5 mL). [b] Decay corrected radiochemical yields of [^{18}F]**226b** determined by radio-TLC on the crude reaction mixture (eluent = MeCN/H_2O, 95:5) or by collection with HPLC – see Chapter 6 for details. *n* = number of individual runs under these conditions. [c] Reaction performed in the absence of $Pd(dba)_2$.

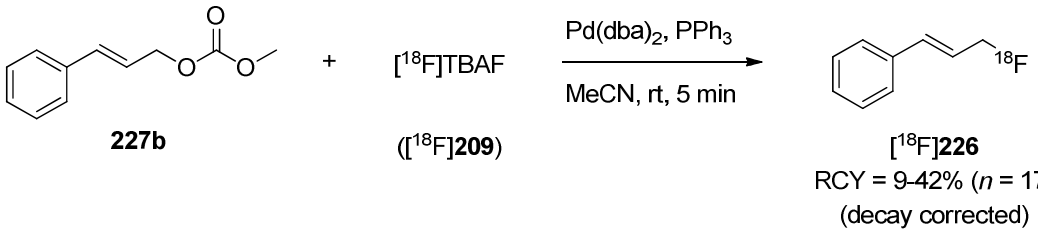
Table 5.2 Palladium-Mediated Allylic [^{18}F]Radiofluorination of Allylic Methyl Carbonate **227b**.

In each case, the allylic methyl carbonate **227b** (5±1 mg), $Pd(dba)_2$ (2±1 mg) and PPh_3 (2±1 mg) were dissolved in 450 μL of the solvent in a borosilicate glass vial containing a v-

shaped stirring bar. A solution of freshly prepared [^{18}F]TBAF in acetonitrile (or tetrahydrofuran, 50 µL, typical radioactivity = 10-50 MBq) was then added in a lead-shielded hot cell and the reaction was stirred at the given temperature for 1-30 minutes. In each experiment, the ^{18}F-labelled allylic fluoride [^{18}F]**226b** was observed as the only radioactive organic product upon crude HPLC analysis (Phenomenex NX 5µm C18 column, MeCN/H_2O, Gradient A, 1 mL/min). The decay corrected radiochemical yields were determined either by radio-TLC on the crude reaction mixture (eluent = MeCN/H_2O, 95:5) or by direct comparison of the radioactivity of the crude mixture injected into the HPLC with that of the product eluted from the column.

As a first experiment, the palladium-mediated [^{18}F]radiofluorination reaction was performed in a 9:1 mixture of acetonitrile and *tert*-butanol (total volume = 0.5 mL). This solvent system resembles the optimised reaction conditions for the 'cold' process where TBAF.(*t*-BuOH)$_4$ (**230**) was identified as the fluoride source of choice. Under these conditions, the desired allylic fluoride [^{18}F]**226b** was delivered in a comparable radiochemical yield of 23% whilst complete recovery of the starting material was observed when the same reaction was performed in the absence of $Pd(dba)_2$ (Table 5.3, Entries 1-2). In order to evaluate the reproducibility of the [^{18}F]radiofluorination process, the reaction described in Entry 1 (Table 5.3) was repeated a number of times with different batches of [^{18}F]TBAF. Whilst the allylic fluoride [^{18}F]**226b** was always afforded as the only radioactive organic product in these experiments, the radiochemical yields varied considerably from 7 to 32% (n = 7, Table 5.3, Entry 1). The inconsistency in the RCY could result from the inherent instability of the ^{18}F-labelled product. As previously demonstrated by our group, allylic fluorides can react with palladium(0) to afford (π-allyl)palladium(II) species resulting from C(sp^3)-F bond cleavage.[254] In addition, cinnamyl fluoride **226b** is a notoriously sensitive compound and has been shown to decompose in contact with borosilicate glass.[261] A broad radiochemical

yield range was also observed when the palladium-mediated [^{18}F]radiofluorination reaction was repeated a number of times using acetonitrile as solvent (Table 5.3, Entry 3). Radio-TLC and HPLC analysis of these experiments after 5 minutes at room temperature indicated that the ^{18}F-labelled allylic fluoride [^{18}F]**226b** was delivered in 9-42% RCY under these conditions (n = 17, Scheme 5.20).

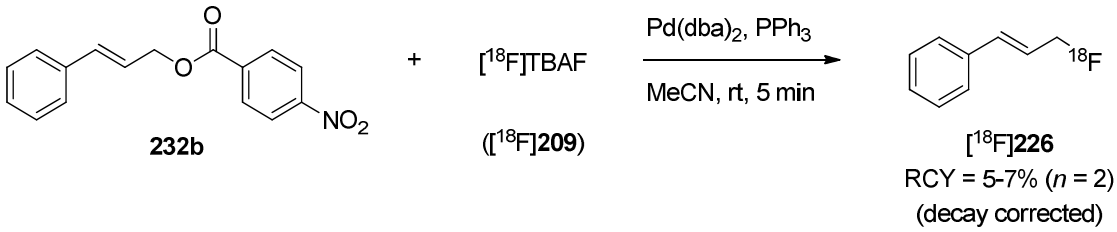


227b ([^{18}F]**209**) [^{18}F]**226**
RCY = 9-42% (n = 17)
(decay corrected)

Scheme 5.20 Palladium-Mediated Allylic [^{18}F]Radiofluorination of Allylic Methyl Carbonate **227b**.

Increasing the reaction time had a minimal effect on the efficiency of the palladium-mediated process. The allylic fluoride [^{18}F]**226b** was delivered in 9-46% (n = 5) radiochemical yield after 10 minutes at room temperature when a 9:1 mixture of acetonitrile and *tert*-butanol was used as the reaction solvent (Table 5.3, Entry 4) whilst a low RCY range of 11-13% (n = 2) was observed with acetonitrile as solvent (Table 5.3, Entry 5). Leaving the reactions for 15 or 30 minutes did not improve the fluorination efficiency although a radiochemical yield of 52% was observed after 30 minutes in one isolated case when acetonitrile was used as the solvent (Table 5.3, Entries 6-8). Notably, substantial formation of the ^{18}F-labelled product was observed within two minutes of reaction with radio-TLC analysis indicating that [^{18}F]**226b** had been furnished in 4-7% (n = 2) and 6-20% (n = 2) radiochemical yield after 60 and 120 seconds respectively (Table 5.3, Entries 9,10). No improvement in the radiochemical yield of the ^{18}F-labelled allylic fluoride product was observed upon performing the reaction at the elevated temperature of 100ºC. [^{18}F]**226b** was delivered in only 6% RCY (n = 1) after 5 minutes under these conditions in acetonitrile/*tert*-butanol (9:1, Table 5.3, Entry 11). In a final screening experiment, the [^{18}F]radiofluorination

of allylic methyl carbonate **227b** was performed in tetrahydrofuran. Whilst this solvent led to the highest yields of allylic fluorides **226** in the 'cold' nucleophilic fluorination process,[255] no C(sp^3)-^{18}F bond formation was observed with [^{18}F]fluoride. HPLC analysis of the crude reaction mixture after 5 minutes at room temperature indicated [^{18}F]TBAF remained unreacted under these conditions with no trace of [^{18}F]**226b** detected (Table 5.3, Entry 12). A similar disparity between the 'cold' and 'hot' palladium-mediated processes was observed upon reacting *para*-nitrobenzoate **232b** with [^{18}F]TBAF under the standard radiolabelling conditions.[yy] This reaction was less efficient than the analogous [^{18}F]radiofluorination of allylic methyl carbonate **227b** and [^{18}F]**226b** was afforded in only 5-7% RCY (n = 2) after 5 minutes at room temperature (Scheme 5.21). By contrast, the non-radioactive palladium-catalysed allylic fluorination of *para*-nitrobenzoate **232b** was significantly higher yielding than the corresponding process with methyl carbonate **227b**.[256][zz]



Scheme 5.21 Palladium-Mediated Allylic [^{18}F]Radiofluorination of Allylic *para*-Nitrobenzoate **232b**.

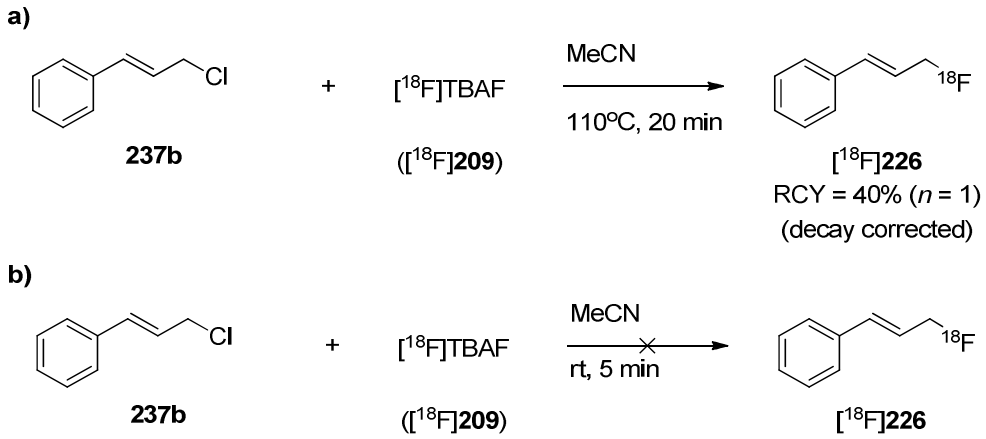
5.5.3 Comparison with Conventional S_N2 [^{18}F]Radiofluorination

At this stage of our investigation, the efficiency of the palladium-mediated allylic [^{18}F]radiofluorination process was compared with conventional S_N2-type radiosyntheses of allylic fluoride [^{18}F]**226b**. In the first control experiment, the commercially-available allylic

[yy] This compound was kindly provided by Charlotte Hollingworth (DPhil, University of Oxford, 2012). reference [256]

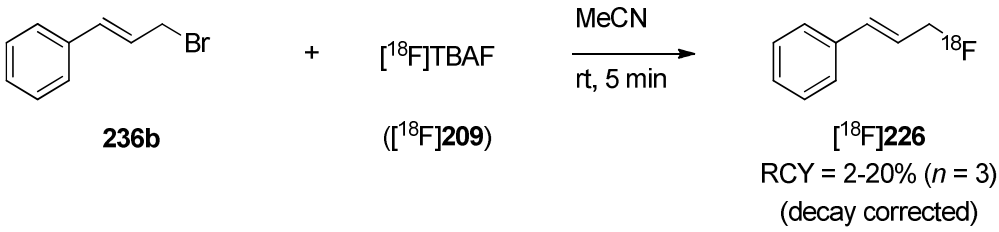
[zz] It should be noted, however, that the isolated yield of the 'cold' process is calculated with respect to the allylic carbonate or *para*-nitrobenzoate starting material whereas the RCY of the 'hot' process relates to the amount of [^{18}F]fluoride consumed. Furthermore, the relative stoichiometries of the reagents are vastly different in each system.

chloride **237b** was heated to 110ºC with [^{18}F]TBAF ([^{18}F]**209**) in acetonitrile. HPLC Analysis after 20 minutes indicated that the nucleophilic [^{18}F]radiofluorination product [^{18}F]**226b** had been formed as the only radioactive organic material in 40% RCY (n = 1) (Scheme 5.22a). However, no trace of the ^{18}F-labelled allylic fluoride was observed when the S_N2 reaction was conducted under the milder conditions used for the palladium-mediated allylic [^{18}F]radiofluorination process (ie. room temperature, 5 minutes, Scheme 5.22b).



Scheme 5.22 Control Reactions with Allylic Chloride **237b** at a) 110ºC and b) room temperature.

By contrast, the more activated allylic bromide **236b** did undergo S_N2-type nucleophilic [^{18}F]radiofluorination when reacted with [^{18}F]TBAF in acetonitrile at room temperature for 5 minutes. The radiochemical yield of the ^{18}F-labelled allylic fluoride [^{18}F]**226b** produced in this reaction (2-20%, n = 3), however, was comparable to those obtained using the palladium-mediated approach (9-42%, n = 17, Scheme 5.23).[aaa]



[aaa] Allylic fluoride [^{18}F]**226b** was delivered in 42% RCY (n = 1) when allylic bromide **236b** was reacted with [^{18}F]TBAF ([^{18}F]**209**) in acetonitrile at 110°C for 20 minutes.

Scheme 5.23 Control Reaction with Allylic Bromide **237b**.

Taken together, these control experiments demonstrate that the palladium-mediated allylic [^{18}F]radiofluorination of methyl carbonate **227b** proceeds under milder conditions than the conventional S_N2-type radiolabelling of the corresponding allylic chloride. Whilst the analogous nucleophilic [^{18}F]radiofluorination of the allylic bromide **236b** occurs with comparable efficiency, the palladium-mediated process utilises a significantly less reactive methyl carbonate starting material. This feature could be important for the direct aliphatic labelling of sensitive substrates where S_N2 nucleophilic [^{18}F]radiofluorination with highly reactive leaving groups is not viable.

5.6 Conclusions

In summary, the palladium-mediated allylic [^{18}F]radiofluorination of methyl carbonate **226b** has been validated using $Pd(dba)_2$ and high specific activity [^{18}F]TBAF ([^{18}F]**209**). This reaction combines transition metal catalysis with ^{18}F-radiochemistry for the first time and, as such, could pave the way for many future C-^{18}F bond-forming processes of relevance for the synthesis of PET radiotracers.

The palladium-mediated [^{18}F]radiofluorination reaction was a remarkably clean process, delivering the allylic fluoride [^{18}F]**226b** as the only radioactive organic product in respectable radiochemical yields up to 52% after only a few minutes at room temperature. However, considerable variation in the radiochemical yields of the ^{18}F-labelled product was observed for the same set of reaction conditions. Control experiments indicated that the palladium-mediated reaction is of comparable efficiency to the conventional S_N2 [^{18}F]radiofluorination of the corresponding allylic bromide **236b**. Whilst further studies are required to investigate the scope and limitations of the transition metal-mediated process with more complex substrates, the mild reaction conditions and relatively benign starting

materials used in this reaction could be of relevance for the direct ^{18}F-labelling of sensitive radiotracer targets.

Furthermore, the use of palladium catalysts bearing chiral ligands could potentially allow for the development of an asymmetric [^{18}F]radiofluorination reaction based on this methodology. An asymmetric variant of the 'cold' palladium-catalysed allylic fluorination reaction was recently reported by Doyle and co-workers using AgF as the fluoride source.[262]

Chapter 6

Experimental Procedures and Characterisation Data

6.1 General Experimental Information

All proton NMR spectra were recorded on either a Bruker DPX200, AV400 or AVII500 spectrometer. Carbon-13 NMR spectra were recorded on either a Bruker AV400 or a Bruker AVII500 spectrometer with a carbon-13 cryoprobe. Fluorine-19 and phosphorus-31 spectra were recorded on a Bruker AV400 or AVII500 spectrometer. Proton and carbon-13 NMR spectra are reported as chemical shifts (δ) in parts per million (ppm) relative to the solvent peak using the Bruker internal referencing procedure (edlock). Fluorine-19 NMR spectra are referenced relative to $CFCl_3$ in $CDCl_3$. Phosphorus-31 NMR spectra are referenced relative to phosphoric acid in D_2O. Coupling constants (*J*) are reported in units of hertz (Hz). The following abbreviations are used to describe multiplicities – s (singlet), d (doublet), t (triplet), q (quartet), quin (quintet), sept (septuplet), m (multiplet), br s (broad singlet). Multiplicities are reported as observed in the spectra. High resolution mass spectra (HRMS, *m/z*) were recorded on a Bruker MicroTOF spectrometer using positive (ESI^+) or negative electrospray ionisation (ESI^-) or on a Micromass GCT spectrometer using either chemical ionisation (CI^+) or field ionisation (FI^+). Infrared spectra were recorded on NaCl discs either as the neat compound or in a solution in dichloromethane using a Bruker Tensor 27 FT-IR spectrometer. Absorptions are reported in wavenumbers (cm^{-1}) and only diagnostic peaks are reported. Melting points of solids were measured on a Griffin apparatus and are uncorrected. Optical rotations were recorded on a Perkin Elmer 241 polarimeter in a 1 dm

cell. $[\alpha]_D^{25}$ Values are given in 10^{-1}degcm^{2}g^{-1}. Enantiomeric excesses were measured using High Performance Liquid Chromatography (HPLC) on a machine supplied by the Waters Corporation using a CHIRALCEL OJ-H column. IUPAC names were obtained using the ACD/I-Lab service. All reported compounds are racemic mixtures unless otherwise indicated.

The following characterisation data are provided for each novel compound:- retention factor (R_f), proton NMR spectra (^{1}H NMR), carbon-13 NMR spectra (^{13}C NMR), infrared spectra (IR) and high resolution mass spectra (HRMS). Fluorine-19 or phosphorus-31 NMR spectra (^{19}F NMR, ^{31}P NMR) are also provided for compounds containing these heteroatoms whilst melting points (Mp) are provided for solids. Optical rotations ($[\alpha]_D^{25}$) are provided for enantioenriched compounds. For known compounds, a minimum of three pieces of characterisation data including proton and carbon-13 NMR spectra are provided. This data is in agreement with literature values. X-Ray crystallography data is included in the Appendix. All compounds used during the study for which a preparation does not appear in this chapter were commercially available.

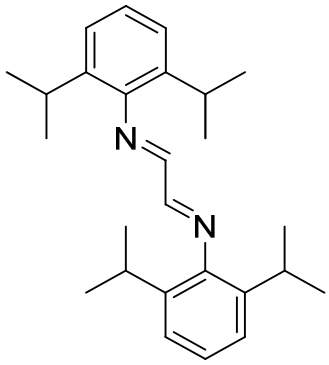
All reactions were performed in dried apparatus with magnetic stirring under an inert atmosphere unless otherwise stated. All solvents were dried on a column of alumina prior to use. Thin layer chromatography (TLC) was performed using Merck aluminium-foil backed plates precoated with Kieselgel 60 F_{254}. The products were visualised using UV fluorescence (254 nm), potassium permanganate or ceric ammonium molybdate stains. Flash column chromatography was performed manually over Merck silica gel C60 (40-60 μm) or on an automated column chromatography machine supplied by Biotage AB using eluent systems as described for each experiment.

6.2 Experimental Data for Chapter 2

6.2.1 Preparation of SIPrAuCl (1)

SIPrAuCl (**1**) was prepared in 5 steps according to the procedures of Arduengo[90] and Sadighi (see Scheme 2.9).[46]

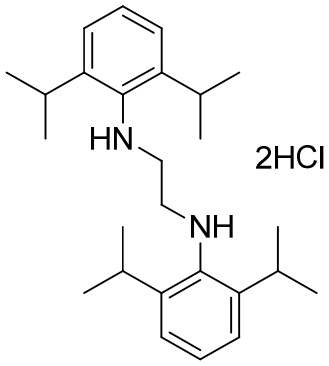
***N*,*N*'-(1*E*,2*E*)-Ethane-1,2-diylidenebis(2,6-diisopropylaniline) (96)** [90]



A mixture of 2,6-diisopropylphenylamine (5.32 mL, 28.0 mmol, 2.25 eq) and 40 % aqueous solution of glyoxal (1.46 mL, 12.7 mmol, 1 eq) in *n*-propanol (20.3 mL) was stirred for 1h at 70°C. After being allowed to cool to room temperature, water (20 mL) was added. The resulting precipitate was collected by filtration, washed with cold methanol and dried *in vacuo* to afford the product (**96**) as a bright yellow solid (4.09 g, yield = 86%).

Mp = 73ºC (lit = 71-73ºC).[90] **^{1}H NMR** (400 MHz, $CDCl_3$) δ: 8.13 (s, 2H, $\underline{H}$C=N), 7.15-7.27 (m, 6H, Ar), 2.97 (sept, 4H, $^3J_{HH}$ = 7.1 Hz, C$\underline{H}$(CH_3)$_2$), 1.24 (d, 24H, d, $^3J_{HH}$ = 7.1 Hz, CH(C$\underline{H}_3$)$_2$). **^{13}C NMR** (101 MHz, $CDCl_3$) δ: 163.1 (H$\underline{C}$=N), 148.0 (*ipso*-Ar), 136.7 (*ortho*-Ar), 125.1 (*meta*-Ar), 123.2 (*para*-Ar), 28.0 ($\underline{C}$H(CH_3)$_2$), 23.4 (CH($\underline{C}$H$_3$)$_2$). **LRMS** (*m*/*z*, ESI$^+$): calculated for $C_{26}H_{37}N_2^+$ ([M+H]$^+$): 377.3, found 377.3.

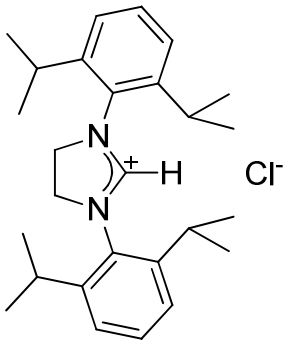
***N,N'*-Bis(2,6-diisopropylphenyl)ethane-1,2-diamine dihydrochloride (97)**[90]



1,2-Diimine (**96**, 5.00 g, 13.2 mmol, 1 eq) in THF/MeOH (50 mL, 3:2) was cooled to 0ºC. Sodium borohydride (1.05 g, 28.0 mmol, 2.1 eq) was added resulting in vivid gas evolution. After 15 min, a further 1.05 g of sodium borohydride was added (28.0 mmol, 2.1 eq). The mixture was stirred at 0ºC for a further 30 minutes before being slowly warmed to room temperature. After 4h, the reaction mixture was quenched with ice water (30 mL) followed by careful addition of 3M HCl (aq, 30 mL). A white solid precipitated, which was collected by filtration, washed with diethyl ether (2×20 mL) and dried *in vacuo*. The product (**97**) was afforded as a white solid (2.56 g, yield = 43%), which required no further purification.

Mp > 250ºC (lit > 250ºC).[90] **^{1}H NMR** (400 MHz, dmso-d_6) δ: 7.25-7.33 (m, 6H, Ar), 3.47 (s, 4H, NC$\underline{H}_2$), 3.36 (sept, 4H, $^{3}J_{HH}$ = 6.8 Hz, C$\underline{H}$(CH_3)$_2$), 1.17 (d, 24H, $^{3}J_{HH}$ = 6.8 Hz, CH(C$\underline{H}_3$)$_2$). *Note: The N$\underline{H}$ proton peaks were not observed.* **^{13}C NMR** (101 MHz, dmso-d_6) δ: 151.0 (*ipso*-Ar), 142.8 (*ortho*-Ar), 128.0 (*para*-Ar), 125.0 (*meta*-Ar), 49.1 (N$\underline{C}H_2$), 27.2 ($\underline{C}$H(CH_3)$_2$) 24.4 (CH($\underline{C}H_3$)$_2$). **LRMS** (*m/z*, ESI$^-$): calculated for $C_{26}H_{40}ClN_2^-$ ([M–2H-Cl]$^-$): 415.3, found 415.3.

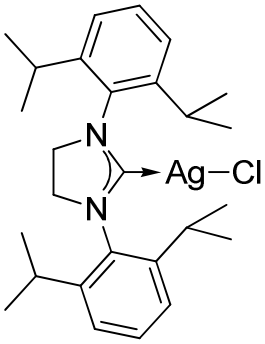
1,3-Bis(2,6-diisopropylphenyl)imidazolidin-2-ylium chloride (SIPrHCl, 98)[90]



Diamine dihydrochloride (**97**, 2.00 g, 4.41 mmol) and one drop of formic acid was stirred in triethyl orthoformate (25 mL) at reflux for 45h. When cooled to room temperature, a solid precipitated, which was collected by filtration, washed with diethyl ether (20 mL) and dried *in vacuo*. The product (**98**) was afforded as a white solid (1.39 g, yield = 74%), which required no further purification.

Mp = 242ºC (lit = 237-240ºC).[90] **^{1}H NMR** (400 MHz, dmso-d_6) δ: 9.54 (s, 1H, NC*H*N), 7.55 (t, 2H, $^3J_{HH}$ = 7.8 Hz, *para*-Ar), 7.42 (d, 4H, $^3J_{HH}$ = 7.8 Hz, *meta*-Ar), 4.54 (s, 4H, NCH_2), 3.09 (sept, 4H, $^3J_{HH}$ = 6.8 Hz, C$H(CH_3)_2$), 1.35 (d, 12H, $^3J_{HH}$ = 6.8 Hz, CH(CH_3)$_2$), 1.20 (d, 12H, $^3J_{HH}$ = 6.8 Hz, CH(CH_3)$_2$). **^{13}C NMR** (101 MHz, dmso-d_6) δ: 160.4 (N*C*HN), 146.5 (*ipso*-Ar), 131.4 (*para*-Ar), 130.2 (*ortho*-Ar), 125.2 (*meta*-Ar), 54.0 (N*C*H_2), 28.6 (*C*H$(CH_3)_2$), 25.3 (CH(*C*H_3)$_2$), 23.7 (CH(*C*H_3)$_2$). **LRMS** (*m*/*z*, ESI$^+$): calculated for $C_{27}H_{39}N_2^+$ ([M-Cl]$^+$): 391.3, found 391.3.

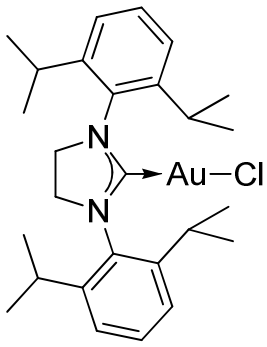
(1,3-Bis(2,6-diisopropylphenyl)imidazolidin-2-ylidene)silver(I) chloride (SIPrAgCl, 99)[46]



Dichloromethane (8.6 mL) was added to SIPrHCl (**98**, 764 mg, 1.34 mmol, 1.67 eq) and silver(I) oxide (186 mg, 800 µmol, 1 eq). The mixture was stirred at room temperature under argon in the dark for 24h before filtration and removal of the solvent *in vacuo*. The resulting yellow crude solid was suspended in diethyl ether (5 mL) and filtered to give the product (**99**) as a white solid (690 mg, yield > 95%).

^{1}H NMR (400 MHz, CD_2Cl_2) δ: 7.45 (t, 2H, $^{3}J_{HH}$ = 7.8 Hz, *para*-Ar), 7.29 (d, 4H, $^{3}J_{HH}$ = 7.8 Hz, *meta*-Ar), 4.08 (s, 4H, NC$\underline{H}_2$), 3.08 (sept, 4H, $^{3}J_{HH}$ = 6.8 Hz, C$\underline{H}$(CH_3)$_2$), 1.35 (d, 12H, $^{3}J_{HH}$ = 6.8 Hz, CH(C$\underline{H}_3$)$_2$), 1.33 (d, 12H, $^{3}J_{HH}$ = 6.8 Hz, CH(C$\underline{H}_3$)$_2$). **^{13}C NMR** (126 MHz, CD_2Cl_2) δ: 208.0 (dd, $^{1}J_{C\text{-}109Ag}$ = 253 Hz, $^{1}J_{C\text{-}107Ag}$ = 220 Hz, $\underline{C}$Ag), 147.3 (*ortho*-Ar), 135.2 (*ipso*-Ar), 130.4 (*para-Ar*), 125.1 (*meta*-Ar), 54.5 (d, $^{3}J_{C\text{-}Ag}$ = 8.6 Hz, N$\underline{C}$H$_2$), 29.3 ($\underline{C}$H(CH_3)$_2$), 25.7 (CH($\underline{C}$H$_3$)$_2$), 24.3 (CH($\underline{C}$H$_3$)$_2$). **LRMS** (*m*/*z*, ESI$^+$): calculated for $C_{29}H_{41}{}^{109}AgN_3ClNa^+$ ([M+MeCN+Na]$^+$): 598.2, found 598.2.

(1,3-Bis(2,6-diisopropylphenyl)imidazolidin-2-ylidene)gold(I) chloride (SIPrAuCl, 1)[46]

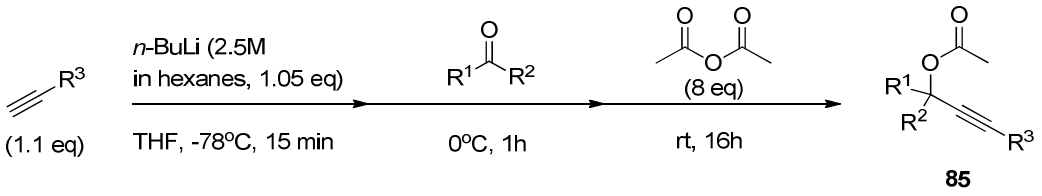


Dichloromethane (20 mL) and dimethyl sulfide (424 µL, 5.77 mmol, 8.5 eq) were added to a mixture of SIPrAgCl (**99**, 363 mg, 678 µmol, 1 eq) and chloro(dimethylsulfide)gold(I) (200 mg, 678 µmol, 1 eq). The mixture was stirred at room temperature in the dark for 60h before filtration and removal of the solvent *in vacuo*. The crude product was washed with diethyl ether (2×10 mL) and dried to give the product (**1**) as a white solid (415 mg, yield > 95%).

^{1}H NMR (400 MHz, CD_2Cl_2) δ: 7.43-7.52 (m, 2H, *para*-Ar), 7.29 (d, 4H, $^3J_{HH}$ = 7.6 Hz, *meta*-Ar), 4.06 (s, 4H, NC$\underline{H}_2$), 3.07 (sept, 4H, $^3J_{HH}$ = 6.8 Hz, C$\underline{H}$(CH_3)$_2$), 1.40 (d, 12H, $^3J_{HH}$ = 6.8 Hz. CH(C$\underline{H}_3$)$_2$), 1.34 (d, 12H, $^3J_{HH}$ = 6.8 Hz, CH(C$\underline{H}_3$)$_2$). **^{13}C NMR** (126 MHz, CD_2Cl_2) δ: 196.3 (C$\underline{C}$Au), 147.3 (*ortho*-Ar), 134.7 (*ipso*-Ar), 130.5 (*para*-Ar), 125.1 (*meta*-Ar), 54.1 (N$\underline{C}H_2$), 29.5 ($\underline{C}$H(CH_3)$_2$), 25.3 (CH($\underline{C}H_3$)$_2$), 24.4 (CH($\underline{C}H_3$)$_2$). **LRMS** (*m/z*, ESI$^+$): calculated for $C_{27}H_{41}AuN_3^+$ ([M–Cl+NH_3]$^+$): 604.3, found 604.2.

6.2.2 Preparation of Propargyl Acetates 85

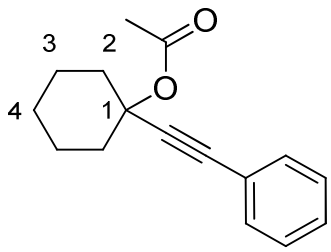
Propargyl acetates **85** were prepared according to the procedure of Zhang.[80]



Scheme 6.1 Preparation of Propargyl Acetates **85**.

General Procedure A: *n*-Butyllithium (2.5 M solution in hexanes, 1.05 eq) was added to a solution of the alkyne (1.1 eq) in tetrahydrofuran (0.25 M) at –78°C. The reaction was stirred for 15 min before the aldehyde or ketone (1 eq) was added. The mixture was allowed to reach 0°C and stirred for 1h. Acetic anhydride (8 eq) was added and the reaction mixture was warmed to room temperature and stirred for 2h. The reaction was quenched with sodium bicarbonate solution (sat. aq.), extracted with diethyl ether (3×) and the combined organic phases were washed with water and brine. After drying with anhydrous magnesium sulfate and filtration, the solvent was removed *in vacuo*. The crude mixture was purified by column chromatography on silica gel.

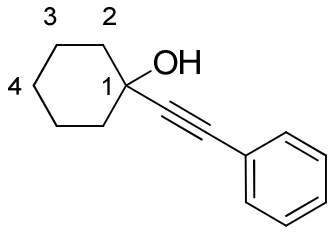
1-(Phenylethynyl)cyclohexyl acetate (85a)[80]



General procedure A was followed using *n*-butyllithium (2.5 M solution in hexanes, 8.40 mL, 21.0 mmol), phenylacetylene (2.42 mL, 22.0 mmol), cyclohexanone (2.07 mL, 20.0 mmol) and acetic anhydride (7.56 mL, 80 mmol) in tetrahydrofuran (84 mL). The resulting crude mixture was purified by column chromatography on silica gel (pet. ether 30-40:diethyl ether, 10:1) to afford the product **85a** as a colourless oil (2.79 g, yield = 58%) along with the propargyl alcohol **93a** as a white solid (683 mg, yield = 17%).

R_f (hexane:ethyl acetate, 10:1) = 0.29. **^{1}H NMR** (400 MHz, $CDCl_3$) δ: 7.43-7.48 (m, 2H, *ortho*-Ph), 7.28-7.31 (m, 3H, *meta*-Ph, *para*-Ph), 2.21-2.26 (m, 2H, *H2*), 2.08 (s, 3H, (C=O)C*H*$_3$), 1.88-1.95 (m, 2H, *H2'*), 1.66-1.71 (m, 4H, *H3*), 1.56 (m, 1H, *H4*), 1.36 (m, 1H, *H4'*). **^{13}C NMR** (101 MHz, $CDCl_3$) δ: 169.3 (*C*=O), 131.8 (*ortho*-Ph), 128.2, 128.1 (*meta*-, *para*-Ph), 122.8 (*ipso*-Ph), 89.1 (*C*≡CPh), 86.2 (C≡*C*Ph), 75.9 (*C1*), 37.1 (*C2*), 25.2 (*C4*), 22.8 (*C3*), 22.1 ((C=O)*C*H$_3$). **IR** (neat): 2250 (C≡C), 1744 (C=O). **LRMS** (*m/z*, ESI$^+$): calculated for $C_{18}H_{21}NNaO_2^+$ ([M+MeCN+Na]$^+$): 306.2, found 306.2.

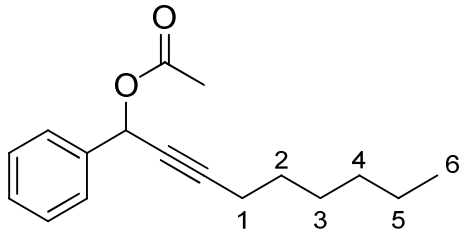
1-(Phenylethynyl)cyclohexanol (93a)[263]



R_f (hexane:ethyl acetate, 10:1) = 0.06. **^{1}H NMR** (400 MHz, $CDCl_3$) δ: 7.41-7.47 (m, 2H, *ortho*-Ph), 7.28-7.33 (m, 3H, *meta*-Ph, *para*-Ph), 2.04, (br s, 1H, O*H*), 1.98-2.03 (m, 2H,

H2), 1.53-1.80 (m, 7H), 1.29 (m, 1H, *H2-4*). **^{13}C NMR** (101 MHz, $CDCl_3$) δ: 131.6 (*ortho*-Ph), 128.2, 128.2 (*meta*-, *para*-Ph), 122.8 (*ipso*-Ph), 92.7 (*C*≡CPh), 84.3 (C≡*C*Ph), 69.1 (*C1*), 40.0 (*C2*), 25.2 (*C4*), 23.4 (*C3*).

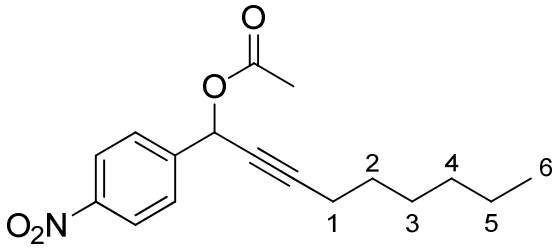
1-Phenylnon-2-yn-1-yl acetate (85b)[264]



General procedure A was followed using *n*-butyllithium (2.5 M solution in hexanes, 2.10 mL, 5.25 mmol), 1-octyne (811 μL, 5.50 mmol), benzaldehyde (508 μL, 5.00 mmol) and acetic anhydride (3.78 mL, 40.0 mmol) in tetrahydrofuran (21 mL). The resulting crude mixture was purified by column chromatography on silica gel (pet. ether 40-60:diethyl ether, 9:1) to afford the product **85b** as a colourless oil (1.15 g, yield = 89%).

R_f (pet. ether 40-60:diethyl ether, 9:1) = 0.38. **^{1}H NMR** (400 MHz, $CDCl_3$) δ: 7.54 (d, 2H, $^{3}J_{HH}$ = 7.6 Hz, *ortho*-Ph), 7.34-7.42 (m, 3H, *meta*-, *para*-Ph), 6.48 (br s, 1H, C*H*(Ph)(OAc)), 2.28 (t, 2H, $^{3}J_{HH}$ = 7.3 Hz, *H1*), 2.10 (s, 3H, (C=O)CH_3), 1.55 (tt, 2H, $^{3}J_{HH}$ = 7.3, 7.1 Hz, *H2*), 1.35-1.44 (m, 2H, *H3*), 1.24-1.34 (m, 4H, *H4*, *H5*), 0.90 (dd, 3H, $^{3}J_{HH}$ = 7.1, 6.8 Hz, *H6*). **^{13}C NMR** (101 MHz, $CDCl_3$) δ: 169.8 (*C*=O), 137.6 (*ipso*-Ph), 128.7 (*para*-Ph), 128.4 (*meta*-Ph), 127.7 (*ortho*-Ph), 88.4 (C≡*C*(C_6H_{13})), 76.6 (*C*≡C(C_6H_{13})), 66.0 (*C*H(Ph)(OAc)), 31.2 (*C4*), 28.5, 28.4 (*C2*, *C3*), 22.5 (*C5*), 21.2 ((C=O)*C*H_3), 18.8 (*C1*), 14.0 (*C6*). **IR** (neat): 2236 (C≡C), 1742 (C=O). **LRMS** (*m*/*z*, ESI$^+$): calculated for $C_{17}H_{22}NaO_2^+$ ([M+Na]$^+$): 281.2, found 281.2.

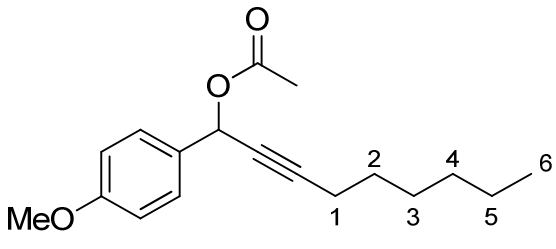
1-(4-Nitrophenyl)non-2-ynyl acetate (85c)



General procedure A was followed using *n*-butyllithium (2.5 M solution in hexanes, 2.10 mL, 5.25 mmol), 1-octyne (811 µL, 5.50 mmol), 4-nitrobenzaldehyde (756 mg, 5.00 mmol) and acetic anhydride (3.78 mL, 40.0 mmol) in tetrahydrofuran (21 mL). The resulting crude mixture was purified by column chromatography on silica gel (hexane:diethyl ether, 9:1) to afford the product **85c** as a yellow oil (1.09 g, yield = 72%).

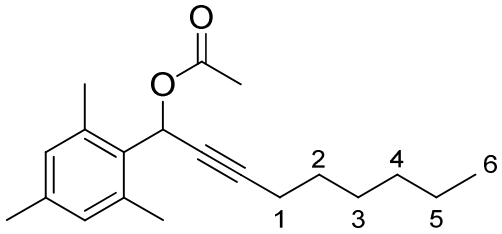
R_f (hexane:diethyl ether, 9:1) = 0.20. **^{1}H NMR** (400 MHz, $CDCl_3$) δ: 8.23 (d, 2H, $^3J_{HH}$ = 8.8 Hz, *ortho*-Ar), 7.68 (d, 2H, $^3J_{HH}$ = 8.8 Hz, *meta*-Ar), 6.50 (t, 1H, $^5J_{HH}$ = 2.0 Hz, CH(Ar)(OAc)), 2.27 (td, 2H, $^3J_{HH}$ = 7.1 Hz, $^5J_{HH}$ = 2.0 Hz, *H1*), 2.13 (s, 3H, (C=O)C*H*$_3$), 1.53 (tt, 2H, $^3J_{HH}$ = 7.3, 7.1 Hz, *H2*), 1.32-1.40 (m, 2H, *H3*), 1.22-132 (m, 4H, *H4*, *H5*), 0.88 (t, 3H, $^3J_{HH}$ = 6.8 Hz, *H6*). **^{13}C NMR** (101 MHz, $CDCl_3$) δ: 169.6 (*C*=O), 147.9, 144.5 (*ipso*-, *para*-Ar), 128.4 (*ortho*-Ar), 123.8 (*meta*-Ar), 89.8 (C≡*C*(C_6H_{13})), 75.6 (*C*≡C(C_6H_{13})), 64.8 (*C*H(Ar)(OAc)), 31.2 (*C4*), 28.5, 28.2 (*C2*, *C3*), 22.5 (*C5*), 21.0 ((C=O)*C*H_3), 18.7 (*C1*), 14.0 (*C6*). **IR** (neat): 2235 (C≡C), 1744 (C=O), 1525 (NO_2), 1350 (NO_2). **HRMS** (*m/z*, ESI^+): calculated for $C_{17}H_{21}NNaO_4^+$ ($[M+Na]^+$): 326.1363, found 326.1351.

1-(4-Methoxyphenyl)non-2-ynyl acetate (85d)



General procedure A was followed using *n*-butyllithium (2.5 M solution in hexanes, 2.10 mL, 5.25 mmol), 1-octyne (811 µL, 5.50 mmol), 4-methoxybenzaldehyde (681 mg, 5.00 mmol) and acetic anhydride (3.78 mL, 40.0 mmol) in tetrahydrofuran (21 mL). The resulting crude mixture was purified by column chromatography on silica gel (hexane:diethyl ether, 9:1) to afford the product **85d** as a yellow oil (881 mg, yield = 61%). **R_f** (hexane:diethyl ether, 9:1) = 0.17. **^{1}H NMR** (400 MHz, $CDCl_3$) δ: 7.47 (dm, 2H, $^3J_{HH}$ = 8.6 Hz, *ortho*-Ar), 6.90 (dm, 2H, $^3J_{HH}$ = 8.6 Hz, *meta*-Ar), 6.43 (t, 1H, $^5J_{HH}$ = 2.0 Hz, C*H*(Ar)(OAc)), 3.82 (s, 3H, OC*H*$_3$), 2.27 (td, 2H, $^3J_{HH}$ = 7.1 Hz, $^5J_{HH}$ = 2.0 Hz, *H1*), 2.08 (s, 3H, (C=O)C*H*$_3$), 1.54 (tt, 2H, $^3J_{HH}$ = 7.3, 7.1 Hz, *H2*), 1.35-1.43 (m, 2H, *H3*), 1.23-.1.35 (m, 4H, *H4*, *H5*), 0.89 (dd, 3H, $^3J_{HH}$ = 7.1, 6.8 Hz, *H6*). **^{13}C NMR** (101 MHz, $CDCl_3$) δ: 170.0 (*C*=O), 159.9 (*para*-Ar), 129.9 (*ipso*-Ar), 129.3 (*ortho*-Ar), 113.8 (*meta*-Ar), 88.1 (C≡*C*(C_6H_{13})), 76.8 (*C*≡C(C_6H_{13})), 65.8 (*C*H(Ar)(OAc)), 55.3 (O*C*H_3), 31.2 (*C4*), 28.5, 28.3 (*C2*, *C3*), 22.5 (*C5*), 21.2 ((C=O)*C*H_3), 18.8 (*C1*), 14.0 (*C6*). **IR** (neat): 2251 (C≡C), 1742 (C=O). **HRMS** (*m*/*z*, FI^+): calculated for $C_{18}H_{24}O_3$ ($[M]^+$): 288.1725, found 288.1720.

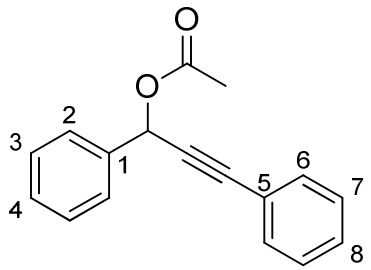
1-Mesitylnon-2-ynyl acetate (85e)



General procedure A was followed using *n*-butyllithium (2.5 M solution in hexanes, 2.10 mL, 5.25 mmol), 1-octyne (811 µL, 5.50 mmol), mesitaldehyde (737 µL, 5.00 mmol) and acetic anhydride (3.78 mL, 40.0 mmol) in tetrahydrofuran (21 mL). The resulting crude mixture was purified by column chromatography on silica gel (hexane:diethyl ether, 9:1) to afford the product **85e** as a pale yellow oil (1.00 g, yield = 67%).

R_f (hexane:diethyl ether, 9:1) = 0.37. **^{1}H NMR** (400 MHz, $CDCl_3$) δ: 6.86 (s, 2H, *meta*-Ar), 6.83 (m, 1H, C*H*(Ar)(OAc)), 2.53 (s, 6H, *ortho*-Ar-C*H*$_3$), 2.27 (s, 3H, *para*-Ar-C*H*$_3$), 2.21 (td, 2H, $^3J_{HH}$ = 7.1, $^5J_{HH}$ = 1.5 Hz, *H1*), 2.07 (s, 3H, (C=O)C*H*$_3$), 1.50 (tt, 2H, $^3J_{HH}$ = 7.3, $^3J_{HH}$ 7.1 Hz, *H2*), 1.31-1.39 (m, 2H, *H3*), 1.21-1.31 (m, 4H, *H4*, *H5*), 0.89 (t, 3H, $^3J_{HH}$ = 7.1 Hz, *H6*). **^{13}C NMR** (101 MHz, $CDCl_3$) δ: 169.8 (*C*=O), 138.1, 137.0, 131.4 (*para*-Ar, *ortho*-Ar, *ipso*-Ar), 129.7 (*meta*-Ar), 87.3 (C≡*C*(C_6H_{13})), 76.4 (*C*≡C(C_6H_{13})), 62.2 (*C*H(Ar)(OAc)), 31.2 (*C4*), 28.5, 28.3 (*C2*, *C3*), 22.5 (*C5*), 21.0, 20.9 ((C=O)*C*H$_3$, *para*-Ar-*C*H$_3$), 18.9 (*C1*), 14.0 0 (*C6*). **IR**: 2232 (C≡C), 1739 (C=O). **HRMS** (*m*/*z*, FI^+): calculated for $C_{20}H_{28}O_2$ ($[M]^+$): 300.2089, found 300.2096.

1,3-Diphenylprop-2-ynyl acetate (85f)[265]

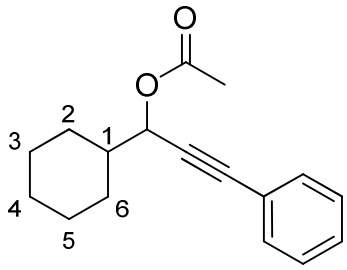


General procedure A was followed using *n*-butyllithium (2.5 M solution in hexanes, 2.10 mL, 5.25 mmol), phenylacetylene (604 µL, 5.50 mmol), benzaldehyde (508 µL, 5.00 mmol) and acetic anhydride (3.78 mL, 40.0 mmol) in tetrahydrofuran (21 mL). The resulting crude mixture was purified by column chromatography on silica gel (hexane:diethyl ether, 9:1) to afford the product **85f** as a yellow oil (1.16 g, yield = 93%).

R_f (hexane:diethyl ether, 9:1) = 0.23. **^{1}H NMR** (400 MHz, $CDCl_3$) δ: 7.66-7.70 (m, 2H, Ph), 7.53-7.57 (m, 2H, Ph), 7.41-7.49 (m, 3H, Ph), 7.34-7.38 (m, 3H, Ph), 6.80 (m, 1H, C*H*(Ph)(OAc)), 2.17 (s, 3H, (C=O)C*H*$_3$). **^{13}C NMR** (101 MHz, $CDCl_3$) δ: 169.6 (*C*=O), 137.0 (*C1*), 131.8, 128.8, 128.7, 128.6, 128.1, 127.7 (*C2*, *C3*, *C4*, *C6*, *C7*, *C8*), 121.9 (*C5*), 86.9 (*C*≡C(Ph)), 85.5 (C≡*C*(Ph)), 65.9 (*C*H(Ph)(OAc)), 20.9 ((C=O)*C*H$_3$). **IR** (neat): 2247

(C≡C), 1741 (C=O). **HRMS** (*m*/*z*, FI$^+$): calculated for $C_{17}H_{14}O_2$ ([M]$^+$): 250.0994, found 250.0994.

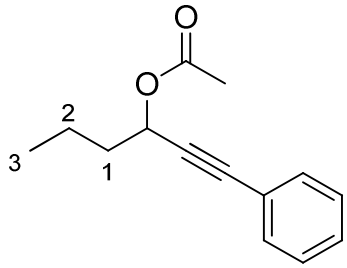
1-Cyclohexyl-3-phenylprop-2-ynyl acetate (85g)



General procedure A was followed using *n*-butyllithium (2.5 M solution in hexanes, 2.10 mL, 5.25 mmol), phenylacetylene (604 µL, 5.50 mmol), cyclohexanecarboxaldehyde (606 µL, 5.00 mmol) and acetic anhydride (3.78 mL, 40.0 mmol) in tetrahydrofuran (21 mL). The resulting crude mixture was purified by column chromatography on silica gel (hexane:diethyl ether, 9:1) to afford the product **85g** as a colourless oil (826 mg, yield = 64%).

R$_f$ (hexane:diethyl ether, 9:1) = 0.22. **^{1}H NMR** (400 MHz, $CDCl_3$) δ: 7.44-7.47 (m, 2H, *ortho*-Ph), 7.29-7.33 (m, 3H, *meta*-, *para*-Ph), 5.46 (d, 1H, $^3J_{HH}$ = 6.1 Hz, C*H*(Cy)(OAc)), 2.13 (s, 3H, (C=O)C*H*$_3$), 1.67-1.96 (m, 6H), 1.13-1.33 (m, 5H, *H1-6*). **^{13}C NMR** (101 MHz, $CDCl_3$) δ: 170.2 (*C*=O), 131.9 (*ortho*-Ph), 128.5 (*para*-Ph), 128.2 (*meta*-Ph), 122.4 (*ipso*-Ph), 85.8 (*C*≡C(Ph)), 85.7 (C≡*C*(Ph)), 68.7 (*C*H(Ph)(OAc)), 42.0 (*C1*), 28.7, 28.2, 26.2, 25.8, 25.7 (*C2-6*), 21.1 ((C=O)*C*H$_3$). **IR** (neat): 2229 (C≡C), 1746 (C=O). **HRMS** (*m*/*z*, FI$^+$): calculated for $C_{17}H_{20}O_2$ ([M]$^+$): 256.1463, found 256.1454.

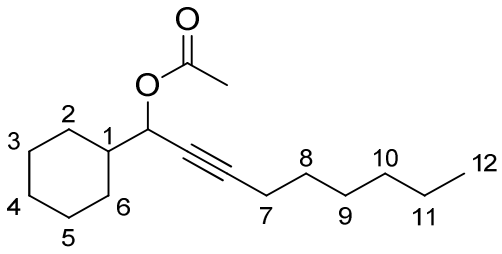
1-Phenylhex-1-yn-3-yl acetate (85h)[266]



General procedure A was followed using *n*-butyllithium (2.5 M solution in hexanes, 2.10 mL, 5.25 mmol), phenylacetylene (604 µL, 5.50 mmol), butyraldehyde (451 µL, 5.00 mmol) and acetic anhydride (3.78 mL, 40.0 mmol) in tetrahydrofuran (21 mL). The resulting crude mixture was purified by column chromatography on silica gel (hexane:diethyl ether, 9:1) to afford the product **85h** as a colourless oil (929 mg, yield = 86%).

R_f (hexane:diethyl ether, 9:1) = 0.27. **^{1}H NMR** (400 MHz, $CDCl_3$) δ: 7.44-7.46 (m, 2H, *ortho*-Ph), 7.28-7.34 (m, 3H, *meta*-, *para*-Ph), 5.62 (t, 1H, $^3J_{HH}$ = 6.8 Hz, C*H*(C_3H_7)(OAc)), 2.12 (s, 3H, (C=O)C*H*$_3$), 1.82-1.88 (m, 2H, *H1*), 1.54 (tq, 2H, $^3J_{HH}$ = 7.6, 7.3 Hz, *H2*), 0.99 (t, 3H, $^3J_{HH}$ = 7.3 Hz, *H3*). **^{13}C NMR** (101 MHz, $CDCl_3$) δ: 170.1 (*C*=O), 131.9 (*ortho*-Ph), 128.5, 128.2 (*meta*-, *para*-Ph), 122.3 (*ipso*-Ph), 86.6 (*C*≡C(Ph)), 85.1 (C≡*C*(Ph)), 64.3 (C*H*(C_3H_7)(OAc)), 36.9 (*C1*), 21.1 ((C=O)*C*H_3), 18.4 (*C2*), 13.7 (*C3*). **IR** (neat): 2236 (C≡C), 1744 (C=O). **HRMS** (*m*/*z*, FI^+): calculated for $C_{14}H_{16}O_2$ ($[M]^+$): 216.1150, found 216.1149.

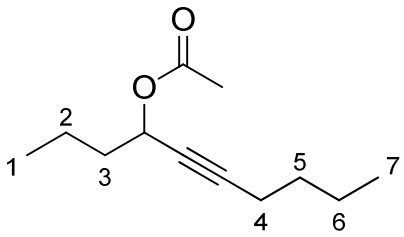
1-Cyclohexylnon-2-yn-1-yl acetate (85i)



General procedure A was followed using *n*-butyllithium (2.5 M solution in hexanes, 2.10 mL, 5.25 mmol), 1-octyne (811 µL, 5.5 mmol), cyclohexanecarboxaldehyde (606 µL, 5.00 mmol) and acetic anhydride (3.78 mL, 40 mmol) in tetrahydrofuran (21 mL). The resulting crude mixture was purified by column chromatography on silica gel (pet. ether 40-60:diethyl ether, 9:1) to afford the product **85i** as a colourless oil (763 mg, yield = 58%).

R_f (hexane:diethyl ether, 9:1) = 0.33. **^{1}H NMR** (400 MHz, $CDCl_3$) δ: 5.18 (dm, 1H, $^3J_{HH}$ = 6.1 Hz, C*H*(Cy)(OAc)), 2.18 (td, 2H, $^3J_{HH}$ = 7.1 Hz, $^5J_{HH}$ = 2.0 Hz, *H7*), 2.05 (s, 3H (C=O)C*H*$_3$), 1.81 (m, 1H, *H1*), 1.70-1.77 (m, 3H, Cy), 1.56-1.68 (m, 2H, Cy), 1.48 (tt, 2H, $^3J_{HH}$ = 7.1, 6.6 Hz, *H8*), 1.00-1.40 (m, 11H, *H9*, *H10*, *H11*, Cy), 0.87 (dd, 3H, *J* = 7.3, 6.6 Hz, *H12*). **^{13}C NMR** (101 MHz, $CDCl_3$) δ: 170.0 (*C*=O), 86.7 (*C*≡C(C_6H_{13})), 76.4 (C≡*C*(C_6H_{13})), 68.7 (*C*H(Cy)(OAc)), 42.0 (*C1*), 31.2, 28.5, 28.4, 28.4, 28.0, 26.2, 25.7, 25.7, 22.5 (*C2-6*, *C8-11*), 21.0 ((C=O)*C*H$_3$), 18.6 (*C7*), 13.9 (*C12*). **IR** (neat): 2248 (C≡C), 1743 (C=O). **HRMS** (*m/z*, FI$^+$): calculated for $C_{17}H_{28}O_2$ ([M]$^+$) 264.2089 found 264.2076.

Dec-5-yn-4-yl acetate (85j)

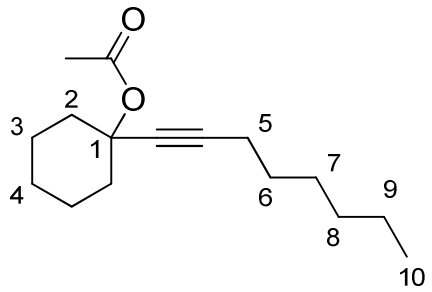


General procedure A was followed using *n*-butyllithium (2.5 M solution in hexanes, 8.40 mL, 21.0 mmol), 1-hexyne (2.52 mL, 22.0 mmol), butyraldehyde (3.61 mL, 20.0 mmol) and acetic anhydride (15.1 mL, 160 mmol) in tetrahydrofuran (84 mL). The resulting crude mixture was purified by column chromatography on silica gel (hexane:diethyl ether, 9:1) to afford the product **85j** as a colourless liquid (3.40 g, yield = 86%).

R_f (hexane:diethyl ether, 9:1) = 0.27. **^{1}H NMR** (400 MHz, $CDCl_3$) δ: 5.29 (tm, 1H, $^3J_{HH}$ = 6.8 Hz, C*H*(C_3H_7)(OAc)), 2.17 (td, 2H, $^3J_{HH}$ = 6.8 Hz, $^5J_{HH}$ = 2.0 Hz, *H4*), 2.01 (s, 3H,

(C=O)C$\underline{H}_3$), 1.59-1.70 (m, 2H, *H3*), 1.28-1.48 (m, 6H, *H2*, *H5*, *H6*), 0.91 (t, 3H, $^3J_{HH}$ = 7.3 Hz), 0.88 (t, 3H, *J* = 7.3 Hz, *H1*, *H7*). **^{13}C NMR** (101 MHz, $CDCl_3$) δ: 169.9 ($\underline{C}$=O), 85.9 ($\underline{C}$≡C(C_4H_9)), 77.5 (C≡$\underline{C}$(C_4H_9)), 64.2 ($\underline{C}$H(C_3H_7)(OAc)), 37.0 (*C3*), 30.4 (*C5*), 21.7 (*C6*), 20.9 ((C=O)$\underline{C}$$H_3$), 18.2 (*C4*), 18.2 (*C2*), 13.5, 13.4 (*C1*, *C7*). **IR** (neat): 2240 (C≡C), 1742 (C=O). **HRMS** (*m/z*, FI^+): calculated for $C_{12}H_{20}O_2$ ($[M]^+$): 196.1463, found 196.1466.

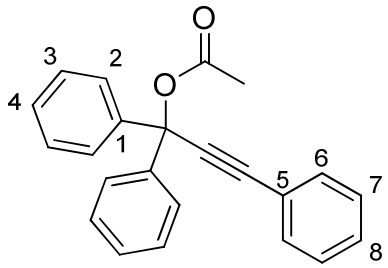
1-(Oct-1-yn-1-yl)cyclohexyl acetate (85k)[96]



General procedure A was followed using *n*-butyllithium (2.5 M solution in hexanes, 2.10 mL, 5.25 mmol), 1-octyne (811 µL, 5.50 mmol), cyclohexanone (518 µL, 5.00 mmol) and acetic anhydride (3.78 mL, 40.0 mmol) in tetrahydrofuran (21 mL). The resulting crude mixture was purified by column chromatography on silica gel (hexane:diethyl ether, 9:1) to afford the product **85k** as a colourless oil (924 mg, yield = 74%).

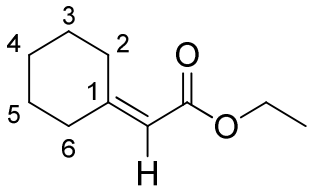
R_f (hexane:diethyl ether, 9:1) = 0.36. **^{1}H NMR** (400 MHz, $CDCl_3$) δ: 2.19 (t, 2H, $^3J_{HH}$ = 7.1 Hz, *H5*), 2.02-2.09 (m, 2H, *H2*), 1.98 (s, 3H, (C=O)C$\underline{H}_3$), 1.72-1.80 (m, 2H, *H2'*), 1.53-1.59 (m, 4H, *H3*), 1.42-1.52 (m, 3H, *H6*, *H8*), 1.31-1.38 (m, 2H, *H7*), 1.19-1.31 (m, 5H, *H4*, *H9, H8*), 0.85 (dd, 3H, $^3J_{HH}$ = 7.1, 6.6 Hz, *H10*). **^{13}C NMR** (101 MHz, $CDCl_3$) δ: 169.1 ($\underline{C}$=O), 86.7 ($\underline{C}$≡C(C_6H_{13})), 80.0 (C≡$\underline{C}$(C_6H_{13})), 75.9 (*C1*), 37.3 (*C2*), 31.2 (*C8*), 28.5, 28.3 (*C6*, *C7*), 25.2 (*C4*), 22.7, 22.4 (*C3*, *C9*), 22.0 ((C=O)$\underline{C}$$H_3$), 18.7 (*C5*), 13.9 (*C10*). **IR** (neat): 2242 (C≡C), 1746 (C=O). **HRMS** (*m/z*, ESI^+): calculated for $C_{16}H_{26}NaO_2^+$ ($[M+Na]^+$): 273.1825, found 273.1824.

1,1,3-Triphenylprop-2-yn-1-yl acetate (85l)



General procedure A was followed using *n*-butyllithium (2.5 M solution in hexanes, 2.10 mL, 5.25 mmol), phenylacetylene (604 µL, 5.50 mmol), benzophenone (911 mg, 5.00 mmol) and acetic anhydride (3.78 mL, 40.0 mmol) in tetrahydrofuran (21 mL). The resulting crude mixture was purified by column chromatography on silica gel (hexane:diethyl ether, 9:1) to afford the product **85l** as a white solid (462 mg, yield = 28%). **Mp** = 75°C. $\mathbf{R_f}$ (hexane:diethyl ether, 9:1) = 0.34. **^{1}H NMR** (400 MHz, $CDCl_3$) δ: 7.59-7.63 (m, 4H, Ph), 7.52-7.55 (m, 2H, Ph), 7.32-7.38 (m, 7H, Ph), 7.27-7.32 (m, 2H, Ph), 2.21 (s, 3H, (C=O)C$\underline{H}_3$). **^{13}C NMR** (101 MHz, $CDCl_3$) δ: 168.0 ($\underline{C}$=O), 142.6 (*C1*), 131.8 (*C6*), 128.6, 128.2, 128.1, 127.7, 126.1 (*C2-4*, *C7*, *C8*), 122.3 (*C5*), 89.4 ($\underline{C}$≡C(Ph)), 88.1 (C≡$\underline{C}$(Ph)), 79.6 ($\underline{C}(Ph)_2(OAc)$), 21.8 ((C=O)$\underline{C}H_3$). **IR** (CH_2Cl_2): 2242 (C≡C), 1752 (C=O). **HRMS** (*m*/*z*, FI^+): calculated for $C_{23}H_{18}O_2$ ($[M]^+$): 326.1307, found 326.1302.

Ethyl cyclohexylideneacetate (86m)[96]

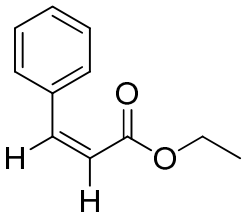


General procedure A was followed using *n*-butyllithium (2.5 M solution in hexanes, 2.10 mL, 5.25 mmol), ethoxyacetylene (50% weight in hexane, 1.07 mL, 5.50 mmol), cyclohexanone (518 µL, 5.00 mmol) and acetic anhydride (3.78 mL, 40.0 mmol) in tetrahydrofuran (21 mL). The resulting crude mixture was purified by column

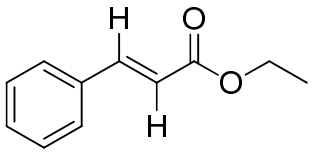
chromatography on silica gel (hexane:diethyl ether, 9:1) to afford the product **86m** as a colourless oil (362 mg, yield = 43%).

R_f (hexane:diethyl ether, 9:1) = 0.23. **^{1}H NMR** (400 MHz, $CDCl_3$) δ: 5.53 (s, 1H, C=C*H*), 4.06 (q, 2H, $^3J_{HH}$ = 7.1 Hz, OC*H*$_2$CH$_3$), 2.75-2.78 (m, 2H, *H2*), 2.11-2.13 (m, 2H, *H6*), 1.48-1.63 (m, 6H, *H3-5*), 1.20 (t, 3H, $^3J_{HH}$ = 7.1 Hz, OCH$_2$C*H*$_3$). **^{13}C NMR** (101 MHz, $CDCl_3$) δ: 166.5 (*C*=O), 163.2 (*C1*), 112.9 (C=*C*H), 59.2 (O*C*H$_2$CH$_3$), 37.8 (*C6*), 29.6 (*C2*), 28.5, 27.6 (*C3*, *C5*), 26.1 (*C4*), 14.1 (OCH$_2$*C*H$_3$). **LRMS** (*m/z*, ESI$^+$): calculated for $C_{10}H_{16}NaO_2^+$ ([M+Na]$^+$): 191.1, found 191.1.

Ethyl 3-phenylacrylate (86n)[267-268]



(*Z*)-**86n**



(*E*)-**86n**

General procedure A was followed using *n*-butyllithium (2.5 M solution in hexanes, 2.10 mL, 5.25 mmol), ethoxyacetylene (50% weight in hexane, 1.07 mL, 5.50 mmol), benzaldehyde (508 μL, 5.00 mmol) and acetic anhydride (3.78 mL, 40.0 mmol) in tetrahydrofuran (21 mL). The resulting crude mixture was purified by column chromatography on silica gel (hexane:diethyl ether, 9:1) to afford the product **86n** as a mixture of diastereoisomers as a colourless oil (*E*/*Z* = 36:64, 610 mg, yield = 69%).

(*Z*)-**86n**[267] :- **R_f** (hexane:diethyl ether, 9:1) = 0.40. **^{1}H NMR** (400 MHz, $CDCl_3$) δ: 7.58-7.61 (m, 2H, *ortho*-Ph), 7.33-7.39 (m, 3H, *meta*-, *para*-Ph), 6.96 (d, 1H, $^3J_{HH}$ = 12.6 Hz, (Ph)C*H*=CH), 5.97 (d, 1H, $^3J_{HH}$ = 12.6 Hz, (Ph)CH=C*H*), 4.19 (q, 2H, $^3J_{HH}$ = 7.1 Hz, OC*H*$_2$CH$_3$), 1.26 (t, 3H, $^3J_{HH}$ = 7.1 Hz, OCH$_2$C*H*$_3$). **^{13}C NMR** (101 MHz, $CDCl_3$) δ: 166.2 (*C*=O), 142.9 ((Ph)*C*H=CH), 134.8 (*ipso*-Ph), 129.6 (*ortho*-Ph), 128.9 (*para*-Ph), 127.9

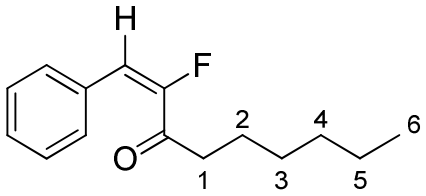
(*meta*-Ph), 119.9 ((Ph)CH=<u>*C*</u>H), 60.2 (O<u>*C*</u>H_2CH_3), 14.0 (OCH_2<u>*C*</u>H_3). **LRMS** (*m/z*, ESI^+): calculated for $C_{11}H_{12}NaO_2^+$ ($[M+Na]^+$): 199.1, found 199.1.

(*E*)-**86n**[268] :- $\mathbf{R_f}$ (hexane:diethyl ether, 9:1) = 0.23. **^{1}H NMR** (400 MHz, $CDCl_3$) δ: 7.70 (d, 1H, $^3J_{HH}$ = 16.0 Hz, (Ph)C<u>*H*</u>=CH), 7.50-7.54 (m, 2H, *ortho*-Ph), 7.35-7.40 (m, 3H, *meta*-, *para*-Ph), 6.45 (d, 1H, $^3J_{HH}$ = 16.0 Hz, (Ph)CH=C<u>*H*</u>), 4.27 (q, 2H, $^3J_{HH}$ = 7.1 Hz, OC<u>*H*</u>$_2CH_3$), 1.34 (t, 3H, $^3J_{HH}$ = 7.1 Hz, OCH_2CH_3). **^{13}C NMR** (101 MHz, $CDCl_3$) δ: 166.8 (<u>*C*</u>=O), 144.4 ((Ph)<u>*C*</u>H=CH), 134.4 (*ipso*-Ph), 130.1, 128.8, 127.9 (*ortho*-, *meta*-, *para*-Ph), 118.2 ((Ph)CH=<u>*C*</u>H), 60.3 (O<u>*C*</u>H_2CH_3), 14.2 (OCH_2<u>*C*</u>H_3). **LRMS** (*m/z*, ESI^+): calculated for $C_{11}H_{12}NaO_2^+$ ($[M+Na]^+$): 199.1, found 199.1.

6.2.3 Rearrangement-Fluorodeacetylation of Propargyl Acetates 85

6.2.3.1 Preliminary Investigations

(*E*)-2-Fluoro-1-phenylnon-1-en-3-one ((*E*)-92b)

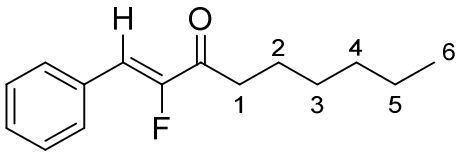


Selectfluor (**82**, 823 mg, 2.32 mmol, 1.2 eq), PPh_3AuCl (19.2 mg, 38.7 μmol, 2 mol%) and silver trifluoromethanesulfonate (24.9 mg, 96.7 μmol, 5 mol%) were added to a solution of 1-phenylnon-2-yn-1-yl acetate (**85b**, 500 mg, 1.94 mmol, 1 eq) in acetonitrile (38.8 mL) and water (48 μL). The mixture was stirred at room temperature for 48h. Water was added and the mixture was extracted with diethyl ether (3×25 mL). The combined organic fractions were washed with brine (50 mL), dried with anhydrous magnesium sulfate, filtered and the solvents removed *in vacuo*. ^{19}F NMR analysis on the crude reaction mixture indicated the presence of the α-fluoroenones **92b** in an *E*/*Z* ratio of 91:9. The crude mixture was purified by column chromatography on silica gel (pet ether 40-60:diethyl ether, gradient = 20:1 to

5:1) to afford the separable α-fluoroenone diastereoisomers (*E*)-**92b** (yellow oil, 187 mg, yield = 41%) and (*Z*)-**92b** (yellow solid, 17 mg, yield = 4%) along with enone (*E*)-**86b** (yellow solid, 106 mg, yield = 25%).

R_f (hexane:diethyl ether, 9:1) = 0.50. **^{1}H NMR** (400 MHz, $CDCl_3$) δ: 7.60-7.64 (m, 2H, *ortho*-Ph), 7.35-7.40 (m, 3H, *meta*-, *para*-Ph), 6.70 (d, 1H, $^3J_{HF}$ = 25.3 Hz, C*H*=CF), 2.65 (dt, 2H, $^3J_{HH}$ = 7.1 Hz, $^4J_{HF}$ = 3.5 Hz, *H1*), 1.63 (tt, 2H, $^3J_{HH}$ = 7.3, 7.1 Hz, *H2*), 1.27-1.36 (m, 6H, *H3-5*), 0.90 (dd, 3H, $^3J_{HH}$ = 6.8, 6.5 Hz, *H6*). **^{13}C NMR** (101 MHz, $CDCl_3$) δ: 195.6 (d, $^2J_{CF}$ = 38 Hz, *C*=O), 153.1 (d, $^1J_{CF}$ = 258 Hz, CH=*C*F), 130.9 (d, $^3J_{CF}$ = 10 Hz, *ipso*-Ph), 130.0 (d, $^4J_{CF}$ = 2 Hz, *ortho*-Ph), 129.2 (*para*-Ph), 128.2 (*meta*-Ph), 119.7 (d, $^2J_{CF}$ = 27 Hz, *C*H=CF), 40.2 (d, $^3J_{CF}$ = 2 Hz, *C1*), 31.6 (*C4*), 28.8 (*C3*), 23.2 (d, $^4J_{CF}$ = 2 Hz, *C2*), 22.5 (*C5*), 14.0 (*C6*). **^{19}F NMR** (377 MHz, $CDCl_3$) δ: −114.9 (dt, $^3J_{HF}$ = 25 Hz, $^4J_{HF}$ = 4 Hz). **IR** (neat): 1708 (C=O). **HRMS** (*m/z*, ESI^+): calculated for $C_{15}H_{19}FNaO^+$ ($[M+Na]^+$): 257.1314, found 257.1312.

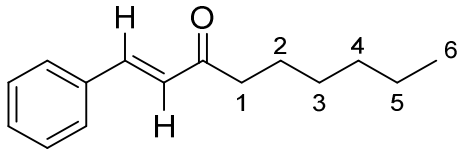
(*Z*)-2-Fluoro-1-phenylnon-1-en-3-one ((*Z*)-92b)



Mp = 30°C. **R_f** (hexane:diethyl ether, 9:1): 0.42. **^{1}H NMR** (400 MHz, $CDCl_3$) δ: 7.66-7.70 (m, 2H, *ortho*-Ph), 7.38-7.44 (m, 3H, *meta*-, *para*-Ph), 6.83 (d, 1H, $^3J_{HF}$ = 36.9 Hz, C*H*=CF), 2.74 (dt, 2H, $^3J_{HH}$ = 7.3 Hz, $^4J_{HF}$ = 2.3 Hz, *H1*), 1.69 (tt, 2H, $^3J_{HH}$ = 7.5, 7.3 Hz, *H2*), 1.27-1.41 (m, 6H, *H3-5*), 0.91 (d, 3H, $^3J_{HH}$ = 7.0, 6.8 Hz, *H6*). **^{13}C NMR** (101 MHz, $CDCl_3$) δ: 195.1 (d, $^2J_{CF}$ = 32 Hz, *C*=O), 154.1 (d, $^1J_{CF}$ = 272 Hz, CH=*C*F), 131.2 (d, $^3J_{CF}$ = 4 Hz, *ipso*-Ph), 130.6 (d, $^4J_{CF}$ = 9 Hz, *ortho*-Ph), 129.7 (*para*-Ph), 128.8 (*meta*-Ph), 114.9 (d, $^2J_{CF}$ = 6 Hz, *C*H=CF), 38.0 (*C1*), 31.6 (*C4*), 28.8 (*C3*), 23.5 (d, $^4J_{CF}$ = 2 Hz, *C2*), 22.5

(*C5*), 14.0 (*C6*). **^{19}F NMR** (377 MHz, $CDCl_3$) δ: −125.0 (d, $^3J_{HF}$ = 37 Hz). **IR** (CH_2Cl_2): 1697 (C=O). **HRMS** (*m/z*, FI^+): calculated for $C_{15}H_{19}FO$ ($[M]^+$): 234.1420, found 234.1414.

(1*E*)-1-Phenylnon-1-en-3-one ((*E*)-86b)[269]



R_f (hexane / diethyl ether, 9:1): 0.26. **^{1}H NMR** (400 MHz, $CDCl_3$) δ: 7.55 (d, 1H, $^3J_{HH}$ = 16.2 Hz, (Ph)C*H*=CH), 7.53-7.57 (m, 2H, *ortho*-Ph), 7.37-7.40 (m, 3H, *meta*-, *para*-Ph), 6.74 (d, 1H, $^3J_{HH}$ = 16.2 Hz, (Ph)CH=C*H*), 2.66 (t, 2H, $^3J_{HH}$ = 7.3 Hz, *H1*), 1.68 (apparent quin, 2H, $^3J_{HH}$ = 7.3 Hz, *H2*), 1.27-1.40 (m, 6H, *H3-5*), 0.90 (dd, 3H, $^3J_{HH}$ = 7.1, 6.6 Hz, *H6*). **^{13}C NMR** (101 MHz, $CDCl_3$) δ: 200.5 (*C*=O), 142.2 ((Ph)*C*H=CH), 134.5 (*ipso*-Ph), 130.3 (*para*-Ph), 128.8, 128.1 (*ortho*-, *meta*-Ph), 126.2 ((Ph)CH=*C*H), 40.9 (*C1*), 31.6 (*C4*), 28.9 (*C3*), 24.3 (*C2*), 22.4 (*C5*), 14.0 (*C6*). **LRMS** (*m/z*, ESI^+): calculated for $C_{15}H_{20}NaO^+$ ($[M+Na]^+$): 239.2, found 239.2.

6.2.3.2 Scope and Limitations

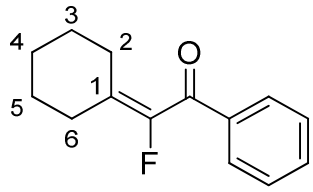


Scheme 6.2 Rearrangement-Fluorodeacetylation of Propargyl Acetates **85**.

General Procedure B: Selectfluor (**82**, 2 eq), SIPrAuCl (**1**, 5 mol%) and silver trifluoromethanesulfonate (12.5 mol%) were added to a solution of the propargyl acetate (1 eq) in acetonitrile (0.05 M). The mixture was stirred at room temperature or 40°C until TLC showed complete consumption of the propargyl acetate (1.5-72h). Water was added and the

mixture was extracted with ethyl acetate (3×). The combined organic fractions were washed with brine, dried with anhydrous magnesium sulfate, filtered and the solvents removed *in vacuo*. The crude mixture was analysed by ^{19}F NMR to give the α-fluoroenone *E*/*Z* ratio and then purified by column chromatography on silica gel.

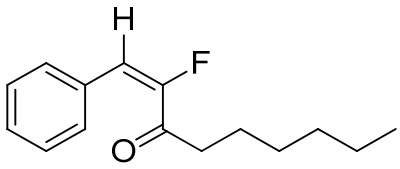
2-Cyclohexylidene-2-fluoro-1-phenylethanone (92a)[270]



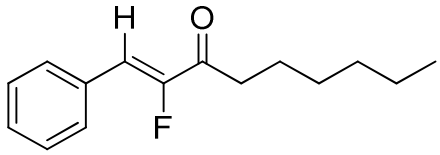
General Procedure B was followed using **85a** (500 mg, 2.06 mmol), Selectfluor (**82**, 1.46 g, 4.13 mmol), SIPrAuCl (**1**, 65 mg, 100 μmol) and AgOTf (66 mg, 0.26 mmol) in acetonitrile (41 mL). The reaction was stirred for 1.5h at 40°C. The resulting crude mixture was purified by column chromatography on silica gel (hexane:diethyl ether, 20:1) to afford the product **92a** as a pale yellow oil (385 mg, yield = 85%).

R_f (pet. ether 30-40:diethyl ether, 9:1) = 0.40. **^{1}H NMR** (400 MHz, $CDCl_3$) δ: 7.87-7.89 (m, 2H, *ortho*-Ph), 7.56 (ddm, 1H, $^3J_{HH}$ = 7.6, 7.3 Hz, *para*-Ph), 7.46 (t, 2H, $^3J_{HH}$ = 7.6 Hz, *meta*-Ph), 2.48-2.52 (m, 2H, *H2*), 2.42-2.45 (m, 2H, *H6*), 1.66-1.74 (m, 2H, *H5*), 1.58-1.66 (m, 4H, *H3*, *H4*). **^{13}C NMR** (101 MHz, $CDCl_3$) δ: 188.7 (d, $^2J_{CF}$ = 36 Hz, *C*=O), 147.8 (d, $^1J_{CF}$ = 251 Hz, C=*C*F), 137.0 (d, $^3J_{CF}$ = 4 Hz, *ipso*-Ph), 133.6 (d, $^2J_{CF}$ = 11 Hz, *C1*), 132.9 (*para*-Ph), 129.3 (d, $^4J_{CF}$ = 5 Hz, *ortho*-Ph), 128.3 (*meta*-Ph), 27.9 (d, $^3J_{CF}$ = 2 Hz, *C2*), 27.6 (d, $^4J_{CF}$ = 2 Hz, *C3*), 27.2 (d, $^4J_{CF}$ = 2 Hz, *C5*), 27.0 (d, $^3J_{CF}$ = 9 Hz, *C6*), 26.0 (*C4*). **^{19}F NMR** (377 MHz, $CDCl_3$) δ: −121.4. **IR** (neat): 1674 (C=O). **HRMS** (*m*/*z*, FI^+): calculated for $C_{14}H_{15}FO$ ($[M]^+$) 218.1107 found 218.1108.

(*E*)- and (*Z*)-2-Fluoro-1-phenylnon-1-en-3-one ((*E*)-92b and (*Z*)-92b)



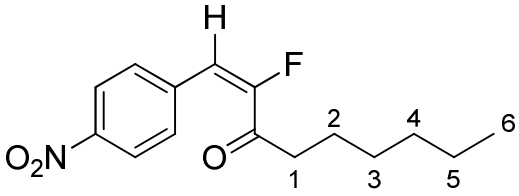
(*E*)-**92b**



(*Z*)-**92b**

General Procedure B was followed using **85b** (500 mg, 1.94 mmol), Selectfluor (**82**, 1.37 g, 3.87 mmol), SIPrAuCl (**1**, 60 mg, 0.10 mmol) and AgOTf (62 mg, 0.24 mmol) in acetonitrile (39 mL). The reaction was stirred for 48h at room temperature. ^{19}F NMR analysis on the crude reaction mixture indicated an *E*/*Z* ratio of 93:7. Purification by column chromatography on silica gel (hexane:diethyl ether, 20:1) afforded the product (*E*)-**92b** as a yellow oil (290 mg, yield = 64%) as well as (*Z*)-**92b** as a yellow solid (24 mg, yield = 6%). For characterisation data of (*E*)-**92b** and (*Z*)-**92b**, see Section 6.2.3.1.

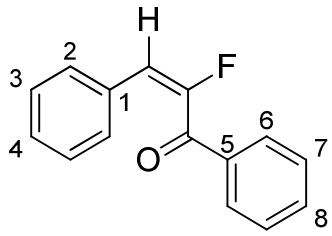
(*E*)-2-Fluoro-1-(4-nitrophenyl)non-1-en-3-one ((*E*)-92c)



General Procedure B was followed using **85c** (500 mg, 1.65 mmol), Selectfluor (**82**, 1.17 g, 3.30 mmol), SIPrAuCl (**1**, 51 mg, 82 µmol) and AgOTf (53 mg, 0.21 mmol) in acetonitrile (33 mL). The reaction was stirred for 20h at 40°C. ^{19}F NMR analysis on the crude reaction mixture indicated an *E*/*Z* ratio of 90:10. Purification by column chromatography on silica gel (hexane:diethyl ether, 20:1) afforded the product (*E*)-**92c** as a yellow oil (295 mg, yield = 64%). **R$_f$** (hexane:diethyl ether, 9:1) = 0.37. **^{1}H NMR** (400 MHz, $CDCl_3$) δ: 8.19 (dm, 2H, $^3J_{HH}$ = 8.6 Hz, *meta*-Ar), 7.70 (d, 2H, $^3J_{HH}$ = 8.6 Hz, *ortho*-Ar), 6.66 (d, 1H, $^3J_{HF}$ = 23.2 Hz, C*H*=CF), 2.70 (dt, 2H, $^3J_{HH}$ = 7.3 Hz, $^4J_{HF}$ = 3.5 Hz, *H1*), 1.61 (tt, 2H, $^3J_{HH}$ = 7.3, 7.1 Hz,

H2), 1.24-1.35 (m, 6H, *H3-5*), 0.88 (t, 3H, $^{3}J_{HH}$ = 6.8 Hz, *H6*). **^{13}C NMR** (101 MHz, $CDCl_3$) δ: 195.5 (d, $^{2}J_{CF}$ = 38 Hz, <u>C</u>=O), 154.0 (d, $^{1}J_{CF}$ = 267 Hz, CH=<u>C</u>F), 147.5 (*para*-Ar), 137.7 (d, $^{3}J_{CF}$ = 12 Hz, *ipso*-Ar), 130.7 (d, $^{4}J_{CF}$ = 3 Hz, *ortho*-Ar), 123.2 (*meta*-Ar), 116.8 (d, $^{2}J_{CF}$ = 29 Hz, <u>C</u>H=CF), 40.0 (d, $^{3}J_{CF}$ = 2 Hz, *C1*), 31.5 (*C4*), 28.6 (*C3*), 22.8 (d, $^{4}J_{CF}$ = 2 Hz, *C2*), 22.4 (*C5*), 14.0 (*C6*). **^{19}F NMR** (377 MHz, $CDCl_3$) δ: −110.8 (dm, $^{3}J_{HF}$ = 23 Hz). **IR** (neat): 1711 (C=O), 1522 (NO_2), 1345 (NO_2). **HRMS** (*m*/*z*, ESI$^+$): calculated for $C_{15}H_{18}FNNaO_3^+$ ([M+Na]$^+$): 302.1163, found 302.1161.

(*E*)-2-Fluoro-1,3-diphenylprop-2-en-1-one ((*E*)-92f)

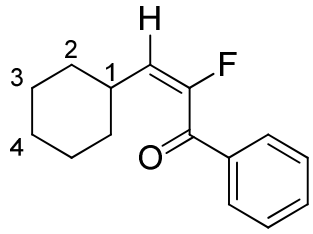


General Procedure B was followed using **85f** (500 mg, 2.00 mmol), Selectfluor (**82**, 1.42 g, 4.00 mmol), SIPrAuCl (**1**, 62 mg, 100 μmol) and AgOTf (64 mg, 0.25 mmol) in acetonitrile (40 mL). The reaction was stirred for 24h at 40°C. ^{19}F NMR analysis on the crude reaction mixture indicated an *E*/*Z* ratio of 92:8. Purification by column chromatography on silica gel (hexane:diethyl ether, 20:1) afforded the product (*E*)-**92f** as a yellow oil (268 mg, yield = 62%).

R_f (hexane:diethyl ether, 9:1) = 0.33. **^{1}H NMR** (400 MHz, $CDCl_3$) δ: 7.92 (d, 2H, $^{3}J_{HH}$ = 8.1 Hz, *H6*), 7.55 (dd, 1H, $^{3}J_{HH}$ = 7.6, 7.3 Hz, *H8*), 7.42 (ddm, 2H, *J* = 8.1, 7.3 Hz, *H7*), 7.31-7.34 (m, 2H, *H2*), 7.22-7.26 (m, 3H, *H3*, *H4*), 6.93 (d, 1H, $^{3}J_{HF}$ = 23.2 Hz, C<u>*H*</u>=CF). **^{13}C NMR** (101 MHz, $CDCl_3$) δ: 188.3 (d, $^{2}J_{CF}$ = 32 Hz, <u>C</u>=O), 153.0 (d, $^{1}J_{CF}$ = 261 Hz, CH=<u>C</u>F), 135.3 (*C5*), 133.8 (*C8*), 130.9 (d, $^{3}J_{CF}$ = 10 Hz, *C1*), 129.6 (d, $^{4}J_{CF}$ = 3 Hz), 129.2 (d, $^{4}J_{CF}$ = 3 Hz, *C2*, *C6*), 128.6 (*C4*), 128.5, 128.3 (*C3*, *C7*), 118.2 (d, $^{2}J_{CF}$ = 25 Hz,

C̲H=CF). **^{19}F NMR** (377 MHz, $CDCl_3$) δ: −107.1 (d, $^3J_{HF}$ = 24 Hz). **IR** (neat): 1677 (C=O). **HRMS** (*m/z*, FI^+): calculated for $C_{15}H_{11}FO$ ($[M]^+$): 226.0794, found 226.0793.

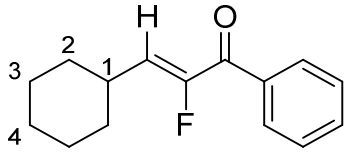
(2*E*)-3-cyclohexyl-2-fluoro-1-phenylprop-2-en-1-one ((*E*)-92g)



General Procedure B was followed using **85g** (500 mg, 1.95 mmol), Selectfluor (**82**, 1.38 g, 3.90 mmol), SIPrAuCl (**1**, 61 mg, 98 μmol) and AgOTf (63 mg, 0.24 mmol) in acetonitrile (39 mL). The reaction was stirred for 48h at 40°C. ^{19}F NMR analysis on the crude reaction mixture indicated an *E*/*Z* ratio of 84:16. Purification by column chromatography on silica gel (hexane:diethyl ether, 20:1) afforded the product (*E*)-**92g** as a yellow oil (307 mg, yield = 68%) as well as (*Z*)-**92g** as a yellow oil (55 mg, yield = 12%).

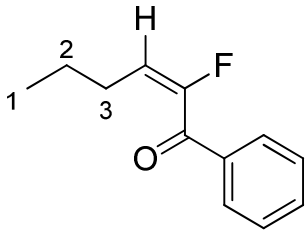
R_f (hexane:diethyl ether, 9:1) = 0.54. **^{1}H NMR** (400 MHz, $CDCl_3$) δ: 7.88-7.92 (m, 2H, *ortho*-Ph), 7.59 (dd, 1H, $^3J_{HH}$ = 7.5, 7.3 Hz, *para*-Ph), 7.47 (ddm, 2H, $^3J_{HH}$ = 8.2, 7.3 Hz, *meta*-Ph), 5.76 (dd, 1H, $^3J_{HF}$ = 23.0 Hz, $^3J_{HH}$ = 10.7 Hz, C*H*̲=CF), 2.74 (tdtd, 1H, $^3J_{HH}$ = 11.0, 10.7, 3.8 Hz, $^4J_{HF}$ = 2.5 Hz, *H1*), 1.77-1.82 (m, 2H, *H2*), 1.63-1.75 (m, 3H, *H3*, *H4*), 1.31 (qt, 2H, $^3J_{HH}$ = 12.6, 3.2 Hz, *H3'*), 1.12-1.24 (m, 3H, *H2'*, *H4'*). **^{13}C NMR** (125 MHz, $CDCl_3$) δ: 188.2 (d, $^2J_{CF}$ = 35 Hz, C̲=O), 152.9 (d, $^1J_{CF}$ = 258 Hz, CH=C̲F), 136.2 (d, $^3J_{CF}$ = 5 Hz, *ipso*-Ph), 133.3 (*para*-Ph), 129.3 (d, $^4J_{CF}$ = 6 Hz, *ortho*-Ph), 128.4 (*meta*-Ph), 127.0 (d, $^2J_{CF}$ = 14 Hz, C̲H=CF), 34.6 (d, $^3J_{CF}$ = 5 Hz, *C1*), 33.0 (d, $^4J_{CF}$ = 2 Hz, *C2*), 25.8 (*C4*), 25.4 (*C3*). **^{19}F NMR** (377 MHz, $CDCl_3$) δ: −107.1 (d, $^3J_{HF}$ = 24 Hz). **IR** (neat): 1678 (C=O). **HRMS** (*m/z*, FI^+): calculated for $C_{15}H_{17}FO$ ($[M]^+$): 232.1263, found 232.1269.

(2*Z*)-3-cyclohexyl-2-fluoro-1-phenylprop-2-en-1-one ((*Z*)-92g)



R_f (hexane:diethyl ether, 9:1) = 0.38. **^{1}H NMR** (400 MHz, $CDCl_3$) δ: 7.79 (d, 2H, $^3J_{HH}$ = 7.8 Hz, *ortho*-Ph), 7.57 (tm, 1H, $^3J_{HH}$ = 7.3 Hz, *para*-Ph), 7.46 (ddm, 2H, $^3J_{HH}$ = 7.8, 7.3 Hz, *meta*-Ph), 5.91 (dd, 1H, $^3J_{HF}$ = 34.9 Hz, $^3J_{HH}$ = 9.6 Hz, C*H*=CF), 2.69 (dddm, 1H, $^3J_{HH}$ = 10.9, 10.4, 9.6 Hz, *H1*), 1.65-1.82 (m, 5H), 1.29-1.42 (m, 2H), 1.14-1.28 (m, 3H, *H2-4*). **^{13}C NMR** (125 MHz, $CDCl_3$) δ: 188.4 (d, $^2J_{CF}$ = 28 Hz, *C*=O), 153.8 (d, $^1J_{CF}$ = 260 Hz, CH=*C*F), 136.4 (*ipso*-Ph), 132.7 (*para*-Ph), 129.4 (d, $^2J_{CF}$ = 13 Hz, *C*H=CF), 129.2 (d, $^4J_{CF}$ = 4 Hz, *ortho*-Ph), 128.3 (*meta*-Ph), 34.3 (d, $^3J_{CF}$ = 2 Hz, *C1*), 32.0 (d, $^4J_{CF}$ = 2 Hz, *C2*), 25.7 (*C3*), 25.4 (*C4*). **^{19}F NMR** (377 MHz, $CDCl_3$) δ: −125.4 (d, $^3J_{HF}$ = 34 Hz). **IR** (neat): 1667 (C=O). **HRMS** (*m*/*z*, FI^+): calculated for $C_{15}H_{17}FO$ ($[M]^+$): 232.1263, found 232.1266.

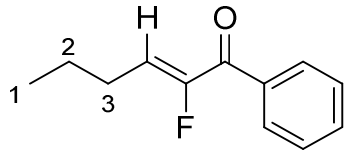
(*E*)-2-Fluoro-1-phenylhex-2-en-1-one ((*E*)-92h)



General Procedure B was followed using **85h** (398 mg, 1.84 mmol), Selectfluor (**82**, 1.30 g, 3.68 mmol), SIPrAuCl (**1**, 57 mg, 92 μmol) and AgOTf (59 mg, 0.23 mmol) in acetonitrile (37 mL). The reaction was stirred for 72h at 40°C. ^{19}F NMR analysis on the crude reaction mixture indicated an *E*/*Z* ratio of 67:33. Purification by column chromatography on silica gel (hexane:diethyl ether, 20:1) afforded the product (*E*)-**92h** as a yellow liquid (145 mg, yield = 42%) as well as (*Z*)-**92h** as a yellow liquid (77 mg, yield = 21%).

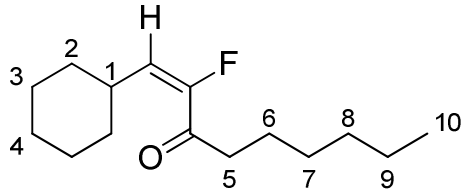
R_f (hexane:diethyl ether, 9:1) = 0.51. **^{1}H NMR** (400 MHz, $CDCl_3$) δ: 7.89-7.92 (m, 2H, *ortho*-Ph), 7.59 (tt, 1H, $^3J_{HH}$ = 7.3 Hz, $^4J_{HH}$ = 2.0 Hz, *para*-Ph), 7.48 (dm, 2H, $^3J_{HH}$ = 7.3 Hz, *meta*-Ph), 5.92 (dt, 1H, $^3J_{HF}$ = 23.0 Hz, $^3J_{HH}$ = 8.1 Hz, C*H*=CF), 2.38 (ddd, 2H, $^3J_{HH}$ = 8.1, 7.3 Hz, $^4J_{HF}$ = 1.8 Hz, *H3*), 1.51 (apparent quin, 2H, $^3J_{HH}$ = 7.3 Hz, *H2*), 0.95 (t, 3H, $^3J_{HH}$ = 7.3 Hz, *H1*). **^{13}C NMR** (101 MHz, $CDCl_3$) δ: 188.2 (d, $^2J_{CF}$ = 35 Hz, *C*=O), 152.8 (d, $^1J_{CF}$ = 257 Hz, CH=*C*F), 136.2 (d, $^3J_{CF}$ = 5 Hz, *ipso*-Ph), 133.3 (*para*-Ph), 129.4 (d, $^4J_{CF}$ = 5 Hz, *ortho*-Ph), 128.4 (*meta*-Ph), 121.7 (d, $^2J_{CF}$ = 17 Hz, *C*H=CF), 27.5 (d, $^3J_{CF}$ = 6 Hz, *C3*), 22.6 (d, $^4J_{CF}$ = 3 Hz, *C2*), 13.6 (*C1*). **^{19}F NMR** (377 MHz, $CDCl_3$) δ: −112.8 (dd, $^3J_{HF}$ = 23 Hz, $^4J_{HF}$ = 2 Hz). **IR** (neat): 1679 (C=O). **HRMS** (*m*/*z*, FI^+): calculated for $C_{12}H_{13}FO$ ($[M]^+$): 192.0950, found 192.0951.

(*Z*)-2-Fluoro-1-phenylhex-2-en-1-one ((*Z*)-92h)



R_f (hexane:diethyl ether, 9:1) = 0.37. **^{1}H NMR** (400 MHz, $CDCl_3$) δ: 7.79-7.83 (m, 2H, *ortho*-Ph), 7.58 (tt, 1H, $^3J_{HH}$ = 7.3 Hz, $^4J_{HH}$ = 2.0 Hz, *para*-Ph), 7.47 (tm, 2H, $^3J_{HH}$ = 7.6 Hz, *meta*-Ph), 6.05 (dt, 1H, $^3J_{HF}$ = 34.1 Hz, $^3J_{HH}$ = 7.8 Hz, C*H*=CF), 2.33 (ddd, 2H, $^3J_{HH}$ = 7.8, 7.3 Hz, $^4J_{HF}$ = 1.8 Hz, *H3*), 1.53 (tq, 2H, $^3J_{HH}$ = 7.3, 7.3 Hz, *H2*), 0.98 (t, 3H, $^3J_{HH}$ = 7.3 Hz, *H1*). **^{13}C NMR** (101 MHz, $CDCl_3$) δ: 187.6 (d, $^2J_{CF}$ = 28 Hz, *C*=O), 155.2 (d, $^1J_{CF}$ = 260 Hz, CH=*C*F), 136.3 (*ipso*-Ph), 132.7 (*para*-Ph), 129.2 (d, $^4J_{CF}$ = 4 Hz, *ortho*-Ph), 128.3 (*meta*-Ph), 124.2 (d, $^2J_{CF}$ = 14 Hz, *C*H=CF), 26.5 (d, $^3J_{CF}$ = 4 Hz, *C3*), 21.6 (d, $^4J_{CF}$ = 2 Hz, *C2*), 13.7 (*C1*). **^{19}F NMR** (377 MHz, $CDCl_3$) δ: −124.8 (d, $^3J_{HF}$ = 34 Hz). **IR** (neat): 1668 (C=O). **HRMS** (*m*/*z*, FI^+): calculated for $C_{12}H_{13}FO$ ($[M]^+$): 192.0950, found 192.0952.

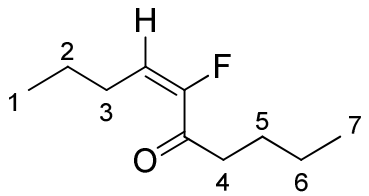
(1*E*)-1-Cyclohexyl-2-fluoronon-1-en-3-one ((*E*)-92i)



General Procedure B was followed using **85i** (323 mg, 1.29 mmol), Selectfluor (**82**, 914 mg, 2.58 mmol), SIPrAuCl (**1**, 40 mg, 65 µmol) and AgOTf (41 mg, 0.16 mmol) in acetonitrile (26 mL). The reaction was stirred for 72h at 40°C. ^{19}F NMR analysis on the crude reaction mixture indicated an *E*/*Z* ratio of 77:23. Purification by column chromatography on silica gel (hexane:diethyl ether, 20:1) afforded the product (*E*)-**92i** as a colourless oil (91 mg, yield = 29%).

R_f (hexane:diethyl ether, 9:1) = 0.59. **^{1}H NMR** (400 MHz, $CDCl_3$) δ: 5.53 (dd, 1H, $^3J_{HF}$ = 23.2 Hz, $^3J_{HH}$ = 10.5 Hz, C*H*=CF), 3.07 (tdm, 1H, $^3J_{HH}$ = 10.9, 10.5 Hz, *H1*), 2.60 (td, 2H, $^3J_{HH}$ = 7.3 Hz, $^4J_{HF}$ = 3.3 Hz, *H5*), 1.56-1.75 (m, 7H), 1.25-1.40 (m, 8H), 1.01-1.23 (m, 3H, *H2-4*, *H6-9*), 0.89 (dd, 3H, *J* = 6.9, 6.6 Hz, *H10*). **^{13}C NMR** (125 MHz, $CDCl_3$) δ: 197.0 (d, $^2J_{CF}$ = 38 Hz, *C*=O), 152.5 (d, $^1J_{CF}$ = 256 Hz, CH=*C*F), 126.7 (d, $^2J_{CF}$ = 15 Hz, *C*H=CF), 39.8 (d, $^3J_{CF}$ = 3 Hz, *C5*), 34.1 (d, $^3J_{CF}$ = 5 Hz, *C1*), 32.8 (d, $^4J_{CF}$ = 2 Hz, *C2*), 31.6, 28.8, 25.8, 25.4 (*C3*, *C4*, *C7*, *C8*), 22.9 (d, $^4J_{HH}$ = 2 Hz, *C6*), 22.5 (*C9*), 14.0 (*C10*). **^{19}F NMR** (377 MHz, $CDCl_3$) δ: −123.3 (d, $^3J_{HF}$ = 23 Hz). **IR** (neat): 1708 (C=O). **HRMS** (*m*/*z*, ESI$^+$): calculated for $C_{15}H_{25}FNaO^+$ ($[M+Na]^+$): 263.1782, found 263.1778.

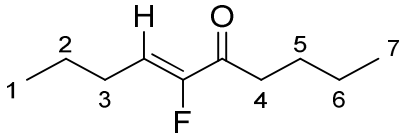
(*E*)-6-Fluorodec-6-en-5-one ((*E*)-92j)



General Procedure B was followed using **85j** (500 mg, 2.55 mmol), Selectfluor (**82**, 1.80 g, 5.09 mmol), SIPrAuCl (**1**, 79 mg, 0.12 mmol) and AgOTf (82 mg, 0.31 mmol) in acetonitrile (51 mL). The reaction was stirred for 72h at 40°C. ^{19}F NMR analysis on the crude reaction mixture indicated an *E*/*Z* ratio of 58:42. Purification by column chromatography on silica gel (hexane:diethyl ether, 50:1) afforded the product (*E*)-**92j** as a pale yellow oil (83 mg, yield = 19%) as well as (*Z*)-**92j** (80 mg, yield = 18%).

R$_f$ (hexane:diethyl ether, 9:1) = 0.61. **^{1}H NMR** (400 MHz, $CDCl_3$) δ: 5.70 (dt, 1H, $^3J_{HF}$ = 22.7 Hz, $^3J_{HH}$ = 8.1 Hz, C*H*=CF), 2.60 (td, 2H, $^3J_{HH}$ = 7.3 Hz, $^4J_{HF}$ = 3.3 Hz, *H4*), 2.49 (dtd, 2H, $^3J_{HH}$ = 8.1, 7.3 Hz, $^4J_{HF}$ = 2.0 Hz, *H3*), 1.59 (tt, 2H, $^3J_{HH}$ = 7.6, 7.3 Hz, *H5*), 1.45 (tq, 2H, $^3J_{HH}$ = 7.6, 7.3 Hz, *H2*), 1.35 (tq, 2H, $^3J_{HH}$ = 7.6, 7.3 Hz, *H6*), 0.93 (dd, 3H, $^3J_{HH}$ = 7.6, 7.3 Hz, *H1*), 0.92 (t, 3H, *J* = 7.3 Hz, *H7*). **^{13}C NMR** (101 MHz, $CDCl_3$) δ: 197.1 (d, $^2J_{CF}$ = 38 Hz, *C*=O), 153.4 (d, $^1J_{CF}$ = 255 Hz, CH=*C*F), 121.3 (d, $^2J_{CF}$ = 18 Hz, *C*H=CF), 39.5 (d, $^3J_{CF}$ = 3 Hz, *C4*), 27.2 (d, $^3J_{CF}$ = 6 Hz, *C3*), 25.2 (d, $^4J_{CF}$ = 2 Hz, *C5*), 22.5 (d, $^4J_{CF}$ = 2 Hz, *C2*), 22.2 (*C6*), 13.8, 13.6 (*C1*, *C7*). **^{19}F NMR** (377 MHz, $CDCl_3$) δ: −121.5 (d, $^3J_{HF}$ = 23 Hz). **IR** (neat): 1708 (C=O). **HRMS** (*m*/*z*, FI$^+$): calculated for $C_{10}H_{17}FO$ ([M]$^+$): 172.1263, found 172.1258.

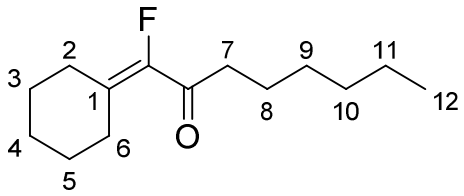
(*Z*)-6-Fluorodec-6-en-5-one ((*Z*)-92j)[271]



R$_f$ (hexane:diethyl ether, 9:1) = 0.44.**^{1}H NMR** (400 MHz, $CDCl_3$) δ: 6.04 (dt, 1H, $^3J_{HF}$ = 34.6 Hz, $^3J_{HH}$ = 7.6 Hz, C*H*=CF), 2.61 (ddd, 2H, $^3J_{HH}$ = 7.6, 7.3 Hz, $^4J_{HF}$ = 1.8 Hz, *H4*), 2.22 (ddt, 2H, $^3J_{HH}$ = 7.6, 7.3 Hz, $^4J_{HF}$ = 2.3 Hz, *H3*), 1.61 (tt, 2H, $^3J_{HH}$ = 7.6, 7.3 Hz, *H5*), 1.49 (tq, 2H, $^3J_{HH}$ = 7.3, 7.3 Hz, *H2*), 1.36 (tq, 2H, $^3J_{HH}$ = 7.6, 7.3 Hz, *H6*), 0.95 (dd, 3H, $^3J_{HH}$ = 7.6, 7.3 Hz), 0.93 (t, 3H, $^3J_{HH}$ = 7.3 Hz, *H1*, *H7*). **^{13}C NMR** (101 MHz, $CDCl_3$) δ: 194.4 (d,

$^{2}J_{CF}$ = 31 Hz, <u>C</u>=O), 153.3 (d, $^{1}J_{CF}$ = 261 Hz, CH=<u>C</u>F), 118.7 (d, $^{2}J_{CF}$ = 13 Hz, <u>C</u>H=CF), 37.5 (*C4*), 26.1 (d, $^{3}J_{CF}$ = 4 Hz, *C3*), 25.7 (d, $^{4}J_{CF}$ = 2 Hz, *C5*), 22.3 (*C6*), 21.7 (d, $^{4}J_{CF}$ = 2 Hz, *C2*), 13.8, 13.7 (*C1*, *C7*). **^{19}F NMR** (377 MHz, $CDCl_3$) δ: −129.9 (d, $^{3}J_{HF}$ = 36 Hz). **IR** (neat): 1714 (C=O). **HRMS** (*m/z*, FI^+): calculated for $C_{10}H_{17}FO$ ($[M]^+$): 172.1263, found 172.1259.

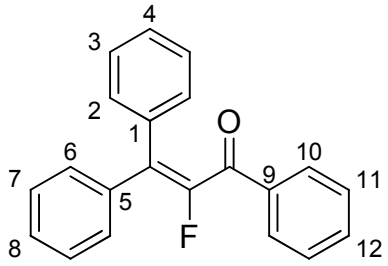
1-Cyclohexylidene-1-fluorooctan-2-one (92k)[96]



General Procedure B was followed using **85k** (250 mg, 1.00 mmol), Selectfluor (**82**, 707 mg, 2.00 mmol), SIPrAuCl (**1**, 31 mg, 50 μmol) and AgOTf (32 mg, 0.13 mmol) in acetonitrile (20 mL). The reaction was stirred for 3.5h at 40°C. Purification by column chromatography on silica gel (hexane:diethyl ether, 20:1) afforded the product **92k** as a yellow oil (131 mg, yield = 58%).

R_f (hexane:diethyl ether, 9:1) = 0.52. **^{1}H NMR** (400 MHz, $CDCl_3$) δ: 2.72-2.76 (m, 2H, *H6*), 2.60 (td, 2H, $^{3}J_{HH}$ = 7.3 Hz, $^{4}J_{HF}$ = 4.1 Hz, *H7*), 2.27-2.33 (m, 2H, *H2*), 1.53-1.67 (m, 8H, *H3*, *H5*, *H8*, *H9*), 1.25-1.36 (m, 6H, *H4*, *H10*, *H11*), 0.88 (dd, 3H, $^{3}J_{HH}$ = 6.8, 6.6 Hz, *H12*). **^{13}C NMR** (101 MHz, $CDCl_3$) δ: 197.3 (d, $^{2}J_{CF}$ = 39 Hz, <u>C</u>=O), 148.3 (d, $^{1}J_{CF}$ = 248 Hz, C=<u>C</u>F), 134.3 (d, $^{2}J_{CF}$ = 13 Hz, *C1*), 40.2 (d, $^{3}J_{CF}$ = 2 Hz, *C7*), 31.6 (*C10*), 28.9 (*C9*), 27.5 (d, J_{CF} = 2 Hz), 27.4 (d, J_{CF} = 10 Hz), 27.2 (d, J_{CF} = 2 Hz), 27.2 (d, J_{CF} = 2 Hz, *C2*, *C3*, *C5*, *C6*), 26.0 (*C4*), 23.3 (d, $^{4}J_{CF}$ = 2 Hz, *C8*), 22.5 (*C11*), 14.0 (*C12*). **^{19}F NMR** (377 MHz, $CDCl_3$) δ: −129.6. **IR** (neat): 1700 (C=O). **HRMS** (*m/z*, ESI^+): calculated for $C_{14}H_{23}FNaO^+$ ($[M+Na]^+$): 249.1625, found 249.1628.

2-Fluoro-1,3,3-triphenylprop-2-en-1-one (92l)



General Procedure B was followed using **85l** (500 mg, 1.53 mmol), Selectfluor (**82**, 1.09 g, 3.06 mmol), SIPrAuCl (**1**, 48 mg, 76 µmol) and AgOTf (49 mg, 0.19 mmol) in acetonitrile (30 mL). The reaction was stirred for 24h at 40°C Purification by column chromatography on silica gel (hexane:diethyl ether, 20:1) afforded the product **92l** as a yellow solid (268 mg, yield = 58%).

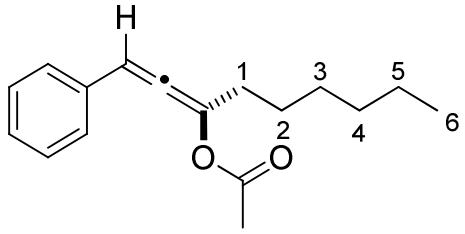
Mp = 80°C. $\mathbf{R_f}$ (hexane:diethyl ether, 9:1) = 0.37. **^{1}H NMR** (400 MHz, $CDCl_3$) δ: 7.89 (d, 2H, $^3J_{HH}$ = 7.8 Hz, *H10*), 7.37-7.53 (m, 8H, Ph), 7.17-7.27 (m, 5H, Ph). **^{13}C NMR** (101 MHz, $CDCl_3$) δ: 189.0 (d, $^2J_{CF}$ = 32 Hz, *C*=O), 149.8 (d, $^1J_{CF}$ = 268 Hz, C=*C*F), 136.4 (d, $^3J_{CF}$ = 5 Hz), 136.0, 135.9 (*C1*, *C5*, *C9*), 133.3 (*C12*), 130.9 (d, $^2J_{CF}$ = 11 Hz, *C*=CF), 130.4 (d, $^4J_{CF}$ = 3 Hz), 130.2 (d, $^4J_{CF}$ = 6 Hz), 129.4 (d, $^4J_{CF}$ = 4 Hz, *C2*, *C6*, *C10*), 128.8, 128.5, 128.3, 128.3, 128.2 (*C3*, *C4*, *C7*, *C8*, *C11*). **^{19}F NMR** (377 MHz, $CDCl_3$) δ: −111.2. **IR** (CH_2Cl_2): 1656 (C=O). **HRMS** (*m/z*, FI^+): calculated for $C_{21}H_{15}FO$ ($[M]^+$): 302.1107, found 302.1111. The structure was unambiguously confirmed by X-ray crystallography. This data is deposited at the Cambridge Crystallographic Data Centre (CCDC): 792124 (see Appendix).

6.2.4 Preparation and Fluorination of Allenyl Acetates 88b and 88o

6.2.4.1 Preparation of Allenyl Acetate 88b

Allenyl acetate **88b** was prepared according to the procedure of Zhang (see Scheme 2.16).[92]

1-Phenylnona-1,2-dien-3-yl acetate (88b)

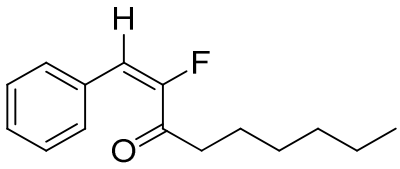


Silver perchlorate (26 mg, 0.13 mmol, 10 mol%) was added to a solution of **85b** (329 mg, 1.27 mmol, 1 eq) in 2-butanone (13 mL). The mixture was stirred at reflux for 2h before cooling to room temperature. After removal of the solvent *in vacuo*, the crude mixture was purified by column chromatography on silica gel (pet. ether 30-40:diethyl ether, 20:1) affording **88b** as a pale yellow oil (148 mg, yield = 45%).

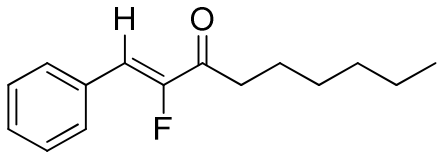
R_f (hexane:diethyl ether, 9:1) = 0.30.**^{1}H NMR** (400 MHz, $CDCl_3$) δ: 7.42-7.46 (m, 2H, *ortho*-Ph), 7.35 (ddm, 2H, $^3J_{HH}$ = 8.1, 7.1 Hz, *meta*-Ph), 7.26 (t, 1H, $^3J_{HH}$ = 7.3 Hz, *para*-Ph), 6.60 (t, 1H, $^5J_{HH}$ = 3 Hz, (Ph)C*H*=C=C), 2.35 (ddd, 2H, $^3J_{HH}$ = 7.3, 7.0 Hz, $^5J_{HH}$ = 3.0 Hz, *H1*), 2.16 (s, 3H, (C=O)CH_3), 1.46-1.54 (m, 2H, *H2*), 1.34-1.41 (m, 2H, *H3*), 1.24-1.32 (m, 4H, *H4*, *H5*), 0.87 (dd, $^3J_{HH}$ = 7.1, 6.8 Hz, *H6*). **^{13}C NMR** (101 MHz, $CDCl_3$) δ: 196.7 (C=*C*=C), 168.7 (*C*=O), 133.9 (*ipso*-Ph), 128.6 (*meta*-Ph), 127.9 (*para*-Ph), 127.8 (*ortho*-Ph), 126.9 ((Ph)*C*H=C=C), 104.5 ((Ph)CH=C=*C*), 31.7, 31.5 (*C1*, *C4*), 28.7 (*C3*), 26.1 (*C2*), 22.6 (*C5*), 21.1 ((C=O)*C*H_3), 14.0 (*C6*). **IR** (neat): 1965 (C=C=C), 1754 (C=O). **HRMS** (*m*/*z*, FI^+): calculated for $C_{17}H_{22}O_2$ ($[M]^+$): 258.1620, found 258.1616.

6.2.4.2 Fluorination of Allenyl Acetate 88b

(*E*)- and (*Z*)-2-Fluoro-1-phenylnon-1-en-3-one ((*E*)-92b and (*Z*)-92b)



(*E*)-**92b**



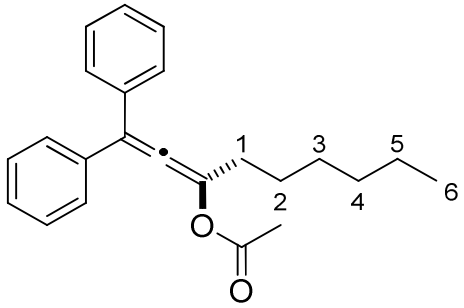
(*Z*)-**92b**

Selectfluor (**82**, 165 mg, 46.4 µmol, 2 eq) was added to a solution of allenyl acetate **88b** (60 mg, 23.3 µmol, 1 eq) in acetonitrile (4.6 mL). The mixture was stirred at rt until TLC showed consumption of the allene (72h). Water was added and the mixture was extracted with ethyl acetate (3×5 mL). The combined organic fractions were washed with brine (15 mL), dried with anhydrous magnesium sulfate, filtered and the solvents removed *in vacuo*. ^{19}F NMR analysis on the crude reaction mixture indicated an *E*/*Z* ratio of 91:9. The crude mixture was purified by column chromatography on silica gel (hexane:diethyl ether, 20:1) to afford α-fluoroenones **92b** as a yellow oil (28 mg, yield = 51%). For characterisation data of (*E*)- and (*Z*)-**92b**, see Section 6.2.3.1.

6.2.4.3 Preparation of Allenyl Acetate 88o

Allenyl acetate **88o** was prepared using General Procedure A (see Section 6.2.2, Scheme 2.18).

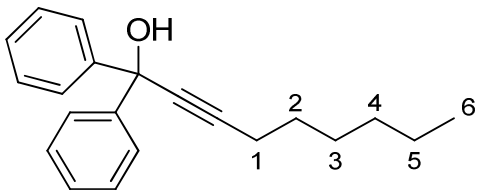
1,1-Diphenylnona-1,2-dien-3-yl acetate (88o)



General procedure A was followed using *n*-butyllithium (2.5 M solution in hexanes, 2.10 mL, 5.25 mmol), 1-octyne (811 μL, 5.50 mmol), benzophenone (911 mg, 5.00 mmol) and acetic anhydride (3.78 mL, 40.0 mmol) in tetrahydrofuran (21 mL). The resulting crude mixture was purified by column chromatography on silica gel (hexane:diethyl ether, 9:1) to afford the allenyl acetate **88o** as a pale yellow oil (491 mg, yield = 29%) as well as the propargyl alcohol **93o** as a pale yellow oil (677 mg, yield = 46%) and the protonated enone **86o** (55 mg, yield = 4%).

R_f (hexane:diethyl ether, 9:1) = 0.28. **^{1}H NMR** (400 MHz, $CDCl_3$) δ: 7.50-7.53 (m, 4H, *ortho*-Ph), 7.34-7.45 (m, 6H, *meta*-, *para*-Ph), 2.49 (dd, 2H, $^3J_{HH}$ = 7.6, 7.3 Hz, *H1*), 2.21 (s, 3H, (C=O)C$\underline{H}_3$), 1.61 (tt, 2H, $^3J_{HH}$ = 7.6, 7.3 Hz, *H2*), 1.35-1.45 (m, 2H, *H3*), 1.26-1.33 (m, 4H, *H4*, *H5*), 0.90 (t, 3H, $^3J_{HH}$ = 6.8 Hz, *H6*). **^{13}C NMR** (101 MHz, $CDCl_3$) δ: 196.5 (C=$\underline{C}$=C), 168.5 ($\underline{C}$=O), 136.5 (*ipso*-Ph), 128.8, 128.2, 127.8 (*ortho*-, *meta*-, *para*-Ph), 126.0 (C=C=$\underline{C}$(C_6H_{13})(OAc)), 118.7 ($\underline{C}$=C=C(C_6H_{13})(OAc)), 32.0, 31.5 (*C1*, *C4*), 28.7 (*C3*), 26.2 (*C2*), 22.5 (*C5*), 21.0 ((C=O)$\underline{C}$H$_3$), 13.9 (*C6*). **IR** (neat): 1957 (C=C=C), 1756 (C=O). **HRMS** (*m*/*z*, ESI^+): calculated for $C_{23}H_{26}NaO_2^+$ ([M+Na]$^+$): 357.1825, found 357.1826.

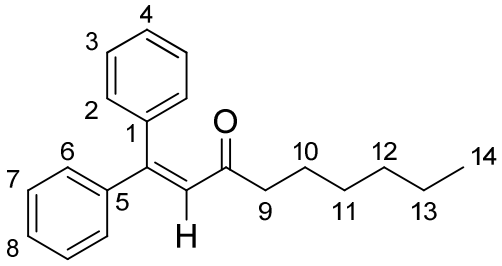
1,1-Diphenylnon-2-yn-1-ol (93o)



R_f (hexane:diethyl ether, 9:1) = 0.13. **^{1}H NMR** (400 MHz, $CDCl_3$) δ: 7.75 (d, 4H, $^3J_{HH}$ = 7.6 Hz, *ortho*-Ph), 7.43 (dd, 4H, $^3J_{HH}$ = 7.6, 7.3 Hz, *meta*-Ph), 7.35 (t, 2H, $^3J_{HH}$ = 7.3 Hz, *para*-Ph), 3.05 (s, 1H, O$\underline{H}$), 2.45 (t, 2H, $^3J_{HH}$ = 7.1 Hz, *H1*), 1.72 (tt, 2H, $^3J_{HH}$ = 7.1, 6.8 Hz, *H2*), 1.54-1.61 (m, 2H, *H3*), 1.40-1.52 (m, 4H, *H4*, *H5*), 1.06 (dd, 3H, $^3J_{HH}$ = 6.8, 6.6 Hz, *H6*). **^{13}C NMR** (101 MHz, $CDCl_3$) δ: 145.5 (*ipso*-Ph), 128.0 (*ortho*-Ph), 127.3 (*para*-Ph), 125.9

(*meta*-Ph), 88.1 (<u>*C*</u>≡C(C_6H_{13})), 83.1 (C≡<u>*C*</u>(C_6H_{13})), 74.3 ((Ph)$_2$<u>*C*</u>(OH)), 31.6 (*C4*), 28.5, 28.4 (*C2*, *C3*), 22.4 (*C5*), 18.7 (*C1*), 13.9 (*C6*). **IR** (neat): 3454 (O-H), 2234 (C≡C). **HRMS** (*m*/*z*, ESI^+): calculated for $C_{21}H_{24}NaO^+$ ($[M+Na]^+$): 315.1719, found 315.1718.

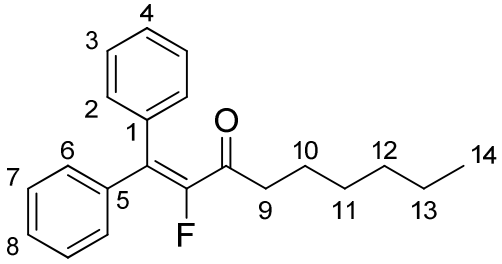
1,1-Diphenylnon-1-en-3-one (86o)



R_f (hexane:diethyl ether, 9:1) = 0.22. **^{1}H NMR** (400 MHz, $CDCl_3$) δ: 7.39-7.43 (m, 3H, Ph), 7.29-7.38 (m, 5H, Ph), 7.19-7.25 (m, 2H, Ph), 6.60 (s, 1H, C=C<u>*H*</u>), 2.24 (dd, 2H, $^3J_{HH}$ = 7.6, 7.3 Hz, *H9*), 1.51 (dd, 2H, $^3J_{HH}$ = 7.3, 7.1 Hz, *H10*), 1.21-1.30 (m, 2H, *H11*), 1.13-1.21 (m, 4H, *H12*, *H13*), 0.87 (t, 3H, $^3J_{HH}$ = 7.1 Hz, *H14*). **^{13}C NMR** (101 MHz, $CDCl_3$) δ: 202.5 (<u>*C*</u>=O), 153.0 (<u>*C*</u>=CH), 141.0, 139.1 (*C1*, *C5*), 129.5, 129.2, 128.5, 128.3, 120.2 (*C2-4*, *C6-8*), 126.7 (C=<u>*C*</u>H), 43.2 (*C9*), 31.5 (*C12*), 28.8 (*C11*), 24.3 (*C10*), 22.4 (*C13*), 14.0 (*C14*). **IR** (neat): 1691 (C=O). **HRMS** (*m*/*z*, ESI^+): calculated for $C_{21}H_{24}NaO^+$ ($[M+Na]^+$): 315.1719, found 315.1710.

6.2.4.4 Fluorination of Allenyl Acetate 88o

2-Fluoro-1,1-diphenylnon-1-en-3-one (92o)



Selectfluor (848 mg, 2.39 mmol, 2 eq) was added to a solution of allenyl acetate **88o** (400 mg, 1.20 mmol, 1 eq) in acetonitrile (24 mL). The mixture was stirred at 40°C until TLC showed consumption of the allene (3.5h). Water was added and the mixture was extracted with ethyl acetate (3 × 15 mL). The combined organic fractions were washed with brine (40 mL), dried with anhydrous magnesium sulfate, filtered and the solvents removed *in vacuo*. The crude mixture was purified by column chromatography on silica gel (hexane:diethyl ether, 20:1) to afford the product **92o** as a yellow oil (272 mg, yield = 73%).

R_f (hexane:diethyl ether, 9:1) = 0.40. **^{1}H NMR** (400 MHz, $CDCl_3$) δ: 7.37-7.43 (m, 3H, Ph), 7.31-7.43 (m, 5H, Ph), 7.18-7.23 (m, 2H, Ph), 2.53 (ddd, 2H, $^3J_{HH}$ = 7.6, 7.3 Hz, $^4J_{HF}$ = 2.8 Hz, *H9*), 1.54-1.61 (m, 2H, *H10*), 1.22-1.34 (m, 6H, *H11-13*), 0.88 (dd, 3H, $^3J_{HH}$ = 7.1, 6.8 Hz, *H14*). **^{13}C NMR** (101 MHz, $CDCl_3$) δ: 195.9 (d, $^2J_{CF}$ = 34 Hz, <u>*C*</u>=O), 150.1 (d, $^1J_{CF}$ = 267 Hz, C=<u>*C*</u>F), 136.8 (d, $^3J_{CF}$ = 6 Hz), 136.5 (*C1*, *C5*), 130.9 (d, $^2J_{CF}$ = 14 Hz, <u>*C*</u>=CF), 130.1 (d, $^4J_{CF}$ = 6 Hz), 129.7 (d, $^4J_{CF}$ = 3 Hz, *C2*, *C6*), 128.8, 128.4, 128.4, 128.1 (*C3*, *C4*, *C7*, *C8*), 40.3 (*C9*), 31.5 (*C12*), 28.7 (*C11*), 23.5 (*C10*), 22.4 (*C13*), 14.0 (*C14*). **^{19}F NMR** (377 MHz, $CDCl_3$) δ: −120.4. **IR** (neat): 1706 (C=O). **HRMS** (*m*/*z*, ESI^+): calculated for $C_{21}H_{23}FNaO^+$ ($[M+Na]^+$): 333.1625, found 333.1628.

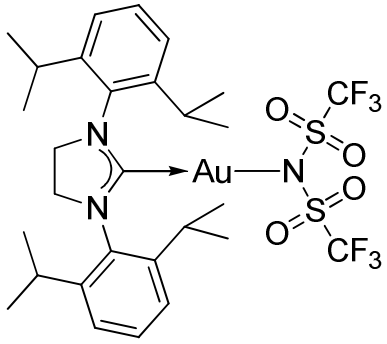
6.3 Experimental Data for Chapter 3

6.3.1 Preparation of Catalysts

6.3.1.1 Preparation of SIPrAuNTf$_2$ (156)

SIPrAuNTf$_2$ (**156**) was prepared according to the procedure of Gagosz (see Scheme 3.31).[161]

[1,3-Bis(2,6-diisopropylphenyl)imidazolidin-2-ylium-2-yl][1,1,1-trifluoro-*N*-[(trifluoromethyl)sulfonyl]methanesulfonamidato-κ*N*]gold(I) (SIPrAuNTf$_2$, 156)[161]



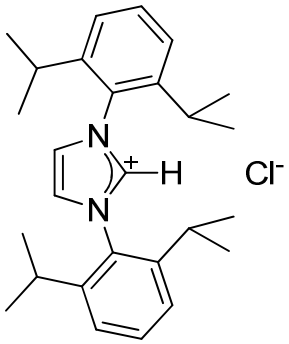
Silver(I) bis[(trifluoromethyl)sulfonyl]azanide (AgNTf$_2$) was prepared according to the procedure of RajanBabu.[272] Silver oxide (1.11 g, 4.79 mmol, 1 eq) was added to a solution of 1,1,1-trifluoro-*N*-[(trifluoromethyl)sulfonyl]methanesulfonamide (HNTf$_2$, 1.35 g, 4.79 mmol, 1 eq) in water (3 mL). The mixture was stirred at room temperature for 19h in the absence of light. The crude reaction mixture was filtered and the filtrate was concentrated *in vacuo*. The crude product was dried under vacuum for 24h, affording AgNTf$_2$ as a white solid (1.85 g, yield = quant) [**Mp** > 250ºC (lit = 249ºC). **^{19}F NMR** (377 MHz, dmso-d$_6$) δ: −78.7].[273] Dichloromethane (2 mL) was added to a mixture of silver(I) bis[(trifluoromethyl)sulfonyl]azanide (AgNTf$_2$, 31 mg, 80 μmol, 1 eq) and SIPrAuCl (**1**, 50 mg, 80 μmol, 1 eq). The mixture was stirred at room temperature for 15 min. The crude reaction mixture was filtered and the filtrate was concentrated *in vacuo*. Recrystallisation from dichloromethane/hexane afforded SIPrAuNTf$_2$ (**156**) as a white solid (63 mg, yield = 90%).

^{1}H NMR (400 MHz, CD_2Cl_2) δ: 7.48 (t, 2H, $^3J_{HH}$ = 7.8 Hz, *para*-Ar), 7.30 (d, 4H, $^3J_{HH}$ = 7.8 Hz, *meta*-Ar), 4.19 (s, 4H, NC$\underline{H}_2$C$\underline{H}_2$N), 3.05 (sept, 2H, $^3J_{HH}$ = 6.8 Hz, C$\underline{H}$(CH_3)$_2$), 3.05 (d, 2H, $^3J_{HH}$ = 7.1 Hz, C$\underline{H}$(CH_3)$_2$), 1.41 (d, 12H, $^3J_{HH}$ = 6.8 Hz, CH(C$\underline{H}_3$)$_2$), 1.37 (d, 12H, $^3J_{HH}$ = 7.1 Hz, CH(C$\underline{H}_3$)$_2$). **^{13}C NMR** (101 MHz, CD_2Cl_2) δ: 190.7 (*C*Au), 147.3 (*ortho*-Ar), 134.1 (*ipso*-Ar), 130.5 (*para*-Ar), 125.1 (*meta*-Ar), 121.9 (q, $^1J_{CF}$ = 322 Hz, *C*F_3), 54.1 (N*C*H_2*C*H_2N), 29.5 (*C*H(CH_3)$_2$), 24.8 (CH(*C*H_3)$_2$), 24.8 (CH(*C*H_3)$_2$). **^{19}F NMR** (377 MHz, CD_2Cl_2) δ: −76.4.

6.3.1.2 Preparation of IPrAuCl (158)

IPrAuCl (**158**) was prepared according to the procedures of Arduengo[90] and Nolan (see Scheme 3.33).[165-166]

1,3-Bis(2,6-diisopropylphenyl)-*1H*-imidazol-3-ium chloride (IPrHCl)[90]

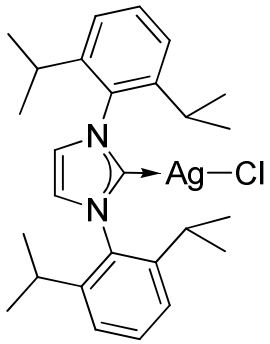


(Chloromethoxy)ethane (MOMCl, 1.22 mL, 13.2 mmol, 1 eq) and two drops of water were added to a solution of 1,2-diimine (**96**, 5.00 g, 13.2 mmol, 1 eq) in tetrahydrofuran (40 mL). The mixture was stirred at 40°C for 16h before being cooled to room temperature. The product IPrHCl precipitated from the reaction mixture and was collected by filtration as a white solid (1.76 g, yield = 31%). No further purification was required.

Mp > 250°C (lit > 255°C).[90] **^{1}H NMR** (400 MHz, dmso-d_6) δ: 10.28 (br s, 1H, NC$\underline{H}$N), 8.60 (d, 2H, $^4J_{HH}$ = 1.5 Hz, NC$\underline{H}$C$\underline{H}$N), 7.69 (d, 2H, $^3J_{HH}$ = 7.8 Hz, *para*-Ar), 7.53 (d, 4H, $^3J_{HH}$ = 7.8 Hz, *meta*-Ar), 2.35 (sept, 4H, $^4J_{HH}$ = 6.8 Hz, C$\underline{H}$(CH_3)$_2$), 1.26 (d, 12H, $^3J_{HH}$ = 6.8

Hz, CH(C<u>*H*</u>$_3$)$_2$), 1.16 (d, 12H, $^3J_{HH}$ = 6.8 Hz, CH(C<u>*H*</u>$_3$)$_2$). **^{13}C NMR** (101 MHz, dmso-d_6) δ: 144.8 (*ortho*-Ar), 139.3 (NC<u>*H*</u>N), 131.9 (*meta*-Ar), 130.1 (*ipso*-Ar), 126.2 (*para*-Ar), 124.7 (N<u>*C*</u>H<u>*C*</u>HN), 28.7 (<u>*C*</u>H(CH$_3$)$_2$), 24.2 (CH(<u>*C*</u>H$_3$)$_2$), 23.1 (CH(<u>*C*</u>H$_3$)$_2$). **LRMS** (*m*/*z*, ESI$^-$): calculated for $C_{27}H_{37}Cl_2N_2^-$ ([M+Cl]$^-$): 459.2, found 459.2.

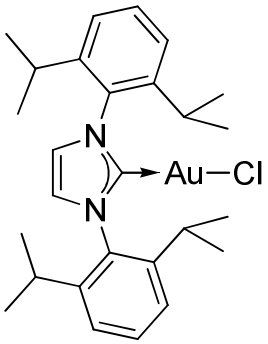
(1,3-Bis(2,6-diisopropylphenyl)imidazol-2-ylidene)silver(I) chloride (IPrAgCl)[166]



Dichloromethane (13 mL), was added to IPrHCl (835 mg, 1.96 mmol, 1 eq) and silver(I) oxide (455 mg, 1.96 mmol, 1 eq). The mixture was stirred at room temperature under argon in the absence of light for 24h before filtration and removal of the solvent *in vacuo*. The resulting crude solid was suspended in diethyl ether (5 mL) and filtered to afford the product as a white solid (626 mg, yield = 60%).

^{1}H NMR (400 MHz, CD_2Cl_2) δ: 7.57 (t, 2H, $^3J_{HH}$ = 7.8 Hz, *para*-Ar), 7.38 (d, 4H, $^3J_{HH}$ = 7.8 Hz, *meta*-Ar), 7.30 (d, 2H, $^4J_{H\text{-}Ag}$ = 2.0 Hz, NC<u>*H*</u>C<u>*H*</u>N), 2.58 (d, 4H, $^3J_{HH}$ = 6.8 Hz, C<u>*H*</u>(CH$_3$)$_3$), 1.30 (d, 12H, $^3J_{HH}$ = 6.8 Hz, CH(C<u>*H*</u>$_3$)$_3$), 1.26 (d, 12H, $^3J_{HH}$ = 6.8 Hz, CH(C<u>*H*</u>$_3$)$_3$). **^{13}C NMR** (126 MHz, CD_2Cl_2) δ: 184.6 (2×d, $^1J_{C\text{-}109Ag}$ = 270 Hz, $^1J_{C\text{-}107Ag}$ = 234 Hz, <u>*C*</u>Ag), 146.1 (*ortho*-Ar), 135.1 (*ipso*-Ar), 131.0 (*para*-Ar), 124.7 (*meta*-Ar), 124.2 (d, $^3J_{C\text{-}Ag}$ = 8 Hz, N<u>*C*</u>H), 29.1 (<u>*C*</u>H(CH$_3$)$_3$), 24.8 (CH(<u>*C*</u>H$_3$)$_3$), 24.1 (CH(<u>*C*</u>H$_3$)$_3$). **LRMS** (*m*/*z*, ESI$^-$): calculated for $C_{27}H_{35}{}^{107}AgClN_2^-$ ([M−H]$^-$): 529.2, found 529.2.

(1,3-Bis(2,6-Diisopropylphenyl)imidazol-2-ylidene)gold(I) chloride (IPrAuCl, 158)[165]



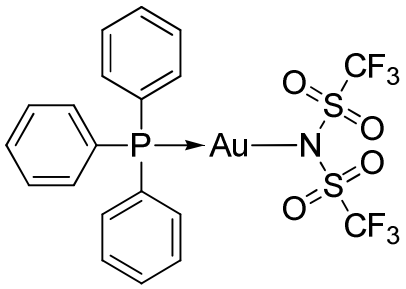
Dichloromethane (10.6 mL) and dimethyl sulfide (210 µL, 2.89 mmol, 8.5 eq) were added to a mixture of IPrAgCl (181 mg, 340 µmol, 1 eq) and chloro(dimethylsulfide)gold(I) (100 mg, 340 µmol, 1 eq). The mixture was stirred at room temperature in the dark for 60h before filtration and removal of the solvent *in vacuo*. The crude product was washed with diethyl ether (2×10 mL) and dried to give IPrAuCl (**158**) as a white solid (201 mg, yield = 95%).

^{1}H NMR (400 MHz, $CDCl_3$) δ: 7.59 (t, 2H, $^{3}J_{HH}$ = 7.8 Hz, *para*-Ar), 7.38 (d, 4H, $^{3}J_{HH}$ = 7.6 Hz, *meta*-Ar), 7.26 (s, 2H, NC*H*C*H*N), 2.58 (sept, 4H, $^{3}J_{HH}$ = 6.8 Hz, C*H*$(CH_3)_2$), 1.36 (d, 12H, $^{3}J_{HH}$ = 6.8 Hz, CH(C*H*$_3)_2$), 1.25 (d, 12H, $^{3}J_{HH}$ = 6.8 Hz, CH(C*H*$_3)_2$). **^{13}C NMR** (126 MHz, $CDCl_3$) δ: 175.7 (*C*Au), 146.3, 134.6 (*ipso*-Ar, *ortho*-Ar), 131.2, 124.8, 123.9 (*meta*-Ar, *para*-Ar, N*C*H*C*HN), 29.4 (*C*H$(CH_3)_2$), 24.7 (CH(*C*H$_3)_2$), 24.3 (CH(*C*H$_3)_2$). **LRMS** (*m*/*z*, ESI$^-$): calculated for $C_{27}H_{37}AuCl_2N_2^-$ ([M+Cl]$^-$): 655.2, found 655.2.

6.3.1.3 Preparation of PPh_3AuNTf_2 (2)

PPh_3AuNTf_2 (**2**) was prepared according to the procedure of Gagosz (see Scheme 3.34).[167]

[1,1,1-Trifluoro-*N*-[(trifluoromethyl)sulfonyl]methanesulfonamidato-κ*N*] (triphenylphosphine)gold(I) (PPh_3AuNTf_2, 2)[167]



Dichloromethane (2.5 mL) was added to a mixture of $AgNTf_2$ (156 mg, 402 μmol, 1 eq) and chloro(triphenylphosphine)gold(I) (PPh_3AuCl, 200 mg, 402 μmol, 1 eq). The mixture was stirred at room temperature for 10 min. The crude reaction mixture was filtered and the filtrate was concentrated *in vacuo*. Recrystallisation from dichloromethane/hexane afforded PPh_3AuNTf_2 (**2**) as a white solid (281 mg, yield = 94%).

^{1}H NMR (400 MHz, $CDCl_3$) δ: 7.48-7.64 (m, 15H, Ph). **^{13}C NMR** (101 MHz, $CDCl_3$) δ: 134.1 (d, $^2J_{CP}$ = 14 Hz, *ortho*-Ph), 132.6 (d, $^4J_{CP}$ = 2 Hz, *para*-Ph), 129.6 (d, $^3J_{CP}$ = 12 Hz, *meta*-Ph), 127.1 (d, $^1J_{CP}$ = 67 Hz, *ipso*-Ph), 116.3 (q, $^1J_{CF}$ = 322 Hz, $\underline{C}F_3$). **^{31}P NMR** (162 MHz, $CDCl_3$) δ: 30.8. **^{19}F NMR** (377 MHz, $CDCl_3$) δ: −75.2.

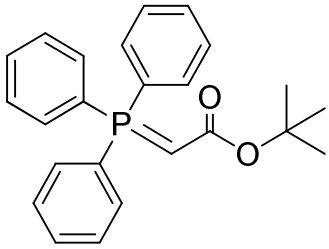
6.3.2 Preparation of Allenoates 102a-j

Some of the experimental results detailed in this section were obtained by Andrew Salisbury (Chemistry Part II, University of Oxford, 2008)[104] and Jonathan E. Ross (Chemistry Part II, University of Oxford, 2010).[206]

6.3.2.1 Preparation of *tert*-Butoxy Phosphorus Ylids 159

tert-Butoxy phosphorus ylids **159** were prepared according to the procedures of Shin (see Schemes 3.35, 3.37 and 3.38).[100]

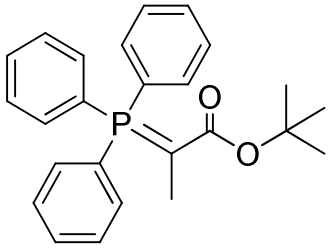
tert-Butyl (triphenylphosphoranylidene)acetate (159a)[274]



tert-Butyl bromoacetate (5.63 mL, 38.1 mmol, 1 eq) was added to a solution of triphenylphosphine (10.0 g, 38.1 mmol, 1 eq) in toluene (45 mL). The mixture was stirred at room temperature for 4h. The white precipitate was collected by filtration, washed with toluene and dried _in vacuo_. The dry solid was dissolved in the minimum amount of methanol and NaOH (aq, 15%) was added until the mixture had a pH > 9. Water (150 mL) was then added and the mixture was left to stand for 1h until a solid precipitated out. Phosphorus ylid **159a** was then collected by filtration as a white solid and dried _in vacuo_ (12.0 g, yield = 84%).

^{1}H NMR (400 MHz, $CDCl_3$) δ: 7.40-7.70 (m, 15H, Ph), 2.78 (br s, 1H, $Ph_3P{=}C\underline{H}$), 1.06 (s, 9H, $C(C\underline{H}_3)_3$). **^{13}C NMR** (101 MHz, $CDCl_3$) δ: 170.8 ($\underline{C}$=O), 133.0 (d, $^{2}J_{CP}$ = 10 Hz, _ortho_-Ph), 132.0 (d, $^{4}J_{CP}$ = 3 Hz, _para_-Ph), 128.6 (d, $^{3}J_{CP}$ = 12 Hz, _meta_-Ph), 128.6 (d, $^{1}J_{CP}$ = 96 Hz, _ipso_-Ph), 78.4 ($\underline{C}(CH_3)_3$), 31.4 (d, $^{1}J_{CP}$ = 122 Hz, $Ph_3P{=}\underline{C}H$), 28.7 ($C(\underline{C}H_3)_3$). **^{31}P NMR** (162 MHz, $CDCl_3$) δ: 16.8. **LRMS** (_m/z_, ESI^+): calculated for $C_{24}H_{26}O_2P^+$ ($[M+H]^+$): 377.2, found 377.2.

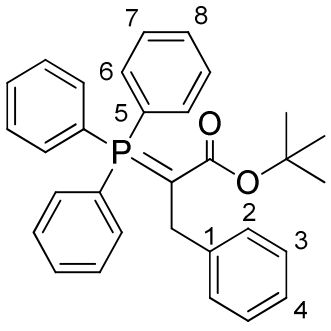
tert-Butyl 2-(triphenylphosphoranylidene)propanoate (159b)[275]



Iodomethane (496 μL, 7.96 mmol, 1.5 eq) was added carefully to a solution of *tert*-butyl (triphenylphosphoranylidene)acetate (**159a**, 2.00 g, 5.31 mmol, 1 eq) in dichloromethane 20 mL) at 0ºC. The mixture was allowed to reach rt and stirred for 16h. The solvent and excess iodomethane were removed *in vacuo* and the crude product was redissolved in dichloromethane (20 mL). An aqueous solution of sodium hydroxide (15%, 20 mL) was added and the biphasic mixture was stirred vigorously for 1h at rt. The layers were separated and the aqueous fraction was extracted with dichloromethane (3×20 mL). The combined organic fractions were combined, dried over anhydrous sodium sulfate, filtered and concentrated *in vacuo*. Purification by column chromatography on silica gel (ethyl acetate) afforded phosphorus ylid **159b** as a bright yellow solid (1.89 g, yield = 91%).

^{1}H NMR (400 MHz, $CDCl_3$) δ: 7.52-7.60 (m, 6H, Ph), 7.42-7.47 (m, 3H, Ph), 7.32-7.40 (m, 6H, Ph), 1.53 (d, 3H, $^{3}J_{HP}$ = 13.9 Hz, P=C(C$\underline{H}_3$)), 0.89 (s, 9H, C(C$\underline{H}_3$)$_3$). **^{13}C NMR** (101 MHz, $CDCl_3$) δ: 170.3 (d, $^{2}J_{CP}$ = 12 Hz, $\underline{C}$=O), 133.3 (d, $^{2}J_{CP}$ = 10 Hz, *ortho*-Ph), 131.2 (d, $^{4}J_{CP}$ = 2 Hz, *para*-Ph), 128.5 (d, $^{1}J_{CP}$ = 72 Hz, *ipso*-Ph), 128.0 (d, $^{3}J_{CP}$ = 12 Hz, *meta*-Ph), 76.1 ($\underline{C}$(CH$_3$)$_3$), 31.4 (d, $^{1}J_{CP}$ = 122 Hz, P=$\underline{C}$(CH$_3$)), 28.3 (C($\underline{C}$H$_3$)$_3$), 12.4 (d, $^{2}J_{CP}$ = 14 Hz, P=C($\underline{C}$H$_3$)). **^{31}P NMR** (162 MHz, $CDCl_3$) δ: 22.3. **LRMS** (*m*/*z*, ESI$^+$): calculated for $C_{25}H_{28}O_2P^+$ ([M+H]$^+$): 391.2, found 391.2.

***tert*-Butyl 3-phenyl-2-(triphenylphosphoranylidene)propanoate (159c)**

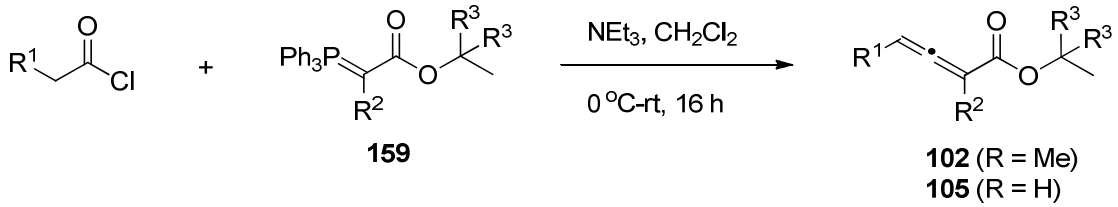


Benzyl bromide (473 μL, 3.98 mmol, 1 eq) was added to a solution of *tert*-butyl (triphenylphosphoranylidene)acetate (**159a**, 1.50 g, 3.98 mmol, 1 eq) and tetra-*n*-butylammonium iodide (147 mg, 39.8 μmol, 10 mol%) in tetrahydrofuran (20 mL). The mixture was stirred at rt for 16h. The solvent was removed *in vacuo* and the crude product was redissolved in diethyl ether (20 mL). An aqueous solution (20 mL) of sodium hydroxide (318 mg, 7.97 mmol, 2 eq) was added and the mixture was stirred at rt for 30 min. The layers were separated and the aqueous fraction was extracted using diethyl ether (3×20 mL). The combined organic fractions were washed with brine (20 mL), dried over anhydrous sodium sulfate and concentrated *in vacuo*. Recrystallisation from Et_2O/hexane afforded the phosphorus ylid **159c** as a yellow solid (1.75 g, yield = 94%).

R_f: (ethyl acetate) = 0.02. **Mp** = 92ºC. **^{1}H NMR** (400 MHz, $CDCl_3$) δ: 7.50-7.57 (m, 9H, P*Ph*$_3$), 7.38-7.42 (m, 6H, P*Ph*$_3$), 7.08 (dd, 2H, $^3J_{HH}$ = 7.3, 7.1 Hz, *H3*), 6.95-7.03 (m, 3H, *H2*, *H4*), 3.37 (d, 2H, $^3J_{HP}$ = 19.2 Hz, C*H*$_2$Ph), 1.01 (s, 9H, C(C*H*$_3$)$_3$). **^{13}C NMR** (125 MHz, $CDCl_3$) δ: 170.7 (*C*=O), 146.1 (*C1*), 133.7 (d, $^3J_{CP}$ = 10 Hz, *C7*), 131.4 (*C8*), 128.4 (d, $^1J_{CP}$ = 67 Hz, *C5*), 128.2 (d, $^2J_{CP}$ = 12 Hz, *C6*), 128.0, 127.4 (*C2*, *C3*), 124.5 (*C4*), 40.4 (d, $^1J_{CP}$ = 115 Hz, P=*C*(Bn)), 32.8 (d, $^2J_{CP}$ = 14 Hz, *C*H$_2$Ph), 28.6 (C(*C*H$_3$)$_3$). **^{31}P NMR** (162 MHz, $CDCl_3$) δ: 22.7. **IR** (CH_2Cl_2): 1702 (C=O). **HRMS** (*m*/*z*, ESI$^+$): calculated for $C_{31}H_{32}O_2P^+$ ($[M+H]^+$): 467.2134, found 467.2125.

6.3.2.2 Preparation of Benzyl-Substituted *tert*-Butyl Allenoates 102b-j and 102n

tert-Butyl and ethyl allenoates **102** and **105** were prepared according to the procedure of Shin.[100]

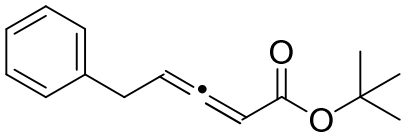


Scheme 6.3 Preparation of *tert*-Butyl and Ethyl Allenoates **102** and **105**.

General Procedure C: Triethylamine (1.7 eq) was added dropwise to a solution of the phosphorus ylid **159** (1.7 eq) in dichloromethane at room temperature. The reaction was stirred at room temperature for 15 min before the dropwise addition of the acid chloride (1 eq) at 0°C. The reaction mixture was warmed to room temperature and stirred overnight. After removal of the solvent *in vacuo*, pentane was added to the semi-solid residue and the mixture was allowed to stand for 2h. It was shaken periodically to facilitate solidification and to complete the extraction of the product. The precipitates were removed by filtration and the filter cake was washed with pentane. The solvent was removed *in vacuo* and the resulting crude mixture was purified by flash column chromatography on silica gel.

*Note:- For allenoates bearing a hydrogen substituent at the 2-position (**102b-d**), separation of the desired allenoate from the isomeric alkyne side-product **108** was not trivial and mixtures of the two were isolated and subjected to further reactions. In most cases, very careful column chromatography allowed for the partial separation of the isomers affording a few milligrams of the pure allenoate **102**. In these instances the analytical data provided are of the pure allenoate.*

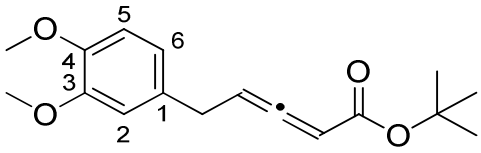
***tert*-Butyl 5-phenylpenta-2,3-dienoate (102b)**



General procedure C was followed using *tert*-butyl (triphenylphosphoranylidene)acetate **159a** (2.00 g, 5.31 mmol, 1.7 eq), 3-phenylpropanoyl chloride (464 µL, 3.12 mmol, 1 eq) and triethylamine (740 µL, 5.31 mmol, 1.7 eq) in dichloromethane (16 mL). The resulting crude mixture was purified by flash column chromatography on silica gel (hexane:diethyl ether, 9:1) to afford the product **102b** and the isomeric alkyne side-product **108b** (allenoate:alkyne = 2.9:1) as a yellow oil (506 mg, corrected yield of **102b** = 55%).

R_f: (hexane:diethyl ether, 9:1) = 0.41. **^{1}H NMR** (400 MHz, $CDCl_3$) δ: 7.21-7.33 (m, 5H, Ph), 5.72 (td, 1H, $^3J_{HH}$ = 7.5 Hz, $^4J_{HH}$ = 6.1 Hz, BnC*H*=C=CH), 5.53 (dt, 1H, $^4J_{HH}$ = 6.1 Hz, $^5J_{HH}$ = 2.5 Hz, BnCH=C=C*H*), 3.51 (ddd, 1H, $^2J_{HH}$ = 15.2 Hz, $^3J_{HH}$ = 7.8 Hz, $^4J_{HH}$ = 2.5 Hz, PhC*H*H'), 3.44 (ddd, 1H, $^2J_{HH}$ = 15.2 Hz, $^3J_{HH}$ = 7.3 Hz, $^4J_{HH}$ = 2.8 Hz, PhCH*H'*), 1.50 (s, 9H, C(CH_3)$_3$). **^{13}C NMR** (101 MHz, $CDCl_3$) δ: 212.2 (C=*C*=C), 165.2 (*C*=O), 138.8 (*ipso*-Ph), 128.5, 128.4, 126.5 (*ortho*-, *meta*-, *para*-Ph), 94.3 (Bn*C*H=C=CH), 90.1 (BnCH=C=*C*H), 80.9 (*C*(CH$_3$)$_3$), 34.2 (Ph*C*H$_2$), 28.1 (C(*C*H$_3$)$_3$). **IR** (neat): 1962 (C=C=C), 1705 (C=O). **HRMS** (*m/z*, CI$^+$): calculated for $C_{15}H_{19}O_2$ ([M+H]$^+$): 231.1385, found 231.1386.

***tert*-Butyl 5-(3,4-dimethoxyphenyl)penta-2,3-dienoate (102c)**



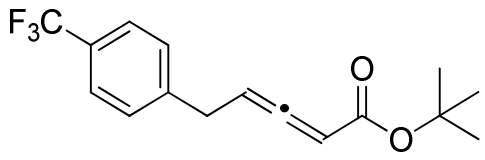
Oxalyl chloride (2 M solution in dichloromethane, 3.75 mL, 7.49 mmol, 1.05 eq) was carefully added to a solution of 3-(3,4-dimethoxyphenyl)propanoic acid (1.50 g, 7.14 mmol,

1 eq) in dichloromethane (15 mL) and dimethylformamide (2 drops) at 0ºC. The reaction mixture was stirred at 0ºC for 3h. The crude 3-(3,4-dimethoxyphenyl)propanoyl chloride was concentrated *in vacuo* and used directly in the next step without further purification.

General procedure C was followed using *tert*-butyl (triphenylphosphoranylidene)acetate **159a** (4.57 g, 12.1 mmol, 1.7 eq), 3-(3,4-dimethoxyphenyl)propanoyl chloride (1.63 g, 7.14 mmol, 1 eq) and triethylamine (1.69 mL, 12.1 mmol, 1.7 eq) in dichloromethane (19 mL). The resulting crude mixture was purified by flash column chromatography on silica gel (hexane:diethyl ether, 1:1) to afford the product **102c** and the isomeric alkyne side-product (allenoate:alkyne = 3.5:1) as an orange oil. (778 mg, corrected yield of **102c** = 29% over two steps).

R_f: (hexane:diethyl ether, 1:1) = 0.35. **^{1}H NMR** (400 MHz, $CDCl_3$) δ: 6.76-6.83 (m, 3H, Ar), 5.70 (td, 1H, $^3J_{HH}$ = 7.3 Hz, $^4J_{HH}$ = 6.1 Hz, $ArCH_2C\underline{H}$=C=CH), 5.50 (m, 1H, $ArCH_2CH$=C=C$\underline{H}$), 3.86 (s, 3H, OC$\underline{H_3}$), 3.83 (s, 3H, OC$\underline{H_3}$), 3.42 (ddd, 1H, $^2J_{HH}$ = 15.7 Hz, $^3J_{HH}$ = 7.3 Hz, $^4J_{HH}$ = 2.5 Hz, ArC$\underline{H}$H'), 3.35 (ddd, 1H, $^2J_{HH}$ = 15.7 Hz, $^3J_{HH}$ = 7.3 Hz, $^4J_{HH}$ = 2.5 Hz, ArCH$\underline{H'}$), 1.46 (s, 9H, C(C$\underline{H_3}$)$_3$). **^{13}C NMR** (125 MHz, $CDCl_3$) δ: 212.3 (C=$\underline{C}$=C), 165.2 ($\underline{C}$=O), 148.9, 147.7 (*C3*, *C4*), 131.3 (*C1*), 120.4 (*C6*)**,** 111.8, 111.0 (*C2*, *C5*), 94.8 ($ArCH_2\underline{C}H$=C=CH), 90.2 ($ArCH_2CH$=C=$\underline{C}$H), 80.8 ($\underline{C}(CH_3)_3$), 55.9 (O$\underline{C}H_3$), 55.8 (O$\underline{C}H_3$), 33.7 (Ar$\underline{C}H_2$), 28.1 (C($\underline{C}H_3)_3$). **IR** (neat): 1961 (C=C=C), 1712 (C=O). **HRMS** (*m/z*, ESI^+): calculated for $C_{17}H_{22}NaO_4^+$ ($[M+Na]^+$): 313.1410 found 313.1410.

***tert*-Butyl 5-[4-(trifluoromethyl)phenyl]penta-2,3-dienoate (102d)**



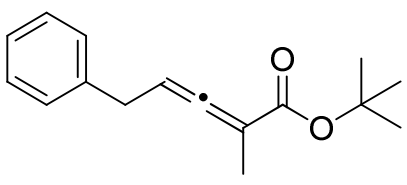
Oxalyl chloride (2 M solution in dichloromethane, 2.41 mL, 4.81 mmol, 1.05 eq) was carefully added to a solution of 3-(4-(trifluoromethyl)phenyl)propanoic acid (1.00 g, 4.58

mmol, 1 eq) in dichloromethane (9.5 mL) and dimethylformamide (2 drops) at 0ºC. The reaction mixture was stirred at 0ºC for 3h. The crude 3-(4-(trifluoromethyl)phenyl)propanoyl chloride was concentrated *in vacuo* and used directly in the next step without further purification.

General procedure C was followed using *tert*-butyl (triphenylphosphoranylidene)acetate **159a** (2.00 g, 5.31 mmol, 1.7 eq), 3-(4-(trifluoromethyl)phenyl)propanoyl chloride (740 mg, 3.13 mmol, 1 eq) and triethylamine (741 μL, 5.31 mmol, 1.7 eq) in dichloromethane (10 mL). The resulting crude mixture was purified by flash column chromatography on silica gel (hexane:diethyl ether, 9:1) to afford a mixture of the product **102d** and the isomeric alkyne side-product (allenoate:alkyne = 2.5:1) as a pale yellow oil (441 mg, corrected yield of **102d** = 34% over two steps).

R_f: (hexane:diethyl ether, 9:1) = 0.24. **^{1}H NMR** (400 MHz, $CDCl_3$) δ: 7.57 (d, 2H, $^3J_{HH}$ = 7.8 Hz, *meta*-Ar), 7.41 (d, 2H, $^3J_{HH}$ = 7.8 Hz, *ortho*-Ar), 5.72 (dt, 1H, $^3J_{HH}$ = 7.1 Hz, $^4J_{HH}$ = 6.8 Hz, $ArCH_2C\underline{H}=C=CH$), 5.54 (m, 1H, $ArCH_2CH=C=C\underline{H}$), 3.52 (m, 2H, $ArC\underline{H}_2$), 1.49 (s, 9H, $C(C\underline{H}_3)_3$). **^{13}C NMR** (125 MHz, $CDCl_3$) δ: 212.4 ($C=\underline{C}=C$), 164.9 ($\underline{C}=O$), 142.9 (*ipso*-Ar), 129.0 (q, $^2J_{CF}$ = 32 Hz, *para*-Ar), 128.9 (*ortho*-Ar), 125.3 (q, $^3J_{CF}$ = 4 Hz, *meta*-Ar), 124.2 (q, $^1J_{CF}$ = 272 Hz, $\underline{C}F_3$), 93.6 ($ArCH_2\underline{C}H=C=CH$), 90.7 ($ArCH_2CH=C=\underline{C}H$), 81.1 ($\underline{C}(CH_3)_3$), 34.0 ($Ar\underline{C}H_2$), 28.1 ($C(\underline{C}H_3)_3$). **^{19}F NMR** (377 MHz, $CDCl_3$) δ: −62.4. **IR** (neat): 1964 (C=C=C), 1715 (C=O). **HRMS** (*m/z*, CI^+): calculated for $C_{16}H_{18}O_2F_3$ ($[M+H]^+$): 299.1259 found 299.1261.

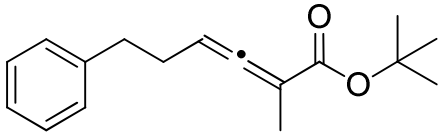
***tert*-Butyl 2-methyl-5-phenylpenta-2,3-dienoate (102e)**



General procedure C was followed using *tert*-butyl 2-(triphenylphosphoranylidene)propanoate **159b** (2.00 g, 5.12 mmol, 1.7 eq), 3-phenylpropionyl chloride (448 μL, 3.01 mmol, 1 eq) and triethylamine (714 μL, 5.12 mmol, 1.7 eq) in dichloromethane (10 mL). The resulting crude mixture was purified by flash column chromatography on silica gel (hexane:diethyl ether, 9:1) to afford the product **102e** as a yellow oil (683 mg, yield = 93%).

R_f: (hexane:diethyl ether, 9:1) = 0.41. **^{1}H NMR** (400 MHz, $CDCl_3$) δ: 7.26-7.33 (m, 5H, Ph), 5.55 (m, 1H, C*H*=C=C(CH_3)), 3.46 (dd, 1H, $^2J_{HH}$ = 15.2 Hz, $^3J_{HH}$ = 8.1 Hz, PhC*H*H'), 3.39 (dd, 1H, $^2J_{HH}$ = 15.2 Hz, $^3J_{HH}$ = 7.1 Hz, PhCH*H'*), 1.82 (d, 3H, $^5J_{HH}$ = 2.8 Hz, CH=C=C(C*H*$_3$)), 1.49 (s, 9H, C(C*H*$_3$)$_3$). **^{13}C NMR** (101 MHz, $CDCl_3$) δ: 210.3 (C=*C*=C), 167.0 (*C*=O), 139.5 (*ipso*-Ph), 128.6, 128.3, 126.3 (*ortho*-, *meta*-, *para*-Ph), 97.3 (Bn*C*H=C=C(CH_3)), 92.5 (BnCH=C=*C*(CH_3)), 80.6 (*C*(CH_3)$_3$), 34.7 (Ph*C*H$_2$), 28.1 (C(*C*H$_3$)$_3$), 15.1 (CH=C=C(*C*H$_3$)). **IR** (neat): 1962 (C=C=C), 1758 (C=O). **HRMS** (*m/z*, CI^+): calculated for $C_{16}H_{21}O_2$ ($[M+H]^+$): 245.1542 found 245.1535.

***tert*-Butyl 2-methyl-6-phenylhexa-2,3-dienoate (102f)**



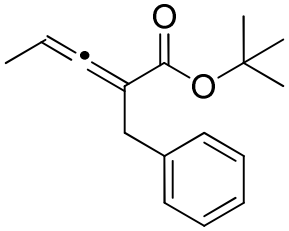
Oxalyl chloride (2 M solution in dichloromethane, 4.73 mL, 2.46 mmol, 1.05 eq) was carefully added to a solution of 4-phenylbutanoic acid (1.48 g, 9.01 mmol, 1 eq) in dichloromethane (18 mL) and dimethylformamide (2 drops) at 0ºC. The reaction mixture was stirred at 0ºC for 3h. The crude 4-phenylbutanoyl chloride was concentrated *in vacuo* and used directly in the next step without further purification.

General procedure C was followed using *tert*-butyl 3-phenyl-2-(triphenylphosphoranylidene)propanoate **159b** (5.98 g, 15.3 mmol, 1.7 eq), 4-

phenylbutanoyl chloride (1.64 g, 9.01 mmol, 1 eq) and triethylamine (2.14 mL, 15.3 mmol, 1.7 eq) in dichloromethane (23 mL). The resulting crude mixture was purified by flash column chromatography on silica gel (hexane:diethyl ether, 9:1) to afford the product **102f** as a colourless oil (1.32 g, yield = 57% over two steps).

R_f: (hexane:diethyl ether, 9:1) = 0.42. **^{1}H NMR** (500 MHz, $CDCl_3$) δ: 7.29 (ddm, 2H, $^3J_{HH}$ = 7.6, 7.3 Hz, *meta*-Ph), 7.19-7.22 (dm, 3H, $^3J_{HH}$ = 7.3 Hz, *ortho*-, *para*-Ph), 5.45 (ddq, 1H, $^3J_{HH}$ = 7.6, 6.9 Hz, $^5J_{HH}$ = 2.8 Hz, C$\underline{H}$=C=C(CH_3)), 2.80 (ddm, 1H, $^2J_{HH}$ = 13.9 Hz, $^3J_{HH}$ = 6.9 Hz, PhC$\underline{H}$H'CH_2), 2.74 (dd, 1H, $^2J_{HH}$ = 13.9 Hz, $^3J_{HH}$ = 7.6 Hz, PhCH$\underline{H'}CH_2$), 2.35-2.48 (m, 2H, PhCH_2C$\underline{H_2}$), 1.76 (d, 3H, $^5J_{HH}$ = 2.8 Hz, CH=C=C(C$\underline{H_3}$)), 1.48 (s, 9H, C(C$\underline{H_3}$)$_3$). **^{13}C NMR** (125 MHz, $CDCl_3$) δ: 209.9 (C=$\underline{C}$=C), 167.2 ($\underline{C}$=O), 141.4 (*ipso*-Ph), 128.4, 128.3 (*ortho*-, *meta*-Ph), 126.0 (*para*-Ph), 97.4 (CH=C=$\underline{C}$(CH_3)), 92.6 ($\underline{C}$H=C=C(CH_3)), 80.4 ($\underline{C}$(CH_3)$_3$), 35.3 (Ph$\underline{C}H_2CH_2$), 29.6 (Ph$CH_2\underline{C}H_2$), 28.1 (C($\underline{C}H_3$)$_3$), 15.1 (CH=C=C($\underline{C}H_3$)). **IR** (neat): 1960 (C=C=C), 1703 (C=O). **HRMS** (*m/z*, ESI$^+$): calculated for $C_{17}H_{22}NaO_2^+$ ([M+Na]$^+$): 281.1512 found 281.1505.

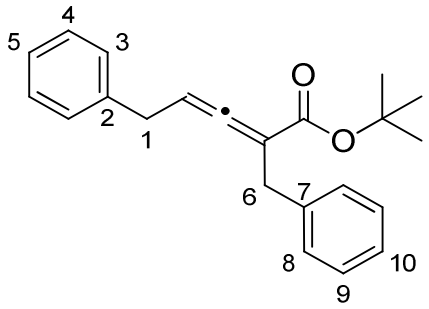
***tert*-Butyl 2-benzylpenta-2,3-dienoate (102g)**



General procedure C was followed using *tert*-butyl 3-phenyl-2-(triphenylphosphoranylidene)propanoate **159c** (1.84 g, 3.95 mmol, 1.7 eq), propanoyl chloride (202 μL, 2.32 mmol, 1 eq) and triethylamine (551 μL, 3.95 mmol, 1.7 eq) in dichloromethane (10 mL). The resulting crude mixture was purified by flash column chromatography on silica gel (hexane:diethyl ether, 9:1) to afford the product **102g** as a colourless oil (564 mg, yield > 95%).

R_f: (hexane:diethyl ether, 9:1) = 0.36. **^{1}H NMR** (400 MHz, $CDCl_3$) δ: 7.17-7.31 (m, 5H, Ph), 5.41 (qt, 1H, $^3J_{HH}$ = 7.3 Hz, $^5J_{HH}$ = 2.3 Hz, $(CH_3)C\underline{H}$=C=C), 3.55 (dd, 1H, $^2J_{HH}$ = 15.2 Hz, $^5J_{HH}$ = 2.3 Hz, PhC$\underline{H}$H'), 3.49 (dd, 1H, $^2J_{HH}$ = 15.2 Hz, $^5J_{HH}$ = 2.3 Hz), 1.69 (d, 3H, $^3J_{HH}$ = 7.3 Hz, (C$\underline{H}_3$)CH=C=C), 1.44 (s, 9H, C(C$\underline{H}_3$)$_3$). **^{13}C NMR** (101 MHz, $CDCl_3$) δ: 211.0 (C=$\underline{C}$=C), 166.4 ($\underline{C}$=O), 139.7 (*ipso*-Ph), 128.8, 128.1, 126.0 (*ortho*-, *meta*-, *para*-Ph), 101.4 ((CH$_3$)CH=C=$\underline{C}$), 89.6 ((CH$_3$)$\underline{C}$H=C=C), 80.7 ($\underline{C}$(CH$_3$)$_3$), 35.4 (Ph$\underline{C}$H$_2$), 28.0 (C($\underline{C}$H$_3$)$_3$), 13.0 (($\underline{C}$H$_3$)CH=C=C). **IR** (neat): 1961 (C=C=C), 1704 (C=O). **HRMS** (*m/z*, CI$^+$): calculated for $C_{16}H_{24}NO_2$ ([M+NH$_4$]$^+$): 262.1807 found 262.1821.

***tert*-Butyl 2-benzyl-5-phenylpenta-2,3-dienoate (102h)**

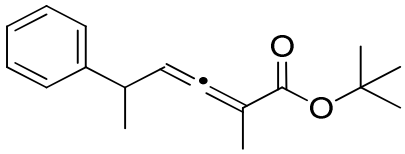


General procedure C was followed using *tert*-butyl 3-phenyl-2-(triphenylphosphoranylidene)propanoate **159c** (1.84 g, 3.94 mmol, 1.7 eq), 3-phenylpropanoyl chloride (344 µL, 2.31 mmol, 1 eq) and triethylamine (549 µL, 3.94 mmol, 1.7 eq) in dichloromethane (10 mL). The resulting crude mixture was purified by flash column chromatography on silica gel (hexane:diethyl ether, 9:1) to afford the product **102h** as a pale yellow oil. (582 mg, yield = 78%).

R_f: (hexane:diethyl ether, 9:1) = 0.33. **^{1}H NMR** (400 MHz, $CDCl_3$) δ: 7.33-7.19 (m, 6H, Ph), 7.13-7.15 (m, 4H, Ph), 5.57 (tt, 1H, $^3J_{HH}$ = 7.3 Hz, $^5J_{HH}$ = 2.5 Hz, BnC$\underline{H}$=C=C), 3.54 (dd, 1H, $^2J_{HH}$ = 15.2 Hz, $^5J_{HH}$ = 2.5 Hz, *H6*), 3.49 (dd, 1H, $^2J_{HH}$ = 15.2 Hz, $^5J_{HH}$ = 2.5 Hz, *H6'*), 3.38 (dd, 1H, $^2J_{HH}$ = 15.4 Hz, $^3J_{HH}$ = 7.3 Hz, *H1*), 3.33 (dd, 1H, $^2J_{HH}$ = 15.4 Hz, $^3J_{HH}$ = 7.3 Hz, *H1'*), 1.47 (s, 9H, C(C$\underline{H}_3$)$_3$). **^{13}C NMR** (125 MHz, $CDCl_3$) δ: 210.9 (C=$\underline{C}$=C), 166.2

(*C*=O), 139.3, 139.0 (*C2*, *C7*), 128.9, 128.6, 128.3, 128.2, 126.4, 126.1 (*C3-5*, *C8-10*), 102.5 (BnCH=C=*C*), 94.3 (Bn*C*H=C=C), 80.8 (*C*$(CH_3)_3$), 35.2, 34.5 (*C1*, *C6*), 28.1 (C(*C*$H_3)_3$). **IR** (neat): 1960 (C=C=C), 1704 (C=O). **HRMS** (*m/z*, ESI^+): calculated for $C_{22}H_{24}NaO_2^+$ ($[M+Na]^+$): 343.1669 found 343.1656.

***tert*-Butyl 2-methyl-5-phenylhexa-2,3-dienoate (102i)**



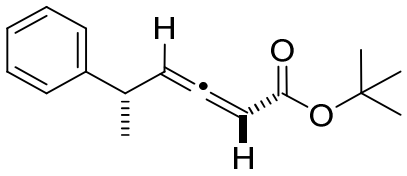
Oxalyl chloride (2 M solution in dichloromethane, 4.80 mL, 9.59 mmol, 1.05 eq) was carefully added to a solution of 3-phenylbutanoic acid (1.50 g, 9.14 mmol, 1 eq) in dichloromethane (19 mL) and dimethylformamide (2 drops) at 0ºC. The reaction mixture was stirred at 0ºC for 3h. The crude 3-phenylbutanoyl chloride was concentrated *in vacuo* and used directly in the next step without further purification.

General procedure C was followed using *tert*-butyl 2-(triphenylphosphoranylidene)propanoate **159b** (2.00 g, 5.13 mmol, 1.7 eq), 3-phenylbutanoyl chloride (551 mg, 3.02 mmol, 1 eq) and triethylamine (715 µL, 5.13 mmol, 1.7 eq) in dichloromethane (10 mL). The resulting crude mixture was purified by flash column chromatography on silica gel (hexane:diethyl ether, 9:1) to afford the product **102i** as a 50:50 diastereoisomeric mixture as a yellow oil (655 mg, yield = 84% over two steps).

(**1:1 Mixture of Diastereoisomers**): $\mathbf{R_f}$: (hexane:diethyl ether, 9:1) = 0.32. **^{1}H NMR** (400 MHz, $CDCl_3$) δ: 7.26-7.36 (m, 8H, Ph), 7.20-7.25 (m, 2H, Ph), 5.62 (dq, 1H, $^3J_{HH}$ = 5.8 Hz, $^5J_{HH}$ = 3.0 Hz, C*H*=C=C), 5.59 (dq, 1H, $^3J_{HH}$ = 6.3 Hz, $^5J_{HH}$ = 3.0 Hz, C*H*=C=C), 3.60 (m, 1H, PhC*H*(CH_3)), 3.56 (m, 1H, PhC*H*(CH_3)), 1.86 (d, 3H, $^5J_{HH}$ = 3.0 Hz, CH=C=C(C*H*$_3$)), 1.84 (d, 3H, $^5J_{HH}$ = 3.0 Hz, CH=C=C(C*H*$_3$)), 1.53 (s, 9H, C(C*H*$_3)_3$), 1.48 (s, 9H, C(C*H*$_3)_3$), 1.40 (d, 3H, $^3J_{HH}$ = 6.8 Hz, PhCH(C*H*$_3$)), 1.35 (d, 3H, $^3J_{HH}$ = 7.1 Hz, PhCH(C*H*$_3$)). **^{13}C**

NMR (125 MHz, $CDCl_3$) δ: 209.4 (C=<u>C</u>=C), 209.4 (C=<u>C</u>=C), 167.3 (<u>C</u>=O), 167.0 (<u>C</u>=O), 145.4 (*ipso*-Ph), 145.0 (*ipso*-Ph), 128.4, 128.3, 127.3, 127.2, 126.5, 126.4 (*ortho*-, *meta*-, *para*-Ph), 98.8, 98.8, 98.5, 98.5 (<u>C</u>H=C=C, CH=C=<u>C</u>), 80.6 (<u>C</u>$(CH_3)_3$), 80.5 (<u>C</u>$(CH_3)_3$), 39.1 (Ph<u>C</u>H(CH_3)), 39.0 (Ph<u>C</u>H(CH_3)), 28.2 (C(<u>C</u>$H_3)_3$), 28.1 (C(<u>C</u>$H_3)_3$), 21.7 (PhCH(<u>C</u>H_3)), 21.3 (PhCH(<u>C</u>H_3)), 15.2 (CH=C=C(<u>C</u>H_3)), 15.1 (CH=C=C(<u>C</u>H_3)). **IR** (neat): 1962 (C=C=C), 1740 (C=O). **HRMS** (*m/z*, CI^+): calculated for $C_{17}H_{23}O_2$ ($[M+H]^+$): 259.1698 found 259.1707.

(±)-(2*S*,5*S*)-*tert*-Butyl 5-phenylhexa-2,3-dienoate ((±)-(2*S*,5*S*)-102j)



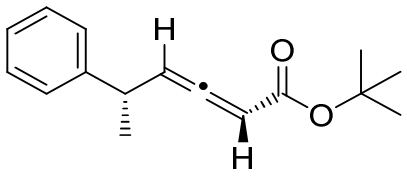
Oxalyl chloride (2 M solution in dichloromethane, 4.80 mL, 9.59 mmol, 1.05 eq) was carefully added to a solution of 3-phenylbutanoic acid (1.50 g, 9.14 mmol, 1 eq) in dichloromethane (19 mL) and dimethylformamide (2 drops) at 0ºC. The reaction mixture was stirred at 0ºC for 3h. The crude 3-phenylbutanoyl chloride was concentrated *in vacuo* and used directly in the next step without further purification.

General procedure C was followed using *tert*-butyl (triphenylphosphoranylidene)acetate **159a** (2.00 g, 5.31 mmol, 1.7 eq), 3-phenylbutanoyl chloride (570 mg, 3.12 mmol, 1 eq) and triethylamine (739 μL, 5.31 mmol, 1.7 eq) in anhydrous dichloromethane (10 mL) at room temperature overnight. The resulting crude mixture was purified and the diastereoisomers and isomeric alkyne side-product partially separated by flash column chromatography on silica gel (hexane:diethyl ether, 50:1) to afford the pure diastereoisomer of the product (±)-(2*S*,5*S*)-**102j** as a colourless oil (54 mg, yield = 7% over two steps) as well as a mixture of both diastereoisomers of **102j** and the isomeric alkyne side-product (114 mg, (±)-(2*S*,5*S*)-

102j: (±)-(2*S*,5*R*)-**102j**: alkyne = 3.3:6.6:1, corrected yield of (±)-(2*S*,5*S*)-**102j** = 5% over two steps, total corrected yield of (±)-(2*S*,5*S*)-**102j** = 13% over two steps, total corrected yield of (2*S*,5*R*)-**102j** = 9% over two steps).

(±)-(2*S*,5*S*)-**102j**: $\mathbf{R_f}$: (hexane:diethyl ether, 9:1) = 0.31. **^{1}H NMR** (400 MHz, $CDCl_3$) δ: 7.30-7.36 (m, 4H, Ph), 7.25 (m, 1H, Ph), 5.78 (dd, 1H, $^3J_{HH}$ = 7.1 Hz, $^4J_{HH}$ = 6.1 Hz, PhCH(CH_3)C*H*=C=C), 5.62 (dd, 1H, $^4J_{HH}$ = 6.1 Hz, $^5J_{HH}$ = 3.3 Hz, PhCH(CH_3)CH=C=C*H*), 3.58 (m, 1H, PhC*H*(CH_3)), 1.53 (s, 9H, C(CH_3)$_3$), 1.39 (d, 3H, $^3J_{HH}$ = 7.1 Hz, PhCH(CH_3)). **^{13}C NMR** (125 MHz, $CDCl_3$) δ: 211.5 (C=*C*=C), 165.4 (*C*=O), 144.9 (*ipso*-Ph), 128.5, 127.2, 126.6 (*ortho*-, *meta*-, *para*-Ph), 100.2 (PhCH(CH_3)*C*H=C=CH), 91.7 PhCH(CH_3)CH=C=*C*H), 80.8 (*C*(CH_3)$_3$), 38.7 (Ph*C*H(CH_3)), 28.2 (C(*C*H_3)$_3$), 21.7 PhCH(*C*H_3)). **IR** (neat): 1961 (C=C=C), 1705 (C=O). **HRMS** (*m/z*, CI^+): calculated for $C_{16}H_{21}O_2$ ($[M+H]^+$): 245.1542 found 245.1544.

***tert*-Butyl (2*S*,5*S*)-5-phenylhexa-2,3-dienoate ((2*S*,5*S*)-102j)**



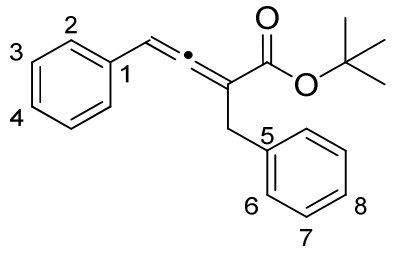
Oxalyl chloride (2 M solution in dichloromethane, 1.28 mL, 2.56 mmol, 1.05 eq) was carefully added to a solution of (*S*)-3-phenylbutanoic acid (Sigma-Aldrich, ee > 97%, 400 mg, 2.44 mmol, 1 eq) in dichloromethane (5.1 mL) and dimethylformamide (2 drops) at 0ºC. The reaction mixture was stirred at 0ºC for 3h. The crude (*S*)-3-phenylbutanoyl chloride was concentrated *in vacuo* and used directly in the next step without further purification.

General procedure C was followed using *tert*-butyl (triphenylphosphoranylidene)acetate **159a** (1.56 g, 4.15 mmol, 1.7 eq), (*S*)-3-phenylbutanoyl chloride (ee > 97%, 446 mg, 2.44

mmol, 1 eq) and triethylamine (578 μL, 4.15 mmol, 1.7 eq) in dichloromethane (6 mL). The resulting crude mixture was purified and the diastereoisomers and isomeric alkyne side-product partially separated by flash column chromatography on silica gel (hexane:diethyl ether, 50:1) to afford the pure diastereoisomer of the product (2*S*,5*S*)-**102j** as a colourless oil (101 mg, yield = 17% over two steps) as well as a mixture of both diastereoisomers of **102j** and the isomeric alkyne side-product (260 mg, (2*S*,5*S*)-**102j** : (2*R*,5*S*)-**102j** : alkyne = 1.6:1.7:1, corrected yield of (2*S*,5*S*)-**102j** = 16% over two steps, total corrected yield of (2*S*,5*S*)-**102j** = 33% over two steps, total corrected yield of (2*R*,5*S*)-**102j** = 17% over two steps).

(2*S*,5*S*)-**102j**: $[\alpha]_D^{25}$ = -65.6 (*c* 1.0, $CHCl_3$). All other characterisation data was identical to the racemic compound (±)-(2*S*,5*S*)-**102j** (see above). The stereochemistry was assigned by mechanistic rationale with reference to the product of cyclisation-oxidative coupling (8*R*,8a*S*)-**109j** (see Section 6.3.3.2).

***tert*-Butyl 2-benzyl-4-phenylbuta-2,3-dienoate (102n)**



General procedure C was followed using *tert*-butyl 3-phenyl-2-(triphenylphosphoranylidene)propanoate **159c** (2.80 g, 6.01 mmol, 1.7 eq), phenylacetyl chloride (468 μL, 3.53 mmol, 1 eq) and triethylamine (837 μL, 6.01 mmol, 1.7 eq) in dichloromethane (17 mL). The resulting crude mixture was purified by flash column chromatography on silica gel (hexane:diethyl ether, 9:1) to afford the product **102n** as a yellow oil (873 mg, yield = 81%).

R_f: (hexane:diethyl ether, 9:1) = 0.33. **^{1}H NMR** (400 MHz, $CDCl_3$) δ: 7.27-7.43 (m, 10H, Ph), 6.57 (t, 1H, $^5J_{HH}$ = 2.3 Hz, PhC*H*=C=C), 3.83 (dd, 1H, $^2J_{HH}$ = 14.9 Hz, $^5J_{HH}$ = 2.3 Hz, PhC*H*H'), 3.78 (dd, 1H, $^2J_{HH}$ = 14.9 Hz, $^5J_{HH}$ = 2.3 Hz, PhCH*H'*), 1.57 (s, 9H, C(CH_3)$_3$). **^{13}C NMR** (125 MHz, $CDCl_3$) δ: 212.9 (C=*C*=C), 165.5 (*C*=O), 139.4 (*C5*), 132.7 (*C1*), 129.0, 128.8, 128.4, 127.7, 127.3, 126.4 (*C2-4*, *C6-8*), 105.7 (PhCH=C=*C*), 98.3 (Ph*C*H=C=C), 81.3 (*C*(CH$_3$)$_3$), 35.8 (Ph*C*H$_2$), 28.2 (C(*C*H$_3$)$_3$). **IR** (neat): 1945 (C=C=C), 1706 (C=O). **HRMS** (*m/z*, ESI$^+$): calculated for $C_{21}H_{22}NaO_2^+$ ([M+Na]$^+$): 329.1512 found 329.1511.

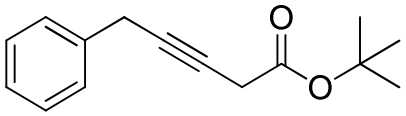
6.3.2.3 Preparation of Alkyne 108b

Alkynes **108** were prepared according to the procedure of Fu.[106]



Scheme 6.4 Synthesis of Alkynes **108**.

***tert*-Butyl 5-phenylpent-3-ynoate (108b)**



Prop-2-yn-1-ylbenzene (249 µL, 2.00 mmol, 1 eq) and copper(I) iodide (19 mg, 100 µmol, 10 mol%) were dissolved in acetonitrile (2.5 mL). *tert*-Butyl diazoacetate (277 µL, 2.00 mmol, 1 eq) was added and the mixture was stirred for 12h at rt. The solvent was removed *in vacuo* and the crude product was passed through a short pad of silica gel (diethyl ether) to afford alkyne **108b** as a yellow oil (442 mg, yield > 95%).

R_f: (hexane:diethyl ether, 9:1) = 0.41. **^{1}H NMR** (400 MHz, $CDCl_3$) δ: 7.38 (dm, 2H, $^3J_{HH}$ = 7.3 Hz, *ortho*-Ph), 7.32 (apparent tm, 2H, $^3J_{HH}$ = 7.3 Hz, *meta*-Ph), 7.24 (tm, 1H, $^3J_{HH}$ = 7.3 Hz, *para*-Ph), 3.64 (br s, 2H, PhC*H*$_2$), 3.25 (t, 2H, $^5J_{HH}$ = 2.4 Hz, C*H*$_2$(C=O)), 1.49 (s, 9H,

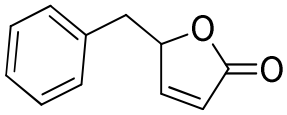
C(C<u>*H*</u>$_3$)$_3$). **^{13}C NMR** (101 MHz, $CDCl_3$) δ: 167.9 (<u>*C*</u>=O), 136.8 (*ipso*-Ph), 128.4, 127.9 (*ortho*-, *meta*-Ph), 126.5 (*para*-Ph), 81.7, 81.0 (Bn<u>*C*</u>≡C, <u>*C*</u>(CH$_3$)$_3$), 74.5 (BnC≡<u>*C*</u>), 27.9 (C(<u>*C*</u>H$_3$)$_3$), 27.3 (Ph<u>*C*</u>H$_2$), 25.1 (<u>*C*</u>H$_2$(C=O)). **IR** (neat): 2227 (C≡C), 1733 (C=O). **HRMS** (*m/z*, ESI$^+$): calculated for $C_{15}H_{18}NaO_2^+$ ([M+Na]$^+$): 253.1199, found 253.1197.

6.3.3 Cyclisation-Intramolecular Arylation of Benzyl-Substituted Allenoates

6.3.3.1 Preliminary Investigations

6.3.3.1.1 Without External Oxidants

5-Benzylfuran-5(2*H*)-one (103b)[100]



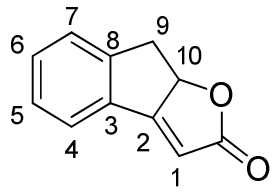
AuCl (10 mg, 43 μmol, 5 mol%) was added to a solution of allenoate **102b** (as a mixture with its isomeric alkyne, allenoate:alkyne 2.2:1, 200 mg, 87 μmol, 1 eq) in dichloromethane (6 mL) at room temperature. The reaction was stirred at room temperature until TLC analysis showed complete consumption of the allenoate (16h). After removal of the solvent *in vacuo*, the crude mixture was purified by column chromatography on silica gel (hexane:diethyl ether, 1:1) to afford butenolide **103b** as a colourless oil (94 mg, yield (based on **102b**) = 90%).

R$_f$: (hexane:diethyl ether, 1:1) = 0.18. **^{1}H NMR** (400 MHz, $CDCl_3$) δ: 7.41 (dd, 1H, $^3J_{HH}$ = 5.7, $^4J_{HH}$ = 1.5 Hz, CH=C<u>*H*</u>(C=O)), 7.26-7.36 (m, 3H, Ph), 7.21-7.24 (m, 2H, Ph), 6.09 (dd, 1H, $^3J_{HH}$ = 5.7, 2.0 Hz, C<u>*H*</u>=CH(C=O)), 5.24 (m, 1H, BnC<u>*H*</u>), 3.17 (dd, 1H, $^2J_{HH}$ = 13.9 Hz, $^3J_{HH}$ = 6.4 Hz, PhC<u>*H*</u>H'), 2.97 (dd, 1H, $^2J_{HH}$ = 13.9 Hz, $^3J_{HH}$ = 7.1 Hz, PhCH<u>*H'*</u>). **^{13}C NMR** (101 MHz, $CDCl_3$) δ: 172.8 (<u>*C*</u>=O), 155.5 (<u>*C*</u>H=CH(C=O)), 134.8 (*ipso*-Ph), 129.4, 128.7, 127.3 (*ortho*-, *meta*-, *para*-Ph), 122.1 (CH=<u>*C*</u>H(C=O)), 83.4 (Bn<u>*C*</u>H), 39.6 (Ph<u>*C*</u>H$_2$). **IR**

(neat): 1762 (C=O). **HRMS** (*m/z*, CI^+): calculated for $C_{11}H_{10}O_2$ ($[M+H]^+$): 175.0759, found 175.0752.

6.3.3.1.2 With Selectfluor

8,8a-Dihydro-2*H*-indeno[2,1-*b*]furan-2-one (109b)

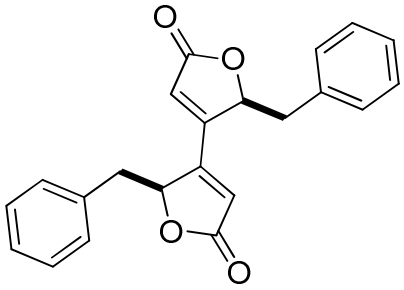


AuCl (11 mg, 49 µmol, 5 mol%) and Selectfluor (**82**, 866 mg, 2.44 mmol, 2.5 eq) were added to a solution of allenoate **102b** (as a mixture with its isomeric alkyne, allenoate:alkyne 2.6:1, 225 mg, 977 µmol, 1 eq) in acetonitrile (6.5 mL) at room temperature. The reaction was stirred at room temperature until TLC analysis showed complete consumption of the allenoate (24h). The reaction mixture was then diluted with dichloromethane and filtered through Celite. After drying over anhydrous sodium sulfate and filtration, the solvent was removed *in vacuo*. The crude mixture was purified by column chromatography on a short pad of silica gel (hexane:ethyl acetate, 7:3) to afford indenofuranone **109b** as a light brown solid (44 mg, yield (based on **102b**) = 36%) as well as bibutenolide (±)-(2*S*,2'*S*)-**110b** as a white solid (24 mg, yield (based on **102b**) = 20%) and bibutenolide (2*R*,2'*S*)-**110b** as a white solid (18 mg, yield (based on **102b**) = 15%).

R_f: (hexane:diethyl ether, 1:1) = 0.22. **Mp** = 50°C. **^{1}H NMR** (400 MHz, $CDCl_3$) δ: 7.63 (m, 1H, *H4*), 7.47 (m, 1H, *H7*), 7.37-7.41 (m, 2H, *H5*, *H6*), 6.02 (d, 1H, $^4J_{HH}$ = 2.2 Hz, *H1*), 5.49 (ddd, 1H, $^3J_{HH}$ = 7.5, 7.3 Hz, $^4J_{HH}$ = 2.2 Hz, *H10*), 3.46 (dd, 1H, $^2J_{HH}$ = 14.5 Hz, $^3J_{HH}$ = 7.5 Hz, *H9*), 2.89 (dd, 1H, $^2J_{HH}$ = 14.5 Hz, $^3J_{HH}$ = 7.3 Hz, *H9'*). **^{13}C NMR** (125 MHz, $CDCl_3$) δ: 175.2, 173.9 (*C*=O, *C2*), 145.7 (*C8*), 131.8 (*C3*), 132.1, 128.4, 126.7, 124.5 (*C4-7*), 108.9 (*C1*), 86.0 (*C10*), 36.5 (*C9*). **IR** (CH_2Cl_2): 1768 (C=O). **HRMS** (*m/z*, CI^+):

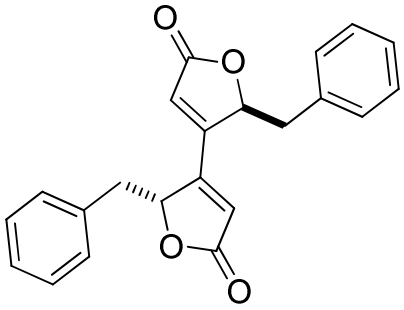
calculated for $C_{11}H_9O_2$ ($[M+H]^+$): 173.0603, found 173.0605. The structure was unambiguously confirmed by X-ray crystallography. This data is deposited at the Cambridge Crystallographic Data Centre (CCDC): 765540 (see Appendix).

(±)-(2*S*,2'S)-2,2'-Dibenzyl-3,3'-bifuran-5,5'(2*H*,2'*H*)-dione ((±)-(2*S*,2'*S*)-110b)



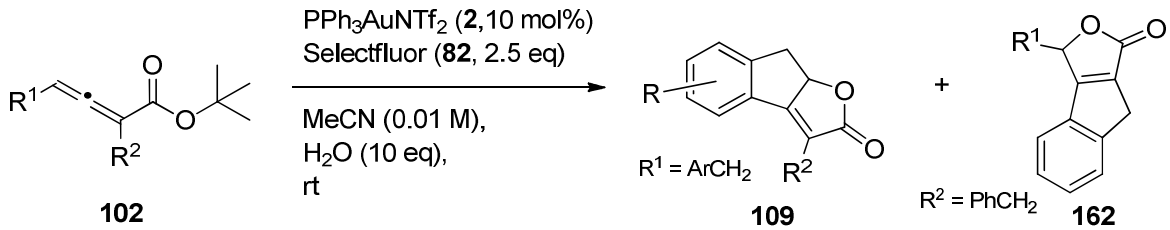
R_f: (hexane:ethyl acetate, 4:1) = 0.10. **Mp** = 154°C. **^{1}H NMR** (400 MHz, $CDCl_3$) δ: 7.26-7.34 (m, 6H, Ph), 7.08-7.14 (m, 4H, Ph), 6.08 (m, 2H, C=C*H*(C=O)), 5.36 (m, 2H, BnC*H*), 3.08 (ddd, 2H, $^2J_{HH}$ = 14.7 Hz, $^3J_{HH}$ = 3.8 Hz, $^4J_{HH}$ = 3.0 Hz, PhC*H*H'), 2.94 (ddd, 2H, $^2J_{HH}$ = 14.7 Hz, $^3J_{HH}$ = 6.8 Hz, $^4J_{HH}$ = 3.3 Hz, PhCH*H'*). **^{13}C NMR** (125 MHz, $CDCl_3$) δ: 170.1 (*C*=O), 155.4 (*C*=CH(C=O)), 134.0 (*ipso*-Ph), 129.4, 128.8, 127.8 (*ortho*-, *meta*-, *para*-Ph), 121.9 (C=*C*H(C=O)), 82.5 (Bn*C*H), 39.4 (Ph*C*H_2). **IR** (CH_2Cl_2): 1753 (C=O). **HRMS** (*m/z*, ESI^+): calculated for $C_{22}H_{18}NaO_4^+$ ($[M+Na]^+$): 369.1097, found 369.1100. The structure and relative stereochemistry were unambiguously assigned by X-ray crystallography. This data is deposited at the Cambridge Crystallographic Data Centre (CCDC): 765543 (see Appendix).

(2*R*,2'*S*)-2,2'-Dibenzyl-3,3'-bifuran-5,5'(2*H*,2'*H*)-dione ((2*R*,2'*S*)-110b)



R_f: (hexane:ethyl acetate, 4:1) = 0.14. **Mp** = 190°C. **^{1}H NMR** (400 MHz, $CDCl_3$) δ: 7.30-7.25 (m, 6H, Ph), 7.10-7.06 (m, 4H, Ph), 6.21 (d, 2H, $^4J_{HH}$ = 1.0 Hz, C=C*H*(C=O)), 5.41 (ddm, 2H, $^3J_{HH}$ = 5.3, 3.8 Hz, BnC*H*), 3.44 (dd, 2H, $^2J_{HH}$ = 14.7 Hz, $^3J_{HH}$ = 3.8 Hz, PhC*H*H'), 2.89 (dd, 2H, $^2J_{HH}$ = 14.7 Hz, $^3J_{HH}$ = 5.3 Hz, PhCH*H'*). **^{13}C NMR** (125 MHz, $CDCl_3$) δ: 170.1 (*C*=O), 154.5 (*C*=CH(C=O)), 133.0 (*ipso*-Ph), 129.5, 128.7, 127.8 (*ortho*-, *meta*-, *para*-Ph), 122.4 (C=*C*H(C=O)), 82.2 (Bn*C*H), 39.5 (Ph*C*H$_2$). **IR** (CH_2Cl_2): 1760 (C=O). **HRMS** (*m/z*, ESI^+) calculated for $C_{22}H_{18}NaO_4^+$ ($[M+Na]^+$): 369.1097, found 369.1095. The structure and relative stereochemistry were unambiguously assigned by X-ray crystallography. This data is deposited at the Cambridge Crystallographic Data Centre (CCDC): 765544 (see Appendix).

6.3.3.2 Scope and Limitations



R^1 = $PhCH_2$, [(*o*-,*m*-OMe)C_6H_3]CH_2, [(*p*-CF_3)C_6H_4]CH_2, Me, $PhCH(CH_3)$, Ph, $PhCH_2CH_2$

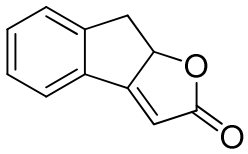
R^2 = H, CH_3, $PhCH_2$

Scheme 6.5 Scope and Limitations of the Cascade Cyclisation-Intramolecular Arylation of Benzyl-Substituted Allenoates **102**.

General Procedure D: PPh_3AuNTf_2 (**2**, 10 mol%) and Selectfluor (**82**, 2.5 eq) were added to a solution of the allenoate **102** (1 eq) in acetonitrile (0.01 M) and water (10 eq). The reaction was stirred at rt until TLC analysis showed complete consumption of the allenoate (1.5-24h). The reaction mixture was then diluted with dichloromethane and filtered through Celite. After drying over anhydrous sodium sulfate and filtration, the solvent was removed *in vacuo*. The resulting crude mixture was purified by column chromatography on a short pad of silica gel.

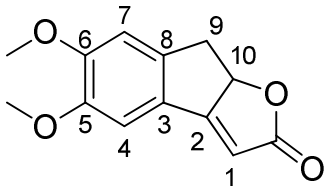
*Note: In some cases (with allenoates **102b-d**), mixtures of the allenoate and the co-spotting isomeric alkyne were used in the cyclisation-oxidative coupling reactions. In these cases, the quantities of reagents was calculated with reference to the combined mass of the two isomers. A control reaction with the pure alkyne **108b** did not afford **109b**, **110b** or **103b** and thus the yields were calculated with respect to the amount of allenoate present.*

8,8a-Dihydro-2*H*-indeno[2,1-*b*]furan-2-one (109b)



General procedure D was followed using allenoate **102b** (as a mixture with its isomeric alkyne, allenoate:alkyne 3.3:1, 250 mg, 1.09 mmol, 1 eq), $Ph_3PAuNTf_2$ (**2**, 80 mg, 0.11 mmol, 10 mol%) and Selectfluor (**82**, 961 mg, 2.71 mmol, 2.5 eq) in acetonitrile (110 mL) and water (195 µL, 10.9 mmol, 10 eq). The resulting crude mixture was purified by column chromatography on a short pad of silica gel (hexane:diethyl ether, 1:1) to afford the product **109b** as a light brown solid (137 mg, yield (based on **102b**) = 95%). For characterisation data of **109b**, see Section 6.3.3.1.2.

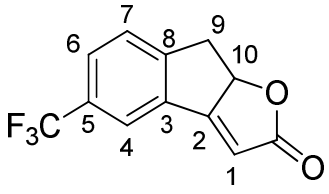
5,6-Dimethoxy-8,8a-dihydro-2*H*-indeno[2,1-*b*]furan-2-one (109c)



General procedure D was followed using allenoate **102c** as a mixture with its isomeric alkyne (allenoate:alkyne 3:1, 250 mg, 861 μmol, 1 eq), $Ph_3PAuNTf_2$ (**2**, 64 mg, 86 μmol, 10 mol%) and Selectfluor (**82**, 763 mg, 2.15 mmol, 2.5 eq) in acetonitrile (85 mL) and water (155 μL, 8.61 mmol, 10 eq). The resulting crude mixture was purified by column chromatography on a short pad of silica gel (hexane:ethyl acetate, 3:7) to afford the product **109c** as a pale orange solid (126 mg, yield (based on **102c**) = 84%).

R_f: (hexane:ethyl acetate, 3:7) = 0.36. **Mp** = 156 °C. **^{1}H NMR** (400 MHz, $CDCl_3$) δ: 7.08 (s, 1H, *H4*), 6.88 (s, 1H, *H7*), 5.86 (d, 1H, $^4J_{HH}$ = 2.0 Hz, *H1*), 5.43 (ddd, 1H, $^3J_{HH}$ = 7.3, 6.8 Hz, $^4J_{HH}$ = 2.0 Hz, *H10*), 3.93 (s, 6H, OC$\underline{H}_3$), 3.38 (dd, 1H, $^2J_{HH}$ = 14.4 Hz, $^3J_{HH}$ = 7.3 Hz, *H9*), 2.85 (dd, 1H, $^2J_{HH}$ = 14.4 Hz, $^3J_{HH}$ = 6.8 Hz, *H9′*). **^{13}C NMR** (101 MHz, $CDCl_3$) δ: 175.7, 174.3 ($\underline{C}$=O, *C2*), 153.0, 149.6 (*C5*, *C6*), 139.6 (*C8*), 124.1 (*C3*), 108.7, 106.3, 105.9 (*C1*, *C4*, *C7*), 85.9 (*C10*), 56.2 (O$\underline{C}H_3$), 56.1 (O$\underline{C}H_3$), 36.3 (*C9*). **IR** (CH_2Cl_2): 1760 ($\underline{C}$=O). **HRMS** (*m/z*, ESI^+): calculated for $C_{13}H_{12}O_4^+$ ($[M+Na]^+$): 255.0628, found 255.0628.

5-(Trifluoromethyl)-8,8a-dihydro-2*H*-indeno[2,1-*b*]furan-2-one (109d)

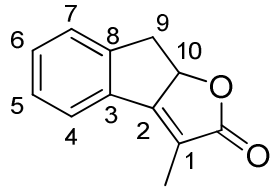


General procedure D was followed using allenoate **102d** as a mixture with its isomeric alkyne (allenoate:alkyne 7:1, 224 mg, 751 μmol, 1 eq), $Ph_3PAuNTf_2$ (**2**, 56 mg, 75 μmol, 10 mol%) and Selectfluor (**82**, 665 mg, 1.88 mmol, 2.5 eq) in acetonitrile (75 mL) and water

(135 μL, 7.51 mmol, 10 eq). The resulting crude mixture was purified by column chromatography on a short pad of silica gel (hexane:diethyl ether, 1:1) to afford the product **109d** as a yellow solid (58 mg, yield (based on **102d**) = 37%).

R_f: (hexane:diethyl ether, 1:1) = 0.27. **Mp**:= 91°C. **^{1}H NMR** (400 MHz, $CDCl_3$) δ: 7.90 (s, 1H, *H4*), 7.73 (d, 1H, $^3J_{HH}$ = 7.8 Hz, *H7*), 7.54 (m, 1H, *H6*), 6.14 (d, 1H, $^4J_{HH}$ = 2.3 Hz, *H1*), 5.52 (ddd, 1H, $^3J_{HH}$ = 7.6, 7.3 Hz, $^4J_{HH}$ = 2.3 Hz, *H10*), 3.54 (dd, 1H, $^2J_{HH}$ = 14.9 Hz, $^3J_{HH}$ = 7.6 Hz, *H9*), 2.94 (dd, 1H, $^2J_{HH}$ = 14.9 Hz, $^3J_{HH}$ = 7.3 Hz, *H9′*). **^{13}C NMR** (125 MHz, $CDCl_3$) δ: 174.5, 171.8 (*C*=O, *C2*), 149.2 (*C8*), 132.5 (*C3*), 131.1 (q, $^2J_{CF}$ = 32 Hz, *C5*), 128.8 (q, $^3J_{CF}$ = 4 Hz, *C6*), 127.3 (*C7*), 123.6 (q, $^1J_{CF}$ = 273 Hz, *C*F_3), 121.5 (q, $^3J_{CF}$ = 4 Hz, *C4*), 110.8 (*C1*), 85.8 (*C10*), 36.6 (*C9*). **^{19}F NMR** (377 MHz, $CDCl_3$) δ: −62.5. **IR** (CH_2Cl_2): 1771 (C=O). **HRMS** (*m/z*, CI^+): calculated for $C_{12}H_8O_2F_3$ ($[M+H]^+$): 241.0476, found 241.0478. The structure was unambiguously confirmed by X-ray crystallography. This data is deposited at the Cambridge Crystallographic Data Centre (CCDC): 765541 (see Appendix).

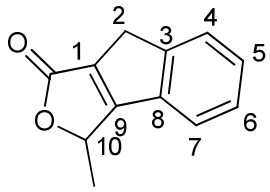
3-Methyl-8,8a-dihydro-2*H*-indeno[2,1-*b*]furan-2-one (109e)[276]



General procedure D was followed using allenoate **102e** (250 mg, 1.02 mmol, 1 eq), $Ph_3PAuNTf_2$ (**2**, 76 mg, 0.10 mmol, 10 mol%) and Selectfluor (**82**, 906 mg, 2.56 mmol, 2.5 eq) in acetonitrile (100 mL) and water (184 μL, 10.2 mmol, 10 eq). The resulting crude mixture was purified by column chromatography on a short pad of silica gel (hexane:diethyl ether, 1:1) to afford the product **109e** as a white solid (133 mg, yield = 70%).

R_f: (hexane:diethyl ether, 1:1) = 0.34. **Mp** = 129°C (lit = 136-137°C).[276] **^{1}H NMR** (400 MHz, $CDCl_3$) δ: 7.60 (m, 1H, *H4*) 7.34-7.43 (m, 3H, *H5-7*), 5.37 (ddq, 1H, $^3J_{HH}$ = 7.6, 7.3 Hz, $^5J_{HH}$ = 2.0 Hz, *H10*), 3.40 (dd, 1H, $^2J_{HH}$ = 14.6 Hz, $^3J_{HH}$ = 7.6 Hz, *H9*), 2.78 (dd, 1H, $^2J_{HH}$ = 14.6 Hz, $^3J_{HH}$ = 7.3 Hz, *H9'*), 2.05 (d, 3H, $^5J_{HH}$ = 2.0 Hz, C*H*$_3$). **^{13}C NMR** (101 MHz, $CDCl_3$) δ: 176.2 (*C*=O), 165.3 (*C2*), 145.2 (*C8*), 132.5 (*C3*), 131.0, 128.1, 126.6, 124.0 (*C4-7*), 118.4 (*C1*), 84.0 (*C10*), 36.4 (*C9*), 9.2 (*C*H$_3$). **IR** (CH_2Cl_2): 1753 (C=O). **HRMS** (*m/z*, CI^+): calculated for $C_{12}H_{11}O_2$ ($[M+H]^+$): 187.0759, found 187.0760. The structure was unambiguously confirmed by X-ray crystallography. This data is deposited at the Cambridge Crystallographic Data Centre (CCDC): 795567 (see Appendix).

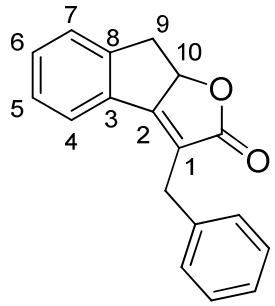
3-Methyl-3,8-dihydro-1*H*-indeno[2,1-*c*]furan-1-one (162g)



General procedure D was followed using allenoate **102g** (200 mg, 818 μmol, 1 eq), $Ph_3PAuNTf_2$ (**2**, 61 mg, 82 μmol, 10 mol%) and Selectfluor (**82**, 725 mg, 2.05 mmol, 2.5 eq) in acetonitrile (82 mL) and water (147 μL, 8.18 mmol, 10 eq). The resulting crude mixture was purified by column chromatography on a short pad of silica gel (hexane:diethyl ether, 1:1) to afford the product **162g** as a white solid (87 mg, yield = 57%).

R_f: (hexane:diethyl ether, 1:1) = 0.21. **Mp** = 141°C. **^{1}H NMR** (400 MHz, $CDCl_3$) δ: 7.62 (m, 1H, *H7*), 7.40-7.50 (m, 3H, *H4-6*), 5.53 (qt, 1H, $^3J_{HH}$ = 6.8 Hz, $^4J_{HH}$ = 2.8 Hz, *H10*), 3.61 (d, 2H, $^4J_{HH}$ = 2.8 Hz, *H2*), 1.70 (d, 3H, $^3J_{HH}$ = 6.8 Hz, C*H*$_3$). **^{13}C NMR** (125 MHz, $CDCl_3$) δ: 174.2 (*C*=O), 168.7 (*C9*), 149.8 (*C3*), 135.8, 135.3 (*C1*, *C8*), 128.9, 127.3, 125.9, 121.6 (*C4-7*), 75.6 (*C10*), 32.2 (*C2*), 19.2 (*C*H$_3$). **IR** (CH_2Cl_2): 1748 (C=O). **HRMS** (*m/z*, ESI^+): calculated for $C_{12}H_{10}NaO_2^+$ ($[M+Na]^+$): 209.0573, found 209.0573.

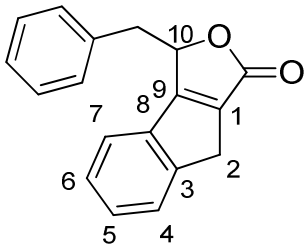
3-Benzyl-8,8a-dihydro-2*H*-indeno[2,1-*b*]furan-2-one (109h)



General procedure D was followed using allenoate **102h** (300 mg, 936 μmol, 1 eq), $Ph_3PAuNTf_2$ (**2**, 69 mg, 94 μmol, 10 mol%) and Selectfluor (**82**, 829 mg, 2.34 mmol, 2.5 eq) in acetonitrile (95 mL) and water (169 μL, 9.36 mmol, 10 eq). The resulting crude mixture was purified by column chromatography on a short pad of silica gel (hexane:diethyl ether, 1:1) to afford the product **109h** as a white solid (67 mg, yield = 27%) and the product **162h** as white solid (106 mg, yield = 43%).

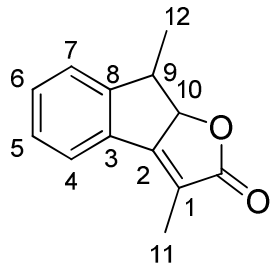
R_f: (hexane:diethyl ether, 1:1) = 0.35. **Mp** = 83°C. **^{1}H NMR** (400 MHz, $CDCl_3$) δ: 7.24-7.41 (m, 8H), 7.07 (m, 1H, *H4-7*, Ph), 5.40 (ddm, 1H, $^3J_{HH}$ = 7.6, 7.3 Hz, *H10*), 3.93 (d, 1H, $^2J_{HH}$ = 15.4 Hz, PhC*H*H'), 3.71 (dd, 1H, $^2J_{HH}$ = 15.4 Hz, $^5J_{HH}$ = 1.2 Hz, PhCH*H'*), 3.42 (dd, 1H, $^2J_{HH}$ = 14.7 Hz, $^3J_{HH}$ = 7.6 Hz, *H9*), 2.84 (dd, 1H, $^2J_{HH}$ = 14.7 Hz, $^3J_{HH}$ = 7.3 Hz, *H9'*). **^{13}C NMR** (125 MHz, $CDCl_3$) δ: 175.8 (*C*=O), 166.1 (*C2*), 145.5 (*C8*), 138.2 (*ipso*-Ph), 132.3 (*C3*), 131.3, 128.9, 128.8, 128.1, 126.7, 126.6, 124.7 (*C4-7*, *ortho*-Ph, *meta*-Ph, *para*-Ph), 122.0 (*C1*), 84.4 (*C10*), 36.5 (*C9*), 30.9 (Ph*C*H_2). **IR** (CH_2Cl_2): 1754 (*C*=O). **HRMS** (*m/z*, CI^+): calculated for $C_{18}H_{15}O_2$ ($[M+H]^+$): 263.1072, found 263.1079.

3-Benzyl-3,8-dihydro-1*H*-indeno[1,2-*c*]furan-1-one (162h)



R_f: (hexane:diethyl ether, 1:1) = 0.23. **Mp** = 148ºC. **^{1}H NMR** (400 MHz, $CDCl_3$) δ: 7.54 (d, 1H, $^3J_{HH}$ = 7.6 Hz, *H4*), 7.39 (m, 1H, *H7*), 7.20-7.31 (m, 6H), 6.76 (m, 1H, *H5*, *H6*, Ph), 5.67 (ddt, 1H, $^3J_{HH}$ = 6.8, 6.3 Hz, $^5J_{HH}$ = 2.3 Hz, *H10*), 3.51 (d, 2H, $^5J_{HH}$ = 2.3 Hz, *H2*), 3.40 (dd, 1H, $^2J_{HH}$ = 14.2 Hz, $^3J_{HH}$ = 6.3 Hz, PhC*H*H'), 3.21 (dd, 1H, $^2J_{HH}$ = 14.2 Hz, $^3J_{HH}$ = 6.8 Hz, PhCH*H'*). **^{13}C NMR** (101 MHz, $CDCl_3$) δ: 172.6 (*C*=O), 168.3 (*C9*), 149.5 (*C3*), 136.2, 136.0 (*ipso*-Ph, *C8*), 134.6 (*C1*), 129.6, 128.7, 128.5, 127.2, 127.1, 125.5, 122.3 (*C4-7*, *ortho*-Ph, *meta*-Ph, *para*-Ph), 79.7 (*C10*), 39.8 (Ph*C*H$_2$), 32.0 (*C2*). **IR** (CH_2Cl_2): 1752 (C=O). **HRMS** (*m/z*, CI$^+$): calculated for $C_{18}H_{15}O_2$ ([M+H]$^+$): 263.1072, found 263.1079. The structure was unambiguously confirmed by X-ray crystallography This data is deposited at the Cambridge Crystallographic Data Centre (CCDC): 765545 (see Appendix).

3,8-Dimethyl-8,8a-dihydro-2*H*-indeno[2,1-*b*]furan-2-one (109i)

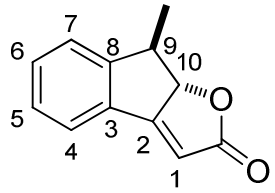


General procedure D was followed using allenoate **102i** (dr = 52:48, 250 mg, 968 μmol, 1 eq), $Ph_3PAuNTf_2$ (**2**, 72 mg, 97 μmol, 10 mol%) and Selectfluor (**82**, 857 mg, 2.42 mmol, 2.5 eq) in acetonitrile (95 mL) and water (174 μL, 9.68 mmol, 10 eq). The resulting crude mixture was purified by column chromatography on a short pad of silica gel (hexane:diethyl

ether, 1:1) to afford the product **109i** as a 55:45 diastereoisomeric mixture as a white solid (157 mg, yield = 81%).

R_f: (hexane:diethyl ether, 1:1) = 0.46. **Mp** = 53°C. **^{1}H NMR** (400 MHz, $CDCl_3$) δ: **Major Diastereoisomer**: 7.61 (m, 1H, *H4*), 7.34-7.49 (m, 3H, *H5-7*), 5.33 (dq, 1H, $^3J_{HH}$ = 7.3 Hz, $^5J_{HH}$ = 2.0 Hz, *H10*), 3.56 (dq, 1H, $^3J_{HH}$ = 7.3, 7.1 Hz, *H9*), 2.09 (d, 3H, $^5J_{HH}$ = 2.3 Hz, *H11*), 0.94 (d, 3H, $^3J_{HH}$ = 7.1 Hz, *H12*). **Minor Diastereoisomer**: 7.61 (m, 1H, *H4*), 7.34-7.49 (m, 3H, *H5-7*), 4.93 (dq, 1H, $^3J_{HH}$ = 7.1 Hz, $^5J_{HH}$ = 2.0 Hz, *H10*), 2.97 (dq, 1H, $^3J_{HH}$ = 6.8, 6.8 Hz, *H9*), 2.07 (d, 3H, $^5J_{HH}$ = 2.0 Hz, *H11*), 1.59 (d, 3H, $^3J_{HH}$ = 6.8 Hz, *H12*). **^{13}C NMR** (125 MHz, $CDCl_3$) δ: **Major & Minor Diastereoisomer**: 176.8 (*C*=O), 176.3 (*C*=O), 163.7 (*C2*), 163.6 (*C2*), 152.3 (*C8*), 149.5 (*C8*), 132.1 (C3), 131.3, 131.1, 128.2, 128.1, 126.0, 124.8, 124.3, 123.8 (*C4-7*), 119.8 (*C1*), 118.1 (*C1*), 91.0 (*C10*), 85.2 (*C10*), 43.3 (*C9*), 40.2 (*C9*), 15.8 (*C11*), 14.5 (*C11*), 9.4 (*C12*), 9.3 (*C12*). *Note: One carbon peak (for C3 in one diastereoisomer) was not observed.* **IR** (CH_2Cl_2): 1754 (C=O). **HRMS** (*m/z*, CI^+): calculated for $C_{13}H_{13}O_2$ ($[M+H]^+$): 201.0916, found 201.0910. The structure was unambiguously confirmed by X-ray crystallography. This data is included in the Appendix.

(±)-(8*R*,8a*S*)-8-Methyl-8,8a-dihydro-2*H*-indeno[2,1-*b*]furan-2-one ((±)-(8*R*,8a*S*)-109j)

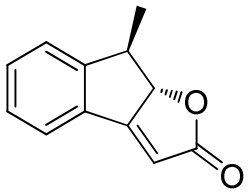


General procedure D was followed using allenoate (±)-(2*S*,5*S*)-**102j** (dr > 95:5, 54 mg, 220 μmol, 1 eq), $Ph_3PAuNTf_2$ (**2**, 16 mg, 22 μmol, 10 mol%) and Selectfluor (**82**, 196 mg, 0.55 mmol, 2.5 eq) in acetonitrile (95 mL) and water (40 μL, 2.2 mmol, 10 eq). The resulting crude mixture was purified by column chromatography on a short pad of silica gel

(hexane:diethyl ether, 1:1) to afford the product (±)-(8*R*,8a*S*)-**109j** as a white solid (dr > 95:5, 34 mg, yield = 83%).

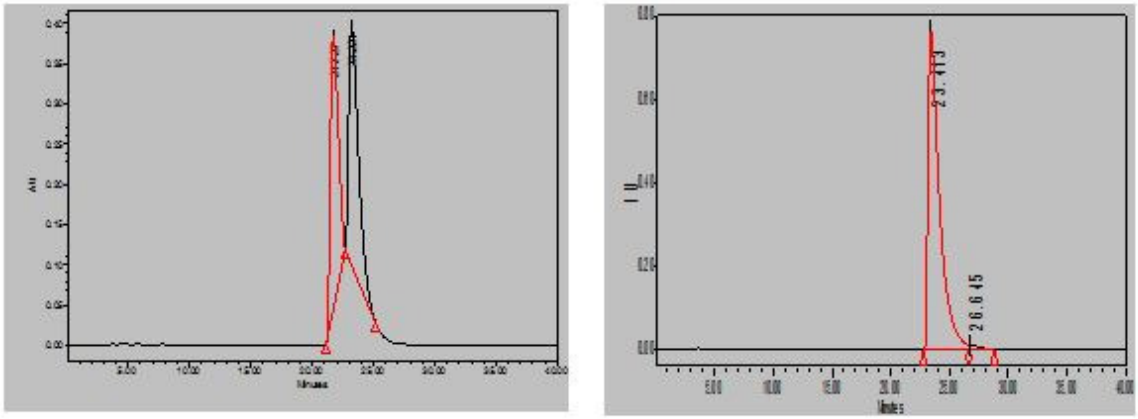
R_f: (hexane:diethyl ether, 1:1) = 0.31. **Mp** = 68°C. **^{1}H NMR** (400 MHz, $CDCl_3$) δ: 7.61 (m, 1H, *H4*), 7.51 (m, 1H, *H7*), 7.36-7.42 (m, 2H, *H5-6*), 6.01 (d, 1H, $^4J_{HH}$ = 2.0 Hz, *H1*), 5.02 (ddm, 1H, $^3J_{HH}$ = 6.8 Hz, $^5J_{HH}$ = 2.0 Hz, *H10*), 3.05 (dq, 1H, $^3J_{HH}$ = 6.8, 6.8 Hz, *H9*), 1.62 (d, 3H, $^3J_{HH}$ = 6.8 Hz, C$\underline{H}_3$). **^{13}C NMR** (125 MHz, $CDCl_3$) δ: 175.2, 172.2 (*C*=O, *C2*), 149.8 (*C8*), 131.3 (*C3*), 132.2, 128.3, 124.9**,** 124.2 (*C4-7*), 108.5 (*C1*), 92.9 (*C10*), 43.3 (*C9*), 15.8 ($\underline{C}H_3$). **IR** (CH_2Cl_2): 1766 ($\underline{C}$=O). **HRMS** (*m/z*, CI^+) calculated for $C_{12}H_{11}O_2$ ($[M+H]^+$): 187.0759, found 187.0766.

(8*R*,8a*S*)-8-Methyl-8,8a-dihydro-2*H*-indeno[2,1-*b*]furan-2-one ((8*R*,8a*S*)-109j)



General procedure D was followed using allenoate (2*S*,5*S*)-**102j** (dr > 95:5, 61 mg, 250 μmol, 1 eq), $Ph_3PAuNTf_2$ (**2**, 18 mg, 25 μmol, 10 mol%) and Selectfluor (**82**, 220 mg, 0.62 mmol, 2.5 eq) in acetonitrile (33 mL) and water (45 μL, 2.5 mmol, 10 eq). The resulting crude mixture was purified by column chromatography on a short pad of silica gel (hexane:diethyl ether, 1:1) to afford the product (8*R*,8a*S*)-**109j** as a white solid (dr > 95:5, 37 mg, yield = 80%) in > 97% enantiomeric excess (major: 23.4 min, minor 26.6 min, CHIRALCEL OJ-H, hexane:isopropanol 97:3, flow rate 1 mL/min).

$[\alpha]_D^{25}$ = −81.0 (*c* 1.0, $CHCl_3$). All other characterisation data was identical to the racemic compound (±)-(8*R*,8a*S*)-**109j** (see above). The structure and relative stereochemistry were unambiguously assigned by X-ray crystallography. This data is deposited at the Cambridge Crystallographic Data Centre (CCDC): 765542 (see Appendix).

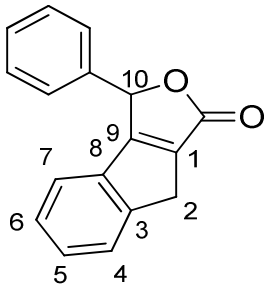


Peak	Time/mins	Area %
1	21.727	47.8
2	23.221	52.2

Peak	Time/mins	Area %
1	23.413	98.8
2	26.645	1.2

Figure 6.1 Chiral HPLC traces for (±)-(8*R*,8a*S*)-**109j** (left) and (8*R*,8a*S*)-**109j** (right)

3-Phenyl-3,8-dihydro-1*H*-indeno[1,2-*c*]furan-1-one (162n)



General procedure D was followed using allenoate **102n** (122 mg, 398 μmol, 1 eq), $Ph_3PAuNTf_2$ (**2**, 29 mg, 40 μmol, 10 mol%) and Selectfluor (**82**, 353 mg, 995 μmol, 2.5 eq) in acetonitrile (40 mL) and water (72 μL, 3.98 mmol, 10 eq). The resulting crude mixture was purified by column chromatography on a short pad of silica gel (hexane:diethyl ether, 1:1) to afford the product **162n** as a white solid (45 mg, yield = 46%).

R_f: (hexane:diethyl ether, 1:1) = 0.49. **Mp** = 84°C. **^{1}H NMR** (400 MHz, $CDCl_3$) δ: 7.61 (d, 1H, $^3J_{HH}$ = 7.6 Hz, *H7*), 7.57-7.37 (m, 6H), 7.32 (d, 1H, $^3J_{HH}$ = 7.6, 7.3 Hz), 7.26 (m, 1H, *H4-6*, Ph), 6.38 (dd, 1H, $^5J_{HH}$ = 3.0, 2.5 Hz, *H10*), 3.72 (br s, 2H, *H2*). **^{13}C NMR** (125 MHz, $CDCl_3$) δ: 172.3 (*C*=O), 168.6 (*C9*), 149.8 (*C3*), 135.9, 135.6 (*ipso*-Ph, *C8*), 134.4 (*C1*), 129.5, 129.1, 129.0, 127.3, 127.2, 125.8, 122.1 (*C4-7*, *ortho*-Ph, *meta*-Ph, *para*-Ph), 80.8

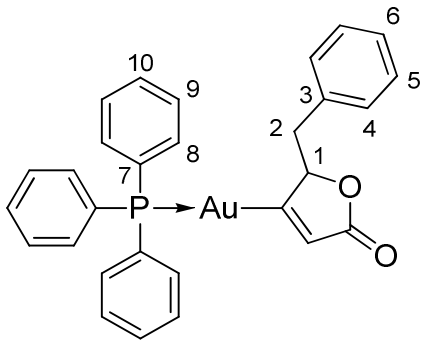
(*C10*), 32.3 (*C2*). **IR** (CH_2Cl_2): 1755 (C=O). **HRMS** (*m/z*, ESI^+): calculated for $C_{17}H_{12}NaO_2^+$ ($[M+Na]^+$): 271.0730, found 271.0731.

6.3.3.3 Preparation and Oxidative Coupling of (Butenolide)gold(I) Complex 104b

6.3.3.3.1 Preparation of (Butenolide)gold(I) Complex 104b

(Butenolide)gold(I) complex **104b** was prepared according to the procedure of Hammond (see Scheme 3.45).[102]

(2-Benzyl-5-oxo-2,5-dihydrofuran-3-yl)(triphenylphosphine)gold(I) (104b)



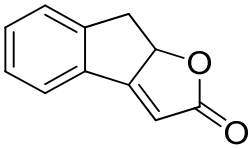
Ph_3PAuCl (90 mg, 0.18 mmol, 1 eq) and AgOTf (46 mg, 0.18 mmol, 1 eq) were added to a solution of allenoate **102b** (as a mixture with its isomeric alkyne, allenoate:alkyne 3.3:1, 65 mg, 0.28 mmol, 1.2 eq of allenoate) in dichloromethane (2 mL). The mixture was stirred at rt for 10 min. After removal of the solvent *in vacuo*, the crude mixture was purified by flash column chromatography on silica gel (hexane:ethyl acetate, 3:1) to afford the product as a white crystalline solid (49 mg, yield = 43%).

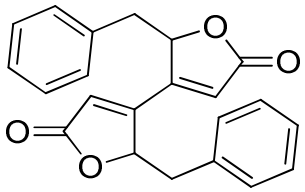
R_f: (hexane:ethyl acetate, 1:1) = 0.30. **Mp** = 50°C. **^{1}H NMR** (400 MHz, $CDCl_3$) δ: 7.39-7.57 (m, 15H, *H8-10*), 7.29-7.31 (m, 2H, *H4*), 6.97-7.07 (m, 3H, *H5*, *H6*), 5.94 (dd, 1H, $^4J_{HP}$ = 3.8 Hz, $^4J_{HH}$ = 1.8 Hz, C=C*H*(C=O)), 5.39 (ddd, 1H, $^3J_{HH}$ = 7.1, 6.1 Hz, $^5J_{HH}$ = 1.8 Hz, *H1*), 3.21 (dd, 1H, $^2J_{HH}$ = 13.9 Hz, $^3J_{HH}$ = 6.1 Hz, *H2*), 3.03 (dd, 1H, $^2J_{HH}$ = 13.9 Hz, $^3J_{HH}$ = 7.1 Hz, *H2′*). **^{13}C NMR** (125 MHz, $CDCl_3$) δ: 206.8 (d, $^2J_{CP}$ = 114 Hz, PAu*C*), 175.5 (d, $^4J_{CP}$ = 10 Hz, *C*=O), 137.5 (*C3*), 134.2 (d, $^2J_{CP}$ = 14 Hz, *C8*), 131.6 (d, $^4J_{CP}$ = 2 Hz, *C10*),

129.8 (d, $^{1}J_{CP}$ = 53 Hz, *C7*), 129.8 (*C4*), 129.2 (d, $^{3}J_{CP}$ = 11 Hz, *C9*), 128.1 (*C5*), 126.4 (*C6*), 125.6 (d, $^{3}J_{CP}$ = 2 Hz, C=<u>C</u>H(C=O)), 96.8 (d, $^{3}J_{CP}$ = 8 Hz, *C1*), 40.8 (*C2*). **^{31}P NMR** (162 MHz, $CDCl_3$) δ: 43.3. **IR** (CH_2Cl_2): 1731 (C=O). **HRMS** (*m/z*, ESI^+) calculated for $C_{29}H_{24}AuNaO_2P^+$ ($[M+Na]^+$): 655.1072, found 655.1073.

6.3.3.3.2 Oxidative Coupling of (Butenolide)gold(I) Complex 104b

8,8a-Dihydro-2*H*-indeno[2,1-*b*]furan-2-one (109b) and 2,2'-Dibenzyl-3,3'-bifuran-5,5'(2*H*,2'*H*)-dione (110b)



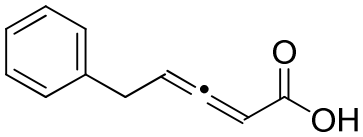


(Butenolide)gold(I) complex (**104b**, 30 mg, 47 μmol, 1 eq) was dissolved in deuterated chloroform (600 μL) and D_2O (8.6 μL, 470 μmol, 10 eq). Selectfluor (**82**, 42 mg, 120 μmol, 2.5 eq) was added and the mixture was stirred at rt with regular monitoring by NMR for 2.5h. Dichloromethane (2 mL) was added and the crude mixture was filtered through Celite, dried over anhydrous Na_2SO_4, filtered and concentrated *in vacuo*. Purification by column chromatography over silica gel (hexane:ethyl acetate, 1:1) afforded indenofuranone **109b** as a light brown solid (3 mg, yield = 37%) and a 63:37 diastereoisomeric mixture of the bibutenolide **110b** as a white solid (5 mg, yield = 60%). For characterisation data of **109b** and **110b**, see Section 6.3.3.1.2.

6.3.3.4 Preparation of β-Fluoro-γ-Butenolides 107

6.3.3.4.1 Preparation of Allenic Acid 157b

5-Phenylpenta-2,3-dienoic acid (157b)



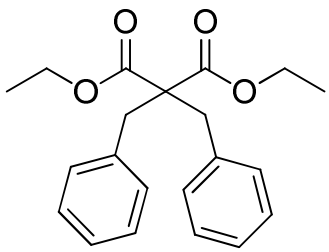
Trifluoroacetic acid (765 μL, 9.99 mmol, 23 eq) was added dropwise to a solution of allenoate **102b** (as a mixture with its isomeric alkyne, allenoate:alkyne = 2.6:1, 100 mg, 434 μmol, 1 eq) in dichloromethane (3.3 mL) at rt. The mixture was stirred for 30 min at rt before being concentrated *in vacuo*. The crude mixture was purified by column chromatography on silica gel (hexane:ethyl acetate 1:1 with a drop of acetic acid) to afford allenic acid **157b** as a yellow oil as a mixture with its isomeric alkyne (allenic acid:alkyne = 3.6:1, 58 mg, overall yield of allenic acid + alkyne = 77%, corrected yield of allenic acid **157b** based on allenoate **102b** = 83%).

R_f: (hexane:ethyl acetate, 1:1) = 0.31. **^{1}H NMR** (500 MHz, $CDCl_3$) δ: 10.47 (br s, 1H, COO*H*), 7.21-7.35 (m, 5H, Ph), 5.94 (td, 1H, $^3J_{HH}$ = 7.6 Hz, $^4J_{HH}$ = 6.1 Hz, C*H*=C=CH(C=O)), 5.63 (dt, 1H, $^4J_{HH}$ = 6.1 Hz, $^5J_{HH}$ = 2.8 Hz, CH=C=C*H*(C=O)), 3.50 (m, 2H, PhCH_2). **^{13}C NMR** (125 MHz, $CDCl_3$) δ: 214.0 (C=*C*=C), 171.0 (*C*=O), 138.3 (*ipso*-Ph), 128.6, 128.5, 126.8 (*ortho*-, *meta*-, *para*-Ph), 95.3 (CH=C=*C*H(C=O)), 88.1 (*C*H=C=CH(C=O)), 33.9 (Ph*C*H_2). **IR** (neat): 1958 (C=C=C), 1686 (C=O). **HRMS** (*m/z*, ESI^+) calculated for $C_{11}H_9Na_2O_2^+$ ($[M-H+2Na]^+$): 219.0392, found 219.0400.

6.3.3.4.2 Preparation of Dibenzyl-Substituted Acid 168

2-Benzyl-3-phenylpropanoic acid (**168**) was prepared according to the procedures of Maslak[277] and Koder (see Scheme 3.52).[278]

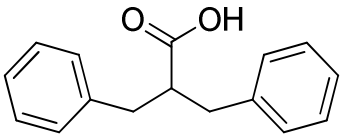
Diethyl dibenzylmalonate (167)[277]



Sodium (2.58 g, 113 mmol, 2.25 eq) was added portionwise to ethanol (46 mL) at rt over 3h. The mixture was stirred until all the metal had dissolved and diethyl malonate (7.59 mL, 50.0 mmol, 1 eq) was added via syringe. After 30 min at rt, the mixture was cooled to 0ºC and a white solid precipitated. Benzyl chloride (12.1 mL, 105 mmol, 2.1 eq) was carefully added via syringe and the reaction was stirred at 0ºC for 1h before being warmed to rt overnight. Hydrochloric acid (1 M, 20 mL) was carefully added and the mixture was extracted into dichloromethane (3×40 mL). The combined organic fractions were washed with brine (100 mL), dried over Na_2SO_4, filtered and concentrated *in vacuo* to afford the product **167** as a colourless oil which required no further purification (17.0 g, yield > 95%).

R_f: (hexane:diethyl ether, 1:1) = 0.62. **^{1}H NMR** (400 MHz, $CDCl_3$) δ: 7.24-7.32 (m, 6H, Ph), 7.19-7.24 (m, 4H, Ph), 4.13 (q, 4H, $^3J_{HH}$ = 7.1 Hz, OC$\underline{H}_2$CH$_3$), 3.26 (s, 4H, PhC$\underline{H}_2$), 1.18 (t, 6H, $^3J_{HH}$ = 7.1 Hz, OCH$_2$C$\underline{H}_3$). **^{13}C NMR** (101 MHz, $CDCl_3$) δ: 170.9 ($\underline{C}$=O), 136.3 (*ipso*-Ph), 130.1 (*ortho*-Ph), 128.1 (*meta*-Ph), 126.8 (*para*-Ph), 61.1 (O$\underline{C}$H$_2$CH$_3$), 60.1 ($\underline{C}$(Bn)$_2$), 39.1 (Ph$\underline{C}$H$_2$), 13.8 (OCH$_2$$\underline{C}H_3$). **LRMS** (*m/z*, ESI$^+$) calculated for $C_{21}H_{24}NaO_4^+$ ([M+Na]$^+$): 363.2, found 363.2.

2-Benzyl-3-phenylpropanoic acid (168)[278]



Potassium hydroxide (10.1 g, 181 mmol, 4.1 eq) was added to a solution of diethyl dibenzylmalonate (**167**, 15.0 g, 44.1 mmol, 1 eq) in ethanol (10 mL) and water (12 mL). The mixture was heated to 90ºC for 20h. After cooling to room temperature, water (40 mL) was added and the mixture was extracted with dichloromethane (2×40 mL). The aqueous phase was treated with hydrochloric acid (1M, 20 mL) and was further extracted with dichloromethane (3×40 mL). The combined organic fractions were dried over anhydrous

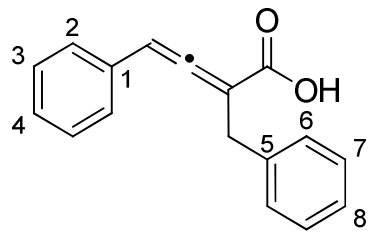
$MgSO_4$, filtered and concentrated *in vacuo*. The crude solid was then heated to 150ºC for 16h to encourage decarboxylation. Recrystallisation from ethanol afforded the product **168** as a yellow solid (7.52 g, yield = 71%).

^{1}H NMR (400 MHz, $CDCl_3$) δ: 7.27-7.32 (m, 4H, *meta*-Ph), 7.21-7.26 (m, 2H, *para*-Ph), 7.15-7.20 (m, 4H, *ortho*-Ph), 2.95-3.05 (m, 3H, C*H*$_2$Ph, C*H*(COOH)), 2.77-2.86 (m, 2H, C*H*$_2$Ph). *Note: The carboxylic acid proton peak was not observed.* **^{13}C NMR** (101 MHz, $CDCl_3$) δ: 180.1 (*C*=O), 138.7 (*ipso*-Ph), 128.9, 128.5 (*ortho*-, *meta*-Ph), 126.5 (*para*-Ph), 49.3 (*C*H(COOH)), 37.7 (*C*H$_2$Ph). **LRMS** (*m/z*, ESI$^-$): calculated for $C_{16}H_{15}O_2^-$ ([M–H]$^-$): 239.1, found 239.1.

6.3.3.4.3 Preparation of β-Fluoro-γ-Butenolide 107n

β-Fluoro-γ-Butenolide **107n** was prepared according to the procedure of Ma (see Scheme 3.56).[279]

2-Benzyl-4-phenylbuta-2,3-dienoic acid (157n)

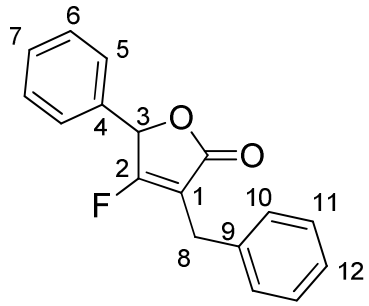


Trifluoroacetic acid (3.75 mL, 49.0 mmol, 30 eq) was added dropwise to a solution of allenoate **102n** (500 mg, 1.63 mmol, 1 eq) in dichloromethane (16 mL) at 0^{o}C. The reaction was allowed to reach room temperature and stirred for 30 min. The volatiles were removed *in vacuo* and the crude reaction mixture was purified by column chromatography on silica gel (hexane:ethyl acetate, 3:2 with a drop of acetic acid) to afford the product **157n** as a white solid (327 mg, yield = 80%).

R_f: (hexane:ethyl acetate, 3:2) = 0.18. **Mp =** 90°C. **^{1}H NMR** (400 MHz, $CDCl_3$) δ: 10.97 (br s, 1H), 7.37-7.20 (m, 10H, Ph), 6.62 (m, 1H, C*H*=C=C(C=O)), 3.74 (dd, 1H, $^2J_{HH}$ = 14.6

Hz, $^{5}J_{HH}$ = 2.2 Hz, PhC*H*H'), 3.68 (dd, 1H, $^{2}J_{HH}$ = 14.6 Hz, $^{5}J_{HH}$ = 2.2 Hz, PhCH*H'*). **^{13}C NMR** (125 MHz, $CDCl_3$) δ: 214.4 (C=*C*=C), 171.9 (*C*=O), 138.7 (*C5*), 131.4 (*C1*), 128.9, 128.8, 128.3, 127.4 (*C2*, *C3*, *C6*, *C7*), 128.0, 126.5 (*C4*, *C8*), 103.8 (CH=C=*C*(C=O)), 98.9 (*C*H=C=C(C=O)), 35.1 (Ph*C*H$_2$). **IR** (CH_2Cl_2): 3055 (O-H), 1944 (C=C=C), 1687 (C=O). **HRMS** (*m/z*, ESI$^+$): calculated for $C_{17}H_{14}NaO_2^+$ ([M+Na]$^+$): 273.0886, found 273.0885.

3-Benzyl-4-fluoro-5-phenylfuran-2(5*H*)-one (107n)



Selectfluor (341 mg, 0.962 mmol, 1.1 eq) was added to a solution of 2-benzyl-4-phenylbuta-2,3-dienoic acid (**157n**, 219 mg, 875 μmol, 1 eq) in acetonitrile (9 mL) and water (157 μL, 9.62 mmol, 10 eq). The reaction was heated to 80^{o}C and stirred for 16h. After cooling to room temperature, water (10 mL) was added and the reaction mixture was extracted with diethyl ether (3×10 mL). The combined organic fractions were washed with brine (20 mL), dried over anhydrous sodium sulfate, filtered and the solvent removed *in vacuo*. Column chromatography on silica gel (hexane:diethyl ether, 4:1) afforded the product **107n** as a white solid (72 mg, yield = 31%).

R$_f$: (hexane:diethyl ether, 1:1) = 0.47. **Mp** = 44°C. **^{1}H NMR** (500 MHz, $CDCl_3$) δ: 7.44-7.40 (m, 3H, Ph), 7.34-7.28 (m, 6H, Ph), 7.26 (m, 1H, Ph), 5.78 (d, 1H, $^{3}J_{HF}$ = 2.5 Hz, *H3*), 3.68 (d, 1H, $^{2}J_{HH}$ = 14.8 Hz, *H8*), 3.64 (d, 1H, $^{2}J_{HH}$ = 14.8 Hz, *H8'*). **^{13}C NMR** (125 MHz, $CDCl_3$) δ: 174.5 (d, $^{1}J_{CF}$ = 249 Hz, *C2*), 170.8 (d, $^{3}J_{CF}$ = 22 Hz, *C*=O), 136.6 (*C9*), 132.1 (*C4*), 130.0, 129.1, 128.8, 128.6, 126.9, 126.7 (*C5-7*, *C6-12*), 108.5 (d, $^{2}J_{CF}$ = 6 Hz, *C1*), 77.7 (d, $^{2}J_{CF}$ = 23 Hz, *C3*), 27.5 (d, $^{3}J_{CF}$ = 3 Hz, *C8*). **^{19}F NMR** (377 MHz, $CDCl_3$) δ:

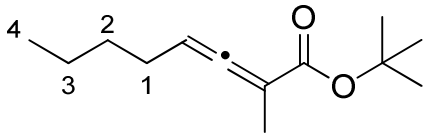
−108.4. **IR** (CH_2Cl_2): 1773 (C=O). **HRMS** (*m/z*, ESI^+): calculated for $C_{17}H_{13}FNaO_2^+$ ($[M+Na]^+$): 291.0792, found 291.0789.

6.4 Experimental Data for Chapter 4

6.4.1 Preparation of *tert*-Butyl Allenoates 102o-u and Ethyl Allenoate 105o

6.4.1.1 Preparation of *tert*-Butyl Allenoates 102o-u

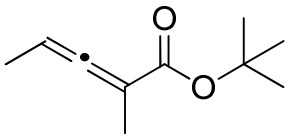
***tert*-Butyl 2-methylocta-2,3-dienoate (102o)**



General procedure C was followed using *tert*-butyl 2-(triphenylphosphoranylidene)propanoate **159b** (16.8 g, 42.8 mmol, 1.7 eq), hexanoyl chloride (3.53 mL, 25.2 mmol, 1 eq) and triethylamine (5.98 mL, 42.8 mmol, 1.7 eq) in dichloromethane (65 mL). The resulting crude mixture was purified by flash column chromatography on silica gel (hexane:diethyl ether, 20:1) to afford the product **102o** as a colourless oil (4.73 g, yield = 89%).

R_f (hexane:diethyl ether, 9:1) = 0.55. **^{1}H NMR** (400 MHz, $CDCl_3$) δ: 5.37 (m, 1H, C*H*C=C=C), 2.08 (dt, 2H, $^3J_{HH}$ = 6.8, 6.1 Hz, *H1*), 1.80 (dm, 3H, $^5J_{HH}$ = 2.8 Hz, CH=C=C(C*H*$_3$)), 1.46 (s, 9H, C(C*H*$_3$)$_3$), 1.35-1.43 (m, 4H, *H2*, *H3*), 0.90 (dd, 3H, $^3J_{HH}$ = 7.1, 6.1 Hz, *H4*). **^{13}C NMR** (101 MHz, $CDCl_3$) δ: 209.8 (C=*C*=C), 167.4 (*C*=O), 96.7 (CH=C=*C*(CH$_3$)), 93.1 (*C*H=C=C(CH$_3$)), 80.3 (*C*(CH$_3$)$_3$), 31.0 (*C1*), 28.1 (C(*C*H$_3$)$_3$), 27.6 (*C2*), 21.9 (*C3*), 15.2 (CH=C=C(*C*H$_3$)), 13.8 (*C4*). **IR** (neat): 1962 (C=C=C), 1706 (C=O). **HRMS** (*m/z*, ESI$^+$): calculated for $C_{13}H_{22}NaO_2^+$ ([M+Na]$^+$): 233.1512, found 233.1513.

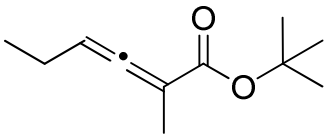
***tert*-Butyl 2-methylpenta-2,3-dienoate (102p)**



General procedure C was followed using *tert*-butyl 2-(triphenylphosphoranylidene)propanoate **159b** (2.40 g, 6.15 mmol, 1.7 eq), propanoyl chloride (316 μL, 3.62 mmol, 1 eq) and triethylamine (857 μL, 6.15 mmol, 1.7 eq) in dichloromethane (9.6 mL). The resulting crude mixture was purified by flash column chromatography on silica gel (hexane:diethyl ether, 20:1) to afford the product **102p** as a colourless oil (242 mg, yield = 40%).

R_f (hexane:diethyl ether, 9:1) = 0.58. **^{1}H NMR** (500 MHz, $CDCl_3$) δ: 5.37 (qq, 1H, $^3J_{HH}$ = 7.3 Hz, $^5J_{HH}$ = 2.8 Hz, C<u>*H*</u>C=C=C(CH_3)(C=O)), 1.81 (d, 3H, $^5J_{HH}$ = 2.8 Hz, CH=C=C(C<u>*H*</u>$_3$)(C=O)), 1.73 (d, 3H, $^3J_{HH}$ = 7.3 Hz, (C<u>*H*</u>$_3$)CH=C=C), 1.47 (s, 9H, C(C<u>*H*</u>$_3$)$_3$). **^{13}C NMR** (125 MHz, $CDCl_3$) δ: 210.4 (C=<u>*C*</u>=C), 167.3 (<u>*C*</u>=O), 96.4 (CH=C=<u>*C*</u>(CH_3)(C=O)), 88.0 (<u>*C*</u>H=C=C(CH_3)(C=O)), 80.4 (<u>*C*</u>(CH_3)$_3$), 28.1 (C(<u>*C*</u>H$_3$)$_3$), 15.2 (CH=C=C(<u>*C*</u>H$_3$)(C=O)), 13.8 ((<u>*C*</u>H$_3$)CH=C=C). **IR** (neat): 1961 (C=C=C), 1704 (C=O). **HRMS** (*m/z*, FI^+): calculated for $C_{10}H_{16}O_2$ ($[M]^+$): 168.1150, found 168.1145.

***tert*-Butyl 2-methylhexa-2,3-dienoate (102q)**

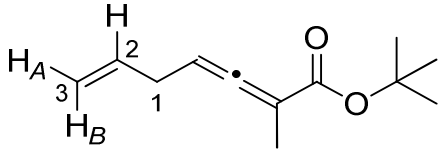


General procedure C was followed using *tert*-butyl 2-(triphenylphosphoranylidene)propanoate **159b** (2.00 g, 5.12 mmol, 1.7 eq), butanoyl chloride (315 μL, 3.01 mmol, 1 eq) and triethylamine (713 μL, 5.12 mmol, 1.7 eq) in dichloromethane (8 mL). The resulting crude mixture was purified by flash column chromatography on silica gel (hexane:diethyl ether, 20:1) to afford the product **102q** as a colourless oil (141 mg, yield = 26%).

R_f (hexane:diethyl ether, 9:1) = 0.47. **^{1}H NMR** (400 MHz, $CDCl_3$) δ: 5.42 (tq, 1H, $^3J_{HH}$ = 6.4 Hz, $^5J_{HH}$ = 2.8 Hz, C<u>*H*</u>C=C=C(CH_3)(C=O)), 2.07 (qd, 2H, $^3J_{HH}$ = 7.3, 6.4 Hz, C<u>*H*</u>$_2$CH$_3$),

1.79 (d, 3H, $^5J_{HH}$ = 2.8 Hz, CH=C=C(C$\underline{H}_3$)(C=O)), 1.44 (s, 9H, C(C$\underline{H}_3$)$_3$), 1.02 (t, 3H, $^3J_{HH}$ = 7.3 Hz, $CH_2C\underline{H}_3$). **^{13}C NMR** (101 MHz, $CDCl_3$) δ: 209.6 (C=$\underline{C}$=C), 167.3 ($\underline{C}$=O), 97.4 (CH=C=$\underline{C}$(CH_3)(C=O)), 94.9 ($\underline{C}$H=C=C(CH_3)(C=O)), 80.2 ($\underline{C}$(CH_3)$_3$), 28.0 (C($\underline{C}H_3$)$_3$), 21.3 ($\underline{C}H_2CH_3$), 15.1 (CH=C=C($\underline{C}H_3$)(C=O)), 13.3 ($CH_2\underline{C}H_3$). **IR** (neat): 1962 (C=C=C), 1703 (C=O). **HRMS** (*m/z*, ESI$^+$): calculated for $C_{11}H_{18}NaO_2^+$ ([M+Na]$^+$): 205.1199, found 205.1195.

***tert*-Butyl 2-methylhepta-2,3,6-trienoate (102r)**



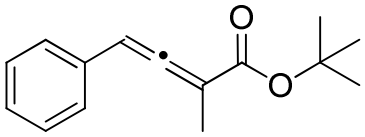
Oxalyl chloride (335 μL, 3.95 mmol, 1.05 eq) was carefully added to a solution of pent-4-enoic acid (384 μL, 3.77 mmol, 1 eq) in dichloromethane (7.5 mL) and dimethylformamide (1 drop) at 0ºC. The reaction mixture was stirred at 0ºC for 3h. The crude pent-4-enoyl chloride was concentrated *in vacuo* and used directly in the next step without further purification.

General procedure C was followed using *tert*-butyl 2-(triphenylphosphoranylidene)propanoate **159b** (2.50 g, 6.40 mmol, 1.7 eq), pent-4-enoyl chloride (3.77 mmol, 1 eq) and triethylamine (892 μL, 6.40 mmol, 1.7 eq) in anhydrous dichloromethane (40 mL). The resulting crude mixture was purified by column chromatography on silica gel (pet ether 40-60:diethyl ether, 20:1) to afford the product **102r** as a pale yellow oil (516 mg, yield = 77% over two steps).

R_f (hexane:diethyl ether, 9:1) = 0.55. **^{1}H NMR** (400 MHz, $CDCl_3$) δ: 5.82 (ddt, 1H, $^3J_{HH}$ = 16.9, 10.1, 6.3 Hz, *H2*), 5.37 (tq, 1H, $^3J_{HH}$ = 7.1 Hz, $^5J_{HH}$ = 2.8 Hz, C$\underline{H}$=C=C(CH_3)), 5.12 (dm, 1H, $^3J_{HH}$ = 16.9 Hz, $H3_B$), 5.02 (dm, 1H, $^3J_{HH}$ = 10.1 Hz, $H3_A$), 2.80 (dd, 2H, $^3J_{HH}$ = 7.1, 6.3 Hz, *H1*), 1.79 (d, 3H, $^5J_{HH}$ = 2.8 Hz, CH=C=C(C$\underline{H}_3$)), 1.43 (s, 9H, C(C$\underline{H}_3$)$_3$). **^{13}C**

NMR (101 MHz, $CDCl_3$) δ: 210.1 (C=<u>*C*</u>=C), 167.1 (<u>*C*</u>=O), 135.5 (*C2*), 115.7 (*C3*), 97.2 (CH=C=<u>*C*</u>(CH_3)), 91.1 (<u>*C*</u>H=C=C(CH_3)), 80.3 (<u>*C*</u>(CH_3)$_3$), 32.1 (*C1*), 28.0 (C(<u>*C*</u>H$_3$)$_3$), 15.0 (CH=C=C(<u>*C*</u>H$_3$)). **IR** (neat): 1962 (C=C=C), 1706 (C=O). **HRMS** (*m/z*, ESI^+): calculated for $C_{12}H_{18}NaO_2^+$ ([M+Na]$^+$): 217.1199, found 217.1203.

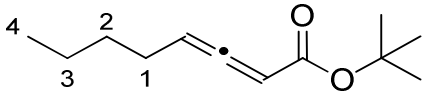
***tert*-Butyl 2-methyl-4-phenylbuta-2,3-dienoate (102s)**



General procedure C was followed using *tert*-butyl 2-(triphenylphosphoranylidene)propanoate **159b** (2.50 g, 6.40 mmol, 1.7 eq), phenylacetyl chloride (498 μL, 3.77 mmol, 1 eq) and triethylamine (892 μL, 6.40 mmol, 1.7 eq) in anhydrous dichloromethane (9.6 mL). The resulting crude mixture was purified by column chromatography on silica gel (pet ether 40-60:diethyl ether, 20:1) to afford the product **102s** as a yellow oil (172 mg, yield = 20%).

R$_f$ (hexane:diethyl ether, 9:1): 0.53. **^{1}H NMR** (500 MHz, $CDCl_3$) δ: 7.22-7.37 (m, 5H, Ph), 6.42 (q, 1H, $^5J_{HH}$ = 2.8 Hz, C<u>*H*</u>=C=C(CH_3)), 1.95 (d, 3H, $^5J_{HH}$ = 2.8 Hz, CH=C=C(C<u>*H*</u>$_3$)), 1.47 (s, 9H, C(C<u>*H*</u>$_3$)$_3$). **^{13}C NMR** (125 MHz, $CDCl_3$) δ: 212.1 (C=<u>*C*</u>=C), 166.3 (<u>*C*</u>=O), 132.9 (*ipso*-Ph), 128.7, 127.4, 127.2 (*ortho*-, *meta*-, *para*-Ph), 100.7 (CH=C=<u>*C*</u>(CH_3)), 96.6 (<u>*C*</u>H=C=C(CH_3)), 81.0 (<u>*C*</u>(CH_3)$_3$), 28.1 (C(<u>*C*</u>H$_3$)$_3$), 15.0 (CH=C=C(<u>*C*</u>H$_3$)). **IR** (neat): 1948 (C=C=C), 1702 (C=O). **HRMS** (*m/z*, ESI^+): calculated for $C_{15}H_{18}NaO_2^+$ ([M+Na]$^+$): 253.1199, found 253.1196.

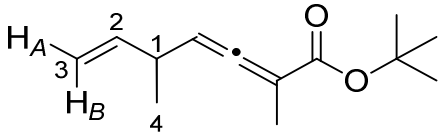
***tert*-Butyl octa-2,3-dienoate (102t)**



General procedure C was followed using *tert*-butyl (triphenylphosphoranylidene)acetate **159a** (12.0 g, 31.9 mmol, 1.7 eq), hexanoyl chloride (2.62 mL, 18.8 mmol, 1 eq) and triethylamine (4.44 mL, 31.9 mmol, 1.7 eq) in dichloromethane (48 mL). The resulting crude mixture was purified by flash column chromatography on silica gel (hexane:diethyl ether, 20:1) to afford the product **102t** and the isomeric alkyne side-product **108t** (allenoate:alkyne = 3.5:1) as a colourless oil (1.70 g, corrected yield of **102t** = 36%).

R_f (hexane:diethyl ether, 9:1) = 0.45. **^{1}H NMR** (500 MHz, $CDCl_3$) δ: 5.55 (td, 1H, $^3J_{HH}$ = 6.9 Hz, $^4J_{HH}$ = 6.0 Hz, $(C_4H_9)C\underline{H}C{=}C{=}CH$), 5.48 (dt, 1H, $^4J_{HH}$ = 6.0 Hz, $^5J_{HH}$ = 2.8 Hz, $(C_4H_9)CH{=}C{=}C\underline{H}$), 2.12 (tdd, 2H, $^3J_{HH}$ = 7.3, 6.9 Hz, $^5J_{HH}$ = 2.8 Hz, *H1*), 1.47 (s, 9H, $C(C\underline{H}_3)_3$), 1.34-1.48 (m, 4H, *H2*, *H3*), 0.91 (t, 3H, $^3J_{HH}$ = 7.3 Hz, *H4*). **^{13}C NMR** (125 MHz, $CDCl_3$) δ: 211.8 ($C{=}\underline{C}{=}C$), 165.6 ($\underline{C}{=}O$), 95.0 ($(C_4H_9)\underline{C}H{=}C{=}CH$), 89.7 ($(C_4H_9)CH{=}C{=}\underline{C}H$), 80.6 ($\underline{C}(CH_3)_3$), 30.9 (*C1*), 28.1 ($C(\underline{C}H_3)_3$), 27.2 (*C2*), 21.9 (*C3*), 13.8 (*C4*). **IR** (neat): 1961 (C=C=C), 1705 (C=O). **HRMS** (*m/z*, ESI^+): calculated for $C_{12}H_{20}NaO_2^+$ ($[M+Na]^+$): 219.1356, found 219.1353.

***tert*-Butyl 2,5-dimethylhepta-2,3,6-trienoate (102u)**



Oxalyl chloride (2 M solution in dichloromethane, 3.57 mL, 7.14 mmol, 1.05 eq) was carefully added to a solution of 3-methylpent-4-enoic acid (826 μL, 6.80 mmol, 1 eq) in dichloromethane (16 mL) and dimethylformamide (1 drop) at 0ºC. The reaction mixture was stirred at 0ºC for 3h. The crude 3-methylpent-4-enoyl chloride was concentrated *in vacuo* and used directly in the next step without further purification.

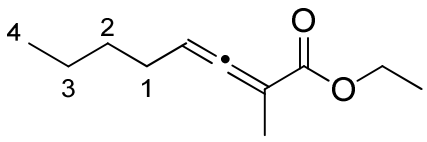
General procedure C was followed using *tert*-butyl 2-(triphenylphosphoranylidene)propanoate **159b** (4.51 g, 11.6 mmol, 1.7 eq), 3-methylpent-4-

enoyl chloride (806 mg, 6.80 mmol, 1 eq) and triethylamine (1.61 mL, 11.6 mmol, 1.7 eq) in anhydrous dichloromethane (40 mL). The resulting crude mixture was purified by column chromatography on silica gel (pet ether 40-60:diethyl ether, 20:1) to afford the product **102u** as a 50:50 diastereoisomeric mixture as a colourless oil (1.08 g, yield = 77% over two steps).

50:50 Mixture of Diastereoisomers: $\mathbf{R_f}$ (hexane:diethyl ether, 9:1) = 0.48. **^{1}H NMR** (400 MHz, $CDCl_3$) δ: 5.76-5.86 (m, 2H, *H2*), 5.36-5.42 (m, 2H, C*H*=C=C(CH_3)), 5.09 (d, 2H, $^3J_{HH}$ = 17.2 Hz, *H3$_B$*), 4.99 (d, 2H, $^3J_{HH}$ = 10.4 Hz, *H3$_A$*), 2.91-3.02 (m, 2H, *H1*), 1.82 (d, 6H, $^5J_{HH}$ = 2.8 Hz, CH=C=C(C*H*$_3$)), 1.46 (s, 18H, C(C*H*$_3$)$_3$), 1.14 (dd, 6H, $^3J_{HH}$ = 6.8 Hz, $^4J_{HH}$ = 2.8 Hz, *H4*). **^{13}C NMR** (125 MHz, $CDCl_3$) δ: 209.1 (C=*C*=C), 209.1 (C=*C*=C), 167.2 (*C*=O), 167.1 (*C*=O), 141.8 (*C2*), 141.8 (*C2*), 113.5 (*C3*), 98.2 (CH=C=*C*(CH_3)), 98.1 (CH=C=*C*(CH_3)), 97.4 (*C*H=C=C(CH_3)), 97.3 (*C*H=C=C(CH_3)), 80.3 (*C*(CH_3)$_3$), 80.3 (*C*(CH_3)$_3$), 36.9 (*C1*), 28.0 (C(*C*H$_3$)$_3$), 19.7 (*C4*), 19.6 (*C4*), 15.0 (CH=C=C(*C*H$_3$)), 14.9 (CH=C=C(*C*H$_3$)). *Note: The peaks for C1, C(CH$_3$)$_3$ and C3 are coincident for each diastereoisomer.* **IR** (neat): 1961 (C=C=C), 1707 (C=O). **HRMS** (*m/z*, ESI$^+$): calculated for $C_{13}H_{20}NaO_2^+$ ([M+Na]$^+$): 231.1356, found 231.1357.

6.4.1.2 Preparation of Ethyl Allenoate 105o

Ethyl 2-methylocta-2,3-dienoate (105o)



General procedure C was followed using ethyl 2-(triphenylphosphoranylidene)propanoate **159d** (2.00 g, 5.52 mmol, 1.7 eq), hexanoyl chloride (454 μL, 3.25 mmol, 1 eq) and triethylamine (769 μL, 5.52 mmol, 1.7 eq) in anhydrous dichloromethane (40 mL). The

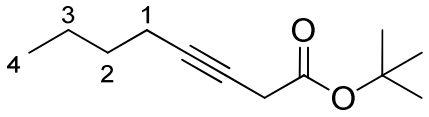
resulting crude mixture was purified by column chromatography on silica gel (pet ether 30-40:diethyl ether, 9:1) to afford the product **105o** as a colourless oil (284 mg, yield = 48%).

R_f (hexane:diethyl ether, 9:1) = 0.53. **^{1}H NMR** (400 MHz, $CDCl_3$) δ: 5.37 (tq, 1H, $^3J_{HH}$ = 6.8 Hz, $^5J_{HH}$ = 3.0 Hz, C*H*=C=C(CH_3)), 4.12 (m, 2H, OC*H*$_2$$CH_3$), 2.04 (td, 2H, $^3J_{HH}$ = 7.1, 6.8 Hz, *H1*), 1.81 (d, 3H, $^5J_{HH}$ = 3.0 Hz, CH=C=C(C*H*$_3$)), 1.22-1.48 (m, 4H, *H2*, *H3*), 1.21 (t, 3H, $^3J_{HH}$ = 7.1 Hz, OCH_2CH_3), 0.85 (t, 3H, $^3J_{HH}$ = 7.3 Hz, *H4*). **^{13}C NMR** (101 MHz, $CDCl_3$) δ: 209.9 (C=*C*=C), 167.8 (*C*=O), 95.4 (CH=C=*C*(CH_3)), 93.5 (*C*H=C=C(CH_3)), 60.5 (O*C*H_2CH_3), 30.8 (*C1*), 27.5 (*C2*), 21.8 (*C3*), 15.0 (CH=C=C(*C*H_3)), 14.0, 13.8 (*C4*, OCH_2CH_3). **IR** (neat): 1961 (C=C=C), 1708 (C=O). **HRMS** (*m/z*, ESI^+): calculated for $C_{11}H_{18}NaO_2^+$ ([M+Na]$^+$): 205.1199, found 205.1198.

6.4.1.3 Preparation of Alkyne 108t

Alkyne **108t** was prepared according to the procedure of Fu (see Scheme 6.4).[106]

***tert*-Butyl oct-3-ynoate (108t)**



1-Hexyne (124 µL, 1.08 mmol, 1 eq) and copper(I) iodide (10 mg, 54 µmol, 10 mol%) were dissolved in acetonitrile (1.5 mL). *tert*-Butyl diazoacetate (150 µL, 1.08 mmol, 1 eq) was added and the mixture was stirred for 12h at rt. The solvent was removed *in vacuo* and the crude product was purified by column chromatography on silica gel (pet ether 30-40:diethyl ether, 20:1) to afford alkyne **108t** as a colourless oil (60 mg, yield = 28%).

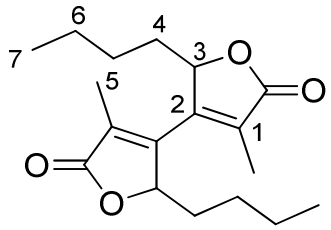
R_f: (hexane:diethyl ether, 9:1) = 0.45. **^{1}H NMR** (500 MHz, $CDCl_3$) δ: 3.15 (t, 2H, $^5J_{HH}$ = 2.5 Hz, C*H*$_2$(C=O)), 2.20 (tt, 2H, $^3J_{HH}$ = 7.3 Hz, $^5J_{HH}$ = 2.5 Hz, *H1*), 1.46 (s, 9H, C(C*H*$_3$)$_3$), 1.37-1.50 (m, 4H, *H2*, *H3*), 0.90 (t, 3H, $^3J_{HH}$ = 7.3 Hz, *H4*). **^{13}C NMR** (125 MHz, $CDCl_3$) δ: 168.2 (*C*=O), 83.6, 81.5 ((C_4H_9)*C*≡C, *C*(CH_3)$_3$), 71.2 ((C_4H_9)C≡*C*), 30.8 (*C2*), 27.9

(C($\underline{C}$H$_3$)$_3$), 27.2 ($\underline{C}$H$_2$(C=O)), 21.9 (*C3*), 18.4 (*C1*), 13.6 (*C4*). **IR** (neat): 2359 (C≡C), 1739 (C=O). **HRMS** (*m/z*, ESI$^+$): calculated for $C_{12}H_{20}NaO_2^+$ ([M+Na]$^+$): 219.1356, found 219.1350.

6.4.2 Cyclisation-Homodimerisation of Allenoates

6.4.2.1 Preliminary Investigations Using Sub-Stoichiometric Gold

2,2'-Dibutyl-4,4'-dimethyl-3,3'-bifuran-5,5'(2*H*,2'*H*)-dione (110o)



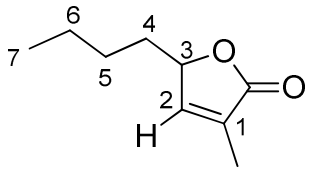
$AuCl_3$ (14 mg, 48 μmol, 5 mol%) was added to a solution of allenoate **102o** (200 mg, 951 μmol, 1 eq) in acetonitrile (6.4 mL). The mixture was stirred at rt for 48h. The crude reaction mixture was concentrated *in vacuo* and purified by column chromatography on silica gel (hexane:diethyl ether, 1:1) to afford a 75:25 diastereoisomeric mixture of the separable bibutenolides **110o** as colourless oils (20 mg, yield = 14%) and butenolide **103o** as a colourless oil (89 mg, yield = 61%).

Major Diastereoisomer: $\mathbf{R_f}$ (hexane:diethyl ether, 1:1) = 0.20. **^{1}H NMR** (400 MHz, $CDCl_3$) δ: 5.04 (m, 2H, *H3*), 1.92 (d, 6H, $^5J_{HH}$ = 1.5 Hz, (C=C)C$\underline{H}_3$)), 1.76 (m, 2H, *H4*), 1.28-1.44 (m, 10H, *H4'*, *H5*, *H6*), 0.89 (t, 6H, $^3J_{HH}$ = 7.1 Hz, *H7*). **^{13}C NMR** (125 MHz, $CDCl_3$) δ: 172.4 ($\underline{C}$=O), 151.1 (*C2*), 129.0 (*C1*), 81.1 (*C3*), 32.9 (*C4*), 26.8 (*C5*), 22.3 (*C6*), 13.8 (*C7*), 10.6 ((C=C)$\underline{C}$H$_3$). **IR** (CH_2Cl_2): 1753 (C=O). **HRMS** (*m/z*, ESI$^+$): calculated for $C_{18}H_{26}NaO_4^+$ ([M+Na]$^+$): 329.1723, found 329.1724.

Minor Diastereoisomer: $\mathbf{R_f}$ (hexane:diethyl ether, 1:1) = 0.14. **^{1}H NMR** (400 MHz, $CDCl_3$) δ: 4.94 (m, 2H, *H3*), 1.82 (s, 6H, (C=C)C$\underline{H}_3$), 1.79 (m, 2H, *H4*), 1.29-1.59 (m, 10H, *H4'*, *H5*, *H6*), 0.92 (t, 6H, $^3J_{HH}$ = 7.3 Hz, *H7*). **^{13}C NMR** (101 MHz, $CDCl_3$) δ: 172.1 ($\underline{C}$=O),

152.0 (*C2*), 129.5 (*C1*), 81.9 (*C3*), 33.1 (*C4*), 27.5 (*C5*), 22.2 (*C6*), 13.8 (*C7*), 10.0 ((C=C)*C*H$_3$). **IR** (CH_2Cl_2): 1756 (C=O). **HRMS** (*m/z*, ESI$^+$): calculated for $C_{18}H_{26}NaO_4^+$ ([M+Na]$^+$): 329.1723, found 329.1720.

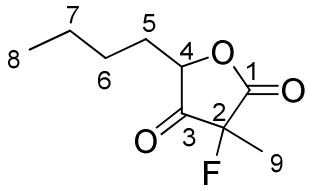
5-Butyl-3-methylfuran-2(5*H*)-one (103o)



R$_f$ (hexane:diethyl ether, 1:1) = 0.42. **^{1}H NMR** (400 MHz, $CDCl_3$) δ: 7.01 (m, 1H, *H2*), 4.81 (tq, 1H, $^3J_{HH}$ = 7.3 Hz, $^5J_{HH}$ = 1.8 Hz, *H3*), 1.83 (dd, 3H, $^4J_{HH}$ = 1.7 Hz, $^5J_{HH}$ = 1.8 Hz, (C=C)C*H*$_3$), 1.64 (m, 1H, *H4*), 1.54 (m, 1H, *H4'*), 1.22-1.39 (m, 4H, *H5*, *H6*), 0.82 (t, 3H, $^3J_{HH}$ = 6.9 Hz, *H7*). **^{13}C NMR** (101 MHz, $CDCl_3$) δ: 174.2 (*C*=O), 148.8 (*C2*), 129.4 (*C1*), 81.0 (*C3*), 32.9 (*C4*), 26.9 (*C5*), 22.2 (*C6*), 13.6 (*C7*), 10.3 ((C=C)*C*H$_3$). **IR** (neat): 1757 (C=O). **HRMS** (*m/z*, ESI$^+$): calculated for $C_9H_{14}NaO_2^+$ ([M+Na]$^+$): 177.0886, found 177.0886.

6.4.2.2 Preparation of the Cyclic Fluorinated β-Ketoester 188

5-Butyl-3-fluoro-3-methylfuran-2,4(3*H*,5*H*)-dione (188)

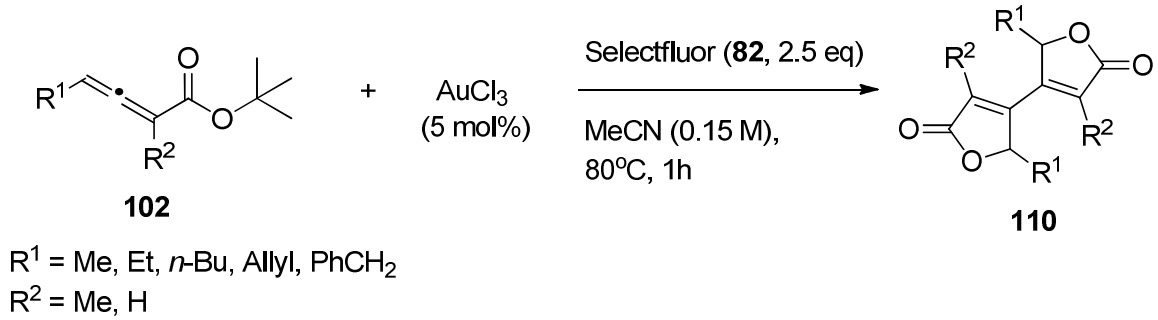


PPh_3AuNTf_2 (**2**, 35 mg, 48 μmol, 10 mol%) and Selectfluor (**82**, 421 mg, 1.19 mmol, 2.5 eq) were added to a solution of allenoate **102o** (100 mg, 4.75 mmol, 1 eq) in acetonitrile (48 mL) and water (428 μL, 23.8 mmol, 50 eq). The mixture was stirred at rt for 24h. The crude reaction mixture was filtered through Celite, dried over Na_2SO_4, filtered and concentrated *in*

vacuo. Purification by column chromatography on silica gel (pet ether 40-60:ethyl acetate, 2:1) afforded a 69:31 mixture of inseparable diastereoisomers of the cyclic fluorinated β-ketoester **188** as a colourless oil (38 mg, yield = 42%).

R_f (hexane:diethyl ether, 1:1) = 0.10. **^{1}H NMR** (400 MHz, $CDCl_3$) δ: **Major Diastereoisomer**: 4.86 (dd, 1H, $^3J_{HH}$ = 8.6, 5.1 Hz, *H4*), 1.96 (m, 1H, *H5*), 1.80 (m, 1H, *H5'*), 1.67 (d, 3H, $^3J_{HF}$ = 23.5 Hz, *H9*), 1.31-1.51 (m, 4H, *H6*, *H7*), 0.92 (t, 3H, $^3J_{HH}$ = 7.1 Hz, *H8*). **Minor Diastereoisomer**: 4.87 (m, 1H, *H4*), 1.96 (m, 1H, *H5*), 1.80 (m, 1H, *H5'*), 1.71 (d, 3H, $^3J_{HF}$ = 22.7 Hz, *H9*), 1.31-1.51 (m, 4H, *H6*, *H7*), 0.91 (t, 3H, $^3J_{HH}$ = 7.1 Hz, *H8*). *Note: Several peaks corresponding to each diastereoisomer overlapped with each other.* **^{13}C NMR** (125 MHz, $CDCl_3$) δ: **Mixture of Diastereoisomers**: 203.1 (*C3*), 203.0 (*C3*), 168.7 (*C1*), 168.5 (*C1*), 84.8 (d, $^1J_{CF}$ = 200 Hz, *C2*), 83.9 (d, $^3J_{CF}$ = 2 Hz, *C4*), 83.5 (d, $^1J_{CF}$ = 196 Hz, *C2*), 82.9 (d, $^3J_{CF}$ = 2 Hz, *C4*), 31.6 (*C5*), 30.6 (*C5*), 27.0 (*C6*), 26.3 (*C6*), 22.1 (*C7*), 22.0 (*C7*), 19.2 (d, $^2J_{CF}$ = 53 Hz, *C9*), 18.9 (d, $^2J_{CF}$ = 53 Hz, *C9*), 13.6 (C8), 13.6 (*C8*). **^{19}F NMR** (377 MHz, $CDCl_3$) δ: **Major Diastereoisomer**: −166.7 (q, $^3J_{HF}$ = 23 Hz). **Minor Diastereoisomer**: −169.3 (q, $^3J_{HF}$ = 24 Hz). **IR** (neat): 1825 (*C1*=O), 1776 (*C3*=O). **HRMS** (*m/z*, ESI$^-$): calculated for $C_9H_{12}FO_3^-$ ([M−H]$^-$): 187.0776, found 187.0774.

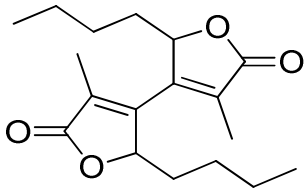
6.4.2.3 Scope and Limitations of the Gold-Catalysed Reaction



Scheme 6.6 Cascade Cyclisation-Homodimerisation of Allenoates **102**.

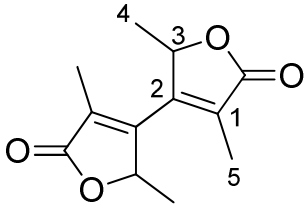
General Procedure E: $AuCl_3$ (5 mol%) and Selectfluor (**82**, 2.5 eq) were added to a solution of allenoate **102** (1 eq) in acetonitrile (0.15M). The reaction was stirred at 80ºC for 1h. The reaction mixture was cooled to rt and then diluted with dichloromethane and filtered through Celite. The crude mixture was purified by column chromatography on silica gel (hexane:diethyl ether 1:1).

2,2'-Dibutyl-4,4'-dimethyl-3,3'-bifuran-5,5'(2*H*,2'*H*)-dione (110o)



General procedure E was followed using allenoate **102o** (200 mg, 951 μmol, 1 eq), $AuCl_3$ (14 mg, 48 μmol, 5 mol%) and Selectfluor (**82**, 842 mg, 2.38 mmol, 2.5 eq) in acetonitrile (6.4 mL). The resulting crude mixture was purified by column chromatography on a short pad of silica gel (hexane:diethyl ether, 1:1) to afford a 52:48 diastereoisomeric mixture of separable bibutenolides **110o** as a colourless oil (114 mg, yield = 78%). For characterisation data of **110o**, see Section 6.4.2.1.

2,2',4,4'-Tetramethyl-3,3'-bifuran-5,5'(2*H*,2'*H*)-dione (110p)

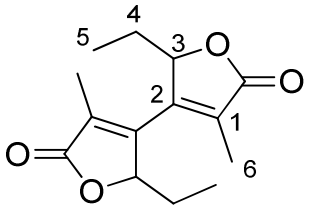


General procedure E was followed using allenoate **102p** (300 mg, 1.78 mmol, 1 eq), $AuCl_3$ (27 mg, 89 μmol, 5 mol%) and Selectfluor (**82**, 1.58 g, 4.46 mmol, 2.5 eq) in acetonitrile (12 mL). The resulting crude mixture was purified by column chromatography on a short pad of

silica gel (pet ether 30-40: ethyl acetate, 1:1) to afford a 50:50 diastereoisomeric mixture of inseparable bibutenolides **110p** as a white solid (71 mg, yield = 36%).

R_f (hexane:ethyl acetate, 1:1) = 0.28. **Mp** = 175ºC (decomp.). **^{1}H NMR** (500 MHz, $CDCl_3$) **Major Diastereoisomer**: δ: 5.17 (qm, 2H, $^3J_{HH}$ = 6.6 Hz, *H3*), 1.93 (d, 6H, $^5J_{HH}$ = 1.3 Hz, *H5*), 1.37 (d, 6H, $^3J_{HH}$ = 6.6 Hz, *H4*). **Minor Diastereoisomer**: δ: 5.07 (qm, 2H, $^3J_{HH}$ = 6.6 Hz, *H3*), 1.83 (d, 6H, $^5J_{HH}$ = 1.6 Hz, *H5*), 1.45 (d, 6H, $^3J_{HH}$ = 6.6 Hz, *H4*). **^{13}C NMR** (125 MHz, $CDCl_3$) δ: **50:50 Mixture of Diastereoisomers**: 172.2 (*C*=O), 171.9 (*C*=O), 152.6 (*C2*), 151.9 (*C2*), 129.4 (*C1*), 128.8 (*C1*), 78.1 (*C3*), 77.3 (*C3*), 18.9 (*C4*), 18.9 (*C4*), 10.4 (*C5*), 10.0 (*C5*). **IR** (CH_2Cl_2): 1749 (C=O). **HRMS** (*m/z*, FI^+): calculated for $C_{12}H_{14}O_4$ ($[M]^+$): 222.0892, found 222.0892.

2,2'-Diethyl-4,4'-dimethyl-3,3'-bifuran-5,5'(2*H*,2'*H*)-dione (110q)

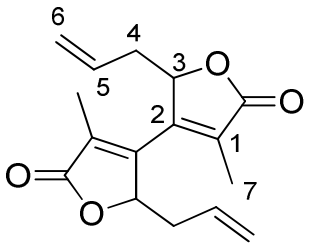


General procedure E was followed using allenoate **102q** (125 mg, 686 μmol, 1 eq), $AuCl_3$ (10 mg, 30 μmol, 5 mol%) and Selectfluor (**82**, 607 mg, 1.71 mmol, 2.5 eq) in acetonitrile (4.6 mL). The resulting crude mixture was purified by column chromatography on a short pad of silica gel (hexane:diethyl ether, 1:1) to afford a 55:45 diastereoisomeric mixture of inseparable bibutenolides **110q** as a colourless oil (68 mg, yield = 79%).

R_f (hexane:ethyl acetate, 1:1) = 0.35. **^{1}H NMR** (400 MHz, $CDCl_3$) **Major Diastereoisomer**: δ: 5.03 (m, 2H, *H3*), 1.90 (d, 6H, $^5J_{HH}$ = 1.8 Hz, *H6*), 1.87 (m, 2H, *H4*), 1.46 (m, 2H, *H4'*), 0.94 (t, 6H, $^3J_{HH}$ = 7.3 Hz, *H5*). **Minor Diastereoisomer**: δ: 4.89 (m, 2H, *H3*), 1.87 (m, 2H, *H4*), 1.81 (d, 6H, $^5J_{HH}$ = 1.6 Hz, *H6*), 1.46 (m, 2H, *H4'*), 1.06 (d, 3H, $^3J_{HH}$ = 7.3 Hz, *H5*). **^{13}C NMR** (125 MHz, $CDCl_3$) δ: **55:45 Mixture of Diastereoisomers**: 172.4 (*C*=O), 172.0

(*C*=O), 151.7 (*C2*), 150.7 (*C2*), 129.6 (*C1*), 129.2 (*C1*), 82.9 (*C3*), 81.9 (*C3*), 26.5 (*C4*), 26.1 (*C4*), 10.6 (*C6*), 10.0 (*C6*), 9.6 (*C5*), 8.5 (*C5*). **IR** (CH_2Cl_2): 1749 (C=O). **HRMS** (*m/z*, ESI^+): calculated for $C_{14}H_{18}NaO_4^+$ ($[M+Na]^+$): 273.1097, found 273.1097.

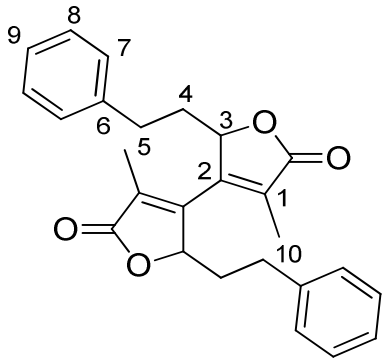
2,2'-Diallyl-4,4'-dimethyl-3,3'-bifuran-5,5'(2*H*,2'*H*)-dione (110r)



General procedure E was followed using allenoate **102r** (250 mg, 1.29 mmol, 1 eq), $AuCl_3$ (20 mg, 64 μmol, 5 mol%) and Selectfluor (**82**, 1.14 g, 3.22 mmol, 2.5 eq) in acetonitrile (8.6 mL). The resulting crude mixture was purified by column chromatography on a short pad of silica gel (hexane:ethyl acetate, 1:1) to afford a 50:50 diastereoisomeric mixture of inseparable bibutenolides **110r** as a colourless oil (82 mg, yield = 46%).

$\mathbf{R_f}$ (hexane:ethyl acetate, 1:1) = 0.40. **^{1}H NMR** (400 MHz, $CDCl_3$) **50:50 Mixture of Diastereoisomers**: δ: 5.76 (ddt, 2H, $^3J_{HH}$ = 16.4, 10.9, 6.8 Hz, *H5*), 5.64 (ddt, 2H, $^3J_{HH}$ = 17.2, 10.1, 6.8 Hz, *H5*), 5.14-5.22 (m, 6H, *H6*), 5.07-5.13 (m, 4H, *H3*, *H6*), 5.03 (tq, 2H, $^3J_{HH}$ = 5.8 Hz, $^5J_{HH}$ = 2.0 Hz, *H3*), 2.54-2.68 (m, 4H, *H4*), 2.24-2.32 (m, 4H, *H4*), 1.87 (d, 6H, $^5J_{HH}$ = 2.0 Hz, *H7*), 1.81 (d, 6H, $^5J_{HH}$ = 2.0 Hz, *H7*). **^{13}C NMR** (101 MHz, $CDCl_3$) δ: **50:50 Mixture of Diastereoisomers**: 172.0 (*C*=O), 171.7 (*C*=O), 151.0 (*C2*), 150.3 (*C2*), 130.7 (*C5*), 130.3 (*C1*), 130.0 (*C5*), 129.8 (*C1*), 120.2 (*C6*), 119.8 (*C6*), 81.1 (*C3*), 80.2 (*C3*), 36.9 (*C4*), 36.9 (*C4*), 10.7 (*C7*), 10.1 (*C7*). **IR** (CH_2Cl_2): 1748 (C=O). **HRMS** (*m/z*, ESI^+): calculated for $C_{16}H_{18}NaO_4^+$ ($[M+Na]^+$): 297.1097, found 297.1092.

4,4'-Dimethyl-2,2'-bis(2-phenylethyl)-3,3'-bifuran-5,5'(2*H*,2'*H*)-dione (110f)



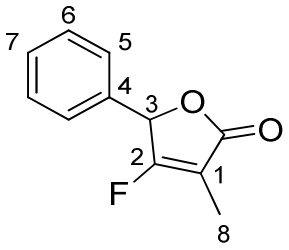
General procedure E was followed using allenoate **102f** (300 mg, 1.16 mmol, 1 eq), $AuCl_3$ (18 mg, 58 μmol, 5 mol%) and Selectfluor (**82**, 1.03 g, 2.90 mmol, 2.5 eq) in acetonitrile (7.7 mL). The resulting crude mixture was purified by column chromatography on a short pad of silica gel (hexane:diethyl ether, 1:1) to afford a 50:50 diastereoisomeric mixture of partially separable bibutenolides **110f** as a white solid (101 mg, yield = 43%).

Single Diastereoisomer: R_f (hexane:diethyl ether, 1:1) = 0.36. **Mp** = 168ºC. **^{1}H NMR** (500 MHz, $CDCl_3$) δ: 7.31 (ddm, 4H, $^3J_{HH}$ = 7.4, 7.1 Hz, *H8*), 7.24 (tm, 2H, $^3J_{HH}$ = 7.4 Hz, *H9*), 7.14 (dm, 4H, $^3J_{HH}$ = 7.1 Hz, *H7*), 4.89 (dm, 2H, $^3J_{HH}$ = 9.5 Hz, *H3*), 2.84 (ddd, 2H, $^2J_{HH}$ = 13.8 Hz, $^3J_{HH}$ = 8.8, 4.5 Hz, *H5*), 2.73 (dt, 2H, $^2J_{HH}$ = 13.8 Hz, $^3J_{HH}$ = 8.5 Hz, *H5'*), 1.87 (dddd, 2H, $^2J_{HH}$ = 14.4 Hz, $^3J_{HH}$ = 8.8, 8.5, 2.5 Hz, *H4*), 1.78 (d, 6H, $^4J_{HH}$ = 1.6 Hz, *H10*), 1.64 (dddd, 2H, $^2J_{HH}$ = 14.4 Hz, $^3J_{HH}$ = 9.5, 8.5, 4.5 Hz, *H4'*). **^{13}C NMR** (125 MHz, $CDCl_3$) δ: 170.3 (*C*=O), 150.7 (*C2*), 139.7 (*C6*), 129.1 (*C1*), 128.8, 128.5 (*C7*, *C8*), 126.7 (*C9*), 79.7 (*C3*), 35.5 (*C4*), 31.4 (*C5*), 10.5 (*C10*). **IR** (CH_2Cl_2): 1749 (C=O). **HRMS** (*m/z*, ESI^+): calculated for $C_{26}H_{26}NaO_4^+$ ($[M+Na]^+$): 425.1723, found 425.1706.

Single Diastereoisomer: R_f (hexane:diethyl ether, 1:1) = 0.31. **Mp** = 136ºC. **^{1}H NMR** (500 MHz, $CDCl_3$) δ: 7.27 (m, 4H, *H8*), 7.21 (tm, 2H, $^3J_{HH}$ = 7.3 Hz, *H9*), 7.10 (dm, 4H, $^3J_{HH}$ = 6.9 Hz, *H7*), 4.77 (dm, 2H, $^3J_{HH}$ = 10.7 Hz, *H3*), 2.87 (ddd, 2H, $^2J_{HH}$ = 13.8 Hz, $^3J_{HH}$ = 7.9, 4.4 Hz, *H5*), 2.77 (ddd, 2H, $^2J_{HH}$ = 13.8 Hz, $^3J_{HH}$ = 8.8, 7.9 Hz, *H5'*), 1.79 (d, 6H, $^4J_{HH}$ = 1.6 Hz, *H10*), 1.76 (m, 2H, *H4*), 1.61 (m, 2H, *H4'*). **^{13}C NMR** (125 MHz, $CDCl_3$) δ: 171.9

(*C*=O), 151.8 (*C2*), 139.5 (*C6*), 129.7 (*C1*), 128.7, 128.7 (*C7*, *C8*), 126.6 (*C9*), 80.3 (*C3*), 35.4 (*C4*), 31.7 (*C5*), 10.1 (*C10*). **IR** (CH_2Cl_2): 1750 (C=O). **HRMS** (*m/z*, ESI^+): calculated for $C_{26}H_{26}NaO_4^+$ ($[M+Na]^+$): 425.1723, found 425.1713.

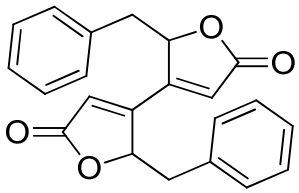
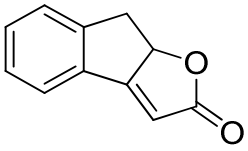
4-Fluoro-3-methyl-5-phenylfuran-2(5*H*)-one (107s)



General procedure E was followed using allenoate **102s** (207 mg, 899 μmol, 1 eq), $AuCl_3$ (14 mg, 45 μmol, 5 mol%) and Selectfluor (**82**, 796 mg, 2.25 mmol, 2.5 eq) in acetonitrile (6 mL). The reaction was stirred at 80ºC for 2h. The resulting crude mixture was purified by column chromatography on silica gel (hexane:diethyl ether, 3:1) to afford the β-fluoro-γ-butenolide **102s** as a yellow oil (45 mg, yield = 26%).

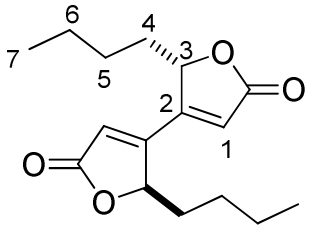
R_f (hexane:diethyl ether, 1:1) = 0.43. **^{1}H NMR** (400 MHz, $CDCl_3$) δ: 7.40-7.45 (m, 3H, *H6*, *H7*), 7.32-7.36 (m, 2H, *H5*), 5.77 (dq, 1H, $^3J_{HF}$ = 3.0 Hz, $^3J_{HH}$ = 1.8 Hz, *H3*), 1.88 (dd, 3H, $^4J_{HF}$ = 2.0 Hz, $^5J_{HH}$ = 1.8 Hz, *H8*). **^{13}C NMR** (101 MHz, $CDCl_3$) δ: 174.3 (d, $^1J_{CF}$ = 296 Hz, *C2*), 171.6 (d, $^3J_{CF}$ = 22 Hz, *C*=O), 132.2 (d, $^3J_{CF}$ = 2 Hz, *C4*), 129.8 (*C7*), 129.0 (*C6*), 126.6 (*C5*), 104.8 (d, $^2J_{CF}$ = 6 Hz, *C1*), 77.7 (d, $^2J_{CF}$ = 23 Hz, *C3*), 6.0 (d, $^3J_{CF}$ = 2 Hz, *C8*). **^{19}F NMR** (377 MHz, $CDCl_3$) δ: −110.0. **IR** (CH_2Cl_2): 1774 (C=O). **HRMS** (*m/z*, ESI^+): calculated for $C_{11}H_9FNaO_2^+$ ($[M+Na]^+$): 215.0479, found 215.0487.

2,2'-Dibenzyl-3,3'-bifuran-5,5'(2*H*,2'*H*)-dione (110b) and 8,8a-Dihydro-2*H*-indeno[2,1-*b*]furan-2-one (109b)

General procedure E was followed using allenoate **102b** (as a mixture with its isomeric alkyne, allenoate:alkyne 2.6:1, 200 mg, 868 μmol, 1 eq), $AuCl_3$ (13 mg, 43 μmol, 5 mol%) and Selectfluor (**82**, 769 mg, 2.17 mmol, 2.5 eq) in acetonitrile (5.8 mL). The resulting crude mixture was purified by column chromatography on a short pad of silica gel (hexane:diethyl ether, 1:1) to afford a 52:48 diastereoisomeric mixture of the separable bibutenolide **110b** as a white solid (66 mg, yield (based on **102b**) = 60%) and the indenofuranone **109b** as a light brown solid (40 mg, yield (based on **102b**) = 37%). For characterisation data of **110b** and **109b**, see Section 6.3.3.1.2.

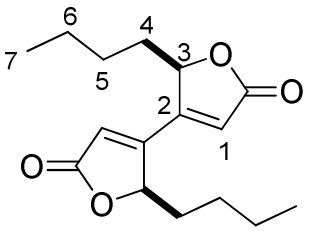
(2*R*,2'*S*)-2,2'-Dibutyl-3,3'-bifuran-5,5'(2*H*,2'*H*)-dione ((2*R*,2'*S*)-(110t))



General procedure E was followed using allenoate **102t** (as a mixture with its isomeric alkyne, allenoate:alkyne = 3.5:1, 200 mg, 1.02 mmol, 1 eq), $AuCl_3$ (15 mg, 55 μmol, 5 mol%) and Selectfluor (**82**, 902 mg, 2.55 mmol, 2.5 eq) in acetonitrile (6.8 mL). The resulting crude mixture was purified by column chromatography on a short pad of silica gel (hexane:diethyl ether, 1:1) to afford a 52:48 diastereoisomeric mixture of separable bibutenolides (2*R*,2'*S*)-**110t** (white solid, 45 mg, dr > 95:5, yield (based on **102t**) = 41%) and (±)-(2*R*,2'*R*)-**110t** (colourless oil, 55 mg, dr > 95:5, yield (based on **102t**) = 50%).

R_f (hexane:diethyl ether, 1:1) = 0.17. **Mp** = 154ºC. **^{1}H NMR** (500 MHz, $CDCl_3$) δ: 6.26 (d, 2H, $^4J_{HH}$ = 1.3 Hz, *H1*), 5.26 (ddd, 2H, $^3J_{HH}$ = 7.6, 4.1 Hz, $^4J_{HH}$ = 1.3 Hz, *H3*), 2.09 (m, 2H, *H4*), 1.66 (m, 2H, *H4'*), 1.29-1.45 (m, 8H, *H5*, *H6*), 0.91 (dd, 6H, $^3J_{HH}$ = 7.3, 6.9 Hz, *H7*). **^{13}C NMR** (125 MHz, $CDCl_3$) δ: 170.7 (*C*=O), 155.5 (*C2*), 121.2 (*C1*), 82.7 (*C3*), 33.6 (*C4*), 26.3 (*C5*), 22.2 (*C6*), 13.8 (*C7*). **IR** (CH_2Cl_2): 1733 (C=O). **HRMS** (*m/z*, ESI^+): calculated for $C_{16}H_{22}NaO_4^+$ ($[M+Na]^+$): 301.1410, found 301.1404. The structure and relative stereochemistry were unambiguously assigned by X-ray crystallography. This data is included in the Appendix .

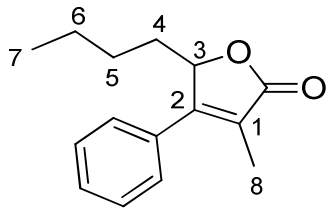
(2*R*,2'*R*)-2,2'-Dibutyl-3,3'-bifuran-5,5'(2*H*,2'*H*)-dione ((±)-(2*R*,2'*R*)-(110t))



R_f (hexane:diethyl ether, 1:1) = 0.09. **^{1}H NMR** (500 MHz, $CDCl_3$) δ: 6.21 (d, 2H, $^4J_{HH}$ = 1.3 Hz, *H1*), 5.30 (ddd, 2H, $^3J_{HH}$ = 7.9, 4.4 Hz, $^4J_{HH}$ = 1.3 Hz, *H3*), 2.01 (m, 2H, *H4*), 1.59 (m, 2H, *H4'*), 1.30-1.48 (m, 8H, *H5*, *H6*), 0.91 (dd, 6H, $^3J_{HH}$ = 7.3, 6.9 Hz, *H7*). **^{13}C NMR** (125 MHz, $CDCl_3$) δ: 170.7 (*C*=O), 156.1 (*C2*), 120.9 (*C1*), 82.2 (*C3*), 33.0 (*C4*), 26.4 (*C5*), 22.2 (*C6*), 13.8 (*C7*). **IR** (CH_2Cl_2): 1740 (C=O). **HRMS** (*m/z*, ESI^+): calculated for $C_{16}H_{22}NaO_4^+$ ($[M+Na]^+$): 301.1410, found 301.1404. The stereochemistry was assigned by comparison with its diastereoisomer (2*R*,2'*S*)-**110t** (see above).

6.4.3 Cyclisation-Intermolecular Arylation of Allenoates

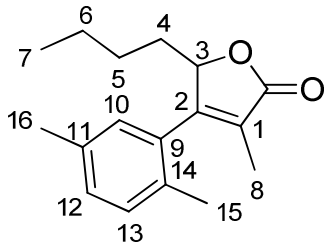
5-Butyl-3-methyl-4-phenylfuran-2(5*H*)-one (192oa)



$Ph_3PAuNTf_2$ (**2**, 35 mg, 48 µmol, 10 mol%) and Selectfluor (**82**, 421 mg, 1.19 mmol, 2.5 eq.) were added to a solution of allenoate **102o** (100 mg, 475 µmol, 1 eq) and benzene (425 µL, 4.75 mmol, 10 eq) in acetonitrile (3.2 mL). The mixture was stirred at rt until TLC showed complete consumption of the allenoate (48h). Dichloromethane (10 mL) was added and the mixture was filtered through Celite. After drying over anhydrous Na_2SO_4 and filtration, the solvent was removed *in vacuo*. The resulting crude mixture was purified by column chromatography on silica gel (pet. ether 30-40:diethyl ether, 4:1 to 1:1) to afford the product **192oa** as a colourless oil (6 mg, yield = 5%) as well as bibutenolides **110o** as a colourless oil (30 mg, dr = 50:50, yield = 41%). For characterisation data of **110o**, see Section 6.4.2.1.

R_f (hexane:diethyl ether, 1:1) = 0.40. **^{1}H NMR** (500 MHz, $CDCl_3$) δ: 7.44-7.52 (m, 3H, *meta*-, *para*-Ph), 7.34 (dm, 2H, $^3J_{HH}$ = 6.6 Hz, o*rtho*-Ph), 5.34 (m, 1H, *H3*), 2.05 (d, 3H, $^5J_{HH}$ = 1.8 Hz, *H8*), 1.81 (m, 1H, *H4*), 1.20-1.50 (m, 5H, *H4'*, *H5, H6*), 0.84 (t, 3H, $^3J_{HH}$ = 7.3 Hz, *H7*). **^{13}C NMR** (125 MHz, $CDCl_3$) δ: 174.6 (*C*=O), 159.5 (*C2*), 131.7 (*ipso*-Ph), 129.7 (*para*-Ph), 129.0 (*meta*-Ph), 127.7 (*ortho*-Ph), 123.7 (*C1*), 81.8 (*C3*), 32.7 (*C4*), 26.6 (*C5*), 22,3 (*C6*), 13.8 (*C7*), 10.0 (*C8*). **IR** (neat): 1749 (C=O). **HRMS** (*m/z*, ESI^+): calculated for $C_{15}H_{18}NaO_2^+$ ($[M+Na]^+$): 253.1199 found 253.1199.

5-Butyl-4-(2,5-dimethylphenyl)-3-methylfuran-2(5*H*)-one (192ob)



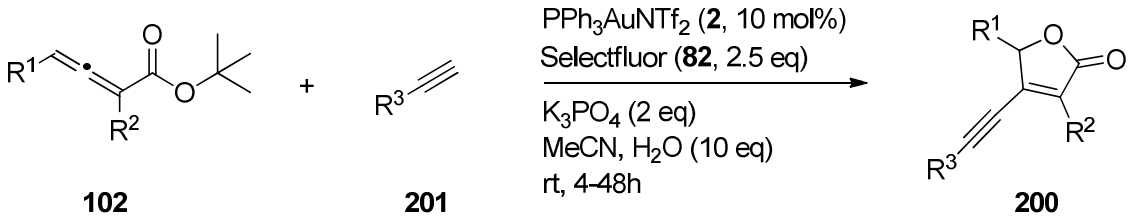
$Ph_3PAuNTf_2$ (**2**, 35 mg, 48 µmol, 10 mol%) and Selectfluor (421 mg, 1.19 mmol, 2.5 eq.) were added to a solution of allenoate **102o** (100 mg, 475 µmol, 1 eq) and *para*-xylene (586 µL, 4.75 mmol, 10 eq) in acetonitrile (3.2 mL). The mixture was stirred at rt until TLC showed complete consumption of the allenoate (20h). Dichloromethane (10 mL) was added and the mixture was filtered through Celite. After drying over anhydrous Na_2SO_4 and filtration, the solvent was removed *in vacuo*. The resulting crude mixture was purified by column chromatography on silica gel (pet. ether 30-40:diethyl ether, 4:1 to 1:1) to afford the product **192ob** as a colourless oil (15 mg, yield = 12%) as well as butenolide **103o** as a colourless oil (5 mg, yield = 7%) and bibutenolides **110o** as a colourless oil (29 mg, dr = 50:50, yield = 40%). For characterisation data of **103o** and **110o**, see Section 6.4.2.1.

R_f (hexane:diethyl ether, 1:1) = 0.46. **^{1}H NMR** (400 MHz, $CDCl_3$) δ: 7.19 (d, 1H, $^3J_{HH}$ = 7.8 Hz), 7.13 (d, 1H, $^3J_{HH}$ = 7.8 Hz, *H12*, *H13*), 6.84 (s, 1H, *H10*), 5.12 (m, 1H, *H3*), 2.35 (s, 3H), 2.18 (s, 3H, *H15*, *H16*), 1.77 (d, 3H, $^5J_{HH}$ = 1.9 Hz, *H8*), 1.64 (m, 1H, *H4*), 1.20-1.54 (m, 5H, *H4', H5*, *H6*), 0.85 (t, 3H, $^3J_{HH}$ = 7.3 Hz, *H7*). **^{13}C NMR** (125 MHz, $CDCl_3$) δ: 174.4 (*C*=O), 162.0 (*C2*), 135.6, 132.2, 131.3 (*C9*, *C11, C14*), 130.7, 129.9 (*C12*, *C13*), 128.1 (*C10*), 125.4 (*C1*), 83.4 (*C3*), 32.4 (*C4*), 27.5 (*C5*), 22,3 (*C6*), 20.9, 19.3 (*C15*, *C16*), 13.8 (*C7*), 9.7 (*C8*). **IR** (neat): 1757 (C=O). **HRMS** (*m/z*, ESI$^+$): calculated for $C_{17}H_{22}NaO_2^+$ ($[M+Na]^+$): 281.1512 found 281.1511.

6.4.4 Cyclisation-Intermolecular Alkynylation of Allenoates

6.4.4.1 Scope and Limitations

The experimental results detailed in this section were obtained by Jonathan E. Ross (Chemistry Part II, University of Oxford, 2010).[206]

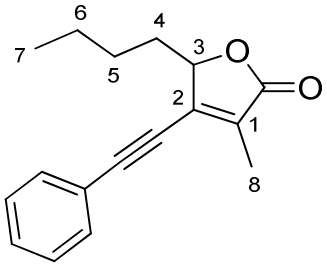


R^1 = Bu, Allyl, CH(Me)CH=CH_2 R^3 = Aryl, Alkyl
R^2 = Me, $PhCH_2$ Silyl
R^3 = H, Me

Scheme 6.7 Cyclisation-Intermolecular Alkynylation of Allenoates.

General Procedure F: $Ph_3PAuNTf_2$ (**2**, 10 mol%), Selectfluor (**82**, 2.5 eq), potassium phosphate tribasic (2 eq) and the alkyne **201** (1.5 eq) were added to a stirring solution of the allenoate **102** (100 mg, 1 eq) in acetonitrile (0.15 M) and water (10 eq). The reaction was stirred at rt until TLC showed complete consumption of the allenoate (4-48h). The reaction mixture was diluted with dichloromethane (20 mL), filtered through Celite, dried over anhydrous Na_2SO_4, filtered again and concentrated *in vacuo*. The resulting crude mixture was purified by column chromatography on silica gel.

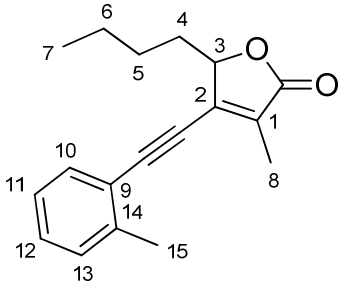
5-Butyl-3-methyl-4-(phenylethynyl)furan-2(5*H*)-one (200a)



General procedure F was followed using allenoate **102o** (100 mg, 475 μmol, 1 eq), alkyne **201a** (78 μL, 0.71 mmol, 1.5 eq), PPh_3AuNTf_2 (**2**, 35 mg, 48 μmol, 10 mol%), Selectfluor (**82**, 421 mg, 1.19 mmol, 2.5 eq) and K_3PO_4 (202 mg, 951 μmol, 2 eq) in acetonitrile (5 mL) and water (86 μL, 4.8 mmol, 10 eq). The mixture was stirred at rt for 4h. The resulting crude mixture was purified by column chromatography on silica gel (pet ether 40-60:diethyl ether, 4:1) to afford the product **200oa** as a yellow oil (114 mg, yield = 94%).

R_f (hexane:diethyl ether, 1:1): 0.54. **^{1}H NMR** (500 MHz, $CDCl_3$) δ: 7.51-7.55 (m, 2H, *ortho*-Ph), 7.38-7.45 (m, 3H, *meta*-, *para*-Ph), 4.92 (m, 1H, *H3*), 2.05 (d, 3H, $^5J_{HH}$ = 1.9 Hz, *H8*), 2.04 (m, 1H, *H4*), 1.66 (m, 1H, *H4'*), 1.44-1.52 (m, 2H, *H5*), 1.34-1.44 (m, 2H, *H6*), 0.93 (t, 3H, $^3J_{HH}$ = 7.3 Hz, *H7*). **^{13}C NMR** (125 MHz, $CDCl_3$) δ: 173.8 (*C*=O), 143.5 (*C2*), 132.0 (*C1*), 131.9, 129.9, 128.6 (*ortho*-, *meta*-, *para*-Ph), 121.5 (*ipso*-Ph), 105.9 (Ph*C*≡C), 82.3 (*C3*), 79.8 (PhC≡*C*), 32.7 (*C4*), 26.6 (*C5*), 22.4 (*C6*), 13.9 (*C7*), 10.3 (*C8*). **IR** (CH_2Cl_2): 2205 (C≡C), 1757 (C=O). **HRMS** (*m/z*, ESI^+): calculated for $C_{17}H_{18}NaO_2^+$ ($[M+Na]^+$): 277.1199, found 277.1200.

5-Butyl-3-methyl-4-[(2-methylphenyl)ethynyl]furan-2(5*H*)-one (200ob)

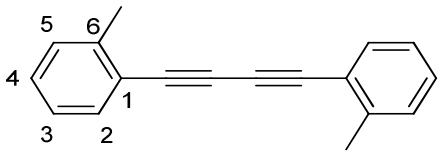


General procedure F was followed using allenoate **102o** (100 mg, 475 μmol, 1 eq), alkyne **201b** (90 μL, 0.71 mmol, 1.5 eq), PPh_3AuNTf_2 (**2**, 35 mg, 48 μmol, 10 mol%), Selectfluor (**82**, 421 mg, 1.19 mmol, 2.5 eq) and K_3PO_4 (202 mg, 951 μmol, 2 eq) in acetonitrile (5 mL) and water (86 μL, 4.8 mmol, 10 eq). The mixture was stirred at rt for 48h. The resulting crude mixture was purified by column chromatography on silica gel (pet ether 40-60:diethyl

ether, 10:1) to afford the product **200ob** as a yellow oil (54 mg, yield = 42%) along with diyne **202b** as a yellow solid (9 mg, yield (relative to **201b**) = 11%).

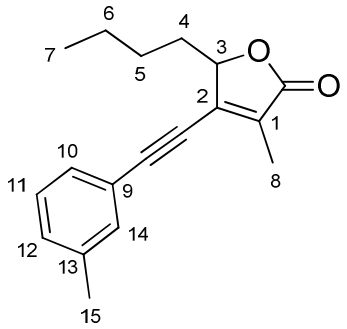
R_f (hexane:diethyl ether, 1:1): 0.33. **^{1}H NMR** (500 MHz, $CDCl_3$) δ: 7.49 (d, 1H, $^3J_{HH}$ = 7.6 Hz, *H13*), 7.19-7.36 (m, 3H, *H10-12*), 4.95 (m, 1H, *H3*), 2.49 (s, 3H, *H15*), 2.06 (s, 3H, *H8*), 2.04 (m, 1H, *H4*), 1.68 (m, 1H, *H4'*), 1.35-1.52 (m, 4H, *H5*, *H6*), 0.93 (t, 3H, $^3J_{HH}$ = 6.8 Hz, *H7*). **^{13}C NMR** (125 MHz, $CDCl_3$) δ: 173.8 (*C*=O), 143.7 (*C2*), 140.5 (*C14*), 131.6 (*C1*), 132.3, 130.0, 129.8, 125.9 (*C10-13*), 121.3 (*C9*), 105.0 (Ar*C*≡C), 83.6 (ArC≡*C*), 82.3 (*C3*), 32.7 (*C4*), 26.5 (*C5*), 22.4 (*C6*), 20.7 (*C15*), 13.8 (*C7*), 10.3 (*C8*). **IR** (CH_2Cl_2): 2200 (C≡C), 1754 (C=O). **HRMS** (*m/z*, ESI^+): calculated for $C_{18}H_{20}NaO_2^+$ ($[M+Na]^+$): 291.1356, found 291.1354.

1,1'-Buta-1,3-diyne-1,4-diylbis(2-methylbenzene) (202b)[280]



R_f (hexane:diethyl ether, 1:1): 0.33. **^{1}H NMR** (400 MHz, $CDCl_3$) δ: 7.14-7.48 (m, 8H, Ar), 2.50 (s, 6H, C*H*$_3$). **^{13}C NMR** (101 MHz, $CDCl_3$) δ: 141.5 (*C6*), 132.9 (*C2*), 129.5 (*C4*), 129.0 (*C5*), 125.6 (*C3*), 121.6 (*C1*), 81.2 (Ar*C*≡C), 77.6 (ArC≡*C*), 20.7 (*C*H$_3$).

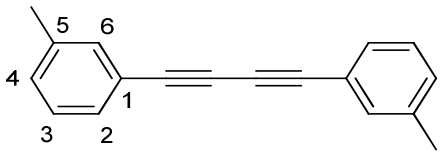
5-Butyl-3-methyl-4-[(3-methylphenyl)ethynyl]furan-2(5*H*)-one (200oc)



General procedure F was followed using allenoate **102o** (100 mg, 475 μmol, 1 eq), alkyne **201c** (92 μL, 0.71 mmol, 1.5 eq), PPh_3AuNTf_2 (**2**, 35 mg, 48 μmol, 10 mol%), Selectfluor (**82**, 421 mg, 1.19 mmol, 2.5 eq) and K_3PO_4 (202 mg, 951 μmol, 2 eq) in acetonitrile (5 mL) and water (86 μL, 4.8 mmol, 10 eq). The mixture was stirred at rt for 48h. The resulting crude mixture was purified by column chromatography on silica gel (pet ether 40-60:diethyl ether, 10:1) to afford the product **200oc** as a yellow oil (91 mg, yield = 71%) along with diyne **202c** (13 mg, yield (relative to **201c**) = 16%).

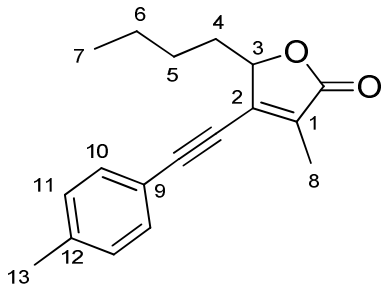
R_f (hexane:diethyl ether, 1:1): 0.34. **^{1}H NMR** (400 MHz, $CDCl_3$) δ: 7.21-7.37 (m, 4H, *H10-12*, *H14*), 4.91 (m, 1H, *H3*), 2.38 (s, 3H, *H15*), 2.05 (d, 3H, $^5J_{HH}$ = 1.5 Hz, *H8*), 2.01 (m, 1H, *H4*), 1.67 (m, 1H, *H4'*), 1.34-1.52 (m, 4H, *H5*, *H6*), 0.93 (t, 3H, $^3J_{HH}$ = 7.1 Hz, *H7*). **^{13}C NMR** (101 MHz, $CDCl_3$) δ: 173.8 (*C*=O), 143.6 (*C2*), 138.4 (*C13*), 132.3 (*C1*), 131.8, 130.8, 129.0, 128.5 (*C10-12*, *C14*), 121.3 (*C9*), 106.2 (Ar*C*≡C), 82.3 (*C3*), 79.4 (ArC≡*C*), 32.7 (*C4*), 26.6 (*C5*), 22.4 (*C6*), 21.2 (*C15*), 13.9 (*C7*), 10.3 (*C8*). **IR** (CH_2Cl_2): 2205 (C≡C), 1757 (C=O). **HRMS** (*m/z*, ESI^+): calculated for $C_{18}H_{20}NaO_2^+$ ($[M+Na]^+$): 291.1356, found 291.1355.

1,1'-Buta-1,3-diyne-1,4-diylbis(3-methylbenzene) (202c)[280]



R_f (hexane:diethyl ether, 1:1): 0.33. **^{1}H NMR** (400 MHz, $CDCl_3$) δ: 7.24-7.27 (m, 4H, Ar), 6.96-7.17 (m, 4H, Ar), 2.26 (s, 6H, C*H*$_3$). **^{13}C NMR** (101 MHz, $CDCl_3$) δ: 138.1 (*C5*), 133.0 (*C4*), 130.1, 129.6 (*C2*, *C6*), 128.3 (*C3*), 121.6 (*C1*), 81.6 (Ar*C*≡C), 73.6 (ArC≡*C*), 21.2 (*C*H$_3$).

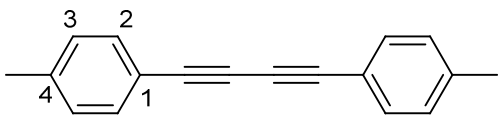
5-Butyl-3-methyl-4-[(4-methylphenyl)ethynyl]furan-2(5*H*)-one (200od)



General procedure F was followed using allenoate **102o** (100 mg, 475 μmol, 1 eq), alkyne **201d** (90 μL, 0.71 mmol, 1.5 eq), PPh_3AuNTf_2 (**2**, 35 mg, 48 μmol, 10 mol%), Selectfluor (**82**, 421 mg, 1.19 mmol, 2.5 eq) and K_3PO_4 (202 mg, 951 μmol, 2 eq) in acetonitrile (5 mL) and water (86 μL, 4.8 mmol, 10 eq). The mixture was stirred at rt for 48h. The resulting crude mixture was purified by column chromatography on silica gel (pet ether 40-60:diethyl ether, 10:1) to afford the product **200od** as a yellow oil (126 mg, yield > 95%) along with diyne **202d** (4 mg, yield (relative to **201d**) = 5%).

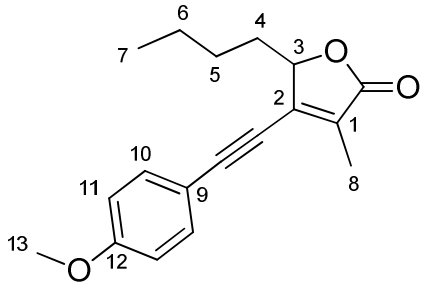
R_f (hexane:diethyl ether, 1:1): 0.32. **^{1}H NMR** (400 MHz, $CDCl_3$) δ: 7.41 (d, 2H, $^3J_{HH}$ = 8.2 Hz, *H10*), 7.19 (d, 2H, $^3J_{HH}$ = 8.2 Hz, *H11*), 4.90 (m, 1H, *H3*), 2.39 (s, 3H, *H13*), 2.03 (d, 3H, $^5J_{HH}$ = 1.9 Hz, *H8*), 2.00 (m, 1H, *H4*), 1.68 (m, 1H, *H4'*), 1.35-1.55 (m, 4H, *H5*, *H6*), 0.92 (t, 3H, $^3J_{HH}$ = 7.3 Hz, *H7*). **^{13}C NMR** (101 MHz, $CDCl_3$) δ: 173.7 (*C*=O), 143.6 (*C2*), 140.3 (*C12*), 131.7 (*C1*), 131.3, 129.3 (*C10*, *C11*), 118.3 (*C9*), 106.3 (Ar*C*≡C), 82.2 (*C3*), 79.2 (ArC≡*C*), 32.6 (*C4*), 26.5 (*C5*), 22.3 (*C6*), 21.5 (*C13*), 13.7 (*C7*), 10.1 (*C8*). **IR** (CH_2Cl_2): 2203 (C≡C), 1755 (C=O). **HRMS** (*m/z*, ESI^+): calculated for $C_{18}H_{20}NaO_2^+$ ($[M+Na]^+$): 291.1356, found 291.1354.

1,1'-Buta-1,3-diyne-1,4-diylbis(4-methylbenzene) (202d)[280]



R_f (hexane:diethyl ether, 1:1): 0.33. **^{1}H NMR** (400 MHz, $CDCl_3$) δ: 7.11-7.48 (m, 8H, Ar), 2.38 (s, 6H, C$\underline{H}_3$). **^{13}C NMR** (101 MHz, $CDCl_3$) δ: 139.5 (*C4*), 132.4 (*C2*), 129.2 (*C3*), 119.0 (*C1*), 81.5 (Ar$\underline{C}$≡C), 73.5 (ArC≡$\underline{C}$), 21.5 ($\underline{C}H_3$).

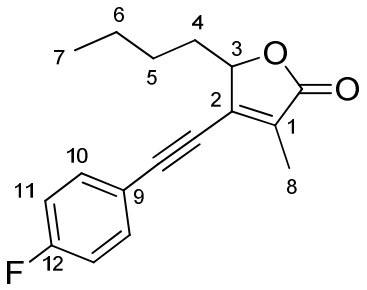
5-Butyl-4-[(4-methoxyphenyl)ethynyl]-3-methylfuran-2(5*H*)-one (200oe)



General procedure F was followed using allenoate **102o** (100 mg, 475 μmol, 1 eq), alkyne **201e** (93 μL, 0.71 mmol, 1.5 eq), PPh_3AuNTf_2 (**2**, 35 mg, 48 μmol, 10 mol%), Selectfluor (**82**, 421 mg, 1.19 mmol, 2.5 eq) and K_3PO_4 (202 mg, 951 μmol, 2 eq) in acetonitrile (5 mL) and water (86 μL, 4.8 mmol, 10 eq). The mixture was stirred at rt for 48h. The resulting crude mixture was purified by column chromatography on silica gel (pet ether 40-60:diethyl ether, 10:1) to afford the product **200oe** as a yellow oil (120 mg, yield = 88%).

R_f (hexane:diethyl ether, 1:1): 0.30. **^{1}H NMR** (500 MHz, $CDCl_3$) δ: 7.46 (d, 2H, $^3J_{HH}$ = 8.6 Hz, *H10*), 6.91 (d, 2H, $^3J_{HH}$ = 8.6 Hz, *H11*), 4.89 (m, 1H, *H3*), 3.84 (s, 3H, *H13*), 2.02 (s, 3H, *H8*), 1.99 (m, 1H, *H4*), 1.62 (m, 1H, *H4'*), 1.42-1.51 (m, 2H, *H5*), 1.32-1.42 (m, 2H, *H6*), 0.92 (t, 3H, $^3J_{HH}$ = 7.2 Hz, *H7*). **^{13}C NMR** (125 MHz, $CDCl_3$) δ: 174.0 ($\underline{C}$=O), 160.8 (*C12*), 143.9 (*C2*), 133.5 (*C11*), 130.8 (*C1*), 114.2 (*C10*), 113.4 (*C9*), 106.4 (Ar$\underline{C}$≡C), 82.3 (*C3*), 78.9 (ArC≡$\underline{C}$), 55.3 (*C13*), 32.7 (*C4*), 26.6 (*C5*), 22.3 (*C6*), 13.8 (*C7*), 10.2 (*C8*). **IR** (CH_2Cl_2): 2205 (C≡C), 1757 (C=O). **HRMS** (*m/z*, ESI^+): calculated for $C_{18}H_{20}NaO_3^+$ ($[M+Na]^+$): 307.1305, found 307.1304.

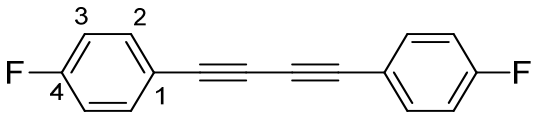
5-Butyl-4-[(4-fluorophenyl)ethynyl]-3-methylfuran-2(5*H*)-one (200of)



General procedure F was followed using allenoate **102o** (100 mg, 475 μmol, 1 eq), alkyne **201f** (82 μL, 0.71 mmol, 1.5 eq), PPh_3AuNTf_2 (**2**, 35 mg, 48 μmol, 10 mol%), Selectfluor (**82**, 421 mg, 1.19 mmol, 2.5 eq) and K_3PO_4 (202 mg, 951 μmol, 2 eq) in acetonitrile (5 mL) and water (86 μL, 4.8 mmol, 10 eq). The mixture was stirred at rt for 48h. The resulting crude mixture was purified by column chromatography on silica gel (pet ether 40-60:diethyl ether, 10:1) to afford the product **200of** as a yellow oil (102 mg, yield = 78%) along with diyne **202f** (4 mg, yield (relative to **201f**) = 5%).

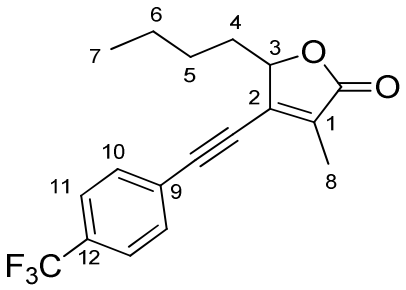
R_f (hexane:diethyl ether, 1:1): 0.32. **^{1}H NMR** (500 MHz, $CDCl_3$) δ: 7.51 (dd, 2H, $^3J_{HH}$ = 8.6 Hz, $^4J_{HF}$ = 5.6 Hz, *H10*), 7.09 (apparent t, 2H, $^3J_{HH}$ = 8.6 Hz, $^3J_{HF}$ = 8.6 Hz, *H11*), 4.91 (m, 1H, *H3*), 2.03 (d, 3H, $^5J_{HH}$ = 1.6 Hz, *H8*), 2.00 (m, 1H, *H4*), 1.64 (m, 1H, *H4'*), 1.35-1.55 (m, 4H, *H5*, *H6*), 0.92 (t, 3H, $^3J_{HH}$ = 7.7 Hz, *H7*). **^{13}C NMR** (125 MHz, $CDCl_3$) δ: 173.6 (*C*=O), 163.3 (d, $^1J_{CF}$ = 252 Hz, *C12*), 143.2 (*C2*), 133.9 (d, $^3J_{CF}$ = 8 Hz, *C10*), 132.0 (*C1*), 117.5 (d, $^4J_{CF}$ = 3 Hz, *C9*), 116.0 (d, $^2J_{CF}$ = 22 Hz, *C11*), 104.7 (Ar*C*≡C), 82.2 (*C3*), 79.5 (ArC≡*C*), 32.7 (*C4*), 26.6 (*C5*), 22.3 (*C6*), 13.8 (*C7*), 10.3 (*C8*). **^{19}F NMR** (377 MHz, $CDCl_3$): −107.9. **IR** (CH_2Cl_2): 2207 (C≡C), 1754 (C=O). **HRMS** (*m/z*, ESI^+): calculated for $C_{17}H_{17}FNaO_2^+$ ($[M+Na]^+$): 295.1105, found 295.1105.

1,1'-Buta-1,3-diyne-1,4-diylbis(4-fluorobenzene) (202f)[280]



R_f (hexane): 0.35. **^{1}H NMR** (500 MHz, $CDCl_3$) δ: 7.52 (ddm, 4H, $^3J_{HH}$ = 8.8 Hz, $^3J_{HF}$ = 5.4 Hz, *H3*), 7.05 (dm, 4H, $^3J_{HH}$ = 8.8 Hz, *H2*). **^{13}C NMR** (125 MHz, $CDCl_3$) δ: 163.0 (d, $^1J_{CF}$ = 252 Hz, *C4*), 134.5 (d, $^3J_{CF}$ = 9 Hz, *C2*), 117.8 (d, $^4J_{CF}$ = 4 Hz, *C1*), 115.9 (d, $^2J_{CF}$ = 22 Hz, *C3*), 80.4 (Ar<u>*C*</u>≡C), 73.5 (ArC≡<u>*C*</u>). **^{19}F NMR** (377 MHz, $CDCl_3$): −108.5.

5-Butyl-3-methyl-4-((4-(trifluoromethyl)phenyl)ethynyl)furan-2(5*H*)-one (200og)

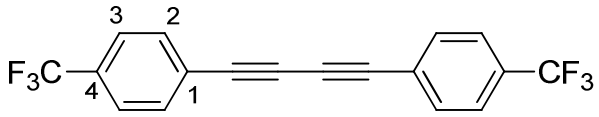


General procedure F was followed using allenoate **102o** (100 mg, 475 μmol, 1 eq), alkyne **201g** (116 μL, 713 μmol, 1.5 eq), PPh_3AuNTf_2 (**2**, 35 mg, 48 μmol, 10 mol%), Selectfluor (**82**, 421 mg, 1.19 mmol, 2.5 eq) and K_3PO_4 (202 mg, 951 μmol, 2 eq) in acetonitrile (5 mL) and water (86 μL, 4.8 mmol, 10 eq). The mixture was stirred at rt for 48h. The resulting crude mixture was purified by column chromatography on silica gel (pet ether 40-60:diethyl ether, 10:1) to afford the product **200og** as a yellow oil (97 mg, yield = 63%) along with diyne **202g** (6 mg, yield (relative to **201g**) = 5%).

R_f (hexane:diethyl ether, 1:1): 0.53. **^{1}H NMR** (500 MHz, $CDCl_3$) δ: 7.66 (d, 2H, $^3J_{HH}$ = 8.5 Hz, *H11*), 7.63 (d, 2H, $^3J_{HH}$ = 8.5 Hz, *H10*), 4.94 (m, 1H, *H3*), 2.06 (d, 3H, $^5J_{HH}$ = 1.3 Hz, *H8*), 2.00 (m, 1H, *H4*), 1.67 (m, 1H, *H4'*), 1.35-1.52 (m, 4H, *H5*, *H6*), 0.93 (t, 3H, $^3J_{HH}$ = 7.1 Hz, *H7*). **^{13}C NMR** (125 MHz, $CDCl_3$) δ: 173.4 (<u>*C*</u>=O), 142.5 (*C2*), 133.3 (*C1*), 132.1 (*C10*), 131.4 (q, $^2J_{CF}$ = 33 Hz, *C12*), 125.5 (q, $^3J_{CF}$ = 3 Hz, *C11*), 125.2 (*C9*), 123.6 (q, $^1J_{CF}$ = 273 Hz, <u>*C*</u>F_3), 103.7 (Ar<u>*C*</u>≡C), 82.2 (*C3*), 81.6 (ArC≡<u>*C*</u>), 32.7 (*C4*), 26.6 (*C5*), 22.4 (*C6*), 13.8 (*C7*), 10.4 (*C8*). **^{19}F NMR** (377 MHz, $CDCl_3$): −63.0. **IR** (CH_2Cl_2): 2200 (C≡C), 1759

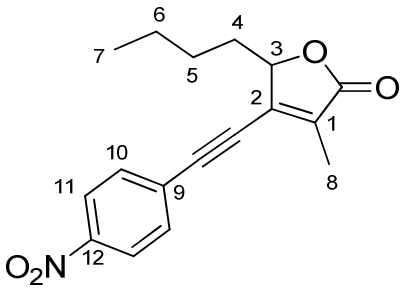
(C=O). **HRMS** (*m/z*, ESI^+): calculated for $C_{18}H_{17}F_3NaO_2^+$ ($[M+Na]^+$): 345.1073, found 345.1074.

1,1'-Buta-1,3-diyne-1,4-diylbis(4-(trifluoromethyl)benzene) (202g)[281]



R_f (hexane): 0.34. **^{1}H NMR** (400 MHz, $CDCl_3$) δ: 7.55-7.70 (m, 8H, Ar). **^{13}C NMR** (125 MHz, $CDCl_3$) δ: 132.8 (*C2*), 131.1 (q, $^2J_{CF}$ = 32 Hz, *C4*), 125.5 (q, $^3J_{CF}$ = 4 Hz, *C3*), 125.2 (*C1*), 123.7 (q, $^1J_{CF}$ = 273 Hz, $\underline{C}F_3$), 81.0 (Ar$\underline{C}$≡C), 75.6 (ArC≡$\underline{C}$). **^{19}F NMR** (377 MHz, $CDCl_3$): −63.0.

5-Butyl-3-methyl-4-[(4-nitrophenyl)ethynyl]furan-2(5*H*)-one (200oh)

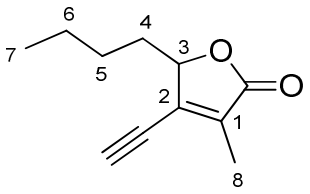


General procedure F was followed using allenoate **102o** (100 mg, 475 μmol, 1 eq), alkyne **201h** (105 mg, 713 μmol, 1.5 eq), PPh_3AuNTf_2 (**2**, 35 mg, 48 μmol, 10 mol%), Selectfluor (**82**, 421 mg, 1.19 mmol, 2.5 eq) and K_3PO_4 (202 mg, 951 μmol, 2 eq) in acetonitrile (5 mL) and water (86 μL, 4.8 mmol, 10 eq). The mixture was stirred at rt for 48h. The resulting crude mixture was purified by column chromatography on silica gel (pet ether 40-60:diethyl ether, 10:1) to afford the product **200oh** as a white solid (64 mg, yield = 45%).

R_f (hexane:diethyl ether, 1:1): 0.49. **Mp** = 87ºC. **^{1}H NMR** (400 MHz, $CDCl_3$) δ: 8.28 (d, 2H, $^3J_{HH}$ = 8.5 Hz, *H11*), 7.68 (d, 2H, $^3J_{HH}$ = 8.5 Hz, *H10*), 4.95 (m, 1H, *H3*), 2.08 (s, 3H, *H8*), 1.99 (m, 1H, *H4*), 1.64 (m, 1H, *H4'*), 1.35-1.55 (m, 4H, *H5*, *H6*), 0.94 (t, 3H, $^3J_{HH}$ =

7.1 Hz, *H7*). **^{13}C NMR** (125 MHz, $CDCl_3$) δ: 173.1 (*C*=O), 147.9 (*C12*), 142.0 (*C2*), 134.2 (*C1*), 132.7 (*C11*), 128.0 (*C9*), 123.8 (*C10*), 102.7 (Ar*C*≡C), 83.9 (ArC≡*C*), 82.1 (*C3*), 32.7 (*C4*), 26.6 (*C5*), 22.4 (*C6*), 13.8 (*C7*), 10.6 (*C8*). **IR** (CH_2Cl_2): 2219 (C≡C), 1755 (C=O), 1523 (NO_2), 1346 (NO_2). **HRMS** (*m/z*, ESI$^+$): calculated for $C_{17}H_{17}NNaO_4^+$ ([M+Na]$^+$): 322.1050, found 322.1053.

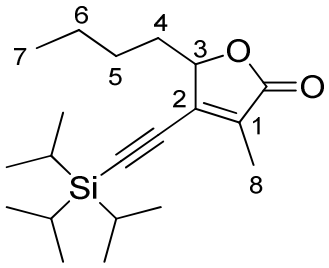
5-Butyl-4-ethynyl-3-methylfuran-2(5*H*)-one (200oi)



General procedure F was followed using allenoate **102o** (100 mg, 475 μmol, 1 eq), alkyne **201i** (101 μL, 713 μmol, 1.5 eq), PPh_3AuNTf_2 (**2**, 35 mg, 48 μmol, 10 mol%), Selectfluor (**82**, 421 mg, 1.19 mmol, 2.5 eq) and NaOH (38 mg, 0.95 mmol, 2 eq) in acetonitrile (5 mL) and water (86 μL, 4.75 mmol, 10 eq). The mixture was stirred at rt for 48h. The resulting crude mixture was purified by column chromatography on silica gel (pet ether 40-60:diethyl ether, 10:1) to afford the product **200oi** as a colourless oil (14 mg, yield = 16%).

R_f (hexane:diethyl ether, 1:1): 0.56. **^{1}H NMR** (500 MHz, $CDCl_3$) δ: 4.86 (m, 1H, *H3*), 3.85 (s, 1H, C≡C*H*), 2.01 (m, 2H, *H4*), 1.56 (s, 3H, *H8*), 1.32-1.49 (m, 4H, *H5*, *H6*), 0.93 (t, 3H, $^3J_{HH}$ = 6.9 Hz, *H7*). **^{13}C NMR** (125 MHz, $CDCl_3$) δ: 173.4 (*C*=O), 142.2 (*C2*), 134.5 (*C1*), 93.6 (C≡*C*H), 82.3 (*C3*), 74.2 (*C*≡CH), 32.4 (*C4*), 26.5 (*C5*), 22.3 (*C6*), 13.8 (*C7*), 10.2 (*C8*). **IR** (CH_2Cl_2): 3298 (C≡C-H), 2108 (C≡C), 1756 (C=O). **HRMS** (*m/z*, ESI$^+$): calculated for $C_{11}H_{14}NaO_2^+$ ([M+Na]$^+$): 201.0886, found 201.0884.

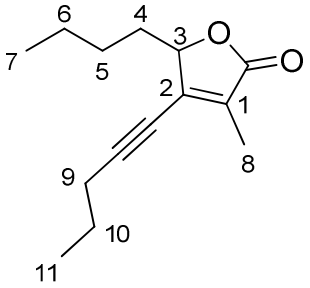
5-Butyl-3-methyl-4-((triisopropylsilyl)ethynyl)furan-2(5*H*)-one (200oj)



General procedure F was followed using allenoate **102o** (100 mg, 475 μmol, 1 eq), alkyne **201j** (160 μL, 713 μmol, 1.5 eq), PPh_3AuNTf_2 (**2**, 35 mg, 48 μmol, 10 mol%), Selectfluor (**82**, 421 mg, 1.19 mmol, 2.5 eq) and K_3PO_4 (202 mg, 951 μmol, 2 eq) in acetonitrile (5 mL) and water (86 μL, 4.75 mmol, 10 eq). The mixture was stirred at rt for 48h. The resulting crude mixture was purified by column chromatography on silica gel (pet ether 40-60:diethyl ether, 10:1) to afford the product **200oj** as a colourless oil (18 mg, yield = 11%).

R_f (hexane:diethyl ether, 1:1): 0.61. **^{1}H NMR** (500 MHz, $CDCl_3$) δ: 4.85 (m, 1H, *H3*), 1.98 (s, 3H, *H8*), 1.92 (m, 1H, *H4*), 1.25-1.45 (m, 5H, *H4'*, *H5*, *H6*), 1.07-1.15 (m, 21H, C*H*(CH_3)$_2$), 0.91 (t, 3H, $^3J_{HH}$ = 7.3 Hz, *H7*). **^{13}C NMR** (125 MHz, $CDCl_3$) δ: 173.9 (*C*=O), 143.6 (*C2*), 132.9 (*C1*), 110.9 (Si*C*≡C), 96.6 (SiC≡*C*), 82.3 (*C3*), 32.5 (*C4*), 26.3 (*C5*), 22.3 (*C6*), 18.5 (CH(CH_3)$_2$), 13.8 (*C7*), 11.0 (*C*H(CH_3)$_2$) 10.3 (*C8*). **IR** (CH_2Cl_2): 2153 (C≡C), 1761 (C=O). **HRMS** (*m/z*, ESI$^+$): calculated for $C_{20}H_{34}NaO_2Si^+$ ([M+Na]$^+$): 357.2220, found 357.2221.

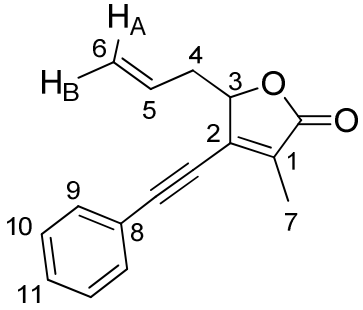
5-Butyl-3-methyl-4-(pent-1-yn-1-yl)furan-2(5*H*)-one (200ok)



General procedure F was followed using allenoate **102o** (100 mg, 475 μmol, 1 eq), alkyne **201k** (70 μL, 713 μmol, 1.5 eq), PPh_3AuNTf_2 (**2**, 36 mg, 48 μmol, 10 mol%), CuOAc, (5.8 mg, 48 μmol, 10 mol%), Selectfluor (**82**, 421 mg, 1.19 mmol, 2.5 eq) and K_3PO_4 (202 mg, 951 μmol, 2 eq) in acetonitrile (5 mL) and water (86 μL, 4.75 mmol, 10 eq). The mixture was stirred at rt for 48h. The resulting crude mixture was purified by column chromatography on silica gel (pet ether 40-60:diethyl ether, 10:1) to afford the product **200ok** as a yellow oil (29 mg, yield = 28%).

R_f (hexane:diethyl ether, 1:1): 0.61. **^{1}H NMR** (500 MHz, $CDCl_3$) δ: 4.78 (m, 1H, *H3*), 2.46 (t, 2H, $^3J_{HH}$ = 6.8 Hz, *H9*), 1.95 (m, 1H, *H4*), 1.93 (s, 3H, *H8*), 1.64 (m, 2H, *H10*), 1.55 (m, 1H, *H4'*), 1.30-1.50 (m, 4H, *H5*, *H6*), 1.04 (t, 3H, $^3J_{HH}$ = 7.6 Hz, *H11*), 0.91 (t, 3H, $^3J_{HH}$ = 6.8 Hz, *H7*). **^{13}C NMR** (125 MHz, $CDCl_3$) δ: 174.2 (*C*=O), 144.6 (*C2*), 130.8 (*C1*), 108.5 ((C_3H_7)*C*≡C), 82.5 (*C3*), 72.0 ((C_3H_7)C≡*C*), 32.5 (*C4*), 26.5 (*C5*), 22.4, 21.9, 21.7 (*C6*, *C9 C10*), 13.8, 13.4 (*C7*, *C11*), 10.0 (*C8*). **IR** (CH_2Cl_2): 2204 (C≡C), 1754 (C=O). **HRMS** (*m/z*, ESI^+): calculated for $C_{14}H_{20}NaO_2^+$ ($[M+Na]^+$): 243.1355, found: 243.1356.

5-Allyl-3-methyl-4-(phenylethynyl)furan-2(5*H*)-one (200ra)

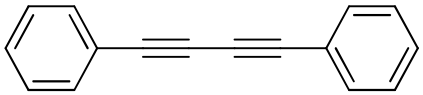


General procedure F was followed using allenoate **102r** (92 mg, 0.48 mmol, 1 eq), alkyne **201a** (78 μL, 0.71 mmol, 1.5 eq), PPh_3AuNTf_2 (**2**, 35 mg, 48 μmol, 10 mol%), Selectfluor (**82**, 421 mg, 1.19 mmol, 2.5 eq) and K_3PO_4 (202 mg, 951 μmol, 2 eq) in acetonitrile (5 mL) and water (86 μL, 4.8 mmol, 10 eq). The mixture was stirred at rt for 48h. The resulting crude mixture was purified by column chromatography on silica gel (pet ether 40-60:diethyl

ether, 8:1) to afford the product **200ra** as a yellow oil (51 mg, yield = 45%) along with diyne **202a** as a yellow solid (21 mg, yield (relative to **201a**) = 29%).

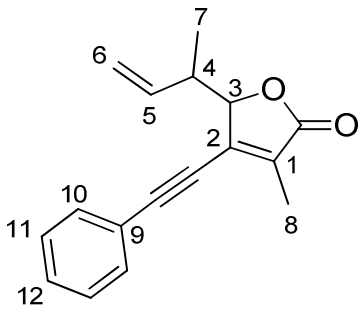
R_f (hexane:diethyl ether, 2:1): 0.43. **^{1}H NMR** (500 MHz, $CDCl_3$) δ: 7.51-7.55 (d, 2H, $^3J_{HH}$ = 6.3 Hz, *H9*), 7.37-7.46 (m, 3H, *H10*, *H11*), 5.75 (ddt, 1H, $^3J_{HH}$ = 17.8, 10.1, 6.8 Hz, *H5*), 5.23 (d, 1H, $^3J_{HH}$ = 17.8 Hz, $H6_A$), 5.18 (d, 1H, $^3J_{HH}$ = 10.1 Hz, $H6_B$), 4.94 (m, 1H, *H3*), 2.80 (m, 1H, *H4*), 2.49 (m, 1H, *H4'*), 2.05 (d, 3H, $^5J_{HH}$ = 1.8 Hz, *H7*). **^{13}C NMR** (125 MHz, $CDCl_3$) δ: 173.5 (*C*=O), 142.6 (*C2*), 132.5 (*C1*), 131.8 (*C9*), 130.9 (*C5*), 130.0 (*C11*), 128.6 (*C10*), 121.4 (*C8*), 119.6 (*C6*), 106.1 (Ph*C*≡C), 81.3 (*C3*), 79.5 (PhC≡*C*), 36.9 (*C4*), 10.3 (*C7*). **IR** (CH_2Cl_2): 2205 (C≡C), 1757 (C=O). **HRMS** (*m/z*, ESI^+): calculated for $C_{16}H_{14}NaO_2^+$ ([M+Na]$^+$): 261.0886, found 261.0889.

1,1'-Buta-1,3-diyne-1,4-diyldibenzene (202a)[282]



R_f (hexane:diethyl ether, 2:1): 0.43. **^{1}H NMR** (400 MHz, $CDCl_3$) δ: 7.20-7.70 (m, 10H, Ph). **^{13}C NMR** (101 MHz, $CDCl_3$) δ: 132.5 (*ortho*-Ph), 129.2, 128.5 (*meta*-, *para*-Ph), 121.8 (*ipso*-Ph), 81.6 (Ph*C*≡C), 73.9 (PhC≡*C*).

5-(But-3-en-2-yl)-3-methyl-4-(phenylethynyl)furan-2(5*H*)-one (200ua)

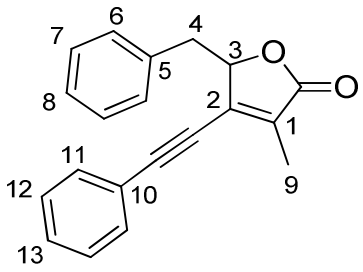


General procedure F was followed using allenoate **102u** (dr = 50:50, 99 mg, 0.48 mmol, 1 eq), alkyne **201a** (78 μL, 0.71 mmol, 1.5 eq), PPh_3AuNTf_2 (**2**, 35 mg, 48 μmol, 10 mol%),

Selectfluor (**82**, 421 mg, 1.19 mmol, 2.5 eq) and K_3PO_4 (202 mg, 951 μmol, 2 eq) in acetonitrile (5 mL) and water (86 μL, 4.8 mmol, 10 eq). The mixture was stirred at rt for 48h. The resulting crude mixture was purified by column chromatography on silica gel (pet ether 40-60:diethyl ether, 8:1) to afford the product **200ua** as a 55:45 diastereoisomeric mixture as a yellow oil (40 mg, yield = 33%) along with diyne **202a** as a yellow solid (17 mg, yield (relative to **201a**) = 23%).

R_f (hexane:diethyl ether, 1:1): 0.56. **^{1}H NMR** (500 MHz, $CDCl_3$) δ: **Major Diastereoisomer**: 7.53 (m, 2H, *H10*), 7.41 (m, 3H, *H11*, *H12*), 5.66 (m, 1H, *H5*), 5.07-5.24 (m, 2H, *H6*), 4.90 (m, 1H, *H3*), 2.85 (m, 1H, *H4*), 2.04 (d, 3H, $^5J_{HH}$ = 1.8 Hz, *H8*), 1.03 (d, 3H, $^3J_{HH}$ = 7.1 Hz, *H7*). **Minor Diastereoisomer**: 7.53 (m, 2H, *H10*), 7.41 (m, 3H, *H11*, *H12*), 5.91 (m, 1H, *H5*), 5.07-5.24 (m, 2H, *H6*), 4.95 (m, 1H, *H3*), 2.85 (m, 1H, *H4*), 2.06 (d, 3H, $^5J_{HH}$ = 1.8 Hz, *H8*), 1.27 (d, 3H, $^3J_{HH}$ = 7.1 Hz, *H7*). **^{13}C NMR** (500 MHz, $CDCl_3$) δ: **Mixture of Diastereoisomers**: 173.7 (*C*=O), 173.6 (*C*=O), 142.1 (*C2*), 141.7 (*C2*), 138.5 (*C5*), 135.5 (*C5*), 132.8 (*C10*), 131.8 (*C1*), 131.8 (*C1*), 129.9, 128.6 (*C11*, *C12*), 121.5 (*C9*), 121.4 (*C9*), 117.6 (*C6*), 116.3 (*C6*), 106.2 (Ph*C*≡C), 106.1 (Ph*C*≡C), 85.3 (*C3*), 84.8 (*C3*), 79.9 (PhC≡*C*), 79.8 (PhC≡*C*), 40.1 (*C4*), 16.3 (*C7*), 12.7 (*C7*), 10.3 (*C8*), 10.2 (*C8*). *Note: The peaks for C4 and C10-12 are coincident for each diastereoisomer*. **IR** (CH_2Cl_2): 2200 (C≡C), 1753 (C=O). **HRMS** (*m/z*, ESI$^+$): calculated for $C_{17}H_{16}NaO_2^+$ ([M+Na]$^+$): 275.1043, found 275.1043.

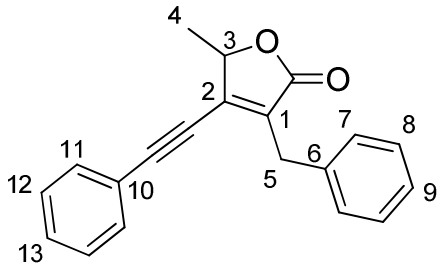
5-Benzyl-3-methyl-4-(phenylethynyl)furan-2(5*H*)-one (200ea)



General procedure F was followed using allenoate **102e** (116 mg, 475 μmol, 1 eq), alkyne **201a** (78 μL, 0.71 mmol, 1.5 eq), PPh_3AuNTf_2 (**2**, 35 mg, 48 μmol, 10 mol%), Selectfluor (**82**, 421 mg, 1.19 mmol, 2.5 eq) and K_3PO_4 (202 mg, 951 μmol, 2 eq) in acetonitrile (5 mL) and water (86 μL, 4.8 mmol, 10 eq). The mixture was stirred at rt for 48h. The resulting crude mixture was purified by column chromatography on silica gel (pet ether 40-60:diethyl ether, 10:1) to afford the product **200ea** as a yellow solid (51 mg, yield = 38%) along with indenofuranone **109e** as a white solid (20 mg, yield = 22%). For characterisation data of **109e**, see Section 6.3.3.2.

R_f (hexane:diethyl ether, 1:1): 0.54. **Mp** = 97ºC. **^{1}H NMR** (500 MHz, $CDCl_3$) δ: 7.23-7.56 (m, 10H, *H6-8*, *H11-13*), 5.18 (m, 1H, *H3*), 3.34 (dd, 1H, $^2J_{HH}$ = 14.4 Hz, $^3J_{HH}$ = 4.6 Hz, *H4*), 3.06 (dd, 1H, $^2J_{HH}$ = 14.4 Hz, $^3J_{HH}$ = 6.6 Hz, *H4'*), 1.97 (d, 3H, $^5J_{HH}$ = 1.5 Hz, *H9*). **^{13}C NMR** (125 MHz, $CDCl_3$) δ: 173.3 (*C*=O), 142.4 (*C2*), 134.7 (*C1*), 132.8 (*C5*), 131.9, 129.9, 129.7, 128.6, 128.3, 127.0 (*C6-8*, *C11-13*), 121.3 (*C10*), 106.5 (Ph*C*≡C), 82.1 (*C3*), 79.8 (PhC≡*C*), 39.0 (*C4*), 10.2 (*C9*). **IR** (CH_2Cl_2): 2205 (C≡C), 1757 (C=O). **HRMS** (*m/z*, ESI^+): calculated for $C_{20}H_{16}NaO_2^+$ ($[M+Na]^+$): 311.1043, found 311.1046. The structure was unambiguously confirmed by X-ray crystallography. This data is deposited at the Cambridge Crystallographic Data Centre (CCDC): 795566 (see Appendix).

3-Benzyl-5-methyl-4-(phenylethynyl)furan-2(5*H*)-one (200ga)



General procedure F was followed using allenoate **102g** (116 mg, 475 μmol, 1 eq), alkyne **201a** (78 μL, 0.71 mmol, 1.5 eq), PPh_3AuNTf_2 (**2**, 35 mg, 48 μmol, 10 mol%), Selectfluor

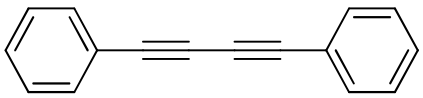
(**82**, 421 mg, 1.19 mmol, 2.5 eq) and K_3PO_4 (202 mg, 951 μmol, 2 eq) in acetonitrile (5 mL) and water (86 μL, 4.8 mmol, 10 eq). The mixture was stirred at rt for 48h. The resulting crude mixture was purified by column chromatography on silica gel (pet ether 40-60:diethyl ether, 10:1) to afford the product **200ga** as a white solid (24 mg, yield = 17%) along with indenofuranone **162g** as a white solid (10 mg, yield = 11%). For characterisation data of **162g**, see Section 6.3.3.2.

R_f (hexane:diethyl ether, 1:1): 0.39. **Mp** = 103ºC. **^{1}H NMR** (400 MHz, $CDCl_3$) δ: 7.21-7.53 (m, 10H, *H7-9*, *H11-13*), 5.01 (q, 1H, $^3J_{HH}$ = 6.6 Hz, *H3*), 3.79 (s, 2H, *H5*), 1.56 (d, 3H, $^3J_{HH}$ = 6.6 Hz, *H4*). **^{13}C NMR** (125 MHz, $CDCl_3$) δ: 172.9 (*C*=O), 145.0 (*C2*), 137.4 (*C1*), 134.2 (*C6*), 132.0, 130.0, 128.9, 128.6, 128.6, 126.7 (*C7-9*, *C11-13*), 121.3 (*C10*), 106.5 (Ph*C*≡C), 79.7 (*C3*), 78.7 (PhC≡*C*), 31.2 (*C5*), 19.0 (*C4*). **IR** (CH_2Cl_2): 2200 (C≡C), 1753 (C=O). **HRMS** (*m/z*, ESI$^+$): calculated for $C_{20}H_{16}NaO_2^+$ ([M+Na]$^+$): 311.1043, found 311.1043.

6.4.4.2 Homodimerisation Reactions of Allenoate 102o and Alkyne 201a

6.3.6.2.1 Homodimerisation of Alkyne 201a

1,1'-Buta-1,3-diyne-1,4-diyldibenzene (202a)[282]

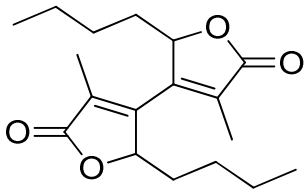


General procedure F was followed using alkyne **201a** (78 μL, 0.71 mmol, 1 eq), PPh_3AuNTf_2 (**2**, 35 mg, 48 μmol, 10 mol%), Selectfluor (**82**, 421 mg, 1.19 mmol, 2.5 eq) and K_3PO_4 (202 mg, 951 μmol, 2 eq) in acetonitrile (5 mL) and water (86 μL, 4.8 mmol, 10 eq) in the absence of an allenoate. The mixture was stirred at rt for 4h. The resulting crude mixture was purified by column chromatography on silica gel (pet ether 40-60:diethyl ether,

10:1) to afford the product **202a** as a yellow solid (71 mg, yield > 95%). For characterisation data of **202a**, see Section 6.4.4.1.

6.4.4.2.2 Homodimerisation of Allenoate 102o

2,2'-Dibutyl-4,4'-dimethyl-3,3'-bifuran-5,5'(2*H*,2'*H*)-dione (110o)



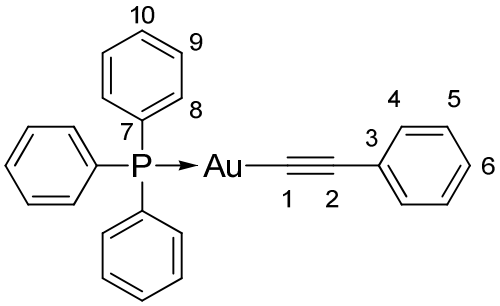
General procedure F was followed using allenoate **102o** (100 mg, 475 μmol, 1 eq), PPh_3AuNTf_2 (**2**, 35 mg, 48 μmol, 10 mol%), Selectfluor (**82**, 421 mg, 1.19 mmol, 2.5 eq) and K_3PO_4 (202 mg, 951 μmol, 2 eq) in acetonitrile (5 mL) and water (86 μL, 4.8 mmol, 10 eq) in the absence of an alkyne. The mixture was stirred at rt for 5d. The resulting crude mixture was purified by column chromatography on silica gel (pet ether 40-60:diethyl ether, 10:1) to afford the product **110o** as a 63:37 diastereoisomeric mixture as a colourless oil (25 mg, yield = 35%). For characterisation data of **110o**, see Section 6.4.2.1.

6.4.4.3 Preparation of Organogold(I) Complexes 203 and 104o

6.4.4.3.1 Preparation of η^1-(Alkynyl)gold(I) Complex 203

η^1-(Alkynyl)gold(I) complex **203** was prepared according to the procedure of Hashmi (see Scheme 4.40a).[208]

(Phenylethynyl)(triphenylphosphine)gold(I) (203)[208]



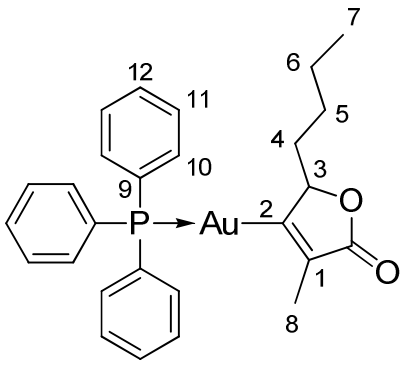
Sodium (5.1 mg, 0.22 mmol, 1.1 eq) was added to ethanol (4 mL) and the mixture was stirred at rt until all the metal had dissolved (15 min). Alkyne **201a** (22 μL, 0.20 mmol, 1 eq) and chloro(triphenylphosphine)gold(I) (100 mg, 202 μmol, 1 eq) were added and the mixture was heated at reflux for 1h. After cooling to rt, the solvent was removed *in vacuo*. Recrystallisation from dichloromethane/hexane afforded the product **203** as a white solid (87 mg, yield = 77%).

^{1}H NMR (500 MHz, $CDCl_3$) δ: 7.44-7.58 (m, 17H, Ph), 7.19-7.27 (m, 3H, Ph). **^{13}C NMR** (125 MHz, $CDCl_3$) δ: 134.3 (d, $^{2}J_{CP}$ = 13 Hz, *C8*), 132.3 (*C4*), 131.5 (*C10*), 129.7 (d, $^{1}J_{CP}$ = 56 Hz, *C7*), 129.1 (d, $^{3}J_{CP}$ = 11 Hz, *C9*), 127.9 (*C5*), 126.8 (*C6*), 124.8 (*C3*), 104.2 (*C2*), 77.1 (*C1*). **^{31}P NMR** (162 MHz, $CDCl_3$) δ: 42.4. **LRMS** (*m/z*, ESI^+): calculated for $C_{26}H_{20}AuNaP^+$ ($[M+Na]^+$): 583.1, found 583.1.

6.4.4.3.2 Preparation of (Butenolide)gold(I) Complex 104o

(Butenelide)gold(I) complex **104o** was prepared according to the procedure of Hashmi (see Scheme 4.40b).[205]

(2-Butyl-4-methyl-5-oxo-2,5-dihydrofuran-3-yl)(triphenylphosphine)gold(I) (104o)



Chloro(triphenylphosphine)gold(I) (70 mg, 0.14 mmol, 1 eq) and silver trifluoromethanesulfonate (36 mg, 0.14 mmol, 1 eq) were added to a solution of ethyl allenoate **105o** (28 mg, 0.16 mmol, 1.1 eq) in anhydrous dichloromethane (1.4 mL) under argon. The mixture was stirred at rt for 2h before water (0.70 mL) was added *via* syringe. The biphasic mixture was stirred vigorously for a further 1.5h and then filtered. The layers were separated and the aqueous layer was extracted with dichloromethane (2×2 mL). The combined organic fractions were dried over anhydrous Na_2SO_4, filtered and concentrated *in vacuo*. Purification by column chromatography on silica gel (pet ether 40-60:diethyl ether, 1:1) afforded the product **104o** as a colourless oil (38 mg, yield = 44%).

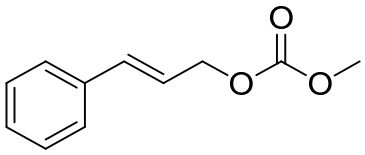
R_f (petrol ether 40-60:diethyl ether, 1:1): 0.11. **^{1}H NMR** (500 MHz, $CDCl_3$) δ: 7.48-7.57 (m, 15H, *H10-12*), 4.93 (tm, 1H, $^3J_{HH}$ = 6.9 Hz, *H3*), 2.03 (t, 3H, $^5J_{HH}$ = 1.3 Hz, *H8*), 1.89 (m, 1H, *H4*), 1.68 (m, 1H, *H4'*), 1.52-1.59 (m, 2H, *H5*), 1.32-1.40 (m, 2H, *H6*), 0.88 (t, 3H, $^3J_{HH}$ = 7.6 Hz, *H7*). **^{13}C NMR** (125 MHz, $CDCl_3$) δ: 200.5 (d, $^2J_{CP}$ = 113 Hz, *C2*), 177.0 (d, $^4J_{CP}$ = 11 Hz, *C*=O), 134.2 (d, $^2J_{CP}$ = 13 Hz, *C10*), 131.7 (d, $^3J_{CP}$ = 2 Hz, *C1*), 131.6 (d, $^4J_{CP}$ = 2 Hz, *C12*), 130.1 (d, $^1J_{CP}$ = 52 Hz, *C9*), 129.3 (d, $^3J_{CP}$ = 11 Hz, *C11*), 90.3 (d, $^3J_{CP}$ = 8 Hz, *C3*), 34.6 (*C4*), 27.9 (*C5*), 22.7 (*C6*), 14.3, 14.0 (*C7*, *C8*). **^{31}P NMR** (162 MHz, $CDCl_3$) δ: 44.4. **IR** (CH_2Cl_2): 1723 (C=O). **HRMS** (*m/z*, ESI^+): calculated for $C_{27}H_{28}AuNaO_2P^+$ ($[M+Na]^+$): 635.1385, found 635.1385.

6.5 Experimental Data for Chapter 5

6.5.1 Preparation of Allylic Carbonate 227b

Allylic methyl carbonate **227b** was prepared according to a procedure modified from Lloyd-Jones *et al* (Scheme 5.15).[283]

Methyl (2*E*)-3-phenylprop-2-en-1-yl carbonate (227b)[283]



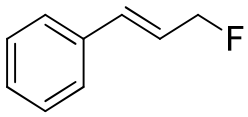
Methyl chloroformate (1.15 mL, 14.9 mmol, 2 eq) was added to a solution of cinnamyl alcohol (1.00 g, 7.45 mmol, 1 eq) in dichloromethane (15 mL) and pyridine (1.81 mL, 22.4 mmol, 3 eq). The mixture was stirred at 0ºC for 4h before being quenched via careful addition of NH_4Cl (sat. aq, 10 mL). The crude solution was extracted with diethyl ether (2×10 mL) and the combined organic fractions were dried over anhydrous Na_2SO_4, filtered and concentrated *in vacuo*. Purification by column chromatography on silica gel (pet ether 40-60:diethyl ether, 4:1) afforded the product **227b** as a colourless oil (1.10 g, yield = 76%). $\mathbf{R_f}$ (hexane:diethyl ether, 4:1): 0.36. **^{1}H NMR** (400 MHz, $CDCl_3$) δ: 7.41 (d, 2H, $^3J_{HH}$ = 7.3 Hz, *ortho*-Ph), 7.34 (t, 2H, $^3J_{HH}$ = 7.3 Hz, *meta*-Ph), 7.28 (tm, 1H, $^3J_{HH}$ = 7.3 Hz, *para*-Ph), 6.70 (d, 1H, $^3J_{HH}$ = 15.9 Hz, PhC*H*=CH), 6.31 (dt, 1H, $^3J_{HH}$ = 15.9, 6.6 Hz, PhCH=C*H*), 4.80 (d, 2H, $^3J_{HH}$ = 6.6 Hz, CH_2), 3.82 (s, 3H, OCH_3). **^{13}C NMR** (101 MHz, $CDCl_3$) δ: 155.6 (*C*=O), 136.0 (*ipso*-Ph), 134.8 (Ph*C*H=CH), 128.6 (*meta*-Ph), 128.2 (*para*-Ph), 126.7 (*ortho*-Ph), 122.4 (PhCH=*C*H), 68.4 (*C*H_2), 54.8 (O*C*H_3). **LRMS** (*m/z*, ESI^+): calculated for $C_{11}H_{12}NaO_3^+$ ($[M+Na]^+$): 215.1, found 215.1.

para-Nitrobenzoate **232b** was kindly provided by Charlotte Hollingworth (DPhil, University of Oxford, 2012).[256]

6.5.2 Preparation of 'Cold' Allylic Fluoride 226b

Allylic fluoride **226b** was prepared according to the procedure of Oshima (see Scheme 5.17).[284]

[(1*E*)-3-Fluoroprop-1-en-1-yl]benzene (226b)[285]



Tetra-*n*-butylammonium fluoride (1M solution in tetrahydrofuran, 16.0 mL, 16.0 mmol, 2 eq) was added to a solution of allylic bromide (**237b**, 1.58 g, 8.00 mmol, 1 eq) in tetrahydrofuran (8 mL). The mixture was stirred at rt for 4h before being quenched in a pH 7.0 buffer solution. The crude product was extracted with diethyl ether (2×10 mL), concentrated *in vacuo* and distilled under reduced pressure (100ºC, 66 Torr) to afford a small amount of the pure product **226b** as a yellow oil (154 mg, yield = 14%).

^{1}H NMR (400 MHz, $CDCl_3$) δ: 7.44 (d, 2H, $^{3}J_{HH}$ = 7.6 Hz, *ortho*-Ph), 7.37 (dd, 2H, $^{3}J_{HH}$ = 7.6, 7.1 Hz, *meta*-Ph), 7.28 (t, 1H, $^{3}J_{HH}$ = 7.3 Hz, *para*-Ph), 6.72 (dd, 1H, $^{3}J_{HH}$ = 15.9 Hz, $^{4}J_{HF}$ = 5.1 Hz, PhC*H*=CH), 6.31 (ddt, 1H, $^{3}J_{HH}$ = 15.9, 6.1 Hz, $^{3}J_{HF}$ = 12.1 Hz, PhCH=C*H*), 5.05 (dd, 2H, $^{2}J_{HF}$ = 47.0 Hz, $^{3}J_{HH}$ = 6.1 Hz, CH_2). **^{13}C NMR** (101 MHz, $CDCl_3$) δ: 135.9 (d, $^{4}J_{CF}$ = 3 Hz, *ipso*-Ph), 134.3 (d, $^{3}J_{CF}$ = 13 Hz, Ph*C*H=CH), 128.6 (*meta*-Ph), 128.3 (*para*-Ph), 126.7 (*ortho*-Ph), 123.5 (d, $^{2}J_{CF}$ = 16 Hz, PhCH=*C*H), 83.4 (d, $^{1}J_{CF}$ = 164 Hz, *C*H_2). **^{19}F NMR** (377 MHz, $CDCl_3$) δ: −210.4 (tdd, $^{2}J_{HF}$ = 47 Hz, $^{3}J_{HF}$ = 12 Hz, $^{4}J_{HF}$ = 5 Hz).

6.5.3 General Experimental Information for Radiochemistry

[^{18}F]TBAF was produced using either manually, using an Advion NanoTek® automated radiosynthesis apparatus controlled by the associated software or using a custom built device developed by GlaxoSmithKline and controlled by software written in Labview.

[^{18}F]Fluoride was produced using a Siemens 11 MeV Eclipse HP cyclotron *via* the ^{18}O(p,n)^{18}F reaction. [^{18}F]Fluoride was separated from ^{18}O-enriched-water using anion exchange cartridges supplied by D&W Inc. (^{18}F Trap & Release, DW-TRC, activated by water (3 mL)) or by Synthra (^{18}F-Separation, 45 mg, activated by water (3 mL)) and eluted with a solution of *n*-Bu_4NHCO_3 (13 mg) in acetonitrile/water (4:1, 0.5 mL). The complex was dried under a gentle stream of nitrogen at 120^{o}C with successive additions of acetonitrile (2×0.5 mL). The resulting [^{18}F]TBAF was dissolved in anhydrous acetonitrile or tetrahydrofuran (1 mL) for use in the nucleophilic radiofluorination reactions.[286]

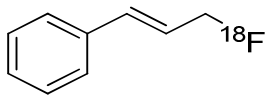
[^{18}F]**226b** was identified by comparison of its radioactive HPLC peak with the UV trace of the non-radioactive reference compound **226b**. Radio-HPLC was conducted on an Agilent 1100 Series or a Gilson HPLC system with an in-line UV detector (254 nm) in series with a NaI crystal radioactivity detector. The HPLC separations were carried out on a Phenomenex NX 5µm C18 column (150×4.60 mm) at room temperature using acetonitrile/water as the mobile phase at a flow rate of 1 mL/min. The following gradient was used:

Gradient A	0-10 min	35-40% acetonitrile (linear increase)
	10-15 min	40-75% acetonitrile (linear increase)
	15-25 min	75% acetonitrile (isocratic)
	25-28 min	75%-35% acetonitrile (linear decrease)
	28-30 min	35% acetonitrile (isocratic)

Radiochemical yields were obtained either by radio-TLC (eluent: MeCN/H_2O, 95:5, LabLogic Systems Ltd. Radio-TLC detector) or by comparison of the radioactivity of the crude reaction mixture injected into the HPLC (20 µL) with that of the product eluted from the column. All radiochemical yields are decay-corrected.

6.5.4 [^{18}F]Radiofluorination of Allylic Methyl Carbonate 227b and *para*-Nitrobenzoate 232b

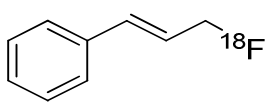
[^{18}F]-[(1*E*)-3-Fluoroprop-1-en-1-yl]benzene ([^{18}F]226b)



A dry 5 mL borosilicate glass vial containing a v-shaped stirring bar was charged with the allylic methyl carbonate **227b** or *para*-nitrobenzoate **232b** (5 mg ± 1 mg), $Pd(dba)_2$ (2 mg ± 1 mg) and triphenylphosphine (2 mg ± 1 mg) in anhydrous acetonitrile or tetrahydrofuran (450 μL). A freshly prepared solution of [^{18}F]TBAF in anhydrous acetonitrile or tetrahydrofuran (50 μL) was added in a lead-shielded hot-cell and the mixture was stirred at at the given temperature (rt or 100ºC) for up to 30 minutes. After quenching with water (500 μL), an aliquot of the crude reaction mixture was taken and analysed by radio-TLC and HPLC. In each reaction, analysis by HPLC ($MeCN/H_2O$ Gradient A, 1 mL/min, 20 μL injected) indicated the formation of [^{18}F]**226b** at a retention time of 14.7 min, which was consistent with the 'cold' reference compound (the HPLC traces are displayed in Figure 5.3). The identity of the peak was confirmed by spiking with the 'cold' reference sample **226b**. Decay corrected radiochemical yields were determined either by radio-TLC on the crude reaction mixture (eluent = $MeCN/H_2O$, 95:5) or by direct comparison of the radioactivity of the crude mixture injected into the HPLC with that of the product eluted from the column (see Table 5.3 for the radiochemical yields of each experiment).

6.5.5 [^{18}F]Radiofluorination of Allylic Chloride 237b and Allylic Bromide 236b

[^{18}F]-[(1*E*)-3-fluoroprop-1-en-1-yl]benzene ([^{18}F]226b)



A dry 5 mL borosilicate glass vial containing a v-shaped stirring bar was charged with the allylic chloride **237b** or bromide **236b** (5 mg ± 1 mg) in anhydrous acetonitrile (450 µL). A freshly prepared solution of [^{18}F]TBAF in anhydrous acetonitrile or tetrahydrofuran (50 µL) was added in a lead-shielded hot-cell and the mixture was stirred at at the given temperature (rt or 110ºC) for up to 20 minutes. After quenching with water (500 µL), an aliquot of the crude reaction mixture was taken and analysed by HPLC. In successful reactions, analysis by HPLC (MeCN/H_2O Gradient A, 1 mL/min, 20 µL injected) indicated the formation of [^{18}F]**226b** at a retention time of 14.7 min, which was consistent with the 'cold' reference compound (the HPLC traces are displayed in Figure 5.3). Decay corrected radiochemical yields were determined by direct comparison of the radioactivity of the crude mixture injected into the HPLC with that of the product eluted from the column (see Schemes 5.22 and Scheme 5.23 for the radiochemical yields of each experiment).

References

[1] S. G. Bratsch, *J. Phys. Chem. Ref. Data* **1989**, *18*, 1-21.
[2] A. S. K. Hashmi, *Chem. Rev.* **2007**, *107*, 3180-3211.
[3] A. Fürstner and P. W. Davies, *Angew. Chem. Int. Ed.* **2007**, *46*, 3410-3449.
[4] Z. Li, C. Brouwer and C. He, *Chem. Rev.* **2008**, *108*, 3239-3265.
[5] A. Arcadi, *Chem. Rev.* **2008**, *108*, 3266-3325.
[6] E. Jiménez-Núñez and A. M. Echavarren, *Chem. Rev.* **2008**, *108*, 3326-3350.
[7] D. J. Gorin, B. D. Sherry and F. D. Toste, *Chem. Rev.* **2008**, *108*, 3351-3378.
[8] A. Fürstner, *Chem. Soc. Rev.* **2009**, *38*, 3208-3221.
[9] S. Sengupta and X. Shi, *ChemCatChem* **2010**, *2*, 609-619.
[10] T. C. Boorman and I. Larrosa, *Chem. Soc. Rev.* **2011**, *40*, 1910-1925.
[11] N. Krause and C. Winter, *Chem. Rev.* **2011**, *111*, 1994-2009.
[12] M. Rudolph and A. S. K. Hashmi, *Chem. Commun.* **2011**, *47*, 6536-6544.
[13] D. J. Gorin and F. D. Toste, *Nature* **2007**, *446*, 395-403.
[14] N. Bartlett, *Gold Bull.* **1998**, *31*, 22-25.
[15] P. Pyykkö, *Angew. Chem. Int. Ed.* **2004**, *43*, 4412-4456.
[16] K. C. Nicolaou, P. G. Bulger and D. Sarlah, *Angew. Chem. Int. Ed.* **2005**, *44*, 4442-4489.
[17] Q. Xu, Y. Imamura, M. Fujiwara and Y. Souma, *J. Org. Chem.* **1997**, *62*, 1594-1598.
[18] R. O. C. Norman, W. J. E. Parr and C. B. Thomas, *J. Chem. Soc., Perkin Trans. 1* **1976**, 1983-1987.
[19] Y. Fukuda and K. Utimoto, *J. Org. Chem.* **1991**, *56*, 3729-3731.
[20] Y. Fukuda and K. Utimoto, *Bull. Chem. Soc. Jpn.* **1991**, *64*, 2013-2015.
[21] J. H. Teles, S. Brode and M. Chabanas, *Angew. Chem. Int. Ed.* **1998**, *37*, 1415-1418.
[22] H. D. Hinton and J. A. Nieuwland, *J. Am. Chem. Soc.* **1930**, *52*, 2892-2896.
[23] S. Antoniotti, E. Genin, V. Michelet and J.-P. Genêt, *J. Am. Chem. Soc.* **2005**, *127*, 9976-9977.
[24] E. Genin, P. Y. Toullec, S. Antoniotti, C. Brancour, J.-P. Genêt and V. Michelet, *J. Am. Chem. Soc.* **2006**, *128*, 3112-3113.
[25] A. Hoffmann-Röder and N. Krause, *Org. Lett.* **2001**, *3*, 2537-2538.
[26] C. J. T. Hyland and L. S. Hegedus, *J. Org. Chem.* **2006**, *71*, 8658-8660.
[27] J. A. Marshall and G. S. Bartley, *J. Org. Chem.* **1994**, *59*, 7169-7171.
[28] N. Krause, M. Laux and A. Hoffmann-Röder, *Tetrahedron Lett.* **2000**, *41*, 9613-9616.
[29] B. Gockel and N. Krause, *Org. Lett.* **2006**, *8*, 4485-4488.
[30] Z. Zhang, C. Liu, R. E. Kinder, X. Han, H. Qian and R. A. Widenhoefer, *J. Am. Chem. Soc.* **2006**, *128*, 9066-9073.
[31] Z. Zhang and R. A. Widenhoefer, *Angew. Chem. Int. Ed.* **2007**, *46*, 283-285.
[32] A. S. K. Hashmi, *Angew. Chem. Int. Ed.* **2008**, *47*, 6754-6756.
[33] D. Benitez, N. D. Shapiro, E. Tkatchouk, Y. Wang, W. A. Goddard and F. D. Toste, *Nature Chem.* **2009**, *1*, 482-486.
[34] B. Lu, C. Li and L. Zhang, *J. Am. Chem. Soc.* **2010**, *132*, 14070-14072.
[35] L. Ye, L. Cui, G. Zhang and L. Zhang, *J. Am. Chem. Soc.* **2010**, *132*, 3258-3259.

[36] L. Ye, W. He and L. Zhang, *J. Am. Chem. Soc.* **2010**, *132*, 8550-8551.
[37] N. Morita and N. Krause, *Angew. Chem. Int. Ed.* **2006**, *45*, 1897-1899.
[38] R. G. Pearson, *J. Am. Chem. Soc.* **1963**, *85*, 3533-3539.
[39] Y. Zhang, J. P. Donahue and C.-J. Li, *Org. Lett.* **2007**, *9*, 627-630.
[40] D. J. Gorin, N. R. Davis and F. D. Toste, *J. Am. Chem. Soc.* **2005**, *127*, 11260-11261.
[41] J. Zhang, C.-G. Yang and C. He, *J. Am. Chem. Soc.* **2006**, *128*, 1798-1799.
[42] G. L. Hamilton, E. J. Kang, M. Mba and F. D. Toste, *Science* **2007**, *317*, 496-499.
[43] G. J. Hutchings, *J. Catal.* **1985**, *96*, 292-295.
[44] B. Nkosi, N. J. Coville, G. J. Hutchings, M. D. Adams, J. Friedl and F. E. Wagner, *J. Catal.* **1991**, *128*, 366-377.
[45] J. A. Akana, K. X. Bhattacharyya, P. Müller and J. P. Sadighi, *J. Am. Chem. Soc.* **2007**, *129*, 7736-7737.
[46] D. S. Laitar, P. Müller, T. G. Gray and J. P. Sadighi, *Organometallics* **2005**, *24*, 4503-4505.
[47] B. C. Gorske, C. T. Mbofana and S. J. Miller, *Org. Lett.* **2009**, *11*, 4318-4321.
[48] J. J. Kennedy-Smith, S. T. Staben and F. D. Toste, *J. Am. Chem. Soc.* **2004**, *126*, 4526-4527.
[49] J. M. Conia and P. Le Perchec, *Synthesis* **1975**, 1-19.
[50] A. S. K. Hashmi, L. Schwarz, J.-H. Choi and T. M. Frost, *Angew. Chem. Int. Ed.* **2000**, *39*, 2285-2288.
[51] G. Dyker, E. Muth, A. S. K. Hashmi and L. Ding, *Adv. Synth. Catal.* **2003**, *345*, 1247-1252.
[52] M. S. Kharasch and H. S. Isbell, *J. Am. Chem. Soc.* **1931**, *53*, 3053-3059.
[53] A. Arcadi, G. Bianchi, M. Chiarini, G. D'Anniballe and F. Marinelli, *Synlett* **2004**, 944-950.
[54] R. M. Zeldin and F. D. Toste, *Chem. Sci.* **2011**, *2*, 1706-1709.
[55] L. S. Fernandez, M. S. Buchanan, A. R. Carroll, Y. J. Feng, R. J. Quinn and V. M. Avery, *Org. Lett.* **2008**, *11*, 329-332.
[56] C. Aubert, O. Buisine and M. Malacria, *Chem. Rev.* **2002**, *102*, 813-834.
[57] S. G. Sethofer, S. T. Staben, O. Y. Hung and F. D. Toste, *Org. Lett.* **2008**, *10*, 4315-4318.
[58] C.-M. Chao, M. R. Vitale, P. Y. Toullec, J.-P. Genêt and V. Michelet, *Chem. Eur. J.* **2009**, *15*, 1319-1323.
[59] E. Comer, E. Rohan, L. Deng and J. A. Porco, *Org. Lett.* **2007**, *9*, 2123-2126.
[60] C. A. Witham, P. Mauleón, N. D. Shapiro, B. D. Sherry and F. D. Toste, *J. Am. Chem. Soc.* **2007**, *129*, 5838-5839.
[61] M. J. Johansson, D. J. Gorin, S. T. Staben and F. D. Toste, *J. Am. Chem. Soc.* **2005**, *127*, 18002-18003.
[62] D. Garayalde, K. Krüger and C. Nevado, *Angew. Chem. Int. Ed.* **2011**, *50*, 911-915.
[63] I. Nakamura, T. Sato and Y. Yamamoto, *Angew. Chem. Int. Ed.* **2006**, *45*, 4473-4475.
[64] K. Molawi, N. Delpont and A. M. Echavarren, *Angew. Chem. Int. Ed.* **2010**, *49*, 3517-3519.
[65] L. Wang, G. Li and Y. Liu, *Org. Lett.* **2011**, *13*, 3786-3789.
[66] A. Buzas and F. Gagosz, *Org. Lett.* **2006**, *8*, 515-518.
[67] B. Gockel and N. Krause, *Eur. J. Org. Chem.* **2010**, *2010*, 311-316.
[68] F. Mo, J. M. Yan, D. Qiu, F. Li, Y. Zhang and J. Wang, *Angew. Chem. Int. Ed.* **2010**, *49*, 2028-2032.
[69] D. Qiu, F. Mo, Z. Zheng, Y. Zhang and J. Wang, *Org. Lett.* **2010**, *12*, 5474-5477.
[70] R. Berger, G. Resnati, P. Metrangolo, E. Weber and J. Hulliger, *Chem. Soc. Rev.* **2011**, *40*, 3496-3508.

[71] P. Jeschke, *ChemBioChem* **2004**, *5*, 570-589.
[72] S. Purser, P. R. Moore, S. Swallow and V. Gouverneur, *Chem. Soc. Rev.* **2008**, *37*, 320-330.
[73] D. O'Hagan, *J. Fluorine Chem.* **2010**, *131*, 1071-1081.
[74] B. E. Smart, *J. Fluorine Chem.* **2001**, *109*, 3-11.
[75] D. O'Hagan, *Chem. Soc. Rev.* **2008**, *37*, 308-319.
[76] P. W. Miller, N. J. Long, R. Vilar and A. D. Gee, *Angew. Chem. Int. Ed.* **2008**, *47*, 8998-9033.
[77] D. B. Harper and D. O'Hagan, *Nat. Prod. Rep.* **1994**, *11*, 123-133.
[78] M. Schuler, F. Silva, C. Bobbio, A. Tessier and V. Gouverneur, *Angew. Chem. Int. Ed.* **2008**, *47*, 7927-7930.
[79] N. Marion and S. P. Nolan, *Angew. Chem. Int. Ed.* **2007**, *46*, 2750-2752.
[80] M. Yu, G. Zhang and L. Zhang, *Org. Lett.* **2007**, *9*, 2147-2150.
[81] M. Yu, G. Zhang and L. Zhang, *Tetrahedron* **2009**, *65*, 1846-1855.
[82] G. Dutheuil, S. Couve-Bonnaire and X. Pannecoucke, *Angew. Chem. Int. Ed.* **2007**, *46*, 1290-1292.
[83] S. Couve-Bonnaire, D. Cahard and X. Pannecoucke, *Org. Biomol. Chem.* **2007**, *5*, 1151-1157.
[84] J. J. Urban, B. G. Tillman and W. A. Cronin, *J. Phys. Chem. A* **2006**, *110*, 11120-11129.
[85] S. Couve-Bonnaire, D. Cahard and X. Pannecoucke, *Org. Biomol. Chem.* **2007**, *5*, 1151-1157.
[86] G. Landelle, M. Bergeron, M. O. Turcotte-Savard and J. F. Paquin, *Chem. Soc. Rev.* **2011**, *40*, 2867-2908.
[87] G. Dutheuil, C. Paturel, X. Lei, S. Couve-Bonnaire and X. Pannecoucke, *J. Org. Chem.* **2006**, *71*, 4316-4319.
[88] A. K. Ghosh, S. Banerjee, S. Sinha, S. B. Kang and B. Zajc, *J. Org. Chem.* **2009**, *74*, 3689-3697.
[89] M. N. Hopkinson, G. T. Giuffredi, A. D. Gee and V. Gouverneur, *Synlett* **2010**, 2737-2742.
[90] A. J. Arduengo, R. Krafczyk, R. Schmutzler, H. A. Craig, J. R. Goerlich, W. J. Marshall and M. Unverzagt, *Tetrahedron* **1999**, *55*, 14523-14534.
[91] W. R. Dolbier Jr, *Guide to Fluorine NMR for Organic Chemists*, John Wiley and Sons, New York, **2009**, p. 70-73.
[92] S. Wang and L. Zhang, *J. Am. Chem. Soc.* **2006**, *128*, 8414-8415.
[93] L. Zhang, *J. Am. Chem. Soc.* **2005**, *127*, 16804-16805.
[94] L. Zhang and S. Wang, *J. Am. Chem. Soc.* **2006**, *128*, 1442-1443.
[95] S. Wang and L. Zhang, *Org. Lett.* **2006**, *8*, 4585-4587.
[96] T. de Haro and C. Nevado, *Chem. Commun.* **2011**, *47*, 248-249.
[97] N. P. Mankad and F. D. Toste, *J. Am. Chem. Soc.* **2010**, *132*, 12859-12861.
[98] D. A. Watson, M. Su, G. Teverovskiy, Y. Zhang, J. García-Fortanet, T. Kinzel and S. L. Buchwald, *Science* **2009**, *325*, 1661-1664.
[99] T. de Haro and C. Nevado, *Adv. Synth. Catal.* **2010**, *352*, 2767-2772.
[100] J.-E. Kang, E.-S. Lee, S.-I. Park and S. Shin, *Tetrahedron Lett.* **2005**, *46*, 7431-7433.
[101] L.-P. Liu, B. Xu, M. S. Mashuta and G. B. Hammond, *J. Am. Chem. Soc.* **2008**, *130*, 17642-17643.
[102] L.-P. Liu and G. B. Hammond, *Chem. Asian. J.* **2009**, *4*, 1230-1236.
[103] M. Seitz and O. Reiser, *Curr. Opin. Chem. Biol.* **2005**, *9*, 285-292.
[104] A. Salisbury, *"Gold Catalysis in the Presence of Electrophilic Fluorinating Reagents"*, Part II (MChem) Thesis, University of Oxford, **2008**.

[105] M. N. Hopkinson, A. Tessier, A. Salisbury, G. T. Giuffredi, L. E. Combettes, A. D. Gee and V. Gouverneur, *Chem. Eur. J.* **2010**, *16*, 4739-4743.
[106] A. Suárez and G. C. Fu, *Angew. Chem. Int. Ed.* **2004**, *43*, 3580-3582.
[107] S. P. Chavan, M. Thakkar and U. R. Kalkote, *Tetrahedron Lett.* **2007**, *48*, 643-646.
[108] A. Tamaki and J. K. Kochi, *J. Organomet. Chem.* **1972**, *40*, C81-C84.
[109] A. Tamaki and J. K. Kochi, *J. Organomet. Chem.* **1973**, *51*, C39-C42.
[110] A. Tamaki and J. K. Kochi, *J. Chem. Soc., Dalton Trans.* **1973**, 2620-2626.
[111] A. Johnson and R. J. Puddephatt, *Inorg. Nucl. Chem. Lett.* **1973**, *9*, 1175-1177.
[112] A. Tamaki and J. K. Kochi, *J. Organomet. Chem.* **1973**, *64*, 411-425.
[113] A. Johnson and R. J. Puddephatt, *J. Organomet. Chem.* **1975**, *85*, 115-121.
[114] C. González-Arellano, A. Corma, M. Iglesias and F. Sánchez, *J. Catal.* **2006**, *238*, 497-501.
[115] A. Corma, E. Gutiérrez-Puebla, M. Iglesias, A. Monge, S. Pérez-Ferreras and F. Sánchez, *Adv. Synth. Catal.* **2006**, *348*, 1899-1907.
[116] C. González-Arellano, A. Abad, A. Corma, H. García, M. Iglesias and F. Sánchez, *Angew. Chem. Int. Ed.* **2007**, *46*, 1536-1538.
[117] P. Li, L. Wang, M. Wang and F. You, *Eur. J. Org. Chem.* **2008**, 5946-5951.
[118] C. González-Arellano, A. Corma, M. Iglesias and F. Sánchez, *Eur. J. Inorg. Chem.* **2008**, *2008*, 1107-1115.
[119] T. Lauterbach, M. Livendahl, A. Rosellón, P. Espinet and A. M. Echavarren, *Org. Lett.* **2010**, *12*, 3006-3009.
[120] A. Corma, R. Juarez, M. Boronat, F. Sanchez, M. Iglesias and H. Garcia, *Chem. Commun.* **2011**, *47*, 1446-1448.
[121] H. A. Wegner, *Chimia* **2009**, *63*, 44-48.
[122] P. Garcia, M. Malacria, C. Aubert, V. Gandon and L. Fensterbank, *ChemCatChem* **2010**, *2*, 493-497.
[123] M. N. Hopkinson, A. D. Gee and V. Gouverneur, *Isr. J. Chem.* **2010**, *50*, 675-690.
[124] M. N. Hopkinson, A. D. Gee and V. Gouverneur, *Chem. Eur. J.* **2011**, *17*, 8248-8262.
[125] T. W. Lyons and M. S. Sanford, *Chem. Rev.* **2010**, *110*, 1147-1169.
[126] E. C. Constable, R. P. G. Henney and T. A. Leese, *J. Organomet. Chem.* **1989**, *361*, 277-282.
[127] E. C. Constable, R. P. G. Henney, P. R. Raithby and L. R. Sousa, *Angew. Chem., Int. Ed. Engl.* **1991**, *30*, 1363-1364.
[128] E. C. Constable and L. R. Sousa, *J. Organomet. Chem.* **1992**, *427*, 125-139.
[129] F. H. Brain and C. S. Gibson, *J. Chem. Soc.* **1939**, 762-767.
[130] G. E. Coates and C. Parkin, *J. Chem. Soc.* **1963**, 421-429.
[131] J. A. J. Jarvis, A. Johnson and R. J. Puddephatt, *J. Chem. Soc., Chem. Commun.* **1973**, 373-374.
[132] A. Tamaki, S. A. Magennis and J. K. Kochi, *J. Am. Chem. Soc.* **1974**, *96*, 6140-6148.
[133] S. Komiya, T. A. Albright, R. Hoffmann and J. K. Kochi, *J. Am. Chem. Soc.* **1976**, *98*, 7255-7265.
[134] S. Komiya and J. K. Kochi, *J. Am. Chem. Soc.* **1976**, *98*, 7599-7607.
[135] P. L. Kuch and R. S. Tobias, *J. Organomet. Chem.* **1976**, *122*, 429-446.
[136] S. Komiya and A. Shibue, *Organometallics* **1985**, *4*, 684-687.
[137] S. Komiya, S. Ozaki and A. Shibue, *J. Chem. Soc., Chem. Commun.* **1986**, 1555-1556.
[138] J. Vicente, M. Dolores Bermúdez and J. Escribano, *Organometallics* **1991**, *10*, 3380-3384.
[139] S. Komiya, T. Sone, S. Ozaki, M. Ishikawa and N. Kasuga, *J. Organomet. Chem.* **1992**, *428*, 303-313.
[140] J. Vicente, M. Dolores Bermúdez and F. J. Carrión, *Inorg. Chim. Acta* **1994**, *220*, 1-3.

[141] O. Schuster, R.-Y. Liau, A. Schier and H. Schmidbaur, *Inorg. Chim. Acta* **2005**, *358*, 1429-1441.
[142] O. Schuster and H. Schmidbaur, *Organometallics* **2005**, *24*, 2289-2296.
[143] N. Komine, K. Ichikawa, A. Mori, M. Hirano and S. Komiya, *Chem. Lett.* **2005**, *34*, 1704-1705.
[144] F. Zamora, P. Amo-Ochoa, B. Fischer, A. Schimanski and B. Lippert, *Angew. Chem. Int. Ed.* **1999**, *38*, 2274-2275.
[145] F. Zamora, E. Zangrando, M. Furlan, L. Randaccio and B. Lippert, *J. Organomet. Chem.* **1998**, *552*, 127-134.
[146] A. K. Sahoo, Y. Nakamura, N. Aratani, K. S. Kim, S. B. Noh, H. Shinokubo, D. Kim and A. Osuka, *Org. Lett.* **2006**, *8*, 4141-4144.
[147] A. Kar, N. Mangu, H. M. Kaiser, M. Beller and M. K. Tse, *Chem. Commun.* **2008**, 386-388.
[148] A. Kar, N. Mangu, H. M. Kaiser and M. K. Tse, *J. Organomet. Chem.* **2009**, *694*, 524-537.
[149] Y. Fuchita, Y. Utsunomiya and M. Yasutake, *J. Chem. Soc., Dalton Trans.* **2001**, 2330-2334.
[150] S. Lavy, J. J. Miller, M. Pažický, A.-S. Rodrigues, F. Rominger, C. Jäkel, D. Serra, N. Vinokurov and M. Limbach, *Adv. Synth. Catal.* **2010**, *352*, 2993-3000.
[151] M. T. Reetz and K. Sommer, *Eur. J. Org. Chem.* **2003**, 3485-3496.
[152] T. de Haro and C. Nevado, *J. Am. Chem. Soc.* **2010**, *132*, 1512-1513.
[153] J. Brand, J. Charpentier and J. Waser, *Angew. Chem. Int. Ed.* **2009**, *48*, 9346-9349.
[154] J. P. Brand and J. Waser, *Angew. Chem. Int. Ed.* **2010**, *49*, 7304-7307.
[155] A. S. K. Hashmi, M. C. Blanco, D. Fischer and J. W. Bats, *Eur. J. Org. Chem.* **2006**, 1387-1389.
[156] S. Fustero, P. Bello, B. Fernández, C. del Pozo and G. B. Hammond, *J. Org. Chem.* **2009**, *74*, 7690-7696.
[157] H. Harkat, A. Y. Dembelé, J.-M. Weibel, A. Blanc and P. Pale, *Tetrahedron* **2009**, *65*, 1871-1879.
[158] H. A. Wegner, S. Ahles and M. Neuburger, *Chem. Eur. J.* **2008**, *14*, 11310-11313.
[159] M. G. Auzias, M. Neuburger and H. A. Wegner, *Synlett* **2010**, 2443-2448.
[160] A. Iglesias and K. Muñiz, *Chem. Eur. J.* **2009**, *15*, 10563-10569.
[161] L. Ricard and F. Gagosz, *Organometallics* **2007**, *26*, 4704-4707.
[162] S. Ma and Z. Yu, *Org. Lett.* **2003**, *5*, 1507-1510.
[163] S. Ma and Z. Yu, *Org. Lett.* **2003**, *5*, 2581-2581.
[164] S. Ma, Z. Yu and Z. Gu, *Chem. Eur. J.* **2005**, *11*, 2351-2356.
[165] P. de Frémont, N. M. Scott, E. D. Stevens and S. P. Nolan, *Organometallics* **2005**, *24*, 2411-2418.
[166] P. de Frémont, N. M. Scott, E. D. Stevens, T. Ramnial, O. C. Lightbody, C. L. B. Macdonald, J. A. C. Clyburne, C. D. Abernethy and S. P. Nolan, *Organometallics* **2005**, *24*, 6301-6309.
[167] N. Mézailles, L. Ricard and F. Gagosz, *Org. Lett.* **2005**, *7*, 4133-4136.
[168] C. Zhou, Z. Ma, Z. Gu, C. Fu and S. Ma, *J. Org. Chem.* **2008**, *73*, 772-774.
[169] L. Cui, G. Zhang and L. Zhang, *Bioorg. Med. Chem. Lett.* **2009**, *19*, 3884-3887.
[170] A. S. K. Hashmi, T. D. Ramamurthi and F. Rominger, *J. Organomet. Chem.* **2009**, *694*, 592-597.
[171] A. S. K. Hashmi, T. D. Ramamurthi, M. H. Todd, A. S.-K. Tsang and K. Graf, *Aust. J. Chem.* **2010**, *63*, 1619-1626.
[172] Y. Peng, L. Cui, G. Zhang and L. Zhang, *J. Am. Chem. Soc.* **2009**, *131*, 5062-5063.
[173] G. Zhang, Y. Peng, L. Cui and L. Zhang, *Angew. Chem. Int. Ed.* **2009**, *48*, 3112-3115.

[174] W. Wang, J. Jasinski, G. B. Hammond and B. Xu, *Angew. Chem. Int. Ed.* **2010**, *49*, 7247-7252.
[175] F. R. Kinder and A. Padwa, *Tetrahedron Lett.* **1990**, *31*, 6835-6838.
[176] A. Padwa and F. R. Kinder, *J. Org. Chem.* **1993**, *58*, 21-28.
[177] J. J. Lingane, *J. Electroanal. Chem.* **1962**, *4*, 332-342.
[178] J. A. Harrison and J. Thompson, *J. Electroanal. Chem. Interfac.* **1975**, *59*, 273-280.
[179] L. H. Skibsted and J. Bjerrum, *Acta. Chem. Scand. A* **1978**, *28*, 764-770.
[180] C. H. Gammons, Y. Yu and A. E. Williams-Jones, *Geochim. Cosmochim. Acta* **1997**, *61*, 1971-1983.
[181] B. Glišić, S. Rajković, Z. Stanić and M. Djuran, *Gold Bull.* **2011**, *44*, 91-98.
[182] D. C. Powers, M. A. L. Geibel, J. E. M. N. Klein and T. Ritter, *J. Am. Chem. Soc.* **2009**, *131*, 17050-17051.
[183] T. Furuya, A. E. Strom and T. Ritter, *J. Am. Chem. Soc.* **2009**, *131*, 1662-1663.
[184] D. C. Powers and T. Ritter, *Nat Chem* **2009**, *1*, 419-419.
[185] P. Tang, T. Furuya and T. Ritter, *J. Am. Chem. Soc.* **2010**, *132*, 12150-12154.
[186] D. C. Powers, D. Benitez, E. Tkatchouk, W. A. Goddard and T. Ritter, *J. Am. Chem. Soc.* **2010**, *132*, 14092-14103.
[187] D. C. Powers, D. Y. Xiao, M. A. L. Geibel and T. Ritter, *J. Am. Chem. Soc.* **2010**, *132*, 14530-14536.
[188] G. J. Chuang, W. Wang, E. Lee and T. Ritter, *J. Am. Chem. Soc.* **2011**, *133*, 1760-1762.
[189] C. Efe, I. N. Lykakis and M. Stratakis, *Chem. Commun.* **2011**, *47*, 803-805.
[190] G. Zhang, L. Cui, Y. Wang and L. Zhang, *J. Am. Chem. Soc.* **2010**, *132*, 1474-1475.
[191] W. E. Brenzovich, D. Benitez, A. D. Lackner, H. P. Shunatona, E. Tkatchouk, W. A. Goddard and F. D. Toste, *Angew. Chem. Int. Ed.* **2010**, *49*, 5519-5522.
[192] A. D. Melhado, W. E. Brenzovich, A. D. Lackner and F. D. Toste, *J. Am. Chem. Soc.* **2010**, *132*, 8885-8887.
[193] W. E. Brenzovich, J.-F. Brazeau and F. D. Toste, *Org. Lett.* **2010**, *12*, 4728-4731.
[194] L. T. Ball, M. Green, G. C. Lloyd-Jones and C. A. Russell, *Org. Lett.* **2010**, *12*, 4724-4727.
[195] R. L. LaLonde, J. W. E. Brenzovich, D. Benitez, E. Tkatchouk, K. Kelley, W. A. Goddard III and F. D. Toste, *Chem. Sci.* **2010**, *1*, 226-233.
[196] T. de Haro and C. Nevado, *Angew. Chem. Int. Ed.* **2011**, *50*, 906-910.
[197] J. Vicente, M.-T. Chicote, M.-D. Abrisqueta and P. G. Jones, *Organometallics* **1997**, *16*, 5628-5636.
[198] M.-A. MacDonald, R. J. Puddephatt and G. P. A. Yap, *Organometallics* **2000**, *19*, 2194-2199.
[199] R.-Y. Liau, A. Schier and H. Schmidbaur, *Organometallics* **2003**, *22*, 3199-3204.
[200] C. Wei and C.-J. Li, *J. Am. Chem. Soc.* **2003**, *125*, 9584-9585.
[201] L. A. Jones, S. Sanz and M. Laguna, *Catal. Today* **2007**, *122*, 403-406.
[202] B. Panda and T. K. Sarkar, *Tetrahedron Lett.* **2010**, *51*, 301-305.
[203] B. Panda and T. K. Sarkar, *Chem. Commun.* **2010**, *46*, 3131-3133.
[204] S. Ma, Z. Shi and Z. Yu, *Tetrahedron Lett.* **1999**, *40*, 2393-2396.
[205] A. S. K. Hashmi, R. Döpp, C. Lothschütz, M. Rudolph, D. Riedel and F. Rominger, *Adv. Synth. Catal.* **2010**, *352*, 1307-1314.
[206] J. E. Ross, *"Gold Catalyzed Oxidative Cross Coupling Reactions"*, Part II (MChem) Thesis, University of Oxford, **2010**.
[207] M. N. Hopkinson, J. E. Ross, G. T. Giuffredi, A. D. Gee and V. Gouverneur, *Org. Lett.* **2010**, *12*, 4904-4907.

[208] A. S. K. Hashmi, C. Lothschütz, R. Döpp, M. Rudolph, T. D. Ramamurthi and F. Rominger, *Angew. Chem. Int. Ed.* **2009**, *48*, 8243-8246.
[209] S. M. Ametamey, M. Honer and P. A. Schubiger, *Chem. Rev.* **2008**, *108*, 1501-1516.
[210] S. M. Ametamey, *Chem. Rev.* **2008**, *108*, 4036-4036.
[211] V. J. Cunningham, C. A. Parker, E. A. Rabiner, A. D. Gee and R. N. Gunn, *Drug Discovery Today: Technologies* **2005**, *2*, 311-315.
[212] Ed. S. Dresel, *PET in Oncology*, Series: *Recent Results in Cancer Research*, *Vol. 170*, (Eds. P. M. Schlag and H. J. Senn), Springer-Verlag, Heidelberg, **2007**.
[213] Y. F. Tai and P. Piccini, *J. Neurol. Neurosurg. Psychiatry* **2004**, *75*, 669-676.
[214] M. F. Di Carli, S. Dorbala, J. Meserve, G. El Fakhri, A. Sitek and S. C. Moore, *J. Nucl. Med.* **2007**, *48*, 783-793.
[215] S. E. Snyder and M. R. Kilbourn in *Handbook of Radiopharmaceuticals*, (Eds. M. J. Welch and C. S. Redvanley), John Wiley and Sons, New York, *Chapter 6*, **2003**, pp. 195-219.
[216] J. Bergman and O. Solin, *Nucl. Med. Biol.* **1997**, *24*, 677-683.
[217] H. Teare, E. G. Robins, E. Arstad, S. K. Luthra and V. Gouverneur, *Chem. Commun.* **2007**, 2330-2332.
[218] H. Teare, E. G. Robins, A. Kirjavainen, S. Forsback, G. Sandford, O. Solin, S. K. Luthra and V. Gouverneur, *Angew. Chem. Int. Ed.* **2010**, *49*, 6821-6824.
[219] L. Cai, S. Lu and V. W. Pike, *Eur. J. Org. Chem.* **2008**, *2008*, 2853-2873.
[220] M.-C. Lasne, C. Perrio, J. Rouden, L. Barré, D. Roeda, F. Dolle and C. Crouzel in *Topics in Current Chemistry: Contrast Agents II*, (Eds. W. Krause), Springer-Verlag, Berlin-Heidelberg, *Vol. 222*, **2002**.
[221] K. Hamacher, H. H. Coenen and G. Stöcklin, *J. Nucl. Med.* **1986**, *27*, 235-238.
[222] J. S. Fowler and T. Ido in *Handbook of Radiopharmaceuticals*, (Eds. M. J. Welch and C. S. Redvanley), John Wiley and Sons, New York, *Chapter 9*, **2003**, pp. 307-322.
[223] S. O. Okarvi, *Eur. J. Nucl. Med. Mol. Imaging* **2001**, *28*, 929-938.
[224] C. Younes, R. Boisgard and B. Tavitian, *Curr. Pharm. Des.* **2002**, *8*, 1451-1466.
[225] M. Glaser and E. Årstad, *Bioconjugate Chem.* **2007**, *18*, 989-993.
[226] F. Dolle, *Curr. Pharm. Des.* **2005**, *11*, 3221-3235.
[227] M. R. Kilbourn, M. J. Welch, C. S. Dence, T. J. Tewson, H. Saji and M. Maeda, *Int. J. Appl. Radiat. Isot.* **1984**, *35*, 591-598.
[228] M. Namavari, A. Bishop, N. Satyamurthy, G. Bida and J. R. Barrio, *Int. J. Appl. Radiat. Instrum. A: Applied Radiation and Isotopes* **1992**, *43*, 989-996.
[229] L. Li, M. N. Hopkinson, R. L. Yona, R. Bejot, A. D. Gee and V. Gouverneur, *Chem. Sci.* **2011**, *2*, 123-131.
[230] P. Biginelli, *Ber. Dtsch. Chem. Ges.* **1891**, *24*, 1317-1319.
[231] I. Ugi, R. Meyr, R. Fetzer and C. Steinbrückner, *Angew. Chem.* **1959**, *71*, 386.
[232] M. Passerini and L. Simone, *Gazz. Chim. Ital.* **1921**, *51*, 126-129.
[233] K. Groebke, L. Weber and F. Mehlin, *Synlett* **1998**, *1998*, 661,663.
[234] H. Bienaymé and K. Bouzid, *Angew. Chem. Int. Ed.* **1998**, *37*, 2234-2237.
[235] C. Blackburn, B. Guan, P. Fleming, K. Shiosaki and S. Tsai, *Tetrahedron Lett.* **1998**, *39*, 3635-3638.
[236] T. G. Murali Dhar, D. Nagarathnam, M. R. Marzabadi, B. Lagu, W. C. Wong, G. Chiu, S. Tyagarajan, S. W. Miao, F. Zhang, W. Sun, D. Tian, Q. Shen, J. Zhang, J. M. Wetzel, C. Forray, R. S. L. Chang, T. P. Broten, T. W. Schorn, T. B. Chen, S. O'Malley, R. Ransom, K. Schneck, R. Bendesky, C. M. Harrell, K. P. Vyas, K. Zhang, J. Gilbert, D. J. Pettibone, M. A. Patane, M. G. Bock, R. M. Freidinger and C. Gluchowski, *J. Med. Chem.* **1999**, *42*, 4778-4793.
[237] V. W. Pike and F. I. Aigbirhio, *J. Chem. Soc., Chem. Commun.* **1995**, 2215-2216.

[238] A. Shah, V. W. Pike and D. A. Widdowson, *J. Chem. Soc., Perkin Trans. 1* **1998**, 2043-2046.
[239] J.-H. Chun, S. Lu, Y.-S. Lee and V. W. Pike, *J. Org. Chem.* **2010**, *75*, 3332-3338.
[240] B. Wang, L. Qin, K. D. Neumann, S. Uppaluri, R. L. Cerny and S. G. DiMagno, *Org. Lett.* **2010**, *12*, 3352-3355.
[241] T. L. Ross, J. Ermert, C. Hocke and H. H. Coenen, *J. Am. Chem. Soc.* **2007**, *129*, 8018-8025.
[242] J. M. Brown and V. Gouverneur, *Angew. Chem. Int. Ed.* **2009**, *48*, 8610-8614.
[243] T. Furuya, H. M. Kaiser and T. Ritter, *Angew. Chem. Int. Ed.* **2008**, *47*, 5993-5996.
[244] K. L. Hull, W. Q. Anani and M. S. Sanford, *J. Am. Chem. Soc.* **2006**, *128*, 7134-7135.
[245] X. Wang, T.-S. Mei and J.-Q. Yu, *J. Am. Chem. Soc.* **2009**, *131*, 7520-7521.
[246] T. Furuya and T. Ritter, *J. Am. Chem. Soc.* **2008**, *130*, 10060-10061.
[247] N. D. Ball and M. S. Sanford, *J. Am. Chem. Soc.* **2009**, *131*, 3796-3797.
[248] T. Furuya, D. Benitez, E. Tkatchouk, A. E. Strom, P. Tang, W. A. Goddard and T. Ritter, *J. Am. Chem. Soc.* **2010**, *132*, 3793-3807.
[249] V. V. Grushin, *Acc. Chem. Res.* **2009**, *43*, 160-171.
[250] D. V. Yandulov and N. T. Tran, *J. Am. Chem. Soc.* **2007**, *129*, 1342-1358.
[251] D. S. Surry and S. L. Buchwald, *Chem. Sci.* **2011**, *2*, 27-50.
[252] A. V. Vorogushin, X. Huang and S. L. Buchwald, *J. Am. Chem. Soc.* **2005**, *127*, 8146-8149.
[253] E. J. Cho, T. D. Senecal, T. Kinzel, Y. Zhang, D. A. Watson and S. L. Buchwald, *Science* **2010**, *328*, 1679-1681.
[254] A. Hazari, V. Gouverneur and J. M. Brown, *Angew. Chem. Int. Ed.* **2009**, *48*, 1296-1299.
[255] C. Hollingworth, A. Hazari, M. N. Hopkinson, M. Tredwell, E. Benedetto, M. Huiban, A. D. Gee, J. M. Brown and V. Gouverneur, *Angew. Chem. Int. Ed.* **2011**, *50*, 2613-2617.
[256] C. Hollingworth, *"Palladium Mediated Allylic Fluorination"*, DPhil Thesis in Preparation, University of Oxford, **2012**.
[257] A. Hazari, *"Palladium Catalyzed Allylic C-F Bond Formation and Activation"*, DPhil Thesis, University of Oxford, **2009**.
[258] N.-U. H. Khan, B. C. Lee, S.-Y. Lee, Y. S. Choe, C.-H. Jun and D. Y. Chi, *J. Label. Compd. Radiopharm.* **2002**, *45*, 1045-1053.
[259] F. Dollé, J. Helfenbein, F. Hinnen, S. Mavel, Z. Mincheva, W. Saba, M.-A. Schöllhorn-Peyronneau, H. Valette, L. Garreau, S. Chalon, C. Halldin, J.-C. Madelmont, J.-B. Deloye, M. Bottlaender, J. Le Gailliard, D. Guilloteau and P. Emond, *J. Label. Compd. Radiopharm.* **2007**, *50*, 716-723.
[260] J. S. Stehouwer, L. M. Daniel, P. Chen, R. J. Voll, L. Williams, S. J. Plott, J. R. Votaw, M. J. Owens, L. Howell and M. M. Goodman, *J. Med. Chem.* **2010**, *53*, 5549-5557.
[261] E. Lee and D. V. Yandulov, *J. Fluorine Chem.* **2009**, *130*, 474-483.
[262] M. H. Katcher and A. G. Doyle, *J. Am. Chem. Soc.* **2010**, *132*, 17402-17404.
[263] T. Ishikawa, T. Mizuta, K. Hagiwara, T. Aikawa, T. Kudo and S. Saito, *J. Org. Chem.* **2003**, *68*, 3702-3705.
[264] A. Bartels, R. Mahrwald and K. Müller, *Adv. Synth. Catal.* **2004**, *346*, 483-485.
[265] T. Schwier, M. Rubin and V. Gevorgyan, *Org. Lett.* **2004**, *6*, 1999-2001.
[266] N. Marion, P. Carlqvist, R. Gealageas, P. de Frémont, F. Maseras and S. P. Nolan, *Chem. Eur. J.* **2007**, *13*, 6437-6451.
[267] S. Liao and B. List, *Angew. Chem. Int. Ed.* **2010**, *49*, 628-631.
[268] K. Zeitler, *Org. Lett.* **2006**, *8*, 637-640.

[269] B. M. Trost and R. C. Livingston, *J. Am. Chem. Soc.* **2008**, *130*, 11970-11978.
[270] H. Hata, T. Kobayashi, H. Amii, K. Uneyama and J. T. Welch, *Tetrahedron Lett.* **2002**, *43*, 6099-6102.
[271] T. Dubuffet, C. Bidon, P. Martinet, R. Sauvêtre and J.-F. Normant, *J. Organomet. Chem.* **1990**, *393*, 161-172.
[272] M. Nandi, J. Jin and T. V. RajanBabu, *J. Am. Chem. Soc.* **1999**, *121*, 9899-9900.
[273] A. Vij, Y. Y. Zheng, R. L. Kirchmeier and J. M. Shreeve, *Inorg. Chem.* **1994**, *33*, 3281-3288.
[274] R. A. Aitken, J. M. Armstrong, M. J. Drysdale, F. C. Ross and B. M. Ryan, *J. Chem. Soc., Perkin Trans. 1* **1999**, 593-604.
[275] C. Li, R. P. Johnson and J. A. Porco, *J. Am. Chem. Soc.* **2003**, *125*, 5095-5106.
[276] Y. Ishii, C. Gao, W. X. Xu, M. Iwasaki and M. Hidai, *J. Org. Chem.* **1993**, *58*, 6818-6825.
[277] P. Maslak, S. Varadarajan and J. D. Burkey, *J. Org. Chem.* **1999**, *64*, 8201-8209.
[278] R. L. Koder, B. R. Lichtenstein, J. F. Cerda, A.-F. Miller and P. L. Dutton, *Tetrahedron Lett.* **2007**, *48*, 5517-5520.
[279] C. Zhou, Z. Ma, Z. Gu, C. Fu and S. Ma, *J. Org. Chem.* **2007**, *73*, 772-774.
[280] S.-N. Chen, W.-Y. Wu and F.-Y. Tsai, *Green Chem.* **2009**, *11*, 269-274.
[281] S. V. Damle, D. Seomoon and P. H. Lee, *J. Org. Chem.* **2003**, *68*, 7085-7087.
[282] C. B. Ziegler, S. M. Harris and J. E. Baldwin, *J. Org. Chem.* **1987**, *52*, 443-446.
[283] J. Lehmann and G. C. Lloyd-Jones, *Tetrahedron* **1995**, *51*, 8863-8874.
[284] K. Hirano, H. Yorimitsu and K. Oshima, *Org. Lett.* **2004**, *6*, 4873-4875.
[285] A. Boukerb, D. Grée, M. Laabassi and R. Grée, *J. Fluorine Chem.* **1998**, *88*, 23-27.
[286] U. Berndt, C. Stanetty, T. Wanek, C. Kuntner, J. Stanek, M. Berger, M. Bauer, G. Henriksen, H.-J. Wester, H. Kvaternik, P. Angelberger and C. Noe, *J. Label. Compd. Radiopharm.* **2008**, *51*, 137-145.

Appendix

X-Ray Crystallography Data

A-1 General Information

In each case, a typical crystal was chosen and mounted on a hair using perfluoropolyether oil and cooled rapidly to 150K in a stream of cold N_2 using an Oxford Cryosystems Cryostream N_2 open flow cooling device.[1] Diffraction data were measured using an Enraf-Nonius Kappa CCD diffractometer (graphite-monochromated MoKα radiation, λ = 0.71073 Å) to a maximum resolution of 0.77 Å. Intensity data were processed using the DENZO-SMN package and were corrected for absorption and other effects using SCALEPACK.[2]

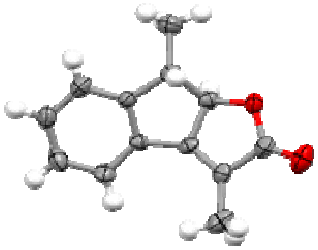
The systematic absences in the intensity data were examined to determine the space group. In each case, the structure was solved using the direct-methods program SIR92,[3] which located all non-hydrogen atoms. Subsequent full-matrix least-squares refinement was carried out using the CRYSTALS[4] program suite to refine coordinates and anisotropic thermal parameters of all non-hydrogen atoms. Hydrogen atoms were located in the difference map and refined before being added to the model using a riding constraint.

The crystallographic data (excluding structure factors) of published crystals has been deposited with the Cambridge Crystallographic Data Centre (CCDC) and copies of these data can be obtained free of charge via www.ccdc.cam.ac.uk/data_request/cif. The relevant crystals and their CCDC Numbers are listed below:

92l	CCDC 792124
109b	CCDC 765540
(±)-(2*S*,2'*S*)-**110b**	CCDC 765543
(2*R*,2'*S*)-**110b**	CCDC 765544
109d	CCDC 765541
109e	CCDC 795567
162h	CCDC 765545
(8*R*,8a*S*)-**109j**	CCDC 765542
200ea	CCDC 795566

The crystallography data for the unpublished crystals **109i** and (2*R*,2'*S*)-**110t** is included in Sections A-2 and A-3 respectively.

A-2 X-Ray data for 109i



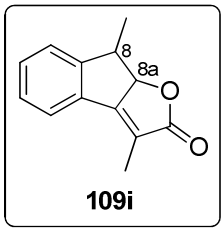


Figure A-1 X-Ray Crystal Structure of **109i** (only the (8*S*,8a*R*) enantiomer is depicted).

Crystal identification	9221606 08lec006
Compound number	**109i**
Empirical formula	C17.33 H16 O2.67
Formula weight	266.98
Temperature	150 K

Wavelength	0.71073 Å
Crystal system	Monoclinic
Space group	P 1 21/c 1
Unit cell dimensions	a = 14.3599(4) Å
	b = 9.8912(3) Å
	c = 14.6614(4) Å
	α = 90°
	β = 93.6037(14)°
	γ = 90°
Volume	2078.34(10) $Å^3$
Z	6
Density (calculated)	1.280 Mg/m^3
Absorption coefficient	0.085 mm^{-1}
F(000)	848
Crystal shape	plate
Crystal colour	colourless
Crystal size	0.51 × 0.42 × 0.21 mm^3
Crystallization solvent	EtOH
Theta range for data collection (θ)	5.1 to 27.5°
Index ranges	−18<=h<=18, −12<=k<=11, −19<=l<=19
Reflections collected	20126
Independent reflections	8003
Completeness to theta max. (θ)	98.5%
Absorption correction	Semi-empirical from equivalents
Max. and min. transmission	0.85 and 0.98
Refinement method	Full-matrix least-squares on F^2
Data/ restraints/ parameters	5758 / 0 / 272
Goodness-of-fit on F^2	0.967
Final R indices [I>2sigma(I)]	R1 = 0.0829, wR2 = 0.2033

R indices (all data)	R1 = 0.0967, wR2 = 0.2080
Largest dif. peak and hole	−0.65 and 0.68 e. $Å^{-3}$

Table A-1 Crystal Data and Refinement Details.

Atom	x	y	z	U_{equiv}
O1	0.12644 (17)	0.4701 (2)	0.60615 (16)	0.0536
C2	0.1404 (2)	0.3574 (3)	0.5776 (2)	0.0397
O3	0.16346 (16)	0.2536 (2)	0.63688 (14)	0.0458
C4	0.1815 (2)	0.1358 (3)	0.58264 (19)	0.0397
C5	0.15520 (19)	0.1760 (3)	0.48644 (18)	0.0308
C6	0.13152 (19)	0.3065 (3)	0.4826 (2)	0.0358
C7	0.0942 (2)	0.3916 (3)	0.4062 (2)	0.0471
C8	0.14094 (19)	0.0512 (3)	0.43412 (19)	0.0313
C9	0.1370 (2)	0.0250 (3)	0.3407 (2)	0.0414
C10	0.1198 (3)	−0.1080 (3)	0.3129 (2)	0.0485
C11	0.1076 (3)	−0.2088 (3)	0.3756 (2)	0.0504
C12	0.1098 (2)	−0.1831 (3)	0.4680 (2)	0.0438
C13	0.1248 (2)	−0.0513 (3)	0.4981 (2)	0.0379
C14	0.1215 (2)	0.0077 (3)	0.5947 (2)	0.0423
C15	0.1504 (3)	−0.0846 (4)	0.6725 (2)	0.0571
O16	0.37992 (15)	0.7516 (2)	0.66063 (14)	0.0438
C17	0.3483 (2)	0.6312 (3)	0.6129 (2)	0.0362
C18	0.4081 (2)	0.5026 (3)	0.61941 (19)	0.0356
C19	0.38204 (19)	0.4413 (3)	0.52560 (19)	0.0321
C20	0.3918 (2)	0.3090 (3)	0.4960 (2)	0.0388
C21	0.3693 (2)	0.2803 (3)	0.4046 (2)	0.0435
C22	0.3402 (2)	0.3786 (3)	0.3428 (2)	0.044
C23	0.3301 (2)	0.5113 (3)	0.3718 (2)	0.0419
C24	0.34932 (19)	0.5409 (3)	0.4635 (2)	0.0322

C25	0.34742 (19)	0.6666 (3)	0.5141 (2)	0.0335
C26	0.36765 (19)	0.7978 (3)	0.5052 (2)	0.0364
C27	0.3865 (2)	0.8533 (3)	0.5968 (2)	0.041
O28	0.40614 (17)	0.9668 (2)	0.62113 (18)	0.0569
C29	0.3809 (2)	0.8792 (3)	0.4208 (2)	0.0495
C30	0.3959 (3)	0.4128 (3)	0.7011 (2)	0.0481

Table A-2 Atomic Coordinates and Equivalent Isotropic Thermal Parameters ($Å^2$) of Non-Hydrogen Atoms.

Atom	x	y	z	U_{iso}
H41	0.2475	0.1107	0.5893	0.0476*
H72	0.0917	0.3409	0.3492	0.0707*
H71	0.1328	0.4711	0.4008	0.0715*
H73	0.0327	0.4213	0.4195	0.0713*
H91	0.1487	0.0914	0.2983	0.0502*
H101	0.1189	−0.1325	0.2501	0.0585*
H111	0.0964	−0.2963	0.3544	0.0593*
H121	0.1008	−0.2515	0.5111	0.0522*
H141	0.0576	0.0315	0.6092	0.0519*
H153	0.1046	−0.1612	0.6694	0.0883*
H152	0.1471	−0.0381	0.7319	0.0870*
H151	0.2145	−0.1182	0.663	0.0874*
H171	0.2854	0.6117	0.6307	0.0417*
H181	0.4756	0.5316	0.6226	0.0430*
H201	0.4134	0.2426	0.5386	0.0459*
H211	0.374	0.1895	0.383	0.0528*
H221	0.3282	0.3548	0.2801	0.0533*
H231	0.3125	0.5808	0.331	0.0509*
H293	0.4364	0.9323	0.428	0.0734*
H292	0.3878	0.817	0.37	0.0736*

H291	0.3277	0.9388	0.4082	0.0739*
H303	0.4332	0.3307	0.696	0.0722*
H302	0.4141	0.4643	0.7568	0.0725*
H301	0.3306	0.3888	0.7023	0.0727*

Table A-3 Atomic Coordinates and Equivalent Isotropic Thermal Parameters (Å^2) of Hydrogen Atoms.

	U^{11}	U^{22}	U^{33}	U^{12}	U^{13}	U^{23}
O1	0.0610 (15)	0.0457 (15)	0.0545 (15)	−0.0019 (11)	0.0072 (11)	−0.0243 (12)
C2	0.0404 (17)	0.041 (2)	0.0385 (17)	−0.0029 (14)	0.0060 (13)	−0.0039 (14)
O3	0.0621 (14)	0.0433 (14)	0.0322 (11)	−0.0063 (11)	0.0029 (10)	−0.0048 (10)
C4	0.0539 (19)	0.0381 (19)	0.0268 (15)	−0.0003 (14)	0.0004 (13)	0.0021 (13)
C5	0.0356 (15)	0.0313 (17)	0.0256 (14)	−0.0037 (12)	0.0036 (11)	−0.0001 (12)
C6	0.0323 (15)	0.0319 (18)	0.0434 (17)	−0.0050 (12)	0.0048 (13)	−0.0041 (13)
C7	0.050 (2)	0.039 (2)	0.052 (2)	0.0019 (14)	−0.0024 (15)	0.0048 (15)
C8	0.0352 (15)	0.0282 (16)	0.0311 (15)	−0.0010 (12)	0.0071 (12)	0.0037 (12)
C9	0.058 (2)	0.0318 (18)	0.0348 (17)	0.0028 (14)	0.0075 (14)	−0.0003 (13)
C10	0.073 (2)	0.043 (2)	0.0298 (17)	0.0056 (16)	0.0041 (15)	−0.0036 (14)
C11	0.071 (2)	0.0294 (19)	0.051 (2)	0.0047 (15)	0.0063 (17)	−0.0008 (15)
C12	0.056 (2)	0.0325 (18)	0.0427 (18)	0.0011 (14)	0.0040 (14)	0.0115 (14)
C13	0.0475 (18)	0.0353 (18)	0.0313 (16)	−0.0034 (13)	0.0043 (13)	0.0041 (13)
C14	0.057 (2)	0.0424 (19)	0.0272 (16)	0.0034 (15)	0.0035 (14)	0.0065 (13)
C15	0.067 (2)	0.062 (3)	0.0416 (19)	0.0029 (18)	−0.0004 (16)	0.0118 (17)
O16	0.0578 (14)	0.0334 (12)	0.0403 (12)	−0.0032 (10)	0.0050 (10)	−0.0074 (10)
C17	0.0387 (16)	0.0319 (17)	0.0380 (17)	−0.0036 (13)	0.0026 (13)	−0.0034 (13)
C18	0.0414 (17)	0.0326 (17)	0.0325 (15)	0.0043 (12)	0.0008 (12)	0.0037 (12)
C19	0.0366 (16)	0.0261 (16)	0.0342 (15)	−0.0017 (12)	0.0063 (12)	−0.0017 (12)
C20	0.0409 (17)	0.0272 (17)	0.0485 (18)	0.0015 (12)	0.0042 (14)	0.0030 (13)
C21	0.0517 (19)	0.0283 (18)	0.051 (2)	−0.0046 (14)	0.0060 (15)	−0.0073 (15)
C22	0.0463 (19)	0.047 (2)	0.0384 (18)	−0.0028 (15)	−0.0036 (14)	−0.0079 (15)

C23	0.0448 (18)	0.045 (2)	0.0350 (17)	0.0048 (14)	−0.0050 (13)	0.0027 (14)
C24	0.0286 (15)	0.0310 (16)	0.0363 (16)	0.0037 (12)	−0.0025 (11)	0.0011 (12)
C25	0.0270 (14)	0.0284 (17)	0.0447 (17)	0.0052 (11)	−0.0014 (12)	0.0061 (13)
C26	0.0320 (16)	0.0277 (17)	0.0493 (18)	0.0075 (12)	−0.0001 (13)	−0.0012 (14)
C27	0.0390 (17)	0.0276 (18)	0.057 (2)	0.0047 (13)	0.0043 (14)	−0.0015 (15)
O28	0.0622 (16)	0.0335 (15)	0.0749 (18)	−0.0059 (11)	0.0024 (13)	−0.0124 (12)
C29	0.048 (2)	0.037 (2)	0.063 (2)	0.0028 (14)	0.0054 (16)	0.0142 (16)
C30	0.064 (2)	0.046 (2)	0.0347 (17)	−0.0029 (16)	0.0072 (15)	0.0075 (15)

Table A-4 Atomic Displacement Parameters ($Å^2$).

O1—C2	1.212 (4)	O16—C17	1.440 (3)
C2—O3	1.372 (4)	O16—C27	1.381 (4)
C2—C6	1.479 (4)	C17—C18	1.535 (4)
O3—C4	1.443 (4)	C17—C25	1.489 (4)
C4—C5	1.491 (4)	C17—H171	0.975
C4—C14	1.548 (4)	C18—C19	1.528 (4)
C4—H41	0.978	C18—C30	1.510 (4)
C5—C6	1.335 (4)	C18—H181	1.01
C5—C8	1.461 (4)	C19—C20	1.389 (4)
C6—C7	1.475 (4)	C19—C24	1.402 (4)
C7—H72	0.973	C20—C21	1.388 (4)
C7—H71	0.968	C20—H201	0.945
C7—H73	0.963	C21—C22	1.375 (4)
C8—C9	1.392 (4)	C21—H211	0.956
C8—C13	1.411 (4)	C22—C23	1.390 (4)
C9—C10	1.394 (4)	C22—H221	0.954
C9—H91	0.928	C23—C24	1.387 (4)
C10—C11	1.375 (5)	C23—H231	0.935
C10—H101	0.952	C24—C25	1.449 (4)

C11—C12	1.377 (5)	C25—C26	1.339 (4)
C11—H111	0.931	C26—C27	1.461 (4)
C12—C13	1.389 (4)	C26—C29	1.497 (4)
C12—H121	0.94	C27—O28	1.206 (4)
C13—C14	1.535 (4)	C29—H293	0.955
C14—C15	1.500 (4)	C29—H292	0.977
C14—H141	0.984	C29—H291	0.973
C15—H153	1.003	C30—H303	0.979
C15—H152	0.989	C30—H302	0.984
C15—H151	0.996	C30—H301	0.968

Table A-5 Bond Length (Å).

O1—C2—O3	120.6 (3)	C17—O16—C27	107.8 (2)
O1—C2—C6	129.2 (3)	O16—C17—C18	119.8 (2)
O3—C2—C6	110.2 (3)	O16—C17—C25	105.2 (2)
C2—O3—C4	107.4 (2)	C18—C17—C25	103.0 (2)
O3—C4—C5	105.2 (2)	O16—C17—H171	107.7
O3—C4—C14	118.5 (3)	C18—C17—H171	110
C5—C4—C14	102.5 (2)	C25—C17—H171	110.9
O3—C4—H41	110.9	C17—C18—C19	99.7 (2)
C5—C4—H41	110.4	C17—C18—C30	116.4 (3)
C14—C4—H41	108.9	C19—C18—C30	116.6 (3)
C4—C5—C6	110.3 (2)	C17—C18—H181	107.4
C4—C5—C8	106.9 (2)	C19—C18—H181	109.5
C6—C5—C8	140.2 (3)	C30—C18—H181	106.8
C2—C6—C5	106.4 (3)	C18—C19—C20	129.2 (3)
C2—C6—C7	121.8 (3)	C18—C19—C24	111.0 (2)
C5—C6—C7	131.6 (3)	C20—C19—C24	119.7 (3)
C6—C7—H72	110.5	C19—C20—C21	118.2 (3)

C6—C7—H71	110	C19—C20—H201	118.9
H72—C7—H71	109.8	C21—C20—H201	122.9
C6—C7—H73	108.4	C20—C21—C22	122.3 (3)
H72—C7—H73	110.3	C20—C21—H211	119.6
H71—C7—H73	107.8	C22—C21—H211	118.1
C5—C8—C9	132.1 (3)	C21—C22—C23	119.9 (3)
C5—C8—C13	106.4 (2)	C21—C22—H221	119.3
C9—C8—C13	121.5 (3)	C23—C22—H221	120.8
C8—C9—C10	117.3 (3)	C22—C23—C24	118.5 (3)
C8—C9—H91	122	C22—C23—H231	121.9
C10—C9—H91	120.6	C24—C23—H231	119.6
C9—C10—C11	121.1 (3)	C19—C24—C23	121.3 (3)
C9—C10—H101	121	C19—C24—C25	106.6 (2)
C11—C10—H101	117.9	C23—C24—C25	132.0 (3)
C10—C11—C12	121.9 (3)	C17—C25—C24	107.3 (2)
C10—C11—H111	118.5	C17—C25—C26	109.6 (3)
C12—C11—H111	119.6	C24—C25—C26	140.4 (3)
C11—C12—C13	118.6 (3)	C25—C26—C27	107.6 (3)
C11—C12—H121	122.1	C25—C26—C29	130.0 (3)
C13—C12—H121	119.2	C27—C26—C29	122.1 (3)
C8—C13—C12	119.5 (3)	C26—C27—O16	109.4 (3)
C8—C13—C14	110.8 (3)	C26—C27—O28	130.4 (3)
C12—C13—C14	129.6 (3)	O16—C27—O28	120.2 (3)
C13—C14—C4	99.0 (2)	C26—C29—H293	110.7
C13—C14—C15	116.5 (3)	C26—C29—H292	108.4
C4—C14—C15	117.1 (3)	H293—C29—H292	107.8
C13—C14—H141	111.9	C26—C29—H291	110.2
C4—C14—H141	111.3	H293—C29—H291	109.2
C15—C14—H141	101.4	H292—C29—H291	110.6
C14—C15—H153	106	C18—C30—H303	109.7

C14—C15—H152	111.1	C18—C30—H302	108.4
H153—C15—H152	108.8	H303—C30—H302	112
C14—C15—H151	108.1	C18—C30—H301	108.6
H153—C15—H151	110.6	H303—C30—H301	109.5
H152—C15—H151	112	H302—C30—H301	108.6

Table A-6 Bond Angles (°).

D—H···*A*	*D*—H	H···*A*	*D*···*A*	*D*—H···*A*
C7—H73···O1^{i}	0.96	2.53	3.445 (4)	159

Symmetry code: (i) $-x, -y+1, -z+1$.

Table A-7: Hydrogen-Bond Geometry (Å, °).

A-3 X-Ray Data for (2*R*,2′*S*)-110t

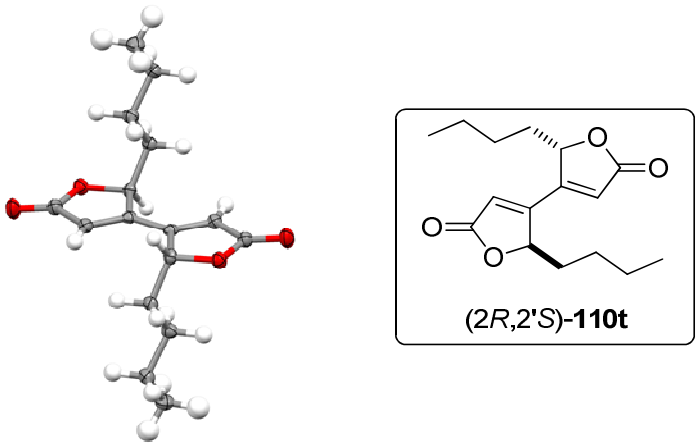


Figure A-2 X-Ray Crystal Structure of (2*R*,2′*S*)-**110t**.

Crystal identification	054GG615MH01
Compound number	(2*R*,2*S*)-**110t**
Empirical formula	C16 H22 O4
Formula weight	278.35
Temperature	150 K
Wavelength	0.71073 Å

Crystal system	Triclinic
Space group	P −1
Unit cell dimensions	a = 7.9377(2) Å
	b = 9.0097(3) Å
	c = 11.5953(4) Å
	α = 96.7063(17)°
	β = 94.5420(16)°
	γ = 114.5456(16)°
Volume	741.63(4) $Å^3$
Z	2
Density (calculated)	1.246 Mg/m^3
Absorption coefficient	0.088 mm^{-1}
F(000)	300
Crystal shape	plate
Crystal colour	colourless
Crystal size	0.32 × 0.25 × 0.12 mm^3
Crystallization solvent	CH_2Cl_2 / hexane
Theta range for data collection (θ)	5.1 to 27.5°
Index ranges	−10<=h<=9, −11<=k<=11, −15<=l<=15
Reflections collected	8704
Independent reflections	3346
Completeness to theta max. (θ)	98.3%
Absorption correction	Semi-empirical from equivalents
Max. and min. transmission	0.93 and 0.99
Refinement method	Full-matrix least-squares on F^2
Data/ restraints/ parameters	3346 / 0 / 181
Goodness-of-fit on F^2	1.0361
Final R indices [I>2sigma(I)]	R1 = 0.0439, wR2 = 0.0595
R indices (all data)	R1 = 0.0753,

	wR2 = 0.749
Largest dif. peak and hole	−0.45 and 0.53 e. $Å^{-3}$

Table A-8 Crystal Data and Refinement Details.

Atom	x	y	z	U_{equiv}
O1	0.28281 (17)	0.01991 (16)	0.78045 (11)	0.0268
C2	0.4448 (2)	−0.0020 (2)	0.82800 (15)	0.0229
C3	0.4325 (2)	0.0090 (2)	0.95803 (14)	0.0205
C4	0.2828 (2)	0.0342 (2)	0.97894 (16)	0.0243
C5	0.1862 (3)	0.0398 (2)	0.86760 (16)	0.0267
O6	0.04424 (18)	0.05778 (19)	0.84774 (13)	0.0381
C7	0.6187 (2)	0.1261 (2)	0.79096 (15)	0.0241
C8	0.6798 (2)	0.3018 (2)	0.85419 (16)	0.0241
C9	0.8413 (3)	0.4262 (2)	0.80292 (18)	0.0315
C10	0.9072 (3)	0.6034 (3)	0.8628 (2)	0.0405
O11	0.07146 (17)	−0.28089 (15)	0.57702 (11)	0.0242
C12	−0.0640 (2)	−0.2111 (2)	0.56378 (15)	0.0206
C13	−0.2421 (2)	−0.3414 (2)	0.48921 (15)	0.0216
C14	−0.2189 (2)	−0.3854 (2)	0.36237 (15)	0.0235
C15	−0.4019 (2)	−0.5077 (2)	0.28770 (15)	0.0254
C16	−0.3773 (3)	−0.5436 (2)	0.16044 (16)	0.0311
C17	0.0397 (2)	−0.0571 (2)	0.51206 (14)	0.0187
C18	0.2085 (2)	−0.0466 (2)	0.49494 (15)	0.0218
C19	0.2305 (2)	−0.1858 (2)	0.53620 (16)	0.0237
O20	0.36365 (18)	−0.21901 (16)	0.53899 (13)	0.0347

Table A-9 Atomic Coordinates and Equivalent Isotropic Thermal Parameters ($Å^2$) of Non-Hydrogen Atoms.

Atom	x	y	z	U_{iso}

H21	0.426	−0.1152	0.7931	0.0249*
H41	0.2392	0.0446	1.0521	0.0293*
H71	0.7213	0.0923	0.8057	0.0284*
H72	0.59	0.1187	0.7068	0.0294*
H81	0.7184	0.3084	0.9388	0.0295*
H82	0.5708	0.3315	0.848	0.0288*
H92	0.9502	0.3961	0.8099	0.0381*
H91	0.8014	0.4173	0.7182	0.0385*
H102	1.0129	0.6765	0.8273	0.0609*
H101	0.9463	0.6136	0.947	0.0609*
H103	0.802	0.6359	0.8522	0.0607*
H121	−0.0929	−0.1800	0.6469	0.0213*
H132	−0.2845	−0.4424	0.5262	0.0259*
H131	−0.3379	−0.2994	0.4917	0.0262*
H142	−0.1245	−0.4330	0.3624	0.0284*
H141	−0.1671	−0.2853	0.3275	0.0291*
H151	−0.4494	−0.6109	0.3206	0.0306*
H152	−0.4958	−0.4614	0.2921	0.0303*
H162	−0.4986	−0.6177	0.1139	0.0467*
H163	−0.2881	−0.5942	0.1554	0.0470*
H161	−0.3240	−0.4400	0.1296	0.0471*
H181	0.3049	0.0376	0.4643	0.0258*

Table A-10 Atomic Coordinates and Equivalent Isotropic Thermal Parameters (Å^2) of Hydrogen atoms

	U^{11}	U^{22}	U^{33}	U^{12}	U^{13}	U^{23}
O1	0.0232 (6)	0.0334 (7)	0.0223 (7)	0.0108 (6)	0.0005 (5)	0.0060 (6)
C2	0.0240 (9)	0.0257 (9)	0.0188 (9)	0.0113 (8)	0.0008 (7)	0.0023 (7)
C3	0.0205 (8)	0.0168 (8)	0.0201 (9)	0.0037 (7)	0.0028 (7)	0.0036 (7)
C4	0.0222 (9)	0.0269 (9)	0.0231 (9)	0.0094 (8)	0.0037 (7)	0.0054 (7)

C5	0.0210 (9)	0.0279 (10)	0.0292 (10)	0.0077 (8)	0.0024 (8)	0.0087 (8)
O6	0.0268 (8)	0.0538 (9)	0.0412 (9)	0.0213 (7)	0.0061 (6)	0.0195 (7)
C7	0.0266 (9)	0.0304 (10)	0.0188 (9)	0.0143 (8)	0.0067 (7)	0.0070 (7)
C8	0.0222 (9)	0.0270 (10)	0.0242 (9)	0.0100 (8)	0.0068 (7)	0.0077 (7)
C9	0.0245 (10)	0.0333 (11)	0.0360 (11)	0.0086 (8)	0.0093 (8)	0.0144 (9)
C10	0.0276 (11)	0.0342 (12)	0.0539 (14)	0.0060 (9)	0.0047 (10)	0.0141 (10)
O11	0.0231 (6)	0.0240 (7)	0.0282 (7)	0.0119 (5)	0.0020 (5)	0.0083 (5)
C12	0.0220 (9)	0.0231 (9)	0.0203 (9)	0.0122 (7)	0.0047 (7)	0.0060 (7)
C13	0.0208 (9)	0.0207 (9)	0.0232 (9)	0.0080 (7)	0.0051 (7)	0.0053 (7)
C14	0.0212 (9)	0.0226 (9)	0.0239 (9)	0.0068 (7)	0.0030 (7)	0.0030 (7)
C15	0.0222 (9)	0.0261 (10)	0.0258 (10)	0.0094 (8)	−0.0003 (7)	0.0021 (8)
C16	0.0287 (10)	0.0319 (11)	0.0279 (10)	0.0110 (9)	−0.0006 (8)	−0.0026 (8)
C17	0.0207 (9)	0.0178 (8)	0.0152 (8)	0.0072 (7)	−0.0008 (6)	0.0002 (6)
C18	0.0204 (8)	0.0223 (9)	0.0227 (9)	0.0094 (7)	0.0017 (7)	0.0032 (7)
C19	0.0218 (9)	0.0224 (9)	0.0269 (10)	0.0099 (8)	0.0009 (7)	0.0036 (7)
O20	0.0250 (7)	0.0327 (8)	0.0524 (9)	0.0176 (6)	0.0032 (6)	0.0104 (7)

Table A-11 Atomic Displacement Parameters ($Å^2$).

O1—C2	1.456 (2)	O11—C12	1.461 (2)
O1—C5	1.355 (2)	O11—C19	1.357 (2)
C2—C3	1.513 (2)	C12—C13	1.522 (2)
C2—C7	1.519 (2)	C12—C17	1.512 (2)
C2—H21	0.997	C12—H121	1.042
C3—C3^{i}	1.462 (3)	C13—C14	1.524 (2)
C3—C4	1.334 (2)	C13—H132	0.992
C4—C5	1.466 (2)	C13—H131	0.98
C4—H41	0.95	C14—C15	1.524 (2)
C5—O6	1.212 (2)	C14—H142	1.007
C7—C8	1.521 (2)	C14—H141	0.974

C7—H71	0.991	C15—C16	1.519 (3)
C7—H72	0.972	C15—H151	0.984
C8—C9	1.528 (2)	C15—H152	0.996
C8—H81	0.992	C16—H162	0.982
C8—H82	1.006	C16—H163	0.99
C9—C10	1.515 (3)	C16—H161	0.976
C9—H92	1.008	C17—C17^{ii}	1.453 (3)
C9—H91	0.992	C17—C18	1.336 (2)
C10—H102	0.983	C18—C19	1.463 (2)
C10—H101	0.983	C18—H181	0.954
C10—H103	0.997	C19—O20	1.212 (2)

Table A-12 Bond Length (Å).

C2—O1—C5	110.18 (13)	C12—O11—C19	109.67 (13)
O1—C2—C3	103.26 (14)	O11—C12—C13	108.67 (14)
O1—C2—C7	108.62 (14)	O11—C12—C17	103.41 (13)
C3—C2—C7	117.02 (15)	C13—C12—C17	116.06 (14)
O1—C2—H21	106.9	O11—C12—H121	108.1
C3—C2—H21	110.7	C13—C12—H121	109.6
C7—C2—H21	109.7	C17—C12—H121	110.5
C2—C3—C3^{i}	122.66 (19)	C12—C13—C14	113.92 (14)
C2—C3—C4	109.17 (15)	C12—C13—H132	108
C3^{i}—C3—C4	128.2 (2)	C14—C13—H132	109.3
C3—C4—C5	108.90 (16)	C12—C13—H131	107.6
C3—C4—H41	127.9	C14—C13—H131	109.9
C5—C4—H41	123.2	H132—C13—H131	107.9
C4—C5—O1	108.49 (15)	C13—C14—C15	112.87 (14)
C4—C5—O6	130.01 (18)	C13—C14—H142	108.1
O1—C5—O6	121.50 (17)	C15—C14—H142	110

C2—C7—C8	114.50 (14)	C13—C14—H141	109.8
C2—C7—H71	107.6	C15—C14—H141	109.2
C8—C7—H71	109.2	H142—C14—H141	106.8
C2—C7—H72	105.8	C14—C15—C16	111.96 (15)
C8—C7—H72	111.1	C14—C15—H151	108.7
H71—C7—H72	108.5	C16—C15—H151	109.8
C7—C8—C9	111.54 (15)	C14—C15—H152	108.9
C7—C8—H81	109.6	C16—C15—H152	109.5
C9—C8—H81	109.6	H151—C15—H152	107.8
C7—C8—H82	109.5	C15—C16—H162	109.9
C9—C8—H82	109.4	C15—C16—H163	109.7
H81—C8—H82	107.1	H162—C16—H163	110.5
C8—C9—C10	113.62 (17)	C15—C16—H161	109.4
C8—C9—H92	109	H162—C16—H161	109.8
C10—C9—H92	108.4	H163—C16—H161	107.5
C8—C9—H91	108.7	C12—C17—C17^{ii}	122.88 (18)
C10—C9—H91	109.5	C12—C17—C18	109.19 (14)
H92—C9—H91	107.4	C17^{ii}—C17—C18	127.9 (2)
C9—C10—H102	109.6	C17—C18—C19	108.76 (15)
C9—C10—H101	110.2	C17—C18—H181	128.1
H102—C10—H101	109.5	C19—C18—H181	123.1
C9—C10—H103	108.7	C18—C19—O11	108.94 (14)
H102—C10—H103	109.5	C18—C19—O20	129.52 (17)
H101—C10—H103	109.3	O11—C19—O20	121.53 (16)

Table A-13 Bond Angles (°).

D—H···*A*	*D*—H	H···*A*	*D*···*A*	*D*—H···*A*
C4—H41···O6^{iii}	0.95	2.49	3.301 (3)	143
C15—H151···O20^{iv}	0.98	2.59	3.446 (3)	145

C18—H181···O20^{v}	0.95	2.46	3.331 (3)	152

Symmetry codes: (iii) $-x, -y, -z+2$; (iv) $-x, -y-1, -z+1$; (v) $-x+1, -y, -z+1$.

Table A-14 Hydrogen-Bond Geometry (Å, °).

A-4 References

1 Cosier, J.; Glazer, A. M. *J. Appl. Cryst.* **1986**, 19, 105.

2 Otwinowski, Z.; Minor, W., "Processing of X-ray Diffraction Data Collected in Oscillation Mode" *Methods Enzymol.* **1997**, 276, Eds. Carter, C. W.; Sweet, R. M. Academic Press.

3 Altomare, A.; Cascarano, G.; Giacovazzo, C.; Guagliardi, A.; Burla, M. C.; Polidori, G.; Camalli, M. *J. Appl. Cryst.* **1994**, 27, 435.

4 Betteridge, P. W.; Carruthers, J. R.; Cooper, R. I.; Prout, K.; Watkin, D. J. *J. Appl. Cryst.* **2003**, 36, 1487.